DISSERTATION

NEW BASE-CATALYZED PROCESSES ENABLE NEW APPROACHES TO C–H FUNCTIONALIZATION REACTIONS

Submitted by

Thomas R. Puleo

Department of Chemistry

In partial fulfillment of the requirements

For the Degree of Doctor of Philosophy

Colorado State University

Fort Collins, Colorado

Fall 2022

Doctoral Committee:

Advisor: Jeffrey Bandar

Andy McNally
Joseph Zadrozny
Delphi Chatterjee

ABSTRACT

NEW BASE-CATALYZED PROCESSES ENABLE NEW APPROACHES TO C–H FUNCTIONALIZATION REACTIONS

Brønsted bases are ubiquitous, inexpensive, and widely available reagents used in synthetic chemistry due to their well-studied and predictable activation mode. This thesis details the discovery and incorporation of new Brønsted base-catalyzed processes into fundamental proton transfer equilibria to enable new approaches to C–H functionalization reactions. The direct functionalization of C–H bonds represents a streamlined and attractive approach to access valuable synthetic targets, and this utility will be highlighted throughout the discussion of each method.

Chapter one describes the discovery and development of a base-catalyzed α-selective styrene deuteration reaction. The mechanistic studies that led to the conceptualization and optimization of this reaction will be highlighted. α-Deuterated styrenes are compounds frequently utilized in the mechanistic studies of alkene functionalization reactions and this work represents the first method to achieve α-selective hydrogen isotope exchange on styrene derivatives.

Chapter two provides an overview of existing approaches to catalytic aryl halide isomerization reactions. A particular focus on base-catalyzed aryl halide isomerization reactions will be provided, as these reports serve as the mechanistic foundation for the reactions developed throughout the remainder of the thesis.

Chapter three describes our discovery and application of a general approach to base-catalyzed aryl halide isomerization. Aryl halides are valuable compounds in synthetic chemistry, and this new catalytic isomerization process unlocks a new mode of reactivity for these

compounds. The scope of this process is demonstrated on several simple aryl bromides and iodides. The second part of this chapter will highlight an application of this process to enable the 4-selective nucleophilic substitution of 3-bromopyridines.

Chapter four describes our approach to achieve nucleophilic C–H etherification of electron-deficient *N*-heteroarenes *via* a base-catalyzed halogen transfer mechanism. 2-Halogenated thiophenes efficiently transfer halogens to *N*-heteroaryl anions to generate *N*-heteroaryl halide intermediates that undergo nucleophilic aromatic substitution with alkoxide nucleophiles. Additionally, C–H etherification can be sequenced with a cascade base-promoted elimination to enable *N*-heteroarene C–H hydroxylation. The scope of process is highly general, and regioselective C–H etherification and hydroxylation is demonstrated on thiazoles, oxazoles, imidazoles, pyridines, pyrimidines, pyridazines, and polyazines.

Chapter five briefly highlights two new C–H functionalization reactions currently being developed that are enabled by base-catalyzed halogen transfer. First, use of this approach to enable the C–H hydroxylation of benzenes will be described. Second, the monoselective and site-selective benzylic C–H etherification of toluenes and polyalkyl benzenes will be detailed. In the final part of the chapter, I will summarize my contributions and discuss the future outlooks on this chemistry.

ACKNOWLEDGEMENTS

There are an innumerable number of people I would like to thank who have helped me on this journey. First, thank you to my Mom and Dad for all your love and support. You instilled a strong work ethic in me, served excellent role models, and always kept me on track when I doubted myself. I would not be where I am today without you. To my stepparents, Joel and Jill, thank you for accepting me into your lives and building a strong relationship with me. Thank you to my sister, Danielle, and my brother, Ken. I have missed you both over the past five years and I look forward to being closer home. To my friend Chris, I do not think someone could come up with two people who are more blatantly different from each other. I believe those differences are what makes our friendship so great, and I consider you my closest friend. Thank you for your support, and I look forward to all the good memories we have ahead.

To my research group, thank you for all the insightful conversations, challenging discussions, and great work in developing our research program. Watching the group grow over the past five years has been one of the most fulfilling experiences of my life. Some people I'd like to particularly thank are Shawn Wright, Spencer Pajk, and Steve Sujansky. Beginning work in a brand-new research group with you three was an absolute joy. Each one of you brought something special to the group that I believe continues to be evident to this day.

I started my college career as a psychology major with little interest in chemistry. That was until I came across a phenomenal professor who sparked my passion for organic chemistry. Dr. Amber Charlebois, thank you for being an excellent mentor and teacher. You saw the chemist in me before I saw it in myself, and I am incredibly grateful for all that you have done for me. I was very fortunate to have several mentors throughout my undergraduate career at Fairleigh Dickinson

University. Dr. Svetlana Bashkova and Dr. Edward Salaski, thank you for taking me in to your research programs mentoring me in my undergraduate career. I have learned so much from all of you and continue to carry the foundation you provided for me.

To my advisor, Professor Jeffrey Bandar, there are too many things to thank you for. Thank you for investing in me and pushing me. Thank you for the countless hours you took to help edit applications, reports, and presentations to advance my career. Thank you for making me a better chemist, scientist, and person. You are fantastic mentor, boss, and advisor. I have had so much fun working with you to come up with new ideas and develop this research program, I look forward to watching how far you go.

TABLE OF CONTENTS

CHAPTER ONE

BASE-CATALYZED α-SELECTIVE DEUTERATION OF STYRENE DERIVATIVES

1.1 Chapter Overview

Upon joining the Bandar Research Group at its inception in 2017, I began working with my colleagues to elucidate important mechanistic features of a base-catalyzed anti-Markovnikov styrene hydroetherification reaction (Figure 1–1, left). The mechanistic experiments I conducted in this research area ultimately led to our conceptualization of an approach to achieve an α-selective styrene deuteration reaction (Figure 1–1, right). This reaction represents the first styrene deuteration method with complete α-selectivity. In Chapter one, the motivation, discovery, and development of this base-catalyzed α-selective styrene deuteration reaction will be described.

Figure 1–1: Overview of the α-selective styrene deuteration reaction that will be covered in Chapter one.

1.2 Deuterium in Synthetic and Medicinal Chemistry

Deuterium is an isotope of hydrogen containing one proton and one neutron and a mass double that of the hydrogen nucleus. The higher mass of deuterium compared to hydrogen results in a significantly lower carbon-deuterium bond frequency (C–D stretch: 2,100 cm^{-1}) compared to carbon-hydrogen bonds (C–H stretch: 3,000 cm^{-1}), rendering C–D bonds stronger than C–H bonds.[1] The additional neutron present in deuterium does not result in a significant increase in steric size around the C–H/C–D bond.[1-2] Therefore, isotopic substitution of C–H bonds to C–D bonds imparts an increase in chemical bond strength without significantly altering the steric or electronic environment around the C–H/C–D bond.

In synthetic chemistry, these properties can provide the basis for mechanistic studies of chemical reactions. One example of this are kinetic isotope effect (KIE) experiments, where C–H to C–D substitution can provide insight into the rate determining step of a chemical reaction. Due to the higher C–D bond strength, if C–D substitution produces a large rate difference in a chemical reaction (e.g. $k_H / k_D = 5$) this indicates a primary KIE where cleavage of the C–H bond is likely involved in the rate-determining step of the reaction. Likewise, if a relatively small rate difference in a chemical reaction upon C–D substitution is observed (e.g. $k_H / k_D = 1.1$), this may be indicative of a secondary KIE, where changes in hybridization or hyperconjugation produce the observed rate difference.[1-3]

Another application of C–D substitution in mechanistic studies is in proton-tracking experiments. Here, deuterium can react similarly to a proton but can be tracked throughout a chemical reaction. Each incorporated deuterium atom imparts a one amu increase in molecular weight, allowing C–H and C–D variants of products to be distinguishable by mass spectrometry.[4] Additionally, deuterium nuclei are not detected in typical proton NMR experiments, and the lack of a ^{1}H signal in an experiment enables determination of the specific carbon where deuterium is incorporated. One example of this is shown in Figure 1–2, where formation of deuterated acetophenone **1–2** in a Wacker oxidation of styrene-α-d_1 (**1–1**) indicates a 1,2-hydride shift occurs in the reaction mechanism.[5]

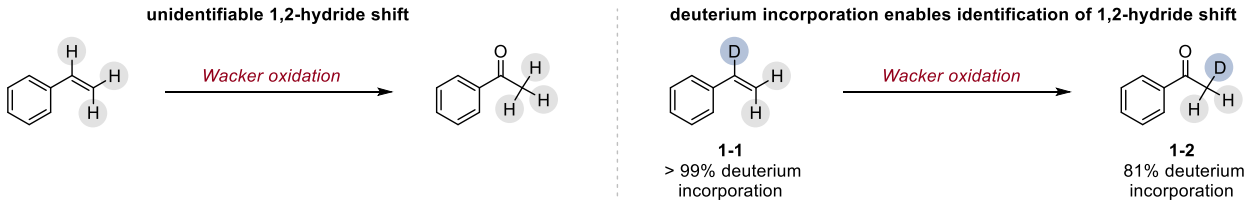

Figure 1–2: Use of selectively deuterated starting materials in proton-tracking experiments.

In medicinal chemistry, isotopic labelling of bioactive molecules with deuterium plays a crucial role in generating analytical standards for mass spectrometry, elucidating the mechanism of drug metabolism, and identifying metabolites in biological samples.[6-9] Additionally, incorporating deuterium into bioactive compounds serves a continually emerging role in the drug discovery and development process. Deuterium incorporation can improve the absorption, distribution, metabolism, and excretion (ADME) profiles of active pharmaceutical ingredients (APIs) while maintaining binding selectivity and affinity. Strategic incorporation of deuterium into APIs can alter the site of metabolic oxidation and reduce the formation of toxic metabolites. Meanwhile, the increased C–D bond strength inhibits oxidative metabolism by cytochrome P-450 enzymes and can increase the half-life or plasma concentration of APIs.[7]

Deutetrabenazine, an FDA-approved treatment for Huntington's chorea, is one example where deuterium incorporation resulted in an improved ADME profile (Figure 1-3). Selective incorporation of deuterium into the metabolically labile C–OCH_3 functional group inhibited oxidative dealkylation. Thus, deuterium incorporation imparted several beneficial effects, increasing the plasma half-life from 4.8 h to 8.6 h and reducing dosing frequency, quantities, and side effects.[10]

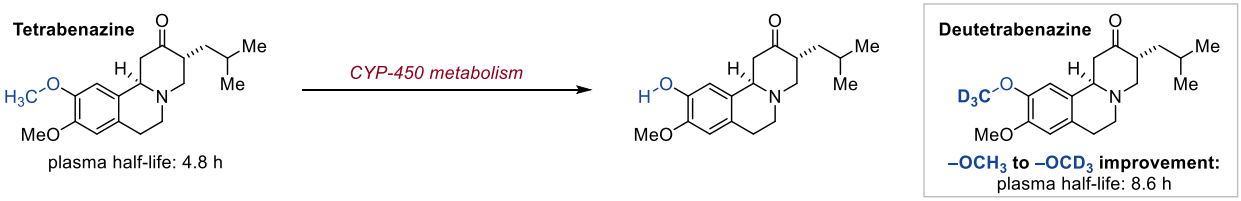

Figure 1–3: Stability of FDA-approved pharmaceuticals Tetrabenazine and Deutetrabenazine toward CYP-450 metabolism.

Given the utility of molecules isotopically labeled with deuterium, it is crucial that synthetic methods are developed to selectively install deuterium onto key classes of molecules.

The following section will describe the value and current methods to access α-deuterated styrene derivatives.

1.3 Value and Methods to Access α-Deuterated Styrene Derivatives

Styrene derivatives (Figure 1–4, left) are prominent precursors in myriad synthetic transformations, including polymerization and asymmetric hydro/dual alkene functionalization reactions.[11-16] Additionally, styrenes with deuterium selectively installed into the α- or β- position of the alkene are often used in KIE or proton-tracking experiments (see Chapter 1.2 for description).[5, 17-22] In particular, styrene-α-d_1 derivatives are a common class of alkenes utilized in these experiments, and access to diverse styrene-α-d_1 derivatives is important to facilitate the study of these transformations. Figure 1–4 displays four α-deuterated styrenes that have been employed in mechanistic studies of alkene functionalization reactions.[17-19, 22]

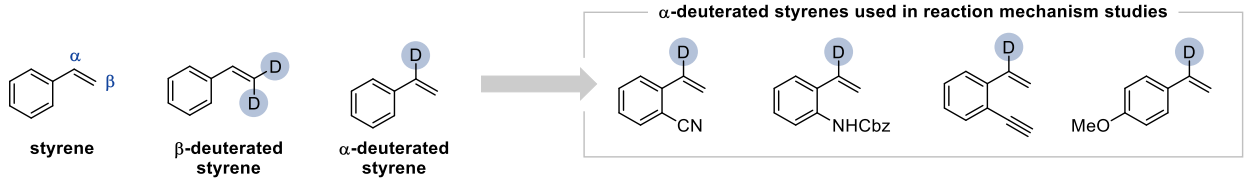

Figure 1–4: Naming convention of isotopically labelled styrenes and selected examples of α-deuterated styrenes used in reaction mechanism studies.

In addition to their application in mechanistic experiments, α-deuterated styrenes can be employed in asymmetric alkene functionalization reactions to access molecules containing chiral deuterated benzylic stereocenters. Notably, the benzylic position in pharmaceuticals is labile to metabolic oxidation, and incorporation of deuterium into these positions is one potential strategy to address this challenge.[23-26] For example, benzylic deuteration of the pharmaceutical procarbazine resulted in decreased testicular toxicity in rat studies. Here, benzylic deuteration of procarbazine slowed the rate of oxidative debenzylation responsible for the formation of toxic metabolites (Figure 1–5).[26] Thus, methods to rapidly access diverse α-deuterated styrenes are

important to facilitate their use in mechanistic studies of alkene functionalization reactions and the study of benzylic deuterated molecules with medicinal applications.

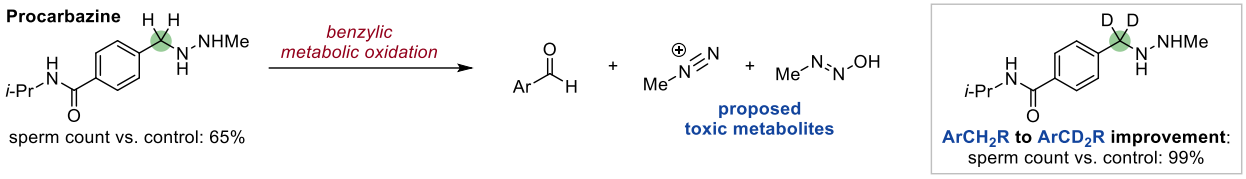

Figure 1–5: Toxicity profile of Procarbazine improves upon benzylic deuteration in rat studies.

A potentially ideal approach to access α- or β-deuterated styrenes is catalytic hydrogen isotope exchange. Hydrogen isotope exchange (HIE) is defined as the isolated process of a C–H bond being converted to a C–D bond (Figure 1–6).[4,27] Although several methods for transition-metal catalyzed alkene HIE have been developed, translation of these methods to styrene derivatives has proven challenging.

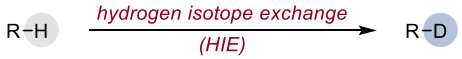

Figure 1–6: General scheme of a hydrogen isotope exchange (HIE) reaction, converting hydrogen (H) to deuterium (D).

In addition to competing arene C–H insertion processes, achieving alkene positional selectively increases the challenges associated with styrene HIE reactions. In this regard, ruthenium deuteride (Ru–D) and iridium deuteride (Ir–D) catalyzed protocols for unselective styrene HIE have been developed that limit competing aromatic deuterium exchange (Figure 1–7).[28-30]

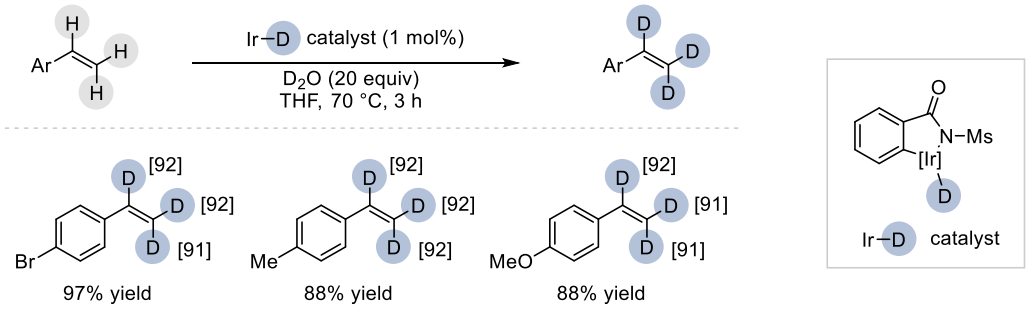

Figure 1–7: Iridium (Ir) deuteride catalyzed protocol for olefin selective deuteration of styrene derivatives. Deuterium incorporation into each position is indicated by the number in brackets.

Castarlenas and Oro developed an impressive rhodium deuteride (Rh–D) catalyzed protocol for highly β-selective styrene HIE (Figure 1–8).[31-32] Here, reversible migratory insertion processes produce two possible intermediates resulting from Markovnikov or anti-Markovnikov insertion. For Markovnikov insertion, rotation of the alkyl group to the necessary conformation for β-hydride elimination is much lower in energy, resulting in β-selective deuteration.

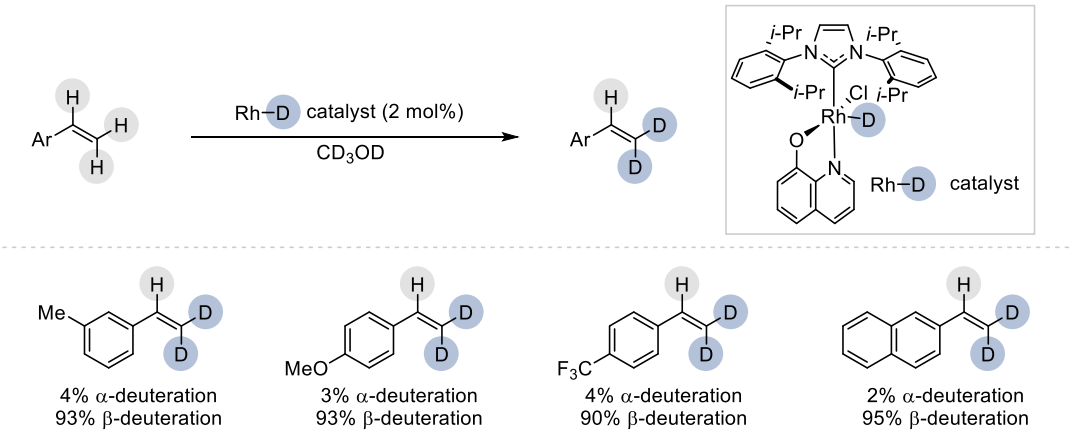

Figure 1–8: Rhodium (Rh) deuteride catalyzed β-selective deuteration of styrene derivatives.

Despite, these impressive developments, no method for α-selective styrene HIE existed prior to our work. Instead, *de novo* synthetic protocols are employed to access α-deuterated styrenes. A common, inefficient, multistep route α-selectively installs deuterium *via* reduction of benzoic acid or benzaldehyde derivatives with $LiAlD_4$ and culminates with a Wittig reaction (Figure 1–9, top).[19,22] Reduction of acetophenone derivatives with $NaBD_4$ or $LiAlD_4$, followed by

elimination of H_2O, is another potential approach (Figure 1–9, bottom).[20, 33-34] Hoveyda developed a Ni-catalyzed α-selective hydroalumination reaction of aryl alkynes that could be leveraged to access α-deuterated styrenes (Figure 1–10, left).[35] Additionally, a Shapiro reaction of tosylhydrazones can be utilized to access α-deuterated styrenes (Figure 1–10, right).[36]

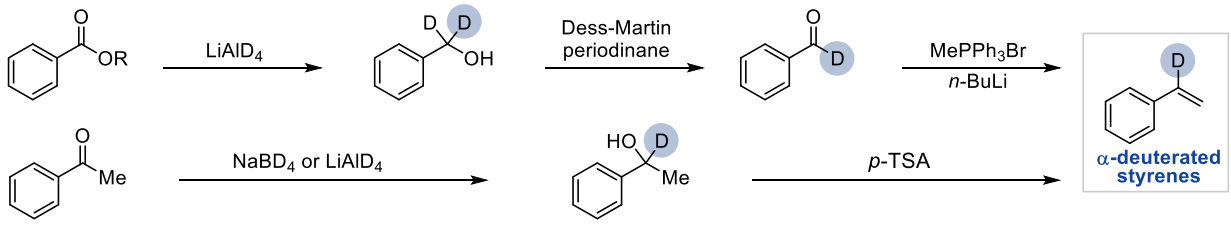

Figure 1–9: General schemes of common *de novo* synthetic routes to access α-deuterated styrenes.

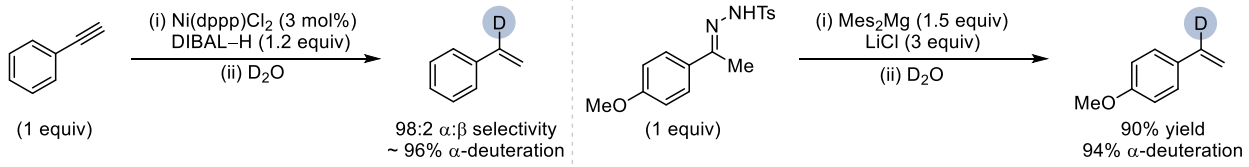

Figure 1–10: Other *de novo* synthetic routes to access α-deuterated styrenes.

At the time I joined the Bandar Research Group in 2017, the group was in the process of developing new base-catalyzed styrene hydrofunctionalization reactions. While studying the mechanism of these reactions, we gained insights that could be applied to enable an α-selective styrene HIE reaction. The following section will describe the mechanistic studies I conducted alongside a postdoctoral researcher in our lab, Dr. Chaosheng Luo, that led to our conceptualization of a method for α-selective styrene deuteration.

1.4 Discovery of a Base-Catalyzed α-Selective Styrene Deuteration Reaction

1.4.1 P_4-t-Bu-Catalyzed Anti-Markovnikov Styrene Hydroetherification Reactions

In 2018, our research group reported the first general method for the direct anti-Markovnikov addition of alcohols across styrene derivatives catalyzed by the organic superbase P_4-*t*-Bu (Figure 1–11).[37-38] Exclusive anti-Markovnikov selectivity is observed due to the inherent

polarity of the olefin, generating a benzylic anion upon alkoxide addition. Use of P_4-*t*-Bu as the base-catalyst is crucial to achieve high reaction yields, and common inorganic bases (e.g. KO-*t*-Bu or KOH) are significantly less effective. This work represents the first general approach for anti-Markovnikov addition of alcohols across styrene derivatives and demonstrated a scope of over 30 electron-poor and electron-neutral styrene derivatives.

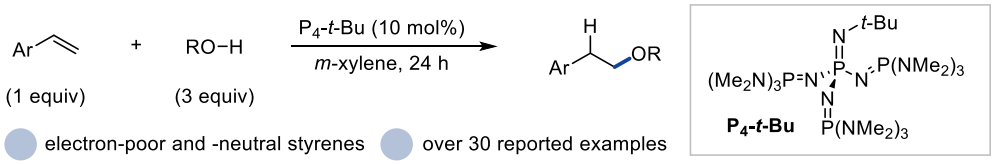

Figure 1–11: Bandar 2018 report of P_4-*t*-Bu catalyzed anti-Markovnikov styrene hydroetherification.

Mechanistic studies revealed alkoxide addition is reversible and under free energy equilibrium control. Anti-Markovnikov hydroetherification of 3-nitrostyrene (**1–3**) with 2-ethyl-1-hexanol (**1–4**) produced a 77% of β-phenethyl ether **1–5** with 23% remaining 3-nitrostyrene (**1–3**). When β-phenethyl ether **1–5**, was subjected to the same reaction conditions, a similar yield of β-phenethyl ether **1–5** and 3-nitrostyrene (**1–3**) was observed (Figure 1–12). These results suggest the reaction is under free energy equilibrium control, and diligent optimization of reaction parameters was required to achieve high equilibrium yields of the β-phenethyl ether.[37]

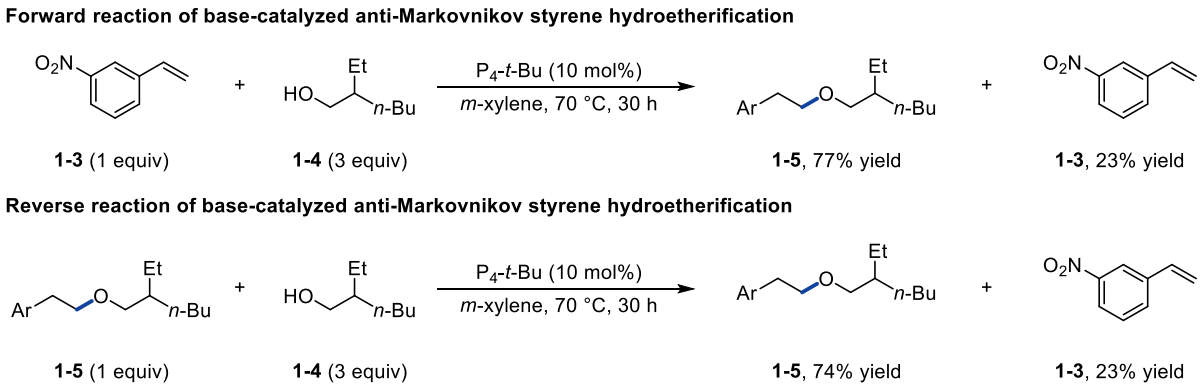

Figure 1–12: Demonstration that base-catalyzed anti-Markovnikov styrene hydroetherification is reversible and under free energy equilibrium control.

One reaction variable that exhibited a pronounced effect on the reaction equilibrium is the identity of the reaction solvent. To demonstrate this effect, I used P$_4$-*t*-Bu-catalyzed methanol (MeOH) addition to 4-(trifluoromethyl)styrene (**1–6**) as a model reaction and measured the equilibrium constant (K_{eq}) for the formation of β-phenethyl ether product **1–7** (Figure 1–13)[41] I measured equilibrium yields of β-phenethyl ether **1–7** in 21% yield (K_{eq} = 0.20) in *m*-xylene and 9% yield (K_{eq} = 0.07) in DMSO (Figure 1–13). This result demonstrates that the K_{eq} for β-phenethyl ether formation is more favorable in non-polar aromatic solvents and less favorable in polar aprotic solvents.

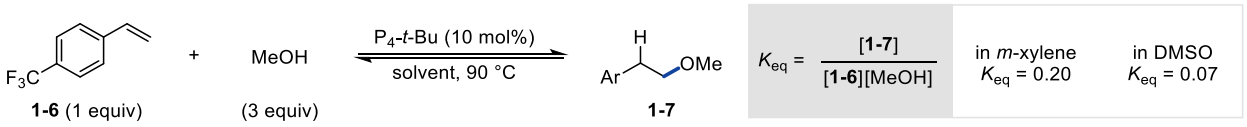

Figure 1–13: Measurement of reaction K_{eq} in *m*-xylene and DMSO solvent.

1.4.2 The Conceptualization and Discovery of a Base-Catalyzed α-Selective Styrene HIE Reaction

Based on the mechanistic studies described in the previous section, we reasoned that the styrene hydroetherification reaction could be translated into an α-selective styrene HIE reaction simply by using deuterated dimethyl sulfoxide (DMSO-d_6) as the solvent and MeOH as the alcohol pronucleophile. In an initial experiment, we found P$_4$-*t*-Bu catalyzed the α-selective deuteration of 4-(trifluoromethyl)styrene (**1–6**) in 88% yield, 99% α-deuterium incorporation, and 0% deuterium incorporation into the β-position or the aromatic ring (Figure 1–14, left). Although P$_4$-*t*-Bu is needed to provide high yields for anti-Markovnikov styrene hydroetherification reactions, we found KO-*t*-Bu to be an equally effective base-catalyst for styrene α-deuteration, producing **1–6–*α–d*$_1$** in 87% yield with 99% α-deuteration. Given the high cost (approximately $14,750/mole) of P$_4$-*t*-Bu, we proceeded developing this reaction using KO-*t*-Bu as an inexpensive and practical catalyst.[41]

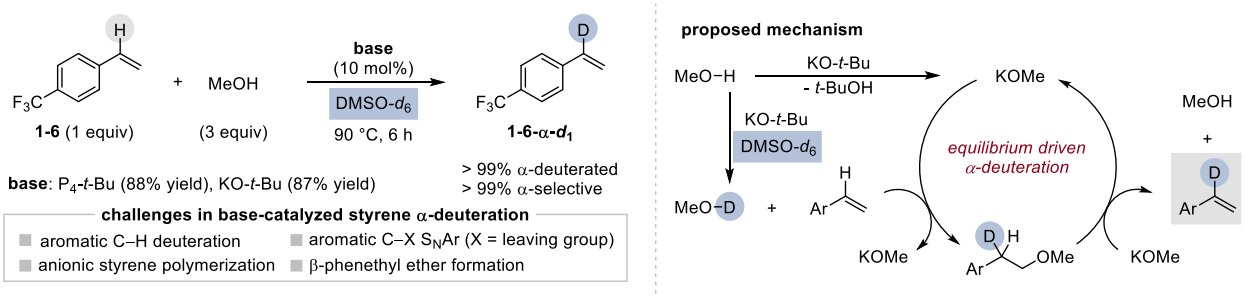

Figure 1–14: Preliminary result (left) and proposed mechanism (right) for base-catalyzed α-selective styrene deuteration.

Our proposed mechanism for this process is detailed in Figure 1–14. First, deuterium scrambling between DMSO-d_6 and MeOH produces MeOD. Second, base-catalyzed anti-Markovnikov addition of MeOD across the styrene produces a β-phenethyl ether intermediate with deuterium selectively incorporated into the benzylic position. Finally, base-catalyzed elimination of MeOH yields the α-deuterated styrene. Use of DMSO-d_6 as the reaction solvent serves a dual role. First, it provides a large excess of deuterium to drive the α-deuteration reaction to high deuterium incorporations. Second, we observed low K_{eq} values for β-phenethyl ether formation in DMSO solvent, producing higher equilibrium yields of the α-deuterated styrene (Figure 1–13).

Although the mechanism for styrene α-deuteration is conceptually straightforward, several other base-promoted processes must be inhibited for this reaction to be applied to a general scope of styrenes. First, basic solutions of DMSO-d_6 can deuterate weakly acidic aromatic C–H bonds.[42-44] Second, alkoxides are known to initiate anionic styrene polymerization reactions.[45-46] Third, styrenes with halogen substituents could potentially undergo competing S_NAr reactions. Finally, the reaction must strongly favor the styrene over the β-phenethyl ether in the equilibrium to obtain high synthetic yields.[37]

These challenges initially precluded the application of this reaction to a general scope of styrene substrates. The following section describes our efforts to overcome these challenges and generalize the scope to a diverse range of styrene derivatives.

1.5 Optimization of Reaction Conditions

Although the reaction conditions in Figure 1–14 were effective for the α-deuteration of 4-(trifluoromethyl)styrene (**1–6**), we found these conditions could not be utilized on a general scope of styrenes. Therefore, we reasoned each styrene substrate would likely require systematic optimization of MeOH concentration and reaction temperature/time to achieve α-selective deuteration in high yields and deuterium incorporation. Instead of empirically optimizing each substrate, we conducted studies on the effects of MeOH concentration and reaction temperature that provided general insights on how to identify effective reaction conditions for each substrate. This section will describe these studies and general insights gained that guided the individual optimization of each substrate.

1.5.1 Effect of the Concentration of MeOH on Styrene α-Deuteration Reactions

To begin, I performed reaction profile analysis studies to investigate how changes in the concentration of MeOH affect the styrene α-deuteration reaction. Using α-deuteration of styrene **1–8** as a model reaction, we tracked the rate of α-deuterium incorporation and styrene mass balance using one equivalent, 0.5 equivalents, and 0.25 equivalents of MeOH (Figure 1–15). Notably, because MeOH elimination is the last step in the proposed mechanism (Figure 1–14, right), only catalytic quantities are needed in this reaction.

When 0.25 equivalents of MeOH are used, the reaction is relatively fast, reaching approximately 80% α-deuterium incorporation after two hours. Meanwhile, the mass balance rapidly approaches 0% under these conditions, with only 20% of styrenes **1–8** or **1–8–α–*d*$_1$**

remaining after two hours. When one equivalent of MeOH is used, the reaction is relatively slow, reaching 80% α-deuterium incorporation after three hours. However, the mass balance is maintained above 97% for the duration of the reaction and 99% α-deuterium incorporation can be reached after ten hours.[41]

The major competing side reaction is this process is anionic styrene polymerization. Thus, the observed positive correlation between the concentration of MeOH and styrene mass balance is likely due to an increased rate of deuteration of the intermediate benzylic anion with MeOD, inhibiting anionic styrene polymerization. Meanwhile, the inverse correlation between the concentration of MeOH and the reaction rate was less clear at the time. Recently, our group published work that investigated this inverse order rate dependence and found it is likely due to the formation of less reactive alkoxide and alcohol hydrogen-bonding clusters.[47] Overall, these studies demonstrate the crucial role of MeOH in controlling the rate of deuterium incorporation and maintaining high mass balance throughout the reaction.

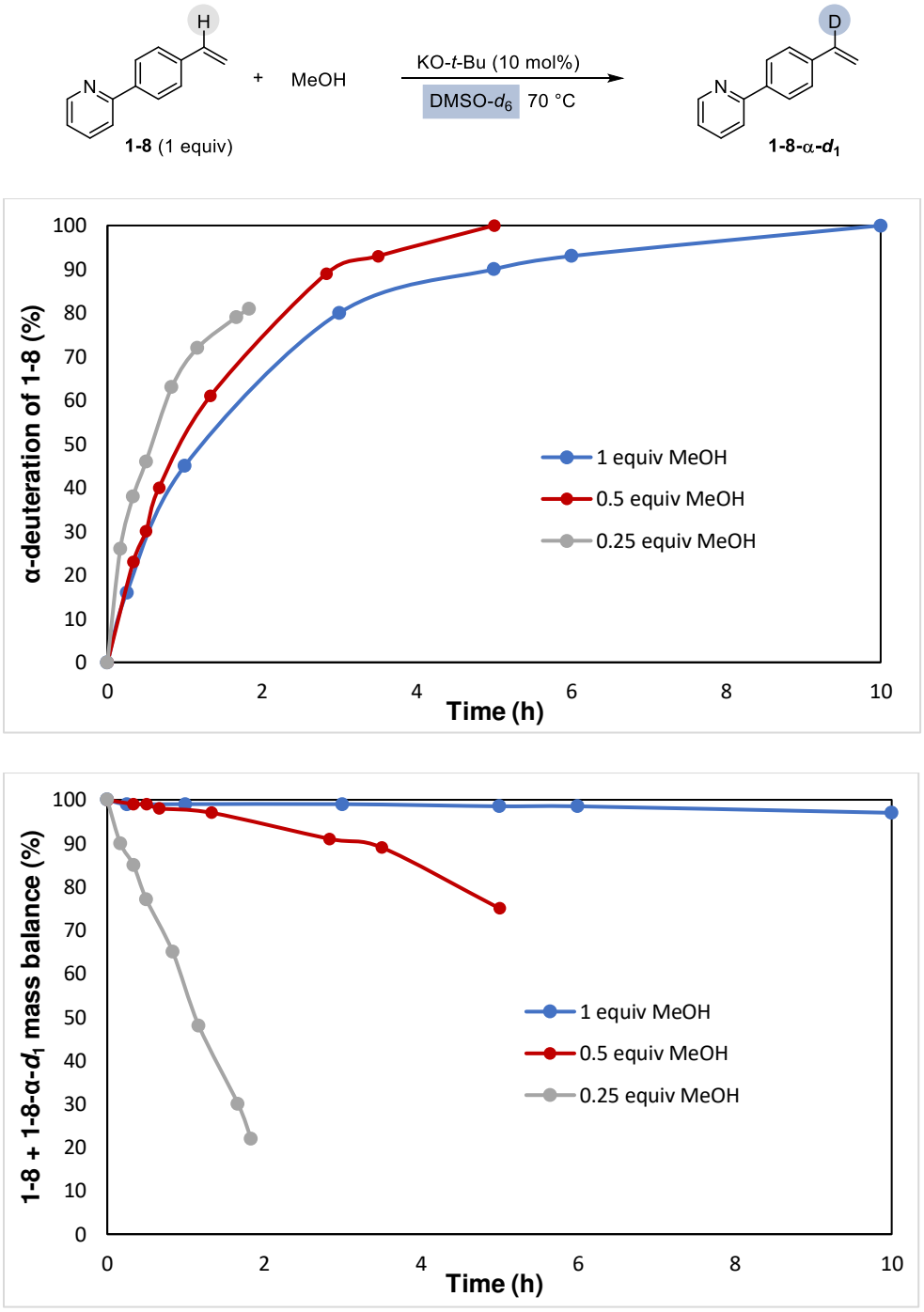

Figure 1–15: Reaction profile for the α-deuteration rate (top) and mass balance (bottom) for substrate **1–8**.

1.5.2 Effect of Reaction Temperature on Styrene α-Deuteration Reactions

In our studies on anti-Markovnikov styrene hydroetherification reactions (Chapter 1.4), we determined the reaction is reversible and under free energy equilibrium control. Thus, factors that control the change in free energy (ΔG) of styrene hydroetherification are crucial to obtain high equilibrium yields of the α-deuterated styrene. According to the Gibbs free energy equation (ΔG = ΔH – TΔS) and the relation of Gibbs free energy to the reaction equilibrium constant ($\ln K_{eq} = -\Delta G/(RT)$), the reaction temperature (T) should significantly impact the K_{eq} of styrene hydroetherification. Simply, these equations suggest lower reaction temperatures should produce higher equilibrium yields of the β-phenethyl ether while higher reaction temperatures should produce higher equilibrium yields of the styrene.

To demonstrate this effect, I conducted the α-deuteration of styrene **1–9** at 40 °C and 70 °C. At 40 °C, **1–9-α–*d*$_1$** was obtained with 99% α-deuteration in 50% yield and concomitant formation of β-phenethyl ether **1–10** in 40% yield (Figure 1–16). When the reaction temperature was increased to 70 °C, the yield of **1–9–α–*d*$_1$** was improved to 75% with 99% α-deuteration and concomitant formation of **1–10** in 20% yield. This study demonstrates that increasing the reaction temperature is one potential approach to improve the equilibrium yields of α-deuterated styrenes.

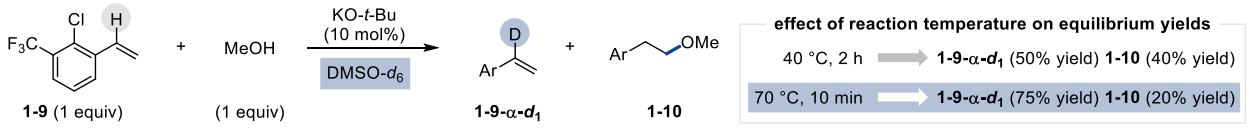

Figure 1–16: Effect of reaction temperature on the equilibrium yields of styrene **1–9–α–*d*$_1$** and β-phenethyl ether **1–10**.

1.5.3 Process for Identifying Effective Reaction Conditions for each Styrene Substrate

Having gained crucial insights into the role of MeOH and reaction temperature on the styrene α-deuteration reaction, we developed a simple process to rapidly identify effective reaction conditions for each substrate. We started by testing one and three equivalents of MeOH at varying

temperatures. If the reaction was sluggish, use of less equivalents of MeOH improved the reaction rate. If the reaction had poor mass balance, use of more equivalents of MeOH improved the mass balance.[41]

The reaction temperature could be adjusted to limit competing side reactions and improve the α-deuterated styrene yield. Use of lower reaction temperatures helped to limit competing aromatic deuteration and anionic styrene polymerization. Meanwhile, higher reaction temperatures could be employed to limit the yield of the corresponding β-phenethyl ether and produce a higher equilibrium yield of the α-deuterated styrene.[41] Overall, conducting a small screen of reaction conditions enabled identification of the specific challenges for each styrene substrate, and the concentration of MeOH and reaction temperature could be adjusted accordingly. Having developed a general strategy to identify effective reaction conditions for each substrate, we next demonstrated the scope of this reaction on a diverse array of styrene derivatives.

1.6 Substrate Scope

Figure 1–17 displays a diverse array of styrenes that undergo α-selective deuteration in high yield and α-deuterium incorporation. I developed this substrate scope while mentoring an undergraduate student in our group, Alivia Strong, who assisted in the identification of reaction conditions and isolation of various substrates. For all substrates, > 95% α-deuterium incorporation was achieved while limiting aromatic deuteration to < 5%. Electron-poor to -neutral styrenes were well-tolerated in the reaction; however electron-rich styrenes (e.g. 4-methoxystyrene) were unreactive. Halogenated styrenes, including *ortho*-substituted bromide (**1–11**), chloride (**1–9** and **1–19**) and iodide (**1–12**) variants undergo α-selective deuteration while avoiding S_NAr reactions. Stilbene derivative **1–16** undergoes selective deuteration on the terminal vinyl group while leaving the internal alkene unlabeled. Meanwhile, a relatively activated stilbene derivative (**1–25**) fully

deuterates both positions of the internal olefin. Ester (**1–13**), amide (**1–14**), and (trifluoromethyl)thio (**1–15**) functional groups in the *meta*- and *para*-positions are also tolerated.

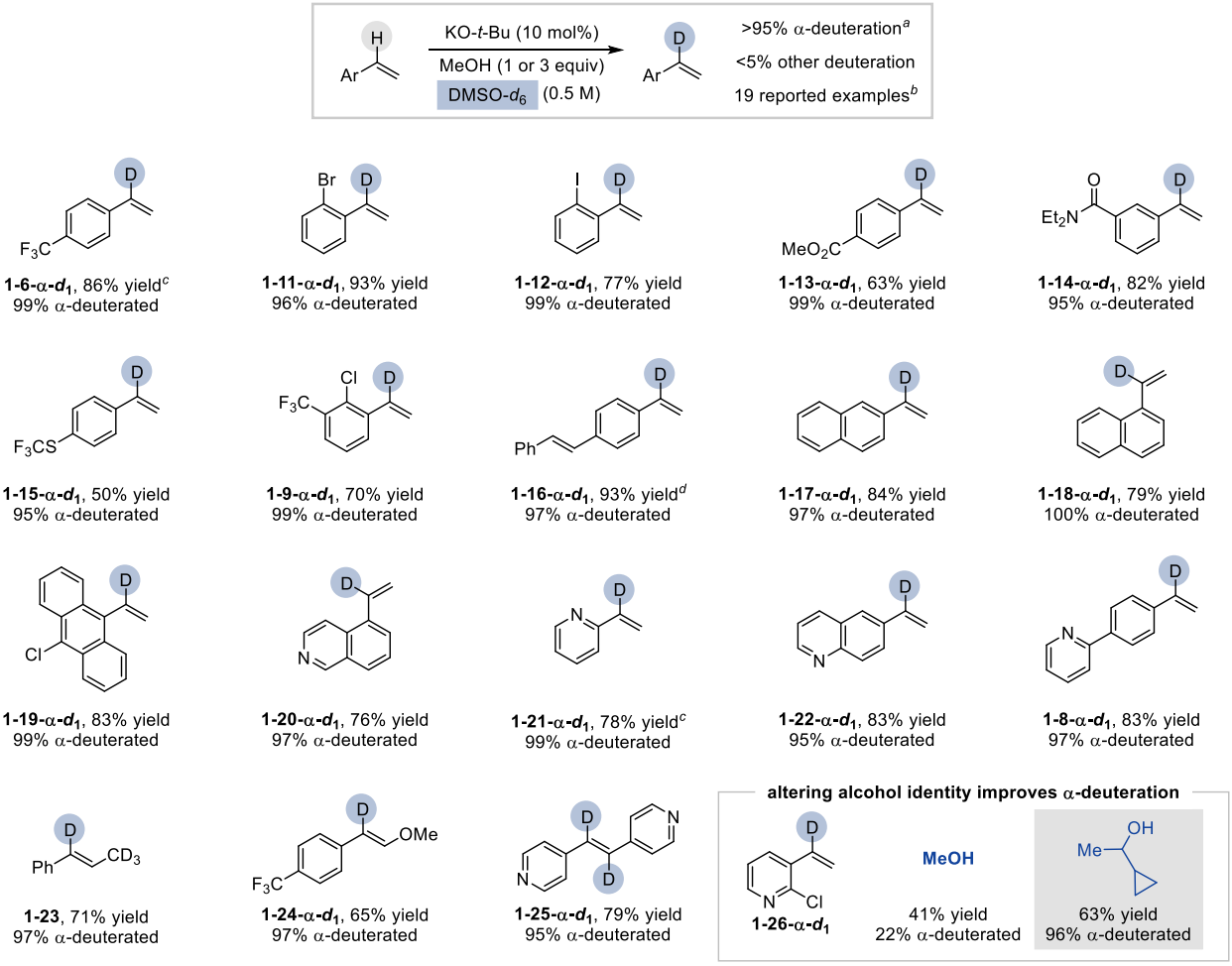

[a]% deuteration determined by ^{1}H and ^{2}H NMR. [b]Yields correspond to the isolated yield of the a-deuterated styrene. Reaction run between 50 °C and 130 °C at 0.5 M of alkene in DMSO-d_6 solvent. [c] ^{1}H NMR yield, isolated yields for product **1-6-α-*d*$_1$** (52%) and **1-21-α-*d*$_1$** (61%) were decreased due to volatility. [d]NaH used instead of KO-*t*-Bu.

Figure 1–17: α-Selective styrene deuteration substrate scope.

Highly α-selective deuteration of naphthalene (**1–17** and **1–18**), anthracene (**1–19**), pyridine (**1–21**), isoquinoline (**1–20**) and quinoline (**1–22**) styrene derivatives was achieved.[41] These substrates are particularly notable because styrenes with extended aromatic systems and heteroarenes contain relatively acidic aromatic C–H bonds. β-Methylstyrene (**1–23**) undergoes α-

and γ-deuteration, likely through a deprotonation process as opposed to alkoxide addition. Meanwhile, a styrene with a β-methoxy substituent (**1–24**) undergoes α-selective deuteration.[41]

Given the crucial role of MeOH in this reaction (see Chapter 1.5.1), we reasoned that strategic modification of the alcohol structure could overcome competing side reactions. Although halogenated styrenes were generally unreactive toward S_NAr under these conditions, more activated 2-chloro-3-vinylpyridine (**1–26**) predominantly underwent S_NAr, with only 21% α-deuteration when MeOH was used. In addition to producing undesired side products, competing S_NAr reactions consume the base-catalyst, shutting down the α-deuteration reaction. I found use of bulkier 1-cyclopropylethanol promotes α-deuteration while limiting competing S_NAr, producing **1–26–*α*–*d*$_1$** in 63% yield with 96% α-deuteration.[41]

A notable substrate scope limitation in this approach are vinyl arenes that possess highly acidic aromatic or benzylic C–H bonds. Although highly α-selective for olefin deuteration, significant deuterium incorporation into non-olefinic positions was observed for these substrates. Figure 1–18 demonstrates three examples of these styrenes, including toluene derivative **1–27**, benzothiophene **1–28**, and dibenzofuran **1–29**.[41] Although this is a limitation to access compounds with deuterium exclusively incorporated in the α-position, there are cases where it is advantageous to have deuterium incorporated into multiple positions (e.g. mass spectrometry standards) and high alkene α-selectivity is still observed.[8]

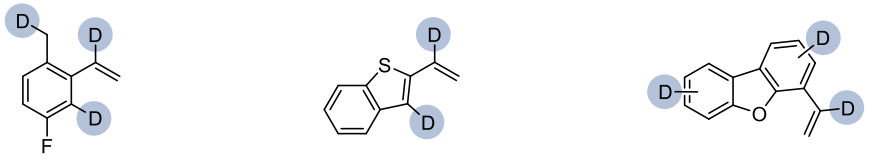

1-27, 76% yield
88% α-deuterated
10% benzylic deuteration
4% aromatic deuteration

1-28, 85% yield
79% α-deuterated
24% aromatic deuteration

1-29, 85% yield
79% α-deuterated
87% aromatic deuteration

Figure 1–18: Styrene substrates that undergo competing aromatic or benzylic deuteration.

1.7 Asymmetric Derivatization of α-Deuterated Styrenes

Having developed a general approach to access diverse α-deuterated styrene derivatives, we next demonstrated the application of these products to access compounds with deuterated benzylic stereocenters. Given the large amount of asymmetric alkene functionalization reactions, α-deuterated styrenes can easily be elaborated to compounds containing chiral deuterated benzylic stereocenters. Chiral benzylic C–H substituted positions are common in pharmaceutical compounds and are often labile to metabolic oxidation (see Chapter 1.2).[23-26] Incorporation of deuterium into these positions is one potential strategy to hinder metabolic oxidation and produce more favorable ADME profiles.

We demonstrated three examples of sequencing base-catalyzed styrene α-deuteration with asymmetric alkene functionalization reactions to access complex compounds with chiral deuterated benzylic stereocenters (Figure 1–19). First, a Sharpless asymmetric dihydroxylation reaction of **1–11–α–*d*$_1$** followed by cyclization with carbonyl diimidazole yielded chiral carbonate derivative **1–30** in 74% yield, 98% ee, and 97% benzylic deuterium incorporation.[11] Instead of a cyclization reaction, the chiral 1,2-diols derived from Sharpless asymmetric dihydroxylation reactions could be elaborated into other complex structures. Thus, activation of the diol derived from **1–17–α–*d*$_1$** with methanesulfonyl chloride (MsCl) followed by substitution with dimethyl malonate yielded chiral cyclopropane **1–31** in 65% yield, 96% ee, and 97% α-deuteration.[48] Finally, a Cu–H-catalyzed Markovnikov selective asymmetric hydroamination reaction of **1–18–α–*d*$_1$** was employed to synthesize a benzylic-d_1 analog of the pharmaceutical, cinacalcet, in 84% yield, 94% ee, and 99% benzylic deuteration.[49]

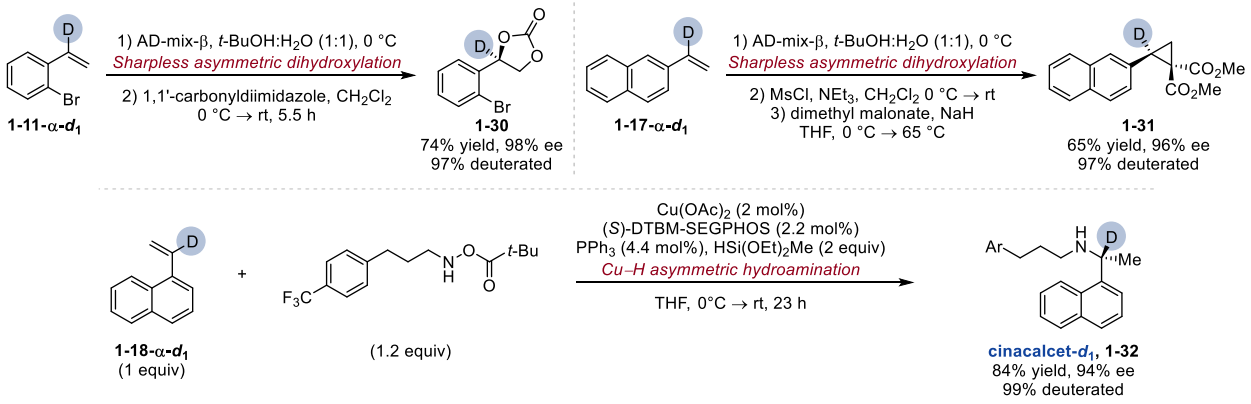

Figure 1–19: Asymmetric elaboration of α-deuterated styrenes.

1.8 Conclusion

The work described throughout Chapter one was published in the *Journal of the American Chemical Society* in 2019.[41] Until this report, no method for α-selective HIE of styrene derivatives existed. By leveraging the mechanistic understanding of base-catalyzed styrene hydroetherification, we conceptualized and developed a general approach to α-selectively deuterate styrene derivatives. Although this work represents a new base-catalyzed approach to alkene C–H functionalization, I sought to develop fundamentally new areas of research within our young research group. In this regard, I discovered and developed new approaches to C–H functionalization reactions enabled by base-catalyzed aryl halide halogen transfer processes. Chapter two will provide the background of base-catalyzed aryl halide isomerization reactions that serve as the mechanistic framework for the remainder of my work that will be described in Chapters three, four, and five.

REFERENCES

[1] Westheimer, F. H. The Magnitude of the Primary Kinetic Isotope Effect for Compounds of Hydrogen and Deuterium. *Chem. Rev.* **1961**, *61*, 265–273.

[2] *Modern Physical Organic Chemistry*; Anslyn, E. V.; Dougherty, D. A. , University Science Books: Sausalito, CA, 2006; Chapter 8, pp. 421-488.

[3] Wiberg, K. B. The Deuterium Isotope Effect. *Chem, Rev.* **1955**, *55*, 713–743.

[4] Atzrodt, J.; Derdau, V.; Kerr, W. J.; Reid, M. Deuterium- and Tritium-Labelled Compounds: Applications in the Life Sciences. *Angew. Chem. Int. Ed.* **2018**, *57*, 1758–1784.

[5] Cornell, C. N.; Sigman, M. S. Discovery of and Mechanistic Insight into a Ligand-Modulated Palladium-Catalyzed Wacker Oxidation of Styrenes Using TBHP. *J. Am. Chem. Soc.* **2005**, *127*, 2796-2797.

[6] Gant, T. G. Using Deuterium in Drug Discovery: Leaving the Label in the Drug. *J. Med. Chem.* **2014**, *57*, 3595-3611.

[7] Harbeson, S. L.; Tung, R. D. Chapter 24 - Deuterium in Drug Discovery and Development. *Annu. Rep. Med. Chem.* **2011**, *46*, 403-417.

[8] Mutlib, A. E. Application of Stable Isotope-Labeled Compounds in Metabolism and in Metabolism-Mediated Toxicity Studies. *Chem. Res. Toxicol.* **2008**, *21*, 1672-1689.

[9] Liu, J. F.; Harbeson, S. L.; Brummel, C. L.; Tung, R.; Silverman, R.; Doller, D. Chapter Fourteen - A Decade of Deuteration in Medicinal Chemistry. *Annu. Rep. Med. Chem.* **2017**, *50*, 519-542.

[10] Tung, R. D. Deuterium medicinal chemistry comes of age. *Future Med. Chem.* **2016**, *8*, 491-494.

[11] Kolb, H. C.; VanNieuwenhze, M. S.; Sharpless, K. B. Catalytic Asymmetric Dihydroxylation. *Chem. Rev.* **1994**, *94*, 2483-2547.

[12] Pirnot, M. T.; Wang, Y.-M.; Buchwald, S. L. Copper Hydride Catalyzed Hydroamination of Alkenes and Alkynes. *Angew. Chem., Int. Ed.* **2016**, *55*, 48-57.

[13] Degennaro, L.; Trinchera, P.; Luisi, R. Recent Advances in the Stereoselective Synthesis of Aziridines. *Chem. Rev.* **2014**, *114*, 7881-7929.

[14] Wong, O. A.; Shi, Y. Organocatalytic Oxidation. Asymmetric Epoxidation of Olefins Catalyzed by Chiral Ketones and Iminium Salts. *Chem. Rev*. **2008**, *108*, 3958-3987.

[15] Chanthamath, S.; Iwasa, S. Enantioselective Cyclopropanation of a Wide Variety of Olefins Catalyzed by Ru(II)−Pheox Complexes. *Acc. Chem. Res.* **2016**, *49*, 2080-2090.

[16] Jui, N. T.; Garber, J. A. O.; Finelli, F. G.; MacMillan, D. W. C. Enantioselective Organo-SOMO Cycloadditions: A Catalytic Approach to Complex Pyrrolidines from Olefins and Aldehydes. *J. Am. Chem. Soc.* **2012**, *134*, 11400-11403.

[17] Maji, A.; Reddi, Y.; Sunoj, R. B.; Maiti, D. Mechanistic Insights on Orthogonal Selectivity in Heterocycle Synthesis. *ACS Catal.* **2018**, *8*, 10111-10118.

[18] Fang, X.; Yu, P.; Cerai, G. P.; Morandi, B. Unlocking Mizoroki−Heck-Type Reactions of Aryl Cyanides Using Transfer Hydrocyanation as a Turnover-Enabling Step. *Chem. - Eur. J.* **2016**, *22*, 15629-15633.

[19] Fra, L.; Millán, A.; Souto, J. A.; Muñiz, K. Indole Synthesis Based On A Modified Koser Reagent. *Angew. Chem., Int. Ed.* **2014**, *53*, 7349-7353.

[20] Walker, K. L.; Dornan, L. M.; Zare, R. N.; Waymouth, R. M.; Muldoon, M. J. Mechanism of Catalytic Oxidation of Styrenes with Hydrogen Peroxide in the Presence of Cationic Palladium(II) Complexes. *J. Am. Chem. Soc.* **2017**, *139*, 12495-12503.

[21] Pryor, W. A.; Henderson, R. W.; Patsiga, R. A.; Carroll, N. Hydrogen Secondary Isotope Effects on the Radical Polymerization of Styrene. *J. Am. Chem. Soc.* **1966**, *88*, 1199-1205.

[22] García-Rubín, S.; González-Rodríguez, C.; García-Yebra, C.; Varela, J. A.; Esteruelas, M. A.; Saá, C. Dihydrobiphenylenes through Ruthenium-Catalyzed [2+2+2] Cycloadditions of Ortho-Alkenylarylacetylenes with Alkynes. *Angew. Chem, Int. Ed.* **2014**, *53*, 1841–1844.

[23] Zhang, Z.; Tang, W. Drug metabolism in drug discovery and development. *Acta Pharm. Sin. B* **2018**, *8*, 721-732.

[24] Guengerich, F. P. Common and Uncommon Cytochrome P450 Reactions Related to Metabolism and Chemical Toxicity. *Chem. Res. Toxicol.* **2001**, *14*, 611-650.

[25] Shetty, H. U.; Nelson, W. L. Chemical aspects of metoprolol metabolism. Asymmetric synthesis and absolute configuration of the 3-[4-(1- hydroxy-2-methoxyethyl)phenoxy]-1-(isopropylamino)-2-propanols, the diastereomeric benzylic hydroxylation metabolites. *J. Med. Chem.* **1988**, *31*, 55-59.

[26] Nelson, S. D.; Trager, W. F. The Use of Deuterium Isotope Effects to Probe the Active Site Properties, Mechanism of Cytochrome P450-Catalyzed Reactions, and Mechanisms of Metabolically Dependent Toxicity. *Drug Metab. Dispos.* **2003**, *31*, 1481-1498.

[27] Atzrodt, J.; Derdau, V.; Kerr, W. J.; Reid, M. C−H Functionalisation for Hydrogen Isotope Exchange. *Angew. Chem., Int. Ed.* **2018**, *57*, 3022-3047.

[28] Hatano, M.; Nishimura, T.; Yorimitsu, H. Selective H/D Exchange at Vinyl and Methylidene Groups with D_2O Catalyzed by an Iridium Complex. *Org. Lett.* **2016**, *18*, 3674-3677.

[29] Rybtchinski, B.; Cohen, R.; Ben-David, Y.; Martin, J. M. L.; Milstein, D. Aromatic vs Aliphatic C-H Bond Activation by Rhodium(I) as a Function of Agostic Interactions: Catalytic H/D Exchange between Olefins and Methanol or Water. *J. Am. Chem. Soc.* **2003**, *125*, 11041-11050.

[30] Tse, S. K. S.; Xue, P.; Lin, Z.; Jia, G. Hydrogen/Deuterium Exchange Reactions of Olefins with Deuterium Oxide Mediated by the Carbonylchlorohydrido-tris(triphenylphosphine)-ruthenium(II) Complex. *Adv. Synth. Catal.* **2010**, *352*, 1512-1522.

[31] Di Giuseppe, A.; Castarlenas, R.; Pérez-Torrente, J. J.; Lahoz, F. J.; Polo, V.; Oro, L. A. Mild and Selective H/D Exchange at the β Position of Aromatic α-Olefins by N-Heterocyclic Carbene−Hydride−Rhodium Catalysts. *Angew. Chem., Int. Ed.* **2011**, *50*, 3938-3942.

[32] Di Giuseppe, A.; Castarlenas, R.; Pérez-Torrente, J. J.; Lahoz, F. J.; Oro, L. A. Hydride-Rhodium(III)-N-Heterocyclic Carbene Catalysts for Vinyl-Selective H/D Exchange: A Structure−Activity Study. *Chem. - Eur. J.* **2014**, *20*, 8391-8403.

[33] Gülak, S.; Gieshoff, T. N.; von Wangelin, A. J. Olefin Assisted Iron-Catalyzed Alkylation of Aryl Chlorides. *Adv. Synth. Catal.* **2013**, *355*, 2197-2202.

[34] Vassilikogiannakis, G.; Orfanopoulos, M. Stereochemistry and Isotope Effects of the [2+2] Photocycloadditions of Arylalkenes to C_{60}. A Stepwise Mechanism. *J. Am. Chem. Soc.* **1997**, *119*, 7394-7395.

[35] Gao, F.; Hoveyda, A. H. α-Selective Ni-Catalyzed Hydroalumination of Aryl- and Alkyl-Substituted Terminal Alkynes: Practical Syntheses of Internal Vinyl Aluminums, Halides, or Boronates. *J. Am. Chem. Soc.* **2010**, *132*, 10961-10963.

[36] Kerr, W. J.; Morrison, A. J.; Pazicky, M.; Weber, T. Modified Shapiro Reactions with Bismesitylmagnesium As an Efficient Base Reagent. *Org. Lett.* **2012**, *14*, 2250-2253.

[37] Luo, C.; Bandar, J. S. Superbase-Catalyzed anti-Markovnikov Alcohol Addition Reactions to Aryl Alkenes. *J. Am. Chem. Soc.* **2018**, *140*, 3547-3550.

[38] Luo, C.; Bandar, J. S. Synthesis of β-Phenethyl Ethers by Base-Catalyzed Alcohol Addition Reactions to Aryl Alkenes. *Synlett* **2018**, *29*, 2218-2224.

[39] Schwesinger, R.; Schlemper, H. Peralkylated Polyaminophosphazenes–Extremely Strong, Neutral Nitrogen Bases. *Angew. Chem., Int. Ed.* **1987**, *26*, 1167-1169.

[40] Puleo, T. R.; Sujansky, S. J.; Wright, S. E.; Bandar, J. S. Organic Superbases in Recent Synthetic Methodology Research. *Chem. Eur. J.* **2021**, *27*, 4216-4229.

[41] Puleo, T. R.; Strong, A. J.; Bandar, J. S. Catalytic α-Selective Deuteration of Styrene Derivatives. *J. Am. Chem. Soc.* **2019**, *141*, 1467-1472.

[42] Hu, Y.; Liang, L.; Wei, W.; Sun, X.; Zhang, X.; Yan, M. A convenient synthesis of deuterium labeled amines and nitrogen heterocycles with KO*t*-Bu/DMSO-d_6. *Tetrahedron* **2015**, *71*, 1425-1430.

[43] Patel, M.; Saunthwal, R. K.; Verma, A. K. Base-Mediated Deuteration of Organic Molecules: A Mechanistic Insight. *ACS Omega* **2018**, *3*, 10612-10623.

[44] Hirono, Y.; Kobayashi, K.; Yonemoto, M.; Kondo, Y. Metal-free deprotonative functionalization of heteroaromatics using organic superbase catalyst. *Chem. Commun.* **2010**, *46*, 7623-7624.

[45] Ntetsikas, K.; Alzahrany, Y.; Polymeropoulos, G.; Bilalis, P.; Gnanou, Y.; Hadjichristidis, N. Anionic Polymerization of Styrene and 1,3-Butadiene in the Presence of Phosphazene Superbases. *Polymers* **2017**, *9*, 538.

[46] Hurley, S. A.; Tait, P. J. T. Anionic polymerization initiated by lithium diethylamide in organic solvents. III. Investigation of the polymerization of styrene. *J. Polym. Sci., Polym. Chem. Ed.* **1976**, *14*, 1565-1580.

[47] Luo, C.; Alegre-Requena, J. V., Sujansky, S. J.; Pajk, S. P.; Gallegos, L. C.; Paton, R. S.; Bandar, J. S. Mechanistic Studies Yield Improved Protocols for Base-Catalyzed Anti-Markovnikov Alcohol Addition Reactions. *J. Am. Chem. Soc.* **2022**, *144*, 9586-9596.

[48] Sapeta, K.; Kerr, M. A. The Cycloaddition of Nitrones with Homochiral Cyclopropanes. *J. Org. Chem.* **2007**, *72*, 8597-8599.

[49] Niu, D.; Buchwald, S. L. Design of Modified Amine Transfer Reagents Allows the Synthesis of α-Chiral Secondary Amines via CuH-Catalyzed Hydroamination. *J. Am. Chem. Soc.* **2015**, *137*, 9716-9721.

CHAPTER TWO

CATALYTIC ARYL HALIDE ISOMERIZATION REACTIONS

2.1 Chapter Overview

Aryl halides are ubiquitous starting materials in synthetic chemistry to reliably and predictably access functionalized arenes.[1-5] The majority of aryl halide substitution reactions occur at the *ipso*-position. Alternatively, catalytic aryl halide isomerization reactions have seen some development to access isomeric substituted arene products. Aryl halide isomerization is defined as the process in which a halogen changes positions on an aromatic ring (Figure 2–1). This chapter will provide the background on current approaches to aryl halide isomerization and selected examples of the utility of this process in synthetic chemistry. In particular, base-catalyzed isomerization reactions will be highlighted, as the mechanistic insights from these approaches serve as the foundation for my work that will be described in Chapters 3, 4, and 5.

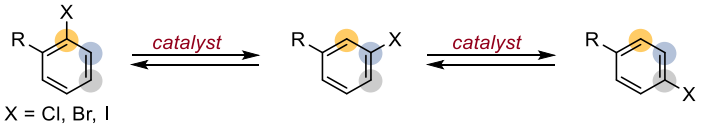

Figure 2–1: General reaction scheme for catalytic aryl halide isomerization.

2.2 Acid-Catalyzed Aryl Halide Isomerization Reactions

Aryl halides can undergo isomerization in the presence of strong acids. In 1962, Olah reported aluminum halides catalyze the isomerization of aryl halides producing a thermodynamic mixture of isomers (Figure 2–2).[6-7] Bromo- and chloroarenes isomerize under these conditions. Interestingly, the mechanism for producing *ortho*- and *para*- isomers of bromoarenes seems to proceed *via* an intermolecular pathway with disproportionated intermediates. Meanwhile, the mechanism for isomerization to the *meta*-isomer proceeds *via* a 1,2-halogen shift mechanism.

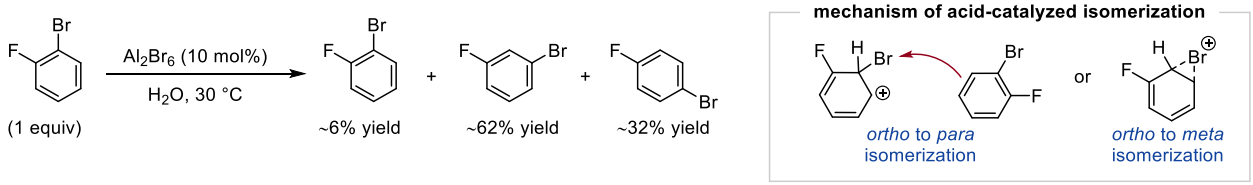

Figure 2–2: Al_2Br_6 catalyzed aryl halide isomerization reported by Olah.

Treatment of bromophenols and bromoanisoles with solvent quantities of superacids promotes isomerization.[8] Dissolution of 2-bromophenol in SbF_5–HF results in complete isomerization to 3-bromophenol (Figure 2–3). The mechanism of the isomerization depended on the superacid solvent employed. Using triflic acid solvent, the isomerization proceeds *via* intermolecular halogen transfer and disproportionated intermediates. Meanwhile, in SbF_5–HF solvent, the isomerization proceeds *via* a 1,2-halogen shift mechanism.

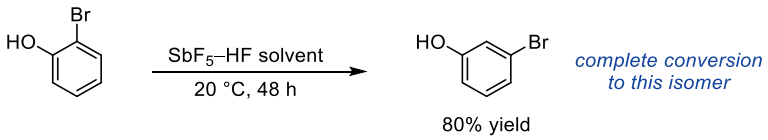

Figure 2–3: Isomerization of 2-bromophenol in superacid SbF_5–HF solvent.

2.3 Base-Catalyzed Aryl Halide Isomerization *via* Intermolecular Halogen Transfer

In contrast to acid-catalyzed aryl halide isomerization, there have been several reports and mechanistic studies on the rearrangement of aryl halides under basic conditions. In 1951 and 1953, Nord disclosed two reports on the unexpected observation that 2-bromothiophene and 2-iodothiophene disproportionate into the corresponding tetrahalothiophene upon treatment with sodium acetylide (Figure 2–4, left).[9-10] In addition to the tetrahalothiophene, a complex mixture of di- and trihalothiophenes were observed in the reaction mixture. Meanwhile, in 1959 Wotiz and Huba disclosed the surprising observation that 1,2,4-tribromobenzene (**2–1**) isomerizes to 1,3,5-tribromobenzene (**2–2**) upon treatment with $NaNH_2$ (Figure 2–4, right).[11] The novelty of these processes at the time of their discovery inspired efforts to study their mechanism.

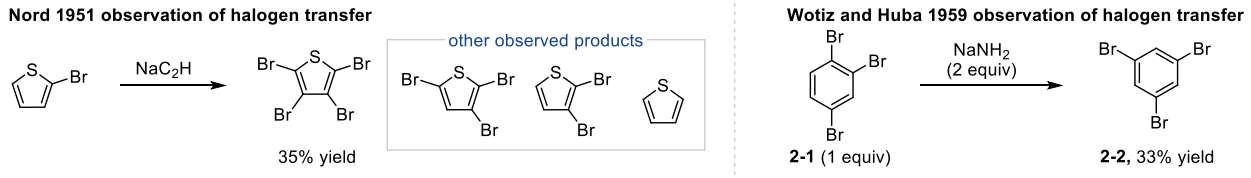

Figure 2–4: Early observations of base-catalyzed halogen transfer.

Despite other related observations and work in this area, it took until the early 1970s for the now widely accepted mechanism for these processes to be elucidated completely by Bunnett.[12-13] Using a series of polyhalobenzene isomerization processes as model reactions, Bunnett designed experiments to distinguish between multiple possible mechanisms.[13-15] The two most compelling proposed mechanisms included rearrangement *via* an aryne intermediate or iterative intermolecular halogen transfer reactions between aromatic rings.

To investigate the possibility of an aryne mechanism, Bunnett used potassium iodide (KI) as an additive in the isomerization reaction of 1,2,4-tribromobenzene (**2–1**) into 1,3,5-tribromobenzene (**2–2**) (Figure 2–5). If isomerization proceeds *via* an aryne intermediate, inclusion of KI should produce iododibromobenzene products. Instead, KI exhibited no effect on the isomerization reaction, producing no iodobenzene products or change in the distribution of bromobenzene isomers.[13]

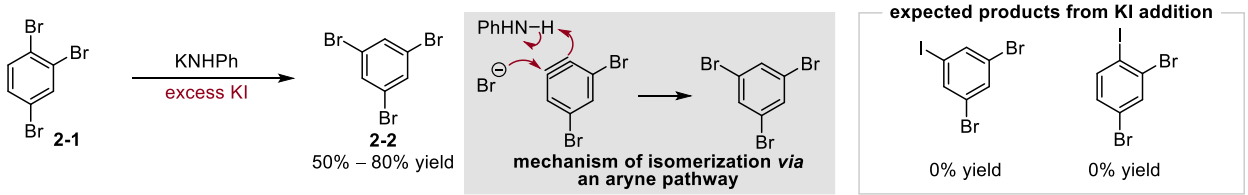

Figure 2–5: Key mechanistic experiment conducted by Bunnett that suggests isomerization does not occur *via* an aryne intermediate.

Several of Bunnett's mechanistic studies strongly support base-catalyzed aryl halide isomerization proceeds *via* intermolecular halogen transfer between aromatic rings. First, in the isomerization of 1,2,4-tribromobenzene (**2–1**) into 1,3,5-tribromobenzene (**2–2**), several

disproportionated products, including dibromobenzenes (**2–5** and **2–6**) as well 1,2,3,5-tetrabromobenzene (**2–3**) and 1,2,4,5-tetrabromobenzene (**2–4**), are observed (Figure 2–6a). Second, reversion of 1,3,5-tribromobenzene (**2–2**) into 1,2,4-tribromobenzene (**2–1**) does not occur under identical reaction conditions, even when substoichiometric quantities of 1,2,4-tribromobenzene (**2–1**) are included. When catalytic quantities of 1,2,3,5-tetrabromobenzene (**2–3**) are included in the reaction, 1,3,5-tribromobenzene (**2–2**) reverts into 1,2,4-tribromobenzene (**2–1**) and establishes a similar equilibrium between the two isomers (Figure 2–6b). This result suggests that 1,2,3,5-tetrabromobenzene (**2–3**) is a key cocatalyst to facilitate isomerization.[14-15]

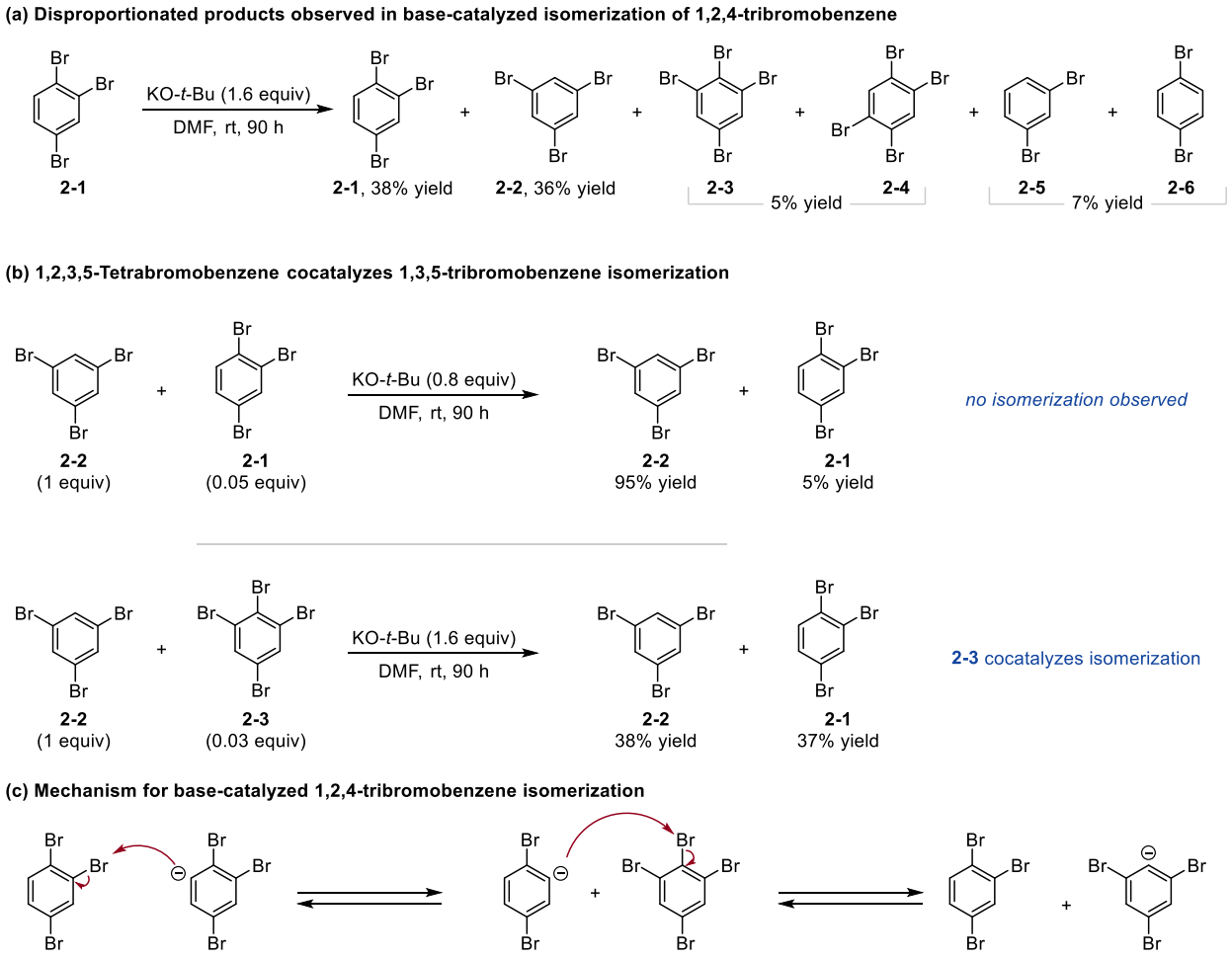

Figure 2–6: Experiments conducted by Bunnett to support that base-catalyzed isomerization occurs through an intermolecular halogen transfer mechanism

These observations, in addition to several other studies by Bunnett, support that isomerization occurs *via* the mechanism depicted in Figure 2–6c.[14] Deprotonation of 1,2,4-tribromobenzene (**2–1**) produces an aryl anion that undergoes electrophilic bromination with a second equivalent of **2–1**, producing 1,2,3,5-tetrabromobenzene (**2–3**) and an aryl anion of 1,4-dibromobenzene (**2–6**). 1,2,3,5-Tetrabromobenzene (**2–3**) then functions as an electrophilic bromine source, and transfers bromine to another aryl anion producing 1,3,5-tribromobenzene (**2–2**). Each of these steps are reversible and establishes a thermodynamic mixture of disproportionated and isomeric products.

Bunnett called this process the "base-catalyzed halogen dance." Although his studies provide significant insight into the mechanism of base-catalyzed aryl halide isomerization, applying this process to synthetic applications is challenging due to the uncontrolled production of a thermodynamic mixture of aryl halide isomers and disproportionated products. Overall, the main application where this mechanistic insight has been applied is in modern "halogen dance" methodology, a topic which will be briefly covered in the following section.

2.4 Halogen Dance Methodology in Modern Synthetic Chemistry

In a modern halogen dance reaction, stoichiometric and irreversible metalation of a halogenated arene with strong lithium bases leads to isomerization to form the most thermodynamically stable metalated haloarene isomer. Treatment of the rearranged and metalated haloarene with a proton source or electrophile produces isomeric aryl halide products, as shown in the example in Figure 2–7. In addition to typically requiring stoichiometric lithium bases under cryogenic conditions, a synthetically useful halogen dance method requires a thermodynamic gradient to drive a selective rearrangement. Halogen dance reactions are broadly developed, and several reviews have been written on the topic.[16-18] In this section, two selected examples of

halogen dance reactions will be described to demonstrate the amenable substrates and reactions that can be achieved.

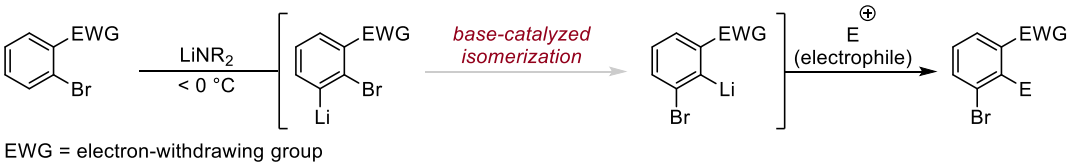

Figure 2–7: General scheme for aromatic electrophilic functionalization *via* halogen dance reactions.

In the first selected example, Schlosser reported a protocol to synthesize 3-fluoro-5-iodopyridine from 3-fluoro-2-(trimethylsilyl)pyridine (**2–7**) *via* a halogen dance approach (Figure 2–8).[19] Treatment of **2–7** with lithium diisopropylamide (LIDA) and I_2 affords 3-fluoro-4-iodo-2-(trimethylsilyl)pyridine (**2–8**). Stoichiometric metalation of **2–8** with LIDA promoted isomerization to metalated pyridine (**2–10**) and H_2O quenching afforded isomeric 3-fluoro-5-iodo-2-(trimethylsilyl)pyridine (**2–11**). Desilylation of **2–11** affords 3-fluoro-5-iodopyridine. The LIDA promoted rearrangement was driven to completion due to the higher thermodynamic stability of the 4-metalated isomer **2–10** compared to the 5-metalated isomer **2–9**.

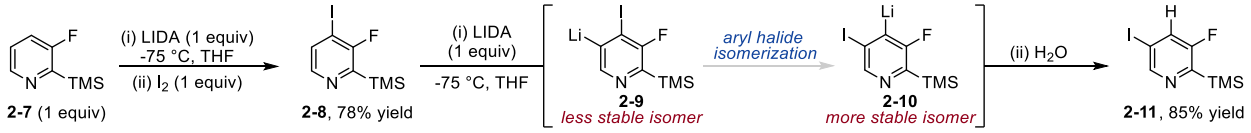

Figure 2–8: Synthesis of an isomeric halogenated pyridine *via* a base-catalyzed halogen dance reaction.

As an additional example, Sammakia utilized two halogen dance rearrangement reactions as key steps in a total synthesis of caerulomycin C (Figure 2–9).[20] Treatment of 3-iodopyridine **2–12** with LIDA promoted complete rearrangement to the more stable 5-iodo-3-metalated pyridine intermediate. Quenching with H_2O produced 5-iodopyridine **2–13** which was subsequently substituted with MeOH and brominated *via* treatment with *n*-BuLi and Br_2 yielding 3-

bromopyridine product **2–14**. Treatment of 3-bromopyridine **2–14** with LIDA promoted a halogen dance rearrangement to the more thermodynamically stable 6-bromopyridine isomer **2–15**. This product could then be transformed into caerulomycin C with three additional synthetic steps.

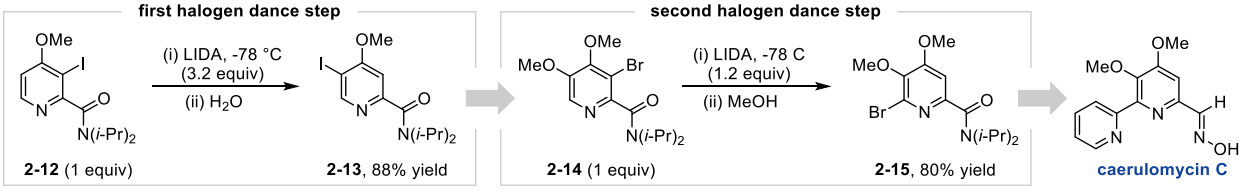

Figure 2–9: Application of base-catalyzed halogen dance methodology to the total synthesis of caerulomycin C.

2.5 Base-Catalyzed Aryl Halide Isomerization *via* Aryne Intermediates

The accepted mechanism in halogen dance reactions and aryl halide isomerization processes is the intermolecular halogen transfer mechanism elucidated by Bunnett (Chapter 2.3).[14] Although this mechanism seems dominant, sporadic reports of aryl halide isomerization occurring through aryne intermediates have been disclosed. Neumann reported treatment of *o*-chlorotoluene with NaOH under high heat produced a 10% yield of *m*-chlorotoluene.[21] Likewise, Bunnett reported the observation that NaOH promotes the isomerization of *para*-halotoluenes to *meta*-halotoluenes *via* an aryne intermediate.[22] Notably, disproportionated products characteristic of an intermolecular halogen transfer isomerization mechanism were not observed in these reports.

We reasoned that if base-catalyzed isomerization of aryl halides *via* aryne intermediates was generalized, it could potentially spur the development of new approaches to aryl halide functionalization reactions. In this regard, we hypothesized that a non-nucleophilic base could catalyze reversible hydrogen halide (HX) elimination *via* aryne intermediates as a complementary approach to base-catalyzed halogen dance methodology (Figure 2–10). This mechanistic hypothesis is the foundation for my work that will be described in Chapter three. Crucial to the mechanistic outline in Figure 2–10 is an understanding of the reactivity of aryne intermediates. In

the following section, an overview of the generation, reactivity, and structure of aryne intermediates is provided.

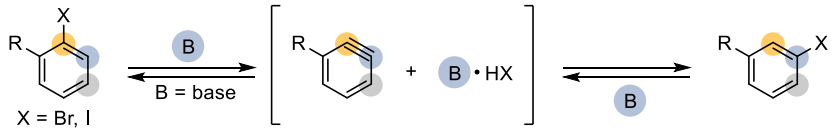

Figure 2–10: General scheme of base-catalyzed aryl halide isomerization *via* aryne intermediates that will be the topic of Chapter three.

2.6 Introduction to the Reactivity of Aryne Intermediates

An aryne intermediate is formally defined as a dehydrogenated aromatic compound possessing a highly strained triple bond within the ring (Figure 2–11).[23] This section will provide an overview of approaches to generate aryne intermediates and the structural effects that govern aryne reactivity.

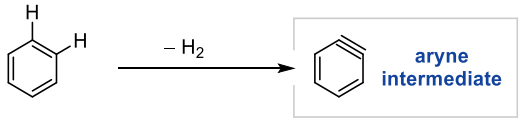

Figure 2–11: Aryne intermediate structure.

2.6.1 Generation of Aryne Intermediates

The high ring strain of arynes renders them highly reactive and precludes their isolation. Thus, arynes are generated and undergo nucleophilic substitution in one reaction pot. Common methods to generate aryne intermediates are presented in Figure 2–12.[23-24] Each approach generates an *ortho*-aromatic anion equivalent that eliminates a good leaving group (e.g. halides, N_2 gas, or triflate). Arguably the mildest approach for aryne generation is treatment of aryl trimethylsilyl triflates with fluoride salts (Figure 2–12, pathway D).

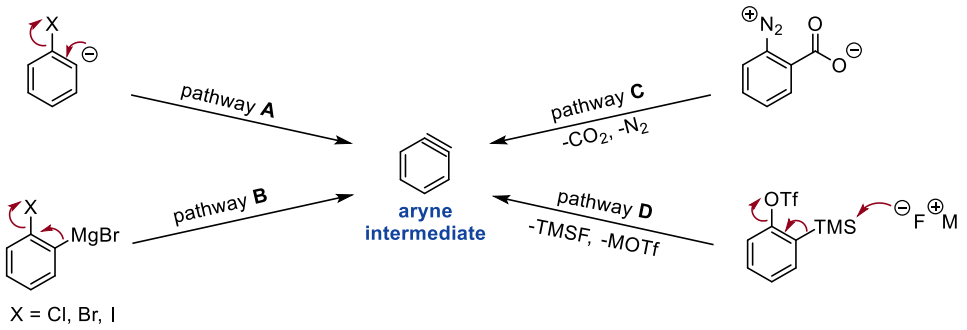

Figure 2–12: Common approaches to generate aryne intermediates.

2.6.2 Structure and Reactivity of Aryne Intermediates

Understanding the structure and reactivity of aryne intermediates towards nucleophiles is crucial to enable their general use in synthetic methods. In this regard, several models have been developed to explain the regioselectivity of nucleophilic addition into unsymmetrical aryne intermediates. Qualitatively, a useful depiction of an aryne is as a polar intermediate, with the alkyne possessing partial positive charge at one site and partial negative charge at another site (Figure 2–13, top). This charge-controlled model of aryne reactivity serves as useful tool for predicting the preferred site of nucleophilic addition into unsymmetrical arynes.[25]

An example for how to use the charge-controlled model is depicted in Figure 2–13. Here, ring substituents are proposed to polarize the aryne and nucleophilic addition occurs at the site with the most positive charge. Thus, 3-fluoro-, 3-chloro-, and 3-methoxybenzynes undergo highly regioselective nucleophilic addition (> 20:1) to produce *meta*-substituted products due to the inductive electron-withdrawing properties of the ring substituents.[25] Although this model enables rapid prediction of the regioselectivity of nucleophile addition for substituted benzynes, it falls short in explaining the regioselectivity observed for heteroaromatic arynes possessing no inductive electron-withdrawing groups. Additionally, accounting for only the charge disparity between each

position of the aryne is not sufficient to explain the observed regioselectivity ($\Delta\Delta G^{\ddagger} \approx 0.2$ kcal/mol).[25]

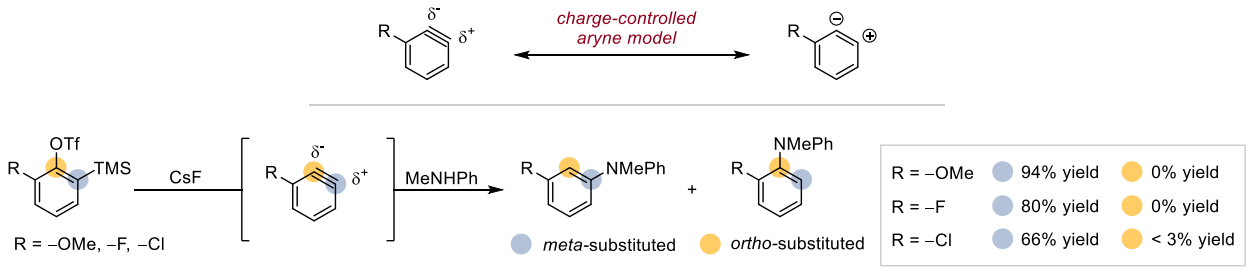

Figure 2–13: The charge-controlled model for aryne reactivity.

A more accurate model for aryne reactivity is the aryne distortion model.[26] The aryne distortion model proposes that the bond angles of the aryne are not equivalent at each position, rendering one site significantly more electrophilic. For example, the calculated bond angles of 3-fluorobenzyne at the 1- and 2-positions is 135 ° and 118 °, respectively (Figure 2–14). Due to this distortion, the 1-position possesses significantly more *p*-character, rendering it more electrophilic. When accounting for this distortion, $\Delta\Delta G^{\ddagger}$ for nucleophilic addition to the 1-position over the 2-position of 3-fluorobenzyne is 4.1 kcal/mol, which sufficiently supports the exclusive *meta*-selectivity observed for *N*-methylaniline addition (Figure 2–14).[25]

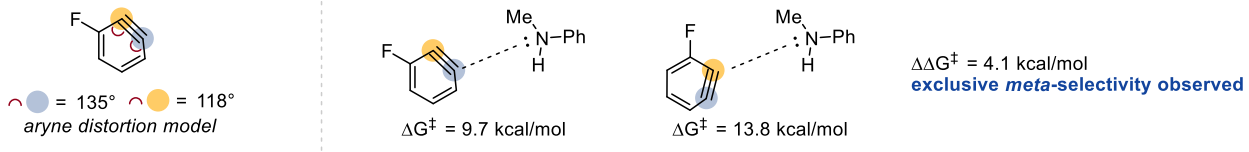

Figure 2–14: The aryne distortion model.

Notably, predictions using the aryne distortion model will often align with those of the charge-controlled model. While the charge-controlled model can be used to rapidly and accurately predict the regioselectivity of benzyne nucleophilic additions, its ability to predict the regioselectivity of nucleophilic addition to heteroaromatic arynes is limited, and the aryne

distortion model is needed. Figure 2–15 displays the calculated bond angles of 3,4-pyridyne and 4,5-indolyne and the predicted site of nucleophilic addition.[26] The magnitude of the difference in bond angle is indicative of how selective nucleophilic addition will be. For example, amination of 3,4-pyridyne (bond angle difference = 0.6°) with morpholine produces a 42:58 mixture 3-amino:4-aminopyridine isomers.[27-28] Amination of 4,5-indolyne (bond angle difference = 4.1°) produces a 91% yield of the 5-substituted product with 12.5:1 5:4-positional selectivity (Figure 2–15).[29-30]

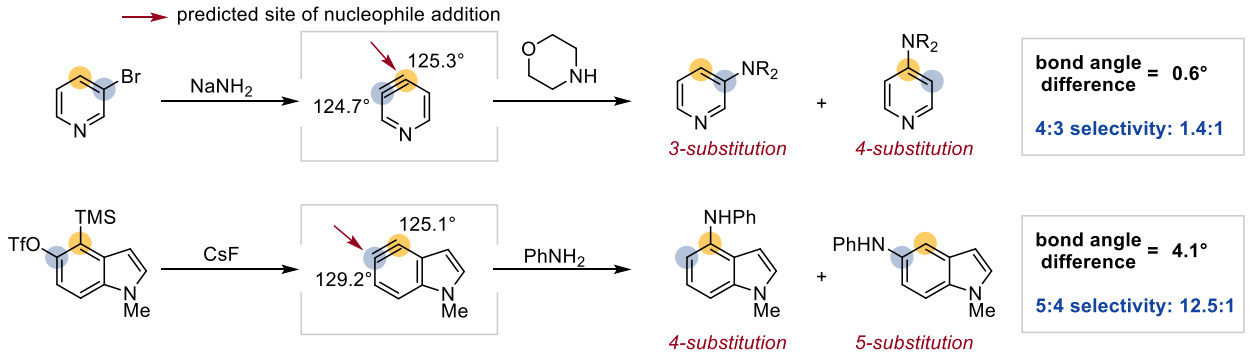

Figure 2–15: Application of the aryne distortion model in predicting the regioselectivity of nucleophilic addition into heteroaromatic aryne intermediates.

2.7 Conclusion

The mechanistic insights from base-catalyzed aryl halide isomerization reactions served as a major inspiration for my work in developing new approaches to C–H functionalization reactions. Chapter three will describe the generalization of base-catalyzed aryl halide isomerization *via* aryne intermediates to simple aryl halides, and the application of this process to enable a new approach to nucleophilic pyridine C–H functionalization reactions. In Chapters 4 and 5, a fundamentally new application of the base-catalyzed halogen dance mechanism to enable C–H functionalization reactions will be described.

REFERENCES

[1] Magano, J.; Dunetz, J. R. Large-Scale Applications of Transition Metal-Catalyzed Couplings for the Synthesis of Pharmaceuticals. *Chem. Rev.* **2011**, *111*, 2177–2250.

[2] Zhang, N.; Samanta, S. R.; Rosen, B. M.; Percec, V. Single Electron Transfer in Radical Ion and Radical-Mediated Organic, Materials and Polymer Synthesis. *Chem. Rev.* **2014**, *114*, 5848–5958.

[3] Seyferth, D. The Grignard Reagents. *Organometallics* **2009**, *28*, 1598–1605.

[4] Twilton, J.; Le, C.; Zhang, P.; Shaw, M. H.; Evans, R. W.; MacMillan, D. W. C. The merger of transition metal and photocatalysis. *Nat. Rev. Chem.* **2017**, *1*, 0052.

[5] Bunnett, J. F. The remarkable reactivity of nucleophiles with aryl halides. *J. Chem. Educ.* **1974**, *51*, 312-315.

[6] Olah, G. A.; Tolgyesi, W. S.; Dear, R. E. A. Friedel-Crafts Isomerization. III. Aluminum Bromide-Catalyzed Isomerization of Bromofluorobenzenes, Bromochlorobenzenes, and Dibromobenzenes. *J. Org. Chem.* **1962**, *27*, 3455–3464.

[7] Olah, G. A.; Meyer, M. W. Friedel-Crafts Isomerization. IV.[1] Aluminum Halide-Catalyzed Isomerization of Halotoluenes. *J. Org. Chem.* **1962**, *27*, 3464–3469.

[8] Jacquesy, J.-C.; Jouannetaud, M.-P. Mechanism of isomerization of *ortho* or *para* bromo phenols in superacids. *Tetrahedron Lett.* **1982**, *23*, 1673–1676.

[9] Vaitiekunas, A.; Nord, F. F. Tetrabromothiophene from 2-Bromothiophene by means of Sodium Acetylide in Liquid Ammonia. *Nature*, **1951**, *168*, 875–876.

[10] Vaitiekunas, A.; Nord, F. F. Studies on the Chemistry of Heterocyclics. XXII. Investigations on the Mechanism of Reactions of 2-Thienyl Halides with Sodium Amide and Sodium Acetylide in Liquid Ammonia. *J. Am. Chem. Soc.*, **1953**, *75*, 1764–1768.

[11] Wotiz, J. H.; Huba, F. Low Temperature Amination of Aromatic Polyhalides. *J. Org. Chem.* **1959**, *24*, 595-598.

[12] Reinecke, M. G.; Adickes, H. W. The case of the ersatz aryne. A new mechanism of cine-substitution. *J. Am. Chem. Soc.* **1968**, *90*, 511-513.

[13] Moyer, C. E.; Bunnett, J. F. Base-Catalyzed Isomerization of Trihalobenzenes. *J. Am. Chem. Soc.* **1963**, *85*, 1891-1893.

[14] Bunnett, J. F. Base-catalyzed halogen dance, and other reactions of aryl halides. *Acc. Chem. Res.* **1972**, *5*, 139–147.

[15] Bunnett, J. F.; Scorrano, G. Mechanism of base-catalyzed isomerization and disproportionation of trihalobenzenes. *J. Am. Chem. Soc*. **1971**, *93*, 1190–1198.

[16] Schnürch, M.; Spina, M.; Khan, A. F.; Mihovilovic, M. D.; Stanetty, P. Halogen Dance Reactions–A review. *Chem. Soc. Rev*. **2007**, *36*, 1046–1057.

[17] Schlosser, M. F. The 2×3 Toolbox of Organometallic Methods for Regiochemically Exhaustive Functionalization. *Angew. Chem., Int. Ed.* **2005**, *44*, 376–393.

[18] Erb, W.; Mongin, F. Halogen 'dance': a way to extend the boundaries of arene deprotolithiation. *Tetrahedron*, **2016**, *72*, 4973–4988.

[19] Marzi, E.; Bobbio, C.; Cottet, F.; Schlosser, M. Converting Core Compounds into Building Blocks: The Concept of Regiochemically Exhaustive Functionalization. *Eur. J. Org. Chem*. **2005**, *2005*, 2116–2123.

[20] Sammakia, T.; Strangeland, E. L.; Whitcomb, M. C. Total Synthesis of Caerulomycin C via the Halogen Dance Reaction. *Org. Lett.* **2002**, *4*, 2385-2388.

[21] Dalman, G. W.; Neumann, F. W. The mechanism of the formation and hydrolysis of phenyl ether in the basic hydrolysis of chlorobenzene. *J. Am. Chem. Soc*. **1968**, *90*, 1601–1605.

[22] Zoratti, M.; Bunnett, J. F. Mechanism of the nonaryne hydroxydehalogenation of unactivated aryl halides. *J. Org. Chem.* **1980**, *45*, 1769–1776.

[23] Pellissier, H.; Santelli, M. The use of arynes in organic synthesis. *Tetrahedron*, **2003**, *59*, 701–730.

[24] Goetz, A. E.; Garg, N. K. Enabling the Use of Heterocyclic Arynes in Chemical Synthesis. *J. Org. Chem.* **2014**, *79*, 846-851.

[25] Medina, J. M.; Mackey, J. L.; Garg, N. K.; Houk, K. N. The Role of Aryne Distortions, Steric Effects, and Charges in Regioselectivities of Aryne Reactions. *J. Am. Chem. Soc.* **2014**, *136*, 15798-15805.

[26] Goetz, A. E.; Bronner, S. M.; Cisneros, J. D.; Melamed, J. M.; Paton, R. S.; Houk, K. N.; Garg, N. K. An Efficient Computational Model to Predict the Synthetic Utility of Heterocyclic Arynes. *Angew. Chem., Int. Ed*. **2012**, *51*, 2758–2762.

[27] Vinter-Pasquier, K; Jamart-Grégoire, B.; Caubére, P. Complex Base-Induced Generation of 3,4-Didehydropyridine Derivatives : New Access to Amino-Pyridines or Pyridones. *Heterocycles*, **1997**, *45*, 2113–2129.

[28] Goetz, A. E.; Garg, N. K. Regioselective reactions of 3,4-pyridynes enabled by the aryne distortion model. *Nat. Chem*. **2013**, *5*, 54–60.

[29] Goetz, A. E.; Shah, T. K.; Garg, N. K. Pyridynes and indolynes as building blocks for functionalized heterocycles and natural products. *Chem. Commun.* **2015**, *51*, 34-45.

[30] Picazo, E.; Houk, K. N.; Garg, N. K. Computational predictions of substituted benzyne and indolyne regioselectivities. *Tetrahedron Lett.* **2015**, *56*, 3511-3514.

CHAPTER THREE

NEW APPROACHES TO PYRIDINE C–H FUNCTIONALIZATION REACTIONS VIA BASE-CATALYZED ARYL HALIDE ISOMERIZATION

3.1 Chapter Overview

This chapter describes our discovery and application of base-catalyzed aryl halide isomerization reactions *via* aryne intermediates. The first part of Chapter three will describe our discovery of a general approach to base-catalyzed aryl halide isomerization *via* reversible hydrogen halide (HX) elimination (Figure 3–1, left). The second part of Chapter three will cover the application of base-catalyzed aryl halide isomerization to enable 4-selective nucleophilic substitution reactions of 3-bromopyridines (Figure 3–1, right). The complementary nature of this approach to other routes to access 4-substituted pyridines will be discussed at the end of this of chapter.

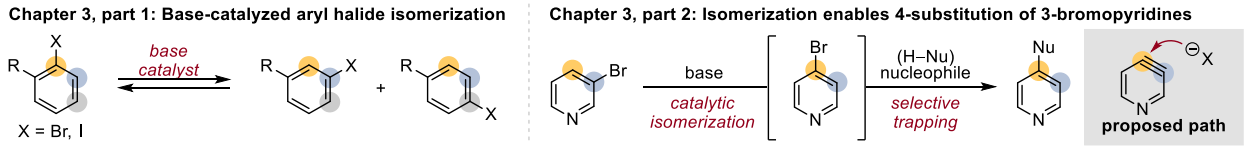

Figure 3–1: Overview of reactions that will be covered in Chapter three.

3.2 Development of a General Approach to Base-Catalyzed Aryl Halide Isomerization

Given sporadic reports of aryl halides rearranging *via* aryne intermediates, we hypothesized strong non-nucleophilic bases could catalyze reversible hydrogen halide elimination producing an isomeric mixture of aryl halides.[1-2] Drawing inspiration from our work in styrene hydroetherification reactions (see Chapter one), we hypothesized P_4-*t*-Bu could be an effective catalyst for aryl halide isomerization.[3-4] P_4-*t*-Bu (pK_a = 30.2 in DMSO) is non-nucleophilic but basic enough to deprotonate aryl halide C–H bonds (pK_a ≈ 36 in DMSO).[5-7] Therefore, we

reasoned P_4-*t*-Bu could generate, but not react with, aryne intermediates allowing isomerization to occur. In an initial result, I discovered P_4-*t*-Bu catalyzes the isomerization of 2-bromobenzotrifluoride (**3–1)** into all possible regioisomers (Figure 3–2a).[8] Likewise, subjection of 3-bromobenzotrifluoride (**3–2**) and 4-bromobenzotrifluoride (**3–3**) to the same reaction conditions interconverts the two isomers but does not form 2-bromobenzotrifluoride (Figure 3–2b). No protodehalogenated or polyhalogenated side products are observed, consistent with rearrangement *via* an aryne intermediate vs. rearrangement *via* a halogen dance mechanism (see Chapter 2.3 and Chapter 2.5).

I demonstrated several simple aryl bromides and iodides undergo isomerization under these reaction conditions (Figure 3–2b). Related 4-iodobenzotrifluoride (**3–4**) undergoes isomerization to 3-iodobenzotrifluoride but to a lesser extent than 4-bromobenzotrifluoride (**3–3**). A variety of other bromoarenes including 1,2-dibromobenzene (**3–5**), 2-bromotrifluoromethoxybenzene (**3–6**), 5-bromobenzothiophene (**3–7**), and 3-bromopyridine (**3–8**) also undergo isomerization. These observations suggest P_4-*t*-Bu-catalyzed aryl halide isomerization is a general and reversible process.[8]

As a broader objective, we questioned if base-catalyzed aryl halide isomerization could be incorporated into other reaction processes to enable new synthetic reactions. The following section will describe our application of base-catalyzed aryl halide isomerization to enable a 4-selective substitution reaction of 3-bromopyridines.

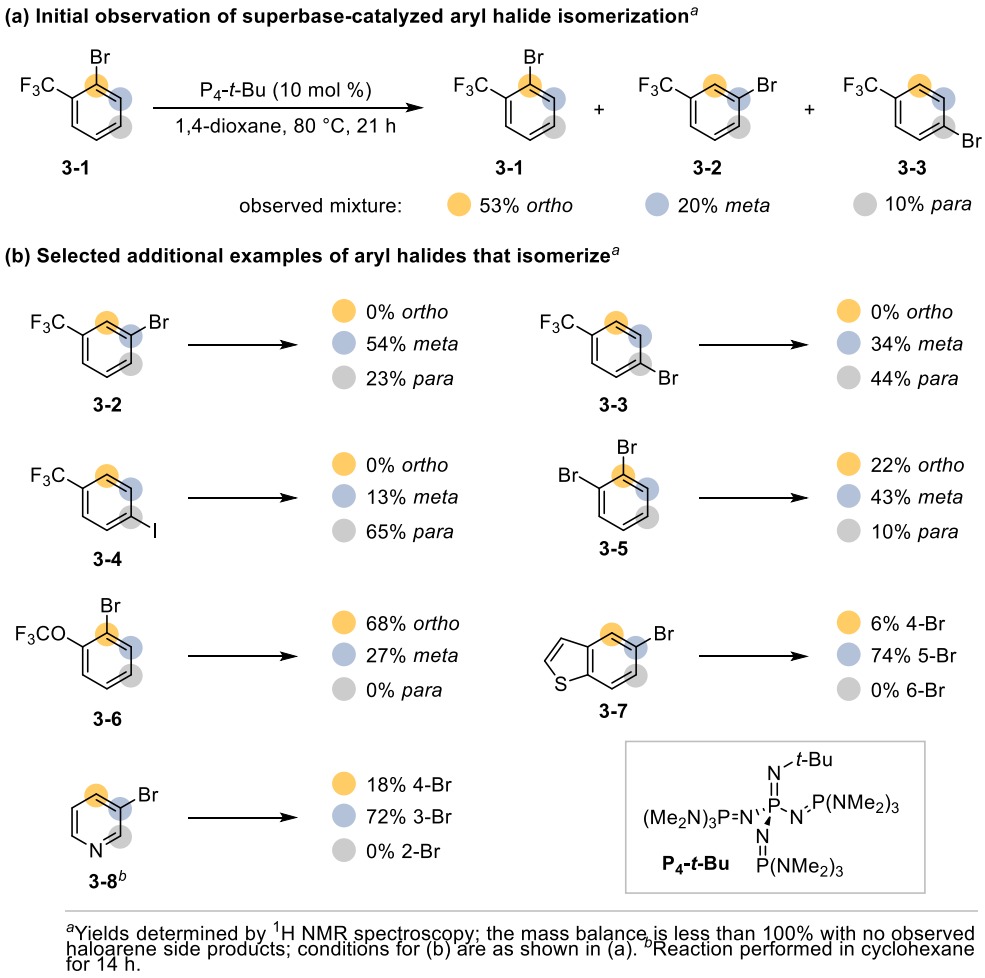

[a]Yields determined by ^{1}H NMR spectroscopy; the mass balance is less than 100% with no observed haloarene side products; conditions for (b) are as shown in (a). [b]Reaction performed in cyclohexane for 14 h.

Figure 3–2: P_4-*t*-Bu-catalyzed aryl halide isomerization.

3.3 Aryl Halide Isomerization Enables 4-Selective Substitution of 3-Bromopyridines

The key challenge in applying base-catalyzed aryl halide isomerization to enable new synthetic reactions is that the isomerization reaction is reversible and there is not a strong thermodynamic driving force to produce a single isomeric aryl halide product. As a halogen migrates around an aromatic ring, we reasoned the differing electronics of isomeric carbon–halogen bonds could provide a source to differentiate interconverting isomers and drive an overall selective transformation. In this regard, we hypothesized pairing 3-bromopyridine isomerization to a tandem nucleophilic aromatic substitution reaction would selectively produce 4-substituted products.

A mechanistic outline for this proposal is displayed in Figure 3–3. Reversible isomerization of 3-bromopyridine *via* a 3,4-pyridyne intermediate produces 4-bromopyridine. The faster rate of nucleophilic aromatic substitution of 4-bromopyridine over 3-bromopyridine could be exploited to produce predominantly 4-substituted products. Challenging to this transformation is avoiding nucleophilic addition to the highly reactive 3,4-pyridyne intermediate.[9] As described in Chapter 2.6, nucleophilic addition across 3,4-pyridyne is only slightly 4-selective, and interception of this intermediate would likely produce a mixture of 3- and 4-substituted products.[10] Overall, this approach offers a complementary route to 4-functionalized pyridines from 3-bromopyridines, which are often more stable and available, commercially and synthetically, than 4-halogenated congeners.[11-14]

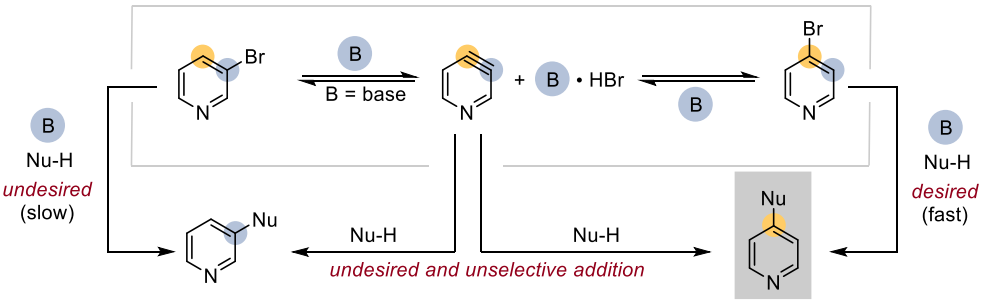

Figure 3–3: Proposed mechanism for the 4-selective substitution of 3-bromopyridines enabled by base-catalyzed aryl halide isomerization.

As this reaction process requires stoichiometric base, I first investigated the use of hydroxide bases as more practical reagents for 3-bromopyridine isomerization. Hydroxide bases are known to generate and be compatible with aryne intermediates and are significantly less expensive and easier to handle than P_4-*t*-Bu.[15] Treatment of 3-bromopyridine (**3–8**) with 18-crown-6-ligated KOH in *N*,*N*-dimethylacetamide (DMAc) solvent produced a 20% yield of 4-bromopyridine (**3–9**) while avoiding competing hydroxide addition (Figure 3–4a). Inclusion of one equivalent of 2-ethyl-1-hexanol (**3–10**) and three equivalents of KOH/18-crown-6 under

similar reaction conditions produced 4-substituted pyridine **3–11** from 3-bromopyridine (**3–8**) in 64% yield with an 8.1:1 ratio of 4:3-substitution products (**3–11:3–12**, Figure 3–4b).[8] Notably, the 4-substitution selectivity observed in this reaction is significantly higher than the expected selectivity for nucleophilic addition to 3,4-pyridyne (Figure 2–15).

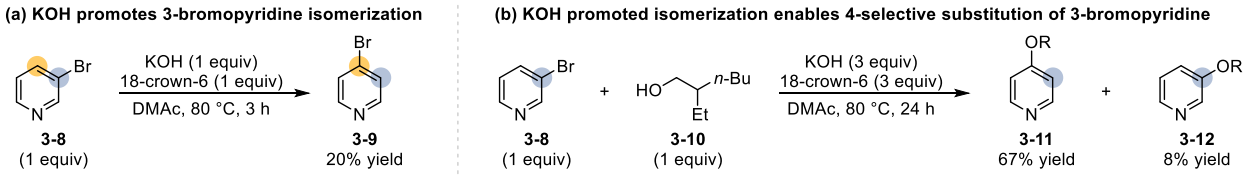

Figure 3–4: Base-catalyzed 3-bromopyridine isomerization enables 4-selective pyridine substitution.

With this promising preliminary result, I next conducted a series of mechanistic studies with the aim to rationally optimize the reaction conditions. The following section will describe the mechanistic and reaction optimization studies we conducted to improve the reaction yield and 4-substitution selectivity.

3.4 Mechanistic Studies and Reaction Optimization

Using the reaction conditions from Figure 3–4 as a foundation, I employed two strategies for optimizing the 4-selective etherification of 3-bromopyridine (**3–8**) with 2-ethyl-1-hexanol (**3-10**, Figure 3–5). Given 3,4-pyridyne is a crucial reaction intermediate, we reasoned modulating the quantity of alcohol nucleophile used in the reaction is important to limit undesired alcohol addition across the aryne intermediate. When one equivalent of 3-bromopyridine (**3–8**) reacts with four equivalents of 2-ethyl-1-hexanol (**3–10**), a 2.4:1 ratio of 4:3-substituted products (**3–11**:**3–12**) was obtained in 54% overall yield (Figure 3–5, left). As higher ratios of 3-bromopyridine : alcohol are used, the 4-substitution selectivity increases. Thus, a 2:1 ratio of 3-bromopyridine (**3–8**) to 2-ethyl-1-hexanol (**3–10**) produced a 95% yield of 4-substituted pyridine **3–11** with 12.6:1 ratio of 4:3-substituted products.[8]

These results indicate that selective trapping of the 3,4-pyridyne intermediate with bromide over the alcohol is crucial. Thus, we hypothesized that added bromide salts may promote more efficient isomerization and hinder undesired interception of 3,4-pyridyne with 2-ethyl-1-hexanol (**3–10**). I found adding 50 mol% of KBr to a reaction using a 1.5:1 ratio of 3-bromopyridine (**3–8**) to 2-ethyl-1-hexanol (**3–10**), increased the yield to 76% with > 14:1 4-selectivity compared to a 67% yield and 8.6:1 4-selectivity in the absence of KBr (Figure 3–5, right). Notably, added halide salts in mechanistic studies of halogen dance reactions imparted no effect on the reaction.[16] Addition of one equivalent of KBr did not improve the yield or selectivity further.[8]

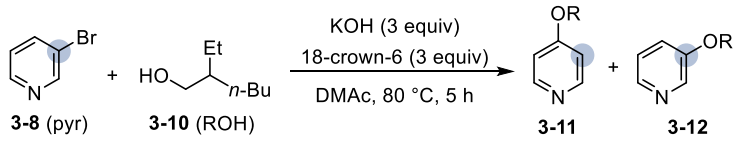

3-8 (pyr) **3-10** (ROH) **3-11** **3-12**

effect of pyridine:alcohol ratio[a]

3-8:3-10	yield	3-11:3-12 ratio
1:4	54%	2.4
1:2	65%	5.5
1:1	64%	8.1
2:1	95%	12.6
4:1	90%	11.9

effect of bromide salt (1.5:1 pyr:ROH)[b]

KBr added	yield	3-11:3-12 ratio
0%	67%	8.6
10%	69%	8.9
20%	73%	11.1
50%	76%	14.2
100%	77%	14.4

[a]Yields and selectivities determined by ^{1}H NMR spectroscopy of the crude reaction mixtures; yields represent total amount of both isomeric products **3-11** and **3-12**. [b]2.0 equiv. of KOH used with a 1 : 1 ratio of **3-8**:**3-10**.

Figure 3–5: Optimization of 4-selective 3-bromopyridine substitution with alcohol nucleophiles.

A reaction profile with the optimized conditions shows the rapid formation of a low concentration of 4-bromopyridine (approximately 5%) that decreases as the reaction reaches completion (Figure 3–6). Subjection of the 3-substituted ether product (**3–12**) to the reaction conditions does not result in mass balance loss, indicating the high 4-selectivity is not a result of selective decomposition or product rearrangement. To further support the generation of 3,4-pyridyne under these conditions, the alcohol was replaced with an excess of furan (**3–13**), a known trap for 3,4-pyridyne intermediates.[17] The corresponding cycloadduct **3–14** was produced 42% yield (Figure 3–7a). I also subjected 3-iodopyridine (**3–15**) to the reaction conditions in the absence

of alcohol. In the presence of excess furan, the cycloadduct **3–14** was formed 24% yield, while in the presence of KBr, 3-bromopyridine (**3–8**) and 4-bromopyridine (**3–9**) formed in 34% overall yield in a 1:1 mixture (Figure 3–7b). The 1:1 mixture of 3-bromopyridine (**3–8**) and 4-bromopyridine (**3–9**) is consistent with the expected regioselectivity for nucleophile addition into 3,4-pyridyne. Overall, these results are consistent with an isomerization pathway *via* a 3,4-pyridyne intermediate and 4-substitution selectivity driven by a facile S_NAr reaction.[8]

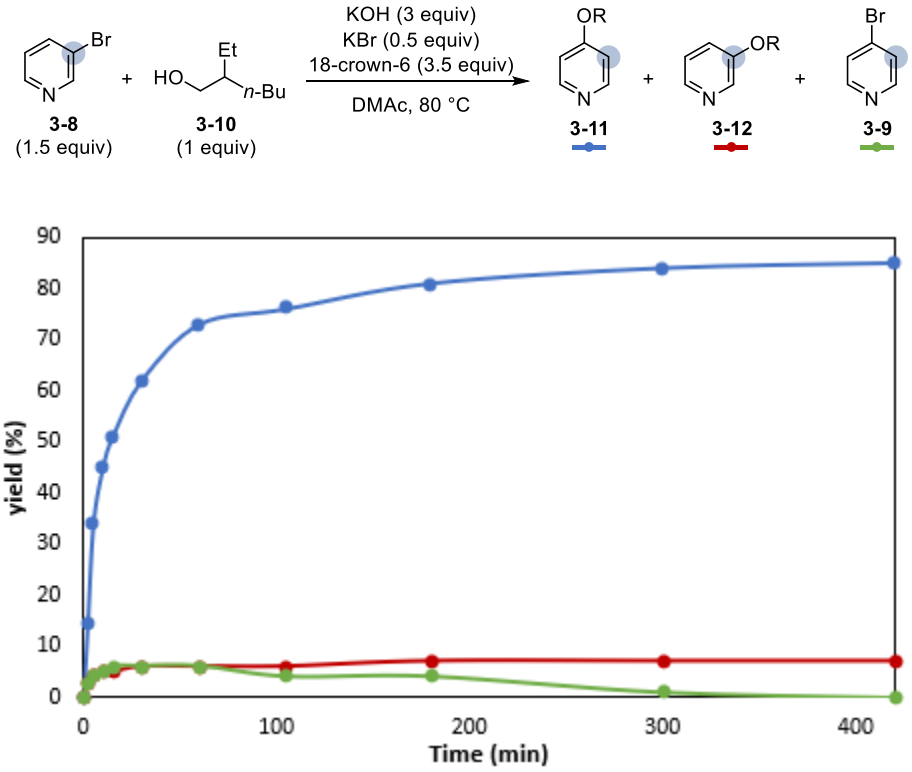

Figure 3–6: Reaction profile analysis of the optimized model reaction.

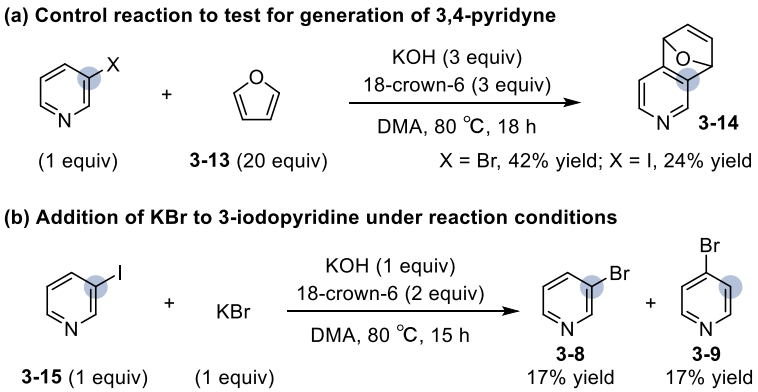

Figure 3–7: Mechanistic experiments that support 3-bromopyridine isomerization proceeds *via* an aryne intermediate.

3.5 Substrate Scope

With optimal reaction conditions identified, I next examined the scope of 3-bromopyridines and nucleophiles that participate in this transformation. The substrate scope for the 4-selective etherification of 3-bromopyridines is presented in Figure 3–8. I examined several primary and secondary alcohols using 1.5 equivalents of simple and inexpensive 3-bromopyridines. Sterically hindered alcohols (**3–16**), aminoalcohols (**3–17**, **3–23**, **3–24**, and **3–27**), alkenols (**3–18**), and a protected sugar (**3–22**) are compatible nucleophiles. 3-Bromopyridines methylated in all positions react in high yield and selectivity (**3–19**, **3–20**, **3–21**), indicating acidic C–H bonds are tolerated on the arene. Notably, 3-bromo-5-methylpyridine (**3–19**) reacts in 70% yield with > 10:1 4-selectivity, indicating that steric hindrance at the 5-position is tolerated. 3-Bromopyridine biaryl substrates also selectively couple in the 4-position (**3–25** and **3–26**). Both 2-alkoxy (**3–23**) and 2-amino (**3–28**) substituents on the pyridine produce 4-subsituted products in good yield and selectivity. Although these 3-bromopyridine substrates isomerize to the corresponding 4-bromopyridine under similar reaction conditions, it is possible the high 4-selectivity could originate from alcohol addition to a distorted 3,4-pyridyne intermediate (see

Chapter 2.6). 3-Bromopyridine substrates with strong electron-withdrawing groups (e.g. 3-bromo-2-(trifluoromethyl)pyridine) undergo direct 3-substitution under these reaction conditions.[8]

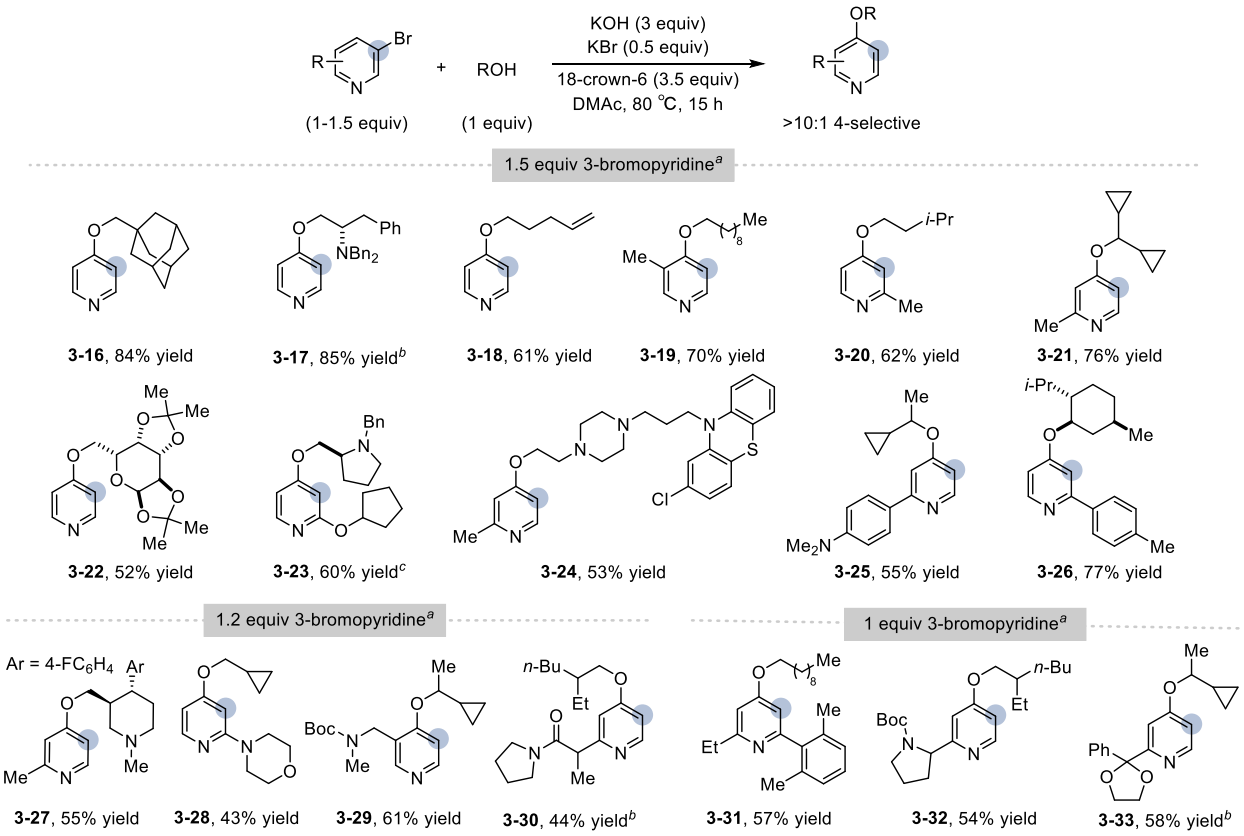

[a]Yields are of purified 4-ether product; regioselectivities determined by ^{1}H NMR spectroscopy of the crude reaction mixture. [b]Selectivity > 6 : 1. [c]P_4-t-Bu (1.3 equiv.) used as base in place of KOH.

Figure 3–8: Substrate scope for 4-selective etherification of 3-bromopyridines.

3-Bromopyridines are often more commercially available and stable than 4-halogenated congeners.[11-14] This advantage was highlighted with substrates **3–29** through **3–33**, where the 3- or 5-bromopyridine was purchased from a commercial source while a 4-halogenated isomer is either not available or significantly more expensive. For example, 3-bromo-5-methylaminopyridine (**3–29**) costs approximately $74/g, whereas the least expensive 4-halogenated congener costs approximately $1001/g. Using 1–1.2 equivalents of these bromopyridines, 4-substituted products including an acidic amide (**3–30**), a 2,6-disubstituted pyridine (**3–31**), a nicotine isomer (**3–32**), and a ketal (**3–33**) can be rapidly accessed.[8] Chapter

3.6 will describe in greater detail the complementarity of this approach compared to other routes to access 4-substituted pyridines.

An additional benefit of this strategy is that an arene's innate halogenation position can be used as an entry to functionalize more difficult to access C–H bonds. I demonstrated this application using 2,6-disubstituted pyridine **3–34** (Figure 3–9), which undergoes mild but unselective electrophilic aromatic bromination in the 3- and 5-positions (**3–35** and **3–36**). Subjecting this isomeric mixture to the reaction conditions from Figure 3–8 provides access to the 4-ether **3–37** through convergence of the regioisomeric bromopyridine mixture.[8]

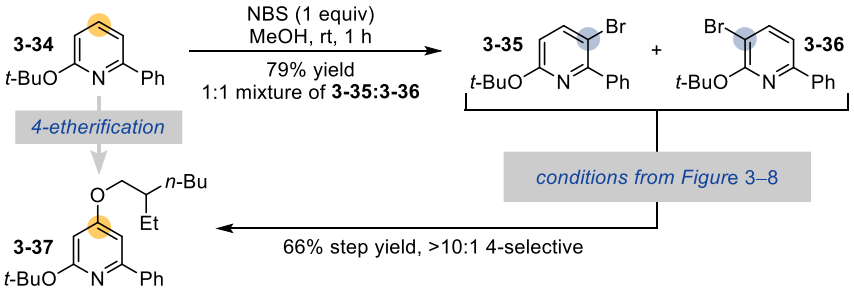

Figure 3–9: Convergence of regioisomeric mixture of 3- and 5-bromopyridine isomers *via* tandem aryl halide isomerization and substitution.

I next examined if amines are amenable to this transformation and found indolines are effective coupling partners (**3–38**, **3–39**, **3–40, 3–41**) and amination can proceed on gram scale in excellent selectivity with these nucleophiles (**3–38**, Figure 3–10). A single isomer of the 5-bromoindoline product **3–39** is obtained, demonstrating the chemoselectivity of aryl halide isomerization. Notably, other amine nucleophiles such as anilines and dialkyl amines produced significantly lower reaction yields and 4-selectivity, indicating aryne substitution is likely the dominant pathway for these nucleophiles.[8]

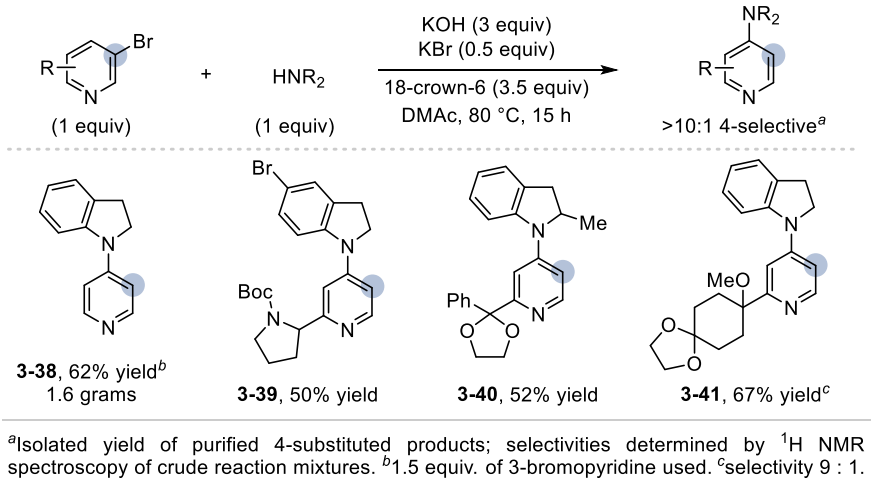

[a]Isolated yield of purified 4-substituted products; selectivities determined by ^{1}H NMR spectroscopy of crude reaction mixtures. [b]1.5 equiv. of 3-bromopyridine used. [c]selectivity 9 : 1.

Figure 3–10: Amine nucleophile substrate scope for 4-selective amination of 3-bromopyridines.

Interestingly, no products arising from substitution of hydroxide are observed in these reactions, even though KOH is used as the base. Hydroxide bases have been observed to be compatible with aryne intermediates and S_NAr reactions using metal hydroxide nucleophiles typically require high reaction temperatures and transition-metal catalysts.[15,18-19] To develop a 4-hydroxylation protocol, we instead hypothesized tandem isomerization/substitution could be further sequenced with a base-promoted elimination step. I found β-hydroxy amide **3–43** is an effective nucleophile for this purpose, undergoing cascade 4-selective etherification and base-promoted elimination of *N*,*N*-dibenzylacrylamide. Thus, treatment of bromopyridine **3–42** with β-hydroxy amide **3–43** under the standard reaction conditions yields 4-pyridone **3–44** in 50% yield and > 10:1 4-selectivity (Figure 3–11).[8]

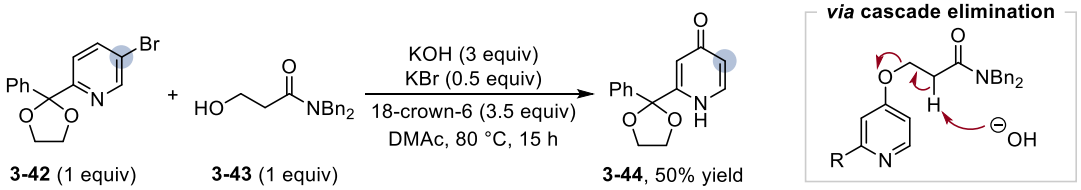

Figure 3–11: 4-Selective hydroxylation of 3-bromopyridines using a β-hydroxyamide nucleophile.

3.6 Methods for Nucleophilic Pyridine C–H Substitution and *cine*-Substitution of 3-Halogenated Pyridines

One unique aspect of this approach is that 3-bromopyridine isomers are utilized to access 4-substituted products. The conventional use of aryl halides is for *ipso*-substitution reactions. Thus, most approaches to access 4-substituted pyridines employ 4-(pseudo)halogenated starting materials. It is common that 3-bromopyridines are more commercially available than the corresponding 4-(pseudo)halogenated pyridine. Additionally, 4-halogenated pyridines can be unstable and undergo self-condensation reactions.[13] Figure 3–12 displays three examples of 3-bromopyridines from Figure 3–8 that are relatively available compared to the corresponding 4-(pseudo)halogenated pyridine.

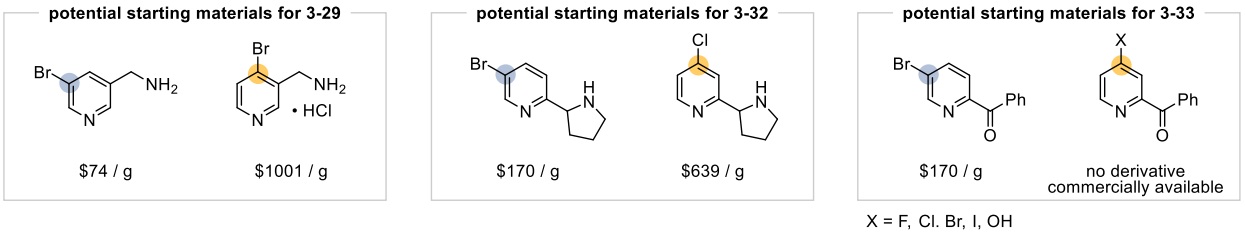

Figure 3–12: Price comparison of the starting materials for 3-bromopyridine substrates in Figure 3–8 to the corresponding 4-(pseudo)halogenated pyridines. Prices were obtained from emolecules.com on March 20th, 2020.

This method would also complement other recently developed methods for 4-selective nucleophilic pyridine C–H functionalization. McNally has developed a powerful heterocyclic phosphonium salt approach to achieve 4-selective pyridine C–H functionalization. In this approach, a triphenylphosphine pseudohalide is selectively installed into the 4-position of pyridines *via* sequential treatment with Tf_2O, PPh_3, and base. The resultant pyridine phosphonium salts are highly versatile intermediates, undergoing nucleophilic substitution with alcohols, amines, thiols, and halogens, amongst other transformations (Figure 3–13).[20-27]

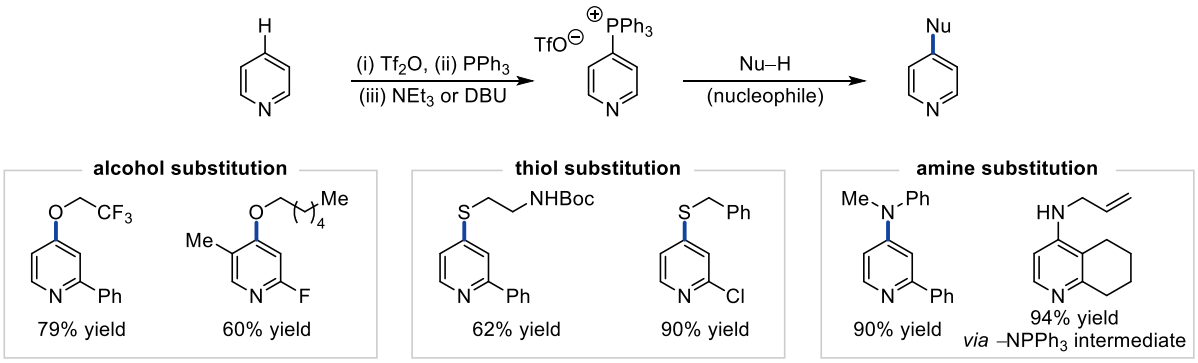

Figure 3–13: McNally's phosphonium salt approach to 4-selective nucleophilic pyridine substitution. Reaction yields correspond to substitution of the pyridine phosphonium salt unless otherwise indicated.

cine-Substitution of 3-bromopyridines is another approach for 4-selective pyridine functionalization. Caubére reported treatment of 3-bromopyridine with $NaNH_2$ base and morpholine produced the corresponding 4-aminopyridine *via* an aryne intermediate in 58% yield with a 42% yield of the corresponding 3-aminopyridine (see Figure 2–15).[28] Dong disclosed an impressive Catellani reaction to converge a mixture and 3- and 5-bromopyridine isomers to a 4-aminopyridine product. Electrophilic aromatic bromination of 2,6-disubstituted pyridine **3–45** with 1,3-dibromo-5,5,-dimethylhydantoin produced a 4.2:1 mixture of bromopyridine isomers **3–46** and **3–47**. Subjection of the mixture to Catellani reaction conditions and *O*-benzoyl hydroxylamine **3–48** promoted 4-selective amination in 83% yield (Figure 3–14).[29]

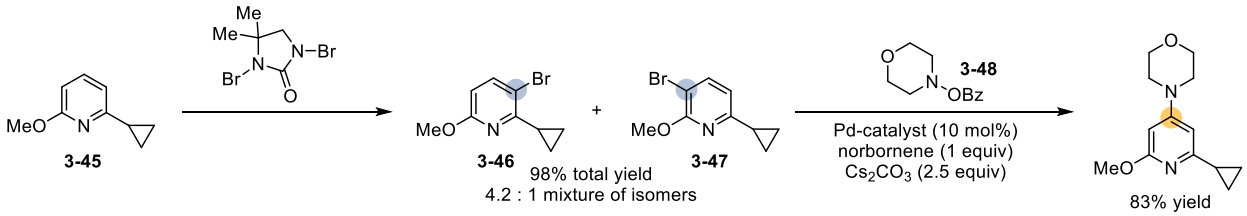

Figure 3–14: Catellani reaction converges a mixture of 3- and 5-bromopyridine isomers to a 4-substituted pyridine.

3.7 Conclusion

This work demonstrates the application of aryl halide isomerization to achieve unconventional selectivity in aryl halide substitution reactions. The differing electronic properties of interconverting 3-bromopyridine and 4-bromopyridine isomers can be differentiated by a tandem substitution reaction, providing a driving force for the selective production of substituted arene products. In contrast, halogen dance methodology requires a thermodynamic gradient between interconverting aryl halide isomers to drive a selective rearrangement prior to treatment with electrophiles. Overall, this work provides a new retrosynthetic option for chemists, enabling the use of one aryl halide isomer as a surrogate to access other isomeric products. Work is ongoing to apply base-catalyzed aryl halide isomerization to enable other new synthetic transformations.

The work described in Chapter three was published in *Chemical Science* in 2020.[35] Throughout my work on this project, I began examining the application of related *intermolecular* base-catalyzed halogen transfer processes to achieve heteroaromatic C–H functionalization reactions. The next chapter will discuss our discovery and application of intermolecular base-catalyzed aromatic halogen transfer to enable the nucleophilic C–H etherification of *N*-heteroarenes.

REFERENCES

[1] Dalman, G. W.; Neumann, F. W. The mechanism of the formation and hydrolysis of phenyl ether in the basic hydrolysis of chlorobenzene. *J. Am. Chem. Soc*. **1968**, *90*, 1601–1605.

[2] Zoratti, M.; Bunnett, J. F. Mechanism of the nonaryne hydroxydehalogenation of unactivated aryl halides. *J. Org. Chem.* **1980**, *45*, 1769–1776.

[3] Luo, C.; Bandar, J. S. Superbase-Catalyzed anti-Markovnikov Alcohol Addition Reactions to Aryl Alkenes. *J. Am. Chem. Soc.* **2018**, *140*, 3547-3550.

[4] Puleo, T. R.; Strong, A. J.; Bandar, J. S. Catalytic α-Selective Deuteration of Styrene Derivatives. *J. Am. Chem. Soc.* **2019**, *141*, 1467-1472.

[5] Schwesinger, R.; Schlemper, H. Peralkylated Polyaminophosphazenes–Extremely Strong, Neutral Nitrogen Bases. *Angew. Chem., Int. Ed.* **1987**, *26*, 1167-1169.

[6] Puleo, T. R.; Sujansky, S. J.; Wright, S. E.; Bandar, J. S. Organic Superbases in Recent Synthetic Methodology Research. *Chem. Eur. J.* **2021**, *27*, 4216-4229.

[7] Shen, K.; Fu, Y.; Li, J.-N.; Liu, L.; Guo, Q.-X. What are the p*K*a values of C−H bonds in aromatic heterocyclic compounds in DMSO? *Tetrahedron* **2007**, *63*, 1568−1576.

[8] Puleo, T. R.; Bandar, J. S. Base-catalyzed aryl halide isomerization enables the 4-selective substitution of 3-bromopyridines. *Chem. Sci.* **2020**, *11*, 10517-10522.

[9] Nathel, N. F. F.; Morrill, L. A.; Mayr, H.; Garg, N. K. Quantification of the Electrophilicity of Benzyne and Related Intermediates. *J. Am. Chem. Soc.* **2016**, *138*, 10402-10405.

[10] Goetz, A. E.; Garg, N. K. Regioselective reactions of 3,4-pyridynes enabled by the aryne distortion model. *Nat. Chem*. **2013**, *5*, 54–60.

[11] *Heterocyclic Chemistry*, Joule, J. A.; Mills, K. Wiley, West Sussex, 5th ed., 2011.

[12] Cañibano, V.; Rodríguez, J. F.; Santos, M.; Sanz-Tejedor, M. A.; Carreño, M. C.; González, G.; García-Ruano, J. L. Mild Regioselective Halogenation of Activated Pyridines with *N*-Bromosuccinimide. *Synthesis*, **2001**, *14*, 2175–2179.

[13] Feast, W. J.; Tsibouklis, J. The Self-Condensation of 4-Bromopyridine. *Polym. Int*. **1994**, *35*, 67–74.

[14] Fisher, E. L.; am Ende, C. W.; Humphrey, J. M. 2,2,2-Trifluoroethoxy Aromatic Heterocycles: Hydrolytically Stable Alternatives to Heteroaryl Chlorides. *J. Org. Chem.* **2019**, *84*, 4904-4909.

[15] Yuan, Y.; Thomé, I.; Kim, S. H.; Chen, D.; Beyer, A.; Bonnamour, J.; Zuidema, E.; Chang, S.; Bolm, C. Dimethyl Sulfoxide/Potassium Hydroxide: A Superbase for the Transition Metal-Free Preparation of Cross-Coupling Products. *Adv. Synth. Catal.* **2010**, *352*, 2892–2898.

[16] Bunnett, J. F. Base-catalyzed halogen dance, and other reactions of aryl halides. *Acc. Chem. Res.* **1972**, *5*, 139–147.

[17] Connon, S. J.; Hegarty, A. F. Substituted 3,4-pyridynes: clean cycloadditions. *J. Chem. Soc., Perkin Trans.* **2000**, *1*, 1245-1249.

[18] Xia, S. Gan, L.; Wang, K.; Li, Z.; Ma, D. Copper-Catalyzed Hydroxylation of (Hetero)aryl Halides under Mild Conditions. *J. Am. Chem. Soc.* **2016**, *138*, 13493-13496.

[19] Fier, P. S.; Maloney, K. M. Direct Conversion of Haloarenes to Phenols under Mild, Transition-Metal-Free Conditions. *Org. Lett.* **2016**, *18*, 2244-2247.

[20] Hilton, M. C.; Dolewski, R. D.; McNally, A. Selective Functionalization of Pyridines via Heterocyclic Phosphonium Salts. *J. Am. Chem. Soc.* **2016**, *138*, 13806-13809.

[21] Dolewski, R. D.; Hilton, M. C.; McNally, A. 4-Selective Pyridine Functionalization Reactions via Heterocyclic Phosphonium Salts. *Synlett.* **2018**, *29*, 8-14.

[22] Anderson, R. G.; Jett, B. M.; McNally, A. Selective formation of heteroaryl thioethers via a phosphonium ion coupling reaction. *Tetrahedron* **2018**, *74*, 3129-3136.

[23] Koniarczyk, J. L.; Hesk, D.; Overgard, A.; Davies, I. W.; McNally, A. A General Strategy for Site-Selective Incorporation of Deuterium and Tritium into Pyridines, Diazines, and Pharmaceuticals. *J. Am. Chem. Soc.* **2018**, *140*, 1990-1993.

[24] Patel, C.; Mohnike, M.; Hilton, M. C.; McNally, A. A Strategy to Aminate Pyridines, Diazines, and Pharmaceuticals via Heterocyclic Phosphonium Salts. *Org. Lett.* **2018**, *20*, 2607-2610.

[25] Anderson, R. G.; Jett, B. M.; McNally, A. A Unified Approach to Couple Aromatic Heteronucleophiles to Azines and Pharmaceuticals. *Angew. Chem. Int. Ed.* **2018**, *57*, 12514-12518.

[26] Zhang, X.; McNally, A. Cobalt-Catalyzed Alkylation of Drug-Like Molecules and Pharmaceuticals Using Heterocyclic Phosphonium Salts. *ACS Catal.* **2019**, *9*, 4862-4866.

[27] Levy, J. N.; Alegre-Requena, J. V.; Liu, R.; Paton, R. S.; McNally, A. Selective Halogenation of Pyridines Using Designed Phosphine Reagents. *J. Am. Chem. Soc.* **2020**, *142*, 11295-11305.

[28] Vinter-Pasquier, K; Jamart-Grégoire, B.; Caubére, P. Complex Base-Induced Generation of 3,4-Didehydropyridine Derivatives : New Access to Amino-Pyridines or Pyridones. *Heterocycles*, **1997**, *45*, 2113–2129.

[29] Dong, Z.; Lu, G.; Wang, J.; Liu, P.; Dong, G. Modular *ipso*/*ortho* Difunctionalization of Aryl Bromides via Palladium/Norbornene Cooperative Catalysis. *J. Am. Chem. Soc.* **2018**, *140*, 8551-8562.

CHAPTER FOUR

NUCLEOPHILIC C–H ETHERIFICATION OF *N*-HETEROARENES ENABLED BY BASE-CATALYZED HALOGEN TRANSFER

4.1 Chapter Overview

In the aryl halide isomerization program described in Chapter three, a formal C–H substitution process is achieved through the *intramolecular* migration of a bromine atom to an unsubstituted carbon.[1] This conceptualization inspired us to design a new form of catalytic *intermolecular* halogen transfer that enables direct nucleophilic heteroarene C–H substitution reactions. This chapter will discuss the design of this intermolecular halogen transfer mechanism and the application of this process to the regioselective nucleophilic C–H etherification of 1,3-azoles, (di)azines, and polyazines (Figure 4–1). The work described in this chapter serves as the foundation for a long-term research program that has developed in our research group. Two new reactions within this research program will be discussed in Chapter five.

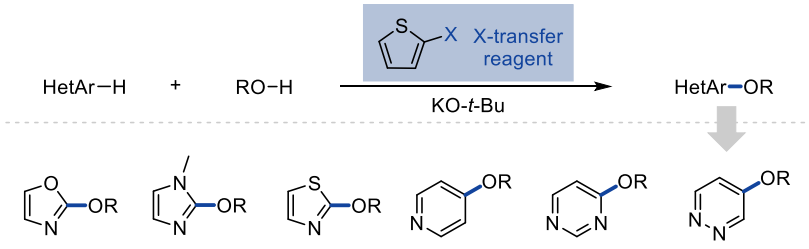

Figure 4–1: *N*-heteroarene C–H etherification reaction that will be covered in Chapter four.

4.2 Value of *N*-Heteroaryl Ethers

Electron-deficient *N*-heteroarenes are valuable compounds in the development of new pharmaceuticals, agrochemicals, and ligands.[2-7] In pharmaceuticals, 5- and 6-membered *N*-heteroarenes can impart several beneficial properties, including improved binding affinity to the desired target, metabolic stability toward CYP-450 metabolism, and aqueous solubility.[3-4] A 2014 analysis found pyridine and thiazole were the most common 5- and 6-membered *N*-heteroaromatic

compounds in pharmaceuticals, respectively, with related diazine and 1,3-azole compounds following closely behind.[2]

Electron-deficient *N*-heteroaryl ethers are an important class of these compounds. Omeprazole, pantoprazole, lansoprazole, dexlansoprazole, esomeprazole, and rabeprazole comprise a series of proton-pump inhibitors used in the treatment of peptic ulcer disease and gastroesophageal reflux disease.[8] Additionally, picoxystrobin and azoxystrobin are two widely used fungicides that contain an *N*-heteroaryl ether structure (Figure 4–2).[5-6]

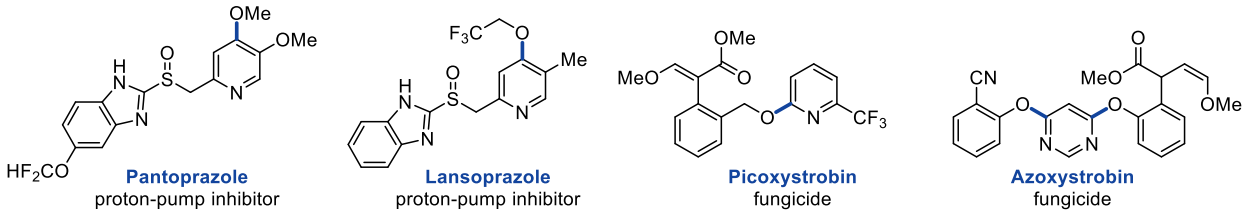

Figure 4–2: Examples of *N*-heteroaryl ethers in pharmaceuticals and agrochemicals.

4.3 Methods to Achieve C–H Etherification of *N*-Heteroarenes

N-Heteroaryl ethers are generally synthesized *via* a substitution reaction of a pre-functionalized arene with an alcohol nucleophile. The C–H etherification of *N*-heteroarenes represents a streamlined approach to access *N*-heteroaryl ethers, bypassing additional synthetic steps to preinstall a suitable leaving group. A key challenge for direct aromatic C−H etherification is the incompatibility of combining a C−H oxidative process with nucleophilic alcohol coupling partners. Thus, existing routes to *N*-heteroaryl ethers almost always require independent synthesis of a functionalized *N*-heteroarene followed by substitution with an alcohol nucleophile. Crucial to these approaches is controlling the selective installation of the functional handle that will undergo substitution.

Directed metalation/halogenation is a highly common approach to access *N*-heteroaryl halides that are common precursors to *N*-heteroaryl ethers (Figure 4–3).[9-12] In this approach,

stoichiometric strong alkyl lithium or lithium amide bases completely deprotonates the arene and treatment with an electrophilic halogen source yields the *N*-heteroaryl halide. Cryogenic temperatures are typically needed to avoid decomposition.[11] Additionally, regioselective metalation generally only occurs on heteroarenes with strong-directing groups that guide *ortho*-metalation.

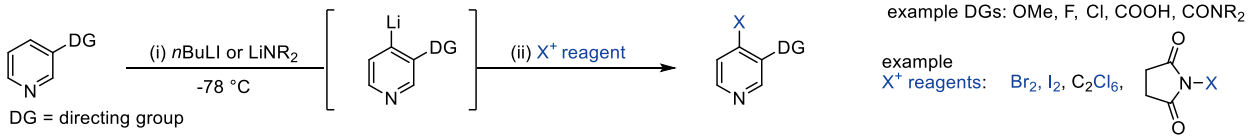

Figure 4–3: General scheme for stoichiometric metalation/halogenation reactions.

In the absence of a strong directing group, achieving regioselective metalation can be challenging. Figure 4–4 demonstrates one example of this, where lithiation of 2-(trifluoromethyl)pyridine with LiTMP followed by treatment with CO_2 produces a mixture of 3- and 4-carboxylic acid products.[13] Notably, metalation selectivity for the 3-position can be improved by increasing the reaction time to six hours.

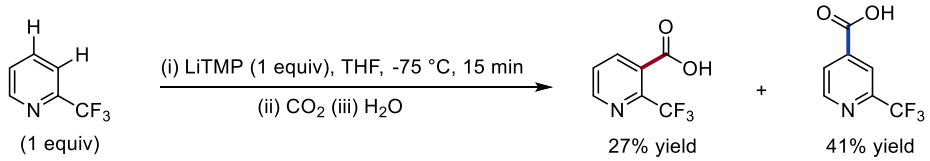

Figure 4–4: Unselective metalation and electrophilic substitution of 2-(trifluoromethyl)pyridine.

Metalation/halogenation sequences that occur in a non-sequential fashion at non-cryogenic temperatures have been reported. Treatment of acidic *N*-heteroarenes with LiO-*t*-Bu, K_3PO_4, or NaO-*t*-Bu and an electrophilic halogenating reagent yields *N*-heteroaryl halides (Figure 4–5).[14-15] Electrophilic halogenating reagents used in this approach include CBr_4, CCl_4, I_2, ICl, 1,2-dibromotetrafluoroethane, and pentafluoroiodobenzene. The scope of these reactions is limited to simple *N*-heteroarenes.

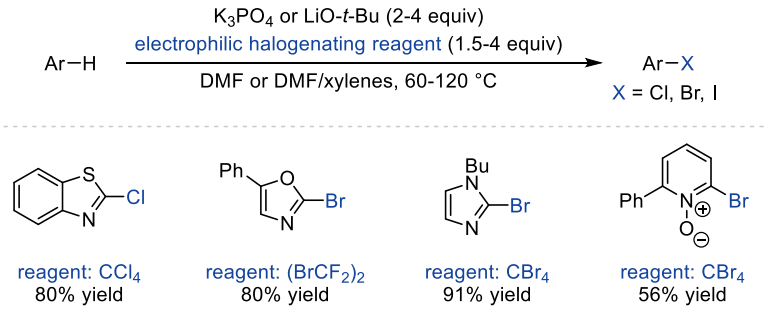

Figure 4–5: Metalation/halogenation of *N*-heteroarenes at non-cryogenic temperatures.

Oxidation of electron-deficient *N*-heteroarenes to the corresponding *N*-oxide is one approach to selectively install halo-, nitro-, cyano-, or sulfonyl functional groups onto heteroarenes that undergo substitution reactions with alcohols to access *N*-heteroaryl ethers.[16-19] Oxidation of *N*-heteroarenes to the *N*-oxide increases the π-nucleophilicity of the aromatic ring, enabling electrophilic aromatic halogenation or nitration.[18] Additionally, *N*-oxides can undergo a series of deoxyfunctionalization reactions *en route* to *N*-heteroaryl ethers.[17-18] Treatment of pyridine *N*-oxides with an electrophile activates the *N*-oxide towards nucleophilic installation of halogens, sulfones, and cyano functional groups at the 2-position. Londregan additionally developed a method to directly couple alcohols to the ring position adjacent to *N*-oxides using the phosphonium salt reagent PyBroP (Figure 4–6).[20] This approach is compatible with the *N*-oxides of pyridines, quinolines, isoquinolines, pyridazines, pyrimidines, pyrazines, and several other related (di)azine compounds.

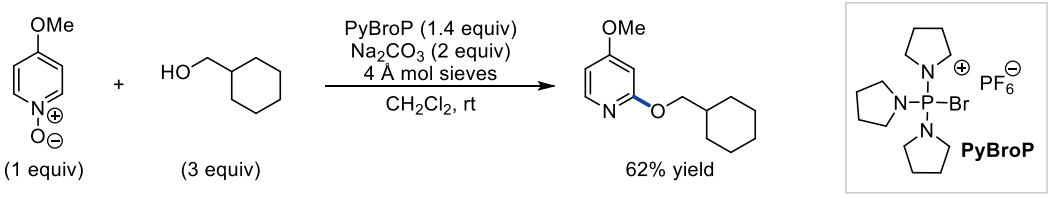

Figure 4–6: Londregan's C–H etherification of azine *N*-oxides.

McNally's heterocyclic phosphonium salts represent a powerful method to access *N*-heteroaryl ethers (see Chapter 3.6 for a description of these methods). The heterocyclic phosphonium salts of pyridines, pyrimidines, and pyridazines can be coupled with alcohol nucleophiles to access *N*-heteroaryl ethers.[21-22] A later publication described the application of this approach to couple alcohols to the 2-position of benzothiazoles.[23]

Hartwig and Fier developed a 2-selective Chichibabin-type pyridine C–H fluorination reaction using AgF_2. The 2-fluoropyridine products can be isolated and substituted with alcohol nucleophiles.[24] Alternatively, a sequential fluorination/substitution approach could be employed to directly access 2-etherified pyridines (Figure 4–7).[25]

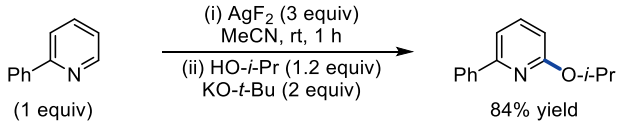

Figure 4–7: Hartwig and Fier's approach to 2-selective pyridine C–H etherification.

The direct substitution of *N*-heteroarene C–H bonds with alcohols is a challenging reaction that has seen limited development. Kanai disclosed a Cu-catalyzed C–H etherification reaction of 1,3-azoles. These reactions were largely intramolecular, and only a few low yielding examples of intermolecular alcohol coupling to benzothiazole and *N*-methylbenzimidazole were reported (Figure 4–8).[26]

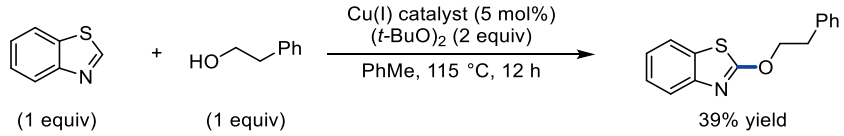

Figure 4–8: Kanai's oxidative C–H etherification of benzofused 1,3-azoles.

Drawing from our experience in 4-selective 3-bromopyridine C–H etherification (see Chapters 3.4 and 3.5), we hypothesized a related *intermolecular* halogen transfer process could be utilized to enable a new and general approach to *N*-heteroarene C–H etherification reactions.

4.4 Reaction Discovery and Optimization

In 1951, Nord disclosed the unexpected observation that 2-bromothiophene disproportionates into tetrabromothiophene under strongly basic conditions (Figure 4–9a).[27-28] Bunnett later elucidated the mechanism of this process occurs through several iterative intermolecular base-catalyzed halogen transfer processes (see Chapter 2.3 for a detailed description of these findings).[29-31] We realized the intermolecular nature of aromatic halogen transfer could be applied to enable a new approach *N*-heteroaromatic C–H etherification. Figure 4–9b displays the mechanism of this approach. Base-catalyzed halogen transfer (X-transfer) from a sacrificial aryl halide (Ar–X) to an *N*-heteroarene (HetAr–H) produces *N*-heteroaryl halide (HetAr–X) intermediates that undergo nucleophilic aromatic substitution with alkoxide nucleophiles to produce *N*-heteroaryl ether products.[32]

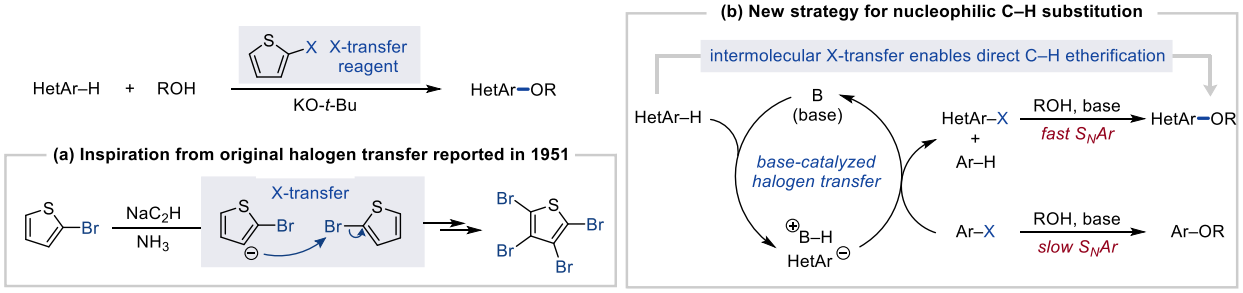

Figure 4–9: Inspiration and mechanism of *N*-heteroarene C–H etherification enabled by base-catalyzed halogen transfer. X-transfer = halogen transfer.

Merging halogen transfer with a substitution reaction is a crucial design feature in this process. First, halogen transfer from the sacrificial aryl halide (Ar–X) to the *N*-heteroarene is likely a reversible process.[30] Selective interception and substitution of the intermediate *N*-heteroaryl

halide with an alcohol nucleophile provides a driving force for the reaction. Second, the generated *N*-heteroaryl halide intermediates are acidic enough to undergo a second halogen transfer reaction, producing polyhalogenated *N*-heteroarene side products.[33] Substitution of the intermediate *N*-heteroaryl halides with alcohol nucleophiles produces *N*-heteroaryl ether products that are significantly less acidic and less prone to undergoing base-catalyzed halogen transfer. Finally, *N*-heteroaryl halides are susceptible to base-promoted protodehalogenation or aryne side reactions, and immediate substitution of the *N*-heteroaryl halide should hinder these deleterious processes.[34-35]

An additional challenge for this method was identification of a sacrificial aryl halide (Ar–X) that efficiently transfers a halogen to transient *N*-heteroaryl anions but does not decompose or undergo nucleophilic substitution under basic conditions. Inspired by Nord's 1951 report, we reasoned 2-halothiophenes could fulfill this role. First, 2-halothiophenes are well-known to participate in halogen dance reactions and thus should be capable of efficient halogen transfer to *N*-heteroaryl anions.[36-37] Second, 2-halothiophenes are relatively electron-rich aromatic compounds that are generally unreactive to nucleophilic aromatic substitution. Finally, 2-halothiophenes are broadly available, commercially and synthetically, presenting an opportunity for structural optimization of the reagent.

With these considerations, I first targeted application of this base-catalyzed halogen transfer approach to the 2-selective C–H etherification of 1,3-azoles. 1,3-Azoles are a class of 5-membered aromatic *N*-heterocycles comprised of oxazoles, imidazoles, and thiazoles (Figure 4–10). A characteristic of each of these heterocycles is that the C–H bond at the 2-position of the ring has the lowest pK_a.[33] Thus, we reasoned base-catalyzed halogen transfer should occur selectively at the 2-position of 1,3-azoles and produce 2-etherified products.

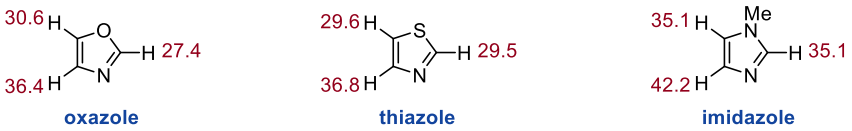

Figure 4–10: Structure and DMSO pK_a values of 1,3-azoles.

Using the C–H etherification of thiazole (**4–1**) with 2-ethyl-1-hexanol (**4–2**) and KO-*t*-Bu base as a model reaction, I first examined several commercially available 2-bromothiophenes as halogen transfer reagents (Figure 4–11a). Use of 2-bromothiophene (**4–4**) as a halogen transfer (X-transfer) reagent provides a 16% yield of the 2-etherified thiazole **4–3** and thiophene as reaction byproduct. Commercially available 2,3-dibromothiophene (**4–5**) produced a slightly higher yield (29% yield) while tetrabromothiophene (**4–6**) produced no yield of **4–3**. Meanwhile, inexpensive 2,5-dibromothiophene (**4–7**, < $40 per mole) was the most effect halogen transfer reagent, producing **4–3** in 74% yield. Common electrophilic halogenating reagents such as CBr_4, Br_2, and NBS produce no product demonstrating the unique efficacy of 2-bromothiophene reagents under these conditions.[32]

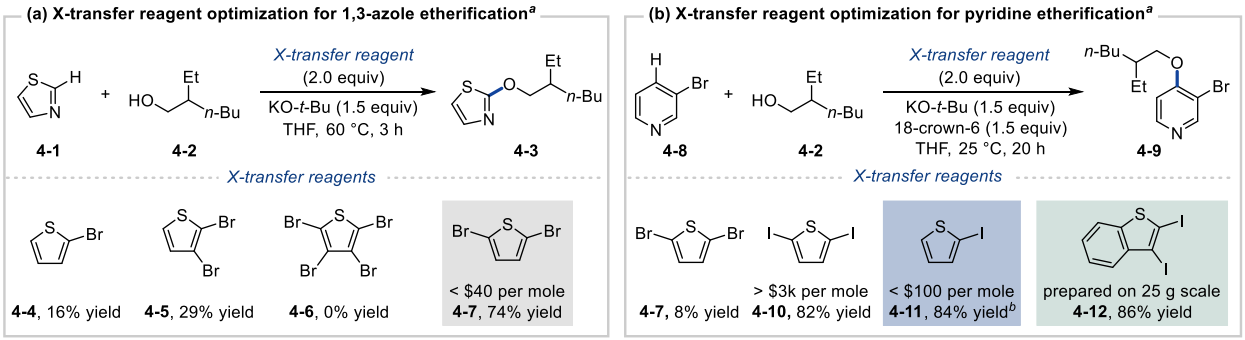

[a]For all reactions, 1 equiv of heteroarene and 1.5 equiv of alcohol used. Yields determined by ^{1}H NMR spectroscopy of the crude reaction mixture. [b]65% yield without 18-crown-6 additive.

Figure 4–11: Optimization of 2-halothiophene structure for *N*-heteroarene C–H etherification.

Next, we reasoned that this C–H etherification strategy could operate on other classes of acidic *N*-heteroarenes such as (di)azine derivatives including pyridines, pyrimidines, and pyridazines (Figure 4–12).[33] We chose 3-bromopyridine C–H etherification with 2-ethyl-1-

hexanol (**4–2**) as a model reaction (Figure 4–11b). Similar to 1,3-azoles, we reasoned etherification would occur at the 4-position of 3-bromopyridine because that is the most thermodynamically acidic C–H bond.

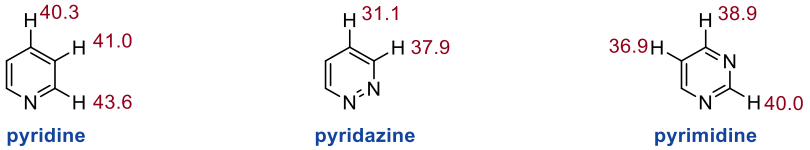

Figure 4–12: Structure and DMSO pK_a values of pyridines, pyrimidines, and pyridazines.

Use of 2,5-dibromothiophene (**4–7**) in this reaction provides a low 12% yield of 4-etherified product **4–9** under the previously optimized reaction conditions (12% at 60 °C and 8% at 25 °C). Since pyridines are less acidic than 1,3-azoles, we suspected lower concentrations of pyridyl anions would require faster halogen transfer for efficient reactivity. In this regard, we hypothesized 2-iodothiophenes would be more active halogen transfer reagents due to the decreased electronegativity and increased polarizability of iodine. Thus, I discovered use of 2,5-diiodothiophene (**4–10**, > $3,000/mole) as a halogen transfer reagent improved the yield of ether **4–9** to 82% at 25 °C. While 2,5-diiodothiophene does improve the yield, significantly less expensive 2-iodothiophene (**4–11**, < $100/mole) was equally effective, producing an 84% yield of ether **4–9**.[32]

When using 2-iodothiophene as a halogen transfer reagent, we observed formation of 3-iodothiophene as major byproduct. 3-Iodothiophene likely forms *via* the base-catalyzed halogen dance mechanism shown in Figure 4–13 (see Chapter 2.3 for a more detailed discussion of base-catalyzed halogen dance isomerization). The instability of 2-iodothiophene and the formation of 2,3-diiodothiophene under the reaction conditions led us to develop 2,3-diiodobenzothiophene (**4–12**, prepared on a 25 g scale) as an alternative halogen transfer reagent for the reaction. Use of 2,3-diiodobenzothiophene (**4–12**) in the model reaction produced an 86% yield of 4-substituted

pyridine **4–9**. Although 2,3-diiodobenzothiophene (**4–12**) produced a yield comparable to 2-iodothiophene (**4–11**), for other substrates we found use of 2,3-diiodobenzothiophene (**4–12**) resulted in significantly improved yields.[32] Chapter 4.6 will provide additional details, insights, and experiments that inspired the development of 2,3-diiodobenzothiophene as a halogen transfer reagent.

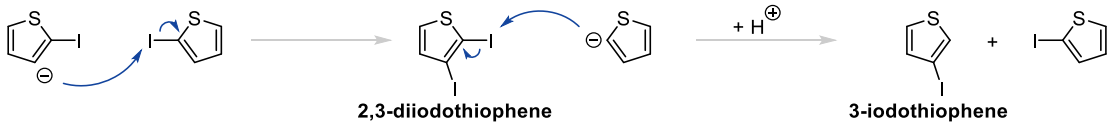

Figure 4–13: Mechanism of base-catalyzed isomerization of 2-iodothiophene into 3-iodothiophene.

Notably, use of 2-iodothiophenes for 1,3-azole C–H etherification was ineffective, producing negligible yields of 2-substituted products. The reason for this is likely due to the poor reactivity of 2-iodo-1,3-azoles towards alkoxide S_NAr. Attempted S_NAr of 2-iodothiazole produced no yield of ether **4–3** and the only observable product was thiazole, resulting from protodehalogenation (Figure 4–14).

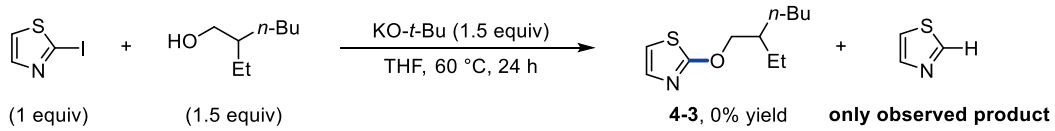

Figure 4–14: Attempted S_NAr reaction of 2-iodothiazole.

4.5 Substrate Scope

Figure 4–15 provides the scope of 1,3-azoles and di(azines) that undergo regioselective C–H etherification using 2,5-dibromothiophene and 2-iodothiophene respectively. High regio- and chemoselectivity (> 10:1) was generally observed. Primary, secondary, and benzylic alcohols are all effective coupling partners, including aminoalcohols, alkenols, and complex alcohols such as the pharmaceutical perphenazine (**4–36**).[32]

Figure 4–15a shows the scope of 1,3-azoles, including thiazoles, oxazoles, imidazoles, and benzofused variants (**4–13** to **4–21**) that undergo 2-selective etherification with 2,5-dibromothiophene (**4–7**) as the halogen transfer reagent. I developed this scope while mentoring another graduate student in the group, Danielle Klaus. 4,5-Dimethylthiazole (**4–13**) undergoes 2-selective etherification while avoiding benzylic oxidation. Etherification of 5-Chloro-1-methylimidazole produces the 2-substituted ether **4–18** with no competing chlorine substitution. 5-(2-bromophenyl)oxazole yields ether **4–15** without competing halogen transfer from the bromophenyl ring, demonstrating the chemoselectivity of the halogen transfer process. Interestingly, a biaryl substrate containing thiazole and pyridine rings (**4–17**) selectively substitutes the thiazole ring with no observed C–H etherification of the pyridine ring.[32]

Figure 4–15b shows the scope of di(azines) that undergo regioselective etherification with 2-iodothiophene (**4–11**) as the halogen transfer reagent. 3-Halopyridines (**4–9**, **4–22**, **4–23**, and **4–24**) undergo 4-selective etherification without competing 3-substitution. Notably, this method complements the 3-bromopyridine substitution reaction discussed in Chapter three, providing access to 4-substituted-3-halopyridine products. Interestingly, 5-bromo-2-iodopyridine (**3–23**) and 2-chloro-5-methoxypyridine (**4–25**) undergo 4-selective etherification in the presence of the reactive 2-halosubstitutents. Pyridines with other electron-withdrawing groups in the 3-position are amenable to this reaction including 3-(thiophenyl)pyridine (**4–26**). Pyridines without electron-withdrawing groups in the 3-position, including 2-phenyl-6-(trifluoromethyl)pyridine (**4–27**), 2,6-bis(trifluoromethyl)pyridine (**4–28**), and 2,6-bis(difluoromethyl)pyridine (**4–29**), yield 4-substituted products exclusively. The high 4-substitution selectivity for these products is intriguing because it is not clear which ring position on these compounds is the most acidic. One possible mechanism for these substrates is that halogen transfer first occurs at the 3- or 5-position of the

ring, followed by rearrangement *via* a halogen dance reaction to the more stable 4-iodopyridine isomer before undergoing substitution.[10, 32]

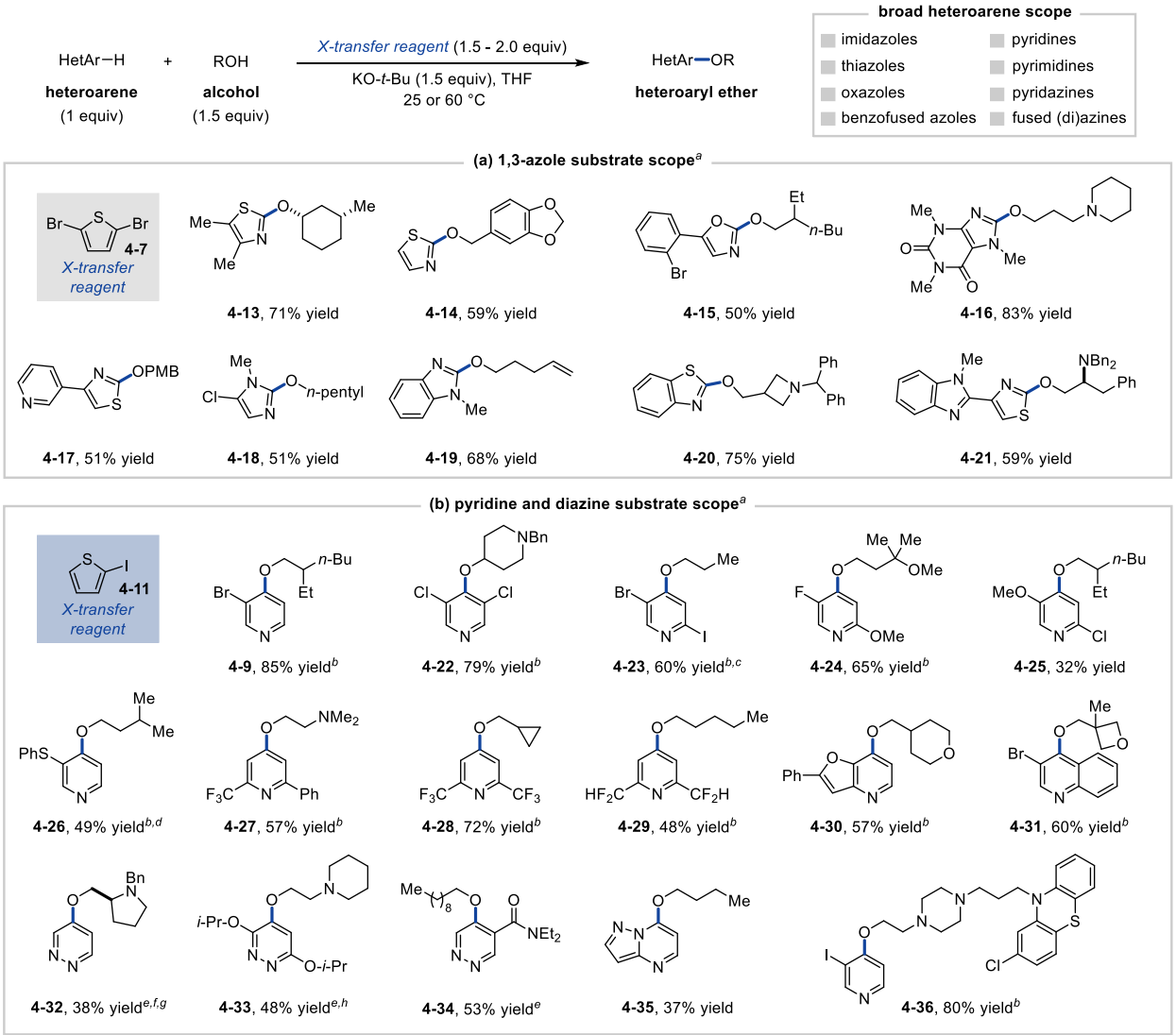

[a]Reactions conducted on 0.5 to 1 mmol scale of heteroarene; yields are of isolated products; reaction conducted at 60 °C for 3 h for (a) and at 25 °C for 20 h for (b). [b]18-crown-6 (1.5 equiv) additive used. [c]Side products (20% total) from 2-substitution of the starting material observed. [d]2 equiv of alcohol used. [e]DMF used as solvent. [f]Reaction conducted at 60 °C. [g]Reaction conducted with 2 equiv pyridazine and 1 equiv alcohol; product forms in 4:1 ratio to other aryl ethers. [h]Product forms in 6:1 ratio to other aryl ethers.

Figure 4–15: Substrate scope for *N*-heteroarene C–H etherification.

Structurally diverse azines and di(azines) are also compatible with this method. Pyridines with fused aromatic rings including furo[3,2-*b*]pyridine (**4–30**), 3-bromoquinoline (**4–31**), and pyrazolo[1,5-*a*]pyrimidine (**4–35**) undergo regioselective C–H etherification without competing

halogenation at other positions. Pyridazine (**4–32**) and derivatives with amide (**4–34**) and 3,6-dialkoxysubstiuents (**4–33**) undergo 4-selective etherification.[32]

Base-promoted heteroarene C–H etherification can be sequenced in a cascade process to other base-promoted reactions to access more complex products. In this regard, reaction of 5-bromo-2-(trifluoromethyl)pyridine (**4–37**) and L-prolinol (**4–38**) produced morpholine fused pyridine **4–39** in 68% yield *via* a base-promoted cascade C–H etherification and C–Br amination process (Figure 4–16).[32]

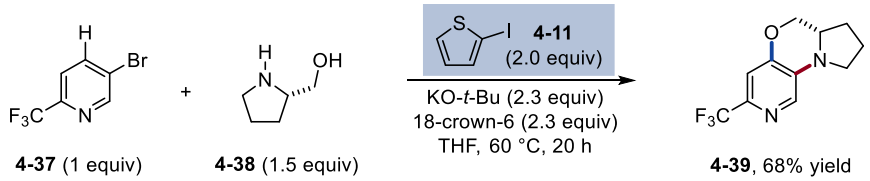

Figure 4–16: Cascade base-promoted C–H etherification and C–Br amination reaction.

While investigating the scope of this reaction, I found some substrates produced low to moderate yields of ether products (Figure 4–17). I examined various bases, solvents, and reaction temperatures, but alteration of these variables produced negligible increases in the yield. Thus, I targeted strategic modification of the halogen transfer reagent to improve the yield for these substrates.

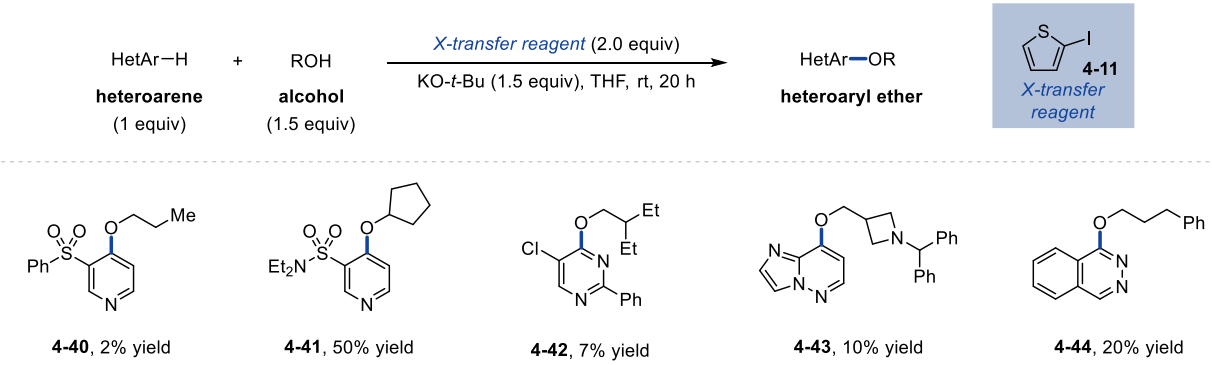

Figure 4–17: Challenging substrates that undergo C–H etherification in low to moderate yields.

4.6 Development of 2,3-Diiodobenzothiophene as an Alternative Halogen Transfer Reagent

While optimizing the di(azine) C–H etherification protocol, I made several observations that provided insights for how the halogen transfer reagent structure could be strategically modified to improve C–H etherification yields. First, 3-iodothiophene is always observed as a major byproduct in every di(azine) etherification reaction (see Figure 4–13 for the reaction mechanism). This byproduct would arise from a halogen dance rearrangement, and disproportionated thiophene products (e.g. 2,3-diiodothiophene and 2,5-diiodothiophene) can be observed when monitoring the reaction over time.[36-37] Subjection of 2-iodothiophene (**4–11**) to the standard reaction conditions in the absence of a (di)azine substrate produced a complex mixture of iodothiophene products after only 10 minutes (Figure 4–18). This observation is surprising given that most of the azine C–H etherification reactions require 10-20 hours to reach completion. Generation of this complex mixture followed by addition of 3-bromopyridine (Figure 4–19) produced a similar yield of the 4-ether **4–9** (80% yield) compared to if the reaction was run normally (84% yield). These observations suggest that 2-iodothiophene is only one of several iodothiophene derivatives that could function as the halogen transfer reagent in di(azine) C–H etherification reactions.

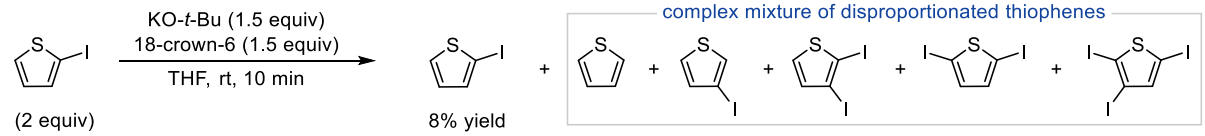

Figure 4–18: Complex mixture of iodothiophene products that form upon subjection of 2-iodothiophene to the reaction conditions in Figure 4–15 in the absence of an *N*-heteroarene substrate.

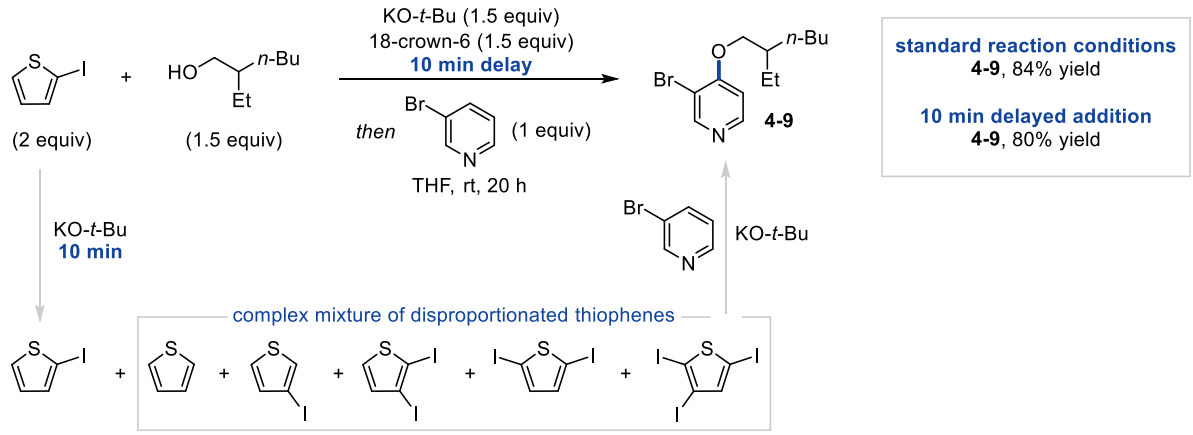

Figure 4–19: Use of the complex mixture of disproportionated thiophenes as the X-transfer reagent produces a similar yield to the standard reaction conditions.

With these insights, I hypothesized 2,3-diiodobenzothiophene (**4–12**) could function as a more effective halogen transfer reagent. The large yield of 3-iodothiophene in the reaction suggests 2,3-diiodothiophene is a dominant halogen transfer reagent. Additionally, fusion of a benzene ring to the acidic 4- and 5-positions of the thiophene ring would prevent disproportionation and increase the reagent stability. Subjection of 2,3-diiodobenzothiophene (**4–12**) to a solution KO-*t*-Bu in THF for 24 h at rt produced low, 8% yield of protodehalogenated product **4–45** with 92% 2,3-diiodobenzothiophene (**4–12**) remaining, demonstrating its improved stability to the reaction conditions (Figure 4–20). 2,3-Diiodobenzothiophene is easily synthesized in three steps on a 25 g scale (Figure 4–21).[38]

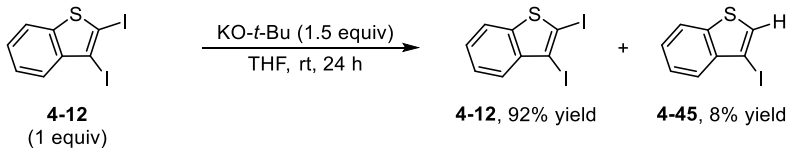

Figure 4–20: Stability of 2,3-diiodobenzothiophene (**4–12**) to the standard reaction conditions in Figure 4–15.

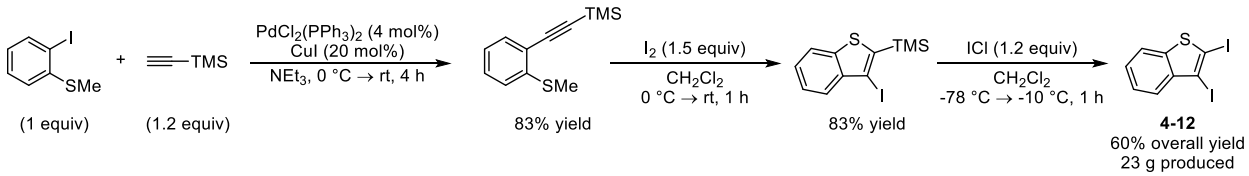

Figure 4–21: Synthesis of 2,3-diiodobenzothiophene (**4–12**).

The enhanced stability of 2,3-diiodobenzothiophene was beneficial in improving the reaction yield for some (di)azine substrate. Figure 4–22 demonstrates five examples where use of 2,3-diiodobenzothiophene (**4–12**) over 2-iodothiophene (**4–11**) resulted in yield improvements in the range of 10% – 70%, including 3-(phenylsulfonyl)pyridine (**4–40**), a sulfonamide-substituted pyridine (**4–41**), 5-chloro-2-phenylpyridimidine (**4–42**), imidazo[1,2-*b*]pyridazine (**4–43**), and phthalazine (**4–44**). Overall, strategic modification of the halogen transfer reagent structure enabled significant yield improvements for these challenging substrates.

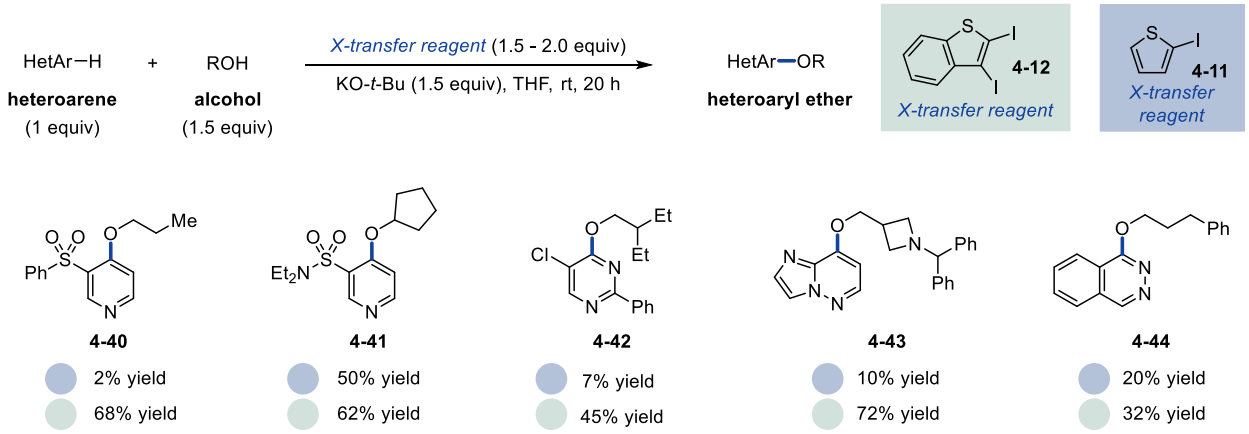

Figure 4–22: Use of 2,3-diiodobenzothiophene (**4–12**) as an X-transfer reagent improves yield for challenging substrates.

4.7 Site-Selective C–H Etherification of Polyazines

A beneficial feature of this method is that no strong directing groups are required to achieve regioselective C–H etherification in a single-step. This aspect is highlighted with 2,6-disubstituted pyridine substrates **4–27**, **4–28**, and **4–29** as well as unsubstituted pyridazine (**4–32**) in Figure 4–15b, where metalation/halogenation protocols would likely produce 3-halopyridine isomers or

mixtures of regioisomers (see Figure 4–4 for a related example).[13] We envisioned the uniquely high regioselectivity for this reaction could be valuable for the selective functionalization of polyazine compounds with multiple possible reactive sites. For example, I found bipyridine **4–46** undergoes 4-selective etherification on the more acidic pyridine ring to produce **4–47** in 62% yield (Figure 4–23a). Attempted metalation/halogenation of this substrate produced a mixture of 4- and 3-iodopyridine products (**4–48** and **4–49**, Figure 4–24). Meanwhile, *N*-oxidation approaches to pyridine functionalization, including McNally's phosphonium salt approach and *N*-oxide chemistry, would likely functionalize the other, more nucleophilic, pyridine ring. Thus, the halogen transfer approach we developed complements the substrate scope of other approaches to access *N*-heteroaryl ethers.[9-19]

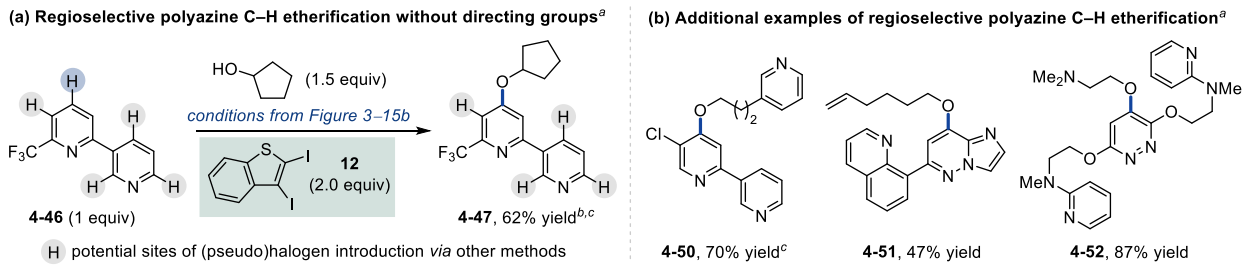

[a]Isolated yields using conditions from Figure 3-15b. [b]Shown product forms in 7:1 ratio to other ether side products. [c]18-Crown-6 additive used.

Figure 4–23: Site-selective C–H etherification of polyazines.

Figure 4–23b shows additional polyazines that undergo regioselective C–H etherification using the conditions from Figure 4–15b. Bipyridine **4–50** undergoes 4-selective etherification on the 3-chloropyridine fragment with an alcohol containing a pendent pyridine. An imdazo[1,2-*b*]pyridazine with an 8-quinolinyl substituent (**4–51**) undergoes selective etherification on the pyridazine ring. Finally, polyazine **4–52** undergoes regioselective etherification on the more acidic pyridazine ring in the presence of two pendent pyridines. Overall, the heteroaryl ether products accessible *via* this approach are rapidly accessed from readily available heteroarenes where a corresponding heteroaryl (pseudo)halide is not readily available, commercially or synthetically.

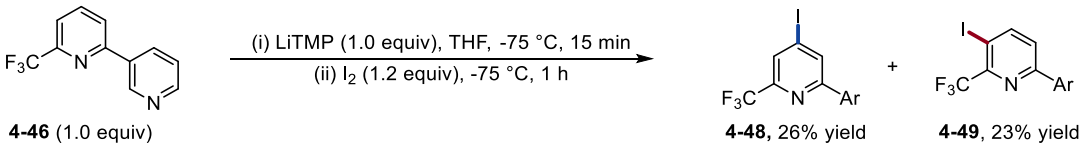

Figure 4–24: Attempted metalation/halogenation of polyazine substrate **4–46**.

4.8 Direct Observation of Halogen Transfer

Base-catalyzed halogen transfer from 2-halothiophenes to *N*-heteroarenes is the key mechanistic process that enables this C–H etherification method. While monitoring these reactions, products arising from halogen transfer from the 2-halothiophene reagents are usually not observed. One exception to this was discovered by another student in our group, Danielle Klaus. When C–H etherification of 3-fluoropyridine (**4–53**) was attempted, 4-iodo-3-methoxypyridine (**4–54**) was obtained as the major product in 41% yield (Figure 4–25). Subjection of 3-fluoro-4-iodopyridine (**4–55**) to KO-*t*-Bu and MeOH also produced 4-iodo-3-methoxypyridine (**4–54**) as the major product in 54% yield. Finally, 3-methoxypyridine (**4–56**) does not undergo iodination under the halogen transfer conditions. Because 2-iodothiophene is the only source of iodine in these reactions, these results demonstrate that halogen transfer and subsequent S_NAr is the operative mechanism for C–H etherification.

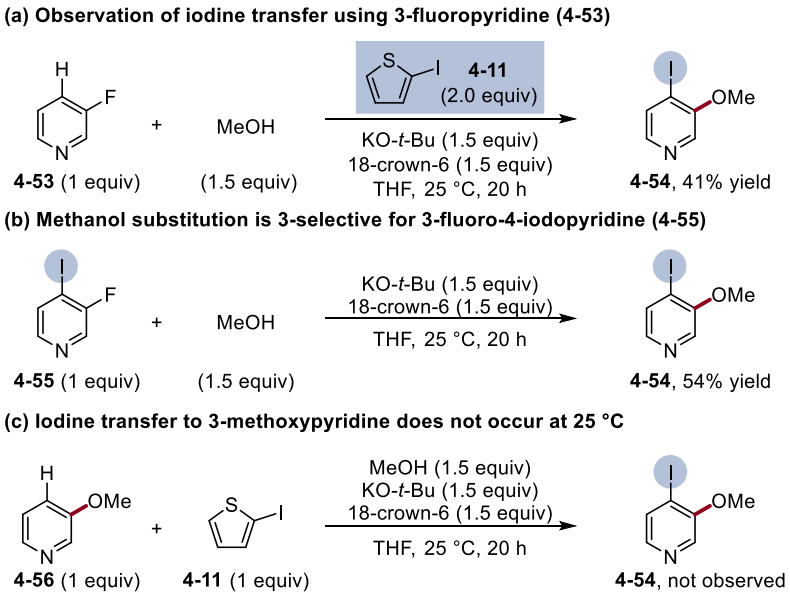

Figure 4–25: Observation of iodine transfer from 2-iodothiophene to 3-fluoropyridine.

4.9 Development of *N*-Heteroarene C–H Hydroxylation

Having successfully developed a general approach to *N*-heteroarene C–H etherification, we next targeted using this approach for *N*-heteroarene C–H hydroxylation. In general, *N*-heteroaryl ethers are not versatile synthetic intermediates and are infrequently used as synthetic handles for the installation of new functional groups. Meanwhile, hydroxylated *N*-heteroarenes are highly dynamic intermediates, capable of participating in cross-coupling reactions after *O*-triflation or undergoing deoxyhalogenation to produce versatile *N*-heteroaryl halides.[39-43] Additionally, hydroxylated *N*-heteroarenes are common structures in medicinally relevant compounds, functional materials, and agrochemicals (Figure 4–26).[7,44] Thus, we reasoned regioselective *N*-heteroarene C–H hydroxylation *via* halogen transfer would be an impactful approach to access a myriad of functionalized *N*-heteroarenes.

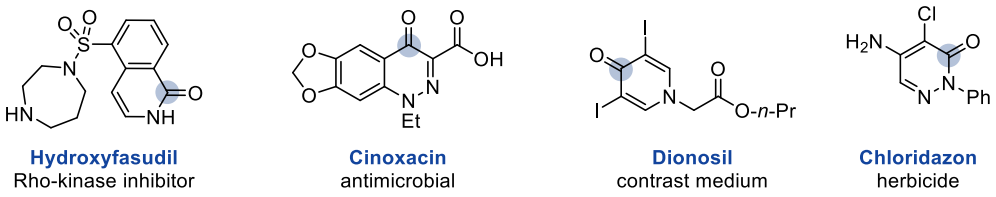

Figure 4–26: Value of hydroxylated *N*-heteroarenes in industrially relevant compounds.

Using C–H hydroxylation of 3-bromopyridine (**4–8**) as a model reaction, I worked with another Ph.D student in our group, Kendelyn Bone, to identify an effective water surrogate for this reaction (Figure 4–27). Replacement of the alcohol nucleophile with water or a metal hydroxide was ineffective producing no yield of 3-bromo-4-pyridione (**4–57**). β-Hydroxyamide (**4–58**), which we successfully used as an H_2O surrogate in the 4-selective hydroxylation of 3-bromopyridines (see Chapter 3.5), produced a low, but promising 8% yield of 3-bromo-4-pyridone (**4–57**) with a similar yield of *N*,*N*-dibenzylacrylamide.[1] With this preliminary result, we next examined other related alcohols including β-hydroxyester **4–59**, 2-cyanoethanol (**4–60**), 2-(trifluoromethyl)ethanol (**4–61**), and 2-phenylethanol (**4–62**). We found 2-phenylethanol was the most effective alcohol for this transformation producing 3-bromo-4-pyridone (**4–57**) in 71% yield with an 84% yield of styrene as a byproduct. Other electronically distinct 2-arylethanols (**4–63**, **4–64**, and **4–65**) did not improve the reaction yield.

Use of 2-phenylethanol (**4–62**) as a water surrogate under halogen transfer conditions enables C–H hydroxylation of a broad scope of (di)azines (**4–66** through **4–80**), polyazines (**4–72**), and 1,3-azoles (**4–81**, **4–82**, and **4–83**). This reaction exhibits a similar substrate scope to the analogous *N*-heteroarene C–H etherification reaction (see Chapters 4.5-4.7). Overall, this heteroarene C–H hydroxylation reaction is an effective approach to regioselectively install the versatile hydroxy functional group onto *N*-heteroarenes (Figure 4–28).

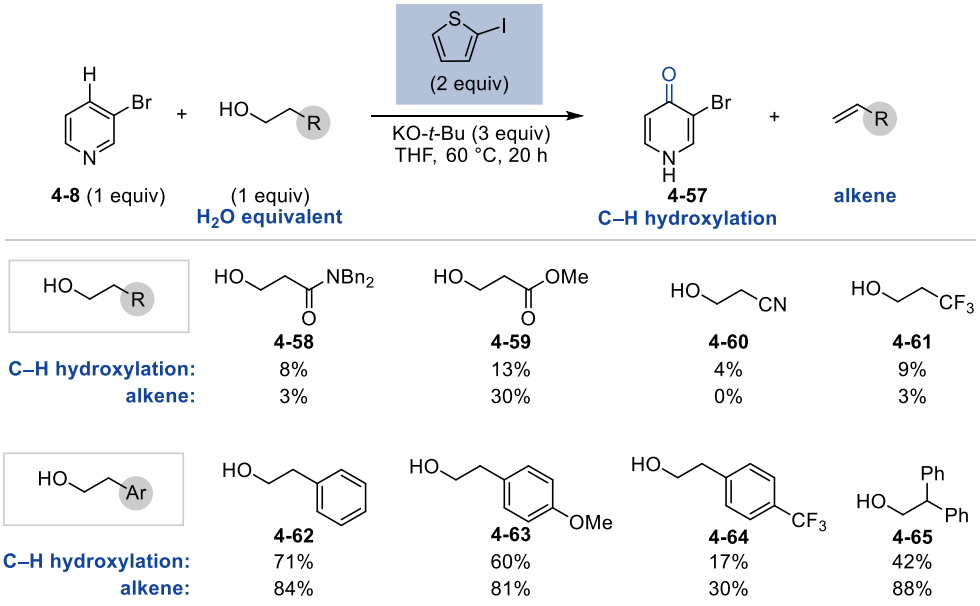

Figure 4–27: Optimization of H_2O surrogate structure for *N*-heteroarene C–H hydroxylation reactions.

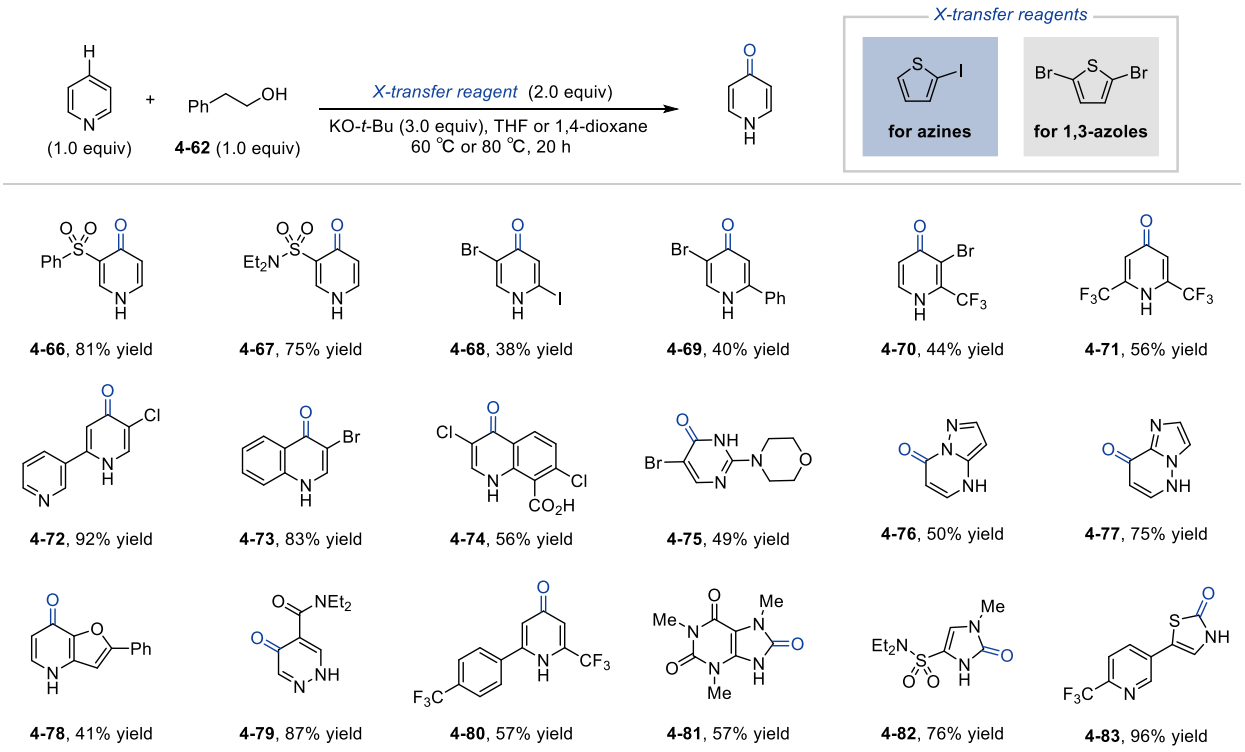

Figure 4–28: Substrate scope for *N*-heteroarene C–H hydroxylation enabled by base-catalyzed X-transfer.

4.10 Conclusion

The *N*-heteroarene C–H etherification work was published in the *Journal of the American Chemical Society* in 2020 and demonstrated 36 total examples of regioselective C–H etherification on 1,3-azoles, (di)azines, and polyazines.[32] The manuscript for *N*-heteroarene C–H hydroxylation is currently being prepared. From these efforts, we realized that base-catalyzed halogen transfer to other C–H bonds could enable a broader range of new C–H functionalization reactions. This strategy is now a prominent area within our research group that will be the subject of several future publications. Chapter five will briefly describe two of these new methods.

REFERENCES

[1] Puleo, T. R.; Bandar, J. S. Base-catalyzed aryl halide isomerization enables the 4-selective substitution of 3-bromopyridines. *Chem. Sci.* **2020**, *11*, 10517-10522.

[2] Vitaku, E.; Smith, D. T.; Njardarson, J. T. Analysis of the Structural Diversity, Substitution Patterns, and Frequency of Nitrogen Heterocycles among U.S. FDA Approved Pharmaceuticals. *J. Med. Chem*. **2014**, *57*, 10257−10274.

[3] Baumann, M.; Baxendale, I. R.; Ley, S. V.; Nikbin, N. An overview of the key routes to the best selling 5-membered ring heterocyclic pharmaceuticals. *Beilstein J. Org. Chem*. **2011**, *7*, 442−495.

[4] Baumann, M.; Baxendale, I. R. An overview of the synthetic routes to the best selling drugs containing 6-membered heterocycles. *Beilstein J. Org. Chem.* **2013**, 2265-2319.

[5] Umetsu, N.; Shirai, Y. Development of novel pesticides in the 21st century. *J. Pestic. Sci.* **2020**, *45*, 54−74.

[6] Jeschke, P. Progress of modern agricultural chemistry and future prospects. *Pest Manage. Sci*. **2016**, *72*, 433−455.

[7] Scott, K. A.; Cox, P. B.; Njardarson, J. T. Phenols in Pharmaceuticals: Analysis of a Recurring Motif. *J. Med. Chem.* **2022**, *65*, 7044-7072.

[8] Strand, D. S.; Kim, D.; Peura, D. A. 25 Years of Proton Pump Inhibitors: A Comprehensive Review. *Gut and Liver* **2017**, *11*, 27-37.

[9] Queguiner, G.; Marsais, F.; Snieckus, V.; Epsztajn, J. Directed Metalation of Pi-Deficient Azaaromatics: Strategies of Functionalization of Pyridines, Quinolines, and Diazines. *Adv. Heterocycl. Chem*. **1991**, *52*, 187−304.

[10] Schlosser, M. The 2×3 Toolbox of Organometallic Methods for Regiochemically Exhaustive Functionalization. *Angew. Chem., Int. Ed*. **2005**, *44*, 376−393.

[11] Balkenhohl, M.; Knochel, P. Regioselective C−H Activation of Substituted Pyridines and other Azines using Mg- and Zn-TMP-Bases. *SynOpen* **2018**, *2*, 78−95.

[12] Balkenhohl, M.; Jangra, H.; Makarov, I. S.; Yang, S.-M.; Zipse, H.; Knochel, P. A Predictive Model Towards Site-Selective Metalations of Functionalized Heterocycles, Arenes, Olefins, and Alkanes using TMPZnCl·LiCl. *Angew. Chem., Int. Ed.* **2020**, *59*, 14992−14999.

[13] Schlosser, M.; Marull, M. The Direct Metalation and Subsequent Functionalization of Trifluoromethyl-Substituted Pyridines and Quinolines. *Eur. J. Org. Chem.* **2003**, *2003*, 1569−1575.

[14] Do, H.-Q.; Daugulis, O. A Simple Base-Mediated Halogenation of Acidic sp^2 C− H Bonds under Noncryogenic Conditions. *Org. Lett.* **2009**, *11*, 421−423.

[15] Liu, X.; Zhao, X.; Liang, F.; Ren, B. *t*-BuONa-mediated direct C−H halogenation of electron-deficient (hetero)arenes. *Org. Biomol. Chem.* **2018**, *16*, 886−890.

[16] *Heterocyclic Chemistry*, Joule, J. A.; Mills, K. Wiley, West Sussex, 5th ed., 2011.

[17] Kutasevich, A. V.; Perevalov, V. P.; Mityanov, V. S. Recent Progress in Non-Catalytic C−H Functionalization of Heterocyclic *N*-Oxides. *Eur. J. Org. Chem*. **2021**, *2021*, 357−373.

[18] Baykov, S. V.; Boyarskiy, V. P. Metal-free functionalization of azine *N*-oxides with electrophilic reagents. *Chem. Heterocycl. Compd*. **2020**, *56*, 814−823.

[19] Wang, Y.; Zhang, L. Recent Developments in the Chemistry of Heteroaromatic *N*-Oxides. *Synthesis* **2015**, *47*, 289−305.

[20] Lian, Y.; Coffey, S. B.; Li, Q.; Londregan, A. T. Preparation of Heteroaryl Ethers from Azine *N*-Oxides and Alcohols. *Org. Lett.* **2016**, *18*, 1362−1365.

[21] Hilton, M. C.; Dolewski, R. D.; McNally, A. Selective Functionalization of Pyridines via Heterocyclic Phosphonium Salts. *J. Am. Chem. Soc.* **2016**, *138*, 13806-13809.

[22] Dolewski, R. D.; Fricke, P. J.; McNally, A. Site-Selective Switching Strategies to Functionalize Polyazines. *J. Am. Chem. Soc.* **2018**, *140*, 8020-8026.

[23] Zi, Y.; Schömberg, F.; Wagner, K.; Vilotijevic, I. C–H Functionalization of Benzothiazoles via Thiazol-2-yl-phosphonium Intermediates. *Org. Lett.* **2020**, *22*, 3407-3411.

[24] Fier, P. S.; Hartwig, J. F. Selective C-H Fluorination of Pyridines and Diazines Inspired by a Classic Amination Reaction. *Science* **2013**, *342*, 956-960.

[25] Fier, P. S.; Hartwig, J. F. Synthesis and Late-Stage Functionalization of Complex Molecules through C−H Fluorination and Nucleophilic Aromatic Substitution. *J. Am. Chem. Soc.* **2014**, *136*, 10139−10147.

[26] Takemura, N.; Kuninobu, Y.; Kanai, M. Copper-Catalyzed C−H Alkoxylation of Azoles. *Org. Lett.* **2013**, *15*, 844−847.

[27] Vaitiekunas, A.; Nord, F. F. Tetrabromothiophene from 2-Bromothiophene by means of Sodium Acetylide in Liquid Ammonia. *Nature*, **1951**, *168*, 875–876.

[28] Vaitiekunas, A.; Nord, F. F. Studies on the Chemistry of Heterocyclics. XXII. Investigations on the Mechanism of Reactions of 2-Thienyl Halides with Sodium Amide and Sodium Acetylide in Liquid Ammonia. *J. Am. Chem. Soc.*, **1953**, *75*, 1764–1768.

[29] Moyer, C. E.; Bunnett, J. F. Base-Catalyzed Isomerization of Trihalobenzenes. *J. Am. Chem. Soc.* **1963**, *85*, 1891-1893.

[30] Bunnett, J. F. Base-catalyzed halogen dance, and other reactions of aryl halides. *Acc. Chem. Res.* **1972**, *5*, 139–147.

[31] Bunnett, J. F.; Scorrano, G. Mechanism of base-catalyzed isomerization and disproportionation of trihalobenzenes. *J. Am. Chem. Soc*. **1971**, *93*, 1190–1198.

[32] Puleo, T. R.; Klaus, D. R.; Bandar, J. S. Nucleophilic C−H Etherification of Heteroarenes Enabled by Base-Catalyzed Halogen Transfer. *J. Am. Chem. Soc.* **2021**, *143*, 12480-12486.

[33] Shen, K.; Fu, Y.; Li, J.-N.; Liu, L.; Guo, Q.-X. What are the p*K*a values of C−H bonds in aromatic heterocyclic compounds in DMSO? *Tetrahedron* **2007**, *63*, 1568−1576.

[34] Dong, Y.; Lipschutz, M. I.; Tilley, T. D. Regioselective, Transition Metal-Free C−O Coupling Reactions Involving Aryne Intermediates. *Org. Lett.* **2016**, *18*, 1530−1533.

[35] Smith, A. J.; Poole, D. L.; Murphy, J. A. The role of organic electron donors in the initiation of BHAS base-induced coupling reactions between haloarenes and arenes. *Sci. China: Chem.* **2019**, *62*, 1425−1438.

[36] Mari, D.; Miyagawa, N.; Okano, K.; Mori, A. Regiocontrolled Halogen Dance of Bromothiophenes and Bromofurans. *J. Org. Chem.* **2018**, *83*, 14126-14137.

[37] Yamane, Y.; Sunahara, K.; Okano, K.; Mori, A. Magnesium Bisamide-Mediated Halogen Dance of Bromothiophenes. *Org. Lett.* **2018**, *20*, 1688-1691.

[38] Mehta, S.; Larock, R. C. Iodine/Palladium Approaches to the Synthesis of Polyheterocyclic Compounds. *J. Org. Chem*. **2010**, *75*, 1652−1658.

[39] Sun, Z.; Wang, H.; Wen, K.; Li, Y.; Fan, E. Solvent-Free or Low-Solvent Large-Scale Preparation of Chloropyrimidine and Analogues. *J. Org. Chem.* **2011**, *76*, 4149–4153.

[40] Tang, P.; Wang, W.; Ritter, T. Deoxyfluorination of Phenols. *J. Am. Chem. Soc.* **2011**, *133*, 11482-11484.

[41] Handa, S.; Ibrahim, F.; Ansari, T. N.; Gallou, F. π-Allylpalladium Species in Micelles of FI-750-M for Sustainable and General Suzuki-Miyaura Couplings of Unactivated Quinoline Systems in Water. *ChemCatChem* **2018**, *10*, 4229-4223.

[42] Sather, A. C.; Lee, H. G.; De La Rosa, V. Y.; Yang, Y.; Müller, P.; Buchwald, S. L. A Fluorinated Ligand Enables Room-Temperature and Regioselective Pd-Catalyzed Fluorination of Aryl Triflates and Bromides. *J. Am. Chem. Soc.* **2015**, *137*, 13433-13438.

[43] Hao, C. Y.; Wang, D.; Li, Y. W.; Dong, L. L.; Jin, Y.; Zhang, X. R.; Zhu, H. Y.; Chang, S. Carbonylative coupling of aryl tosylates/triflates with arylboronic acids under CO atmosphere. *RSC Adv.* **2016**, *6*, 86502-86509.

[44] Zhang, Y.; Pike, A. Pyridones in drug discovery: Recent advances. *Bioorg. Med. Chem. Lett.* **2021**, 38, 127849.

CHAPTER FIVE

APPLICATION OF BASE-CATALYZED HALOGEN TRANSFER AS A GENERAL APPROACH TO C–H FUNCTIONALIZATION REACTIONS

5.1 Chapter Overview

Having applied base-catalyzed halogen transfer to enable *N*-heteroarene C–H etherification and hydroxylation, we next targeted new C–H functionalization reactions for other mildly acidic C–H bonds. This chapter will briefly discuss two methods that have evolved out of this approach: benzene C–H hydroxylation and benzylic C–H etherification of toluene derivatives (Figure 5–1). In the final part of this chapter, I will summarize my contributions and discuss future outlooks on this chemistry.

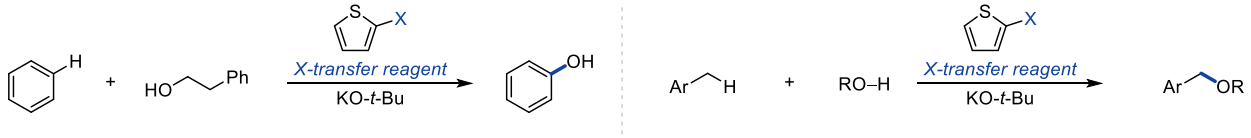

Figure 5–1: X-transfer enabled benzene C–H hydroxylation and benzylic C–H etherification reactions that will be the topic of Chapter five.

5.2 C–H Hydroxylation of Benzenes

Phenols are highly versatile products in synthetic chemistry. In addition to their prevalence in medicinally relevant compounds (Figure 5–2), phenols can participate in several important synthetic transformations, including *O*-alkylation and electrophilic aromatic substitution.[1-2] Additionally, *O*-triflation of phenols produces triflate intermediates which can be used to forge C–C, C–O, C–N, and C–S, amongst other, chemical bonds.[3]

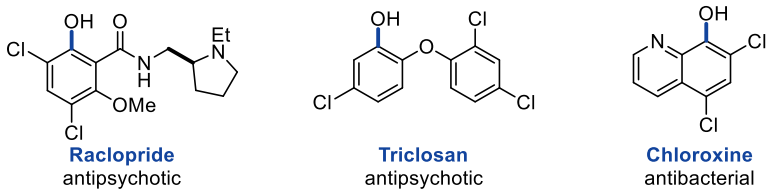

Figure 5–2: Examples of phenols in medicinally relevant compounds.

Phenols are commonly synthesized *via* substitution of aryl (pseudo)halides or oxidation of aromatic organoboron compounds.[4-7] Crucial to these approaches is selective installation of the functional handle prior to substitution/oxidation to the phenol. In this regard, aromatic deprotonation sequenced to halogenation/borylation is useful approach, but requires a strong directing group to achieve high selectivity.[8-10] Iridium-catalyzed borylation is another frequently used approach, installing boron functional groups at the least sterically encumbered positions.[11-12]

Although there are several approaches to benzene C–H hydroxylation, new methods that offer complementary substrate compatibility and selectivity are highly impactful.[13-14] This is highlighted by two recent aromatic C–H hydroxylation reactions reported in *Science*. Han disclosed an impressive Fe-catalyzed benzene C–H hydroxylation reaction (Figure 5–3, right), however few examples of benzenes with electron-withdrawing groups were demonstrated.[15] Meanwhile, Yu recently reported a Pd-catalyzed C–H hydroxylation reaction of benzoic acid derivatives that selectively installs –OH adjacent to the carboxylic acid (Figure 5–3, left).[16]

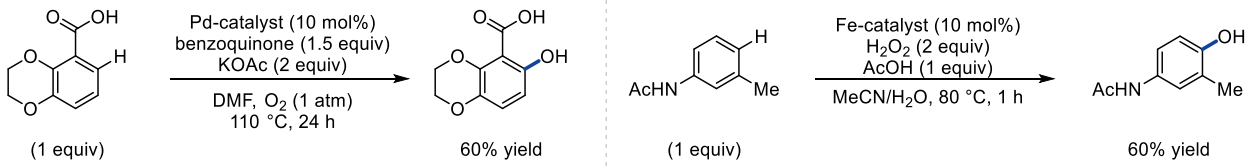

Figure 5–3: Examples of recent benzene C–H hydroxylation methods.

Drawing from our experience on *N*-heteroarene C–H hydroxylation (Chapter 4.9), we reasoned this reaction could be translated to electron-deficient benzene derivatives.[17] Benzenes with electron-withdrawing groups possess similar pK_a values as *N*-heteroarenes (Figure 5–4, see Figure 4–10 and 4–12 for comparison).[18] Additionally, we reasoned sequencing cascade S_NAr with 2-phenylethanol (**5–1**) and base-promoted elimination of styrene would react similarly to produce phenols.

Figure 5–4: pK_a values in DMSO of various benzenes substituted with electron-withdrawing groups.

Working with Kendelyn Bone, we developed a preliminary scope of benzenes that undergo regioselective C–H hydroxylation using 2-iodo-3-bromobenzothiophene (**5–2**) as a halogen transfer reagent (Figure 5–5). Notably, 2-iodo-3-bromobenzothiophene exhibits similar reactivity to 2,3-diiodobenzothiophene used for *N*-heteroarene C–H etherification reactions (Chapter 4.6) but can be synthesized in fewer steps and in greater yield. Diphenylsulfone (**5–3**) and an oxidized phenothiazine derivative (**5–4**) undergo selective hydroxylation *ortho* to the sulfone. Hydroxylation of cyanobenzenes (**5–5**, **5–6**, **5–7**, **5–8**, **5–9**, and **5–14**) occurs at positions directly adjacent to the cyano group. Interestingly, poly(trifluoromethyl)benzenes (**5–12**, **5–13**) undergo selective C–H hydroxylation at the less acidic 4-position. A benzotriazole with an amide substituent (**5–10**) and a sulfonamide derivative (**5–11**) produce phenol products without competing hydrolysis.

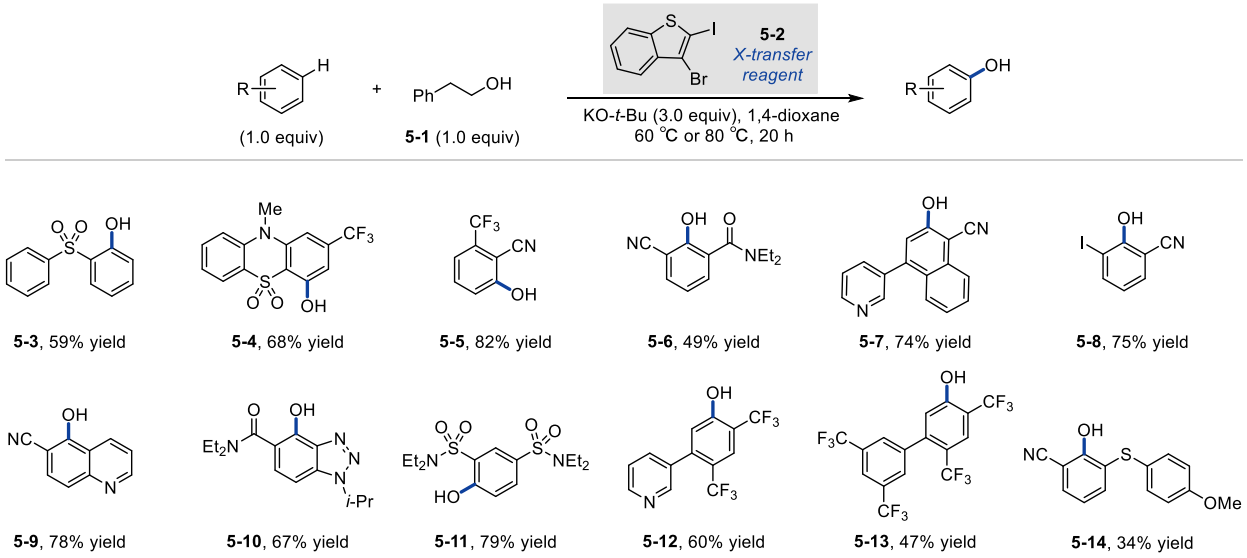

Figure 5–5: Preliminary substrate scope for benzene C–H hydroxylation.

Overall, this approach provides a complementary method to selectively access phenolic products. Several substrates in this scope (e.g. **5–4**, **5–13**, and **5–12**) would likely produce mixtures of products using metalation/halogenation or borylation reactions. Kendelyn Bone is currently working to complete development of this method.

5.3 Benzylic C–H Etherification of Toluene Derivatives

Benzyl ethers are important compounds in the development of new pharmaceuticals, and several bioactive compounds possess benzyl ether motifs (Figure 5–6).[19] In addition to their contribution to the overall design of a pharmaceutical, benzylic ether linkages can undergo oxidative debenzylation to facilitate the metabolism and excretion of the drug.[20] The benzylic position of pharmaceuticals is labile to metabolic oxidation and benzylic substitution can alter the metabolic profile of biologically active molecules.[19]

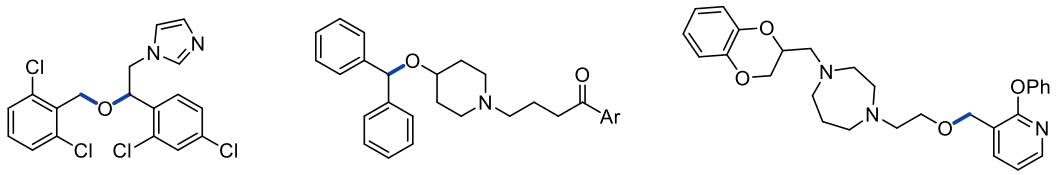

Figure 5–6: Examples of benzyl ethers in pharmaceuticals and bioactive compounds.

Few synthetic methods for direct intermolecular substitution of benzylic C–H bonds with alcohol nucleophiles exist. Electrochemical methods have been developed that directly substitute benzylic C–H bonds with alcohols but the scope of these reactions are limited to simple alkyl arenes and alcohols.[22,23] Yoon disclosed a photoredox based approach in which electron-rich alkyl benzenes undergo sequenced oxidation, benzylic deprotonation, benzylic oxidation, and alcohol addition to produce benzyl ether products (Figure 5–7, top).[24] This approach is limited to electron-rich alkyl benzenes, and toluene derivatives are generally incompatible substrates due to competitive overoxidation. Stahl developed a "radical relay" approach to benzylic C–H etherification using an *N*-centered radical generated from *N*-fluorobenzenesulfonimide (NFSI) to promote HAT from the benzylic position and a Cu-catalyst to facilitate C–O bond formation.[25,26] Much like Yoon's approach, this reaction is incompatible with toluene derivatives and demonstrates few arenes with strongly electron-withdrawing substituents, although some *N*-heterocyclic derivatives are tolerated (Figure 5–7, bottom).

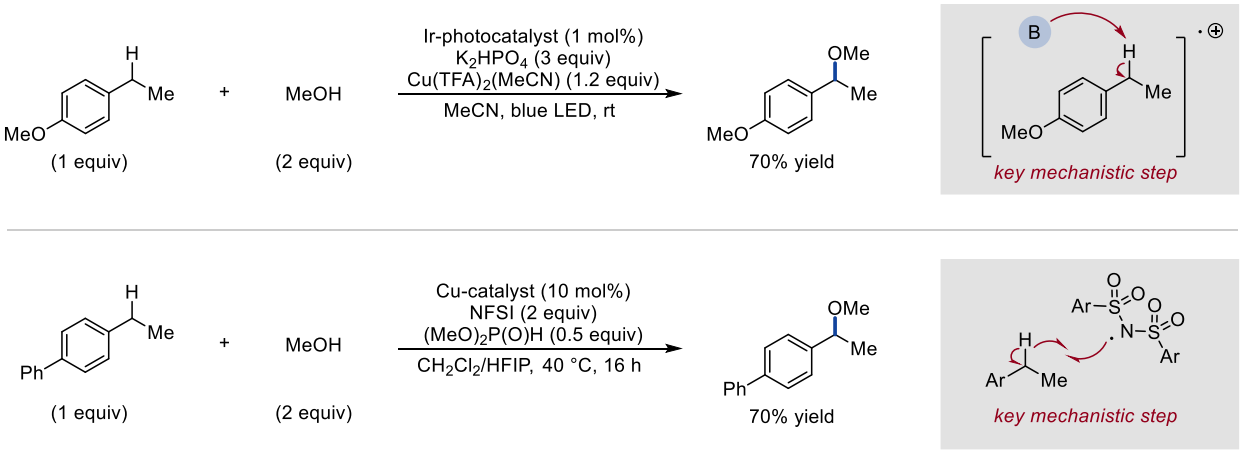

Figure 5–7: Yoon's (top) and Stahl's (bottom) recently reported methods for benzylic C–H etherification.

Two-step benzylic bromination and base-promoted alcohol substitution is a highly common approach to access benzylic ethers.[27] Although robust, this approach is incapable of selectively brominating of polyalkyl benzenes (Figure 5–8). Additionally, the electrophilic brominating reagents typically employed in these reactions (e.g. NBS and Br_2) could potentially undergo competing electrophilic aromatic bromination with electron-rich toluenes. Sequencing benzylic bromination reactions to nucleophilic substitution also appears to be challenging as the benzyl bromide products are always individually isolated.

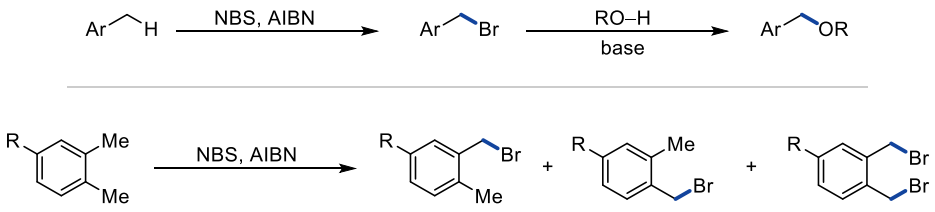

Figure 5–8: A common approach to access benzyl ethers *via* benzylic bromination (top). Challenge of benzylic bromination on polyalkyl benzenes (bottom).

We reasoned toluenes with electron-withdrawing groups are acidic enough to be deprotonated by alkoxide bases and that base-catalyzed halogen transfer could enable a benzylic C–H etherification reaction.[28] I discovered use of 2-iodothiophene (**5–15**) or 2-iodo-3-

phenylbenzothiophene (**5–16**) as halogen transfer reagents enables the monoselective benzylic C–H etherification of toluene derivatives. Use of 2-iodo-3-phenylbenzothiophene results in significantly improved yields for some substrates, and efforts are ongoing to understand the nature of this improvement. Figure 5–9a displays the current substrate scope I developed while mentoring a younger Ph.D student in our group, Yuka Shimuzu, using KO-*t*-Bu or LiO-*t*-Bu as the base and 2-ethyl-1-hexanol as the model alcohol. Halogenated toluenes (**5–17**, **5–18**, **5–19**) undergo monoselective etherification in good yield. Heterocyclic methyl arenes including 7-chloro-8-methylquinoline (**5–26**), 5-cyano-1,2-dimethylpyrrole (**5–29**), and 3-methylbenzothiophene (**5–24**) participate in the reaction. Notably, 2-bromo-6-methylpyridine (**5–25**) undergoes benzylic etherification despite being reactive toward S_NAr. Toluenes with electron-donating groups including 4-bromo-3-methoxytoluene (**5–20**) and 2-bromo-5-(dimethylamino)toluene (**5–23**) are also compatible with these conditions. Toluenes with *para*-electron-withdrawing groups including 4-(trifluoromethyl)toluene (**5–22**) and 4-(thiophenyl)toluene (**5–21**) undergo benzylic C–H etherification. Finally, biaryl toluene with an amide functional group (**5–30**) undergoes selective etherification without competing amide alcoholysis. Yuka Shimuzu and a postdoctoral researcher in our lab, Dr. Michael Delost, are currently developing this substrate scope further.

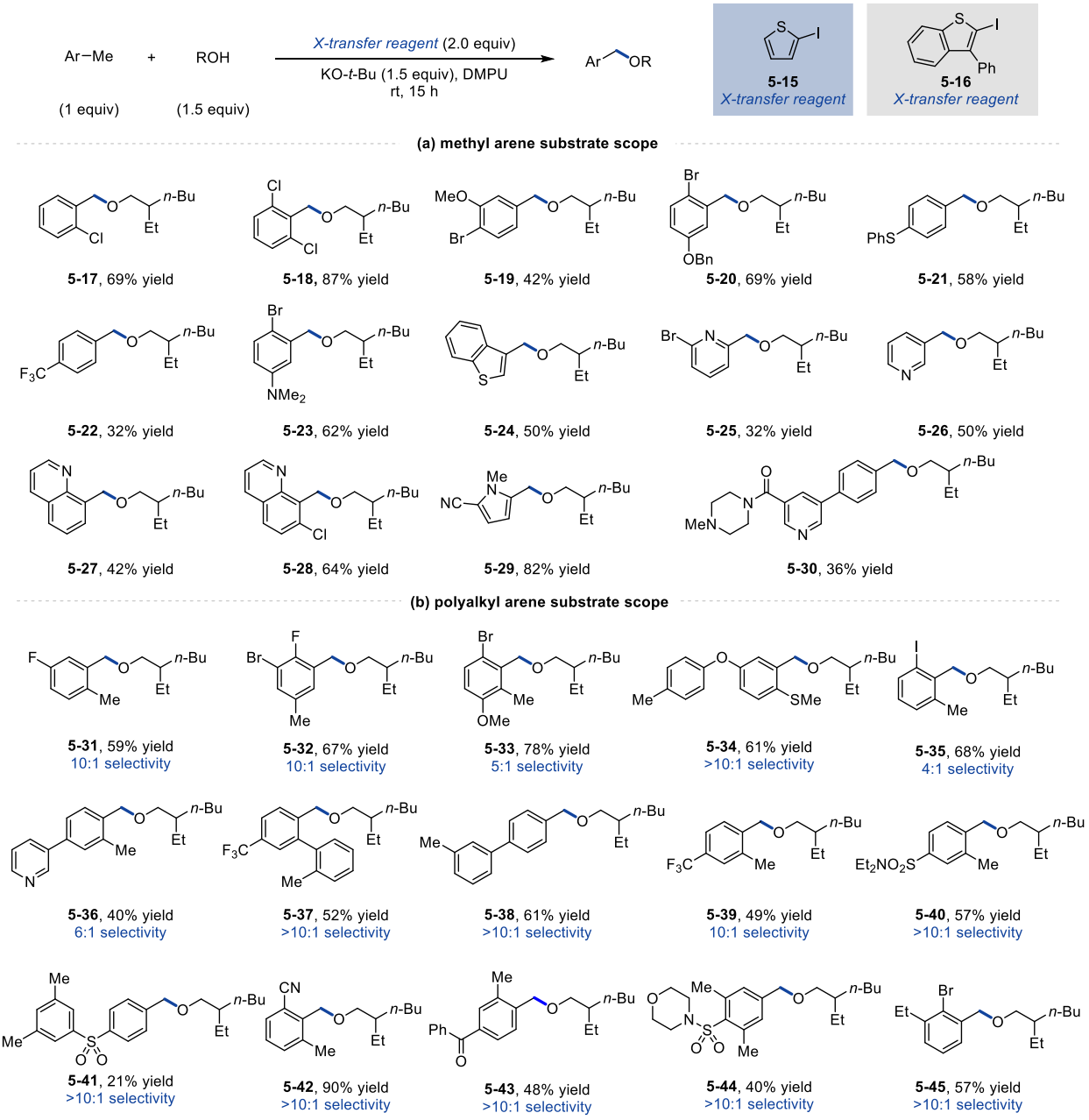

Figure 5–9: Current benzylic C–H etherification substrate scope.

Next, I applied this approach to enable site-selective C–H etherification of polyalkyl benzenes. For these substrates, etherification occurs at the most acidic benzylic position and only minor electronic differences between benzylic positions is required for site-selective etherification. Figure 5–9b shows the current substrate scope of polyalkyl benzenes with most examples proceeding with > 10:1 site-selectivity. 3,4-Dimethylfluorobenzene (**5–31**) undergoes selective

etherification at the 3-position. Other polyalkyl benzenes with halogen (**5–32, 5–35**), thioether (**5–34**), pyridine (**5–36**), or alkoxy (**5–33, 5–34**) electron-withdrawing groups undergo site-selective C–H etherification. Etherification of biphenyl compounds with alkyl groups on each ring (**5–37**, **5–38**) occurs at the most acidic site. Dialkyl benzenes with strong electron-withdrawing substituents including 2,3-dimethylcyanobenzene (**5–42**), 3,4-dimethylbenzenesulfonamide (**5–40**), 3,4-dimethylbenzotrifluoride (**5–37**), benzophenone derivative (**5–43**), and sulfone derivative (**5–41**) are effective substrates. Notably, 2,4,6-trimethylbenzenesulfonamide (**5–44**) undergoes selective etherification at the 4-methyl position, likely due to steric effects. Finally, etherification of 2-methyl-6-ethylbromobenzene (**5–45**) occurs exclusively at the methyl position. Work is ongoing to develop the substrate scope of this reaction.

The high site-selectivity observed for these substrates is remarkable and highlights a distinct benefit of this unique approach to achieve benzylic oxidation. Benzylic C–H deprotonation with KO-*t*-Bu base is likely an endothermic process. According to the Hammond postulate, the selectivity of this endothermic deprotonation is likely very sensitive to the stability of the benzyl anion intermediates. This directly contrasts with radical-type oxidation processes where HAT is relatively exothermic, and the site-selectivity is less sensitive to the stability of the benzylic radical. Attempted benzylic bromination of 3,4-dimethylfluorobenzene (**5–46**) produced a mixture of 3-(methylbromo)-, 4-(methylbromo)- and 3,4-(methylbromo)fluorobenzene products (Figure 5–10). Thus, the uniquely fast rate of halogen transfer from 2-iodothiophenes to low concentrations of benzylic anions enables the site-selective benzylic etherification of polyalkyl benzenes.

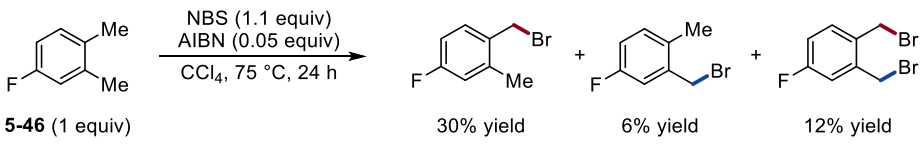

Figure 5–10: Benzylic bromination reaction of 3,4-dimethylfluorobenzene.

Notably, the benzylic deprotonation and halogen transfer mechanistic step cannot be conducted in isolation. Benzylic deprotonation of 1-methylnaphthalene (**5–47**) with the base combination of *n*-BuLi, KO-*t*-Bu, and 2,2,6,6-tetramethylpiperidine (TMPH) followed by sequential treatment with Br_2 produces no yield of the corresponding benzyl bromide (**5–48**, Figure 5–11).[29] Instead, the generated benzyl bromide product is unstable under the reaction conditions, undergoing nucleophilic substitution with TMPH (**5–49**) and the benzyl anion of 1-methylnaphthalene (**5–50**). This challenge has additionally been documented in previous reports.[30]

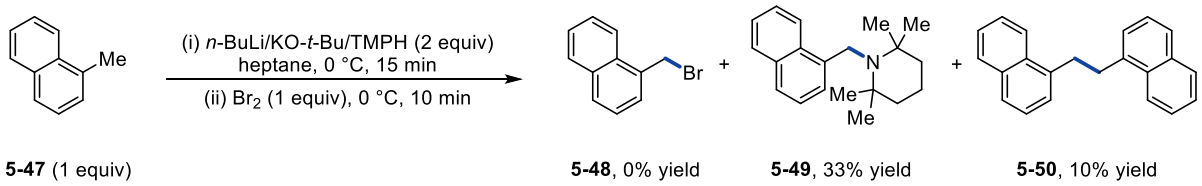

Figure 5–11: Attempted benzylic bromination *via* deprotonation of 1-methylnaphthalene.

The discovery that 2-iodothiophenes can serve as a base- and nucleophile compatible oxidant that selectively halogenates carbanions enables a unique and complementary approach to achieve benzylic C–H oxidation. The high site-selectivity demonstrated on polyalkyl benzenes arises from site-selective benzylic deprotonation. The generated benzyl halide intermediate is unstable under basic conditions, and nucleophilic substitution with the desired nucleophile must occur in the same reaction. Thus, the combination of benzylic deprotonation, halogen transfer, and nucleophilic substitution steps is crucial for the success of this approach and is the key principle that enables the site-selective benzylic C–H etherification of toluenes.

Finally, I discovered that treatment of more electron-deficient toluene derivatives with an excess of 2-iodothiophene, KO-*t*-Bu, and *n*-propanol promotes selective oxidation of the benzylic position to acetals. Site-selective acetalization of biaryl (**5–51**) occurs at the more acidic benzylic

position, and sequenced acidic deprotection yields the corresponding aldehyde (**5–52**) in 96% yield and > 10:1 site-selectivity (Figure 5–12). This development is notable because aldehydes are highly diversifiable functional groups, and we expect this approach will serve as an attractive approach to selectively functionalize polyalkyl benzene derivatives.[31-33]

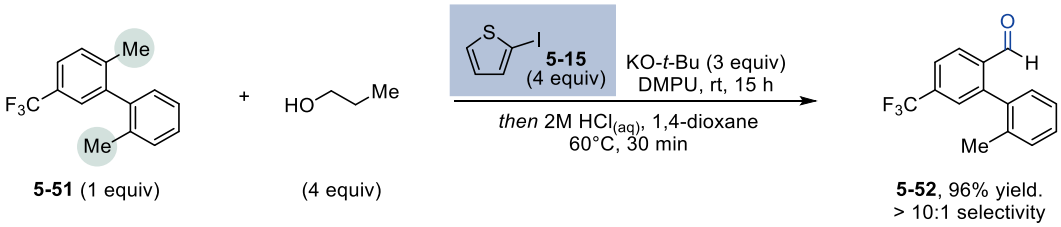

Figure 5–12: Site-selective oxidation of a polyalkyl benzene to an aldehyde.

Overall, this reaction represents the first general approach to directly substitute toluene benzylic C–H bonds with alcohol nucleophiles. In addition to streamlining the synthesis of benzylic ethers, the combination of deprotonation, halogen transfer, and substitution reaction processes enables site-selective benzylic oxidation of polyalkyl benzenes. Currently, a postdoctoral researcher, Dr. Michael Delost, and a Ph.D student, Yuka Shimizu, are completing this work.

5.4 Conclusions and Outlook

The methods described throughout this thesis demonstrate that base-catalyzed halogen transfer is a general platform for the development of C–H functionalization reactions. Efforts are ongoing in our research group to apply this approach to other classes of compounds with mildly acidic C–H bonds. The unique approach to achieving C–H functionalization by sequencing compatible base deprotonation, halogen transfer, and substitution processes streamlines synthetic procedures and enables new synthetic transformations. The success of each mechanistic step in these processes is contingent on the other and cannot be conducted in isolation for the methods described above to be selective and high yielding. The application of this principle is what enables

site-selective C–H etherification of *N*-heteroarenes and polyalkyl arenes with multiple potential reactive sites. The approach of stringing deprotonation, halogen transfer, and nucleophilic substitution together to enable challenging C–H functionalization reactions is currently a significant motivation in our research group, and serves as the foundation for several reactions currently under development.

REFERENCES

[1] Scott, K. A.; Cox, P. B.; Njardarson, J. T. Phenols in Pharmaceuticals: Analysis of a Recurring Motif. *J. Med. Chem.* **2022**, *65*, 7044-7072.

[2] Kumar, L.; Mahajan, T.; Sharma, V.; Agarwal, D. D. Environmentally-Benign and Rapid Bromination of Industrially-Important Aromatics Using an Aqueous $CaBr_2$−Br_2 System as an Instant and Renewable Brominating Reagent. *Ind. Eng. Chem. Res.* **2011**, *50*, 705-712.

[3] Qiu, Z.; Li, C.-J. Transformations of Less-Activated Phenols and Phenol Derivatives via C–O Cleavage. *Chem. Rev.* **2020**, *120*, 10454-10515.

[4] Cheng, G.; Zeng, X.; Cui, X. Benzoquinone-Promoted Aerobic Oxidative Hydroxylation of Arylboronic Acids in Water. *Synthesis* **2014**, *46*, 295−300.

[5] Molander, G. A.; Cavalcanti, L. N. Oxidation of Organotrifluoroborates via Oxone. *J. Org. Chem*. **2011**, *76*, 623−630.

[6] Xia, S.; Gan, L.; Wang, K.; Li, Z.; Ma, D. Copper-Catalyzed Hydroxylation of (Hetero)aryl Halides under Mild Conditions. *J. Am. Chem. Soc.* **2016**, *138*, 13493−13496.

[7] Fier, P. S.; Maloney, K. M. Synthesis of Complex Phenols Enabled by a Rationally Designed Hydroxide Surrogate. *Angew. Chem., Int. Ed.* **2017**, *56*, 4478−4482.

[8] Queguiner, G.; Marsais, F.; Snieckus, V.; Epsztajn, J. Directed Metalation of Pi-Deficient Azaaromatics: Strategies of Functionalization of Pyridines, Quinolines, and Diazines. *Adv. Heterocycl. Chem*. **1991**, *52*, 187−304.

[9] Schlosser, M. The 2×3 Toolbox of Organometallic Methods for Regiochemically Exhaustive Functionalization. *Angew. Chem., Int. Ed*. **2005**, *44*, 376−393.

[10] Balkenhohl, M.; Knochel, P. Regioselective C−H Activation of Substituted Pyridines and other Azines using Mg- and Zn-TMP-Bases. *SynOpen* **2018**, *2*, 78−95.

[11] Ishiyama, T.; Takagi, J.; Ishida, K.; Miyaura, N.; Anastasi, N. R.; Hartwig, J. F. Mild Iridium-Catalyzed Borylation of Arenes. High Turnover Numbers, Room Temperature Reactions, and Isolation of a Potential Intermediate. *J. Am. Chem. Soc.* **2002**, *124*, 390-391.

[12] Preshlock, S. M.; Ghaffari, B.; Maligres, P. E.; Krska, S. W.; Maleczka, R. E. Jr.; Smith, M. R. III. High-Throughput Optimization of Ir-Catalyzed C–H Borylation: A Tutorial for Practical Applications. *J. Am. Chem. Soc.* **2013**, *135*, 7572-7582.

[13] Iqbal, Z.; Joshi, A.; De, S. R. Recent Advancements on Transition-Metal-Catalyzed, Chelation-Induced *ortho*-Hydroxylation of Arenes. *Adv. Synth. Catal.* **2020**, *362*, 5301-5351.

[14] Alonso, D. A. Nájera, C.; Pastor. I. M.; Yus, M. Transition-Metal-Catalyzed Synthesis of Hydroxylated Arenes. *Chem. Eur. J.* **2010**, *16*, 5274-5284.

[15] Cheng, L.; Wang, H.; Cai, H.; Zhang, J. Gong, X.; Han, W. Iron-catalyzed arene C−H hydroxylation. *Science* **2021**, *374*, 77-81.

[16] Li, Z.; Wang, Z.; Chekshin, N.; Qian, S.; Qiao, J. X.; Cheng, P. T.; Yeung, K.-S.; Ewing, W. R.; Yu, J.-Q. A tautomeric ligand enables directed C–H hydroxylation with molecular oxygen. *Science* **2021**, *372*, 1452-1457.

[17] Puleo, T. R.; Klaus, D. R.; Bandar, J. S. Nucleophilic C−H Etherification of Heteroarenes Enabled by Base-Catalyzed Halogen Transfer. *J. Am. Chem. Soc.* **2021**, *143*, 12480-12486.

[18] Shen, K.; Fu, Y.; Li, J.-N.; Liu, L.; Guo, Q.-X. What are the p*K*a values of C−H bonds in aromatic heterocyclic compounds in DMSO? *Tetrahedron* **2007**, *63*, 1568−1576.

[19] Roughley, S. D.; Jordan, A. M. The Medicinal Chemist's Toolbox: An Analysis of Reactions Used in the Pursuit of Drug Candidates. *J. Med. Chem.* **2011**, *54*, 3451-3479.

[20] Tompson, T. N. Optimization of metabolic stability as a goal of modern drug design. *Med. Res. Rev*. **2001**, *21*, 412–449.

[21] Gant, T. G. Using Deuterium in Drug Discovery: Leaving the Label in the Drug. *J. Med. Chem.* **2014**, *57*, 3595-3611.

[22] Wang, H.; Liang, K.; Xiong, W.; Samanta, S.; Li, W.; Lei, A. Electrochemical oxidation-induced etherification via C(sp^3)─H/O─H cross-coupling. *Sci. Adv.* **2020**, *6*.

[23] Chowdhury, S.; Pandey, S. A Catalyst/Oxidant/Base Free Benzylic Csp^3–H Alkoxylation of toluidines via Electro-oxidative Csp^3–O-Coupling with Alcohols. *Asian J. Org. Chem.* **2021**, *10*, 2902-2906.

[24] Lee, B. J.; DeGlopper, K. S.; Yoon, T. P. Site-Selective Alkoxylation of Benzylic C−H Bonds by Photoredox Catalysis. *Angew. Chem. Int. Ed.* **2020**, *59*, 197-202.

[25] Hu, H.; Chen, S.-J.; Mandal, M.; Pratik, S. M.; Buss, J. A.; Krska, S. W.; Cramer, C. J.; Stahl, S. S. Copper-catalysed benzylic C–H coupling with alcohols via radical relay enabled by redox buffering. *Nature Catalysis* **2020**, *3*, 358-367.

[26] Leibler, I. N.-M. Tekle-Smith, M. A.; Doyle, A. G. A general strategy for C(sp^3)–H functionalization with nucleophiles using methyl radical as a hydrogen atom abstractor. *Nat Commun* **2021**, *12*, 6950.

[27] Steiner, A.; Roth, P. M. C.; Strauss, F. J.; Gauron, G.; Tekautz, G.; Winter, M.; Williams, J. D.; Kappe, C. O. Multikilogram per Hour Continuous Photochemical Benzylic Brominations Applying a Smart Dimensioning Scale-up Strategy. *Org. Process Res. Dev.* **2020**, *24*, 2208-2216.

[28] Sim, B. A.; Griller, D.; Wayner, D. D. M. Reduction potentials for substituted benzyl radicals: pKa values for the corresponding toluenes. *J. Am. Chem. Soc.* **1989**, *111*, 754-755.

[29] Manvar, A.; Fleming, P.; O'Shea, D. F. General Ambient Temperature Benzylic Metalations Using Mixed-Metal Li/K-TMP Amide. *J. Org. Chem.* **2015**, *80*, 8727-8738.

[30] Clark, R. D.; Jahangir, A. Lateral Lithiation Reactions Promoted by Heteroatomic Substituents. *Org. React.* **1995**, *47*, 1.

[31] Melvin, P. R.; Ferguson, D. M.; Schimler, S. D.; Bland, D. C.; Sanford, M. S. Room Temperature Deoxyfluorination of Benzaldehydes and α-Ketoesters with Sulfuryl Fluoride and Tetramethylammonium Fluoride. *Org. Lett.* **2019**, *21*, 1350-1353.

[32] Maercker, A. The Wittig Reaction. *Org. React.* **1965**, *14*, 270-490.

[33] Afanasyev, O. I.; Kuchuk, E.; Usanov, D. L.; Chusov, D. Reductive Amination in the Synthesis of Pharmaceuticals. *Chem. Rev.* **2019**, *119*, 11857-11911.

APPENDIX ONE

BASE-CATALYZED α-SELECTIVE DEUTERATION OF STYRENE DERIVATIVES: EXPERIMENTAL

A1.1 General Information

General Reagent Information: All reactions to prepare α-deuterated styrenes were performed under a nitrogen atmosphere. DMSO-d_6 was purchased from Cambridge Isotopes Inc. and was stored over activated 4Å molecular sieves. Potassium *tert*-butoxide (KO-*t*-Bu) was purchased from Acros (product #192860) and used as purchased. Anhydrous methanol was purchased from Sigma-Aldrich and used as purchased. DMSO-d_6, KO-*t*-Bu, and MeOH were stored in a nitrogen filled glovebox and used immediately if brought outside the glovebox. Tetrahydrofuran and dichloromethane were deoxygenated and dried by passage over packed columns of neutral alumina and copper (II) oxide under positive pressure of nitrogen or argon. NaH was purchased from Acros as a 60% dispersion in mineral oil and was stored in a desiccator with $CaSO_4$ as the desiccant. 1-*tert*-Butyl-4,4,4-tris(dimethylamino)-2,2-bis[tris(dimethylamino)-phosphoranylidenamino]-2λ^5,4λ^5-catenadi(phosphazene) (P_4-*t*-Bu) was purchased from a Sigma-Aldrich as a 0.8M solution in hexanes and was stored in a -30 °C freezer inside a nitrogen filled glovebox. Before use, the P_4-*t*-Bu solution was allowed to warm to room temperature and homogenize if any solid was evident. AD-mix-β was purchased from Sigma-Aldrich and used as received. (*S*)-DTBM-SEGPHOS was purchased from Strem Chemicals and stored in a nitrogen filled glovebox. (*R*)-DTBM-SEGPHOS was purchased from Sigma-Aldrich and stored inside a nitrogen filled glovebox. $Cu(OAc)_2$ was purchased from Aldrich and used as received. PPh_3 was purchased from Combi-Blocks and used as received. (*S*)-(+)-α-methoxy-α-(trifluoromethyl)phenylacetyl chloride was purchased from Matrix Scientific and used as received. All other solvents and reagents were purchased from

Sigma-Aldrich, Combi-Blocks, TCI, Acros Organics, Matrix, or Alfa-Aesar and used as received unless otherwise noted. Flash Chromatography was performed on 40-63 μm silica gel (SiliaFlash® F60 from Silicycle).

General Analytical Information: All reported compounds were characterized by ^{1}H, ^{2}H, ^{13}C and ^{19}F (as appropriate) NMR spectroscopy, FTIR spectroscopy and mass spectrometry. Melting point analysis was conducted if the compound was solid. Optical rotation analysis was conducted if the compound was chiral. Enantiomeric excess of compounds **1–30** and **1–31** was determined by chiral HPLC on a Shimadzu Prominence UFLC instrument using the given conditions. ^{1}H NMR, ^{13}C NMR, and ^{19}F NMR spectra were obtained on a Bruker Advanced NEO or Varian Inova 400 spectrometer. ^{1}H NMR data is reported as follows: chemical shift (δ ppm), multiplicity (s = singlet, d = doublet, t = triplet, q = quartet, dd = doublet of doublets, td = triplet of doublets, m = multiplet), coupling constant (Hz), and integration. ^{13}C NMR data is reported as follows: chemical shift (δ ppm), multiplicity (if applicable, q = quartet, T = 1:1:1 triplet). All ^{1}H NMR signals are reported as chemical shifts (δ ppm) relative to residual $CHCl_3$, CH_2Cl_2, or DMSO at 7.26 ppm, 5.32 ppm, or 2.50 ppm respectively. ^{13}C NMR signals are reported as chemical shifts (δ ppm) relative to $CDCl_3$, CD_2Cl_2, or DMSO-d_6 at 77.23 ppm, 53.84 ppm, or 39.52 ppm respectively. α,α,α-Trifluorotoluene (δ -63.72 ppm) internal standard was added to all ^{19}F NMR samples. Chemical shifts for ^{2}H NMR are reported as chemical shifts (δ ppm) relative to residual CD_3CN (1.94 ppm). High resolution mass spectra (HRMS) were recorded on an Agilent 6210 TOF interfaced to a DART 100 or APCI source provided by Colorado State University Central Instrumentation Facility. If the substrate would not ionize using LC-MS methods, a GC-MS method was used on an Agilent 5977A GC/MSD system. IR spectra were recorded using a Thermo Scientific Nicolet

iS-50 FTIR Spectrometer and reported as frequency of absorption (cm^{-1}). Melting point analyses were conducted using a Mel-Temp capillary melting point apparatus. The specific rotation of chiral molecules was measured using a Rudolph Research Analytical Autopol III polarimeter. Thin-layer chromatography analysis was performed on silica gel 60Å F_{254} plates (250 µm, SiliaPlate from Silicycle, #TLG-R10014B-323) and interpreted using UV light (254 nm) or $KMnO_4$ stain.

A1.2 Equilibrium Studies and K_{eq} Calculations

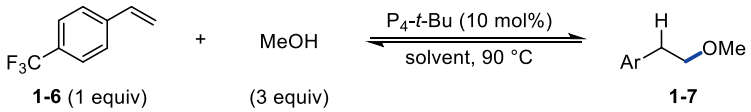

General Process: The equilibrium constant (K_{eq}) for the above reaction was calculated in both DMSO and *m*-xylene. To do so, the reaction was run in both the forward (starting from **1–6**) and reverse (starting from **1–7**) directions until both reactions converged to the same yields of styrene **1–6** and the corresponding methyl ether (**1–7**). The yields of the styrene and methyl ether were determined by ^1H NMR using trimethoxybenzene as the internal standard. The final concentration of methanol was calculated by subtracting the final concentration of **1–7** from the starting concentration of methanol. The K_{eq} of the reaction was calculated using the following equation:

$$K_{eq} = \frac{[\mathbf{1\text{-}7}]}{[\mathbf{1\text{-}6}][MeOH]}$$

Forward reaction general procedure: In a nitrogen filled glovebox, 1-(trifluoromethyl)-4-vinylbenzene (**1–6**) (43.0 mg, 0.25 mmol, 1 eq) was weighed into an oven-dried 4 mL vial (ThermoFisher, C4015-1). The appropriate solvent (DMSO or *m*-xylene, 0.5 mL), anhydrous MeOH (30 µl, 0.75 mmol, 3 eq) and P_4-*t*-Bu (31 µl of a 0.8M solution in hexanes, 0.025 mmol, 0.1 eq) was then added in that order. The vial was capped with a screw top PTFE-lined cap (ThermoFisher, C4015-1A), removed from the glovebox and placed in a preheated 90 °C

aluminum reaction block for 6 h (DMSO) or 3 h (*m*-xylene). After the indicated time, the reaction was immediately quenched with acetic acid while at 90 °C. Trimethoxybenzene was weighed into each vial and used to calculate the equilibrium quantities of **1–6** and **1–7**.

Reverse reaction general procedure: In a nitrogen filled glovebox, 1-(2-methoxyethyl)-4-(trifluoromethyl)benzene **(1–7)** (51.0 mg, 0.25 mmol, 1 eq) was weighed into an oven-dried 4 mL vial (ThermoFisher, C4015-1) and constituted in the appropriate solvent (DMSO or *m*-xylene, 0.5 mL). Anhydrous MeOH (20 µl, 0.5 mmol, 2 eq) and P_4-*t*-Bu (31 µl of 0.8M solution in hexanes, 0.025 mmol, 0.1 eq) was then added in that order. The vial was capped with a PTFE-lined screw cap (ThermoFisher, C4015-1A), removed from the glovebox and placed in a preheated 90 °C aluminum reaction block for 6 h (DMSO) or 3 h (*m*-xylene). After the indicated time, each reaction was immediately quenched with acetic acid while at 90°C. Trimethoxybenzene was weighed into each vial and used to calculate the equilibrium quantities of **1–6** and **1–7**.

Example spectra: Provided below are example spectra used to calculate K_{eq} for a reaction run in the forward and reverse direction in DMSO and *m*-xylene.

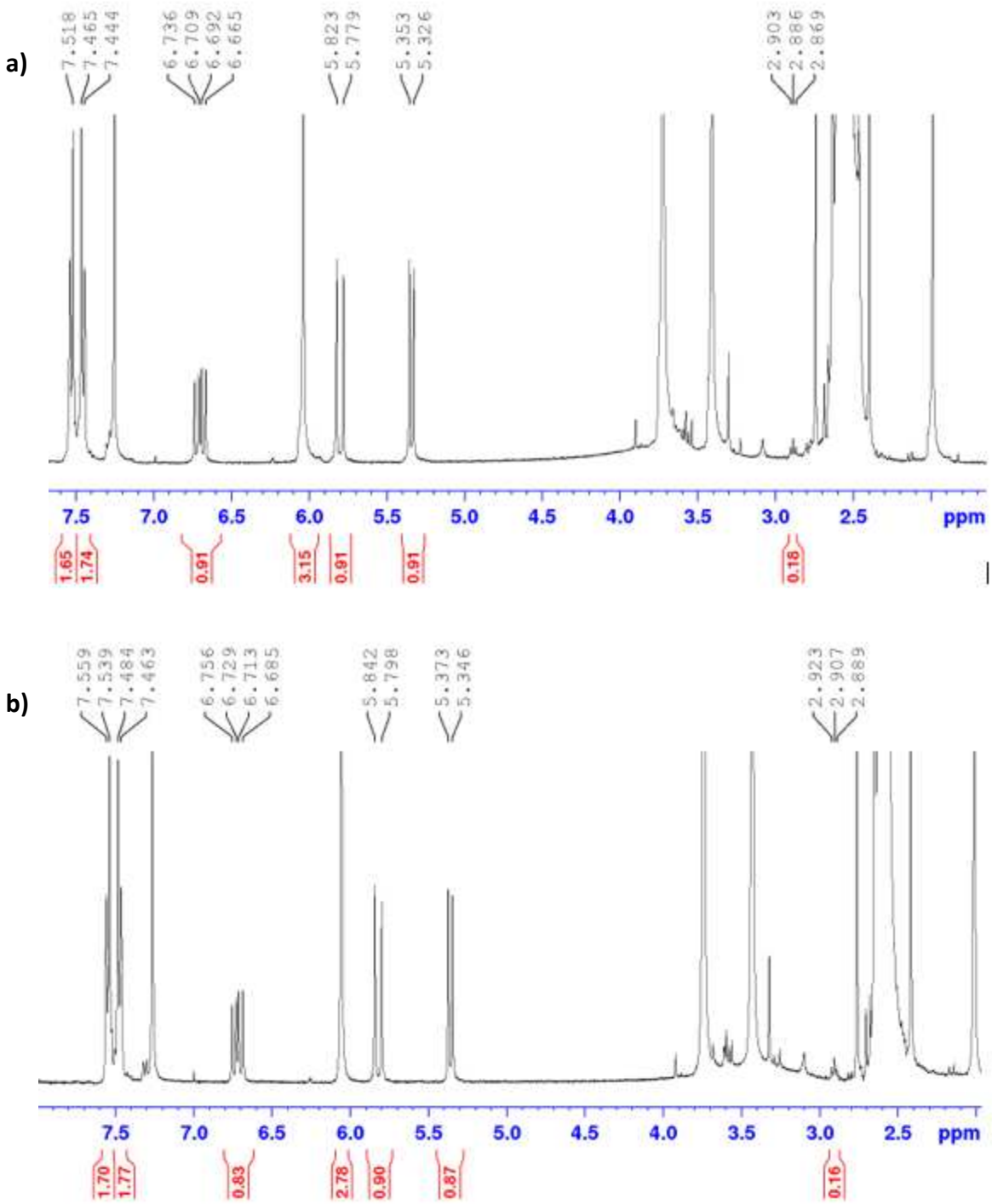

Figure A1–1 : In DMSO **(a)**: Forward reaction (0.25 mmol scale and 0.26 mmol TMB as internal standard, 91% yield of **1–6**, 9% yield of **1–7**. **(b)**: Reverse reaction (0.25 mmol scale and 0.23 mmol TMB as internal standard, 90% yield of **1–6**, 8%yield of **1–7**.

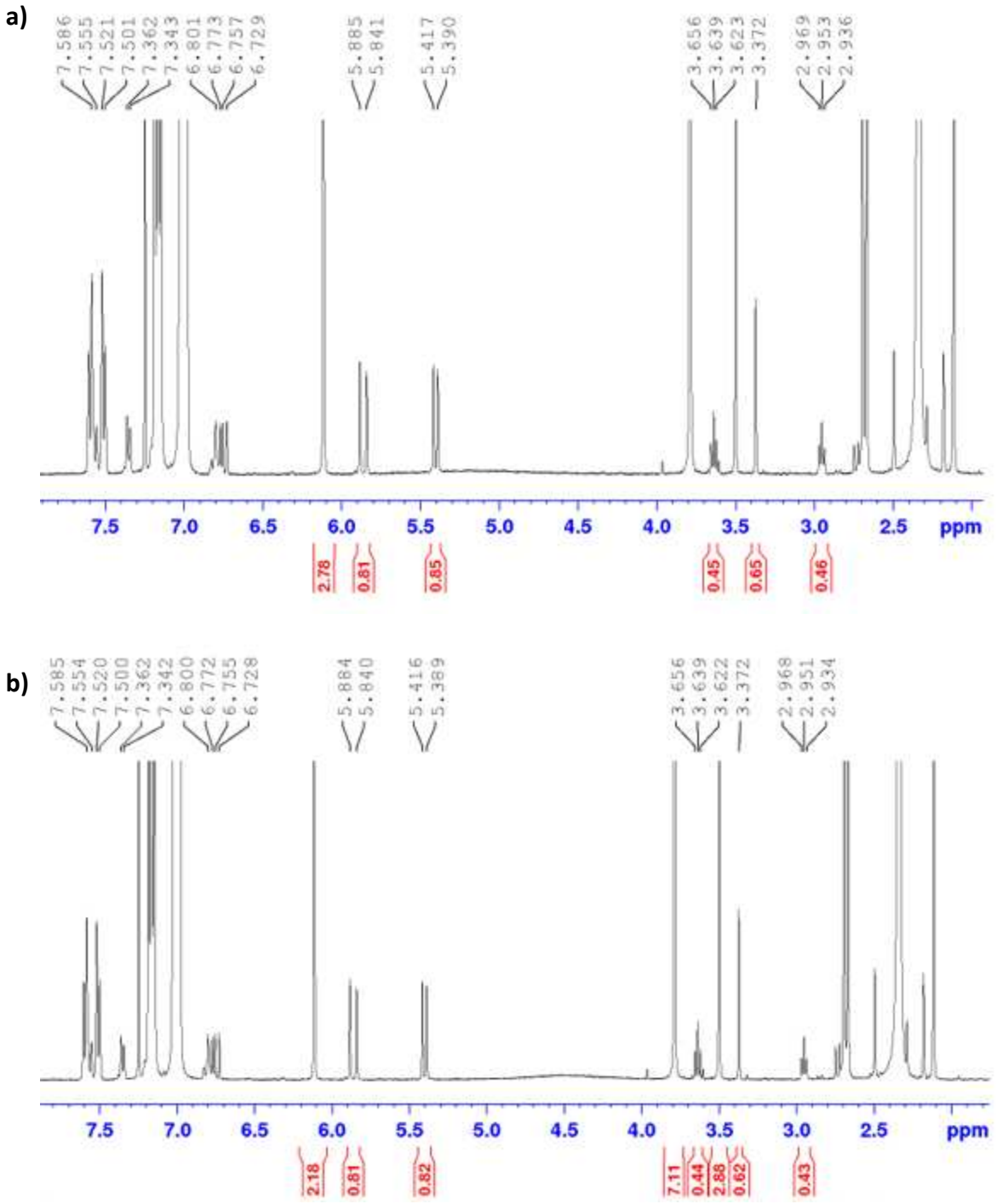

Figure A1–2: In *m*-xylene **(a)**: Forward reaction (0.25 mmol scale and 0.23 mmol TMB as internal standard, 81% yield of **1–6**, 22% yield of **1–7**. **(b)**: Reverse reaction (0.25 mmol scale and 0.18 mmol TMB as internal standard, 81% yield of **1–6**, 21% yield of **1–7**.

	forward		backward		K_{eq}
solvent	styrene (%)	ether (%)	styrene (%)	ether (%)	
m-xylene	81	22	81	21	0.20
DMSO	91	9	90	8	0.07

Figure A1–3 : Equilibrium proportions of **1–6** (styrene) and **1–7** (ether) and K_{eq} value for the addition of methanol to 1-(trifluoromethyl)-4-vinylbenzene in DMSO and *m*-xylene.

A1.3 Initial α-Deuteration Discovery

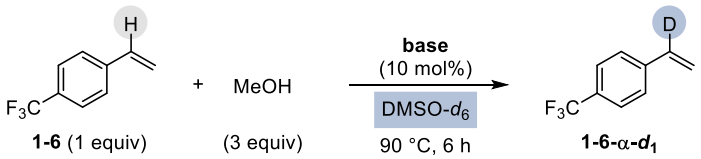

Procedure: 1-(trifluoromethyl)-4-vinylbenzene (**1–6**) (43.0 mg, 0.25 mmol, 1 eq) was weighed into an oven dried 4 mL vial (ThermoFisher, C4015-1) in a nitrogen filled glovebox. MeOH (30 µl, 0.75 mmol, 3 eq), DMSO-d_6 (0.5 mL), and either KO-*t*-Bu (2.8 mg, 0.025 mmol, 0.1 eq) or P_4-*t*-Bu (31 µl, 0.025 mmol, 0.1 eq) were then added in that order. The vial was sealed with a PTFE-lined screw cap (ThermoFisher, C4015-1A), removed from the glovebox, and placed into a pre-heated 90 °C silicon oil bath. The reaction solution was stirred for 6 h and then was quenched with acetic acid while at 90 °C. Trimethoxybenzene internal standard was then weighed into each vial and a ^{1}H NMR (400 MHz, $CDCl_3$) spectrum was taken to determine the yield and α-deuterium incorporation in each reaction. For full characterization of **1–6–α–*d*$_1$** see Section A1.5.

Note: Provided below are example ^{1}H NMR spectra of starting styrene (**1–6**) and the crude reaction mixture containing α-deuterated product **1–6–α–*d*$_1$**. The chemical shift of the α-proton for 4-trifluoromethyl styrene (**1–6**) is 6.75 ppm.[4]

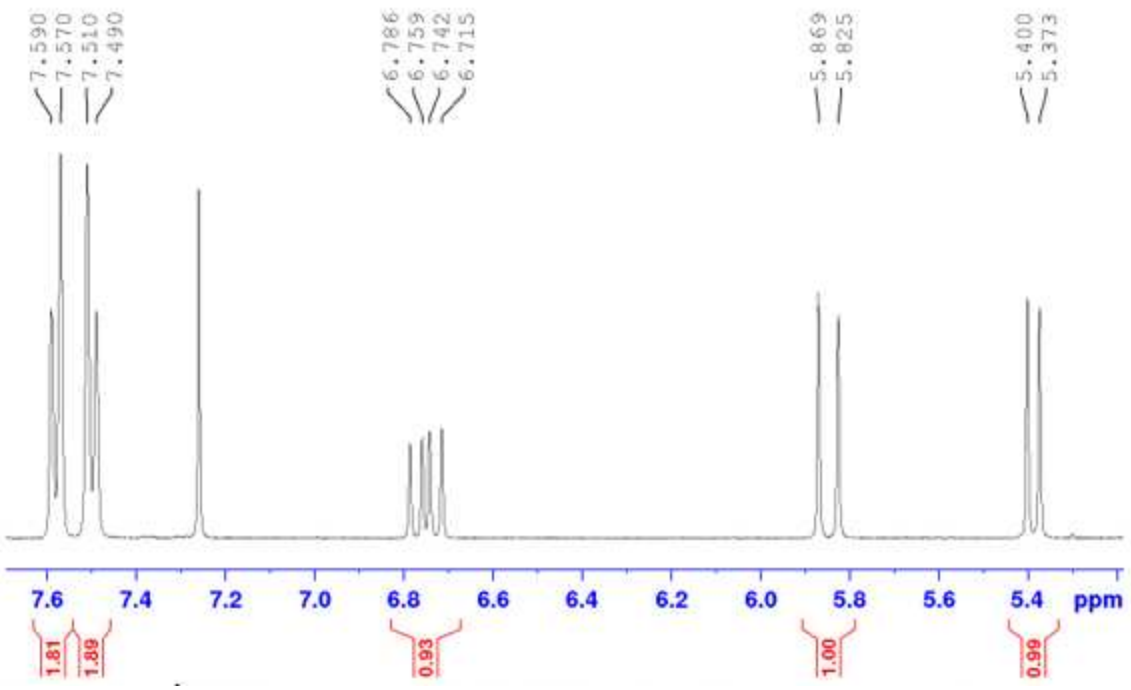

Figure A1–4: ^{1}H NMR spectrum (400 MHz, $CDCl_3$) of 1-(trifluoromethyl)-4-vinylbenzene.

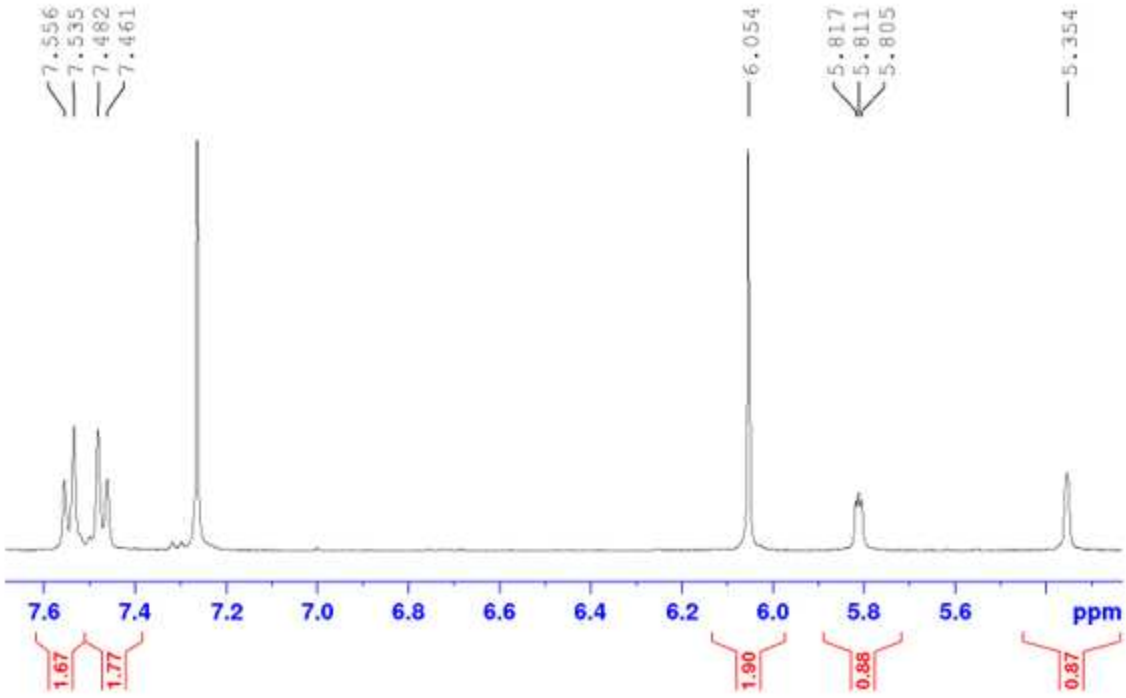

Figure A1–5: Preliminary α-deuteration reaction of 1-(trifluoromethyl)-4-vinylbenzene with P_4-*t*-Bu as the base (0.25 mmol scale; trimethoxybenzene (26.7 mg, 0.16 mmol) used as internal standard, 88% ^{1}H NMR yield, >99% α-deuteration).

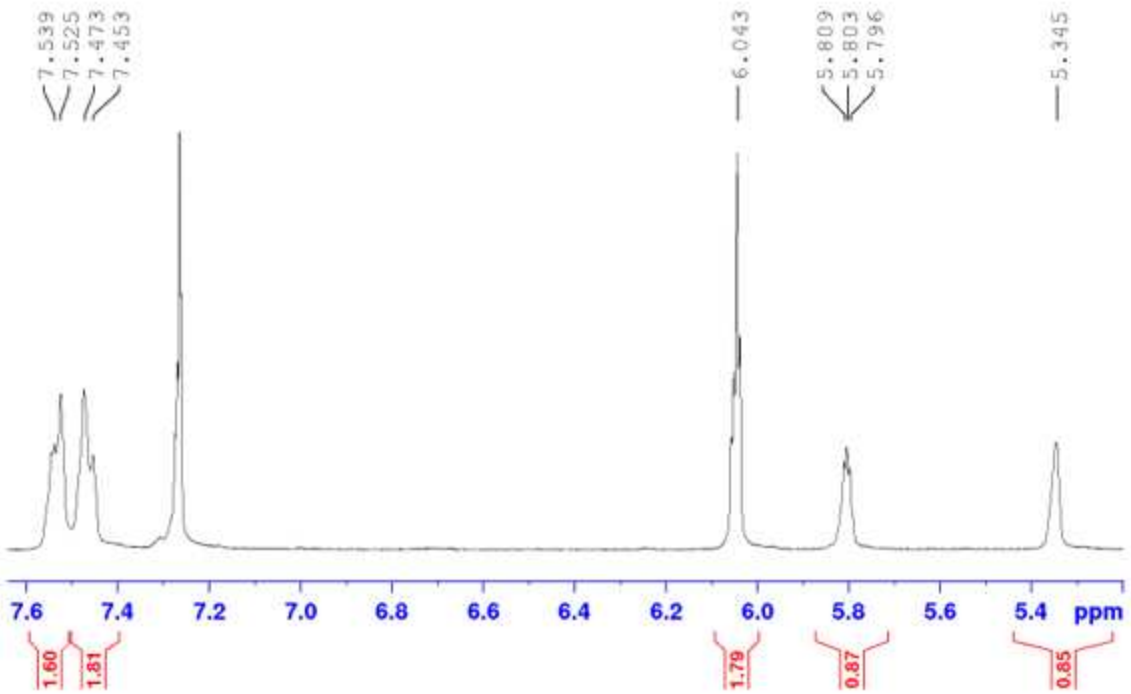

Figure A1–6 : Preliminary α-deuteration reaction of 1-(trifluoromethyl)-4-vinylbenzene with KO-*t*-Bu as the base (0.25 mmol scale; trimethoxybenzene (25.1 mg, 0.15 mmol) used as internal standard, 87% ^{1}H NMR yield, >99% α-deuteration).

A1.4 General Procedure for Preparation of *α*-Deuterated Styrenes

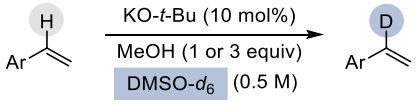

General procedure for 1 mmol scale reactions: KO-*t*-Bu, methanol and DMSO-d_6 were stored in a nitrogen filled glovebox until use. Outside of the glovebox, an oven-dried 4 mL vial (ThermoFisher, C4015-1) was charged with a magnetic stir bar and KO-*t*-Bu (11.2 mg, 0.1 mmol, 0.1 eq) and sealed with a PTFE-lined screw cap (ThermoFisher, C4015-1A). The vial was then evacuated and backfilled with nitrogen three times and left under positive pressure with a nitrogen balloon after the third cycle. A separate vial was then charged with the appropriate vinyl arene (1 mmol, 1 eq), methanol (1 or 3 mmol, 1 or 3 eq), and DMSO-d_6 (2.0 mL). This solution was sparged with nitrogen for three minutes, and then transferred to the vial containing KO-*t*-Bu via syringe.

The cap was then parafilmed, and the vessel was placed into a preheated silicon oil bath. The reactions were monitored by observing the disappearance of the *α*-proton by ^{1}H NMR spectroscopy (***Caution*:** the reactions were observed to be air sensitive and care should be taken to not introduce air to the system while taking aliquots.) After the indicated time, the reaction solution was quenched with acetic acid before allowing to cool to rt. The crude reaction mixture was washed with H_2O (30 mL), extracted with EtOAc (3 x 30 mL), dried over Na_2SO_4, and concentrated *in vacuo* unless otherwise noted. All substrates were purified by silica gel chromatography using the given conditions. The percentage of deuterium incorporation into the α-position was determined by integrating one terminal vinyl peak assumed to have a value of 1.0, to the residual α-proton signal. The percentage of deuterium incorporation into other positions was determined by integrating ^{2}H NMR signals to the calibrated α-deuterium signal (value determined by ^{1}H NMR). **Note:** ^{1}H NMR experiments with relaxation delays of 1 s and 5 s were taken to ensure that delay was not a factor in the depleted integration of the α-proton signal for all substrates. Both experiments showed the same percentage of α-deuterium incorporation.

Note on process used for identification of reaction conditions for each styrene substrate: Suitable conditions for preparative scale reactions could generally be found by testing 1 or 3 equivalents of MeOH at varying temperatures on a 0.1 mmol scale. For relatively electron-deficient substrates, a lower temperature (e.g. **1–21** was originally tested at 40 °C) was initially tested and suitable conditions could be identified from there. For relatively electron-rich substrates, a higher temperature (e.g. **1–17** was originally tested at 120 °C) was initially tested and suitable reaction conditions could be identified from there. If aromatic deuteration was an issue, it was found that lower temperatures and extended reactions times generally improved α-positional

selectivity. If the corresponding methyl ether comprised a significant amount of the mass balance, it was found that increasing the temperature generally improved the yield of the styrene.

A1.5 Characterization Data for α-Deuterated Styrenes

Note on nomenclature: The names provided for the structures below were obtained from ChemDraw Professional 16.0.

1-(trifluoromethyl)-4-(vinyl-1-*d*)benzene (1–6–α–d_1)

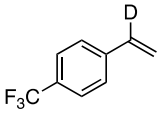

1-(trifluoromethyl)-4-(vinyl-1-*d*)benzene was prepared according to the general procedure using 1-(trifluoromethyl)-4-vinylbenzene (172.2 mg, 1 mmol, 1 eq), MeOH (40 µl, 1 mmol, 1 eq), KO-*t*-Bu (11.2 mg, 0.1 mmol, 0.1 eq), and DMSO-d_6 (2.0 mL). The solution was stirred at 90 °C for 1.5 h. Trimethoxybenzene internal standard (61.2 mg, 0.36 mmol) was added to the solution prior to purification to determine the ^{1}H NMR yield (86% yield). The crude reaction mixture was loaded directly onto a silica gel column and eluted with hexanes to afford the title compound as a clear oil (89.9 mg, 52% isolated yield, 99% α-deuteration, 1% other deuteration). **^{1}H NMR** (400 MHz, $CDCl_3$) δ 7.58 (d, J = 8.2 Hz, 2H), 7.50 (d, J = 8.2 Hz, 2H), 6.75 (dd, J_1 = 11.0 Hz, J_2 = 17.6 Hz, 0.01H), 5.84 (m, 1H), 5.39 (s, 1H). **^{13}C NMR** (101 MHz, $CDCl_3$) δ 141.1, 135.6 (T), 129.9 (q), 126.6, 125.8 (q), 123.1, 116.6. **^{2}H NMR** (62 MHz, CH_3CN) δ 7.66 (0.01D), 6.83 (0.99D). **^{19}F NMR** (376 MHz, $CDCl_3$) δ -63.5 (3F). **HRMS** (APCI) $[M+H]^+$ calcd. for $[C_9H_7DF_3]^+$ 174.0641, 174.0633 found. **IR** (neat, cm^{-1}) 3094, 2936, 2241, 1618, 1401, 1321, 1164, 1113, 1065, 1016, 918, 845.

1-bromo-2-(vinyl-1-*d*)benzene (1–11–α–d_1)

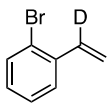

1-bromo-2-(vinyl-1-*d*)benzene was prepared according to the general procedure on a 2 mmol scale using 1-bromo-2-vinylbenzene (366.1 mg, 2 mmol, 1 eq), MeOH (64.1 mg,

2 mmol. 1 eq), KO-*t*-Bu (22.4 mg, 0.2 mmol, 0.1 eq), and DMSO-d_6 (4.0 mL). The solution was stirred at 70 °C for 2 h. The crude reaction mixture was loaded directly onto a silica gel column and eluted with hexanes to afford the title compound as a clear oil (330.4 mg, 90% yield, 97% α-deuteration, 0% other deuteration). **^{1}H NMR** (400 MHz, DMSO-d_6) δ 7.56 (m, 2H), 7.29 (t, J = 7.6 Hz, 1H), 7.12 (t, J = 7.6 Hz, 1H), 7.07 (dd, 0.03H), 5.71 (m, 1H), 5.37 (m, 1H). **^{13}C NMR** (101 MHz, $CDCl_3$) δ 137.7, 135.7 (T), 133.1, 129.3, 127.7, 127.0, 123.8, 116.7. **^{2}H NMR** (62 MHz, CH_3CN) δ 7.10 (0.97D). **HRMS** (APCI) $[M+H]^+$ calcd. for $[C_8H_7DBr]^+$ 183.9872, 183.9881 found. **IR** (neat, cm^{-1}) 3057, 2924, 2853, 2253, 1612, 1587, 1560, 1467, 1431, 1402, 1025, 916, 832, 756, 727, 660. Note: The α-deuterium incorporation was determined by ^{1}H NMR with DMSO-d_6 as the solvent. In $CDCl_3$ the α-proton overlaps with aromatic protons.

2-chloro-1-(trifluoromethyl)-3-(vinyl-1-*d*)benzene (1–9–α–d_1)

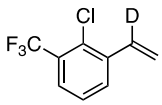

2-chloro-1-(trifluoromethyl)-3-(vinyl-1-*d*)benzene was prepared according to the general procedure using 2-chloro-1-(trifluoromethyl)-3-vinylbenzene (206.6 mg, 1 mmol, 1 eq), MeOH (40 µl, 1 mmol, 1 eq), KO-*t*-Bu (11.2 mg, 0.1 mmol, 0.1 eq), and DMSO-d_6 (2.0 mL). The solution was stirred at 70 °C for 10 min. The crude reaction mixture was loaded directly onto a silica gel column and eluted with hexanes to afford the title compound as a clear oil (144.2 mg, 70% yield, 97% α-deuteration, 0% other deuteration). **^{1}H NMR** (400 MHz, $CDCl_3$) δ 7.73 (d, J = 7.9 Hz, 1H), 7.62 (d, J = 7.8 Hz, 1H), 7.34 (t, J = 7.9 Hz, 1H), 7.18 (dd, J_1 = 11.0 Hz, J_2 = 17.4 Hz, 0.03H), 5.76 (m, 1H), 5.49 (s, 1H). **^{13}C NMR** (101 MHz, $CDCl_3$) δ 138.4, 132.5 (T), 131.1, 130.3, 129.3 (q), 127.0 (q), 126.7, 123.1 (q), 118.3. **^{2}H NMR** (62 MHz, CH_3CN) δ 7.21 (0.98D). **^{19}F NMR** (376 MHz, $CDCl_3$) δ -63.5 (3F). **GCMS** calcd. for $[C_9HDClF_3]^+$ 207.0, 207.0 found. **IR** (neat, cm^{-1}) 3093, 2918, 2360, 2341, 1581, 1428, 1399, 1316, 1170, 1125, 1086, 1049, 924, 802, 733.

1-iodo-2-(vinyl-1-*d*)benzene (1–12–α–d_1)

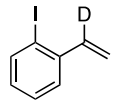

1-iodo-2-(vinyl-1-*d*)benzene was prepared according to the general procedure using 1-iodo-2-vinylbenzene (230 mg, 1 mmol, 1 eq), MeOH (120 µl, 3 mmol, 3 eq), KO-*t*-Bu (11.2 mg, 0.1 mmol, 0.1 eq), and DMSO-d_6 (2.0 mL). The solution was stirred at 100 °C for 2 h. Silica gel chromatography (2% EtOAc/hexanes) yielded the title compound as a clear oil (177.9 mg, 77% yield, 99% α-deuteration, 1% other deuteration). **^{1}H NMR** (400 MHz, $CDCl_3$) δ 7.84 (d, J = 7.9 Hz, 1H), 7.52 (d, J = 7.8 Hz, 1H), 7.32 (t, J = 7.5 Hz, 1H), 6.95 (t, J = 7.6 Hz, 1H), 6.91 (dd, 0.01H), 5.63 (m, 1H), 5.33 (s, 1H). **^{13}C NMR** (101 MHz, $CDCl_3$) δ 140.9, 140.5 (T), 139.7, 129.5, 128.6, 126.6, 116.9, 99.9. **^{2}H NMR** (62 MHz, CH_3CN) δ 7.92 (0.01D), 6.93 (0.99D). **HRMS** (APCI) $[M+H]^+$ calcd. for $[C_8H_7DI]^+$ 231.9733, 231.9722 found. **IR** (neat, cm^{-1}) 3052, 2922, 2245, 1610, 1583, 1555, 1462, 1430, 1400, 1010, 916, 756, 646.

methyl 4-(vinyl-1-*d*)benzoate (1–13–α–d_1)

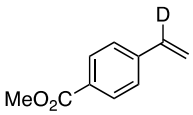

Methyl 4-(vinyl-1-*d*)benzoate was prepared according to the general procedure using methyl 4-vinylbenzoate (162.2 mg, 1 mmol, 1eq), MeOH (40 µl, 1 mmol, 1 eq), KO-*t*-Bu (11.2 mg, 0.1 mmol, 0.1 eq), and DMSO-d_6 (2.0 mL). The solution was stirred at 50 °C for 12 h. Silica gel chromatography (15% EtOAc/hexanes) yielded the title compound as a white solid (103.0 mg, 63% yield, 99% α-deuteration, 0% other deuteration). **Melting Point**: 33-34 °C. **^{1}H NMR** (400 MHz, $CDCl_3$) δ 7.98 (d, J = 8.2 Hz, 2H), 7.45 (d, J = 8.2 Hz, 2H), 6.74 (dd, J_1 = 10.8 Hz, J_2 = 17.6 Hz, 0.01H), 5.84 (s, 1H), 5.36 (s, 1H), 3.90 (s, 3H). **^{13}C NMR** (101 MHz, $CDCl_3$) δ 166.9, 141.9, 135.7 (T), 129.9, 129.3, 126.1, 116.3, 52.2. **^{2}H NMR** (62 MHz, CH_3CN)

δ 6.80 (0.99D). **HRMS** (DART) $[M+H]^+$ calcd. for $[C_{10}H_{10}DO_2]^+$ 164.0822, 164.0820 found. **IR** (neat, cm^{-1}) 2949, 2848, 2230, 1713, 1606, 1436, 1275, 1180, 1102, 1015, 962, 931, 861, 779, 710.

_N_,_N_-diethyl-3-(vinyl-1-_d_)benzamide (1–14–α–d_1)

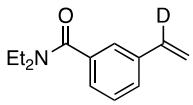

_N_,_N_-diethyl-3-(vinyl-1-_d_)benzamide was prepared according to the general procedure using _N_,_N_-diethyl-3-vinylbenzamide (203.3 mg, 1 mmol, 1 eq), MeOH (40 µl, 1 mmol, 1 eq), KO-_t_-Bu (11.2 mg, 0.1 mmol, 0.1 eq), and DMSO-d_6 (2.0 mL). The solution was stirred at 100 °C for 24.5 h. Silica gel chromatography (50% EtOAc/hexanes) yielded the title compound as a viscous clear oil (151.7 mg, 74% yield, 98% α-deuteration, 0% other deuteration). **^{1}H NMR** (400 MHz, $CDCl_3$) δ 7.41-7.43 (m, 2H), 7.34 (t, J = 7.5 Hz, 1H), 7.23-7.25 (m, 1H), 6.71 (dd, J_1 = 11.1 Hz, J_2 = 17.7 Hz, 0.02H), 5.77 (s, 1H), 5.29 (s, 1H), 3.27-3.56 (m, 4H), 1.12-1.26 (m, 6H). **^{13}C NMR** (101 MHz, $CDCl_3$) δ 171.1, 137.8, 137.6, 135.9 (T), 128.6, 126.9, 125.6, 124.1, 114.6, 43.3, 39.2, 14.3, 12.9. **^{2}H NMR** (62 MHz, CH_3CN) δ 6.82 (0.98D). **HRMS** (DART) $[M+H]^+$ calcd. for $[C_{13}H_{17}DNO]^+$ 205.1451, 205.1458 found. **IR** (neat, cm^{-1}) 2972, 2934, 2234, 1626, 1433, 1290, 1098, 909, 802, 707.

(trifluoromethyl)(4-(vinyl-1-_d_)phenyl)sulfane (1–15–α–d_1)

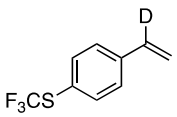

(trifluoromethyl)(4-(vinyl-1-_d_)phenyl)sulfane was prepared according to the general procedure using (trifluoromethyl)(4-vinylphenyl)sulfane (204.2 mg, 1 mmol, 1 eq), MeOH (121 µl, 3 mmol, 3 eq), KO-_t_-Bu (11.2 mg, 0.1 mmol, 0.1 eq), and DMSO-d_6 (2.0 mL). The solution was stirred at 80 °C for 3 h. The crude reaction mixture was loaded directly onto a silica gel column and eluted with hexanes to afford the title compound as a clear oil (102.4 mg, 50% yield, 95% α-deuteration, 0% other deuteration). **^{1}H NMR** (400 MHz, $CDCl_3$) δ 7.62 (d,

J = 8.2, 2H), 7.45 (d, J = 8.2, 2H), 6.73 (dd, J_1 = 10.9 Hz, J_2 = 17.6 Hz, 0.05H), 5.84 (m, 1H), 5.38 (s, 1H). **^{13}C NMR** (101 MHz, $CDCl_3$) δ 140.2, 136.7, 135.5 (T), 129.7 (q), 127.3, 123.5, 116.4. **^{2}H NMR** (62 MHz, CH_3CN) δ 6.84 (0.95D). **^{19}F NMR** (376 MHz, $CDCl_3$) δ -43.83 (3F). **HRMS** (APCI) $[M + H]^+$ calcd. for $[C_9H_7DF_3S]$ 206.0362, 206.0358 found. **IR** (neat, cm^{-1}) 3092, 2926, 2359, 2239, 1491, 1396, 1118, 1102, 1014, 916, 839.

(*E*)-1-styryl-4-(vinyl-1-*d*)benzene (1–16–α–d_1)

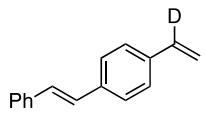

(*E*)-1-styryl-4-(vinyl-1-*d*)benzene was prepared using a modified procedure. (*E*)-1-styryl-4-vinylbenzene (206.3 mg, 1.0 mmol, 1.0 eq) and NaH (60% dispersion, 8.0 mg, 0.2 mmol, 0.2 eq) was weighed into a 4 mL oven-dried vial (ThermoFisher, C4015-1). The vial was sealed with a PTFE lined screw cap (ThermoFisher, C4015-1A) and parafilmed. The vial was evacuated and backfilled three time with N_2 using a nitrogen balloon and left under positive pressure after the third cycle. MeOH (121 µl, 3 mmol, 3 eq) and d_6-DMSO (2.0 mL) was measured into a separate vial, bubbled with N_2 for three minutes, and then added to the NaH/(*E*)-1-styryl-4-(vinyl-1-*d*)benzene mixture via syringe. The rest of the procedure was carried out in accordance with the general procedure. The solution was stirred at 90 °C for 24 h. Silica gel chromatography (3% EtOAc/hexanes) yielded the title compound as a pale yellow solid (192.5 mg, 93% yield, 97% α-deuteration, 0% other deuteration). **Melting Point**: 159-162 °C. **^{1}H NMR** (400 MHz, $CDCl_3$) δ 7.48-7.53 (m, 4H), 7.34-7.42 (m, 4H), 7.24-7.28 (m, 1H), 7.11 (s, 2H), 6.72 (dd, J_1 = 10.8 Hz, J_2 = 17.5 Hz, 0.03H), 5.76 (s, 1H), 5.25 (s, 1H). **^{13}C NMR** (101 MHz, $CDCl_3$) δ 137.3, 137.1, 137.0, 136.2 (T), 128.7, 128.6, 128.3, 127.7, 126.7, 126.6, 126.5, 113.6. **^{2}H NMR** (62 MHz, CH_3CN) δ 6.80 (0.97D). **HRMS** (APCI) $[M+H]^+$ calcd. for $[C_{16}H_{14}D]$ 208.1237,

208.1227 found. **IR** (neat, cm^{-1}) 3080, 3053, 3021, 2923, 2360, 2341, 2226, 1607, 1508, 1389, 1448, 1401, 966, 903, 828, 757, 733, 690.

2-(vinyl-1-*d*)naphthalene (1–17–α–d_1)

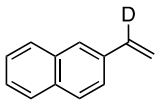

2-(vinyl-1-*d*)naphthalene was prepared according to the general procedure using 2-vinylnaphthalene (154.2 mg, 1 mmol, 1 eq), MeOH (121µl, 3 mmol, 3 eq), KO-*t*-Bu (11.2 mg, 0.1 mmol, 0.1 eq), and DMSO-d_6 (2.0 mL). The solution was stirred at 130 °C for 4 h. Silica gel chromatography (hexanes) yielded the title compound as a white powder (133.0 mg, 86% yield, 97% α-deuteration, 4% other deuteration). **Melting Point**: 64-65 °C. **^{1}H NMR** (400 MHz, $CDCl_3$) δ 7.80-7.84 (m, 3H), 7.77 (s, 1H), 7.66 (dd, J_1 = 8.6 Hz, J_2 = 1.7 Hz, 1H), 7.44-7.50 (m, 2H), 6.91 (dd, J_1 = 10.8 Hz, J_2 = 17.6 Hz, 0.03H), 5.89 (m, 1H), 5.36 (s, 1H). **^{13}C NMR** (101 MHz, $CDCl_3$) δ 136.8 (T), 135.2, 133.8, 133.5, 128.3, 128.2, 127.9, 126.5, 126.4, 126.1, 123.3, 114.2. **^{2}H NMR** (62 MHz, CH_3CN) δ 7.85 (0.04D), 6.93 (0.97D). **HRMS** (APCI) $[M+H]^+$ calcd. for $[C_{12}H_9D]^+$ 156.0924, 156.0886 found. **IR** (neat, cm^{-1}) 3053, 2922, 2852, 2361, 2341, 1613, 1590, 1571, 1505, 1185, 894, 861, 820, 749.

1-(vinyl-1-*d*)naphthalene (1–18–α–d_1)

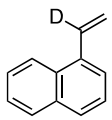

1-(vinyl-1-*d*)naphthalene was prepared according to the general procedure using 1-vinylnapthalene (154.2 mg, 1 mmol, 1 eq), MeOH (121 µl, 3 mmol, 3 eq), KO-*t*-Bu (11.2 mg, 0.1 mmol, 0.1 eq), and DMSO-d_6 (2.0 mL). The solution was stirred at 130 °C for 4 h. Silica gel chromatography (hexanes eluent) yielded the title compound as a clear oil (122.2 mg, 79% yield, 99% α-deuteration, 0% other deuteration). **^{1}H NMR** (400 MHz, $CDCl_3$) δ 8.15 (d, J = 8.2 Hz, 1H), 7.88 (d, J = 8.1 Hz, 1H), 7.82 (d, J = 8.2 Hz, 1H), 7.66 (d, J = 7.1 Hz, 1H), 7.46-7.56

(m, 3H), 5.82 (m, 1H), 5.51 (s, 1H). **^{13}C NMR** (101 MHz, $CDCl_3$) δ 135.7, 134.3 (T), 133.8, 131.1, 128.7, 128.3, 126.3, 125.9, 125.8, 123.9, 123.8, 117.1. **^{2}H NMR** (62 MHz, CH_3CN) δ 7.57 (0.99D). **HRMS** (APCI) $[M+H]^+$ calcd. for $[C_{12}H_{10}D]^+$ 156.0924, 156.0952 found. **IR** (neat, cm^{-1}) 3045, 2924, 2852, 2242, 1609, 1590, 1409, 1337, 914, 797, 773.

9-chloro-10-(vinyl-1-*d*)anthracene (1–19–α–d_1)

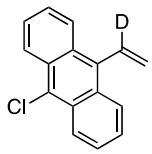

9-chloro-10-(vinyl-1-*d*)anthracene was prepared according to the general procedure using 9-chloro-10-vinylanthracene (238.7 mg, 1 mmol, 1 eq), MeOH (40 µl, 1 mmol, 1 eq), KO-*t*-Bu (11.2 mg, 0.1 mmol, 0.1 eq), and DMSO-d_6 (2.0 mL). The solution was stirred at 70 °C for 45 min. Silica gel chromatography (hexanes) yielded the title compound as a yellow solid (199.6 mg, 83% yield, 99% α-deuteration, 0% other deuteration). **Melting Point**: 111-114 °C. **^{1}H NMR** (400 MHz, CD_2Cl_2) δ 8.54 (d, J = 8.8 Hz, 2H), 8.37 (d, J = 8.8 Hz, 2H), 7.61-7.65 (m, 2H), 7.52-7.56 (m, 2H), 6.06 (s, 1H), 5.61 (s, 1H). **^{13}C NMR** (101 MHz, CD_2Cl_2) δ 134.0, 133.3 (T), 130.1, 128.9, 128.4, 127.1, 126.8, 126.0, 125.2, 123.8. **^{2}H NMR** (62 MHz, CH_3CN) δ 7.54 (0.99D). **HRMS** (APCI) $[M+H]^+$ calcd. for $[C_{16}H_{11}DCl]^+$ 240.0690, 240.0661 found. **IR** (neat, cm^{-1}) 3078, 3038, 2981, 2921, 2222, 1619, 1439, 1420, 1327, 1258, 925, 757.

2-(4-(vinyl-1-*d*)phenyl)pyridine (1–8–α–d_1)

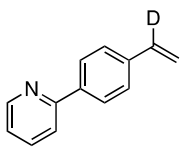

2-(4-(vinyl-1-*d*)phenyl)pyridine was prepared according to the general procedure using 2-(4-vinylphenyl)pyridine (181.2 mg, 1 mmol, 1 eq), MeOH (40 µl, 1 mmol, 1 eq), KO-*t*-Bu (11.2 mg, 0.1 mmol, 0.1 eq), and DMSO-d_6 (2.0 mL). The solution was stirred at 70 °C for 24 h. Silica gel chromatography (30% EtOAc/hexanes) yielded the title compound as a pale yellow oil (151.6 mg, 83% yield, 97% α-deuteration, 4% other deuteration).

^{1}H NMR (400 MHz, $CDCl_3$) δ 8.69 (d, J = 4.6 Hz, 1H), 7.98 (d, J = 8.2 Hz, 2H), δ 7.71-7.76 (m, 2H), 7.52 (d, J = 8.2 Hz, 2H), 7.22 (m, 1H), 6.77 (dd, J_1 = 11.0 Hz, J_2 = 17.7 Hz, 0.03H), 5.82 (s, 1H), 5.30 (s, 1H). **^{13}C NMR** (101 MHz, $CDCl_3$) 157.2, 149.9, 139.9, 138.4, 136.9, 136.3 (T), 127.2, 126.8, 122.3, 120.6, 114.5. **^{2}H NMR** (62 MHz, CH_3CN) δ 7.85 (0.04D), 6.84 (0.97D). **HRMS** (DART) $[M+H]^+$ calcd. for $[C_{13}H_{11}DN]^+$ 183.1033, 183.1041 found. **IR** (neat, cm^{-1}) 3083, 3049, 3007, 2232, 1612, 1587, 1572, 1465, 1433, 908., 850, 783, 739.

2-(vinyl-1-*d*)pyridine (1–21–α–d_1)

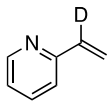

2-(vinyl-1-*d*)pyridine was prepared according to the general procedure using 2-vinylpyridine (105.1 mg, 1 mmol, 1 eq), MeOH (20 µl, 0.5 mmol, 0.5 eq), KO-*t*-Bu (11.2 mg, 0.1 mmol, 0.1 eq), and DMSO-d_6 (2.0 mL). The solution was stirred at 50 °C for 12.5 h. Trimethoxybenzene internal standard (79.3 mg, 0.47 mmol) was added to the solution prior to purification to determine the ^{1}H NMR yield (78% yield). The crude reaction mixture was loaded directly onto a silica gel column and eluted with a gradient of hexanes to 20% Et_2O/hexanes to afford the title compound as a clear oil (65.2 mg, 61% isolated yield, >99% α-deuteration, 0% other deuteration). **^{1}H NMR** (400 MHz, $CDCl_3$) δ 8.58 (d, J = 4.6 Hz, 1H), δ 7.64 (td, J_1 = 7.7 Hz, J_2 = 1.8 Hz, 1H), 7.34 (d, J = 7.8 Hz, 1H), 7.15 (m, 1H), 6.82 (dd, J_1 = 11.0 Hz, J_2 = 17.6 Hz, 0.01H), 6.20 (s, 1H), 5.48 (s, 1H). **^{13}C NMR** (101 MHz, $CDCl_3$) δ 155.9, 149.7, 136.8 (T), 136.6, 122.6, 121.4, 118.2. **^{2}H NMR** (62 MHz, $CDCl_3$) δ 6.83 (0.99D). **HRMS** (DART) $[M+H]^+$ calcd. for $[C_7H_7DN]$ 107.0720, 107.0735 found. **IR** (neat, cm^{-1}) 3077, 3005, 2926, 2218, 1586, 1563, 1470, 1432, 1150, 925, 796, 730.

5-(vinyl-1-*d*)isoquinoline (1–20–α–d_1)

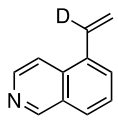

5-(vinyl-1-*d*)isoquinoline was prepared according to the general procedure using 5-vinylisoquinoline (155.2 mg, 1 mmol, 1 eq), MeOH (40 µl, 1 mmol, 1 eq), KO-*t*-Bu (11.2 mg, 0.1 mmol, 0.1 eq), and DMSO-d_6 (2.0 mL). The solution was stirred at 60 °C for 6 h. Silica gel chromatography (30% EtOAc/hexanes) yielded the title compound as a pale yellow oil (118.1 mg, 76% yield, 97% α-deuteration, 0% other deuteration). **^{1}H NMR** (400 MHz, $CDCl_3$) δ 9.24 (s. 1H), 8.54 (d, J = 6.0 Hz, 1H), 7.82-7.90 (m, 3H), 7.57 (t, J = 7.4 Hz, 1H), 7.36 (dd, J_1 = 11.0 Hz, J_2 = 17.4 Hz, 0.03H), 5.83 (s, 1H), 5.53 (s, 1H). **^{13}C NMR** (101 MHz, $CDCl_3$) δ 153.3, 143.5, 134.6, 133.8, 132.5 (T), 129.0, 127.7, 127.5, 127.2, 118.2, 116.8. **^{2}H NMR** (62 MHz, CH_3CN) δ 7.49 (0.97D). **HRMS** (APCI) $[M+H]^+$ calcd. for $[C_{11}H_9DN]^+$ 157.0876, 157.0871 found. **IR** (neat, cm^{-1}) 3055, 3026, 2923, 2851, 1616, 1584, 1487, 1367, 915, 809, 755, 686.

6-(vinyl-1-*d*)quinoline (1–22–α–d_1)

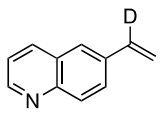

6-(vinyl-1-*d*)quinoline was prepared according to the general procedure using 6-vinylquinoline (155.2 mg, 1 mmol, 1 eq), MeOH (40 µl, 1 mmol, 1 eq), KO-*t*-Bu (11.2 mg, 0.1 mmol, 0.1 eq), and DMSO-d_6 (2.0 mL). The solution was stirred at 60 °C for 13.5 h. Silica gel chromatography (40% EtOAc/hexanes) yielded the title compound as a pale yellow oil (131.5 mg, 84% yield, 95% α-deuteration, 4% other deuteration). **^{1}H NMR** (400 MHz, $CDCl_3$) δ 8.86 (d, J = 4.3 Hz, 1H), 8.04-8.11 (m, 2H), 7.86 (d, J = 8.9 Hz, 1H), 7.70 (s, 1H), 7.37 (dd, J_1 = 4.2 Hz, J_2 = 8.2 Hz, 1H), 6.88 (dd, J_1 = 10.9 Hz, J_2 = 17.6 Hz, 0.05H), 5.89 (m, 1H), 5.39 (s, 1H). **^{13}C NMR** (101 MHz, $CDCl_3$) δ 150.2, 148.2, 136.1 (T), 136.0, 135.8, 135.6, 129.7, 128.4, 125.8, 121.4, 115.2. **^{2}H NMR** (62 MHz, CH_3CN) δ 8.19 (0.04D), 6.91 (0.95D). **HRMS** (DART)

$[M+H]^+$ calcd. for $[C_{11}H_9DN]^+$ 157.0876, 157.0880 found. **IR** (neat, cm^{-1}) 3016, 2923, 2233, 1585, 1498, 908, 888, 837, 795, 775.

prop-1-en-1-yl-1,3,3,3-*d*$_4$ benzene (1–23)

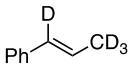

Prop-1-en-1-yl-1,3,3,3-d_4 benzene was prepared according to the general procedure using (*Z*)-prop-1-en-1-ylbenzene (118.2 mg, 1 mmol, 1 eq), MeOH (40 µl, 1 mmol, 1 eq), KO-*t*-Bu (11.2 mg, 0.1 mmol, 1 eq), and DMSO-d_6 (2.0 mL). The solution was stirred at 60 °C for 21.5 h. The crude reaction mixture was loaded directly onto a silica gel column and eluted with hexanes to afford an isomeric mixture (*E*/*Z* approximately 97:3) of the title compound as a clear oil (81.6 mg, 67% yield, 97% β-methyl deuteration, 95% α-deuteration, 0% other deuteration). Note: "*" denotes minor isomer. **^{1}H NMR** (400 MHz, $CDCl_3$) δ 7.28-7.35 (m, 4H), 7.20 (t, J = 7.1 Hz, 1H), 6.41 (d, J = 15.8 Hz, 0.05H), 6.23 (m, 1H), 5.79* (m, 0.03H), 1.86 (m, 0.10H). **^{13}C NMR** (101 MHz, $CDCl_3$) δ 138.1, 131.0 (T), 129.0, 128.7, 126.9, 125.6, 17.9 (m). **^{2}H NMR** (62 MHz, CH_3CN) δ 6.47 (1D), 1.82 (3D). **GCMS** calcd. for $[C_9H_6D_4]^+$ 122.1, 122.1 found. **IR** (neat, cm^{-1}) 3080, 3058, 3023, 2924, 2223, 2110, 1494, 1446, 930, 769, 692.

1-(2-methoxyvinyl-1-*d*)-4-(trifluoromethyl)benzene (1–24–α–*d*$_1$)

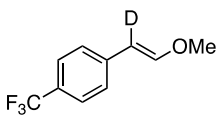

1-(2-methoxyvinyl-1-*d*)-4-(trifluoromethyl)benzene was prepared using a slightly modified procedure. Inside a nitrogen filled glovebox, 1-(2-methoxyvinyl)-4-(trifluoromethyl)benzene (101.0 mg, 0.5 mmol, 1 eq), MeOH (20 µl, 0.5 mmol, 1 eq), KO-*t*-Bu (5.6 mg, 0.05 mmol, 0.1 eq) and DMSO-d_6 (1.0 mL) were added to an oven-dried 4 mL vial (ThermoFisher, C4015-1). The vial was sealed with a PTFE lined screw cap (ThermoFisher, C4015-1A) and then removed from the glovebox. The solution was placed into a

preheated 100 °C aluminum reaction block for 26 h. The reaction solution was quenched with acetic acid before allowing to cool to rt. The crude reaction mixture was washed with H_2O (20 mL), extracted with EtOAc (3 x 20 mL), dried with Na_2SO_4 and concentrated *in vacuo*. Silica gel chromatography (1% EtOAc/hexanes) yielded an isomeric mixture (*E/Z* approximately 2:1) of the title compound as a clear oil (65.8 mg, 65% yield, 97% α-deuteration, 0% other deuteration). Note: "*" denotes minor isomer. **^{1}H NMR** (400 MHz, $CDCl_3$) δ 7.65* (d, J = 8.1 Hz, 1H), 7.49-7.53 (m, 3H), 7.31 (d, J = 8.0 Hz, 2H), 7.13 (s, 1H), 6.24* (s, 0.48H), 5.82 (d, J = 12.9 Hz, 0.01H), 5.25* (d, J = 7.0 Hz, 0.01H), 3.82* (s, 1.5H), 3.72 (s, 3H). **^{13}C NMR** (101 MHz, $CDCl_3$) δ 150.6, 149.8, 140.2, 139.4, 128.1, 127.6, 127.4, 127.3, 127.1, 125.8 (q), 125.0 (q), 124.9, 123.1, 123.0, 103.9, 103.7, 103.3, 61.0, 56.7. **^{2}H NMR** (62 MHz, CH_3CN) δ 5.95 (1D), 5.35* (1D). **^{19}F NMR** (376 MHz, $CDCl_3$) δ -63.29 (3F), -63.31* (3F). **IR** (neat, cm^{-1}) 3011, 2937, 1641, 1613, 1321, 1104, 1065, 841. **HRMS** (APCI) $[M+H]^+$ calcd. for $[C_{10}H_9DF_3O]^+$ 204.0747, 204.0737 found. A HMBC 2D-NMR was acquired to confirm that the α-position (and not the β-position) was deuterated. The 3-bond correlation between the $-OCH_3$ carbon and the β-proton (see section A1.7) is consistent with the signal that disappears due to incorporation of deuterium and does not correspond to the β-proton.

(*E*)-1,2-di(pyridin-4-yl)ethene-1,2-*d*$_2$ (1–25–α–*d*$_1$)

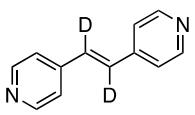

(*E*)-1,2-di(pyridin-4-yl)ethene-1,2-d_2 was prepared according to the general procedure using (*E*)-1,2-di(pyridin-4-yl)ethene (182.2 mg, 1 mmol, 1 eq), MeOH (202 µl, 5 mmol, 5 eq), KO-*t*-Bu (11.2 mg, 0.1 mmol, 0.1 eq), and DMSO-d_6 (2.0 mL). The solution was stirred at 60 °C for 72 h. Silica gel chromatography (10% MeOH/CH_2Cl_2) yielded the title compound as a yellow solid (144.0 mg, 79% yield, 95% α-deuteration, 0% other deuteration).

Melting Point: 151-152 °C. **^{1}H NMR** (400 MHz, DMSO-d_6) δ 8.61 (d, J = 6.0 Hz, 4H), 7.62 (d, J = 6.0 Hz, 4H), 7.54 (s, 0.09 H). **^{13}C NMR** (101 MHz, $CDCl_3$) δ 150.4, 143.3, 130.1 (T), 121.1. **^{2}H NMR** (62 MHz, CH_3CN) δ 7.43 (0.95D). **HRMS** (DART) $[M+H]^+$ calcd. for $[C_{12}H_9N_2D_2]^+$ 185.1048, 185.1048 found. **IR** (neat, cm^{-1}) 3020, 2923, 2362, 2341, 1594, 1409, 819, 542.

A1.6 Influence of MeOH on Reaction Kinetics and Mass Balance

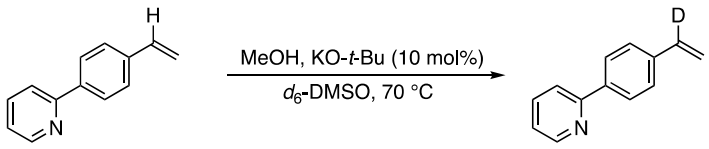

General Procedure: Outside of the glovebox, 2-(4-vinylphenyl)pyridine (**1–8**) (181.2 mg, 1 mmol, 1 eq) was weighed to three oven-dried 4 mL vial (ThermoFisher, C4015-1). Inside of a nitrogen filled glovebox, the appropriate quantity of MeOH (40 µl, 1 mmol, 1 eq; (20 µl, 0.5 mmol, 0.5 eq; or 10 µl, 0.25 mmol, 0.25 eq) and DMSO-d_6 (2.0 mL) were added to each vial. The solutions were then added to an oven-dried 4 mL vial (ThermoFisher, C4015-1) containing KO-*t*-Bu (11.2 mg, 0.1 mmol, 0.1 eq) and approximately 0.35 mmol of trimethoxybenzene. The solution was agitated until homogenous and then divided into eight separate 0.25 mL portions into eight oven-dried 4 mL vials (ThermoFisher, C4015-1) and sealed with PTFE lined screw cap (ThermoFisher, C4015-1A). The solutions were removed from the glovebox and placed into a preheated 70 °C aluminum reaction block. For each reaction time point in the tables below, a separate reaction solution was quenched with acetic acid at 70 °C and an ^{1}H NMR spectrum was acquired. The ^{1}H NMR (400 MHz, $CDCl_3$) spectrum was used to determine the percentage of deuterium incorporation into the α-position and the overall quantity of styrene (indicated as NMR yield below).

Time (min)	α-deuteration (%)	NMR Yield (%)
15	16	99
60	45	99
90	53	99
180	80	99
300	90	98.5
360	93	98.5
600	100	97

Figure A1–7: Results of α-deuteration reaction of **1–8** using 1 equiv MeOH.

Time (min)	α-deuteration (%)	NMR Yield (%)
10	15	99
20	23	99
30	30	99
40	40	98
80	61	97
170	89	91
210	93	89
300	100	75

Figure A1–8: Results of α-deuteration reaction of **1–8** using 0.5 equiv MeOH.

Time (min)	α-deuteration (%)	NMR Yield (%)
10	26	90
20	38	85
30	46	77
50	63	65
70	72	48
100	79	30
110	81	22

Figure A1–9: Results of α-deuteration reaction of **1–8** using 0.25 equiv MeOH.

A1.7 Overcoming S_NAr for 2-chloro-3-vinylpyridine

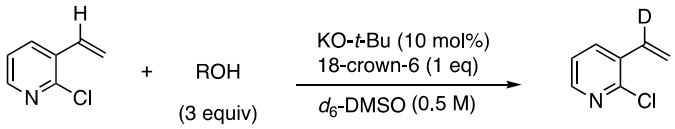

2-chloro-3-(vinyl-1-*d*)pyridine (1–26–α–d_1)

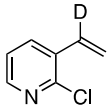

2-chloro-3-vinyl pyridine (69.8 mg, 0.5 mmol, 1 eq) was weighed into an oven-dried 4 mL vial (ThermoFisher, C4015-1). The vial was sealed and brought into a nitrogen filled glovebox where 1-cyclopropyl ethanol (147 µl, 1.5 mmol, 3 eq) or anhydrous MeOH (61 µl, 1.5 mmol, 3 eq) was added followed by DMSO-d_6 (1.0 mL), 18-crown-6 ether (132.2 mg, 0.5 mmol, 1 eq), and KO-*t*-Bu (11.2 mg, 1 mmol, 1 eq). The vials were capped, removed from glovebox and placed into a pre-heated 40 °C silicon oil bath and stirred for 1 h. The reaction solutions were quenched with acetic acid after 1 h while at 40 °C. The reaction solutions were then washed with H_2O (20 mL) and extracted with EtOAc (3 x 20 mL), dried over Na_2SO_4, and

concentrated *in vacuo*. Silica gel chromatography (2% EtOAc/hexanes) yielded the title compound as a light yellow oil. **Note**: provided below are regions of the isolated alkene ^{1}H NMR spectra using both alcohols for comparison of the degree of deuterium incorporation.

Using MeOH: (30.1 mg, 43% yield, 21% α-deuteration, 0% other deuteration).

Using 1-cyclopropylethanol: (44.1 mg, 63% yield, 96% α-deuteration, 0% other deuteration)

^{1}H NMR (400 MHz, $CDCl_3$) δ 8.30 (dd, J_1 = 4.7 Hz, J_2 = 1.8 Hz, 1H), 7.87 (dd, J_1 = 7.8 Hz, J_2 = 1.8 Hz, 1H), 7.23 (dd, J_1 = 7.8 Hz, J_2 = 4.7 Hz, 1H), 7.03 (dd, J_1 = 17.5 Hz, J_2 = 11.0 Hz, 0.04H), 5.78 (m, 1H), 5.49 (s, 1H). **^{13}C NMR** (101 MHz, $CDCl_3$) δ 150.2, 148.8, 135.1, 132.5, 131.9 (T), 122.9, 118.7. **^{2}H NMR** (CH_3CN, 62 MHz) δ 7.01 (0.96D). **HRMS** (APCI): $[M+H]^+$ calcd. for $[C_7H_6DClN]^+$ 141.0330, 141.0334 found. **IR** (neat, cm^{-1}) 3090, 3045, 2926, 2853, 1555, 1381, 1134, 1063, 922, 803, 682.

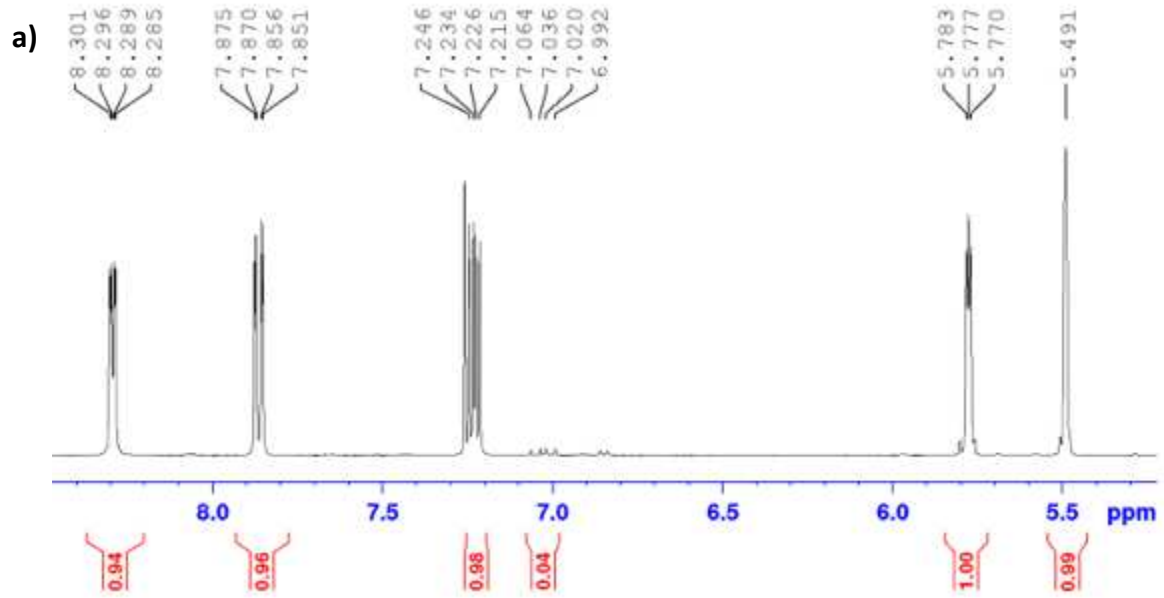

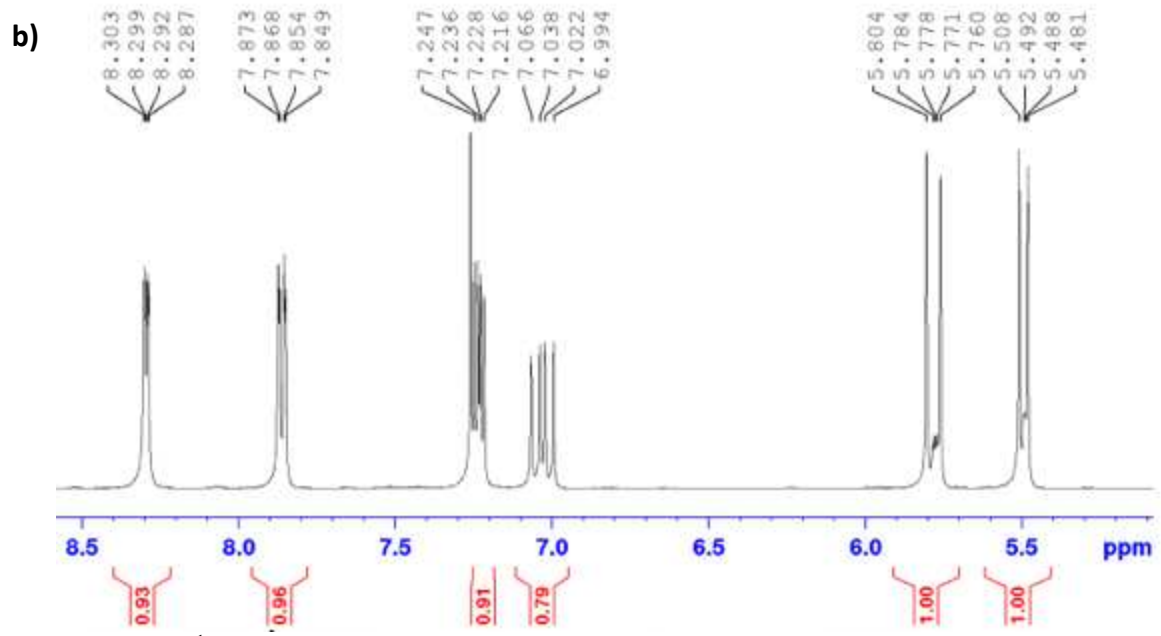

Figure A1–10: ^{1}H NMR spectra of 1-cyclopropylethanol **(a)** and MeOH **(b)** conditions.

A1.8 Enantioselective Derivatization of α-Deuterated Styrenes

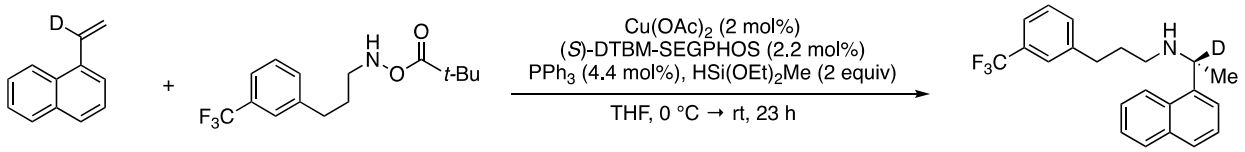

(*R*)-*N*-(1-(naphthalen-1-yl)ethyl-1-*d*)-3-(3-(trifluoromethyl)phenyl)propan-1-amine (1-32)

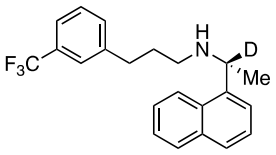

This procedure was adopted from a literature report.[1] Inside a nitrogen filled glovebox, $Cu(OAc)_2$ (3.7 mg, 0.02 mmol), (*S*)-DTBM-SEGPHOS (26.0 mg, 0.022 mmol), PPh_3 (11.5 mg, 0.044 mmol) and THF (1.0 mL) were added to an oven-dried 4 mL vial (ThermoFisher, C4015-1). The vial was sealed with a screw cap lined with a PTFE septum (ThermoFisher, C4015-1A), removed from the glovebox, and stirred under ambient conditions until the solution was homogenous. The solution was then taken back into the glovebox and $HSi(OEt)_2Me$ (320 µl, 2.0 mmol) was added. This solution (0.5 mL, corresponding to 2 mol% L*CuH and 2.0 equiv of silane) was taken up into an air tight syringe

and removed from the glovebox and transferred to a solution of 1-(vinyl-1-*d*)naphthalene (77.6 mg, 0.5 mmol, 1 eq), *O*-pivaloyl-*N*-(3-(3-(trifluoromethyl)phenyl)propyl)hydroxylamine (182.0 mg, 0.6 mmol, 1.2 eq), and THF (0.5 mL) under an N_2 atmosphere at 0 °C. The reaction was stirred at 0 °C for 9 h and then rt for 14 h. The reaction solution was then diluted with CH_2Cl_2 and washed with 3M K_2CO_3 (*aq*, 3 x 30 mL). The organic layer was dried over Na_2SO_4 and then concentrated *in vacuo*. Silica gel chromatography (30% EtOAc/hexanes to 50% EtOAc/hexanes) yielded the title compound as a light yellow oil (149.7 mg, 84% yield, 94% ee). Benzylic deuteration was assumed to be >99%, corresponding to that of the 1-(vinyl-1-*d*)naphthalene starting material. **^{1}H NMR** (400 MHz, $CDCl_3$) δ 8.19 (d, J = 8.2 Hz, 1H), 7.88 (m, 1H), 7.76 (d, J = 8.2 Hz, 1H), 7.64 (d, J = 7.2 Hz, 1H),7.46-7.54 (m, 3H), 7.42-7.44 (m, 2H), 7.30-7.37 (m, 2H), 2.56-2.77 (m, 4H), 1.80-1.88 (m, 2H), 1.49 (s, 3H), 1.40 (s, 1H). **^{13}C NMR** (101 MHz, $CDCl_3$) δ 143.3, 141.3, 134.2, 132.0, 131.5, 130.8 (q), 129.2, 128.9, 127.4, 126.0, 125.9, 125.5, 125.2 (q), 123.1, 122.8, 53.5 (T), 47.4, 33.7, 32.1, 23.7. **^{2}H NMR** (62 MHz, CH_3CN) δ 4.56 (0.97D). **^{19}F NMR** (376 MHz, $CDCl_3$) δ -63.5 (3F). **HRMS** (DART) $[M+H]^+$ calcd. for $[C_{22}H_{22}DF_3N]^+$ 359.1845, 359.1850 found. **IR** (neat, cm^{-1}) 3047, 2927, 2859, 1449, 1326, 1159, 1119, 1072, 797, 776, 702. **Specific Rotation**: $[\alpha]_D^{22} = +22.5°$.

Procedure for ee determination of 1–32: isolated compound **1–32** was subsequently acylated with (*S*)-2-chloro-2-methoxy-2-phenylacetyl chloride to determine the enantiomeric excess. All procedural steps were conducted open to air. (*R*)-*N*-(1-(naphthalen-1-yl)ethyl-1-*d*)-3-(3-(trifluoromethyl)phenyl)propan-1-amine (35.8 mg, 0.1 mmol, 1 eq) was weighed into an oven-dried 4 mL vial and constituted in dry CH_2Cl_2 (1.0 mL). (*S*)-2-chloro-2-methoxy-2-phenylacetyl chloride (21 µl, 0.12 mmol, 1.2 eq) was added followed by triethylamine (21 µl, 0.15 mmol, 1.5

eq). The solution was stirred at rt for 14 h. The reaction solution was diluted with CH_2Cl_2 (40 mL) and washed once with H_2O (30 mL), once with saturated aqueous $NaHCO_3$ (30 mL) and then dried over Na_2SO_4. The organic solution was concentrated *in vacuo*. The ee (%) was determined by ^1H NMR spectroscopy using the relative integration of the (-OMe) peaks of the diastereomers compared to a racemic sample of acylated **25** (See section A1.7). The observed ee value (94%) is similar to that reported by Buchwald.[1]

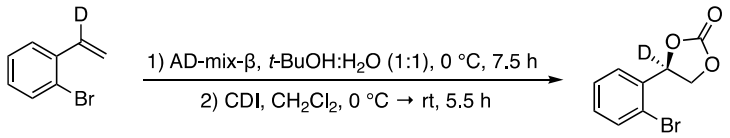

(*R*)-4-(2-bromophenyl)-1,3-dioxolan-2-one-4-*d* (1–30)

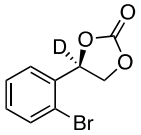

AD-mix-β (700 mg) was weighed into a 25 mL round bottom flask and constituted in *t*-BuOH (2.0 mL) and H_2O (2.5 mL). The slurry was cooled to 0 °C and 1-bromo-2-(vinyl-1-*d*)benzene (92.1 mg, 0.5 mmol, 1 eq in 0.5 mL *t*-BuOH) was added. The reaction mixture was stirred at 0 °C for 7.5 h. Na_2SO_3 (about 30 mg) was then added, and the solution was allowed to stir an additional 30 min at rt. The solution was then washed with H_2O (30 mL) and extracted with EtOAc (3 x 30 mL). The organic layer was washed once with brine (20 mL), dried over Na_2SO_4, and concentrated *in vacuo*. The crude material was then transferred into an oven-dried 10 mL round bottom flask, constituted in dry CH_2Cl_2 (2.0 mL) and cooled to 0 °C. Next, 1,1'-carbonyldiimidazole (162.2 mg, 1.0 mmol, 2 eq) was added over 3 min. The solution was allowed to warm to rt and stirred for 5.5 h. The reaction solution was directly loaded onto a silica gel column and eluted with 10% EtOAc/hexanes to afford the title compound as a clear oil (89.9 mg, 74% yield, 98% ee). Benzylic deuteration was assumed to be 97%, corresponding to that of the 1-bromo-2-(vinyl-1-*d*)benzene starting material. **^{1}H NMR** (400 MHz, $CDCl_3$) δ 7.60 (d, J = 7.9 Hz, 1H), 7.50 (d, J = 7.9 Hz, 1H), 7.42 (t, J = 7.6 Hz, 1H), 7.28 (t, J = 7.7 Hz, 1H), 5.95 (t, J = 7.9 Hz,

0.03H), 4.98 (d, J = 8.6 Hz, 1H), 4.24 (d, J = 8.6 Hz, 1H). **^{13}C NMR** (101 MHz, $CDCl_3$) δ 154.8, 136.4, 133.3, 130.8, 128.4, 126.2, 120.4, 76.4 (T), 70.7. **^{2}H NMR** (62 MHz, CH_3CN) δ 5.99. **HRMS** (DART) $[M+NH_4]^+$ calcd. for $[C_9H_9DBrNO_3]^+$ 260.9985, 260.9991 found. **IR** (neat) 3067, 2918, 1797, 1470, 1198, 1058, 752. **Specific Rotation**: $[\alpha]_D^{23}$ = -54.1°. **HPLC** analysis: Chiralcel AD-3 (Hex/EtOH = 90/10, 0.6 mL/min, 210 nm, 50 °C), 14.7 min (major), 15.5 min (minor), 98% ee.

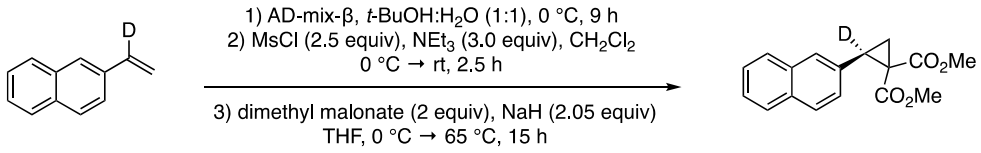

Step 1: AD-mix-β (1.40 g) was weighed into a 50 mL round bottom flask and constituted in *t*-BuOH/H_2O (10 mL of a 1:1 ratio). The slurry was cooled to 0 °C and 2-vinylnaphthalene-α-d_1 (155.2 mg, 1.0 mmol, 1 eq) was added. The reaction solution was stirred at 0 °C for 9 h. A scoop of Na_2SO_3 (about 30 mg) was then added, and the solution was allowed to stir an additional 30 min at rt. The solution was then washed with H_2O (30 mL) and extracted with EtOAc (3 x 30 mL). The organic layer was washed with brine, dried over Na_2SO_4, and concentrated *in vacuo*. Silica gel chromatography (60% EtOAc/hexanes to 100% EtOAc) yielded (*R*)-1-(naphthalen-2-yl)ethane-1-*d*-1,2-diol as a white solid (186 mg, 98% yield). **^{1}H NMR** (400 MHz, $CDCl_3$) δ 7.83-7.86 (m, 4H), 7.46-7.52 (m, 3H), 3.87 (dd, J_1 = 7.4 Hz, J_2 = 11.2 Hz, 1H), 3.77 (dd, J_1 = 4.7 Hz, J_2 = 11.2 Hz, 1H), 2.54 (s, 1H), 1.99 (dd, J_1 = 4.7 Hz, J_2 = 7.4 Hz, 1H).

Step 2: (*R*)-1-(naphthalen-2-yl)ethane-1-*d*-1,2-diol (186 mg, 0.98 mmol, 1 eq) was weighed into an oven-dried 10 mL round bottom flask and constituted in dry CH_2Cl_2 (5.0 mL). The solution was cooled to 0 °C and triethylamine (410 µl, 2.94 mmol, 3.0 eq) was added followed by a solution of

methanesulfonyl chloride (190 µl, 2.45 mmol, 2.5 eq in 1.3 mL of CH_2Cl_2). The solution was stirred at 0°C for 1 h, warmed to rt, and stirred for an additional 1.5 h. The reaction solution was then poured into 1M HCl (30 mL) and extracted CH_2Cl_2 (3 x 30 mL). The organic layer was washed with saturated aqueous $NaHCO_3$ (30 mL) and brine (20 mL). The organic layer was then dried over Na_2SO_4 and concentrated *in vacuo*. Silica gel chromatography (30% EtOAc/hexanes to 40% EtOAc/hexanes) yield (*R*)-1-(naphthalen-2-yl)ethane-1,2-diyl-1-*d* dimethanesulfonate as a white solid (295.3 mg, 86% yield). **^{1}H NMR** (400 MHz, $CDCl_3$) δ 7.86-7.94 (m, 4H), 7.54-7.59 (m, 2H), 7.50 (dd, J_1 = 1.8 Hz, J_2 = 8.5 Hz, 1H), 4.64 (1H), 4.48 (1H), 3.11 (s, 3H), 2.87 (s, 3H).

dimethyl (*R*)-2-(naphthalen-2-yl)cyclopropane-1,1-dicarboxylate-2-*d* (1–29)[2]

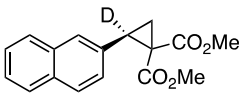

Step 3: A 60% dispersion of NaH (70.2 mg, 1.8 mmol, 2.05 eq) was weighed into an oven-dried 50 mL round bottom flask and sealed with a septum. The flask was evacuated and backfilled 3 times with N_2 gas and left under positive pressure. Dry THF (5.0 mL) was added via syringe and the slurry was cooled to 0 °C. Dimethyl malonate (195 µl, 1.7 mmol, 2 eq) was then added slowly. The solution was allowed to stir for 30 min at 0 °C. (*R*)-1-(naphthalen-2-yl)ethane-1,2-diyl-1-*d* dimethanesulfonate (295.3 mg, 0.86 mmol, 1 eq in 8.0 mL of THF) was then added dropwise to the NaH solution. The reaction mixture was allowed to warm to rt and was then placed in a pre-heated 65 °C silicon oil bath and stirred for 15 h. The reaction solution was quenched with H_2O (30 mL) and extracted EtOAc (3 x 30 mL). The organic layer was washed with 1.0M NaOH (30 mL) and brine (20 mL), dried over Na_2SO_4, and then concentrated *in vacuo*. Silica gel chromatography (5% EtOAc/hexanes to 10% EtOAc/hexanes) yielded the title compound as a white solid (186.1 mg, 76% yield for the step, 65% yield overall, 96% ee). Benzylic deuteration was assumed to be 97%, corresponding to that of the 2-(vinyl-1-

d)naphthalene starting material. **Melting Point**: 84-86 °C. **^{1}H NMR** (400 MHz, $CDCl_3$) δ 7.74-7.80 (m, 3H), 7.64 (s, 1H), 7.43-7.47 (m, 2H), 7.33 (dd, J_1 = 8.5 Hz, J_2 = 1.8 Hz, 1H), 3.82 (s, 3H), 3.30 (s, 3H), 2.33 (d, J = 5.2 Hz, 1H), 1.83 (d, J = 5.2 Hz, 1H). **^{13}C NMR** (101 MHz, $CDCl_3$) δ 170.4, 167.2, 133.3, 132.8, 132.2, 128.0, 127.9, 127.8, 127.3, 126.8, 126.3, 126.1, 53.0, 52.4, 37.5, 32.7 (T), 19.4. **^{2}H NMR** (62 MHz, CH_3CN) δ 3.30 (0.97D). **HRMS** (APCI) $[M+H]^+$ calcd. for $[C_{17}H_{16}DO_4]^+$ 286.1190, 286.1162 found. **IR** (neat, cm^{-1}) 3059, 2951, 2846, 1739, 1712, 1435, 1336, 1264, 1121, 750. **Specific Rotation**: $[\alpha]_D^{23}$ = +191.4°. **HPLC** analysis: Chiralcel OJ-3 (Hex/EtOH = 80/20, 0.8 mL/min, 210 nm, 50 °C), 10.2 min (minor), 11.2 min (major), 96% ee.

A1.9 Additional Examples of Styrene α-Deuteration

During the course of the development of the reported substrate scope, we found additional examples of styrene derivatives that underwent highly a-selective deuteration. We also discovered that electron-rich styrenes fail to undergo any a-deuteration. These findings, along with examples of vinyl arenes that undergo competitive side deuteration, are reported in Figure S5 below. The reported values were obtained following the general procedure provided in Section A1.6.

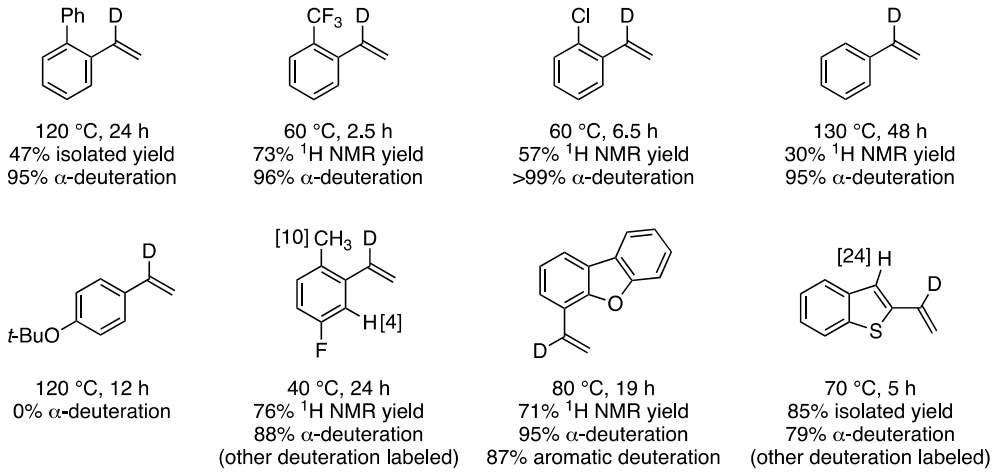

Figure A1–11: Additional examples of styrene α-deuteration. Yield determined by isolation or ^{1}H NMR spectroscopy using trimethoxybenzene as an internal standard.

A1.10 Preparation of Aryl Alkene Substrates

1-Bromo-2-vinylbenzene, 2-vinylpyridine, and (*E*)-1,2-di(pyridin-4-yl)ethene were purchased from Combi-Blocks and used as received. (*Z*)-prop-1-en-1-ylbenzene was purchased from TCI and used as received. (*E*)-1-styryl-4-vinylbenzene, 1-iodo-2-vinylbenzene, methyl 4-vinylbenzoate, (trifluoromethyl)(4-vinylphenyl)sulfane, 4-vinyl-1,1'-biphenyl, 1-(trifluoromethyl)-4-vinylbenzene, 2-(4-vinylphenyl)pyridine, 1-vinylnaphthalene, 9-chloro-10-vinylanthracene, 6-vinylquinoline, 5-vinylisoquinoline and 2-chloro-3-vinylpyridine were prepared according to the general procedure below unless otherwise noted. 1-(2-Methoxyethenyl)-4-trifluoromethylbenzene was made according to the general procedure below with methoxymethyltriphenylphosphonium chloride as the ylide precursor.[3-15] Characterization of the aryl alkenes matched reported literature data.

General procedure for styrene preparation: Methyltriphenylphosphonium bromide (1.2-1.5 eq) was added to an oven or flame-dried round bottom flask (methyltriphenylphosphonium bromide was dried for at least 1 hour *in vacuo* at 100 °C prior to use). The flask was then evacuated and backfilled with N_2 gas (3 times). Anhydrous THF (20 mL per 1 gram of aldehyde) was added via syringe and the solution was cooled to 0 °C. KO-*t*-Bu (1.2-1.5 eq) constituted in anhydrous THF or *n*-butyl lithium (1.6M in hexanes, 1.2-1.5 eq) was then added via syringe, forming the observed yellow phosphonium ylide. The solution was stirred for 15 min at 0°C and then the appropriate aldehyde (1M in THF) was added dropwise. The reaction was allowed to stir at 0 °C until all of the aldehyde was consumed as indicated by TLC analysis (approximately 15 to 30 min). The reaction solution was quenched with H_2O and extracted with ethyl acetate (3 x reaction volume).

The organic layer was dried over Na_2SO_4 and concentrated *in vacuo*. Silica gel chromatography was used to purify all substrates.

2-chloro-1-(trifluoromethyl)-3-vinylbenzene

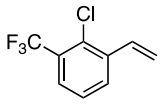

2-chloro-1-(trifluoromethyl)-3-vinylbenzene was made according to the general procedure with 2-chloro-3-trifluoromethylbenzaldehyde (2.00 g, 9.6 mmol, 1 eq), methyltriphenylphosphonium bromide (4.45 g, 12.5 mmol, 1.3 eq), and KO-*t*-Bu (1.51 g, 13.4 mmol, 1.4 eq) and THF (50 mL). Purification by silica gel chromatography (hexanes) yielded the title compound as a clear oil (971 mg, 49% yield). **^{1}H NMR** (400 MHz, $CDCl_3$) δ 7.73 (d, J = 7.8 Hz, 1H), 7.62 (d, J = 7.7 Hz, 1H), 7.34 (t, J = 7.8 Hz, 1H), 7.18 (dd, J_1 = 11.0 Hz, J_2 = 17.4 Hz, 1H), 5.76 (d, J = 17.4 Hz, 1H), 5.49 (d, J = 11.0 Hz, 1H). **^{13}C NMR** (101 MHz, $CDCl_3$) δ 138.5, 132.9, 131.1, 130.4, 129.3 (q), 127.0 (q), 126.7, 123.0 (q), 118.6. **^{19}F NMR** (376 MHz, $CDCl_3$) δ -63.5 (3F). **GCMS** calcd. for $[C_9H_6ClF_3]^+$ 206.0, 206.0 found. **IR** (neat, cm^{-1}): 3094, 3025, 2992, 1435, 1404, 1318, 1129, 1096, 1049, 805.

***N,N*-diethyl-3-vinylbenzamide**

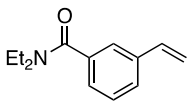

3-Vinylbenzoic acid (2.0 g, 13.5 mmol, 1 eq), N-(3-dimethylaminopropyl)-N′-ethylcarbodiimide hydrochloride (3.88 g, 20.3 mmol, 1.5 eq), and 1-hydroxybenzotriazole hydrate were added to a round bottom flask and constituted in CH_2Cl_2 (30 mL). The solution was cooled to 0 °C and *N*,*N*-diethylamine (1.8 mL, 17.6 mmol, 1.3 eq) and triethylamine (2.8 mL, 20.3 mmol, 1.5 eq) were added via syringe. The reaction solution was allowed to warm to rt and stirred for 23 h. The mixture was washed with H_2O and extracted CH_2Cl_2 (3 x 50 mL). The organic layer was dried over Na_2SO_4 and then concentrated *in vacuo*. Silica gel

chromatography yielded the title compound as a viscous clear oil (2.48 g, 90% yield). Spectroscopic characterization matched that of reported literature.[16]

A1.11: References

[1] Niu, D.; Buchwald, S. L. *J. Am. Chem Soc.* **2015**, *137* (30), 9716-9721.
[2] Chu, Z.-Y.; Liang, D.; Li, Z.-H.; Zheng, Y.-S.; Liu, J.-K. *Tetrahedron Lett.* **2018**, *59* (8), 715-718.
[3] Bezou, P.; Hilberer, A.; Hadziioannou, G. *Synthesis* **1996** (4), 449-451.
[4] Acheson, R. M.; Lee, G. C. M. *J. Chem. Soc. Perkin Trans. I*, **1987**, 2321.
[5] Yokoyama, A.; Maruyama, T.; Tagami, K.; Masu, H.; Katagiri, K.; Azumaya, I.; Yokozawa, T. *Org. Lett.* **2008**, *10*, 3207-3210.
[6] Shao, X.; Wang, X.; Yang, T.; Lu, Long; Shen, Q. *Angew. Chem. Int. Ed.* **2013**, *52*, 3457-3460.
[7] Bejot, R.; He, A.; Falck, J. R.; Mioskowski, C. *Angew. Chem. Int. Ed.* **2007**, *46*, 1719-1722.
[8] Molander, G. A.; Brown, A. R. *J. Org. Chem.* **2006**, *71*, 9681-9686.
[9] Mizuno, H.; Takaya, J.; Iwasawa, N. *J. Am. Chem. Soc.* **2011**, *133*, 1251-1253.
[10] Khan, Z. A.; Iwaoka, M.; Wirth, T. *Tetrahedron* **2010**, *66*, 6639-6646.
[11] Gülak, S.; Gieshoff, T. N.; Jacobi von Wangelin, A. *Adv. Synth. Catal.* **2013**, *355*, 2197-2202.
[12] Cong, F.; Wei, Y.; Tang, P. *Chem. Commun.* **2018**, *54*, 4473.
[13] Chen, D.; Xu, G.; Zhou, Q.; Chung, L.-W.; Tang, W. *J. Am. Chem. Soc.* **2017**, *139*, 9767.
[14] Lafaye, K.; Nicolas, L.; Guérinot, A.; Reymond, Reymond, S.; Cossy, J. *Org. Lett.* **2014**, *16*, 4972-4975.
[15] Kondo, M.; Kochi, T.; Kakiuchi, F. *J. Am. Chem. Soc.* **2011**, *133*, 32-34.
[16] Wang, Y.-M.; Buchwald, S. L. *J. Am. Chem. Soc.* **2016**, *138*, 5024-5027.

A1.12 Copies of NMR Spectra

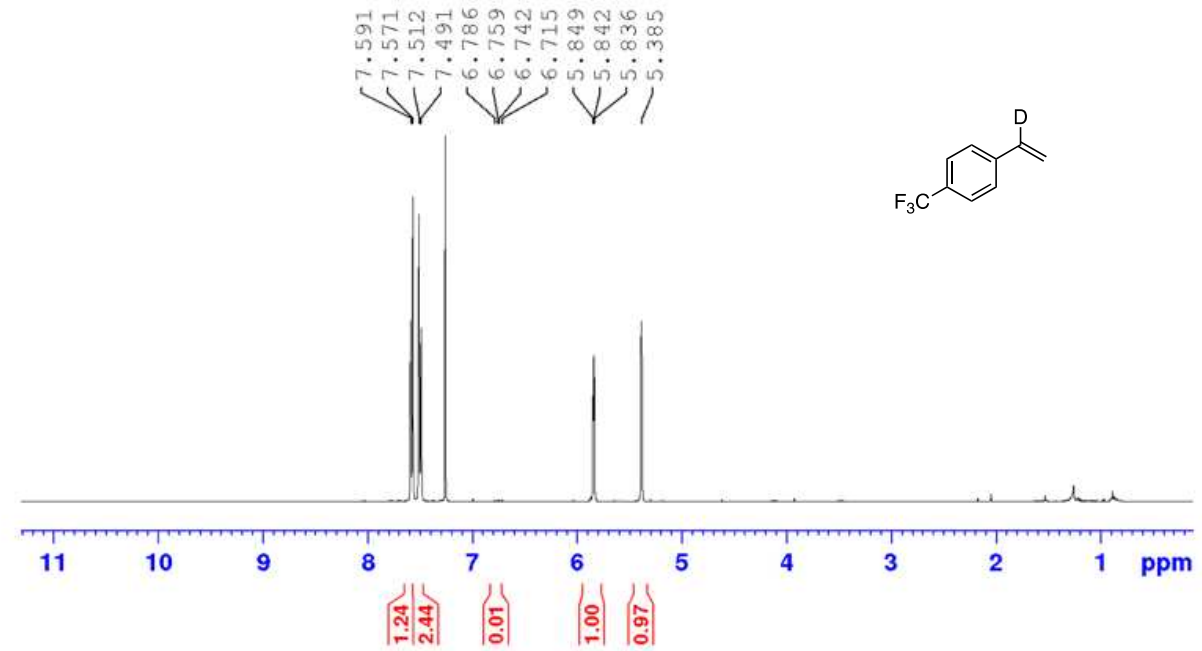

^{1}H NMR spectrum (400 MHz, $CDCl_3$)

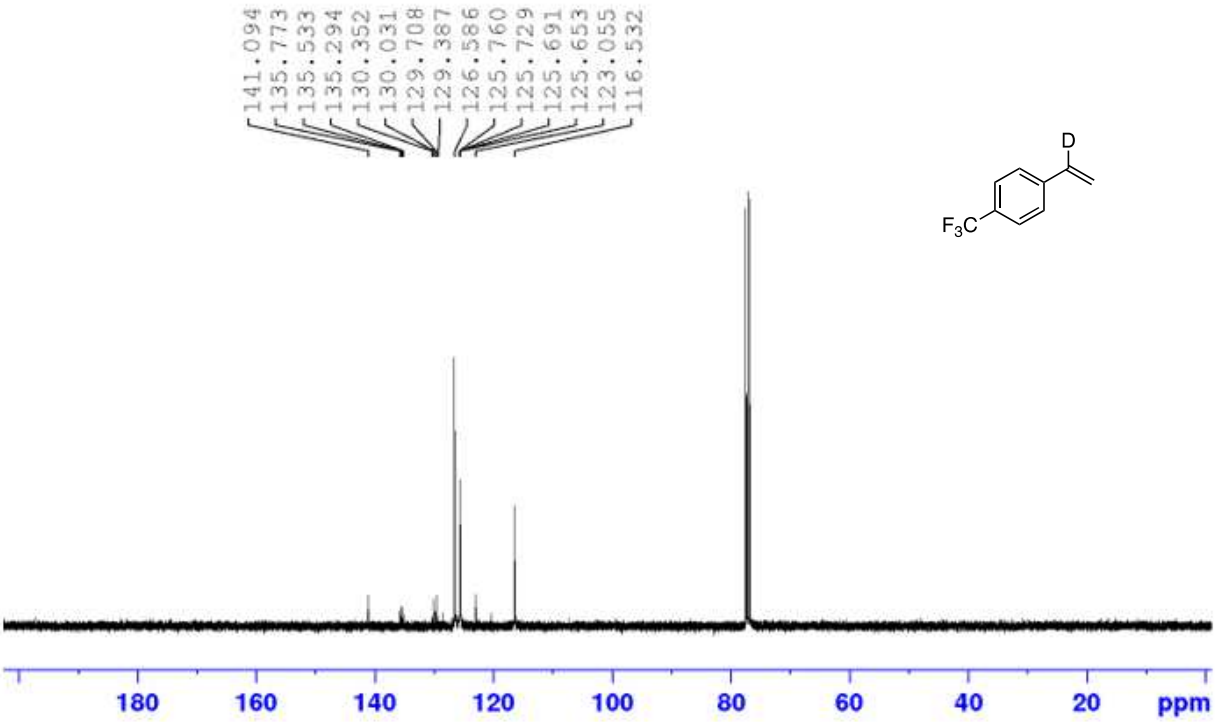

^{13}C NMR spectrum (101 MHz, $CDCl_3$)

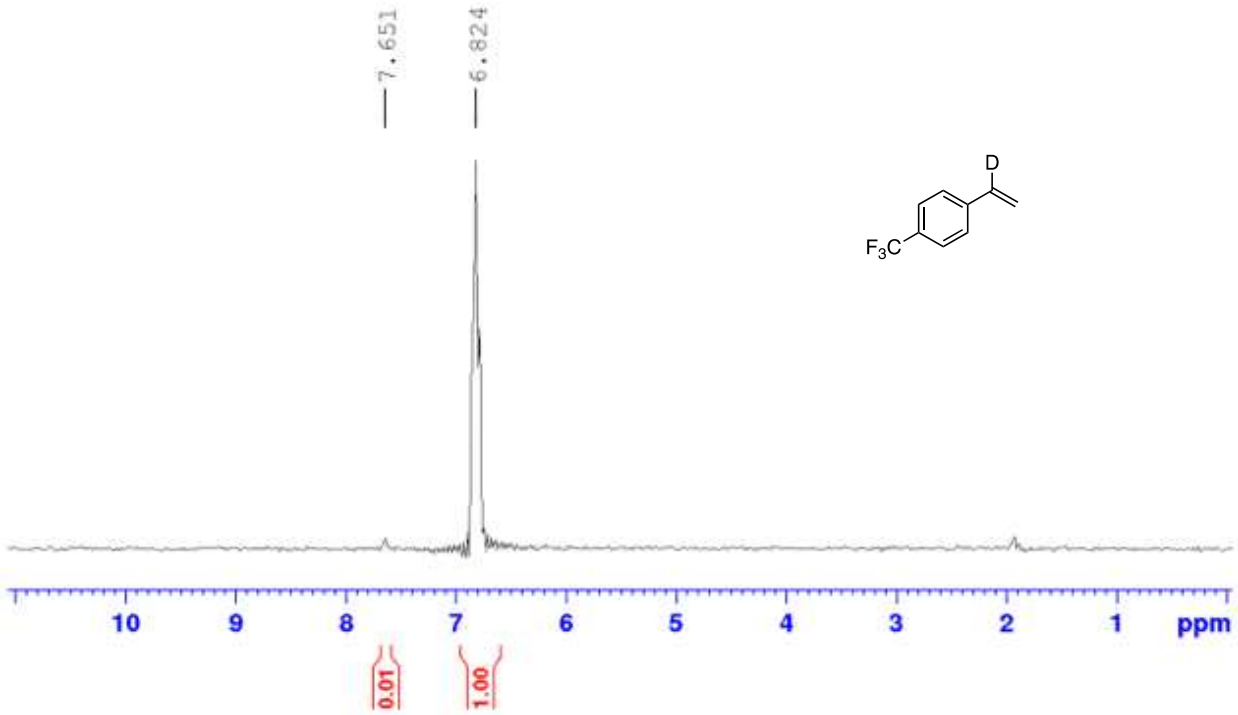

^{2}H NMR spectrum (62 MHz, CH_3CN)

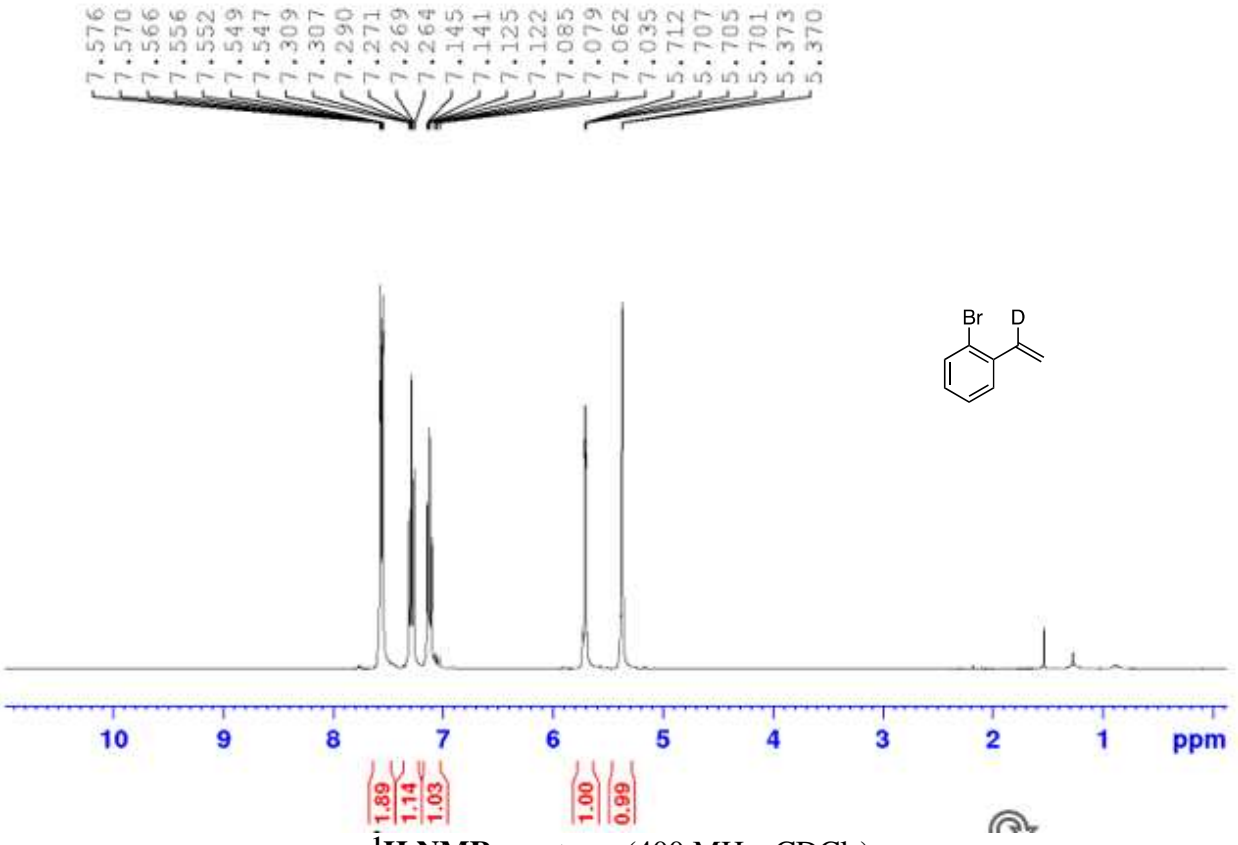

^{1}H NMR spectrum (400 MHz, $CDCl_3$)

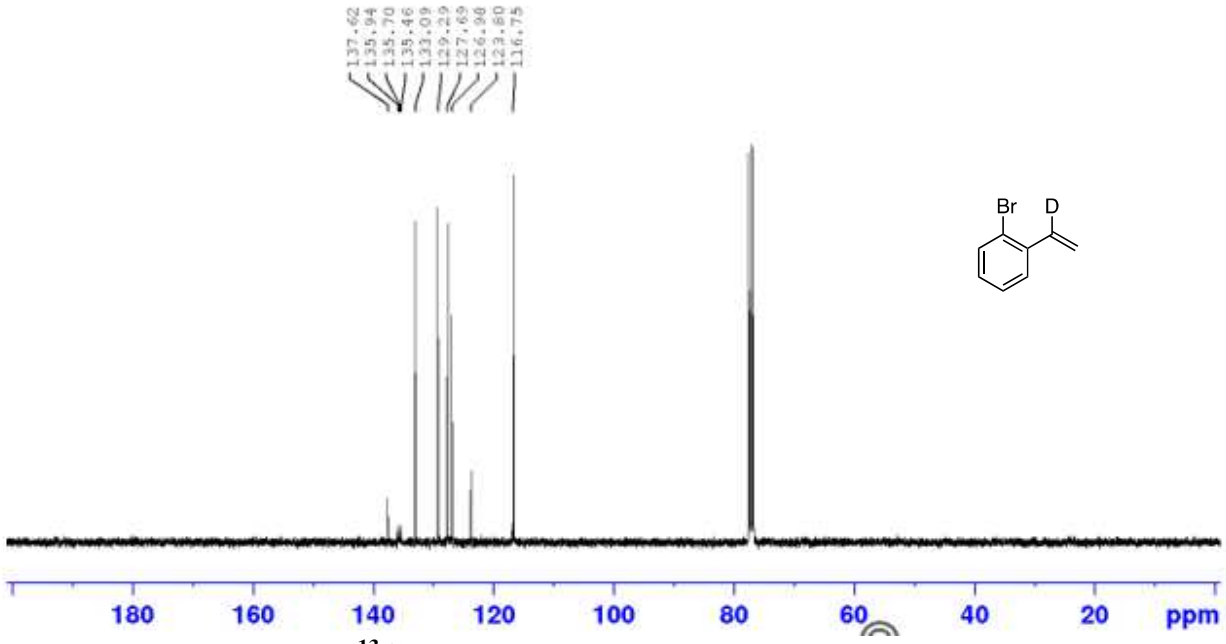

^{13}C NMR spectrum (101 MHz, $CDCl_3$)

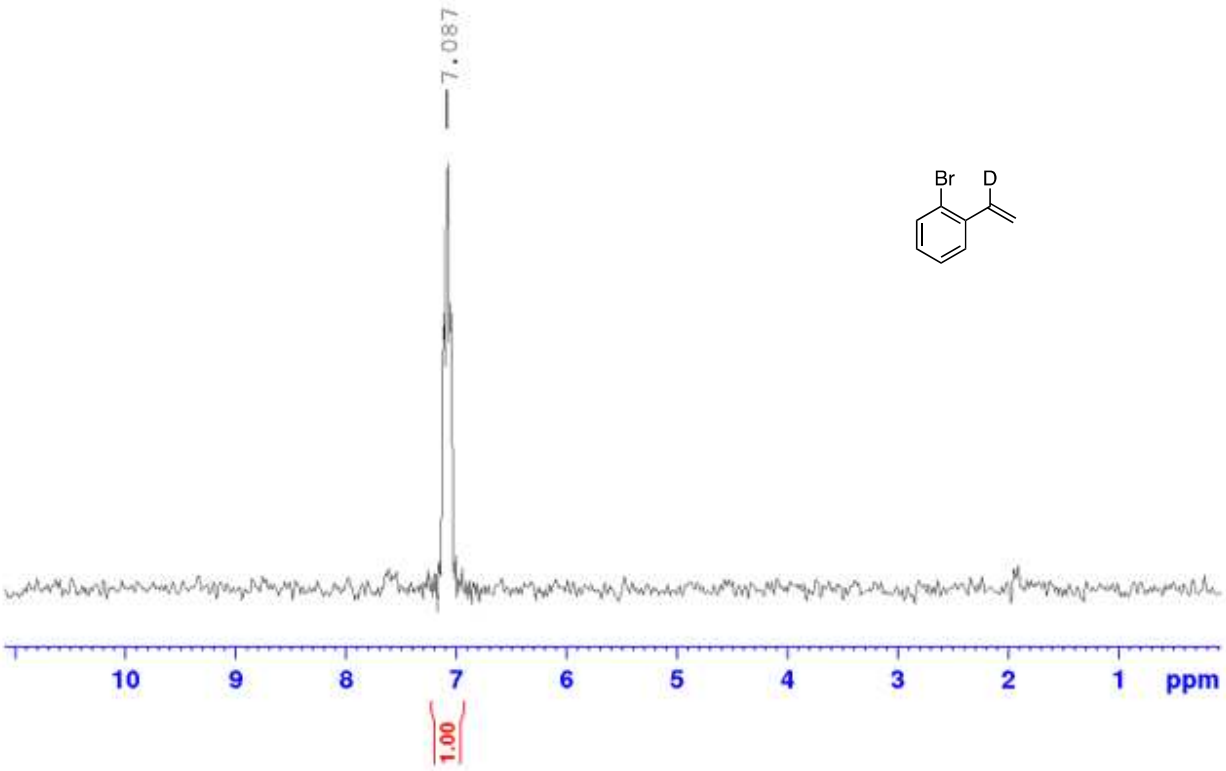

^{2}H NMR spectrum (62 MHz, CH_3CN)

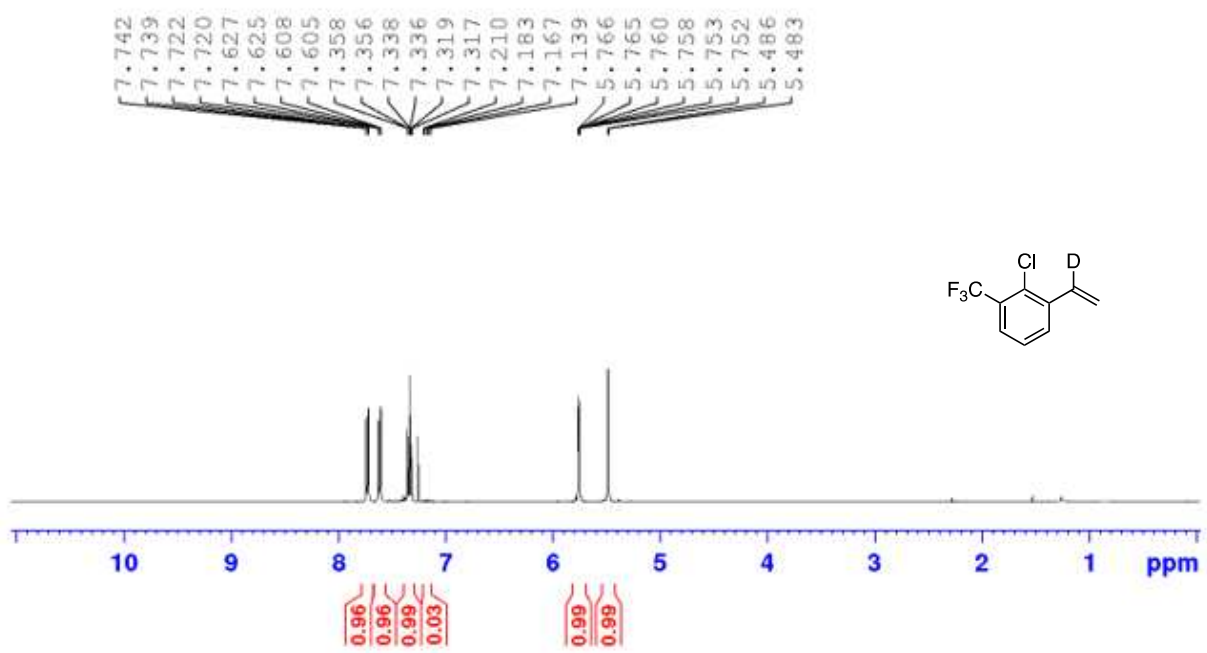

^{1}H NMR spectrum (400 MHz, $CDCl_3$)

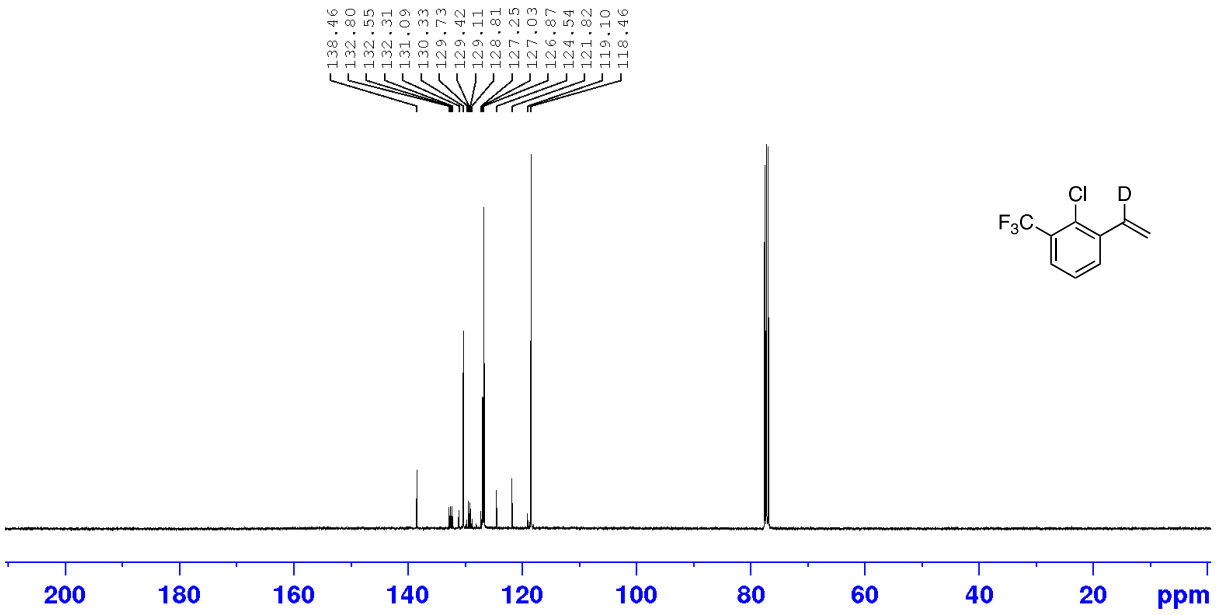

^{13}C NMR spectrum (101 MHz, $CDCl_3$)

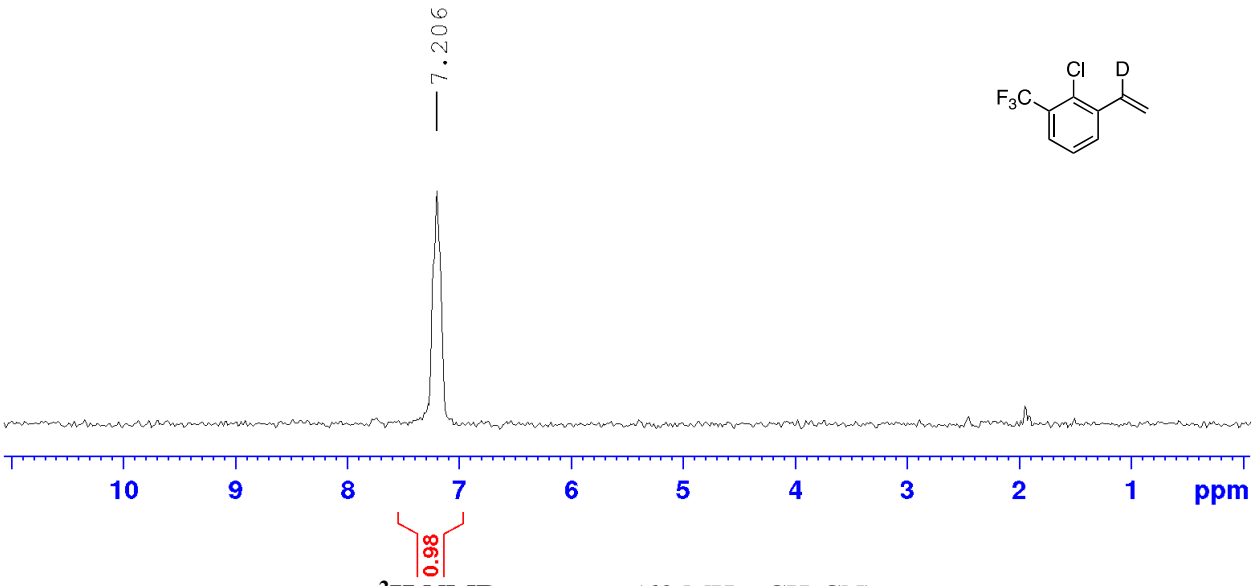

^{2}H NMR spectrum (62 MHz, CH_3CN)

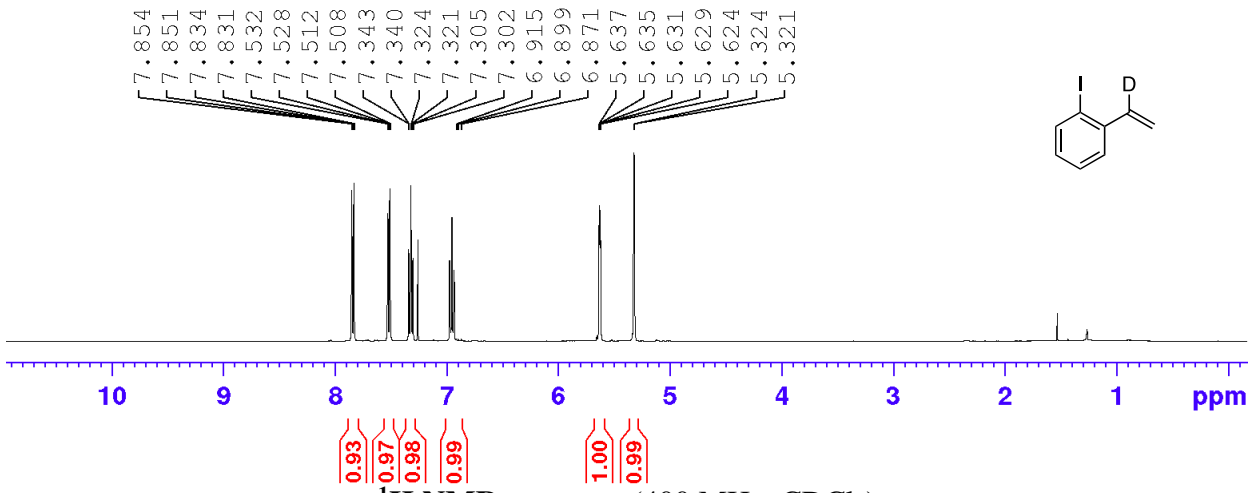

^{1}H NMR spectrum (400 MHz, $CDCl_3$)

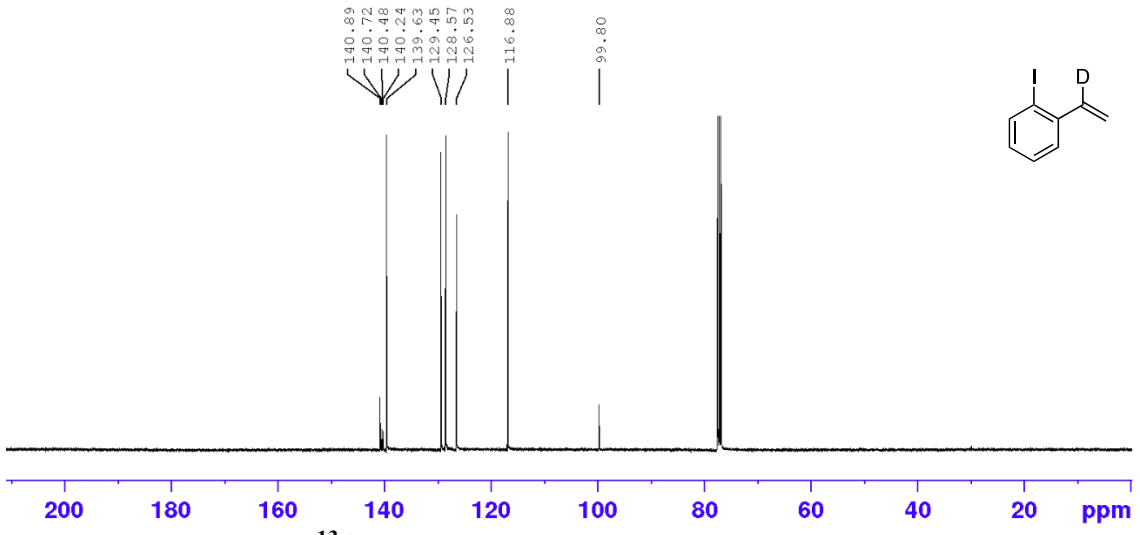

^{13}C NMR spectrum (101 MHz, $CDCl_3$)

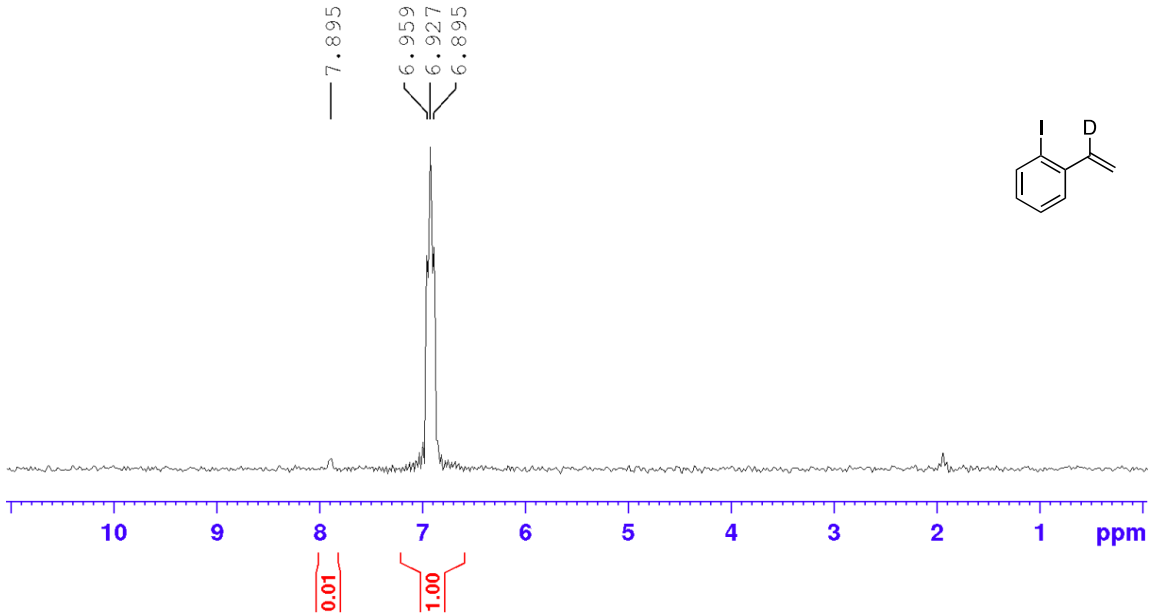

^{2}H NMR spectrum (62 MHz, CH_3CN)

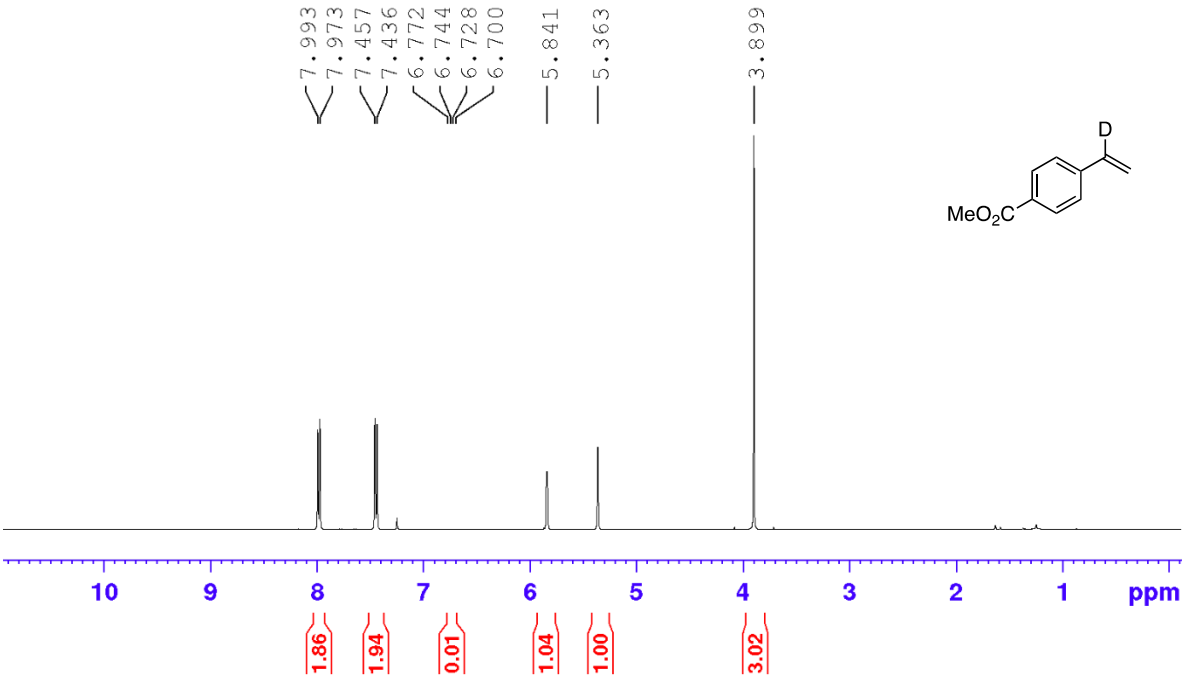

^{1}H NMR spectrum (400 MHz, $CDCl_3$)

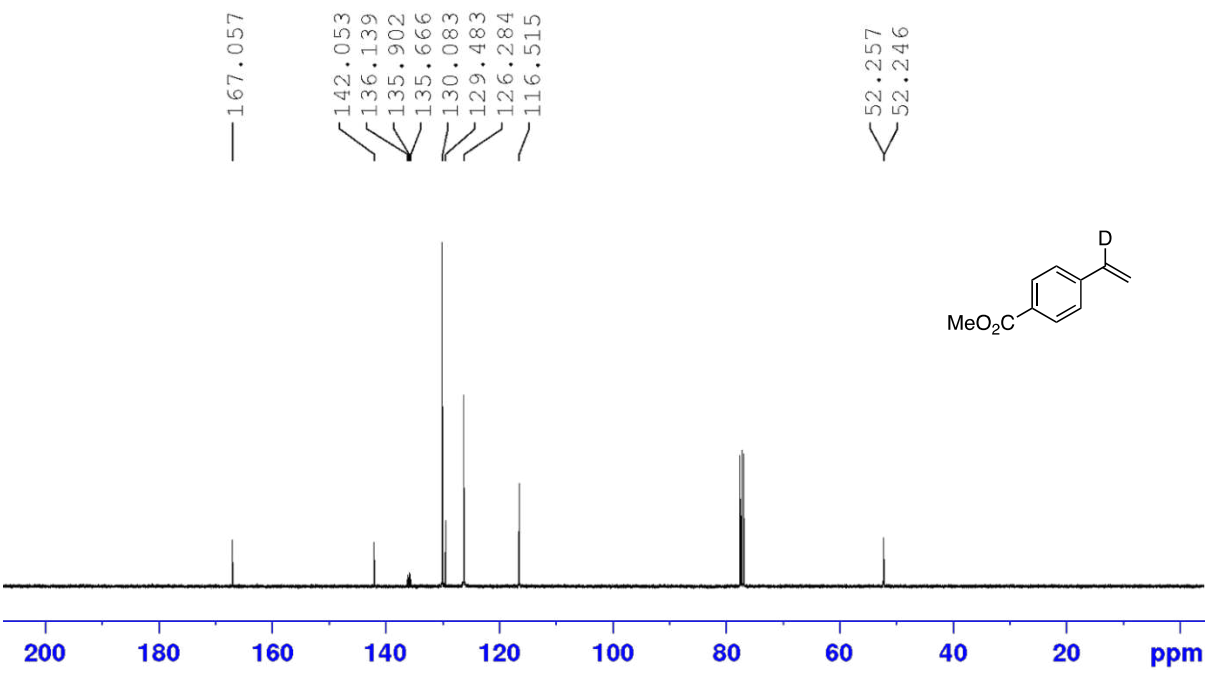

^{13}C NMR spectrum (101 MHz, $CDCl_3$)

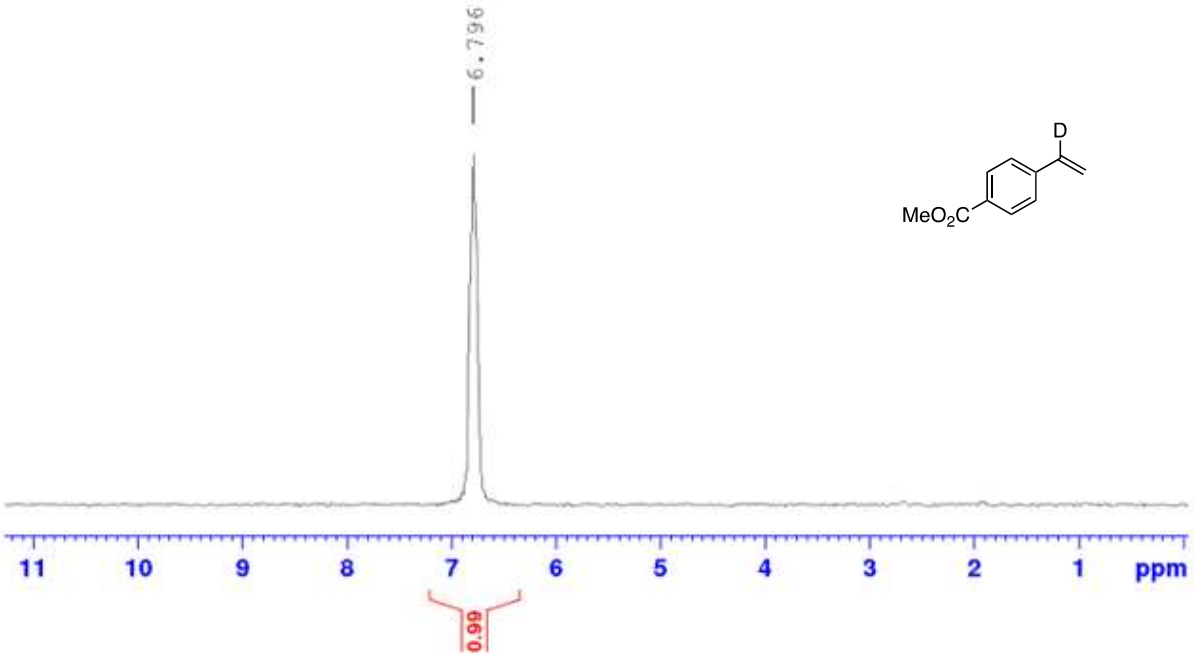

^{2}H NMR spectrum (62 MHz, CH_3CN)

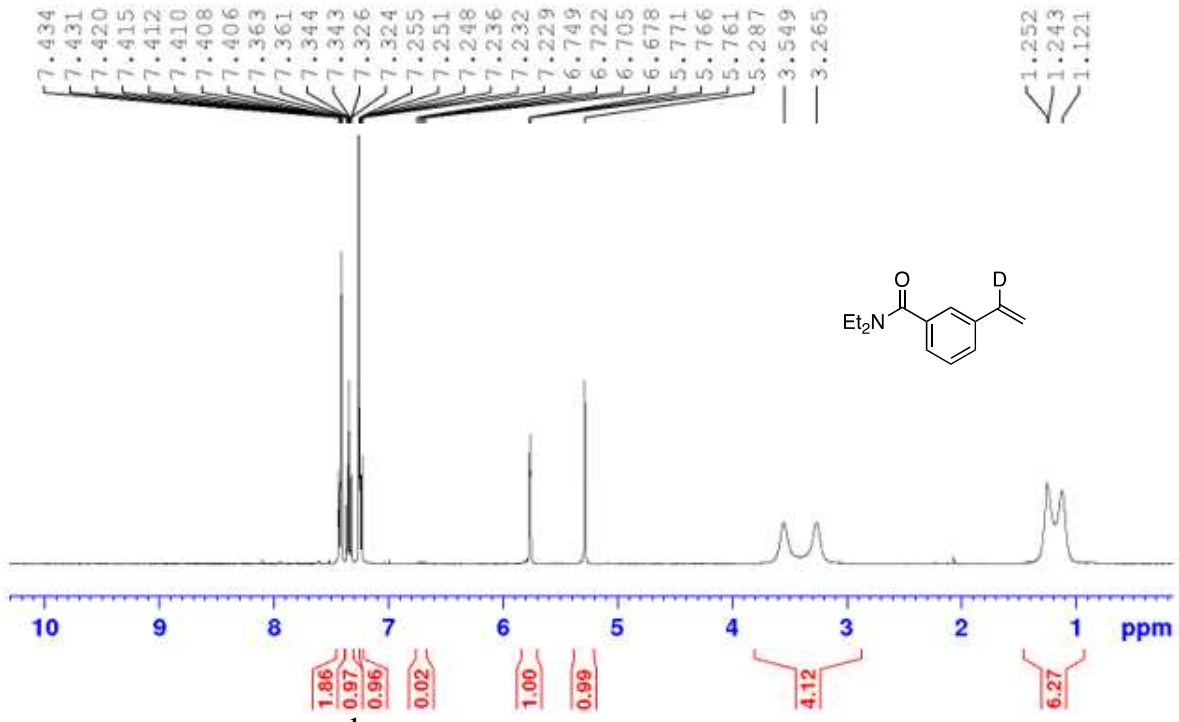

^{1}H NMR spectrum (400 MHz, $CDCl_3$)

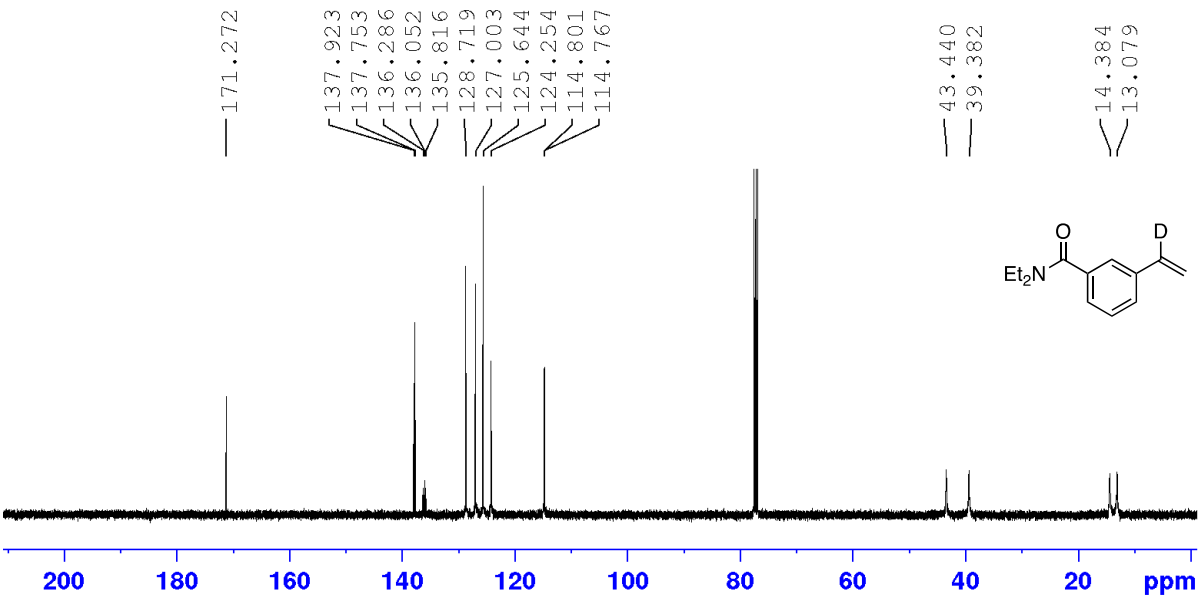

^{13}C NMR spectrum (101 MHz, $CDCl_3$)

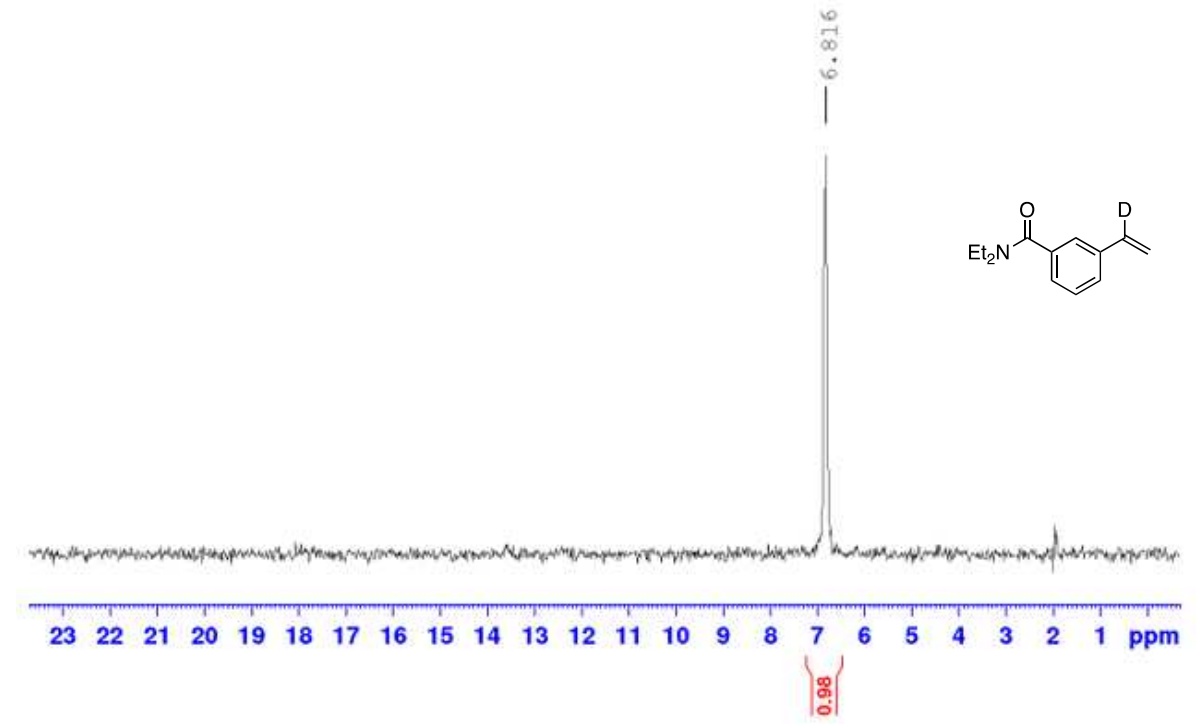

^{2}H NMR spectrum (62 MHz, CH_3CN)

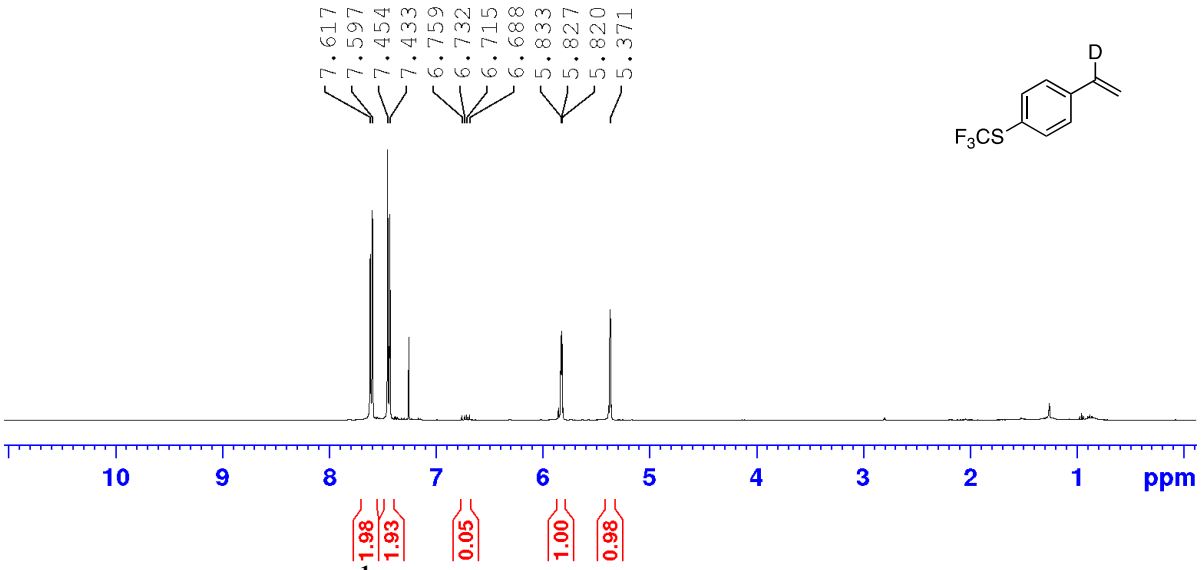

^{1}H NMR spectrum (400 MHz, $CDCl_3$)

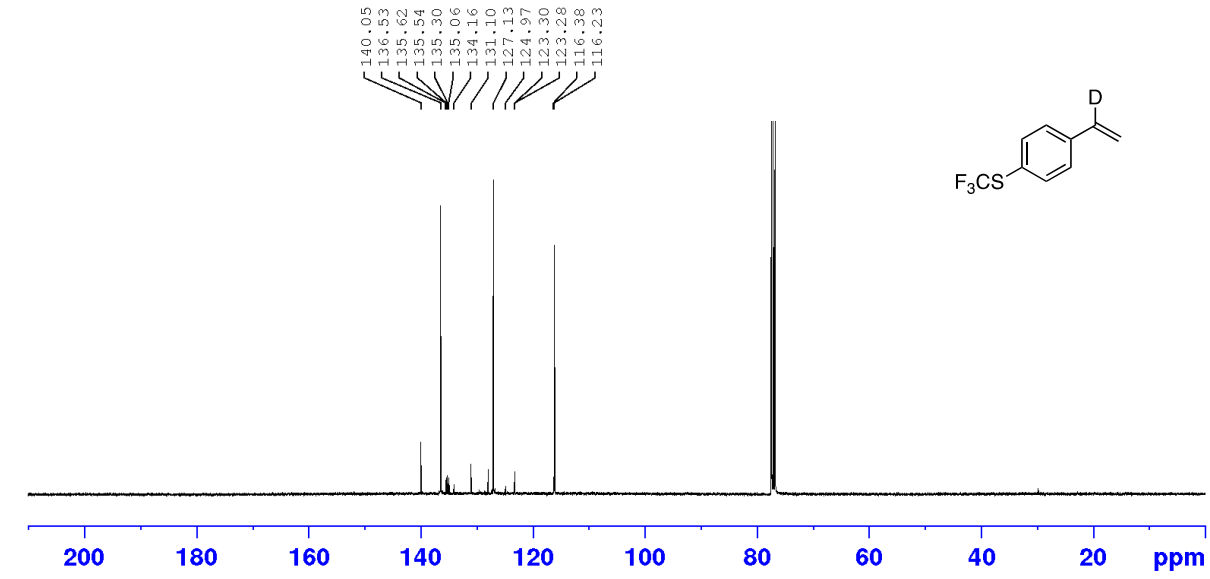

^{13}C NMR spectrum (101 MHz, $CDCl_3$)

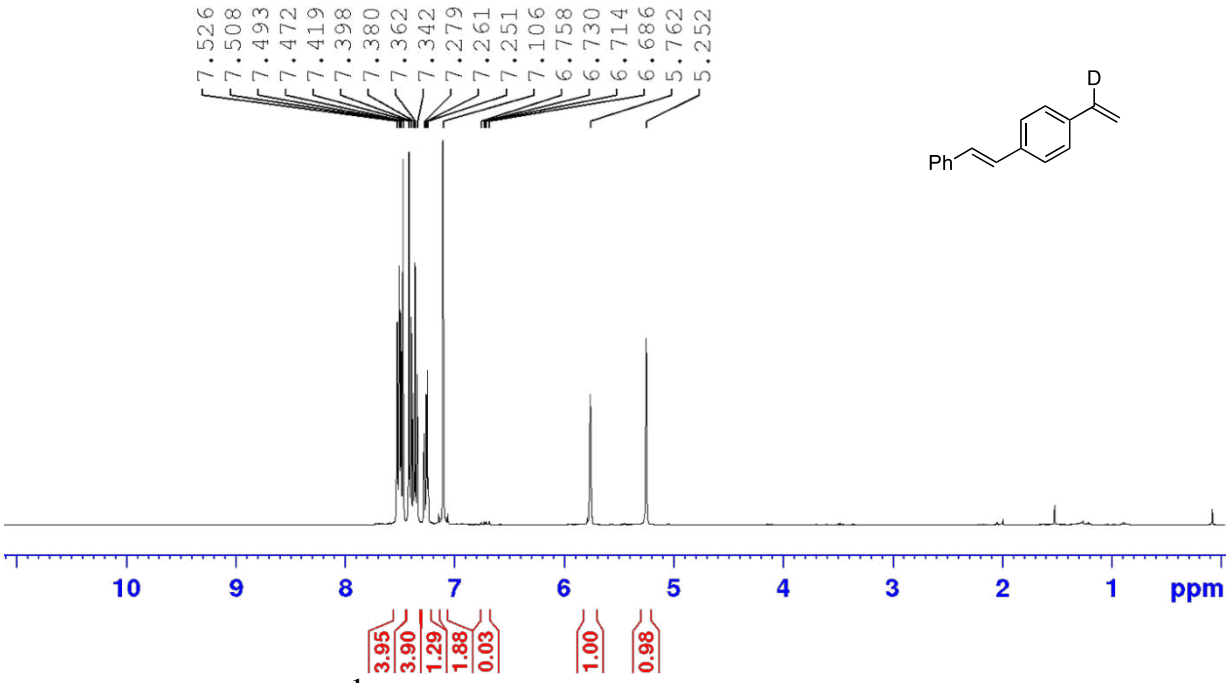

^{1}H NMR spectrum (400 MHz, $CDCl_3$)

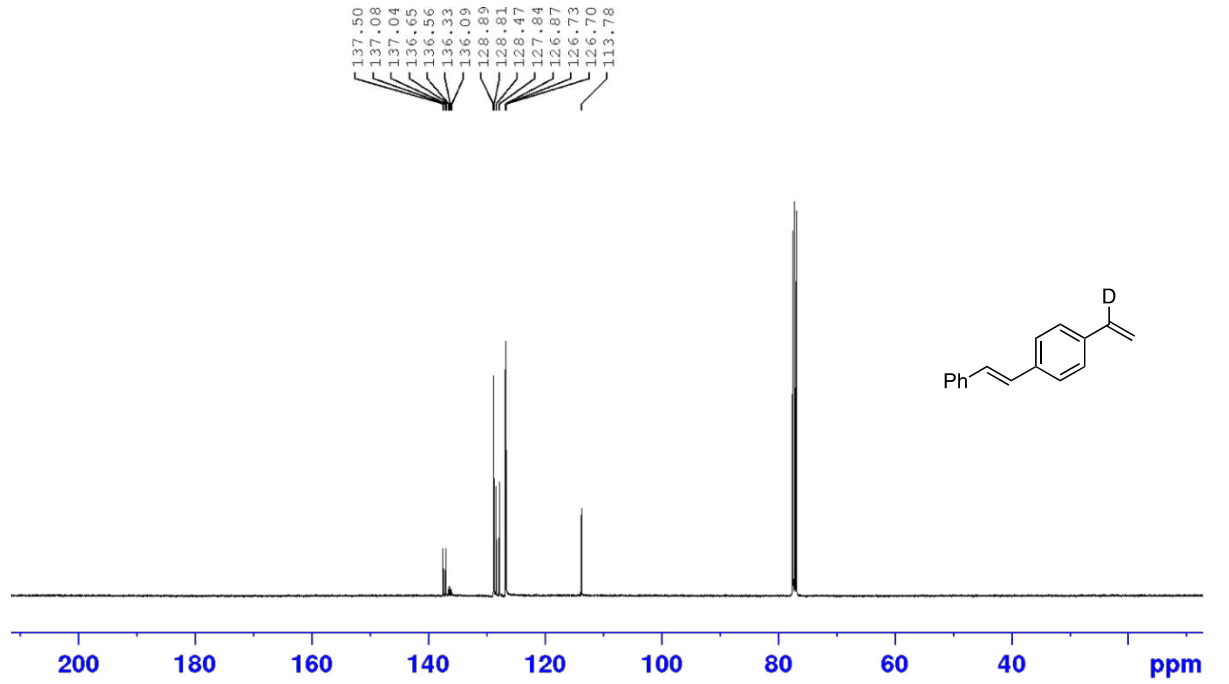

^{13}C NMR spectrum (101 MHz, $CDCl_3$)

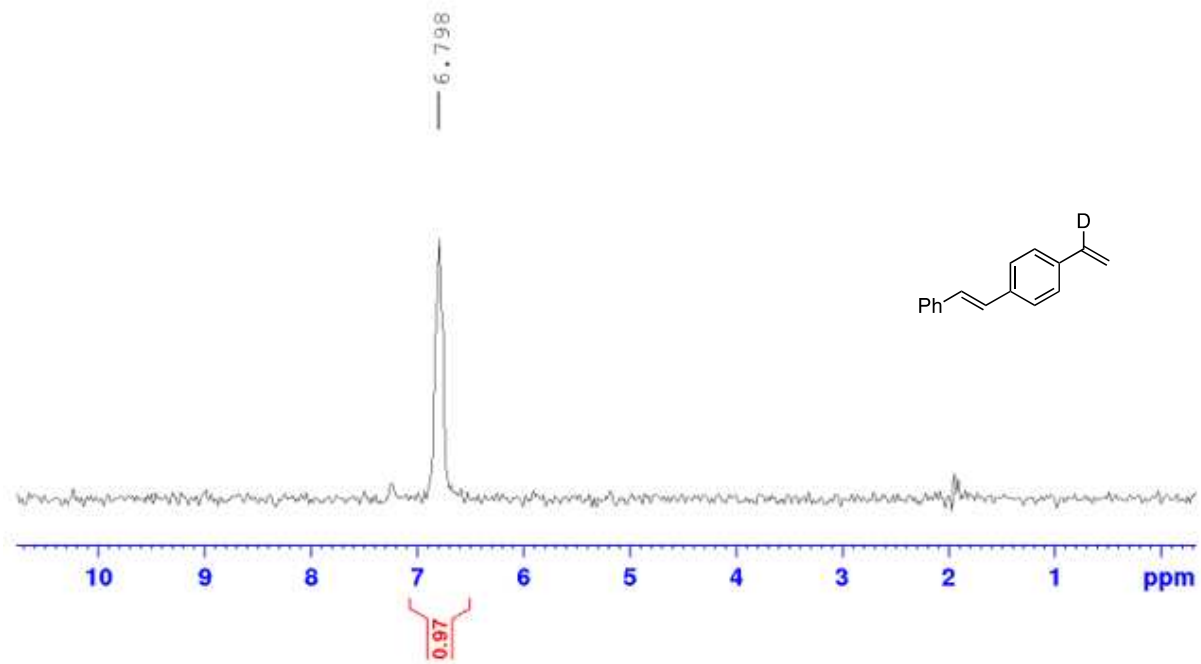

^{2}H NMR spectrum (62 MHz, CH_3CN)

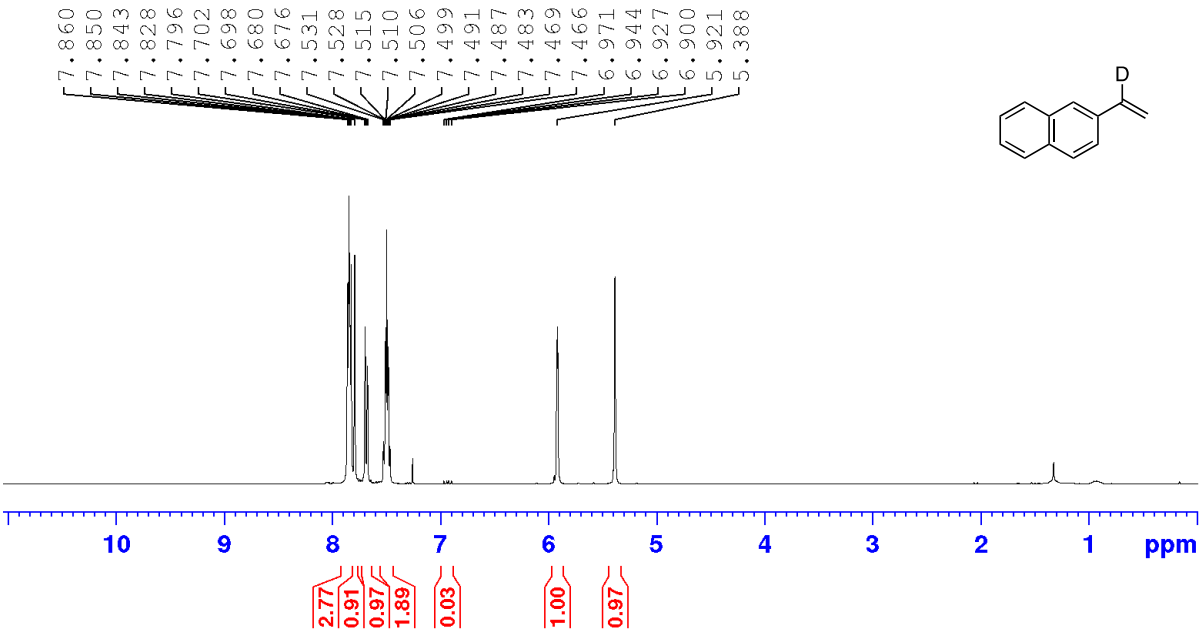

^{1}H NMR spectrum (400 MHz, $CDCl_3$)

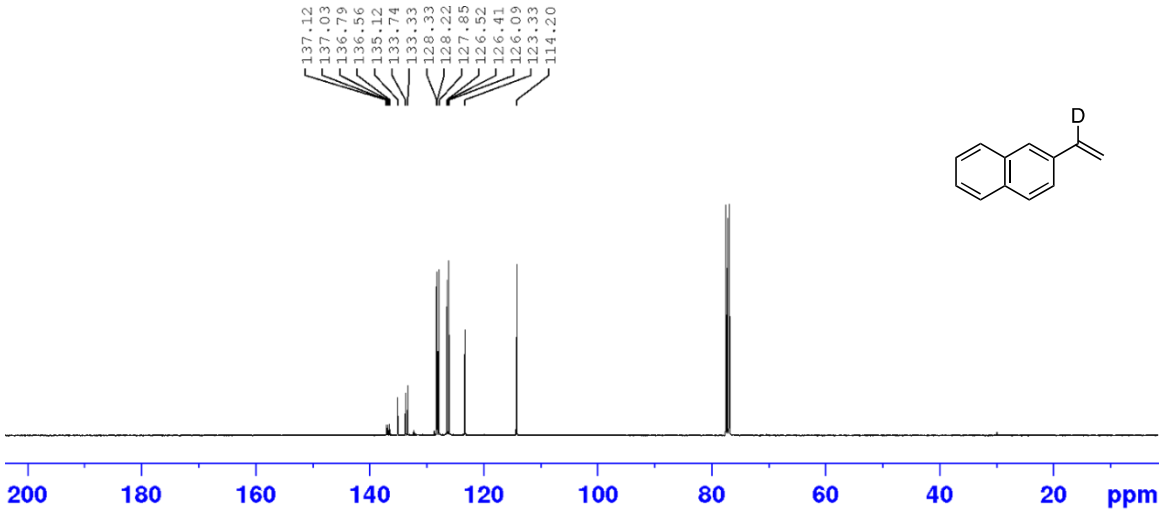

^{13}C NMR spectrum (400 MHz, $CDCl_3$)

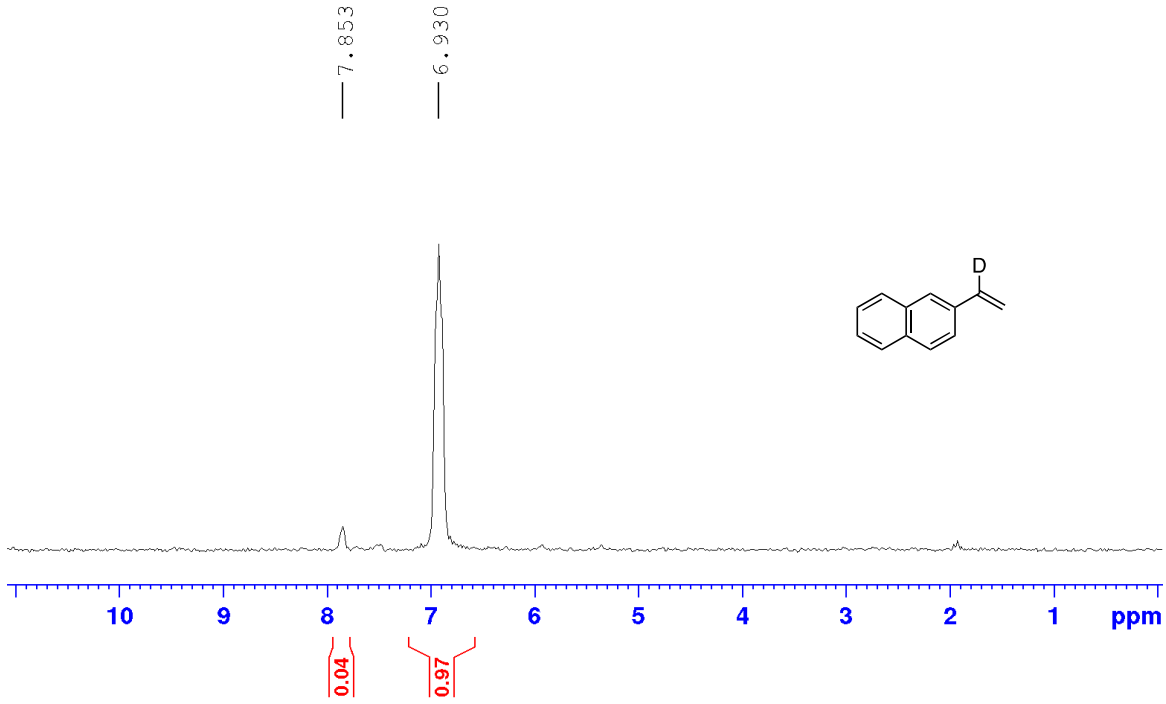

^{2}H NMR spectrum (62 MHz, CH_3CN)

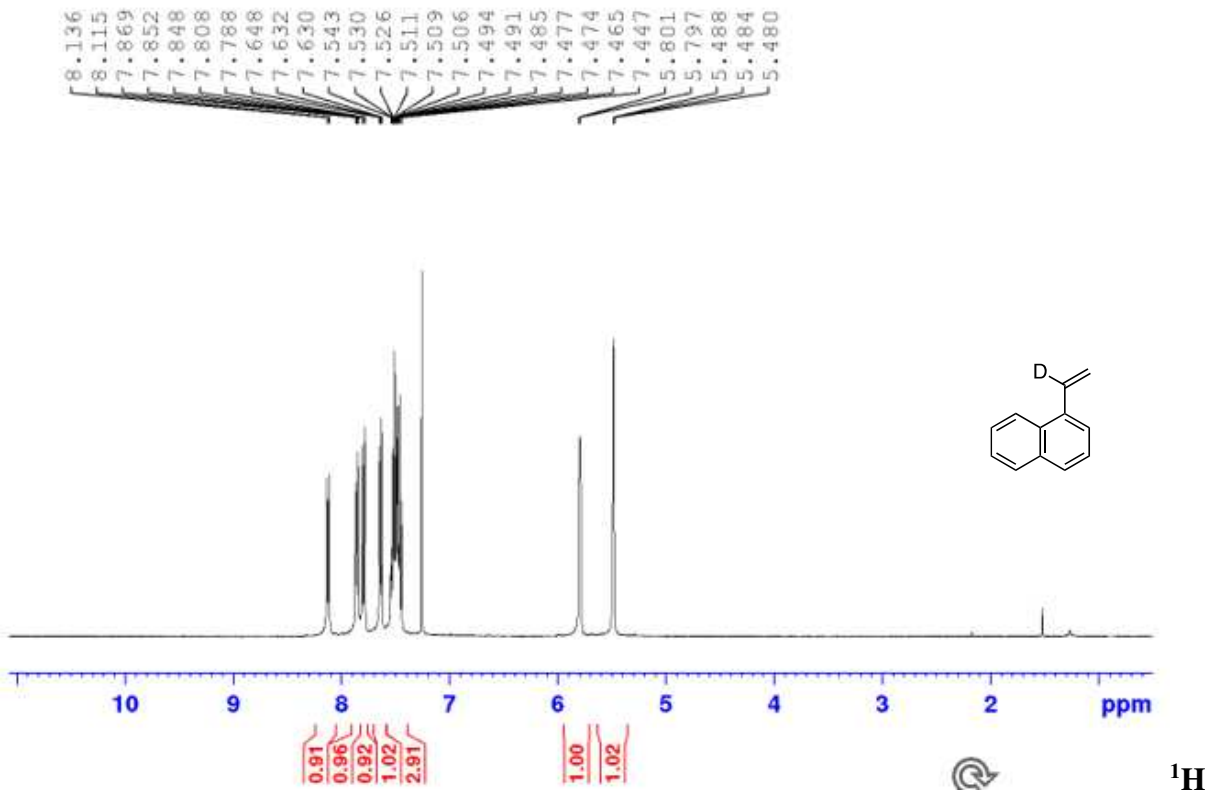

^{1}H NMR spectrum (400 MHz, $CDCl_3$)

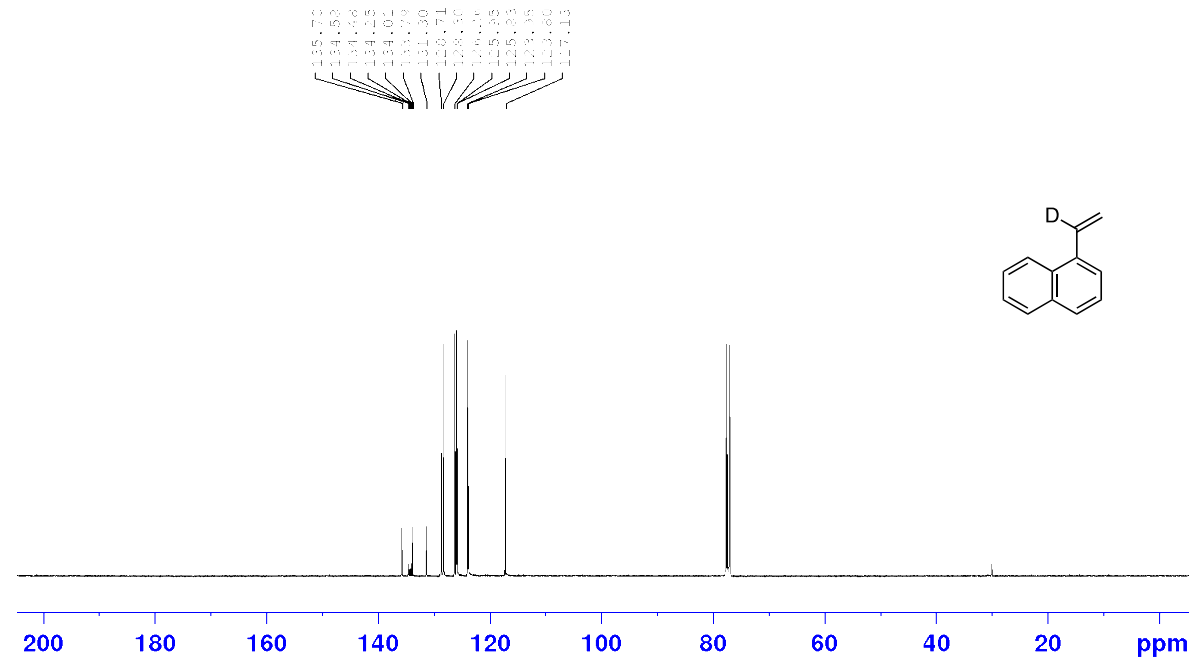

^{13}C NMR spectrum (101 MHz, $CDCl_3$)

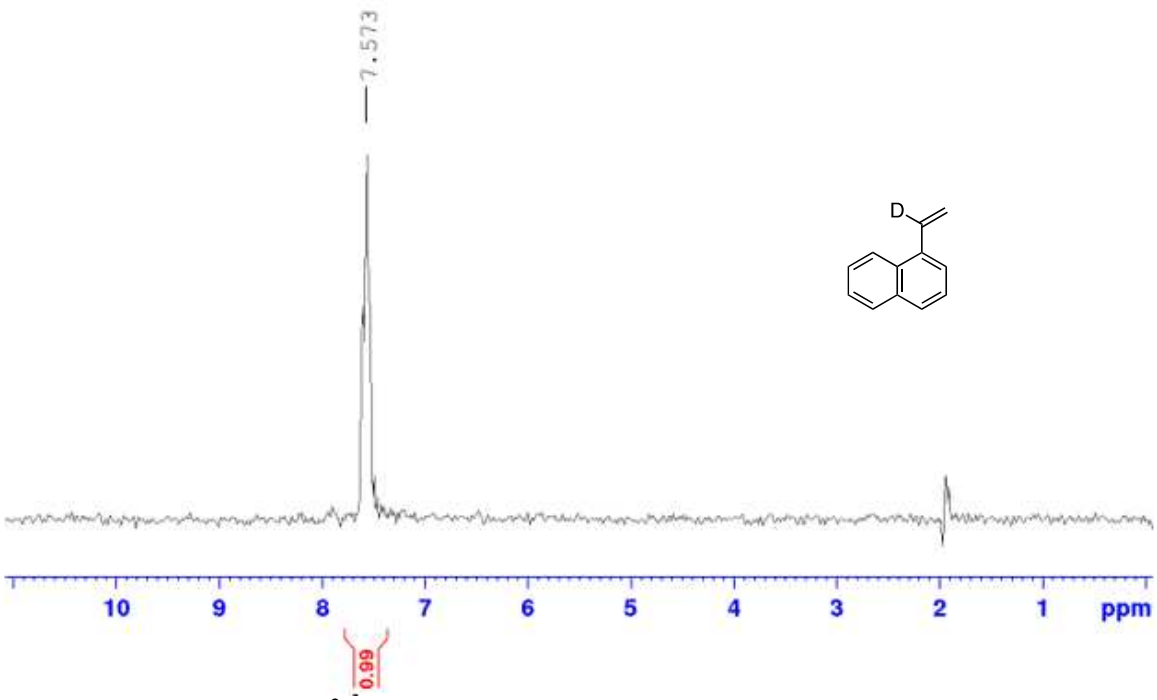

^{2}H NMR spectrum (62 MHz, CH_3CN)

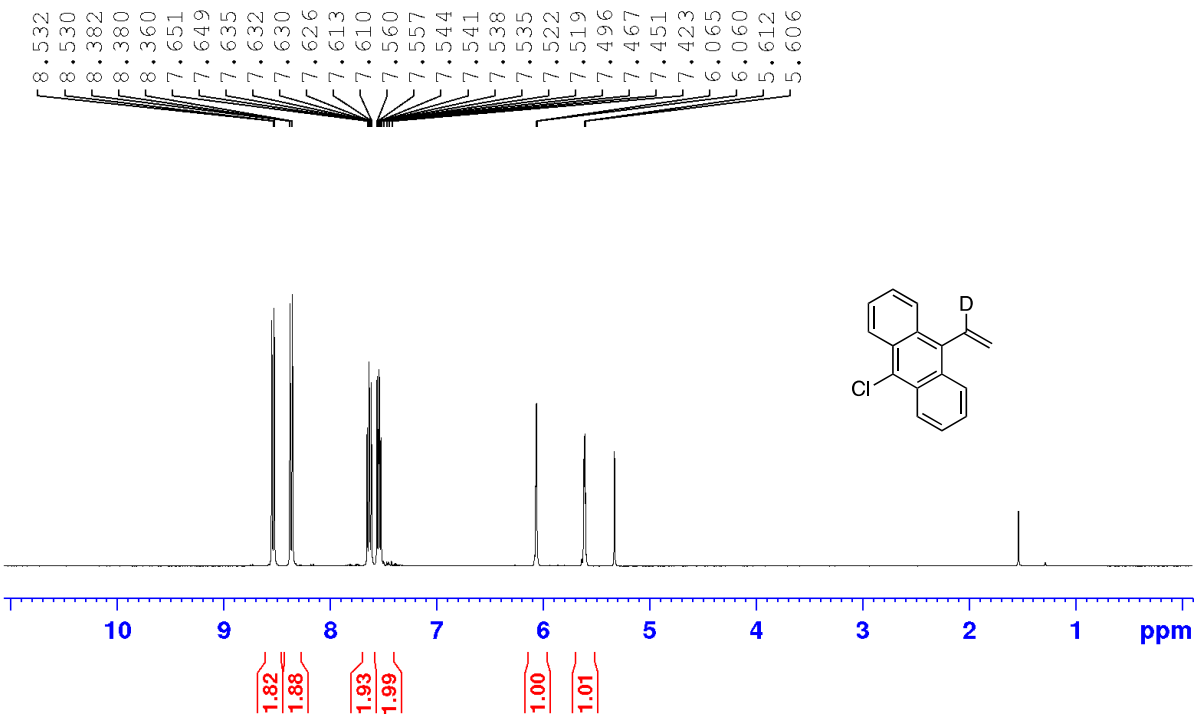

^{1}H NMR spectrum (400 MHz, CH_2Cl_2)

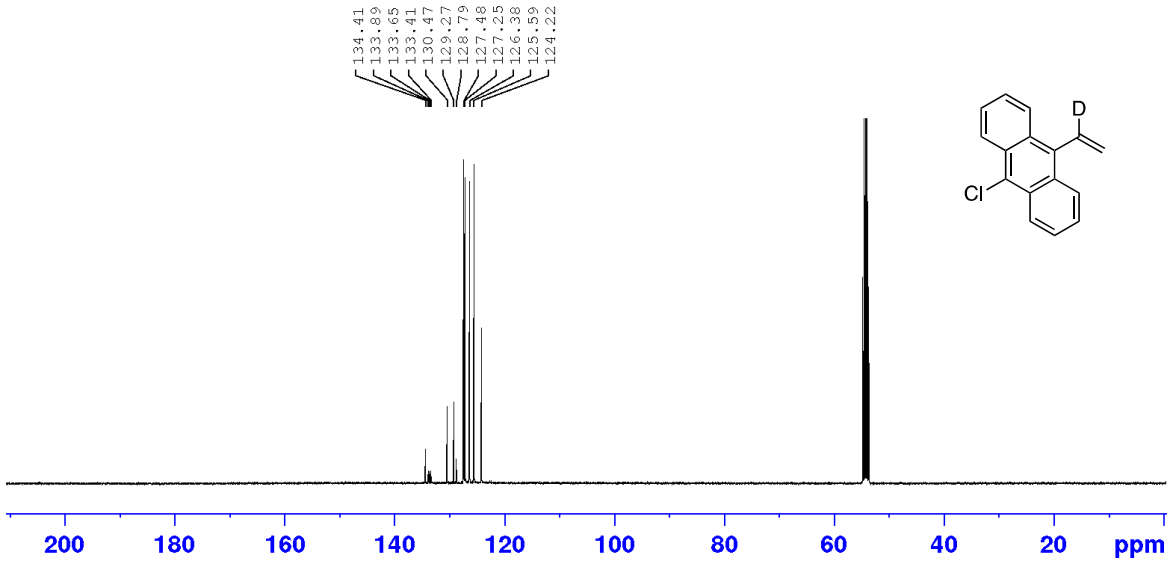

^{13}C NMR spectrum (101 MHz, CH_2Cl_2)

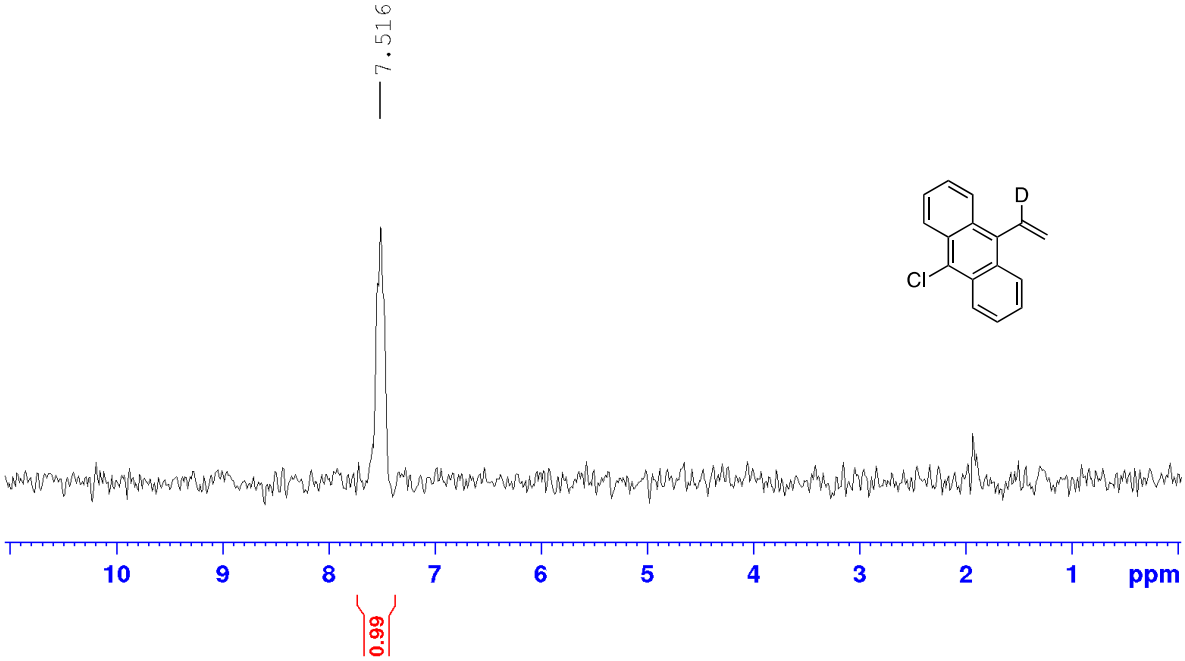

^{2}H NMR spectrum (62 MHz, CH_3CN)

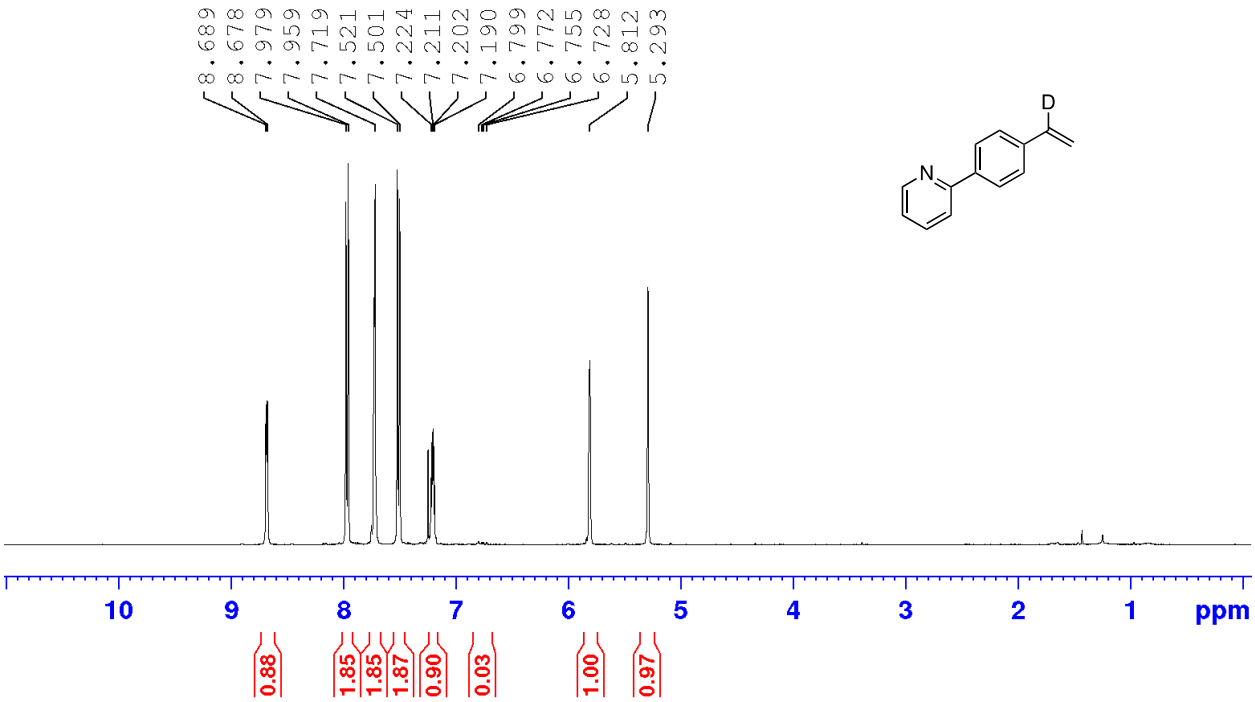

^{1}H NMR spectrum (400 MHz, $CDCl_3$)

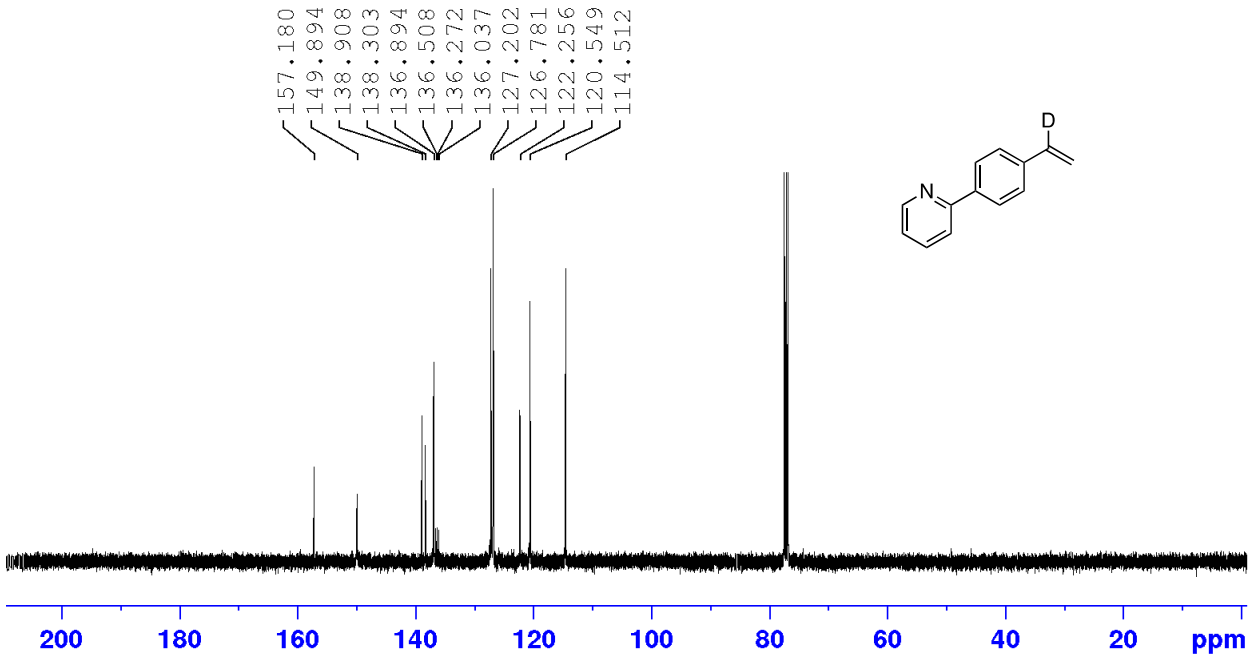

^{13}C NMR spectrum (101 MHz, $CDCl_3$)

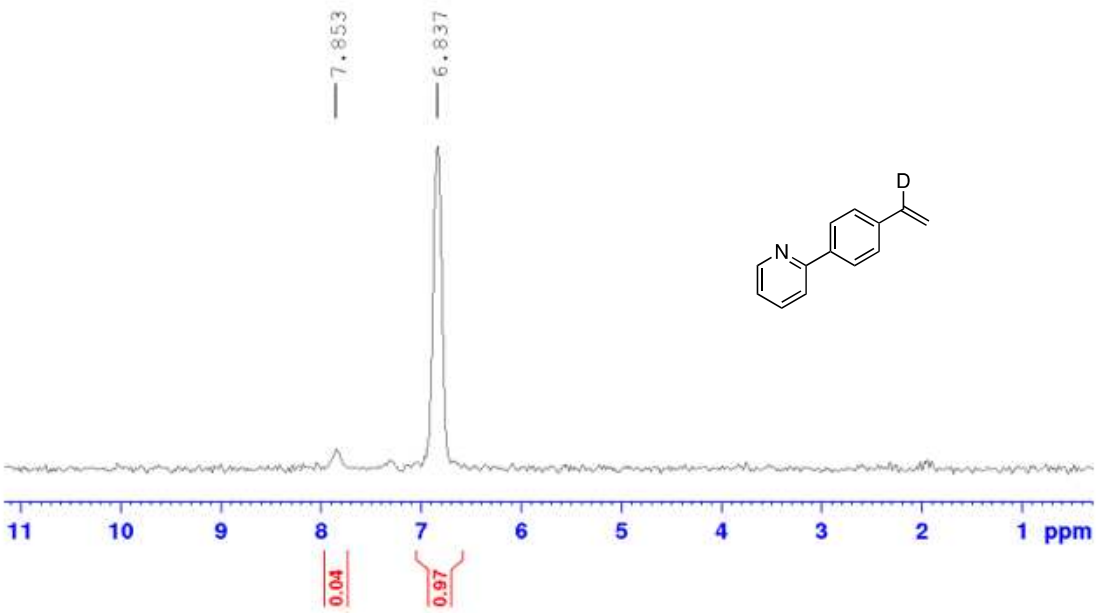

^{2}H NMR spectrum (62 MHz, $CDCl_3$)

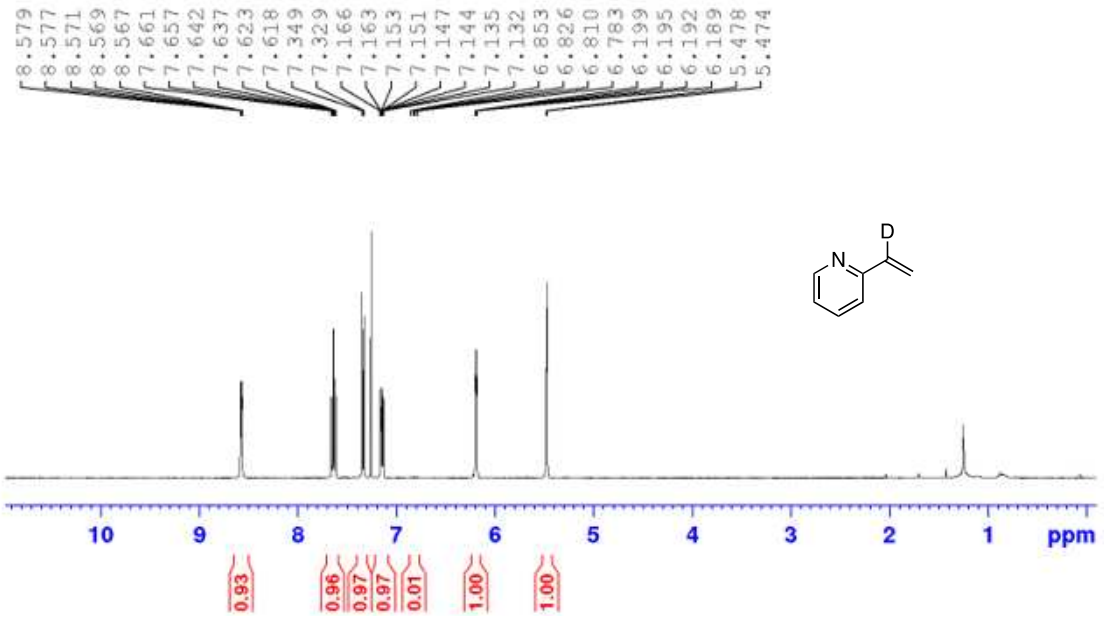

^{1}H NMR spectrum (400 MHz, $CDCl_3$)

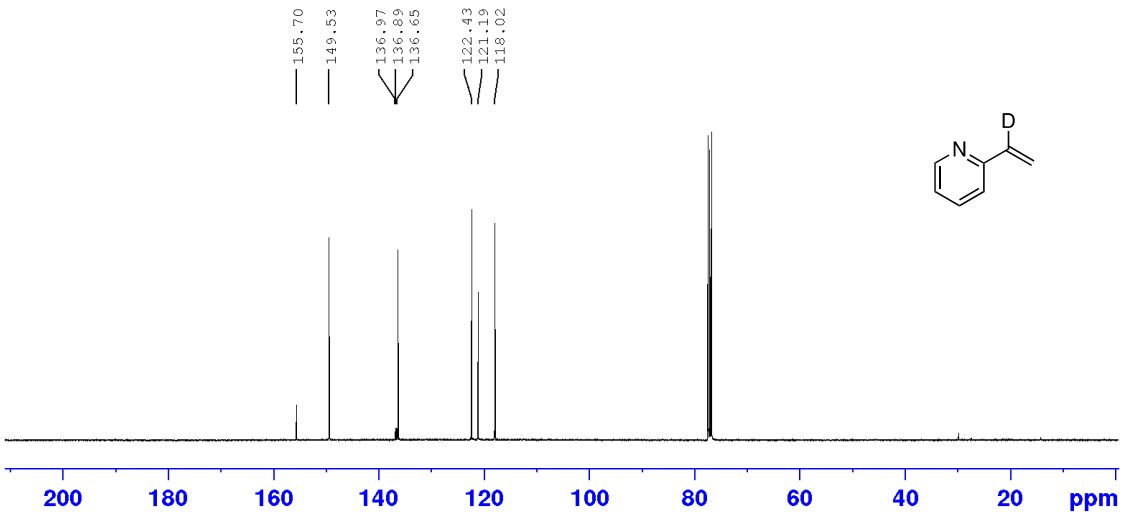

^{13}C NMR spectrum (101 MHz, $CDCl_3$)

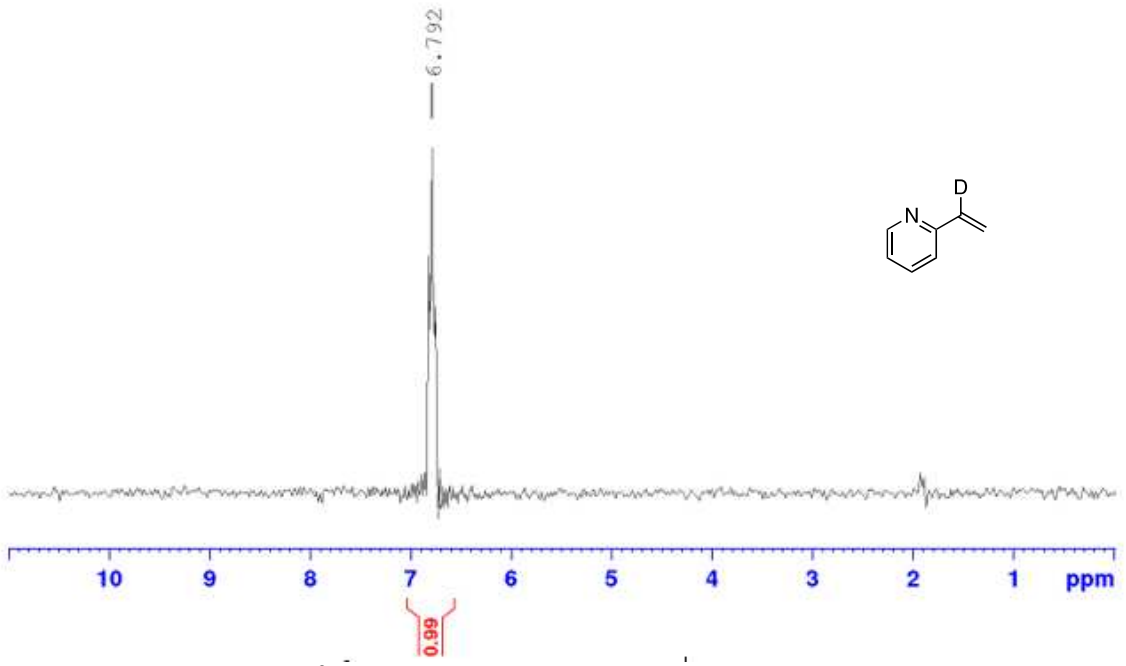

^{2}H NMR spectrum (62 MHz, CH_3CN)

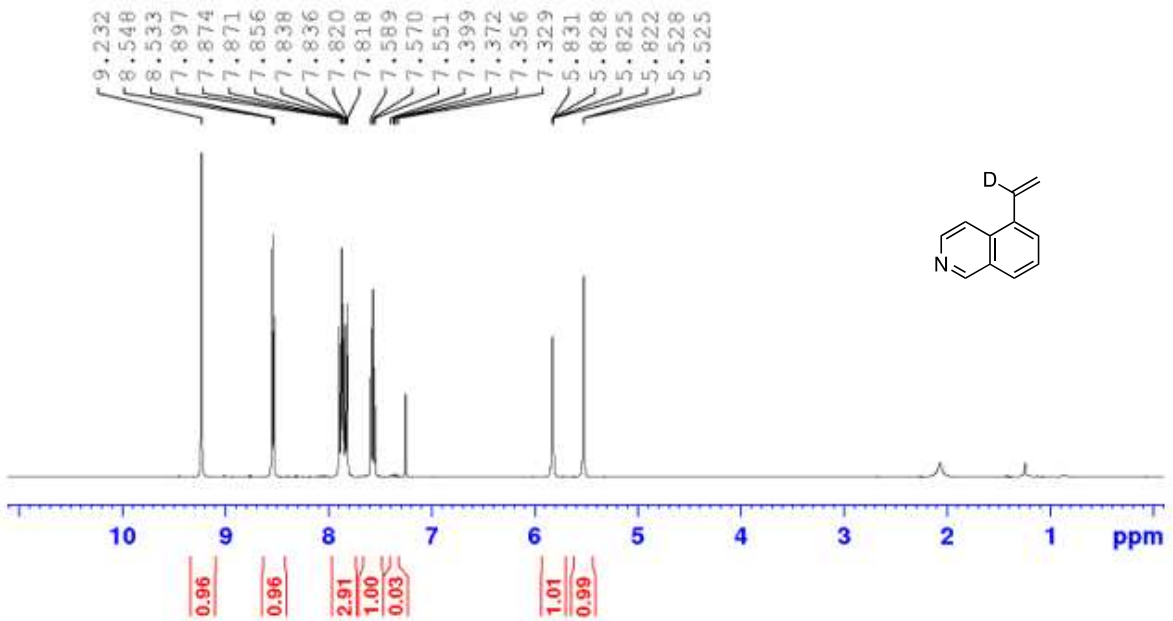

^{1}H NMR spectrum (400 MHz, $CDCl_3$)

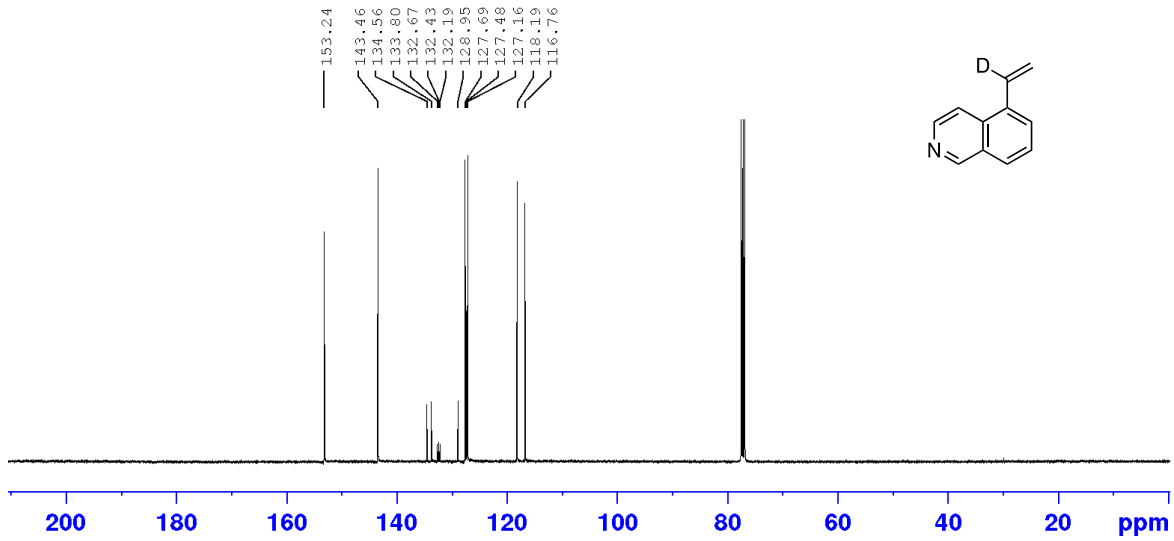

^{13}C NMR spectrum (101 MHz, $CDCl_3$)

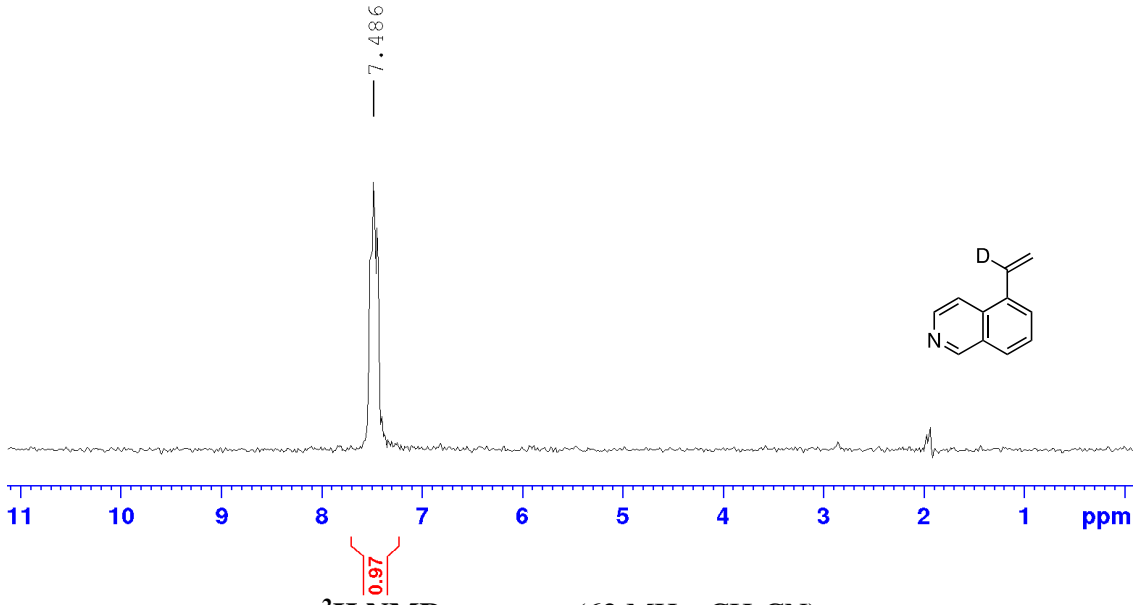

^{2}H NMR spectrum (62 MHz, CH_3CN)

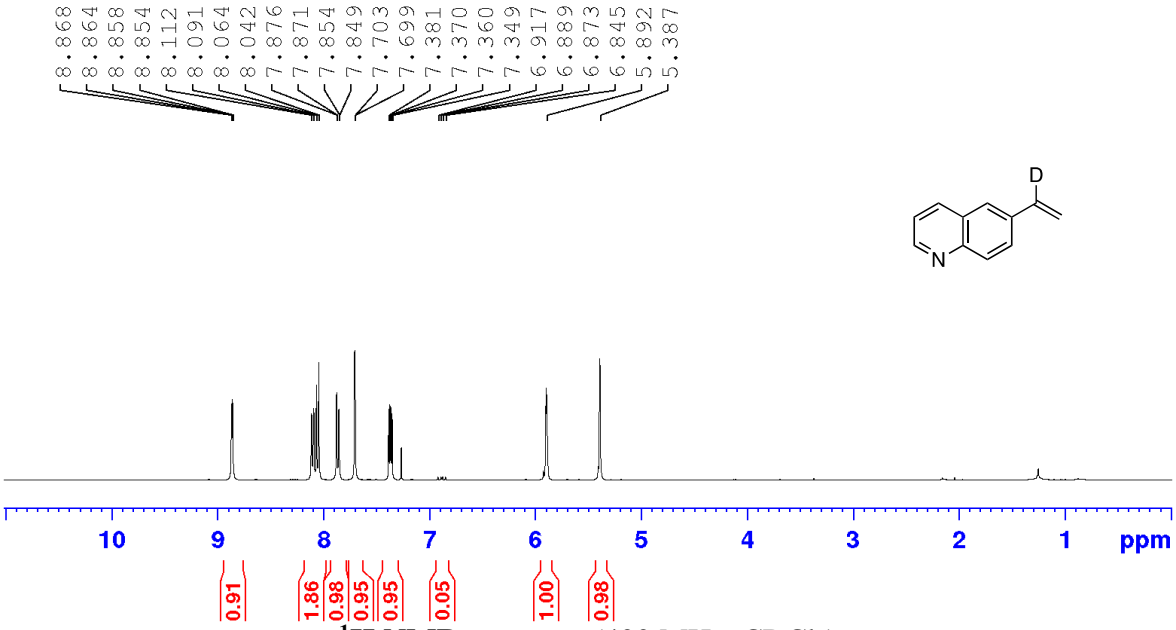

^{1}H NMR spectrum (400 MHz, $CDCl_3$)

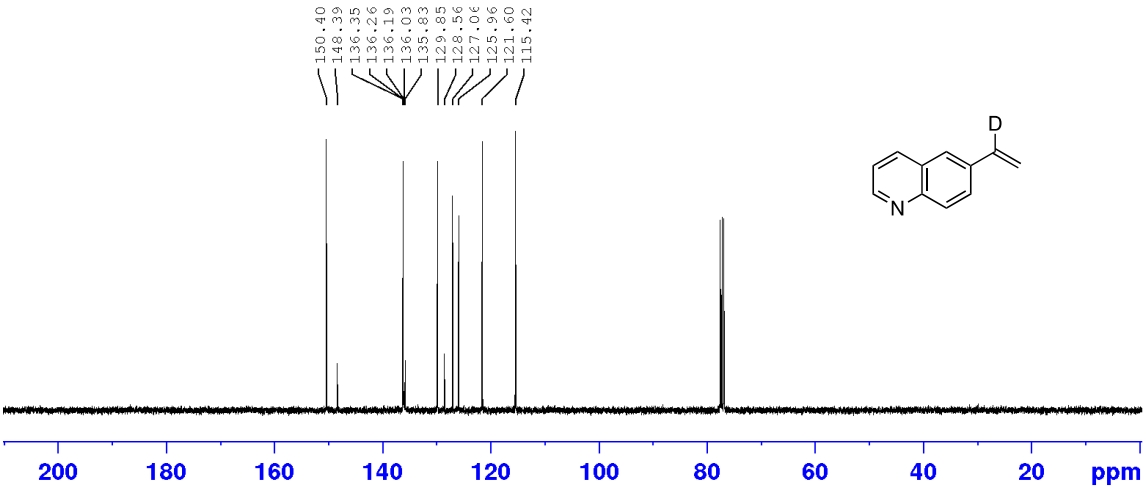

^{13}C NMR spectrum (101 MHz, $CDCl_3$)

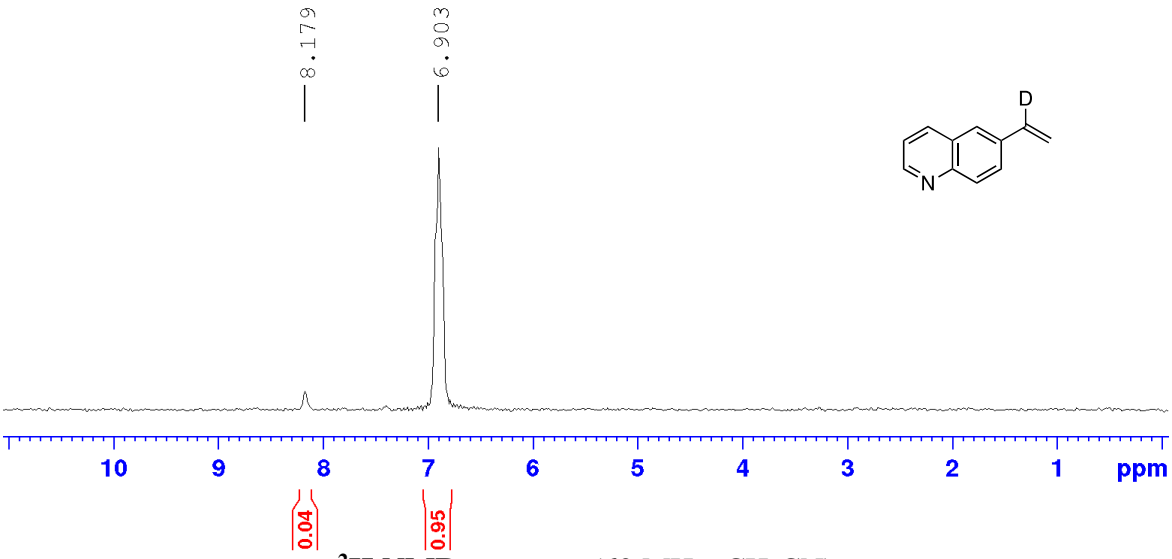

^{2}H NMR spectrum (62 MHz, CH_3CN)

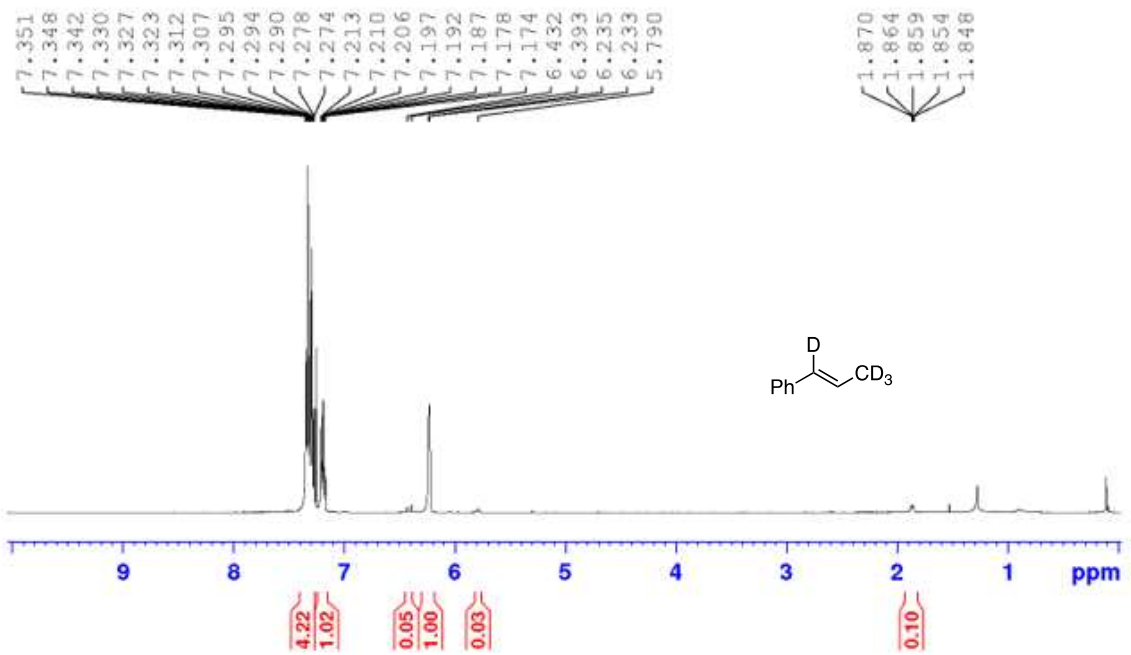

^{1}H NMR spectrum (400 MHz, $CDCl_3$)

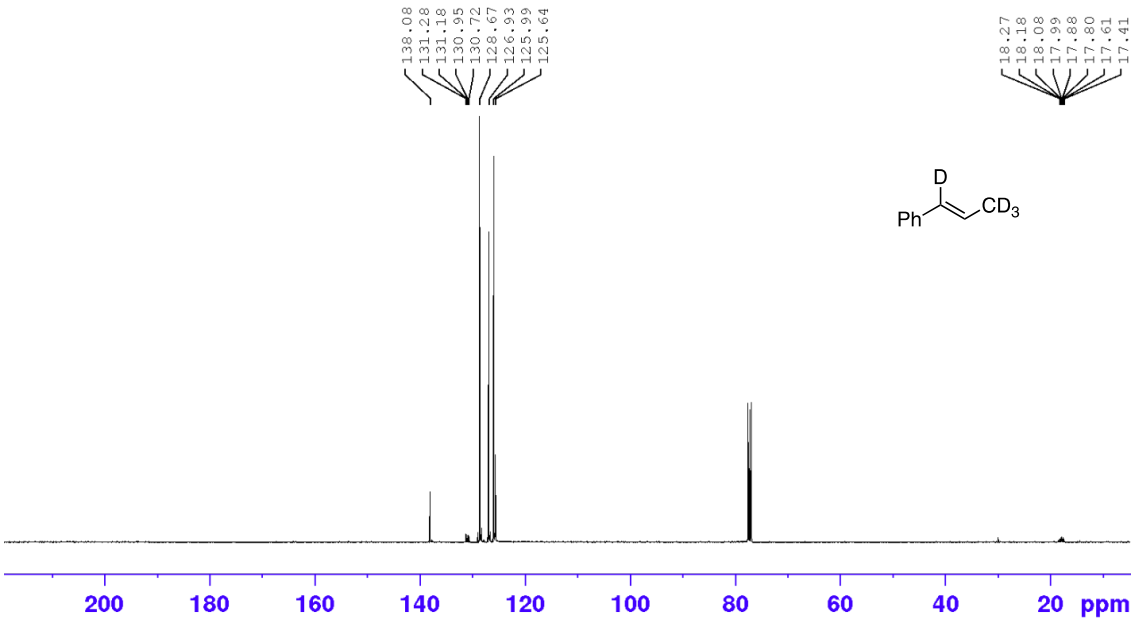

^{13}C NMR spectrum of (101 MHz, $CDCl_3$)

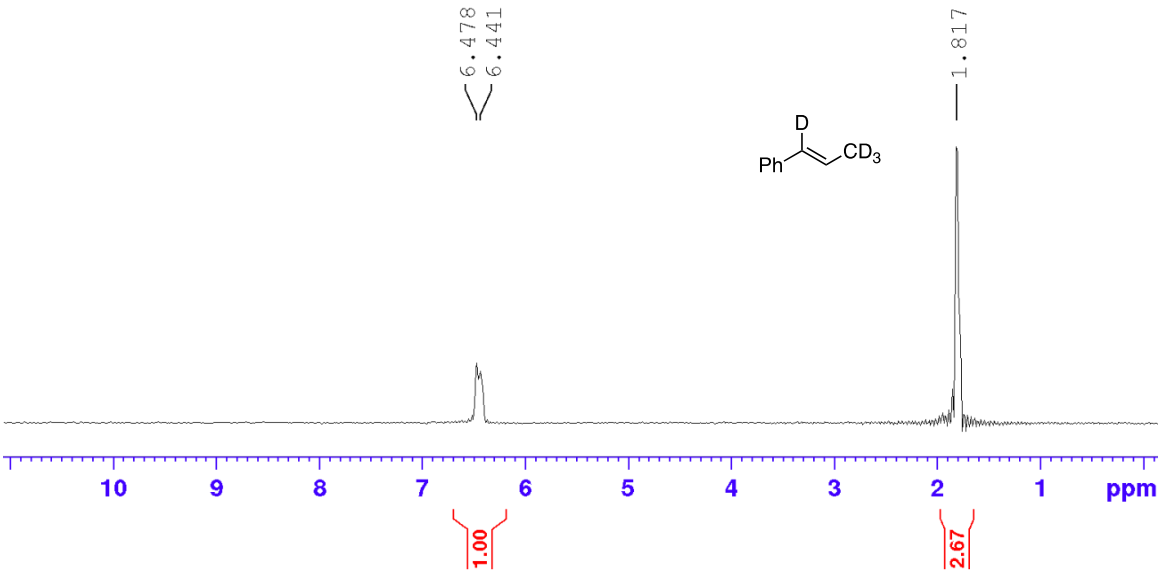

^{2}H NMR spectrum of (62 MHz, CH_3CN)

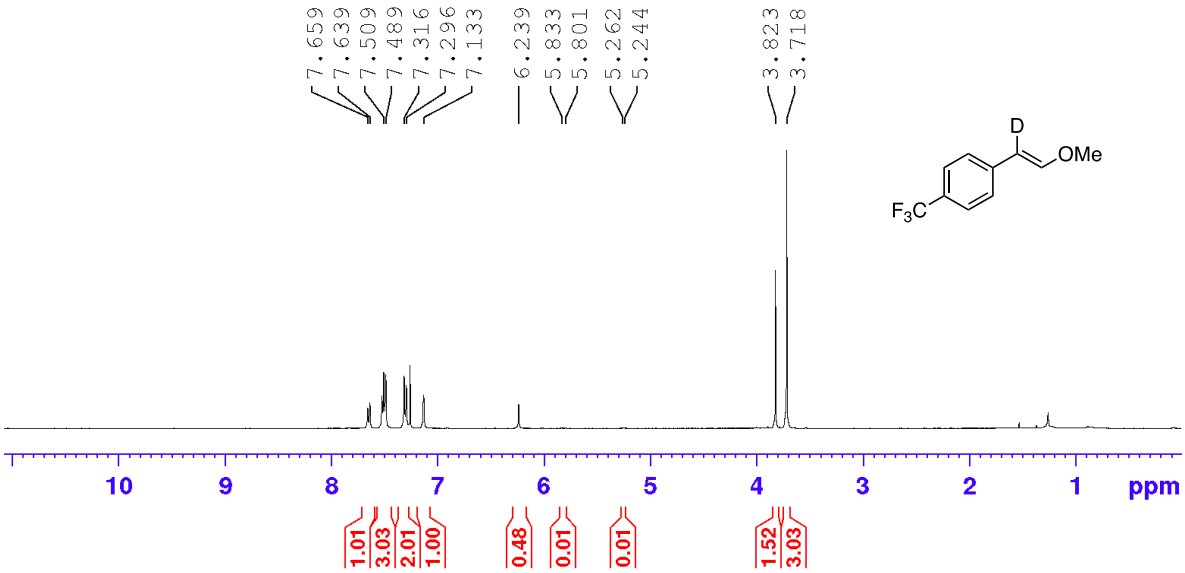

^{1}H NMR spectrum (400 MHz, $CDCl_3$)

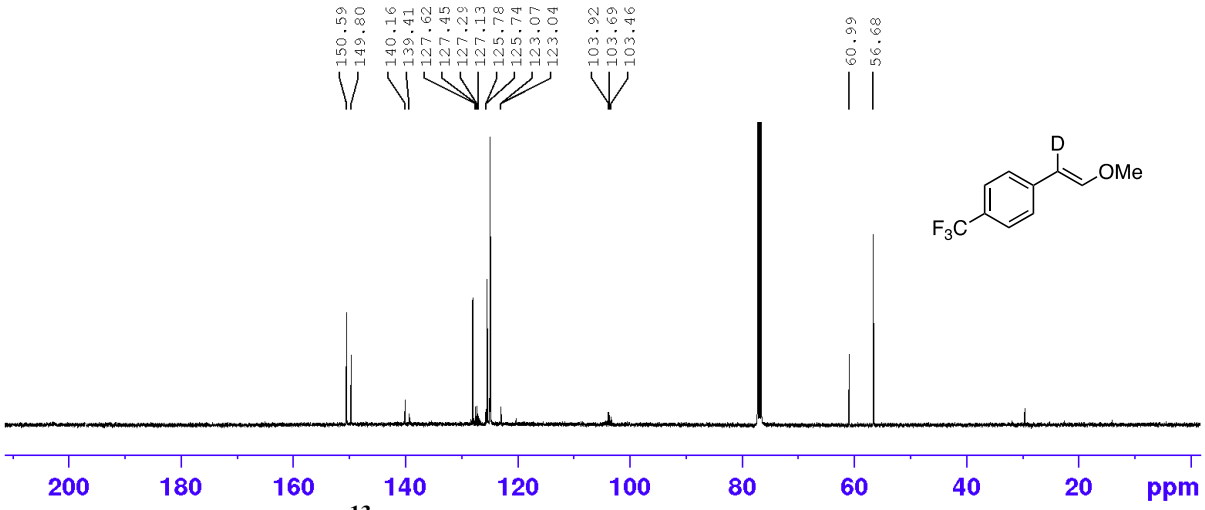

^{13}C NMR spectrum (101 MHz, $CDCl_3$)

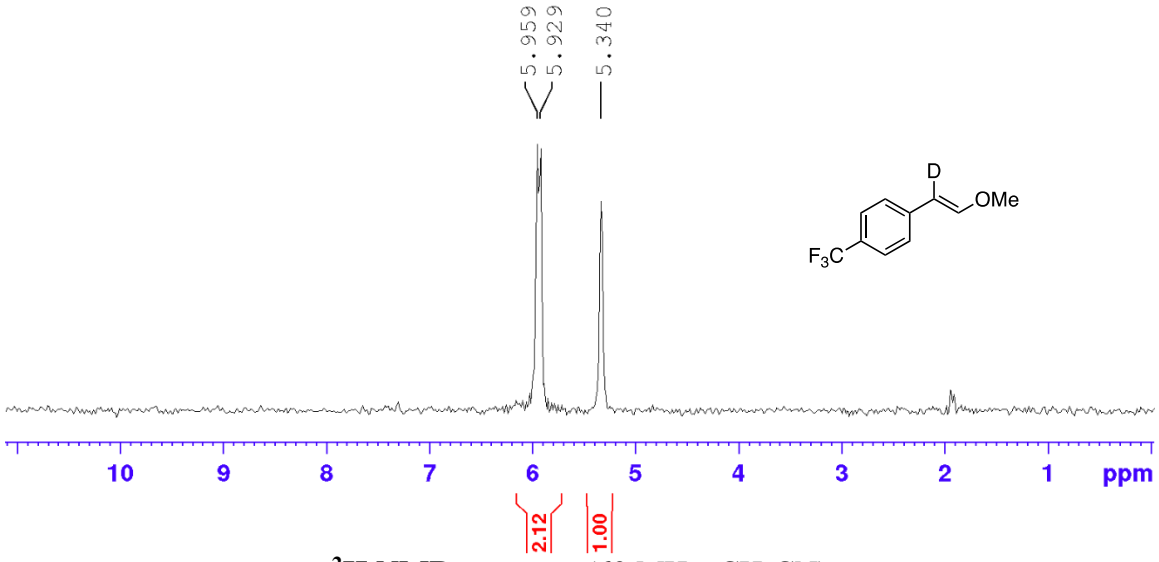

^{2}H NMR spectrum (62 MHz, CH_3CN)

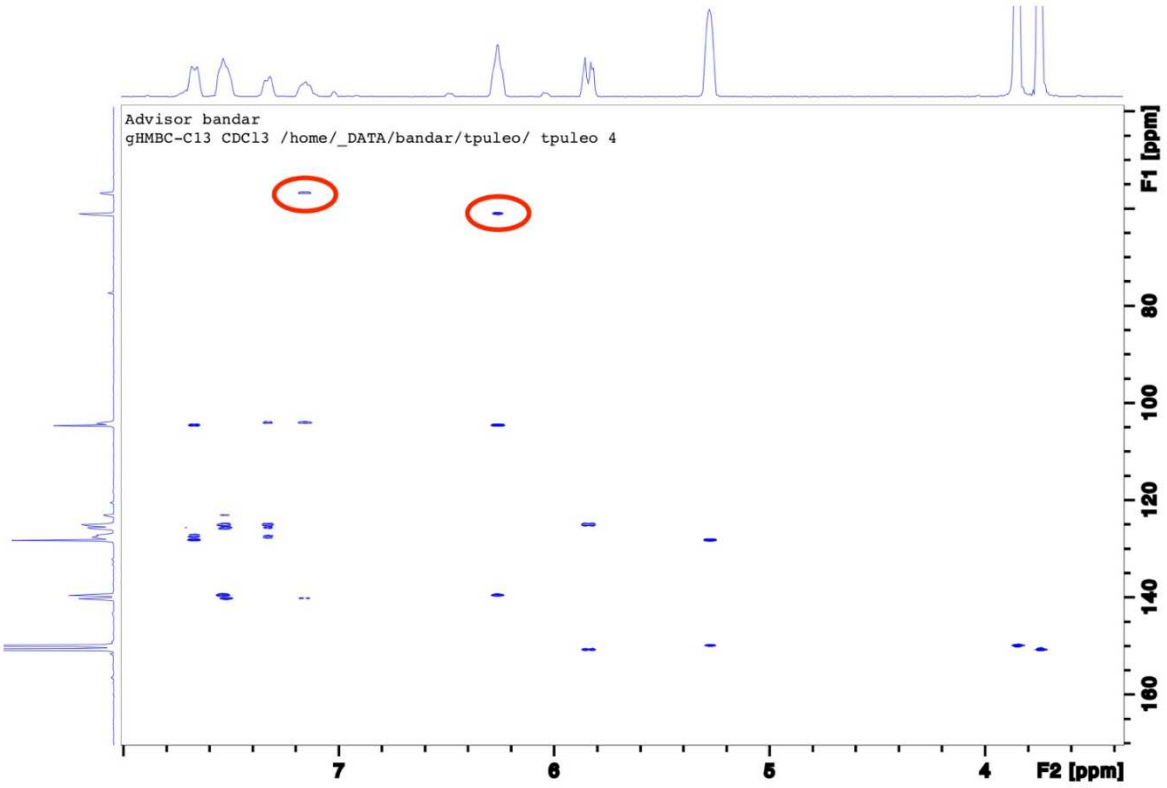

2D HMBC NMR spectrum of **1–24**. The circled signals correlate to the (-OMe) ^{13}C NMR and the β ^{1}H NMR 3-bond correlation.

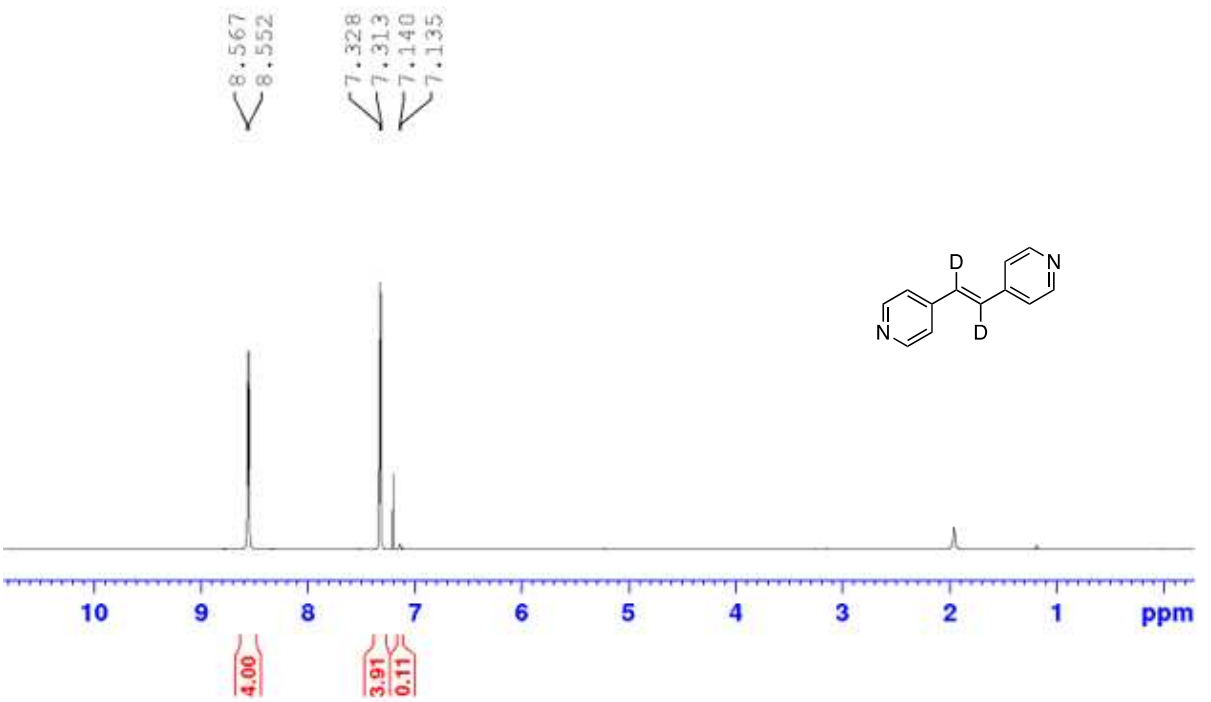

^{1}H NMR spectrum (400 MHz, $CDCl_3$)

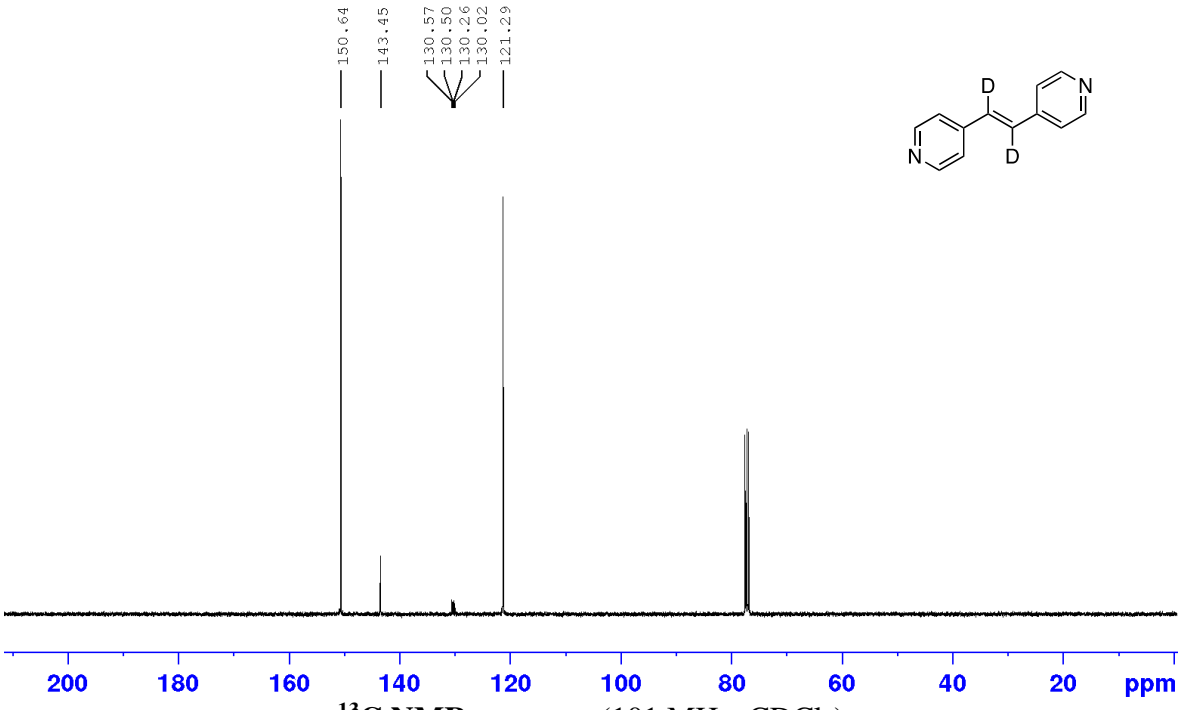

^{13}C NMR spectrum (101 MHz, $CDCl_3$)

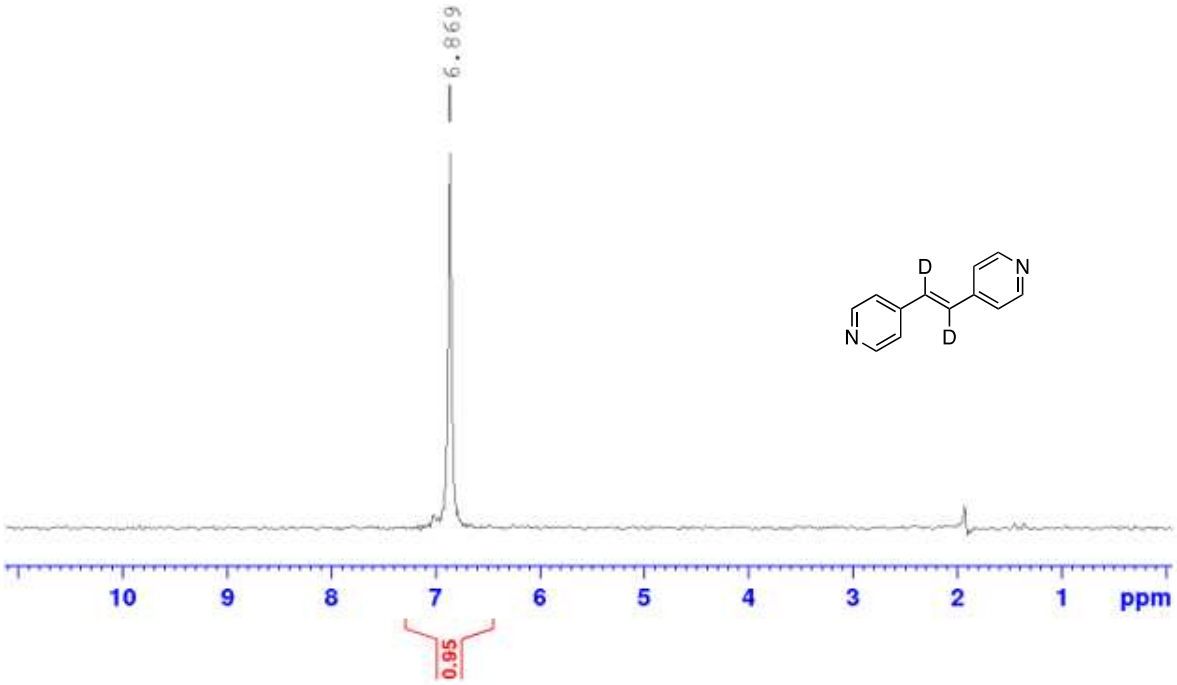

^{2}H NMR spectrum (62 MHz, CH_3CN)

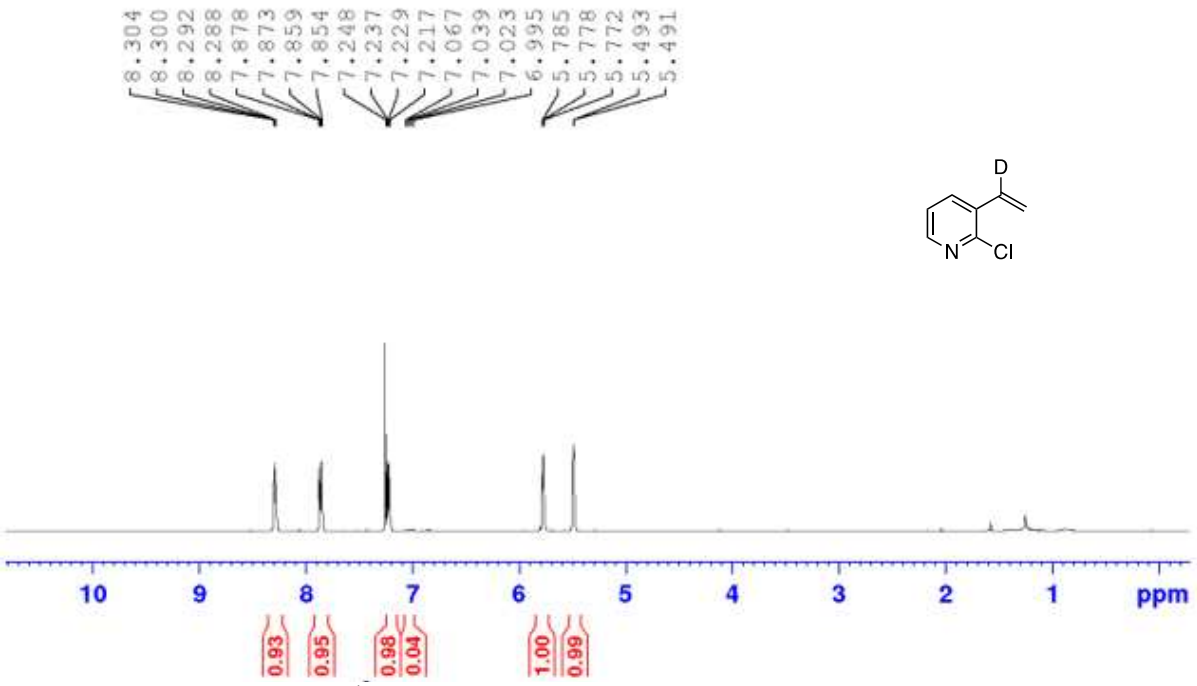

^{1}H NMR spectrum (400 MHz, $CDCl_3$)

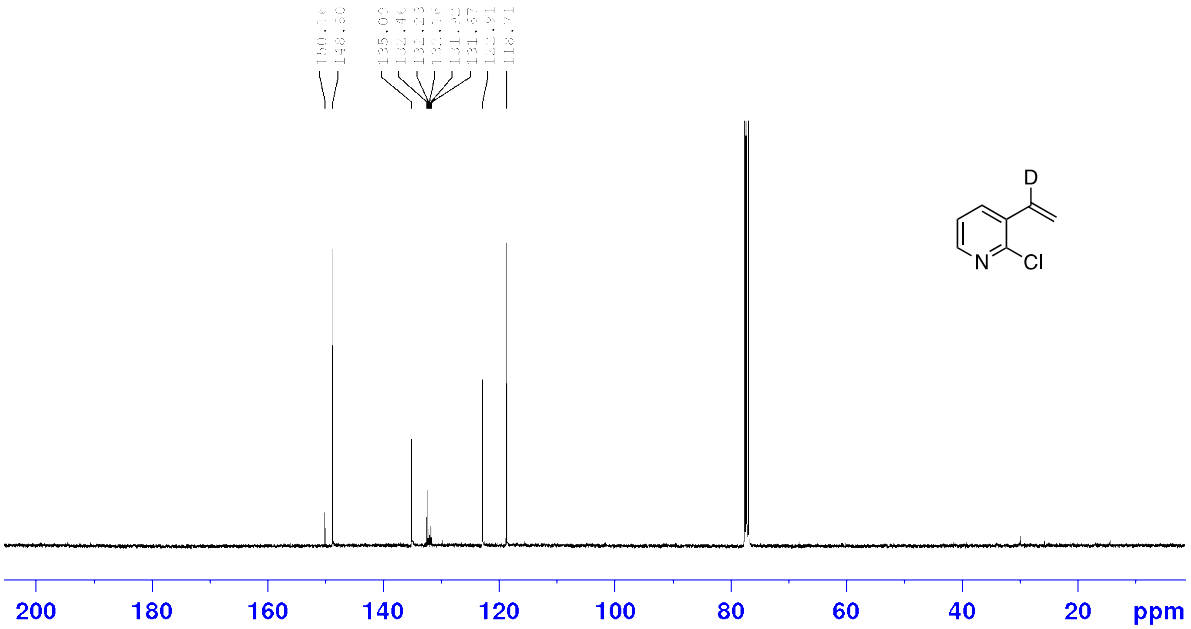

^{13}C NMR spectrum of (101 MHz, $CDCl_3$)

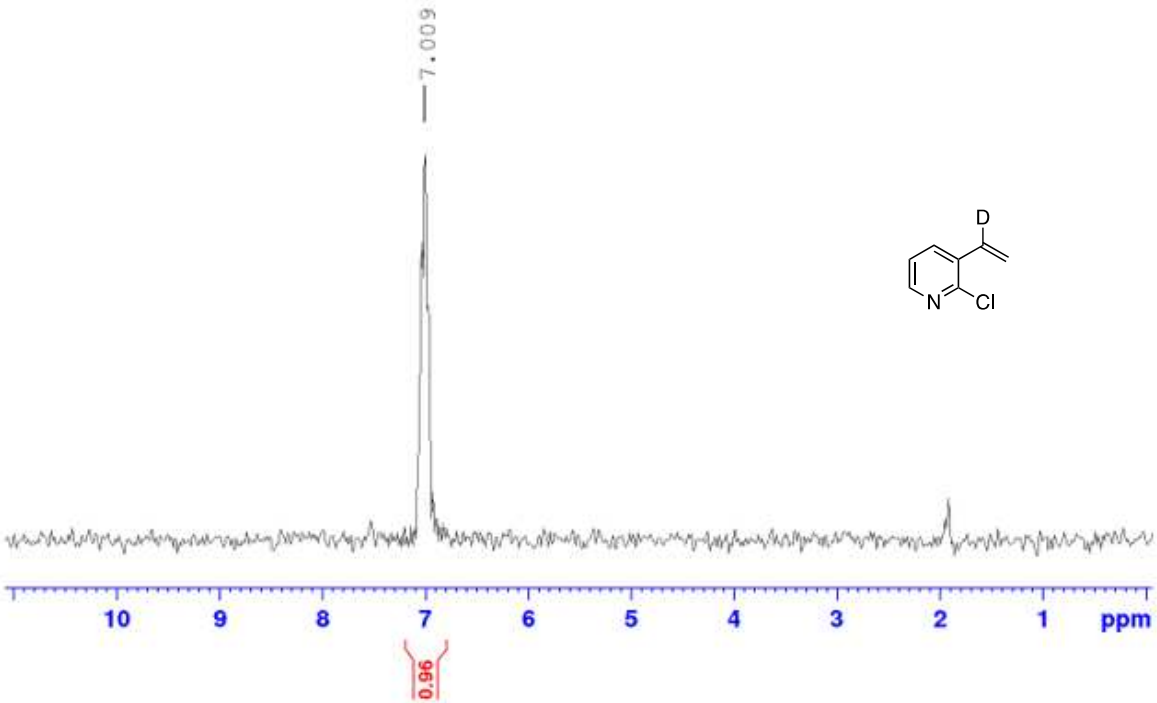

^{2}H NMR spectrum (62 MHz, CH_3CN)

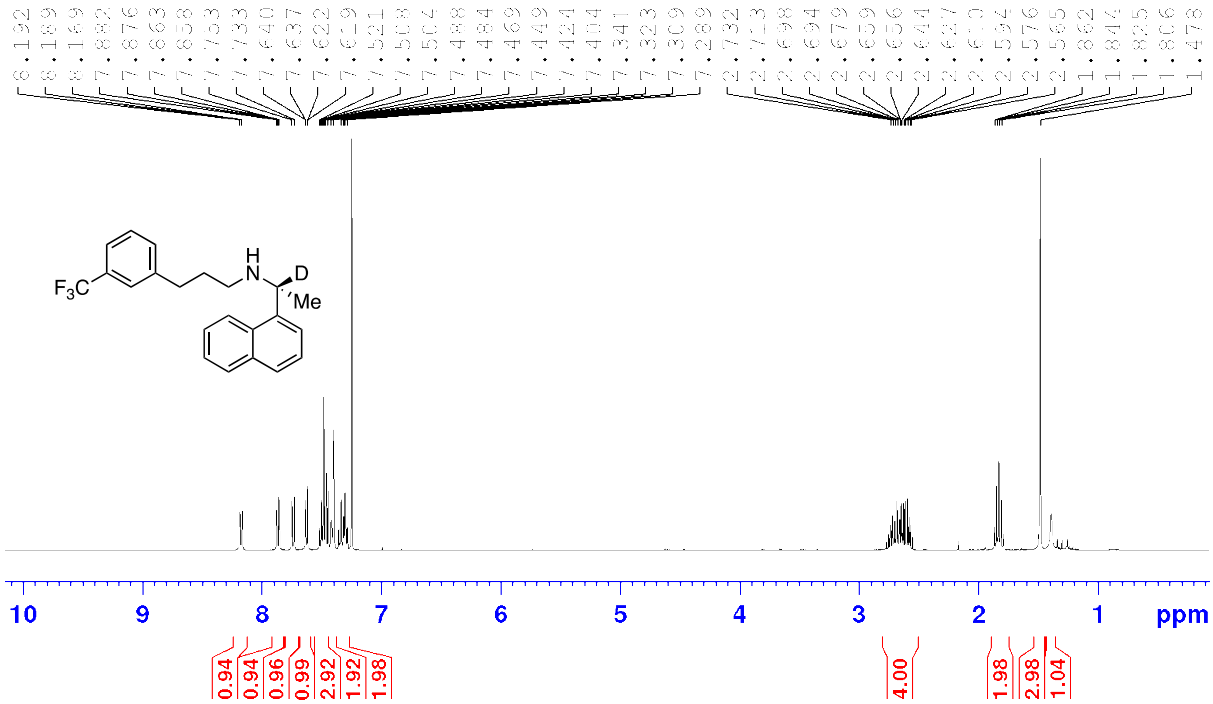

^{1}H NMR spectrum (400 MHz, $CDCl_3$)

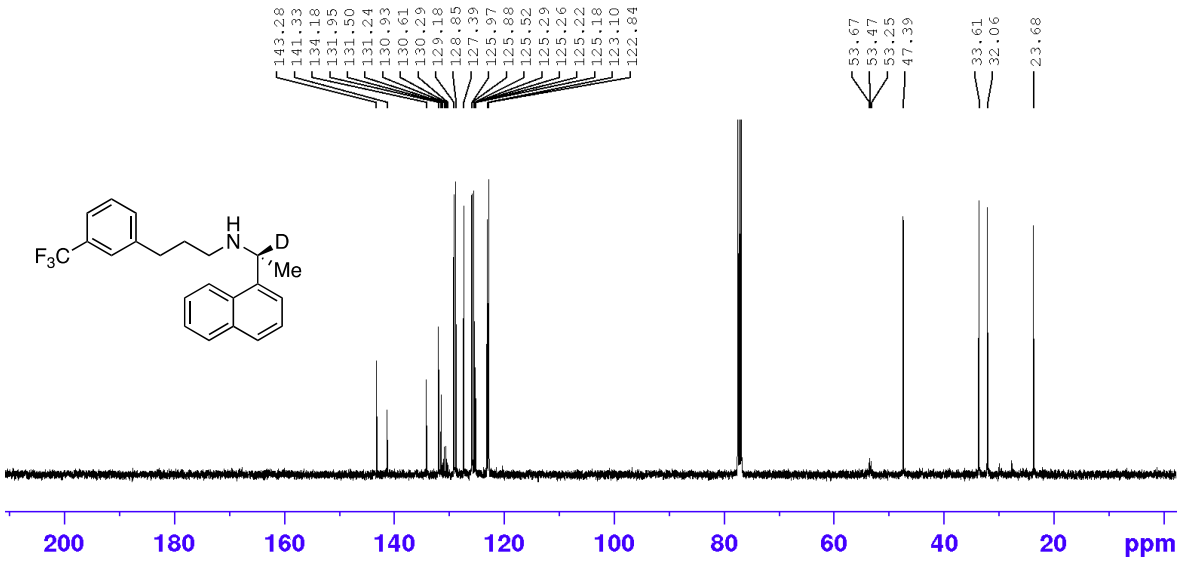

^{13}C NMR spectrum (101 MHz, $CDCl_3$)

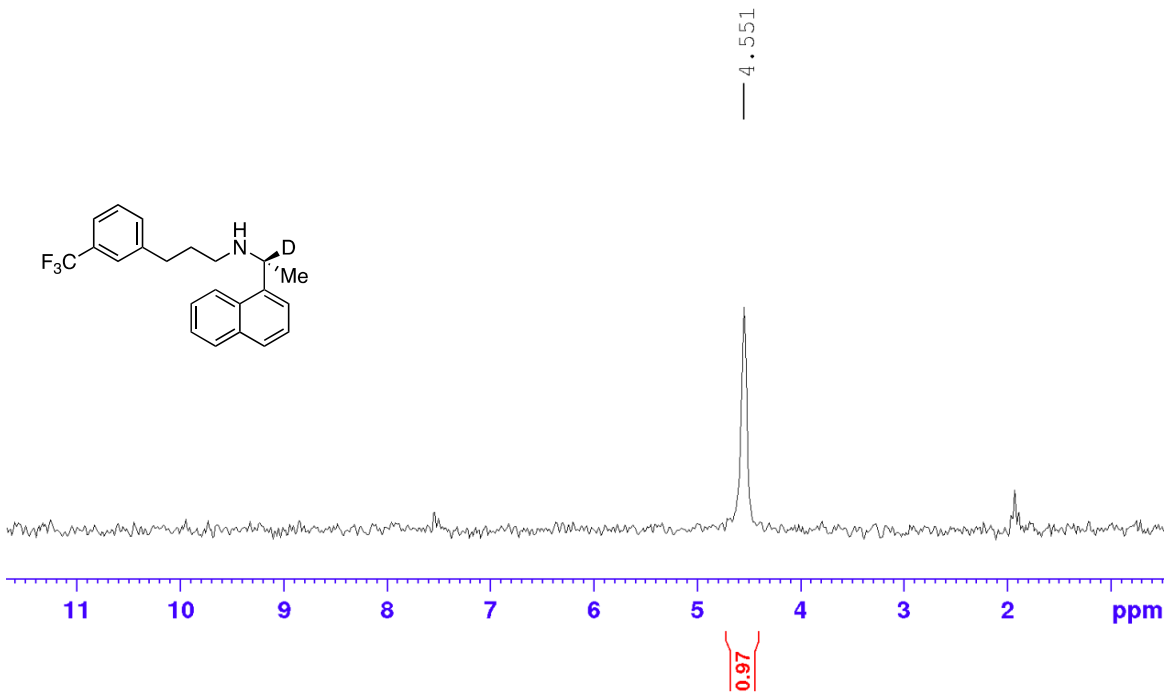

^{2}H NMR spectrum (62 MHz, CH_3CN)

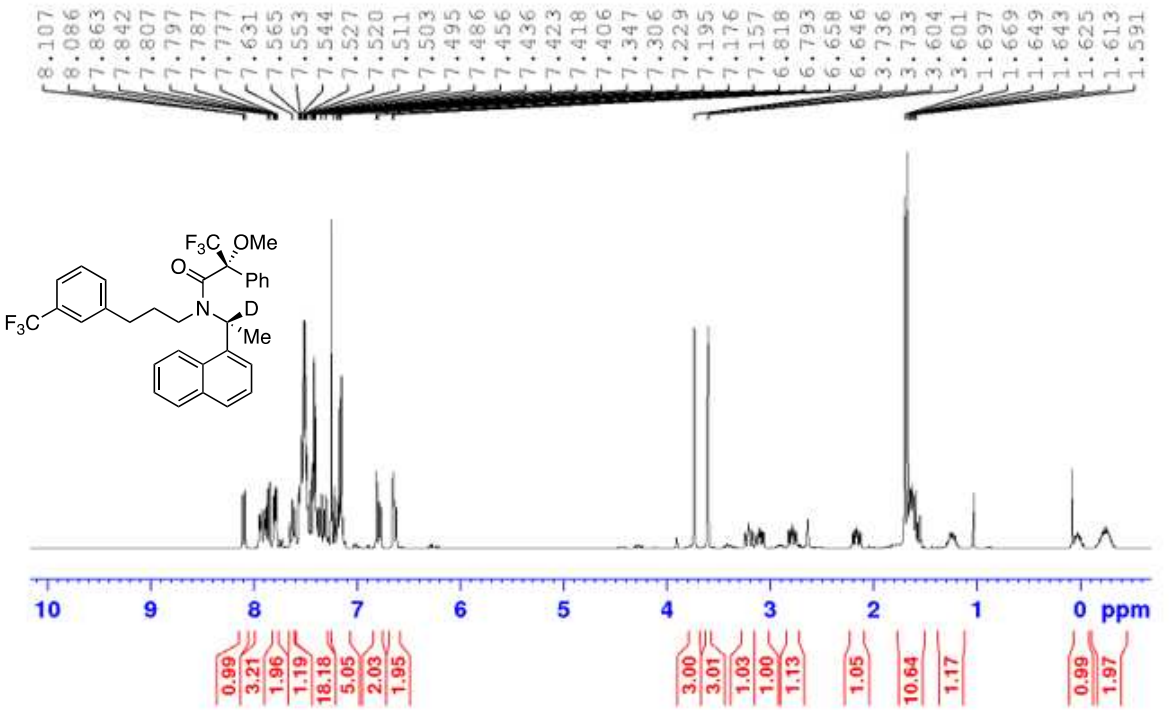

^{1}H NMR spectrum (400 MHz, $CDCl_3$)

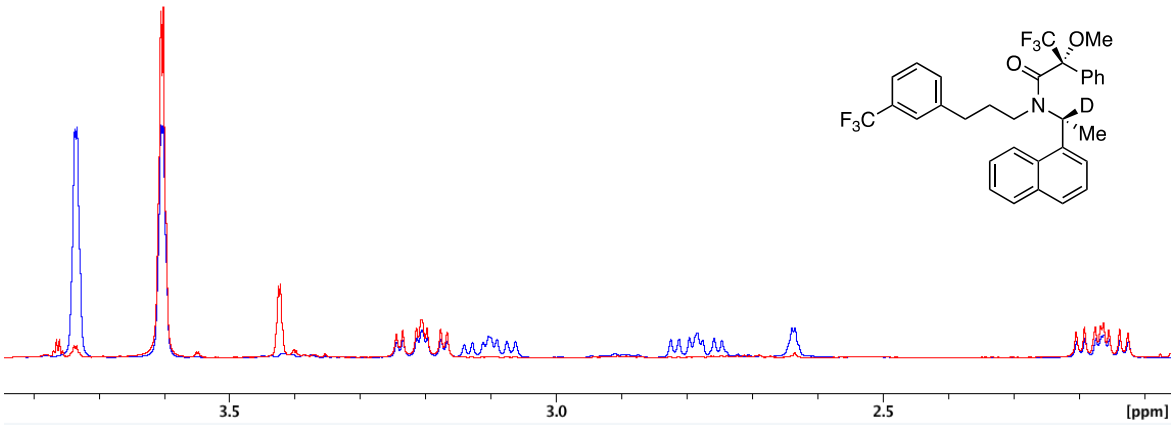

^{1}H NMR overlay of acylated **racemic** compound (blue) and **chiral** compound (red) (400 MHz, $CDCl_3$)

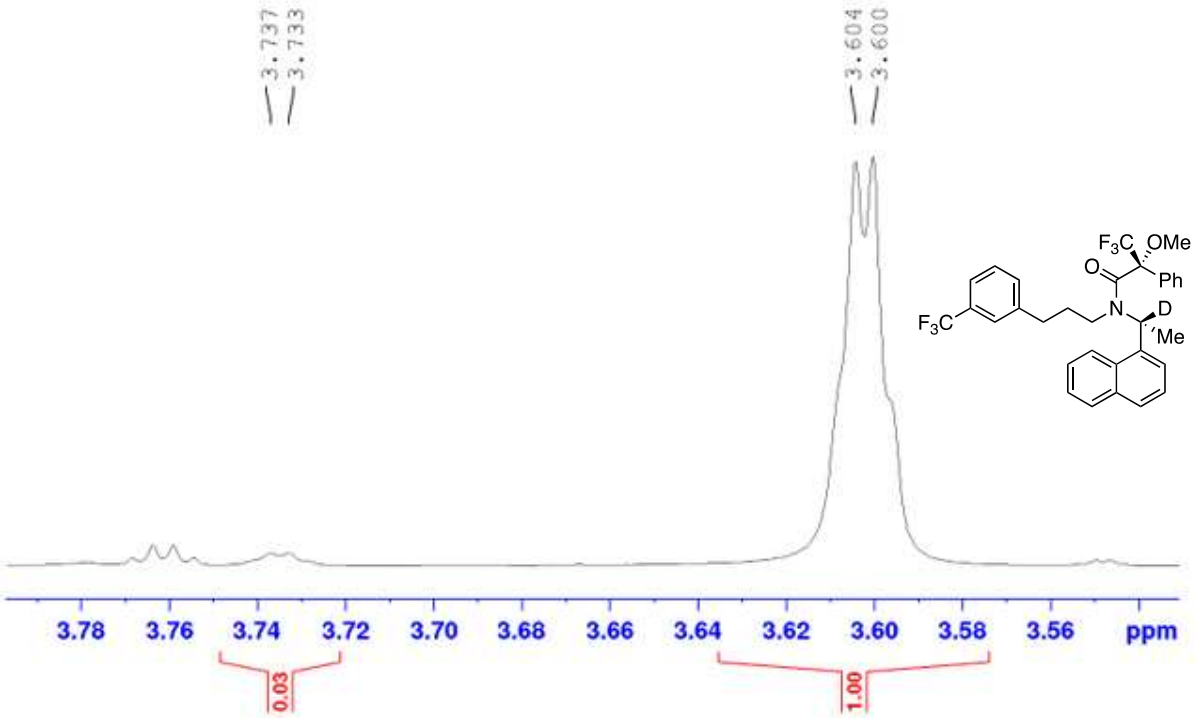

^{1}H NMR spectrum of -OMe signals for acylated chiral compound used for ee determination (400 MHz, $CDCl_3$).

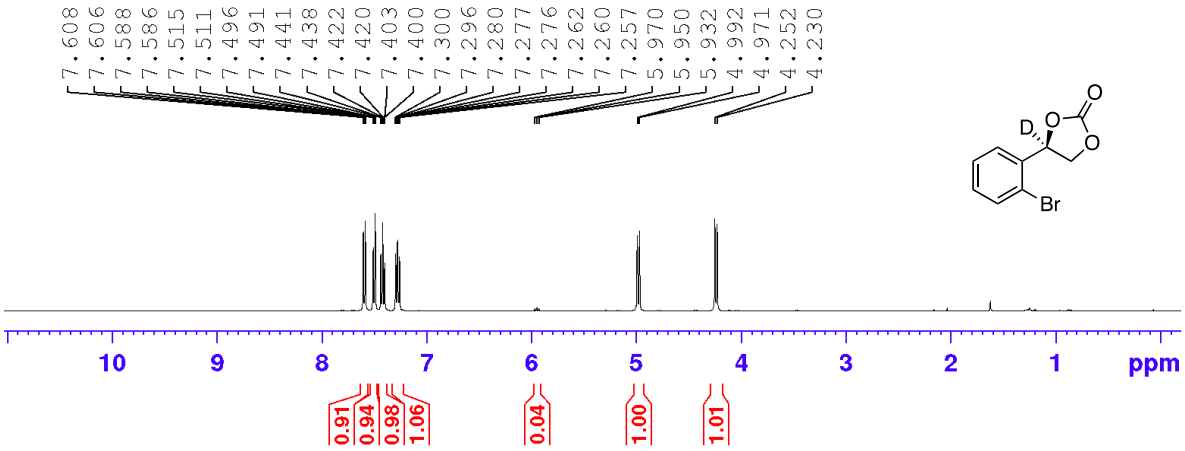

^{1}H NMR spectrum (400 MHz, $CDCl_3$)

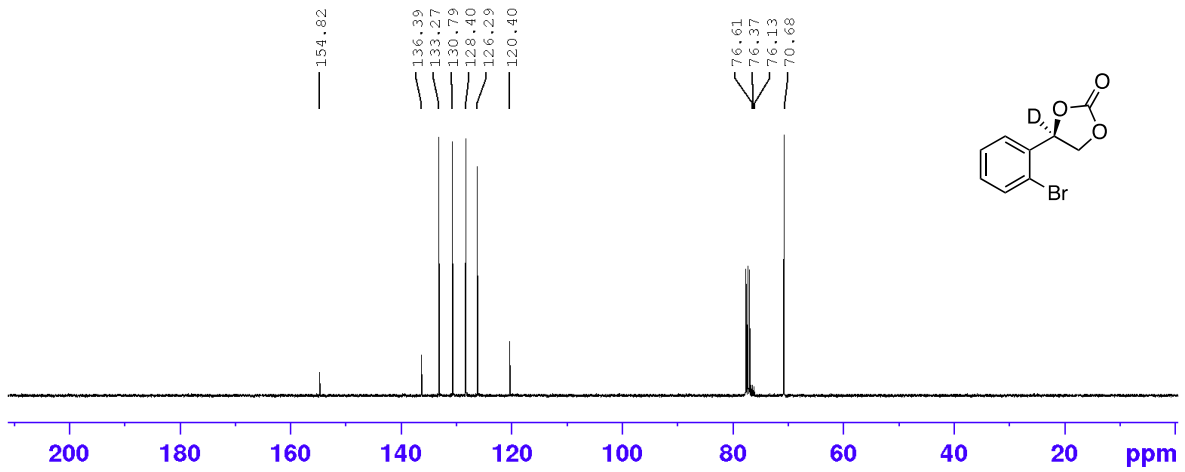

^{13}C NMR spectrum (101 MHz, $CDCl_3$)

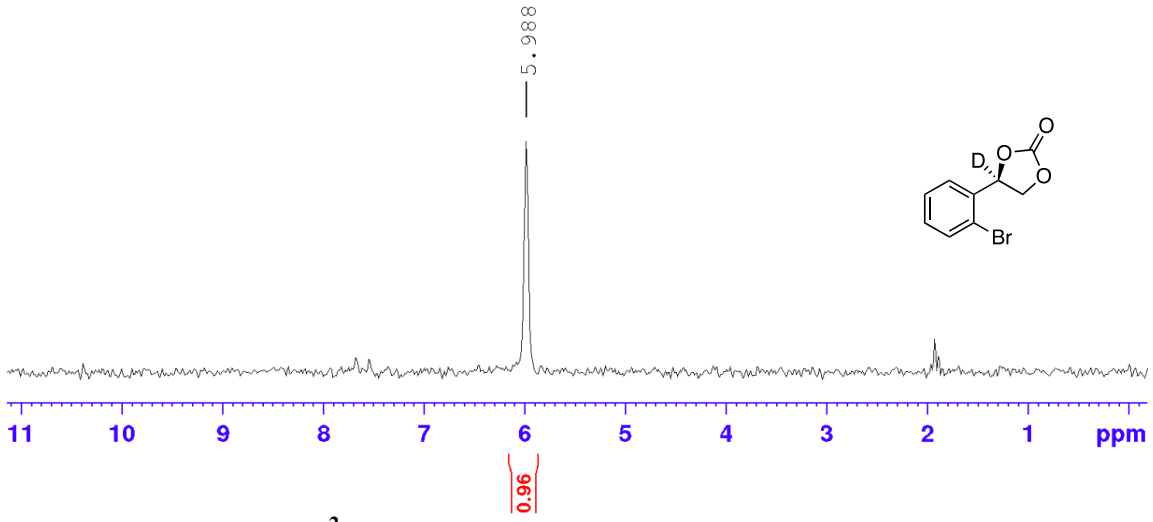

^{2}H NMR spectrum (62 MHz, CH_3CN)

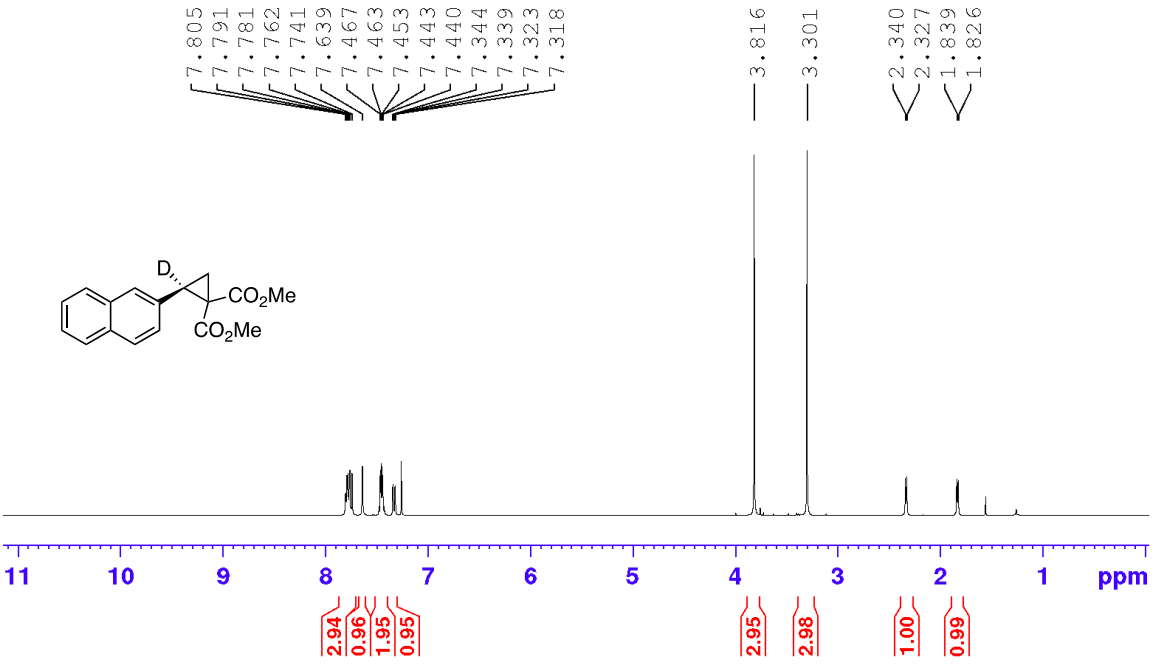

^{1}H NMR spectrum (400 MHz, $CDCl_3$)

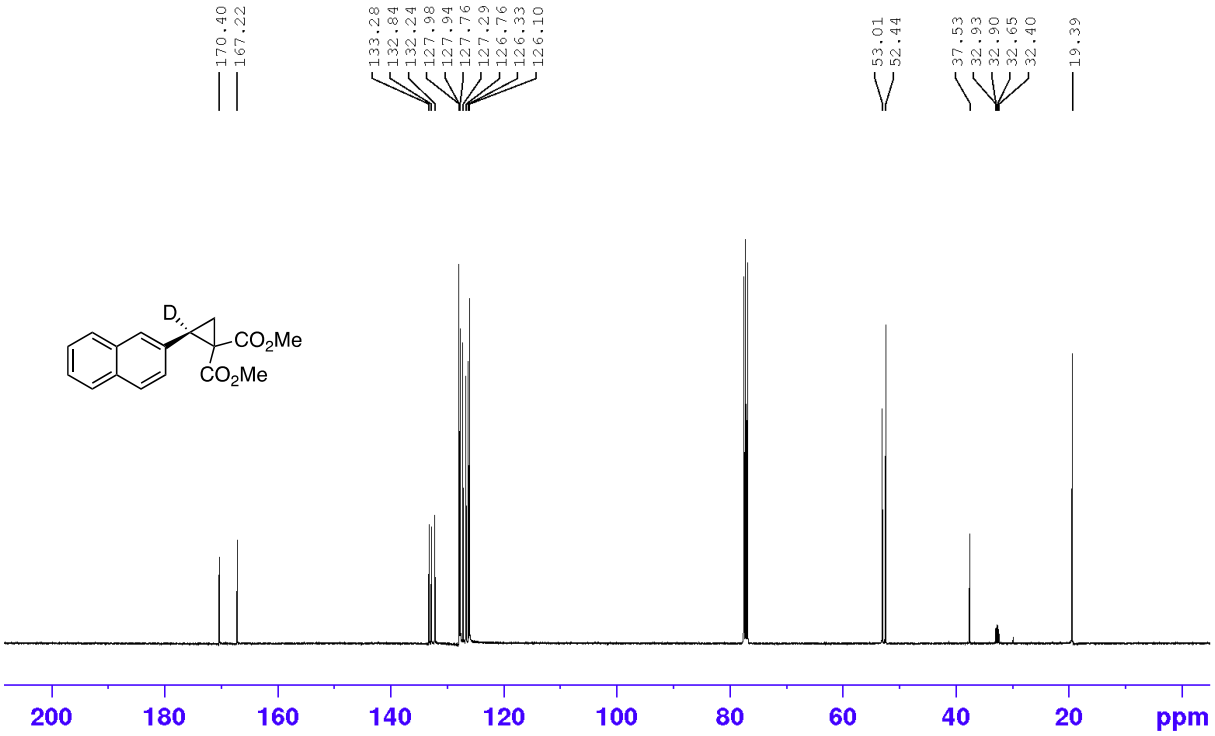

^{13}C NMR spectrum (101 MHz, $CDCl_3$)

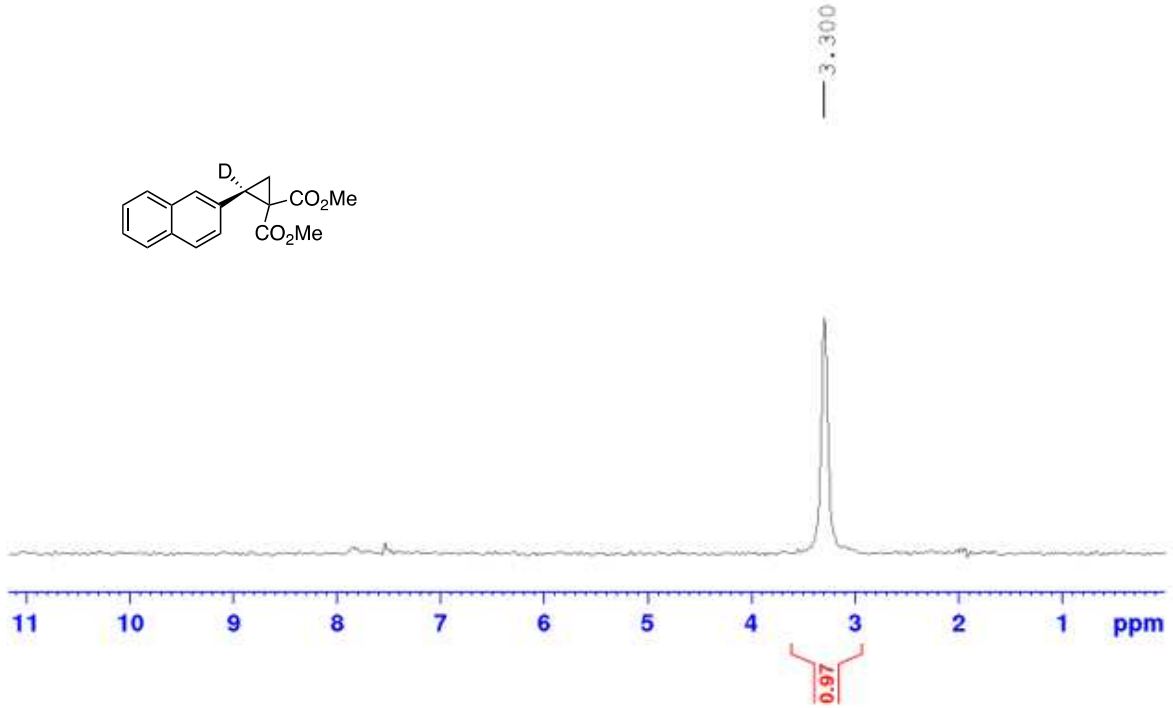

^{2}H NMR spectrum (62 MHz, CH_3CN)

XIII: Copies of Chiral HPLC Chromatograms

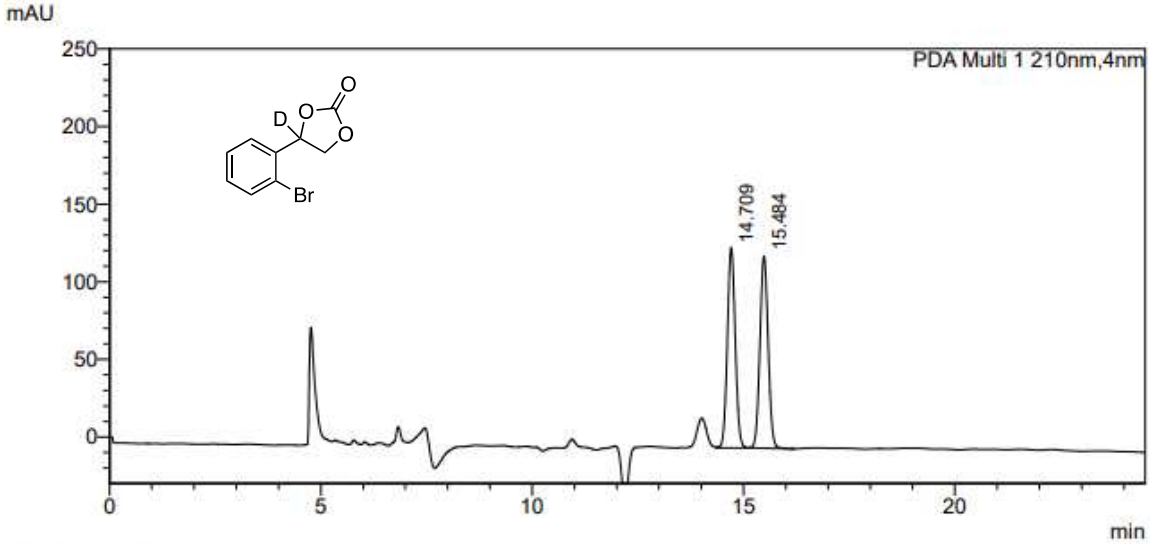

<Peak Table>

PDA Ch1 210nm

Peak#	Ret. Time	Area	Height	Conc.	Unit	Mark	Name
1	14.709	1674699	129153	0.000			
2	15.484	1676379	123744	0.000			
Total		3351078	252898				

Chiral HPLC of racemate

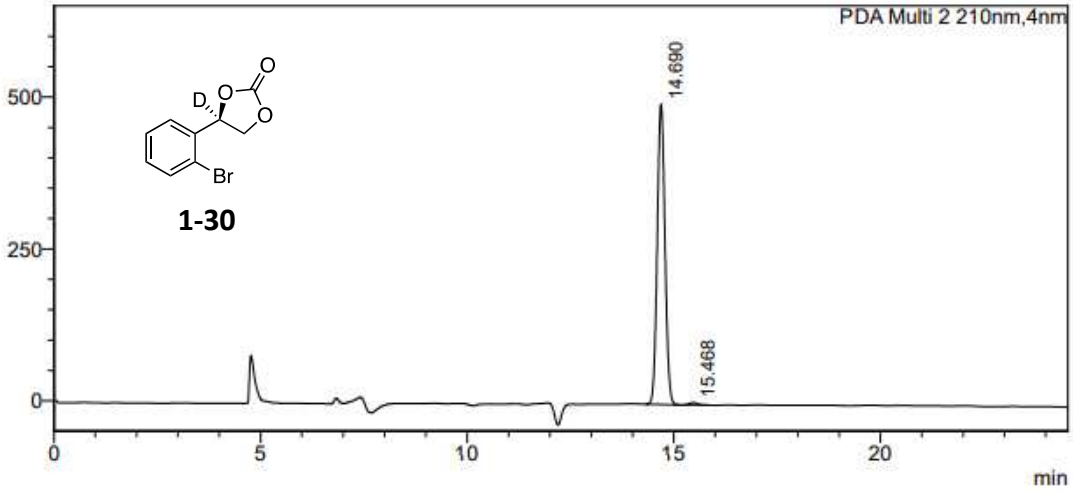

<Peak Table>

PDA Ch2 210nm

Peak#	Ret. Time	Conc.	ID#	Name	Area%
1	14.690	99.192			99.192
2	15.468	0.808			0.808
Total					100.000

Chiral HPLC of **1-30**

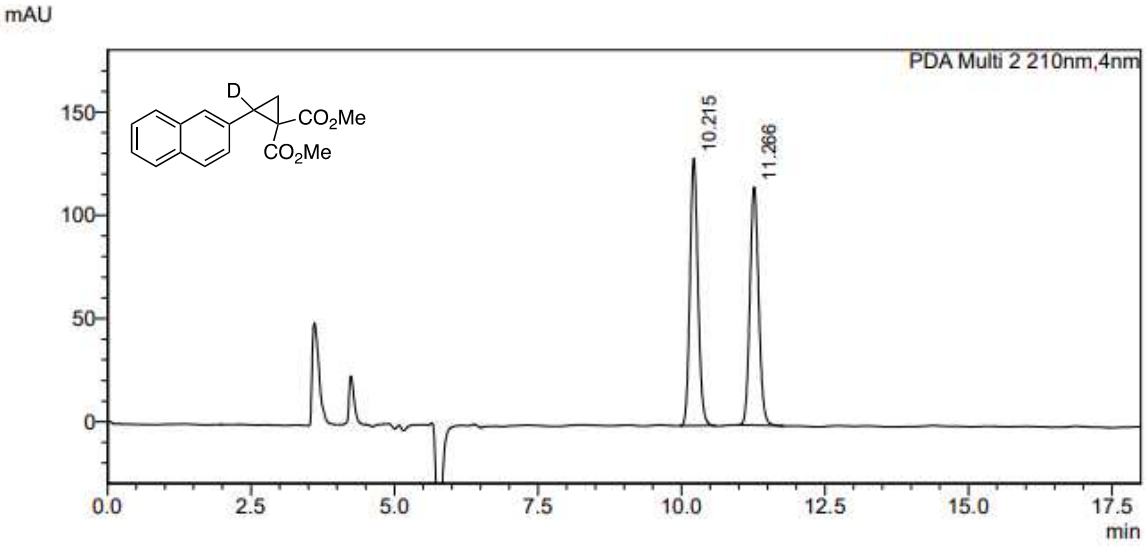

<Peak Table>

PDA Ch2 210nm

Peak#	Name	ID#	Area%
1			50.675
2			49.325
Total			100.000

Chiral HPLC of racemate

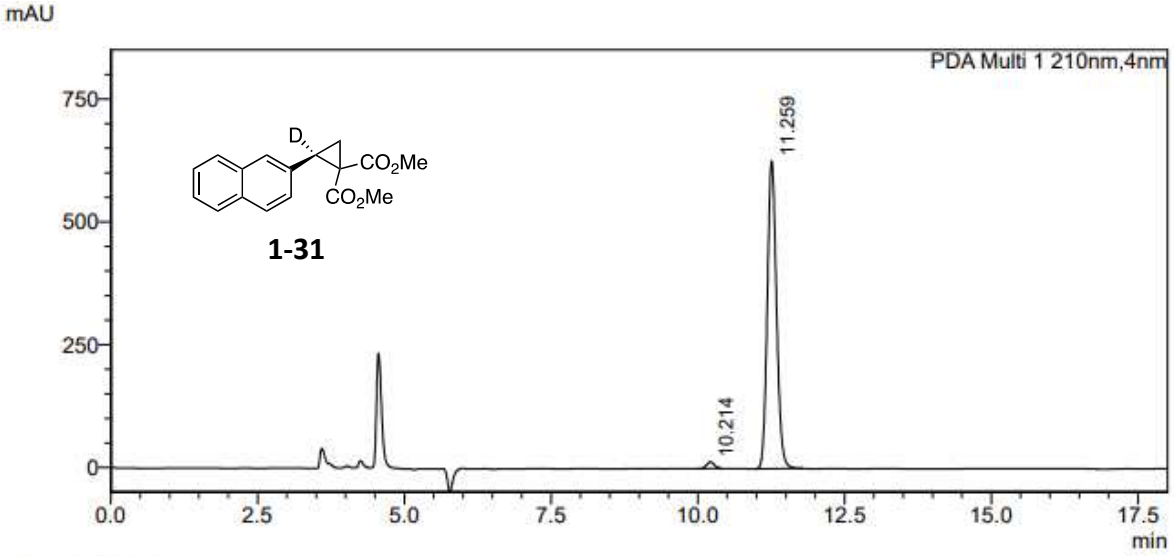

<Peak Table>

PDA Ch1 210nm

Peak#	Ret. Time	Name	ID#	Area%
1	10.214			1.808
2	11.259			98.192
Total				100.000

Chiral HPLC of **1-31**

APPENDIX TWO

NEW APPROACHES TO PYRIDINE C–H FUNCTIONALIZATION REACTIONS VIA BASE-CATALYZED ARYL HALIDE ISOMERIZATION: EXPERIMENTAL

A2.1 General Information

General Reagent Information: All reactions were performed under a N_2 atmosphere unless otherwise noted. Anhydrous *N,N*-dimethylacetamide (DMAc) (Catalog # 375230010) was purchased from Sigma Aldrich in a Sure/Seal® bottle stored over 4 Å molecular sieves and used as received. Potassium hydroxide (KOH) was purchased from Millipore Sigma (Catalog # 8143530100) as an 85% purity powder and used as purchased. Potassium bromide (KBr) (Catalog # A16339) was purchased from Alfa Aesar in 99.8% purity. Prior to use, KBr was dried *in vacuo* at 100 °C for 24 h. 1,4,7,10,13,16-Hexaoxacyclooctadecane (18-crown-6) was purchased from Chem-Impex (Catalog # 03901) and used as purchased. Anhydrous 2-ethyl-1-hexanol was purchased from Sigma-Aldrich (Catalog # 538051) and stored over 4 Å molecular sieves. 3-Bromopyridine was purchased from Chem-Impex (Catalog # 27044) and used as purchased. KOH, KBr, and 18-crown-6 were all stored at room temperature (rt) inside a N_2 filled glovebox and used immediately if brought outside the glovebox. Tetrahydrofuran, dichloromethane, and toluene were deoxygenated and dried by passage over packed columns of neutral alumina and copper (II) oxide under positive pressure of N_2. NaH was purchased from Acros as a 60% dispersion in mineral oil and was stored in a desiccator with $CaSO_4$ as the desiccant. 1-*tert*-Butyl-4,4,4-tris(dimethylamino)-2,2-bis[tris(dimethylamino)-phosphoranylidenamino]-2λ^5,4λ^5-catenadi(phosphazene) (P_4-*t*-Bu) was purchased from Millipore Sigma as a 0.8 M solution in hexanes and was stored in a -30 °C freezer inside a N_2 filled glovebox. Before use, the P_4-*t*-Bu solution was allowed to warm to rt and homogenize if any solid was evident. All other solvents

and reagents were purchased from Millipore Sigma, Combi-Blocks, TCI, Acros Organics, Matrix Scientific, Alfa-Aesar, or Synthonix and used as received unless otherwise noted. Flash Chromatography was performed on 40-63 μm silica gel (SiliaFlash® F60 from Silicycle). Preparative thin-layer chromatography (PTLC) was performed on silica gel 60Å F254 plates (20 x 20 cm, 1000 μm, SiliaPlate from Silicycle, #TLG-R10011B-341) and visualized with UV light (254 nm).

General Analytical Information: All reported compounds were characterized by ^{1}H, ^{13}C, and ^{19}F (if applicable) NMR spectroscopy, FTIR spectroscopy and mass spectrometry. Melting point analysis was conducted if the compound was solid. ^{1}H NMR, ^{13}C NMR, and ^{19}F NMR spectra were obtained on a Bruker Advanced NEO or Varian Inova 400 spectrometer. ^{1}H NMR data is reported as follows: chemical shift (δ ppm), multiplicity (s = singlet, br s = broad singlet, d = doublet, t = triplet, q = quartet, dd = doublet of doublets, td = triplet of doublets, m = multiplet), coupling constant (Hz), and integration. ^{13}C NMR data is reported as follows: chemical shift (δ ppm), multiplicity (if applicable, d = doublet), and coupling constant (Hz). All ^{1}H NMR signals are reported as chemical shifts (δ ppm) relative to residual $CHCl_3$, DMSO, or MeOH at 7.26 ppm, 2.50 ppm, or 3.34 ppm, respectively. ^{13}C NMR signals are reported as chemical shifts (δ ppm) relative to $CDCl_3$, CD_3OD, or DMSO-d_6 at 77.23 ppm, 49.86 ppm, or 39.52 ppm, respectively. ^{19}F NMR signals are reported as chemical shifts relative to added α,α,α-trifluorotoluene internal standard calibrated to -63.72 ppm. High resolution mass spectra (HRMS) were recorded on an Agilent 6210 TOF interfaced to a DART 100 source provided by Colorado State University Central Instrumentation Facility. IR spectra were recorded using a Thermo Scientific Nicolet iS-50 FTIR Spectrometer and reported as frequency of absorption (cm^{-1}). Melting point analyses were conducted using a Mel-Temp capillary melting point apparatus. The specific rotation of chiral

molecules was measured using a Rudolph Research Analytical Autopol III polarimeter. Thin-layer chromatography analysis was performed on silica gel 60Å F_{254} plates (250 μm, SiliaPlate from Silicycle, #TLG-R10014B-323) and interpreted using UV light (254 nm).

Note on nomenclature: The names provided for the structures below were obtained from ChemDraw Professional 16.0.

A2.2 Base-Catalyzed Isomerization of Aryl Halides

General Procedure: An oven-dried 4 mL vial (ThermoFisher, C4015-1) was charged with a magnetic stir bar. Inside a N_2 filled glovebox, the appropriate aryl bromide/iodide (0.1 mmol, 1.0 equiv), 1,4-dioxane (0.4 mL, 0.25 M), and P_4-*t*-Bu (13 μl, 0.1 equiv) were added to the vial in successive order. The vial was sealed with a PTFE-lined screw cap (ThermoFisher, C4015-1A), removed from the glovebox, and placed into a preheated 80 °C aluminum reaction block. The reaction solution was stirred at 80 °C for 21 h. Upon completion of the given reaction time, the reaction solution was cooled to rt. 1,3,5-Trimethoxybenzene (TMB) internal standard was measured into the solution and ^{1}H NMR spectroscopy (400 MHz, $CDCl_3$) of the crude solution was used to determine the percentage of each aryl halide isomer in solution. The identity of each isomer within the spectrum was determined by ^{1}H NMR analysis of an authentic sample of the isomer. The figures below provide an overlay of the ^{1}H NMR spectra of the authentic regioisomers on the top, and the ^{1}H NMR spectrum of the crude reaction solutions on the bottom. ***Note***: the signal at $\delta = 6.08$ ppm corresponds to the 1,3,5-trimethoxybenzene internal standard.

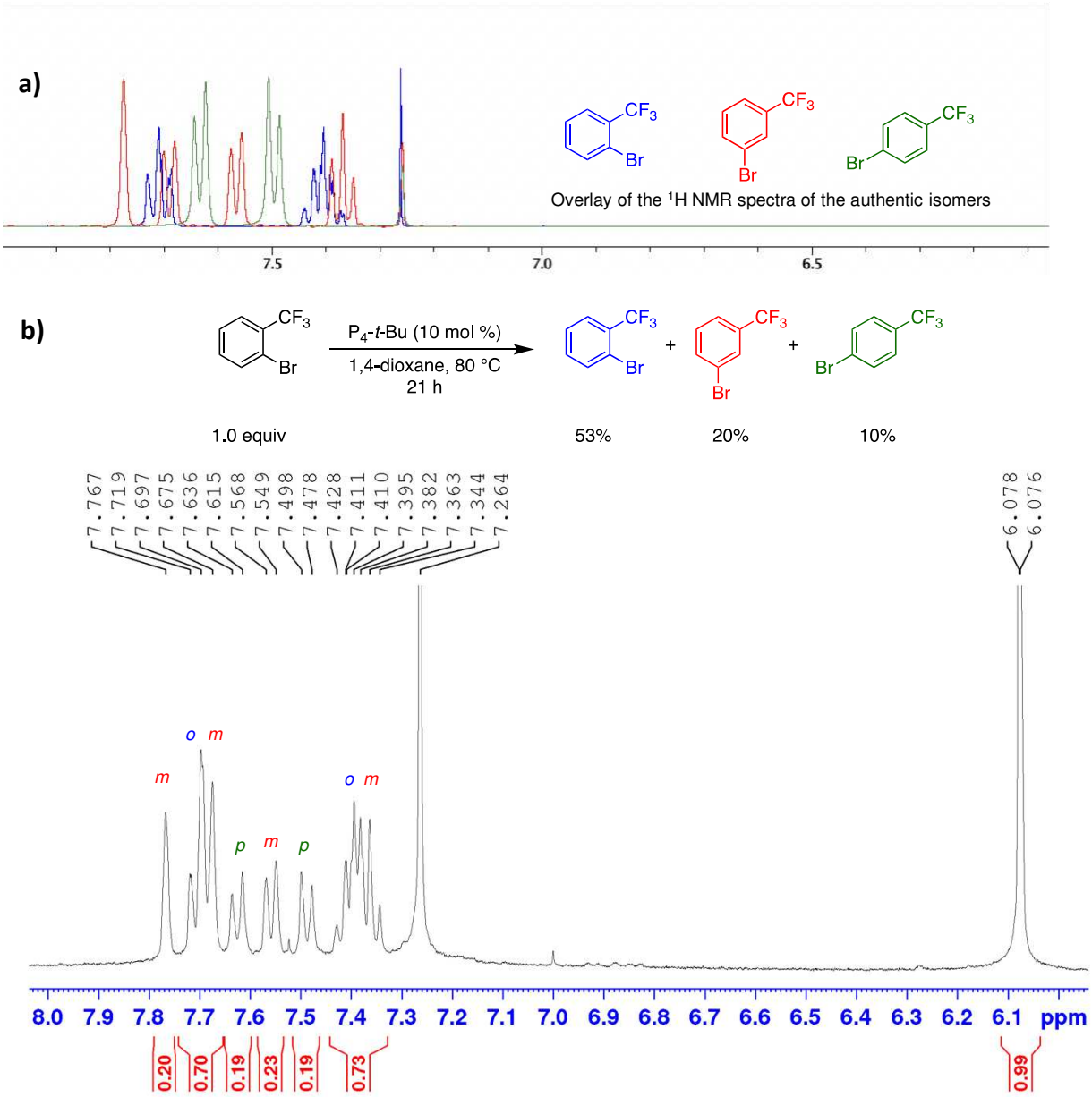

Figure A2–1: (**a**) Overlay of the ^{1}H NMR spectra of the authentic isomers of 1-bromo-2-(trifluoromethyl)benzene, 1-bromo-3-(trifluoromethyl)benzene and 1-bromo-4-(trifluoromethyl)benzene. (**b**) ^{1}H NMR spectrum of the crude reaction solution of 1-bromo-2-(trifluoromethyl)benzene base-catalyzed isomerization; the reaction was run according to the general procedure; 5.5 mg (0.033 mmol) of TMB was added to the reaction solution: 53% 1-bromo-2-(trifluoromethyl)benzene, 20% 1-bromo-3-(trifluoromethyl)benzene, 10% 1-bromo-4-(trifluoromethyl)benzene.

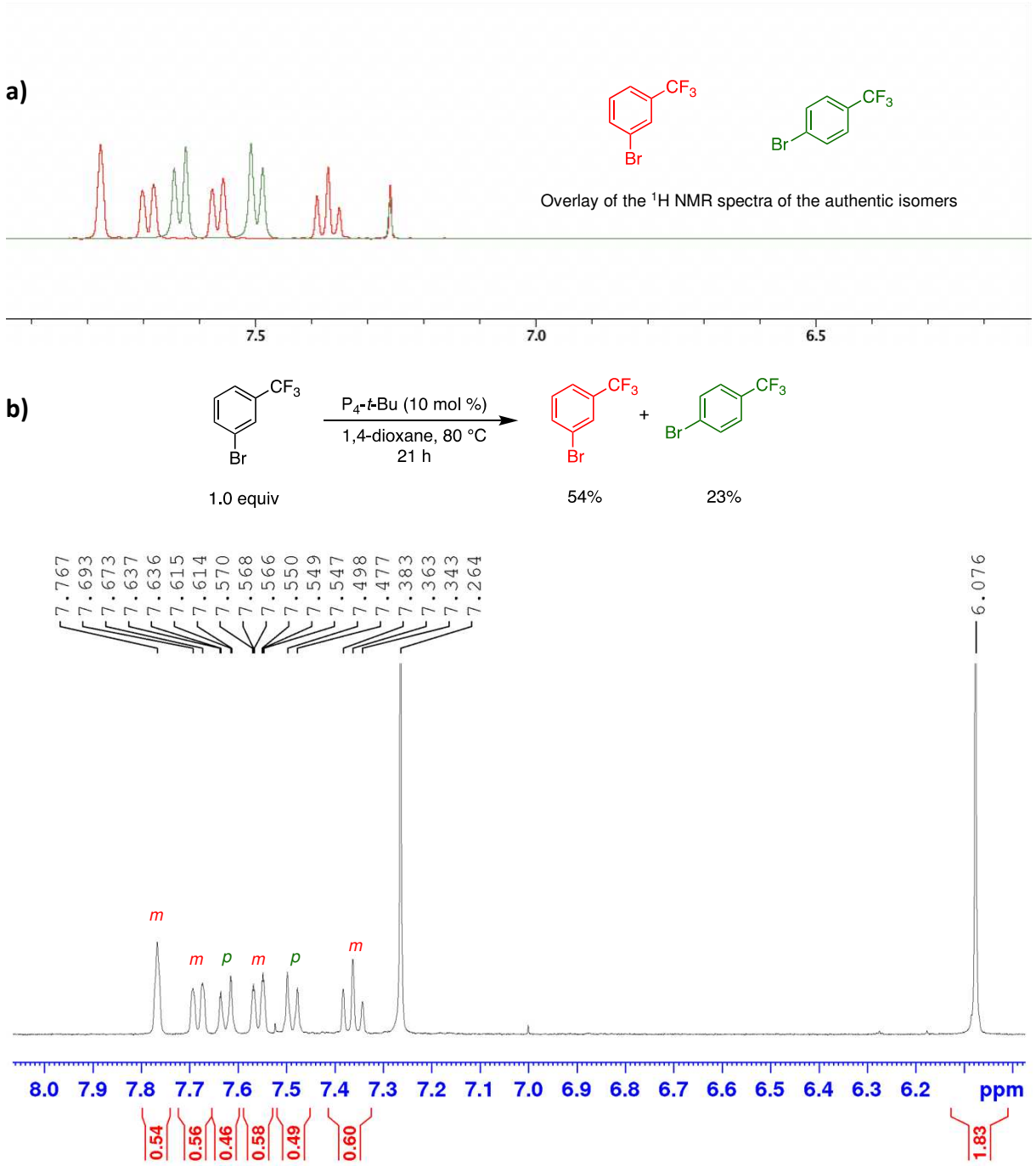

Figure A2–2: (**a**) Overlay of the ^{1}H NMR spectra of the authentic isomers of 1-bromo-3-(trifluoromethyl)benzene and 1-bromo-4-(trifluoromethyl)benzene. (**b**) ^{1}H NMR spectrum of the crude reaction solution of 1-bromo-3-(trifluoromethyl)benzene base-catalyzed isomerization; the reaction was run according to the general procedure; 10.3 mg (0.061 mmol) of TMB was added to the reaction solution: 54% 1-bromo-3-(trifluoromethyl)benzene and 23% 1-bromo-4-(trifluoromethyl)benzene.

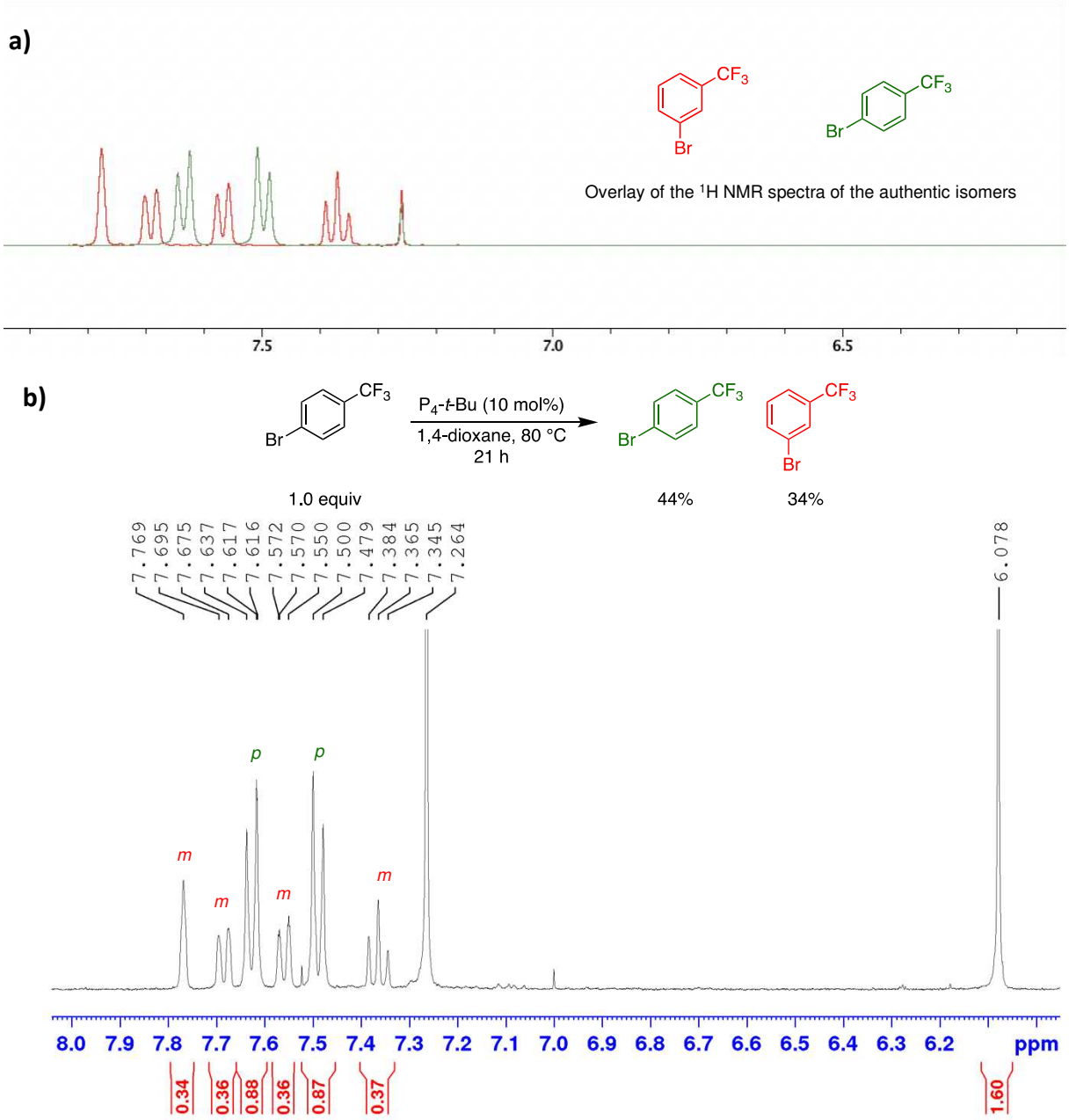

Figure A2–3: (**a**) Overlay of the ^{1}H NMR spectra of the authentic isomers of 1-bromo-4-(trifluoromethyl)benzene and 1-bromo-3-(trifluoromethyl)benzene. (**b**) ^{1}H NMR spectrum of the crude reaction solution of 1-bromo-4-(trifluoromethyl)benzene base-catalyzed isomerization; the reaction was run according to the general procedure; 8.9 mg (0.053 mmol) of TMB was added to the reaction solution: 44% 1-bromo-4-(trifluoromethyl)benzene and 34% 1-bromo-3-(trifluoromethyl)benzene.

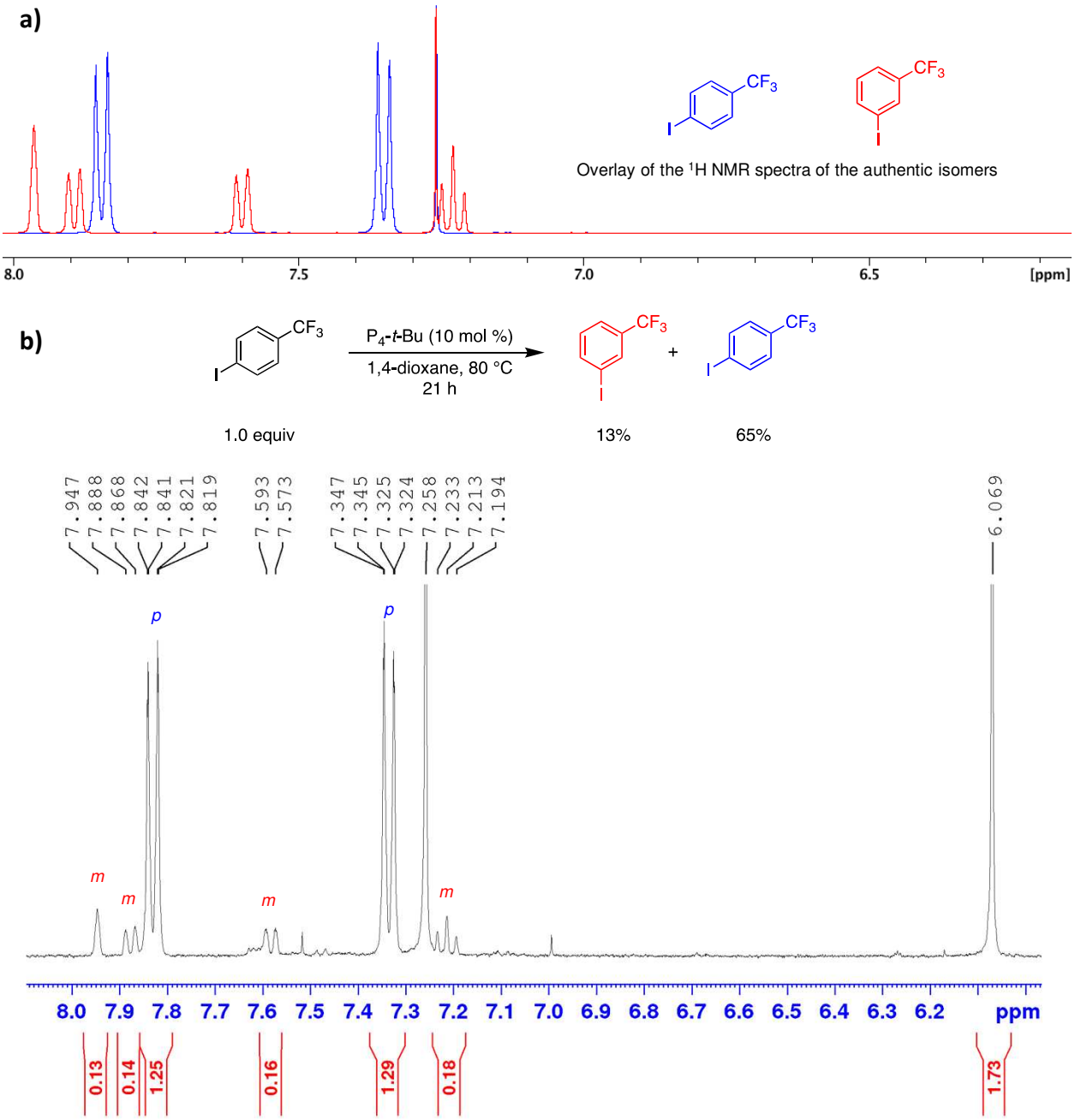

Figure A2–4: (**a**) Overlay of the ^{1}H NMR spectra of the authentic isomers of 1-iodo-4-(trifluoromethyl)benzene and 1-iodo-3-(trifluoromethyl)benzene. (**b**) ^{1}H NMR spectrum of the crude reaction solution of 1-iodo-4-(trifluoromethyl)benzene base-catalyzed isomerization; the reaction was run according to the general procedure; 9.7 mg (0.058 mmol) of TMB was added to the reaction solution: 65% 1-iodo-4-(trifluoromethyl)benzene and 13% 1-iodo-3-(trifluoromethyl)benzene.

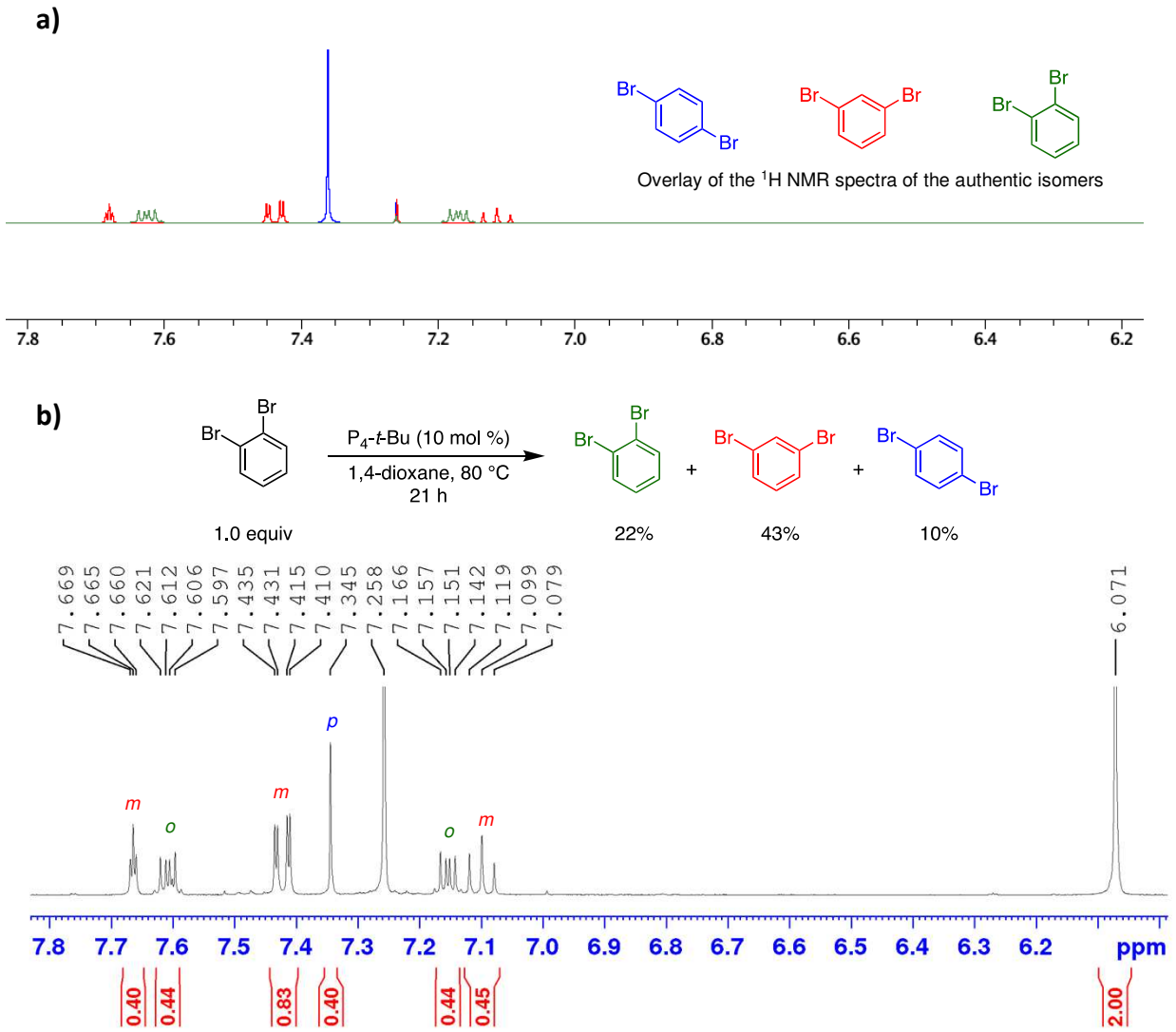

Figure A2–5: (**a**) Overlay of the ^{1}H NMR spectra of the authentic isomers of 1,2-dibromobenzene, 1,3-dibromobenzene, and 1,4-dibromobenzene. (**b**) ^{1}H NMR spectrum of the crude reaction solution of 1,2-dibromobenzene base-catalyzed isomerization; the reaction was run according to the general procedure; 11.2 mg (0.067 mmol) of TMB was added to the reaction solution: 22% 1,2-dibromobenzene, 43% 1,3-dibromobenzene, 10% 1,4-dibromobenzene.

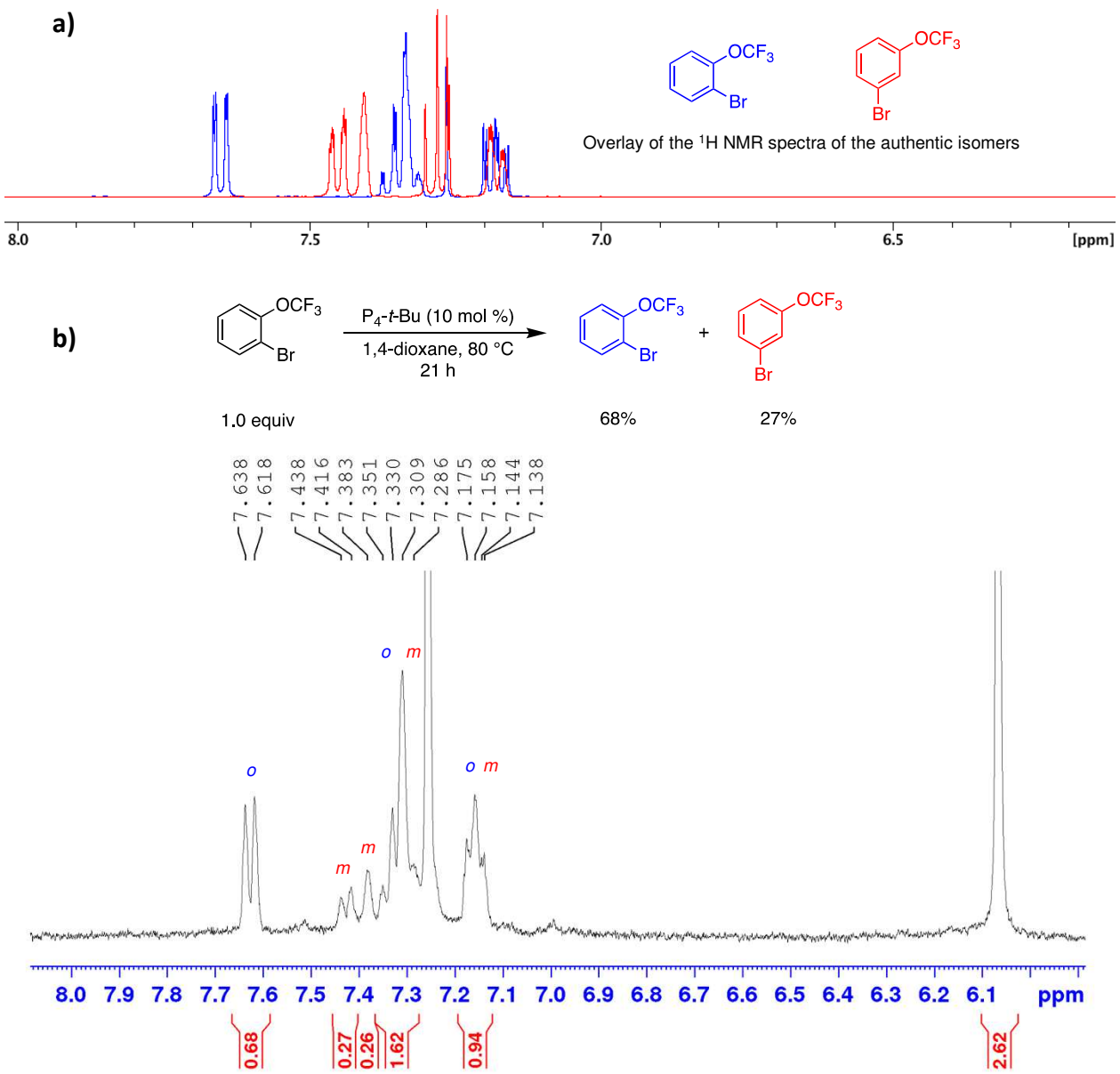

Figure A2–6: (**a**) Overlay of the ^{1}H NMR spectra of the authentic isomers of 1-bromo-2-(trifluoromethoxy)benzene and 1-bromo-3-(trifluoromethoxy)benzene. (**b**) ^{1}H NMR spectrum of the crude reaction solution of 1-bromo-2-(trifluoromethoxy)benzene base-catalyzed isomerization; the reaction was run according to the general procedure; 14.7 mg (0.087 mmol) of TMB was added to the reaction solution: 68% 1-bromo-2-(trifluoromethoxy)benzene and 27% 1-bromo-3-(trifluoromethoxy)benzene.

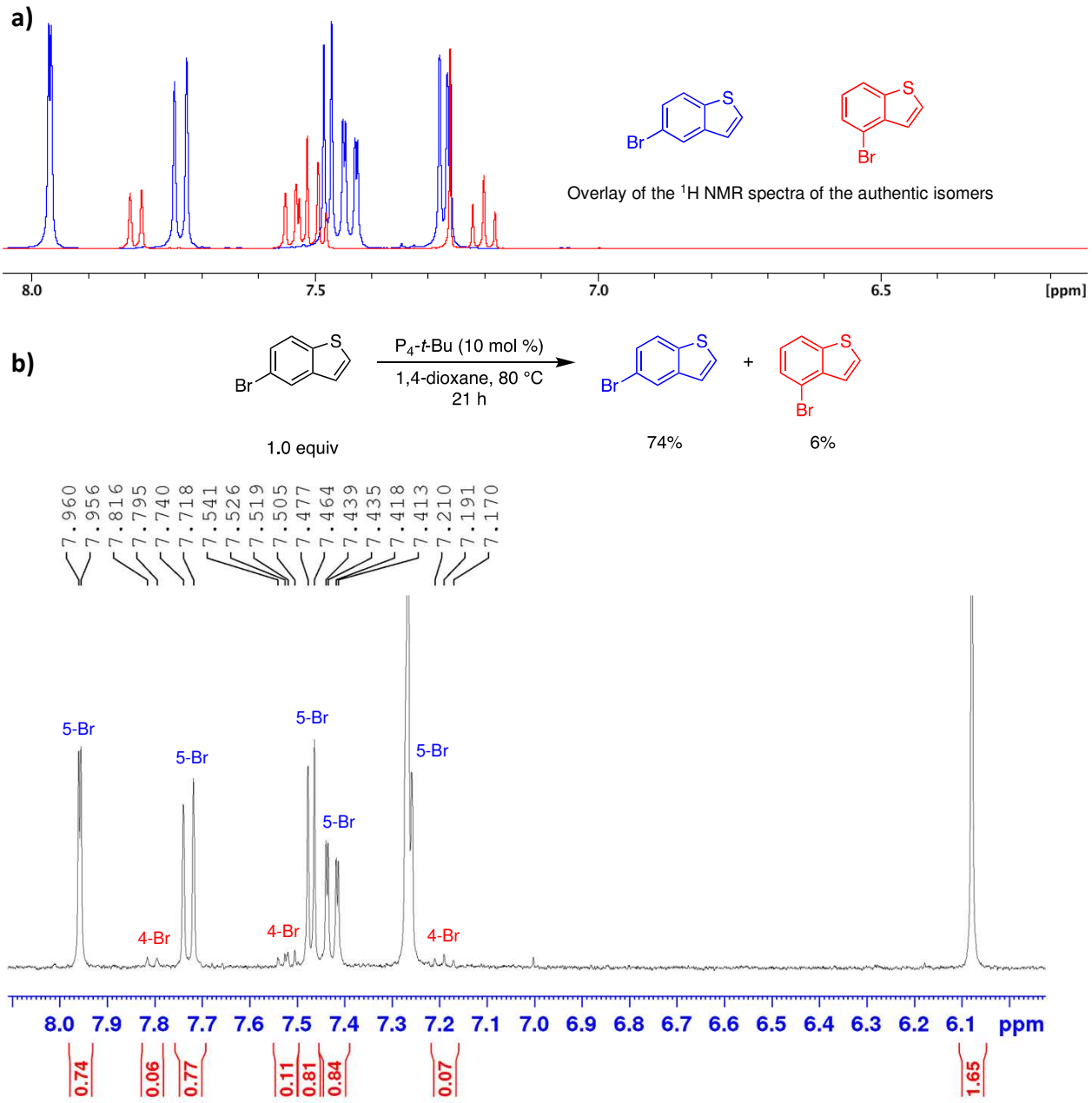

Figure A2–7: (**a**) Overlay of the ^{1}H NMR spectra of the authentic isomers of 5-bromobenzo[*b*]thiophene and 4-bromobenzo[*b*]thiophene. (**b**) ^{1}H NMR spectrum of the crude reaction solution of 5-bromobenzo[*b*]thiophene base-catalyzed isomerization; the reaction was run according to the general procedure using 38 µl (0.03 mmol, 0.3 equiv) of P_4-*t*-Bu; 9.3 mg (0.055 mmol) of TMB was added to the reaction solution: 74% 5-bromobenzo[*b*]thiophene and 6% 4-bromobenzo[*b*]thiophene.

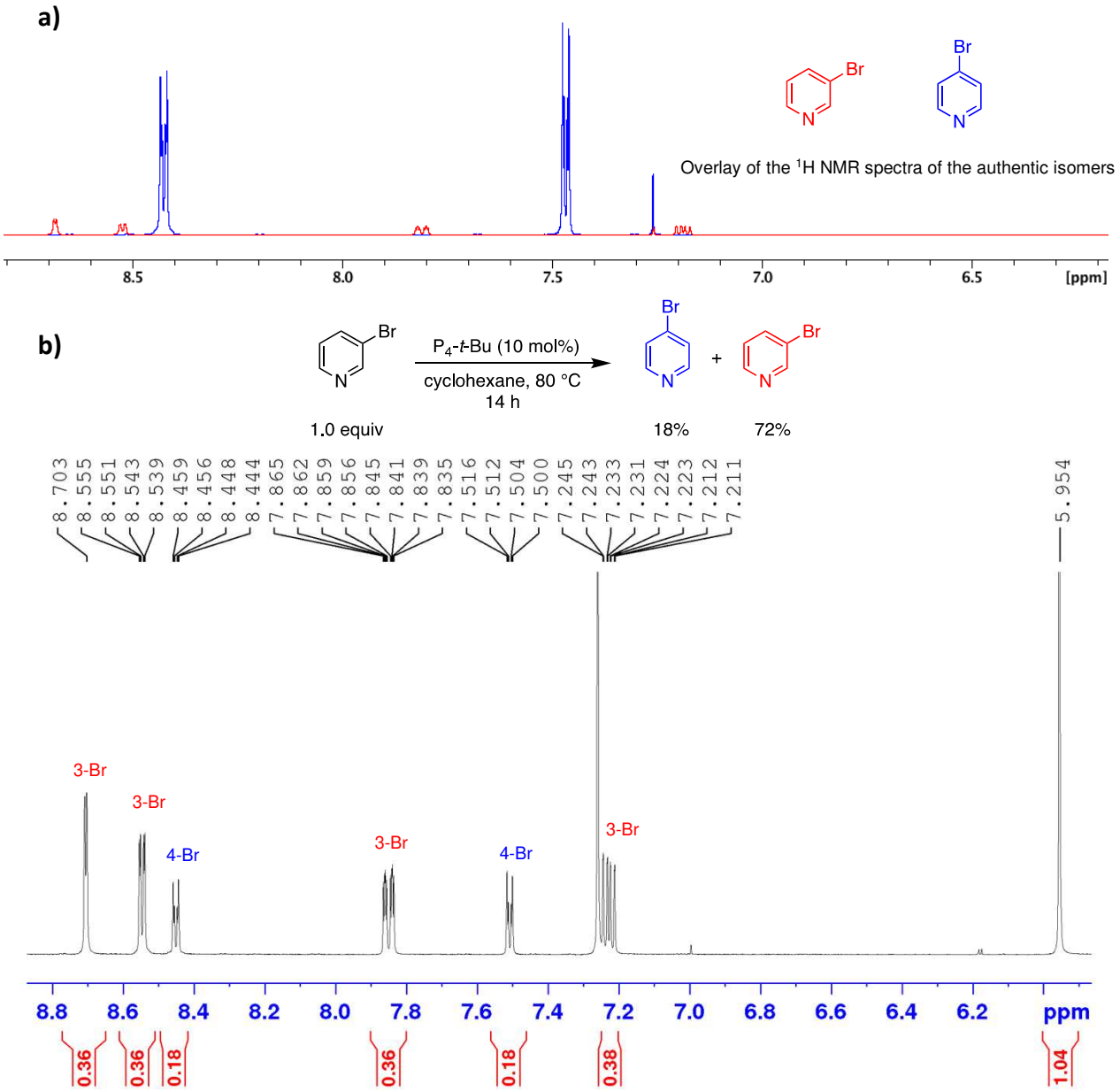

Figure A2–8: (**a**) ^{1}H NMR spectra of the authentic isomers of 3-bromopyridine and 4-bromopyridine. (**b**) ^{1}H NMR spectrum of the crude reaction solution of 3-bromopyridine base-catalyzed isomerization; the reaction was run according to the general procedure with stirring for 14 h at 80 °C in cyclohexane solvent (0.2 mL, 0.5 M), the reaction was quenched with acetic acid (ca. 250 µl) and 11 µl (0.10 mmol) of 1,1,2,2-tetrachloroethane (δ = 5.95 ppm) was added as internal standard to the reaction solution: 72% 3-bromopyridine and 18% 4-bromopyridine.

A2.3 Optimization of the 4-Selective Etherification of 3-Bromopyridine

(a) Evaluation of changes in optimal base, solvent, temperature, and concentration

Preliminary experiments varying base and solvent suggested KOH with 18-crown-6 in DMAc could promote a 4-selective etherification reaction between 3-bromopyridine and 2-ethyl-1-hexanol. The optimal conditions were identified using pyridine:alcohol stoichiometry studies and KBr additive experiments that are described below in Section A2.3b and A2.3c, respectively. The optimized conditions are provided in the table below in comparison to specific changes of reagents or conditions used.

General procedure for condition variation: Inside a N_2 filled glovebox, a 4 mL vial (ThermoFisher, C4015-1) was charged with a magnetic stir, 3-bromopyridine (1.0 – 1.5 equiv), 2-ethyl-1-hexanol (13.0 mg, 0.1 mmol, 1.0 equiv), solvent (see Figure A2–9 below), KBr (6.0 mg, 0.05 mmol, 0.5 equiv.), 18-crown-6 (92.5 mg, 0.35 mmol, 3.5 equiv), and base (see Figure A2–9 below) in successive order. The vial was sealed with a PTFE-lined screw cap (ThermoFisher, C4015-1A), removed from the glovebox, and placed into a preheated 80 °C aluminum reaction block. The solution was stirred for 15 h at 80 °C and then allowed to cool to rt. 1,3,5-Trimethoxybenzene internal standard was then measured into the crude solution. A small aliquot was then removed and injected into a NMR tube and constituted in $CDCl_3$ (0.6 mL). ^1H NMR spectroscopy (400 MHz, $CDCl_3$) was used to determine the 4:3 selectivity and yield of each reaction using the process described in Section A2.3b.

standard conditions:

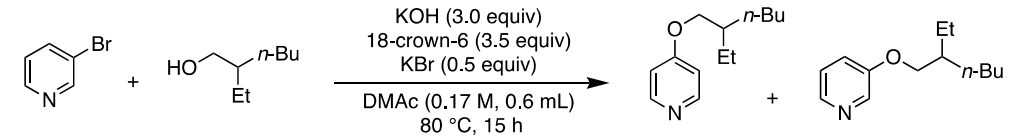

0.15 mmol
1.5 equiv

0.1 mmol
1.0 equiv

3-11 **3-12**

Entry	Change from the "standard conditions"	yield of 3-11	4:3 selectivity
1	none	88%	>10:1
2	3.0 equiv NaOH used instead of KOH	0%	-
3	3.0 equiv CsOH · H_2O used instead of KOH	86%	>10:1
4	2.0 equiv of KOH/18-crown-6	81%	10:1
5	1.2 equiv P_4-*t*-Bu at rt instead of KOH at 80 °C	62%	4.4:1
6[a]	2.0 equiv KO-*t*-Bu/18-crown-6 used instead of KOH	62%	10:1
7	no 18-crown-6	40%	4.0:1
8[b]	0.5 M instead of 0.17 M in DMAc	84%	7.1:1
9[b]	1.0M instead of 0.17 M in DMAc	77%	4.5:1
10	99.8% KOH Pellets used instead of 85% KOH	86%	>10:1
11	Reaction run at 40 °C instead of 80 °C	70%	8.8:1
12	Reaction run open to air	66%	10:1
13	DME used as solvent instead of DMAc	28%	1.6:1
14	PhMe used as solvent instead of DMAc	20%	1.1:1

Figure A2–9: Evaluation of the base, solvent, temperature, and concentration for the 4-selective etherification of 3-bromopyridine. [a]An 18% yield of 4-(*tert*-butoxy)pyridine was observed; this undesired side product was difficult to separate from the desired ether using silica gel chromatography. [b]Large quantities of solid precipitated from the reaction solution inhibiting adequate mixing.

(b) Effect of 3-bromopyridine and alcohol equivalency on substitution selectivity

Purpose: This experiment was performed to evaluate how the equivalency ratio of 3-bromopyridine:alcohol impacts the yield and 4-selectivity of the model substitution reaction.

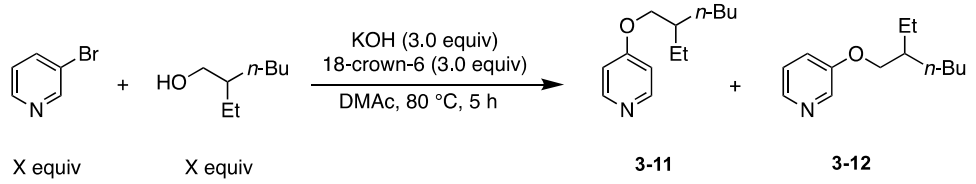

Procedure: An oven-dried 4 mL vial (ThermoFisher, C4015-1) was charged with a magnetic stir bar. Inside a N_2 filled glovebox, the vial was charged with appropriate quantity of 3-bromopyridine (see Figure A2–10), the appropriate quantity of 2-ethyl-1-hexanol (see Figure A2–10), DMAc (1.5 mL, 0.17 M in the limiting reagent), 18-crown-6 (198.2 mg, 0.75 mmol, 3.0 equiv), and KOH (42.1 mg, 0.75 mmol, 3.0 equiv) in successive order. The vials were sealed with a PTFE-lined screw cap (ThermoFisher, C4015-1A), removed from the glovebox, and placed into a preheated 80 °C aluminum reaction block. The reaction solutions were stirred at 80 °C for 5 h, at which point the solutions were removed from the aluminum reaction block and allowed to cool to rt. 1,3,5-Trimethoxybenzene internal standard was then added to each solution, and the yield of **3–11** and **3–12** under each condition was determined via analysis of the crude solutions by ^{1}H NMR spectroscopy (400 MHz, $CDCl_3$).

Evaluation of ^{1}H NMR yield and 4:3 substitution selectivity: Authentic samples of **3–11** and **3–12** were synthesized in order to accurately determine the 4:3 selectivity. The ^{1}H NMR spectra of the crude solutions of entries **1** and **6** from Figure A2–10 are provided in Figure A2–11 and

Figure A2–9, respectively, to provide an example for how the yields of **3–11** and **3–12** were determined.

Entry	Equivalents of 3-bromopyridine	Equivalents of 2-ethyl-1-hexanol	yield of 3-11	yield of 3-12	4:3 selectivity
1	1.0	4.0	38%	16%	2.4:1
2	1.0	3.0	52%	14%	3.7:1
3	1.0	2.0	55%	10%	5.5:1
4	1.0	1.0	57%	7%	8.1:1
5	2.0	1.0	88%	7%	12.6:1
6	3.0	1.0	90%	7%	12.9:1
7	4.0	1.0	83%	7%	11.9:1

Figure A2–10 Results of the study on the effect of the equivalents ratio of 3-bromopyridine to 2-ethyl-1-hexanol on the selectivity and yield of the title reaction. **Note**: Under the conditions of entries **5, 6,** and **7** an appreciable yield of 4-bromopyridine (≈ 25% yield) was observed.

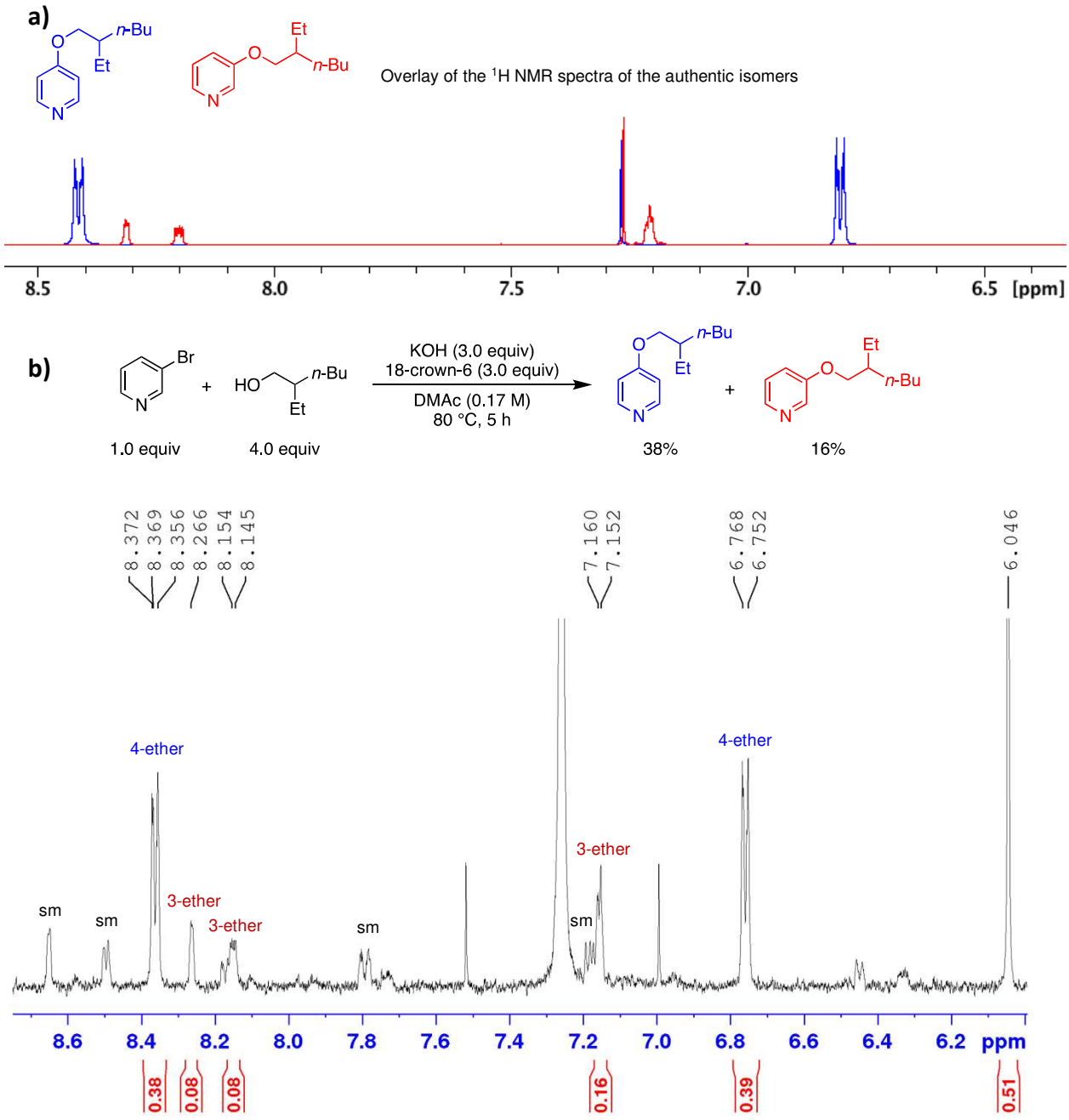

Figure A2–11: (**a**) Overlay of the ^{1}H NMR spectra of authentic 4-((2-ethylhexyl)oxy)pyridine and 3-((2-ethylhexyl)oxy)pyridine. (**b**) ^{1}H NMR spectrum of the crude reaction solution from entry **1** in Figure A2–10. The reaction was run according to the general procedure; 14.2 mg (0.084 mmol) of 1,3,5-trimethoxybenzene used as internal standard: 38% yield of 4-((2-ethylhexyl)oxy)pyridine and 16% yield of 3-((2-ethylhexyl)oxy)pyridine (2.4:1 selectivity); sm = starting material.

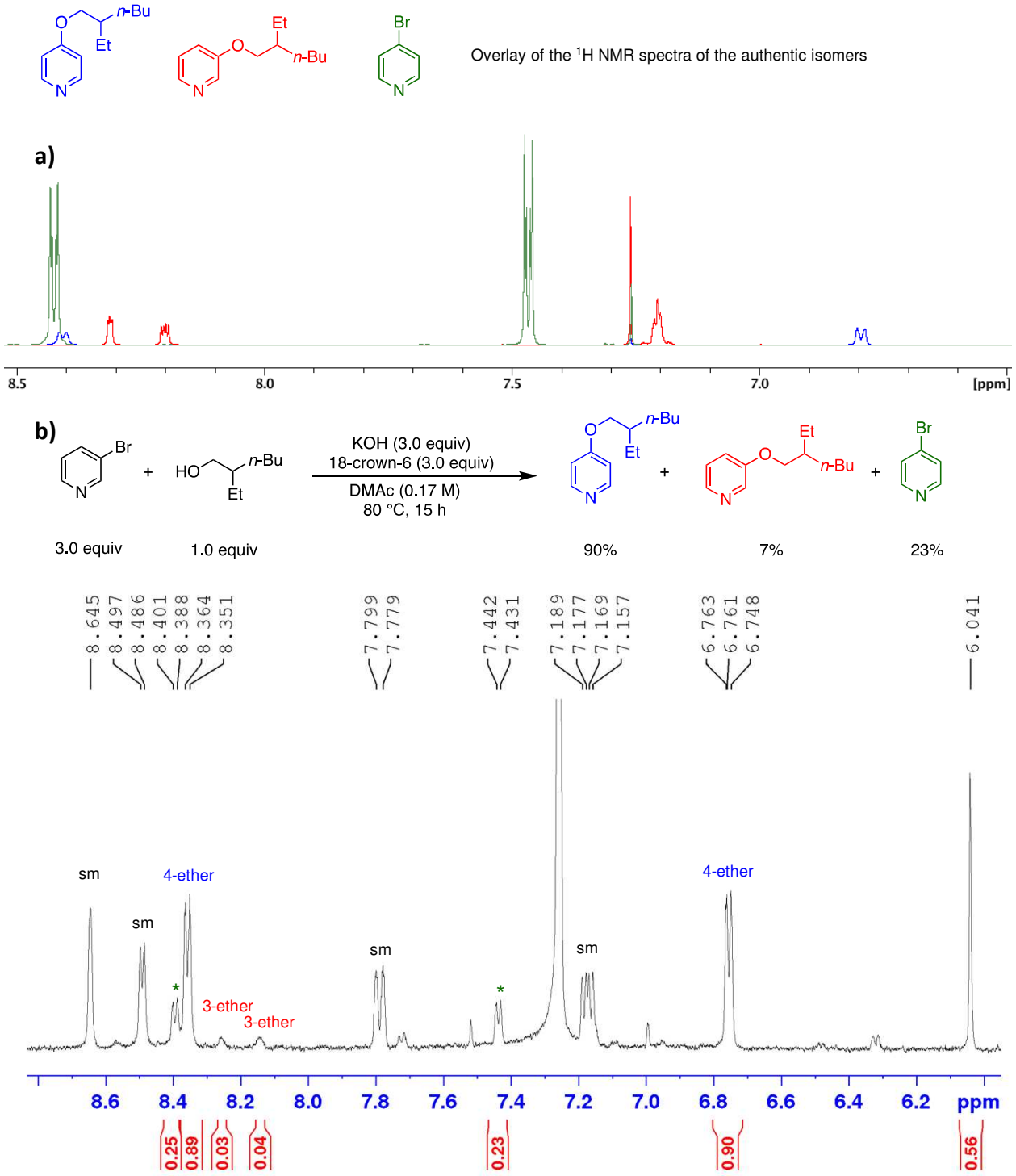

Figure A2–12: (**a**) Overlay of the ^{1}H NMR spectra of authentic 4-((2-ethylhexyl)oxy)pyridine and 3-((2-ethylhexyl)oxy)pyridine. (**b**) ^{1}H NMR spectrum of the crude reaction solution from entry **6** in Figure A2–10. The reaction was run according to the general procedure; 15.8 mg (0.094 mmol) of 1,3,5-trimethoxybenzene used as internal standard: 90% yield of 4-((2-ethylhexyl)oxy)pyridine

and 7% yield of 3-((2-ethylhexyl)oxy)pyridine (>10:1 selectivity) with 23% yield of 4-bromopyridine (marked with green asterisk); sm = starting material.

(c) Effect of KBr on the product yield, selectivity, and mass balance

Purpose: This experiment was performed to evaluate how added KBr impacts the yield and 4-selectivity of the model substitution reaction. Note that these reactions were run with 2.0 equiv of KOH and the experiments in Section A2.3b were run with 3.0 equiv of KOH.

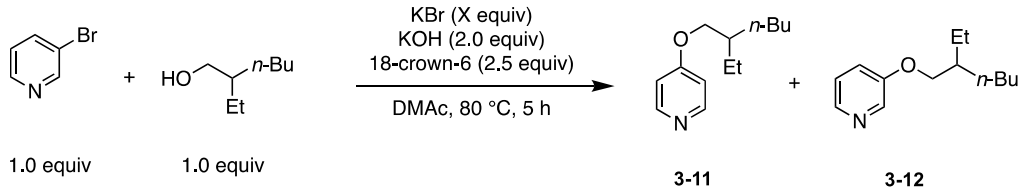

Procedure: An oven-dried 4 mL vial (ThermoFisher, C4015-1) was charged with a magnetic stir bar. Inside a N_2 filled glovebox, the vial was charged with 3-bromopyridine (39.5 mg, 0.25 mmol, 1.0 equiv), 2-ethyl-1-hexanol (32.6 mg, 0.25 mmol, 1.0 equiv), DMAc (1.5 mL, 0.17 M), 18-crown-6 (165.2 mg, 0.625 mmol, 2.5 equiv), the appropriate quantity of KBr (see Figure A2–13), and KOH (28.1 mg, 0.50 mmol, 2.0 equiv) in successive order. The vials were sealed with a PTFE-lined screw cap (ThermoFisher, C4015-1A), removed from the glovebox, and placed into a preheated 80 °C aluminum reaction block. The reaction solutions were stirred at 80 °C for 5 h, at which point the reaction vials were removed from the aluminum reaction block and allowed to cool to rt. 1,3,5-Trimethoxybenzene internal standard was then added to each solution, and the

yield of **10** and **11** under each condition was determined via analysis of the crude solutions by ^{1}H NMR spectroscopy (400 MHz, $CDCl_3$).

Entry	Equivalents of KBr	yield of 3-11	yield of 3-12	4:3 selectivity	Mass balance
1	0	60%	7%	8.6:1	72%
2	0.1	62%	7%	8.9:1	75%
3	0.2	67%	6%	11.1:1	78%
4	0.3	65%	5%	13.0:1	78%
5	0.4	72%	5%	14.4:1	84%
6	0.5	71%	5%	14.2:1	81%
7[a]	1.0	72%	5%	14.4:1	81%

Figure A2–13: Results of the effect of added KBr on the product yield, selectivity, and mass balance for the model reaction. [a]3.0 equiv of 18-crown-6 (198.2 mg, 0.75 mmol) used.

Results: A significant increase in yield of the 4-ether product and 4:3 selectivity were observed as the equivalents of KBr increased up to 0.5 equiv (see Figure A2–13).

A2.4 Description of Mechanistic Studies on 3-Bromopyridine Isomerization

(a) Furan cycloaddition experiment under optimized basic conditions

Purpose: A known trap for 3,4-pyridyne is a cycloaddition reaction with furan.[1] We included an excess of furan under the reaction conditions to observe if the [4+2] cycloaddition adduct (**3–14** below) is formed.

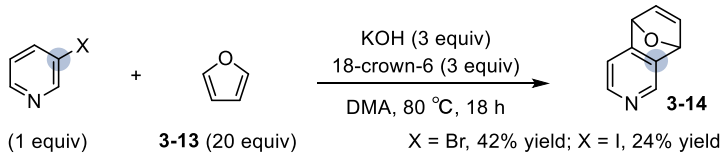

Procedure: An oven-dried 4 mL vial (ThermoFisher, C4015-1) was charged with a magnetic stir bar. Inside a N_2 filled glovebox, the vial was charged with 3-bromopyridine (15.8 mg, 0.1 mmol, 1.0 equiv), furan (146 μl, 2.0 mmol, 20 equiv), DMAc (0.6 mL, 0.17 M) 18-crown-6 (79.3 mg, 0.3 mmol, 3.0 equiv), and KOH (16.8 mg, 0.3 mmol, 3.0 equiv) in successive order. The vial was sealed with a PTFE-lined screw cap (ThermoFisher, C4015-1A), removed from the glovebox, and placed into a preheated 80 °C aluminum reaction block. The solution was stirred at 80 °C for 18 h, at which point the reaction vial was removed from the aluminum reaction block and allowed to cool to rt. 1,3,5-Trimethoxybenzene internal standard (8.9 mg, 0.053 mmol) was then added to the solution, and the yield of **3–14** was determined by ^{1}H NMR spectroscopy (400 MHz, $CDCl_3$, 42% yield). The observed ^{1}H NMR and ^{13}C NMR signals are consistent with literature reports for **2–32**.[1] **^{1}H NMR** (400 MHz, $CDCl_3$) δ 8.45 (s, 1H), δ 8.29 (d, J = 4.6 Hz, 1H), 7.24 (d, J = 4.6 Hz, 1H), 7.06 (dd, J = 1.8 Hz, 5.6 Hz, 1H), 6.99 (dd, J = 1.8 Hz, 5.6 Hz, 1H), 5.82 (m, 1H), 5.73 (m, 1H). **^{13}C NMR** (101 MHz, $CDCl_3$) δ 159.2, 147.8, 143.8, 142.3, 140.2, 116.5, 82.1, 81.0.

(b) Effect of the addition of KCl and KI on product yield and selectivity

Purpose: After observing that KBr improved the product yield and selectivity for the model etherification reaction, we next investigated how addition of potassium iodide (KI) and potassium chloride (KCl) impacts the yield and selectivity of the reaction.

Procedure: An oven-dried 4 mL vial (ThermoFisher, C4015-1) was charged with a magnetic stir bar. Inside a N_2 filled glovebox, the vial was charged with 3-bromopyridine (39.5 mg, 0.25 mmol, 1.0 equiv), 2-ethyl-1-hexanol (32.6 mg, 0.25 mmol, 1.0 equiv), DMAc (1.5 mL, 0.25 M), 18-crown-6 (165.2 mg, 0.625 mmol, 3.5 equiv), and KCl (18.7 mg, 0.25 mmol, 1.0 equiv), KBr (29.8 mg, 0.25 mmol, 1.0 equiv) or KI (41.5 mg, 0.25 mmol, 1.0 equiv) in successive order. KOH (42.1

mg, 0.75 mmol, 3.0 equiv) was then added. The vials were sealed with a PTFE-lined screw cap (ThermoFisher, C4015-1A), removed from the glovebox, and placed into a preheated 80 °C aluminum reaction block. The reaction solutions were stirred at 80 °C for 15 h, at which point they were removed from the aluminum reaction block and allowed to cool to rt. 1,3,5-Trimethoxybenzene internal standard was then added to each solution, and the yield of **3–11** and **3–12** under each condition was determined via analysis of the crude solutions by ^{1}H NMR spectroscopy (400 MHz, $CDCl_3$).

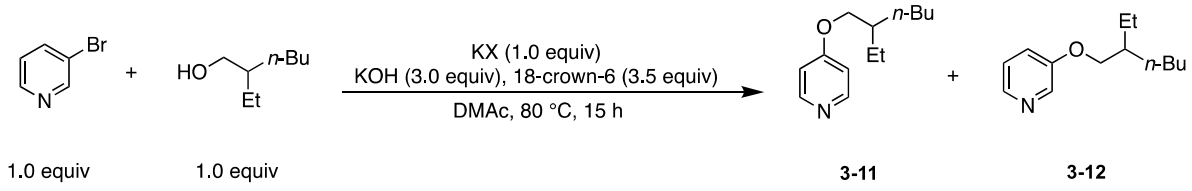

KX	yield of 3-11	yield of 3-12	4:3 selectivity
KCl	60%	7%	8.6:1
KBr	80%	7%	>10:1
KI	57%	7%	8.1:1
no KX	57%	7%	8.3:1

Figure A A2–14: Results of the effect of halide salt addition on the 4-selectivity and product yield.

Results: Addition of KCl or KI had a negligible effect on the yield and 4-selectivity of the reaction. The yield and 4-selectivity under either condition was comparable to a control in which no halide salt was included. Addition of KBr to the reaction improved the yield of the 4-alkoxylated product and the 4-selectivity of the reaction.

(c) Determination of the reaction profile

Purpose: This experiment was performed to analyze components of the reaction solution at different time points to observe the formation and consumption of potential reaction intermediates.

Procedure: An oven-dried 25 mL round bottom flask was charged with a magnetic stir bar, 3-bromopyridine (237 mg, 1.5 mmol, 1.5 equiv), and dibenzyl ether (99.2 mg, 0.5 mmol, 0.5 equiv, used as internal standard). The flask was then brought into a N_2 filled glovebox and 2-ethyl-1-hexanol (130.2 mg, 1 mmol, 1.0 equiv), DMAc (6.0 mL, 0.17 M), KBr (59.5 mg, 0.5 mmol, 0.5 equiv), 18-crown-6 (1.19g, 4.5 mmol, 4.5 equiv), and KOH (224.4 mg, 4.0 mmol, 4.0 equiv) were added to the flask in successive order. The flask was sealed with a Fisherbrand® red septum stopper (Cat. No. FB57875) and the edges of the septum were lined with Parafilm®. The flask was put under positive pressure using a balloon filled with N_2, and then placed into a preheated 80 °C silicon oil bath. At the given time intervals (see Figure A2–15), a small aliquot (ca. 25 μl) of the reaction solution was removed using a syringe, injected into an NMR tube, and constituted in $CDCl_3$ (0.6 mL). The mass balance, selectivity, and amount of 4-bromopyridine, **3–11**, and **3–12** was then determined via ^1H NMR (400 MHz, $CDCl_3$) using the dibenzyl ether (which is inert under the reaction conditions) as the internal standard.

Time (min)	4-bromopyridine (%)	3-11 (%)	3-12 (%)	4:3 selectivity
2	3%	14%	3%	4.7:1
5	4%	34%	4%	8.5:1
10	5%	45%	5%	9.0:1
15	6%	51%	5%	10.2:1
30	6%	62%	6%	10.3:1
60	6%	73%	6%	12.2:1
105	4%	76%	6%	12.7:1
180	4%	81%	7%	11.6:1
300	1%	84%	7%	12.0:1
420	0%	85%	7%	12.1:1

Figure A2–15: Results of the reaction profile on the 4-selective etherification of 3-bromopyridine.

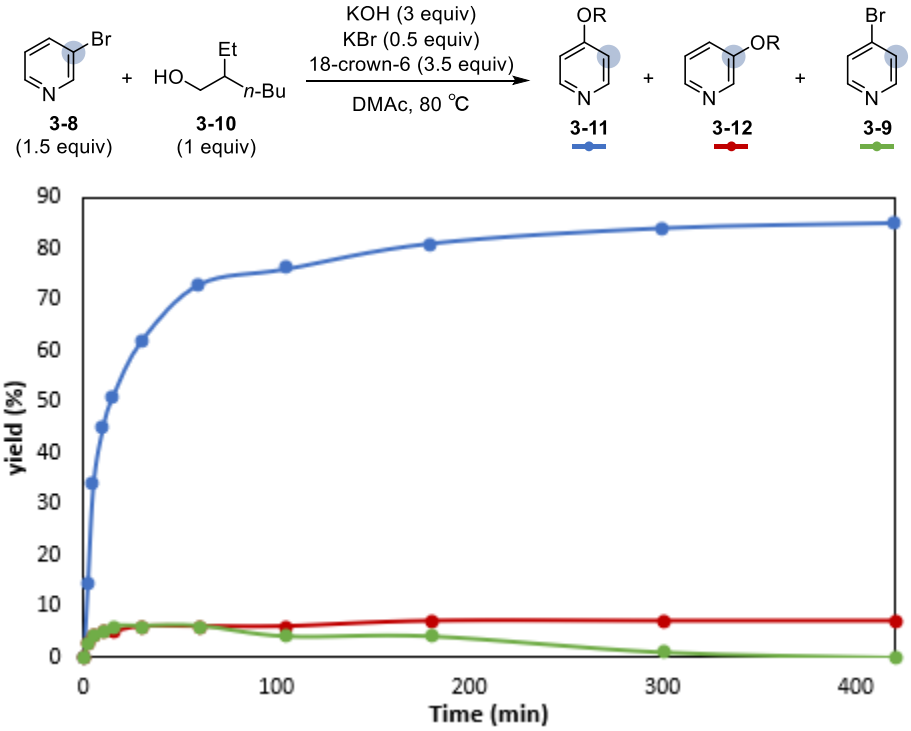

Figure A2–16. Reaction profile obtained for the model etherification reaction of 3-bromopyridine.

Result: Upon monitoring the reaction over time, we observed a buildup of 4-bromopyridine that is ultimately consumed by the end of the reaction. No other discernable intermediates were observed.

(d) Conversion of 3-iodopyridine to 4- and 3-bromopyridine with KBr additive

Purpose: A possible explanation for the positive effect of KBr on the yield and selectivity of the etherifcation reaction is addition of bromide to a 3,4-pyridyne intermediate. We sought to investigate if there is a yield of 3- or 4-bromopyridine when 3-iodopyridine is stirred under the basic reaction conditions in the presence of KBr.

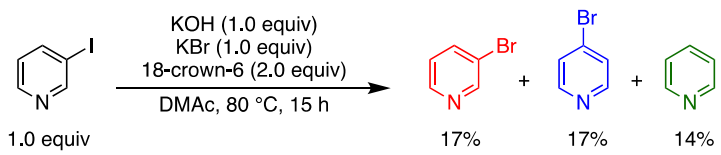

Procedure: An oven-dried 4 mL vial (ThermoFisher, C4015-1) was charged with a magnetic stir bar. Inside a N_2 filled glovebox, the vial was charged with 3-iodopyridine (20.5 mg, 0.10 mmol, 1.0 equiv), DMAc (1.5 mL, 0.25 M), 18-crown-6 (52.8 mg, 0.20 mmol, 2.0 equiv), KBr (11.9 mg, 0.10 mmol, 1.0 equiv), and KOH (5.6 mg, 0.10 mmol, 1.0 equiv) in successive order. The vials were sealed with a PTFE-lined screw cap (ThermoFisher, C4015-1A), removed from the glovebox, and placed into a preheated 80 °C aluminum reaction block. The reaction solutions were stirred at 80 °C for 15 h, at which point they were removed from the aluminum reaction block and allowed to cool to rt. 1,3,5-Trimethoxybenzene internal standard (15.0 mg, 0.089 mmol) was then added to the solution, and the yield of 3-bromopyridine and 4-bromopyridine was determined via analysis of the crude solution by ^{1}H NMR spectroscopy (400 MHz, $CDCl_3$).

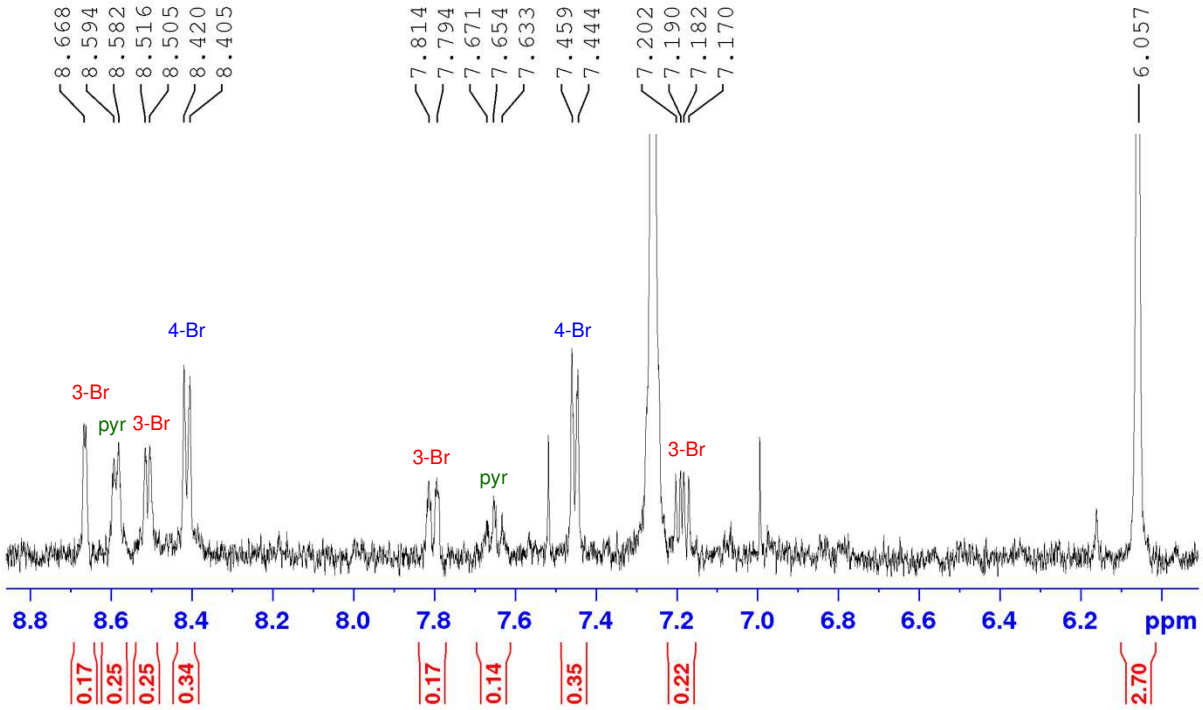

Figure A2–17: ^{1}H NMR spectrum of the crude reaction solution of the base-catalyzed substitution of 3-iodopyridine with KBr; 17% yield of 3-bromopyridine (marked in red), 17% yield of 4-bromopyridine (marked in blue), and 14% yield of pyridine (marked in green). **Note:** To support

the identity that corresponds to each ^{1}H NMR signal above, we mixed authentic 3-bromopyridine, 4-bromopyridine, 3-iodopyridine, and 4-iodopyridine into 4 separate ^{1}H NMR samples of the crude solution. Only in the cases of 3-iodopyridine and 4-iodopyridine were new signals observed.

Supplementary Experiments and Notes: To corroborate that 3,4-pyridyne is generated under the reaction conditions for 3-iodopyridine, we performed a trapping experiment with furan analogous to Section A2.4a. Additionally, we stirred 3-iodopyridine under the conditions above with exclusion of KOH; under these conditions we observed no conversion of 3-iodopyridine.

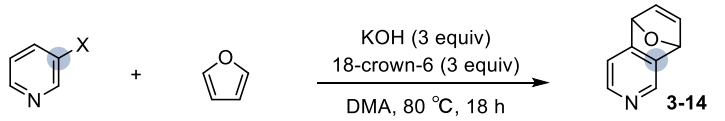

Procedure: An oven-dried 4 mL vial (ThermoFisher, C4015-1) was charged with a magnetic stir bar. Inside a N_2 filled glovebox, the vial was charged with 3-iodopyridine (20.5 mg, 0.1 mmol, 1.0 equiv), furan (146 µl, 2.0 mmol, 20 equiv), DMAc (0.6 mL, 0.17 M) 18-crown-6 (79.3 mg, 0.3 mmol, 3.0 equiv), and KOH (16.8 mg, 0.3 mmol, 3.0 equiv) in successive order. The vial was sealed with a PTFE-lined screw cap (ThermoFisher, C4015-1A), removed from the glovebox, and placed into a preheated 80 °C aluminum reaction block. The solution was stirred at 80 °C for 18 h, at which point the solution was removed from the aluminum reaction block and allowed to cool to rt. 1,3,5-Trimethoxybenzene internal standard (8.8 mg, 0.052 mmol) was then added to the solution, and the yield of **3–14** was determined by ^{1}H NMR spectroscopy (400 MHz, $CDCl_3$, 24% yield).

(d) Observation of the isomerization of 3-bromopyridine substrates

Purpose: To demonstrate that diverse 3-bromopyridines isomerize to 4-bromopyridines under the optimal reaction conditions, we subjected several substrates to the basic conditions in the absence of alcohol nucleophile.

Procedure: An oven-dried 4 mL vial (ThermoFisher, C4015-1) was charged with a magnetic stir bar. Inside a N_2 filled glovebox, the vial was charged with the appropriate 3- or 5-bromopyridine substrate (0.1 mmol, 1.0 equiv), DMAc (0.6 mL, 0.17 M), KBr (6.0 mg, 0.05 mmol, 0.5 equiv), 18-crown-6 (1.0-1.5 equiv), and KOH (5.6 mg, 0.1 mmol, 0.1 equiv) in successive order. The vial was sealed with a PTFE lined screw cap (ThermoFisher, C4015-1A), removed from the glovebox, and placed into a preheated 80 °C aluminum reaction block. The reaction solutions were stirred at 80 °C for 4 h. The reaction solutions were removed from the aluminum reaction block and allowed to cool to rt. 1,3,5-Trimethoxybenzene internal standard was then measured into each solution, and the yield of the starting material and the corresponding 4-bromopyridine was determined via analysis of the crude solutions by ^{1}H NMR spectroscopy (400 MHz, $CDCl_3$). **Note**: the structure of the corresponding 4-bromopyridine was confirmed by ^{1}H NMR analysis of authentic samples of the appropriate 4-bromopyridine or by direct isolation and ^{1}H NMR characterization of the 4-bromopyridine from the reaction solution. An overlay of the ^{1}H NMR spectra of the authentic 3-bromopyridine and 4-bromopyridine isomer for each substrate is provided above the ^{1}H NMR spectrum of each crude reaction solution.

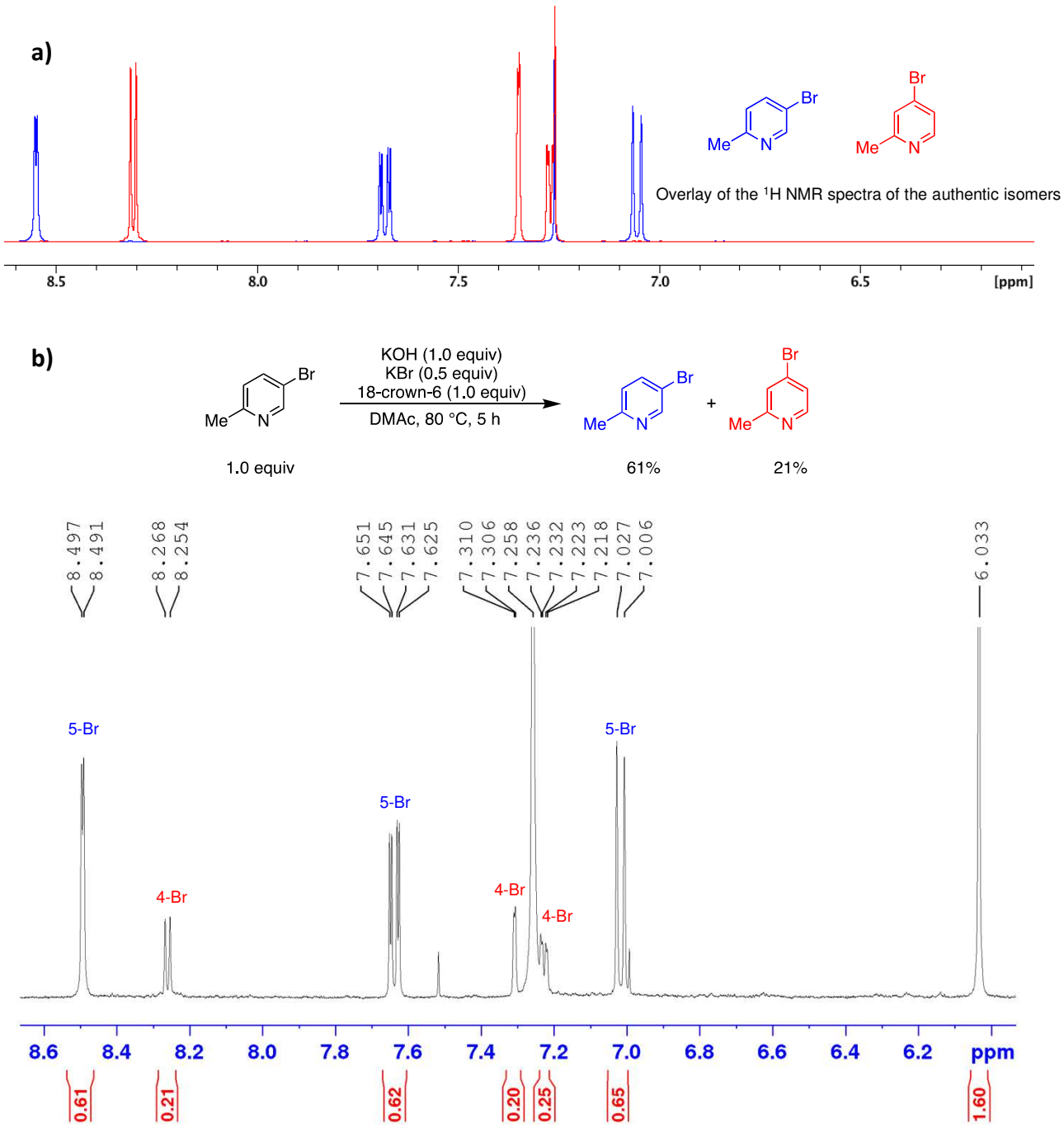

Figure A2–18: (**a**) ^{1}H NMR spectra of the authentic isomers of 5-bromo-2-methylpyridine and 4-bromo-2-methylpyridine. (**b**) ^{1}H NMR spectrum of the crude reaction solution of 5-bromo-2-methylpyridine base-catalyzed isomerization. The reaction was run according to the general procedure on 0.25 mmol scale using 43.0 mg (0.25 mmol) of 5-bromo-2-methylpyridine; 22.3 mg (0.133 mmol) of 1,3,5-trimethoxybenzene was added as internal standard to the reaction solution: 61% 2-methyl-5-bromopyridine and 21% 2-methyl-4-bromopyridine.

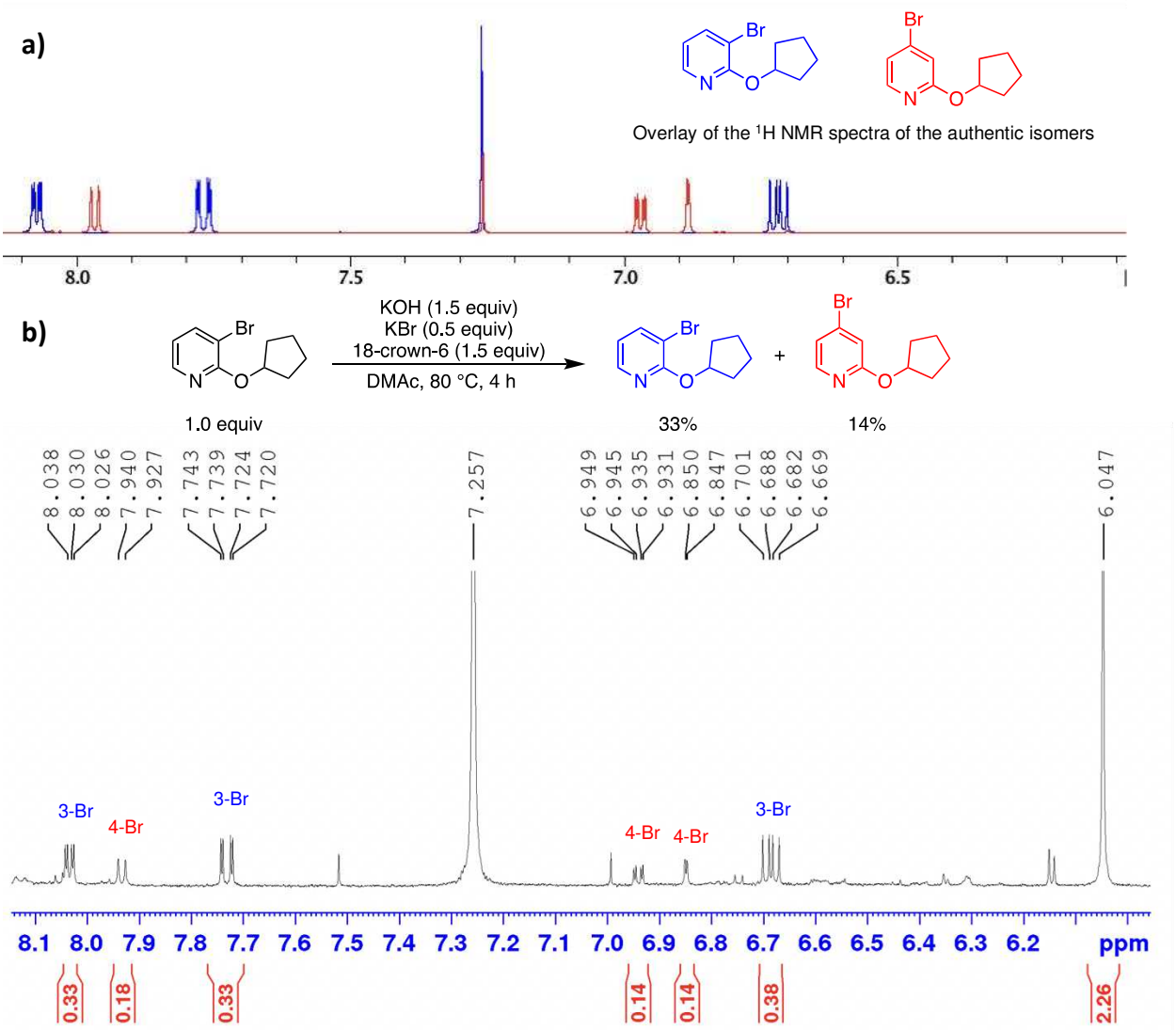

Figure A2–19: (**a**) ^{1}H NMR spectra of the authentic isomers of 3-bromo-2-(cyclopentyloxy)pyridine and 4-bromo-2-(cyclopentyloxy)pyridine. (**b**) ^{1}H NMR spectrum of the crude reaction solution of 3-bromo-2-(cyclopentyloxy)pyridine base-catalyzed isomerization; the reaction was run according to the general procedure using 1.5 equiv of KOH (8.4 mg, 0.15 mmol) and 1.5 equiv of 18-crown-6 (39.6 mg, 0.15 mmol); 12.7 mg (0.076 mmol) of 1,3,5-trimethoxybenzene was added as internal standard: 33% 3-bromo-2-(cyclopentyloxy)pyridine and 14% 4-bromo-2-(cyclopentyloxy)pyridine.

a)

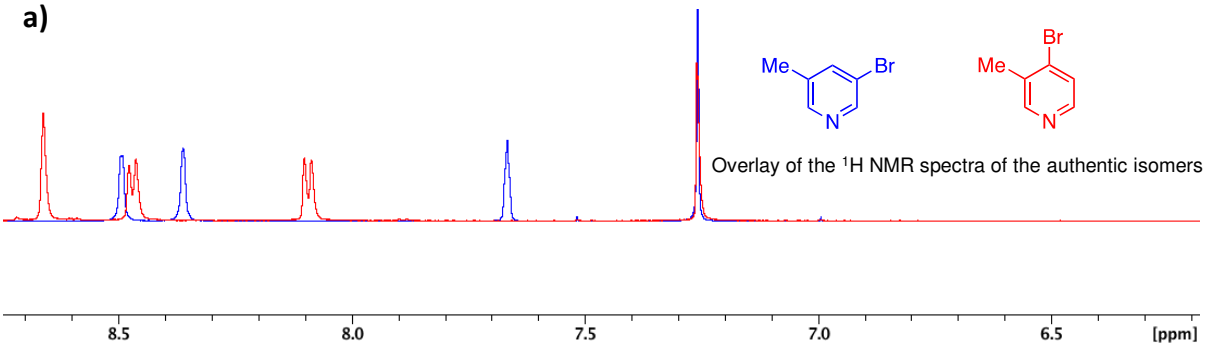

Overlay of the ^{1}H NMR spectra of the authentic isomers

b)

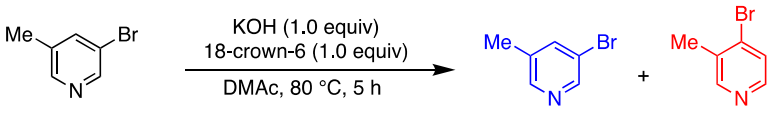

1.0 equiv

35%

13%

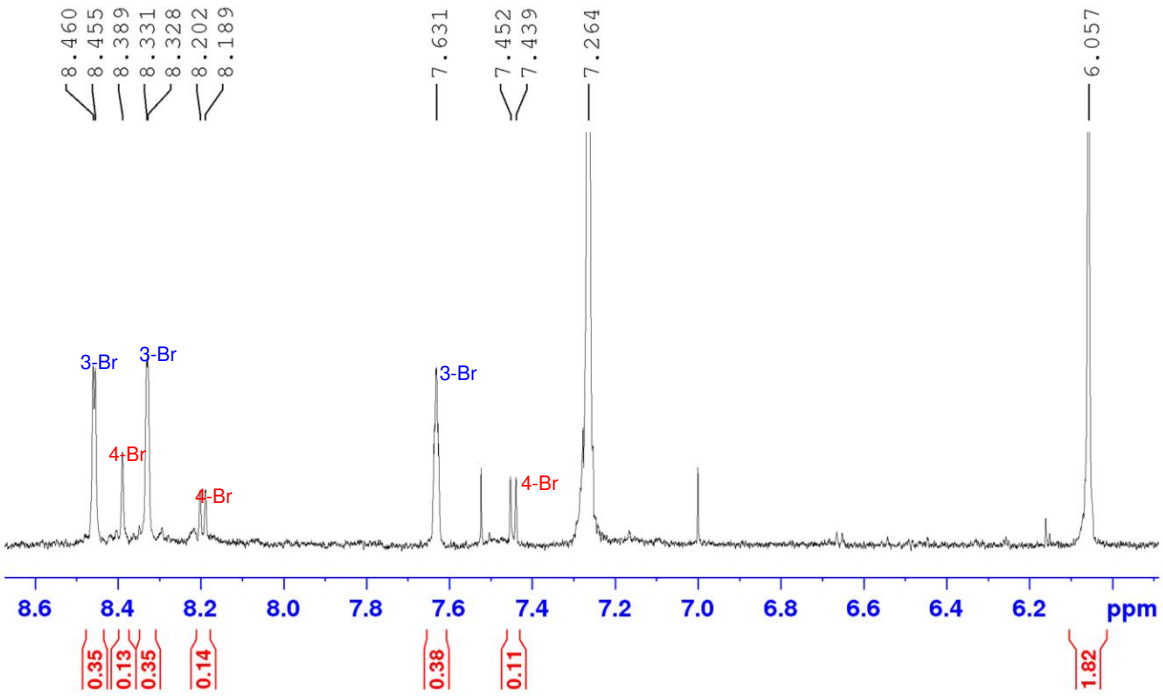

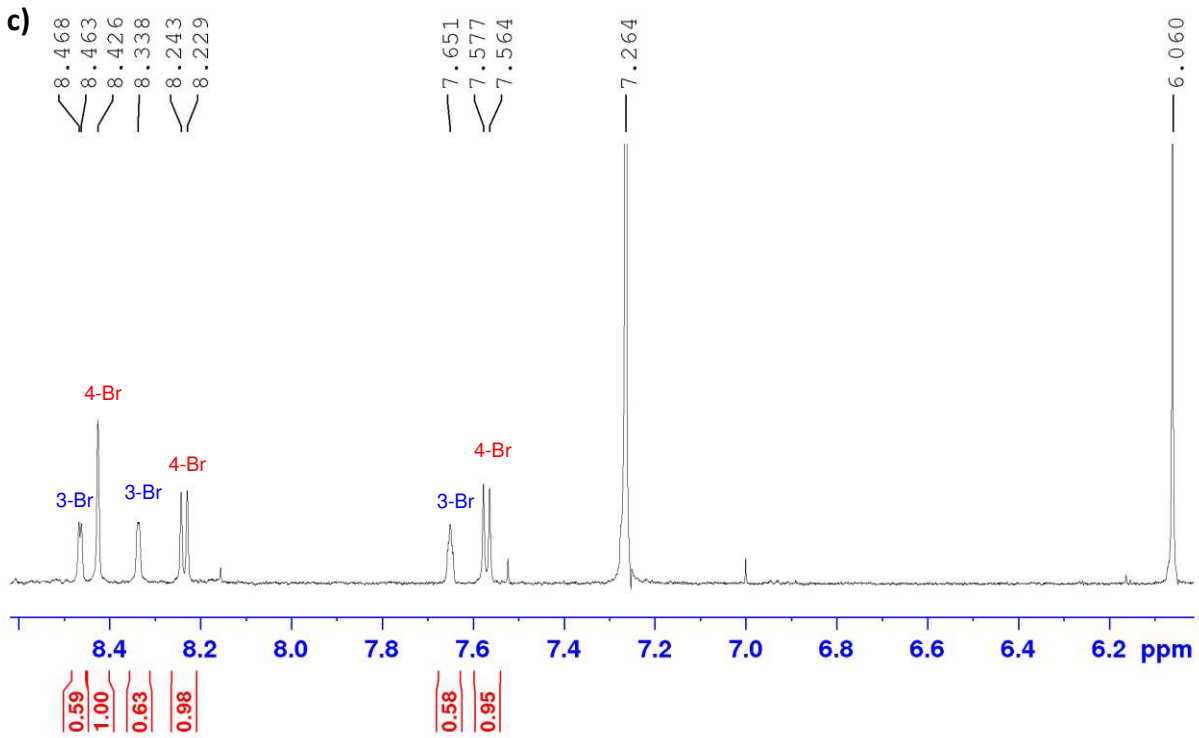

Figure A2–20: (**a**) ^{1}H NMR spectra of the authentic isomers of 3-bromo-5-methylpyridine and 4-bromo-3-methylpyridine. (**b**) ^{1}H NMR spectrum of the crude reaction solution of 3-bromo-5-methylpyridine base-catalyzed isomerization; the reaction was run according to the general procedure; 10.2 mg (0.061 mmol) of 1,3,5-trimethoxybenzene was added as internal standard to the reaction solution: 35% 3-bromo-5-methylpyridine and 13% 4-bromo-3-methylpyridine. **(c)** ^{1}H NMR spectrum of the crude reaction solution of 3-bromo-5-methylpyridine base-catalyzed isomerization with a small quantity of authentic 4-bromo-3-methylpyridine spiked into it. We note that the spectrum of 4-bromo-3-methylpyridine from (**a**) above does not overlay onto the ^{1}H NMR spectrum of the crude solution. When authentic 4-bromo-3-methylpyridine was spiked into the ^{1}H NMR sample of the crude solution, we observed an increase in the signals we labeled as corresponding to the 4-bromo-3-methylpyridine isomer. This is shown in spectrum (c).

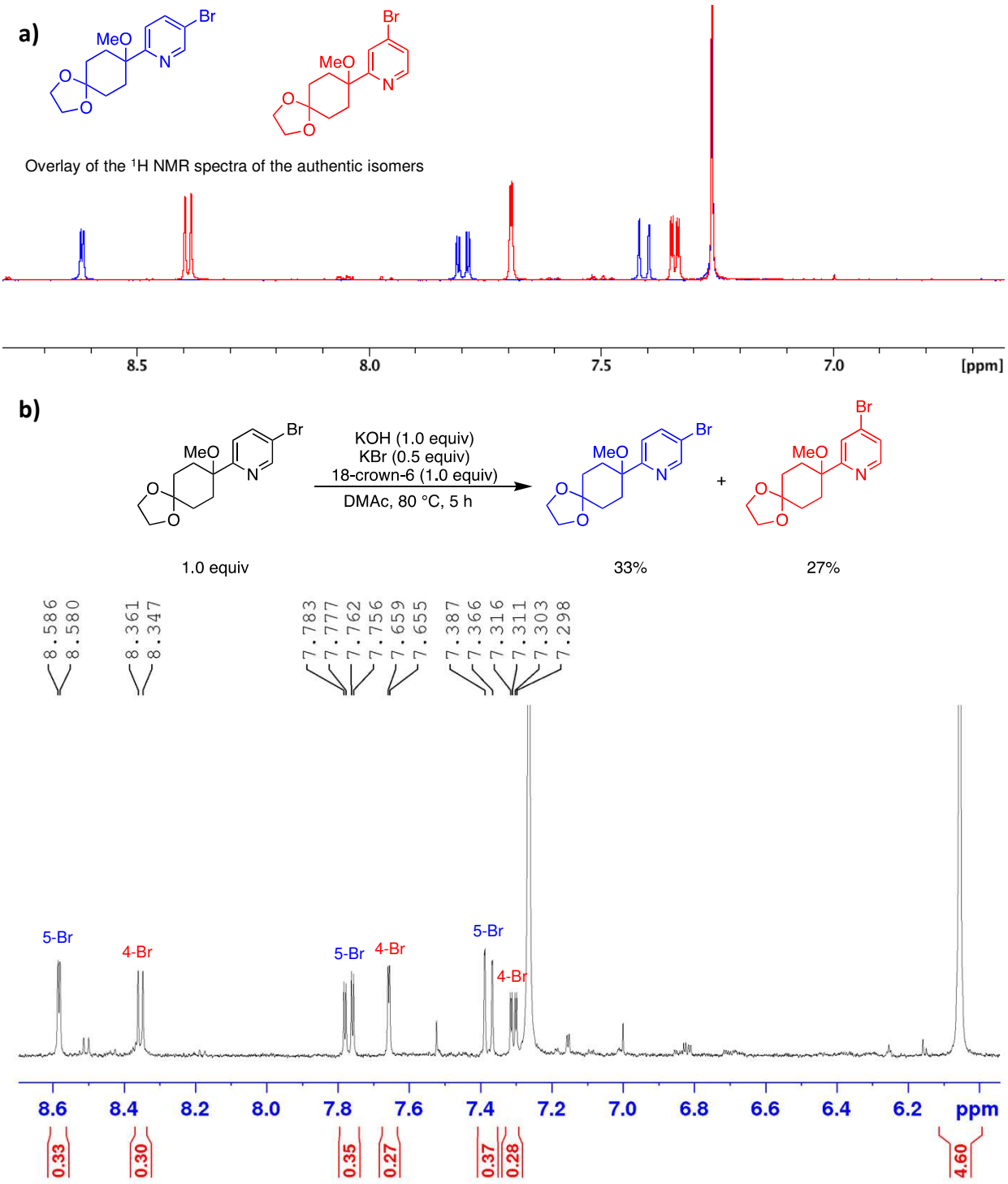

Figure A2–21: (**a**) ^{1}H NMR spectra of the authentic isomers of 5-bromo-2-(8-methoxy-1,4-dioxaspiro[4.5]decan-8-yl)pyridine and 4-bromo-2-(8-methoxy-1,4-dioxaspiro[4.5]decan-8-yl)pyridine. (**b**) ^{1}H NMR spectrum of the crude reaction solution of 5-bromo-2-(8-methoxy-1,4-dioxaspiro[4.5]decan-8-yl)pyridine base-catalyzed isomerization; the reaction was run according to the general procedure; 25.6 mg (0.152 mmol) of 1,3,5-trimethoxybenzene was added as internal standard to the reaction solution: 33% 5-bromo-2-(8-methoxy-1,4-dioxaspiro[4.5]decan-8-yl)pyridine and 27% 4-bromo-2-(8-methoxy-1,4-dioxaspiro[4.5]decan-8-yl)pyridine.

(e) Control test for the decomposition of 3-((2-ethylhexyl)oxy)pyridine (3–12) under reaction conditions

Purpose: To determine if the 3-alkoxypyridines are stable under the reaction conditions.

Procedure: An oven-dried 4 mL vial (ThermoFisher, C4015-1) was charged with a magnetic stir bar. Inside a N_2 filled glovebox, the vial was charged with 3-((2-ethylhexyl)oxy)pyridine (20.8 mg, 0.1 mmol, 1.0 equiv), 2-ethyl-1-hexanol (3.3 mg, 0.025 mmol, 0.25 equiv), DMAc (0.6 mL, 0.17 M), KBr (6.0 mg, 0.05 mmol, 0.5 equiv), 18-crown-6 (26.4 mg, 0.1 mmol, 1.0 equiv), and KOH (5.6 mg, 0.1 mmol, 1.0 equiv) in successive order. The vial was sealed with a PTFE-lined screw cap (ThermoFisher, C4015-1A), removed from the glovebox, and placed into a preheated 80 °C aluminum reaction block. The reaction solution was stirred at 80 °C for 15 h. The solution was removed from the aluminum reaction block and allowed to cool to rt. 1,3,5-Trimethoxybenzene internal standard (13.9 mg, 0.083 mmol) was then added to the solution, and the yield of 3-((2-ethylhexyl)oxy)pyridine was determined via analysis of the crude solution by ^{1}H NMR spectroscopy (400 MHz, $CDCl_3$).

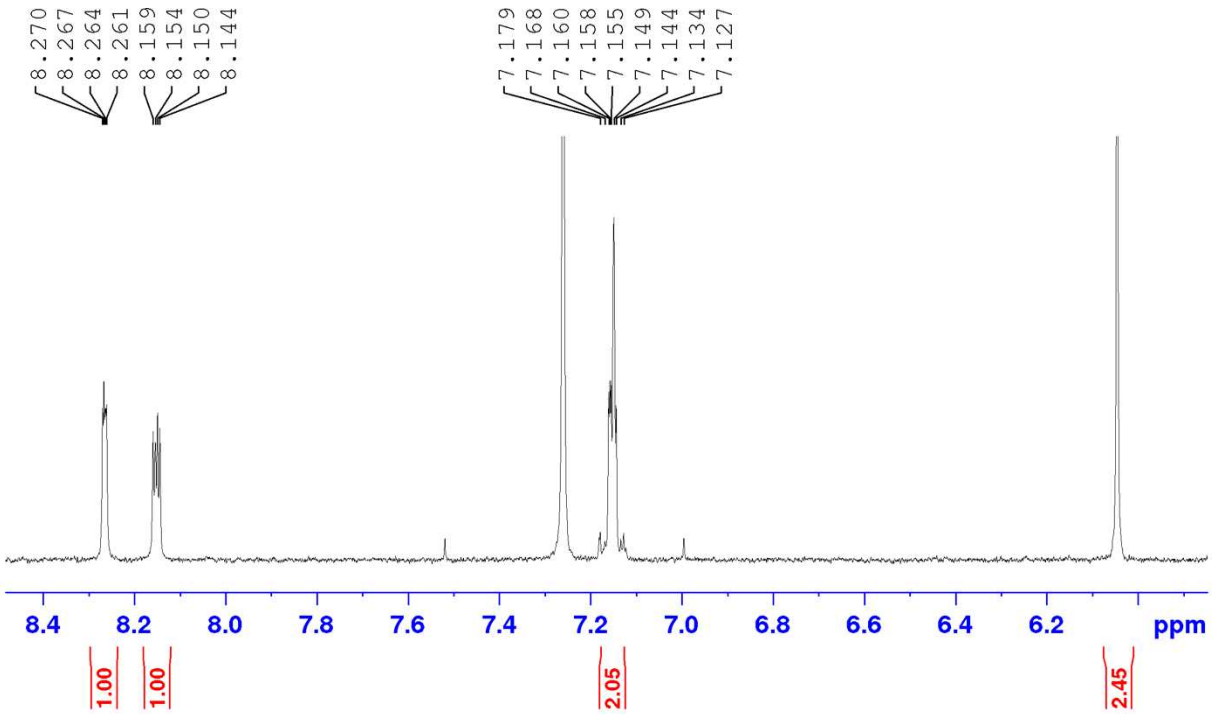

Figure A2–22: ^{1}H NMR spectrum for the subjection of **3–12** to the standard reaction conditions. 13.9 mg (0.083 mmol) of 1,3,5-trimethoxybenzene was added to reaction solution as internal standard. 100% of **3–12** can be accounted for in the ^{1}H NMR spectrum with no observable decomposition products.

A2.5 General Procedure for the 4-Selective Substitution of 3/5-Bromopyridines

General procedure for 1 mmol scale reactions: KOH, KBr, and 18-crown-6 were stored in a N_2 filled glovebox at rt and used immediately upon removal from the glovebox. Outside of the glovebox, an oven-dried 25 or 50 mL round bottom flask was charged with a magnetic stir bar, 18-crown-6 (925.1 mg, 3.5 mmol, 3.5 equiv), KBr (59.5 mg, 0.5 mmol, 0.5 equiv), and KOH (168.3 mg, 3.0 mmol, 3.0 equiv). The flask was then sealed with a Fisherbrand® red septum stopper (Cat. No. FB57875) and the edges of the septum were then sealed with Parafilm®. The flask was evacuated and backfilled three times with N_2 and left under positive pressure using either a N_2 balloon or a Schlenk line. DMAc (4.0 mL) was then added via syringe under N_2 and the

solution was stirred at rt (***Note***: there is usually some insoluble solid that remains in the bottom of the flask). The 3/5-bromopyridine substrate (1.0-1.5 mmol, 1.0-1.5 equiv) and the alcohol substrate (1.0 mmol, 1.0 equiv) were measured into a separate vessel and constituted in DMAc (2.0 mL). This substrate solution was then sparged with N_2 for 3 min and then transferred into the reaction flask via a syringe under N_2. The reaction solution was then placed into a preheated 80 °C silicon oil bath and stirred for 15 h. The solution was then allowed to cool to rt, and 1,3,5-trimethoxybenzene internal standard was measured into the solution. ^{1}H NMR spectroscopy of the crude reaction solution was used to determine the selectivity of the reaction (see discussion below). The solution was then poured into a 250 mL separatory funnel containing water (60 mL). The product was extracted with ethyl acetate (3 x 40 mL) and the organic layers were dried over Na_2SO_4. The Na_2SO_4 was filtered off and the organic layer was concentrated *in vacuo*. All substrates were purified by silica gel chromatography using the given conditions. **Note**: in some cases, residual DMAc co-eluted with the desired product; this can be removed by extended drying *in vacuo*. The results below are reported in the format: (mass of isolated product, percent isolated yield, 4:3 substitution selectivity of crude reaction mixture).

Determining the selectivity of the reaction: The selectivity of each reaction was determined by analyzing the crude reaction solutions by ^{1}H NMR spectroscopy and determining the yield of both 4- and 3-isomeric products. If the identity of the 3-isomeric product was ambiguous in the ^{1}H NMR spectrum, an authentic sample was synthesized, or the 3-isomeric product was purified from the reaction mixture to ensure the correct peaks were used for the analysis. Below are examples of our process to determine the selectivity of the reaction. The top portion of the figure is an overlay of the authentic 3-substituted and 4-substituted isomers. The bottom portion of the figure shows the

^{1}H NMR spectrum of the crude reaction solution and the yield of both the 4-substituted isomer and the 3-substituted isomer relative to 1,3,5-trimethoxybenzene (TMB) internal standard.

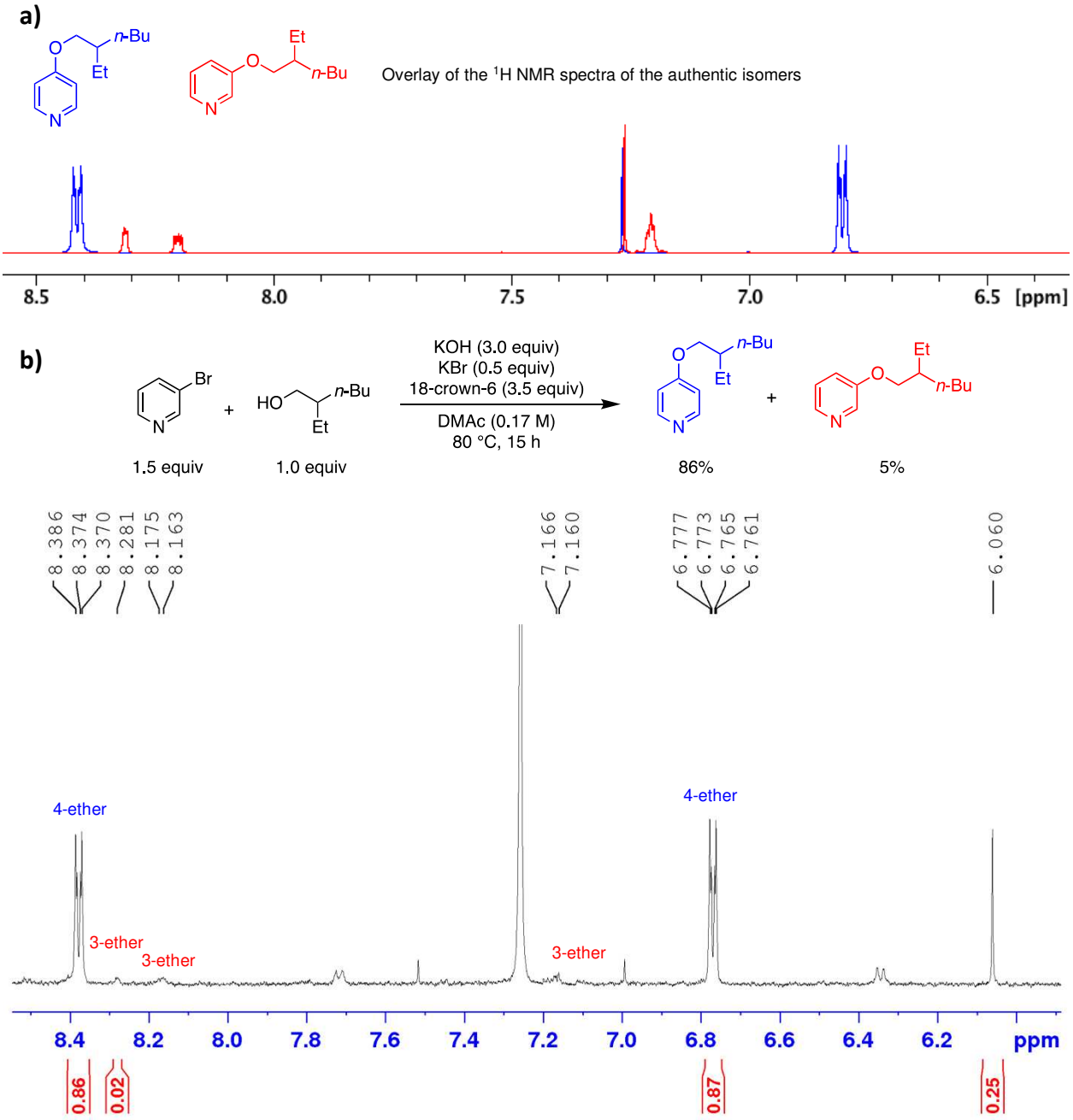

Figure A2–23: (**a**) Overlay of the ^{1}H NMR spectra of 4-((2-ethylhexyl)oxy)pyridine (blue) and 3-((2-ethylhexyl)oxy)pyridine (red). (**b**) ^{1}H NMR spectrum of the crude reaction solution of **3–11** used to determine the 4-selectivity. The reaction was run according to the general procedure; 27.5 mg (0.164 mmol) of TMB was added as internal standard: 86% yield of 4-((2-ethylhexyl)oxy)pyridine and 5% yield of 3-((2-ethylhexyl)oxy)pyridine (>10:1 selectivity).

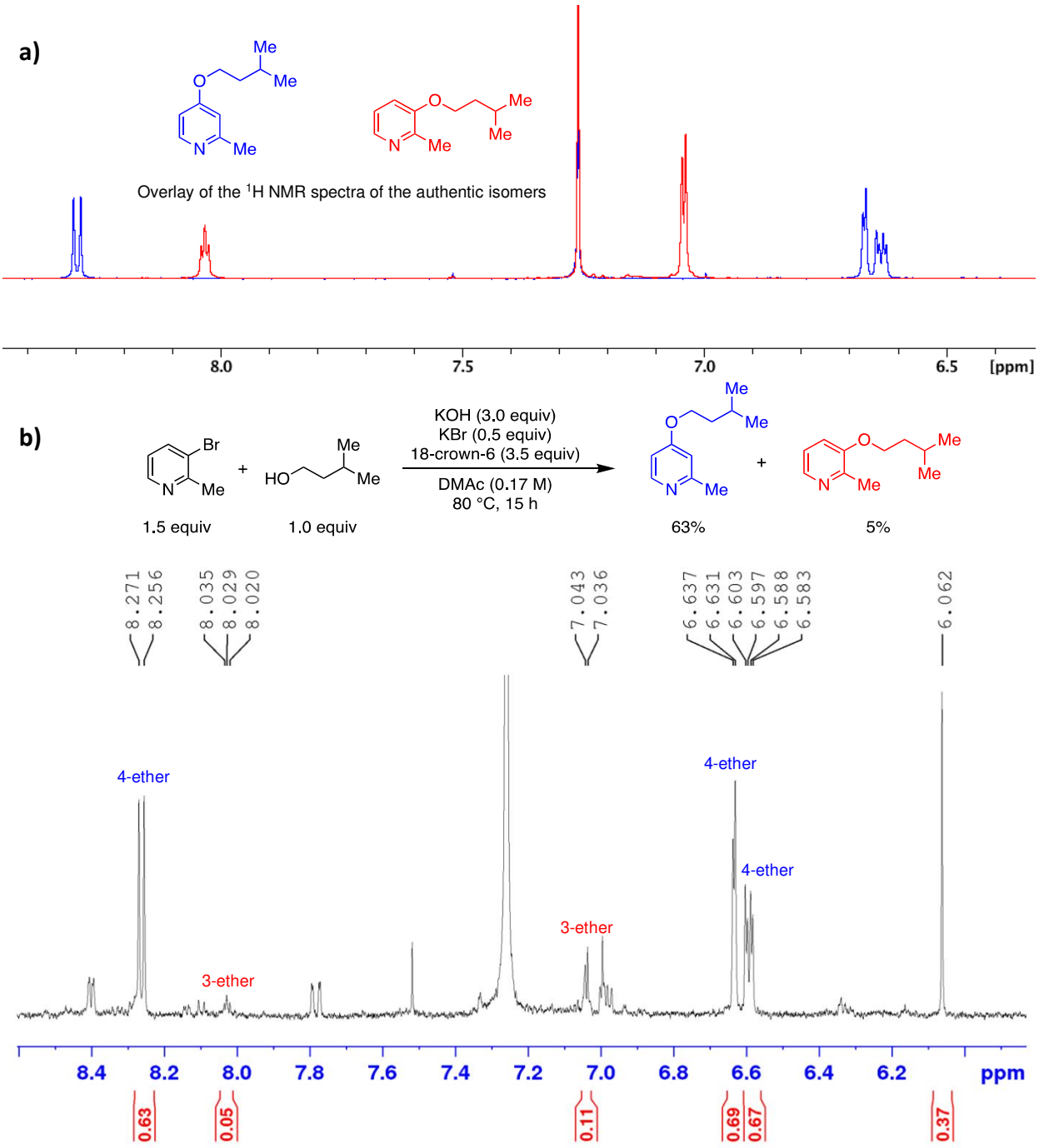

Figure A2–24: (**a**) Overlay of the ^{1}H NMR spectra of 4-(isopentyloxy)-2-methylpyridine (blue) and 3-(isopentyloxy)-2-methylpyridine (red). (**b**) ^{1}H NMR spectrum of the crude reaction solution used to determine the 4-selectivity. Reaction run according to the general procedure; 20.8 mg (0.124 mmol) of TMB was added as internal standard: 63% yield of 4-(isopentyloxy)-2-methylpyridine and 5% yield of 3-(isopentyloxy)-2-methylpyridine (>10:1 selectivity).

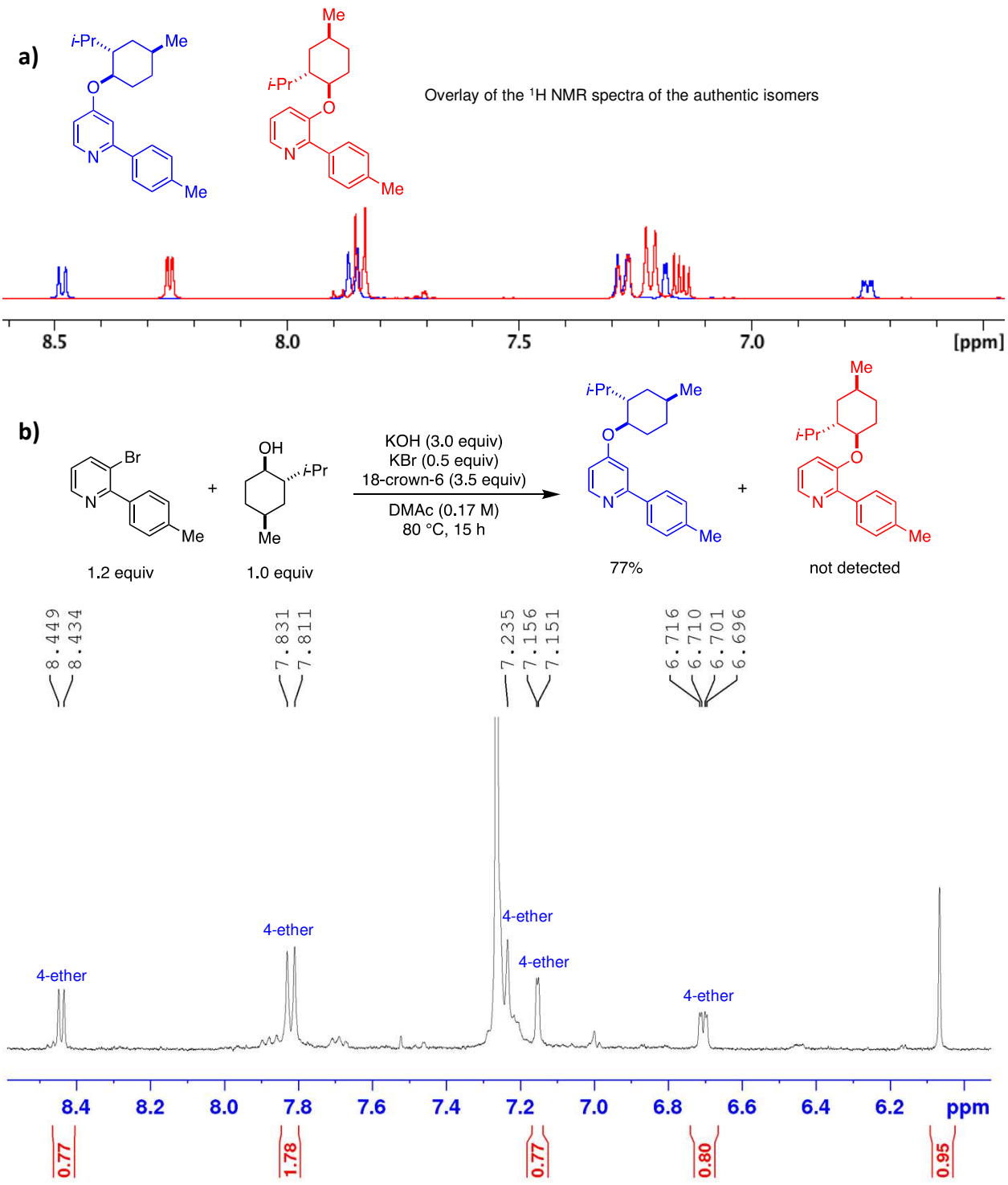

Figure A2–25: **(a)** Overlay of the ^{1}H NMR spectra of authentic 4-(((1*R*,2*S*,4*S*)-2-isopropyl-4-methylcyclohexyl)oxy)-2-(*p*-tolyl)pyridine (blue) and 3-(((1*R*,2*S*,4*S*)-2-isopropyl-4-methylcyclohexyl)oxy)-2-(*p*-tolyl)pyridine (red). **(b)** ^{1}H NMR spectrum of the crude reaction solution. Reaction run according to the general procedure on a 0.5 mmol scale; 26.7 mg (0.159 mmol) of TMB was added as internal standard: 77% yield of 4-(((1*R*,2*S*,4*S*)-2-isopropyl-4-

methylcyclohexyl)oxy)-2-(*p*-tolyl)pyridine and no observed yield of 3-(((1*R*,2*S*,4*S*)-2-isopropyl-4-methylcyclohexyl)oxy)-2-(*p*-tolyl)pyridine (>10:1 selectivity).

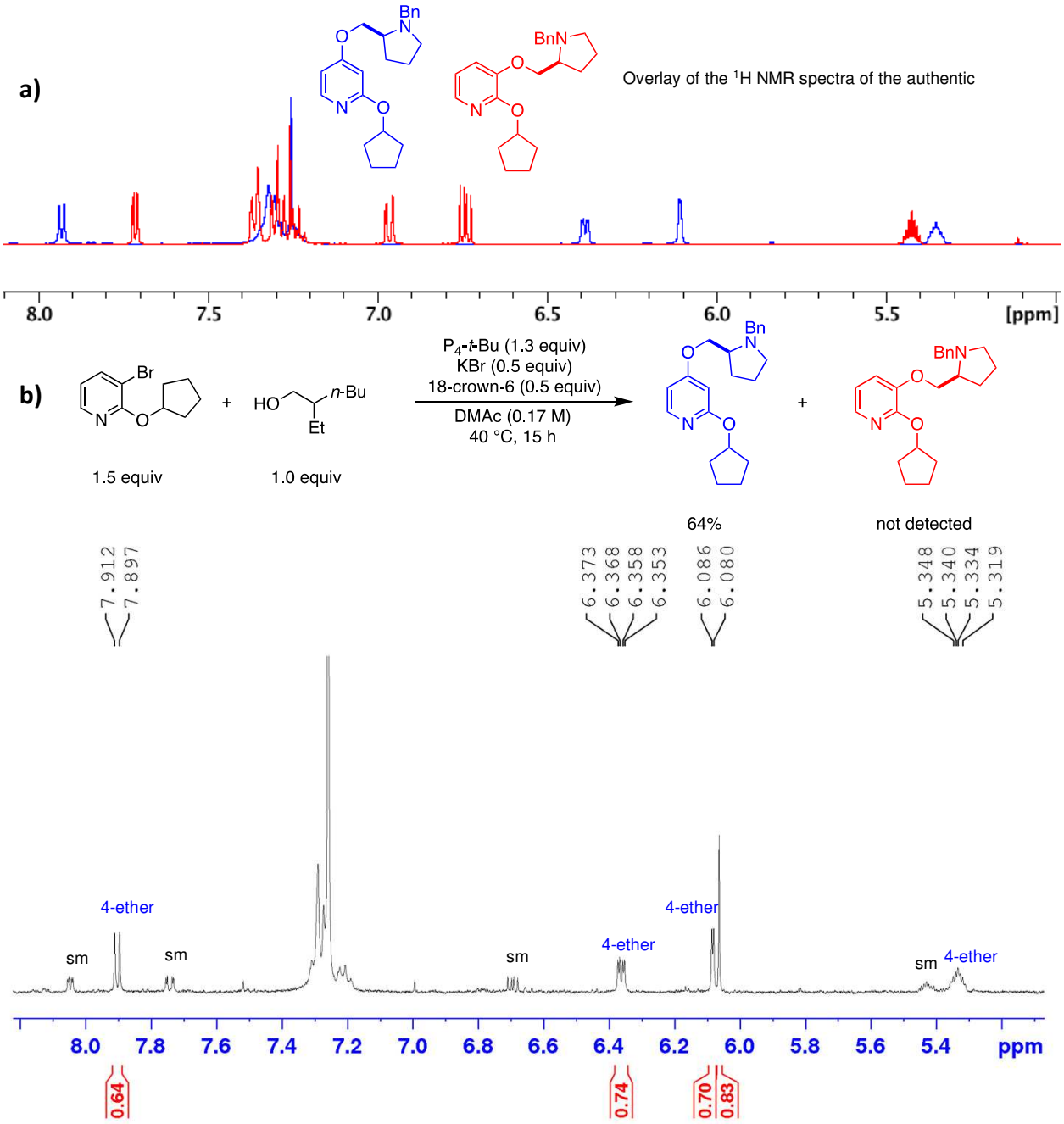

Figure A2–26: **(a)** Overlay of the ^{1}H NMR spectra of authentic (*S*)-4-((1-benzylpyrrolidin-2-yl)methoxy)-2-(cyclopentyloxy)pyridine (blue) and (*S*)-3-((1-benzylpyrrolidin-2-yl)methoxy)-2-(cyclopentyloxy)pyridine (red). **(b)** ^{1}H NMR spectrum of the crude reaction solution. Reaction run according to a modified procedure on a 0.25 mmol scale (see Section A2.6); 11.7 mg (0.070 mmol) of TMB was added as internal standard: 64% yield of (*S*)-4-((1-benzylpyrrolidin-2-yl)methoxy)-

2-(cyclopentyloxy)pyridine and no detected yield of (*S*)-3-((1-benzylpyrrolidin-2-yl)methoxy)-2-(cyclopentyloxy)pyridine (>10:1 selectivity); sm = starting material.

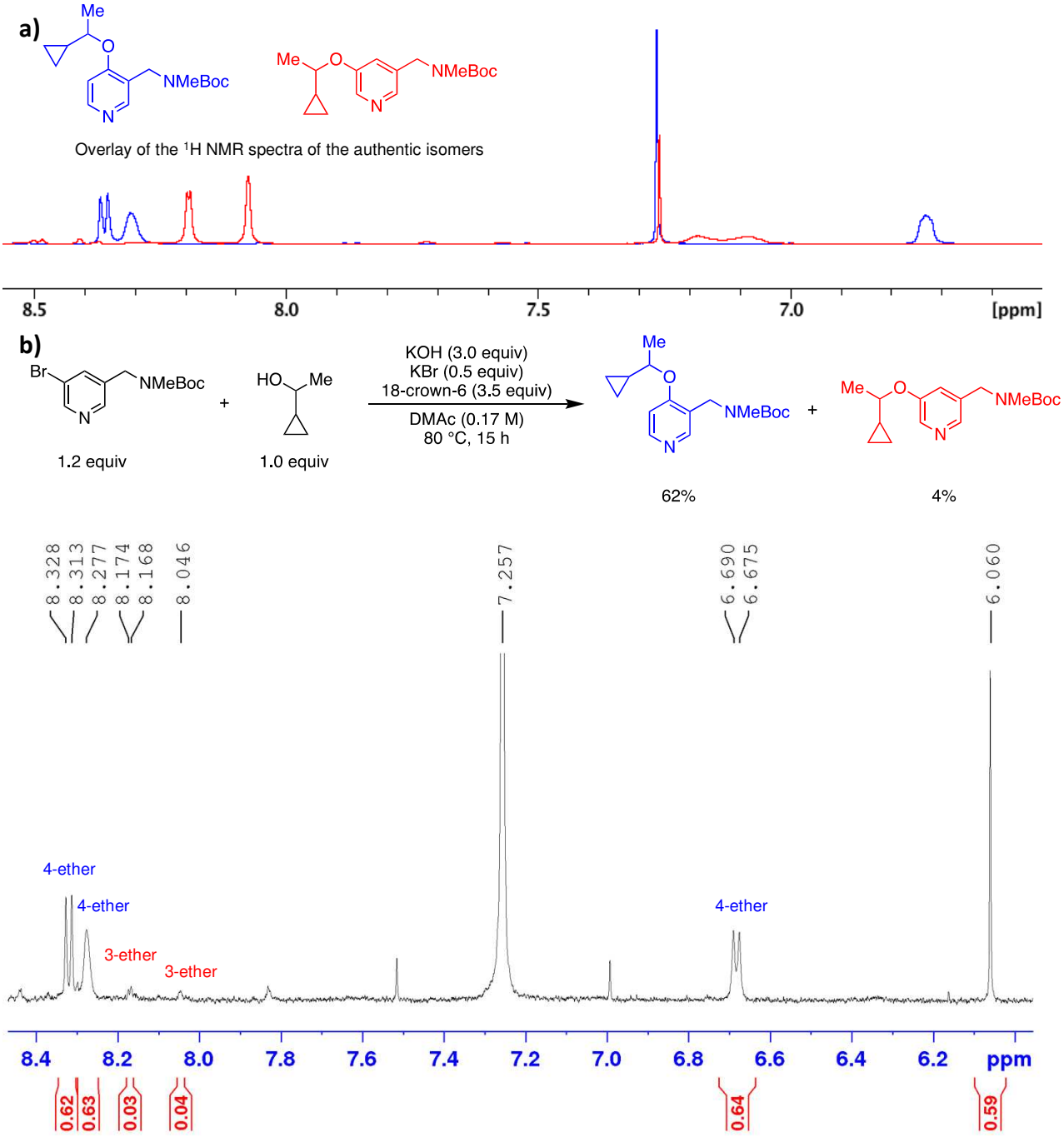

Figure A2–27: **(a)** Overlay of the ^{1}H NMR spectra of authentic *tert*-butyl ((4-(1-cyclopropylethoxy)pyridin-3-yl)methyl)(methyl)carbamate (blue) and *tert*-butyl ((5-(1-cyclopropylethoxy)pyridin-3-yl)methyl)(methyl)carbamate (red, broad signals due to rotamers). **(b)** ^{1}H NMR spectrum of the crude reaction solution. Reaction run according to the general procedure; 33.3 mg (0.198 mmol) of TMB was added as internal standard: 62% yield of *tert*-butyl ((4-(1-cyclopropylethoxy)pyridin-3-yl)methyl)(methyl)carbamate (blue) and 4% yield of *tert*-butyl ((5-(1-cyclopropylethoxy)pyridin-3-yl)methyl)(methyl)carbamate (>10:1 selectivity).

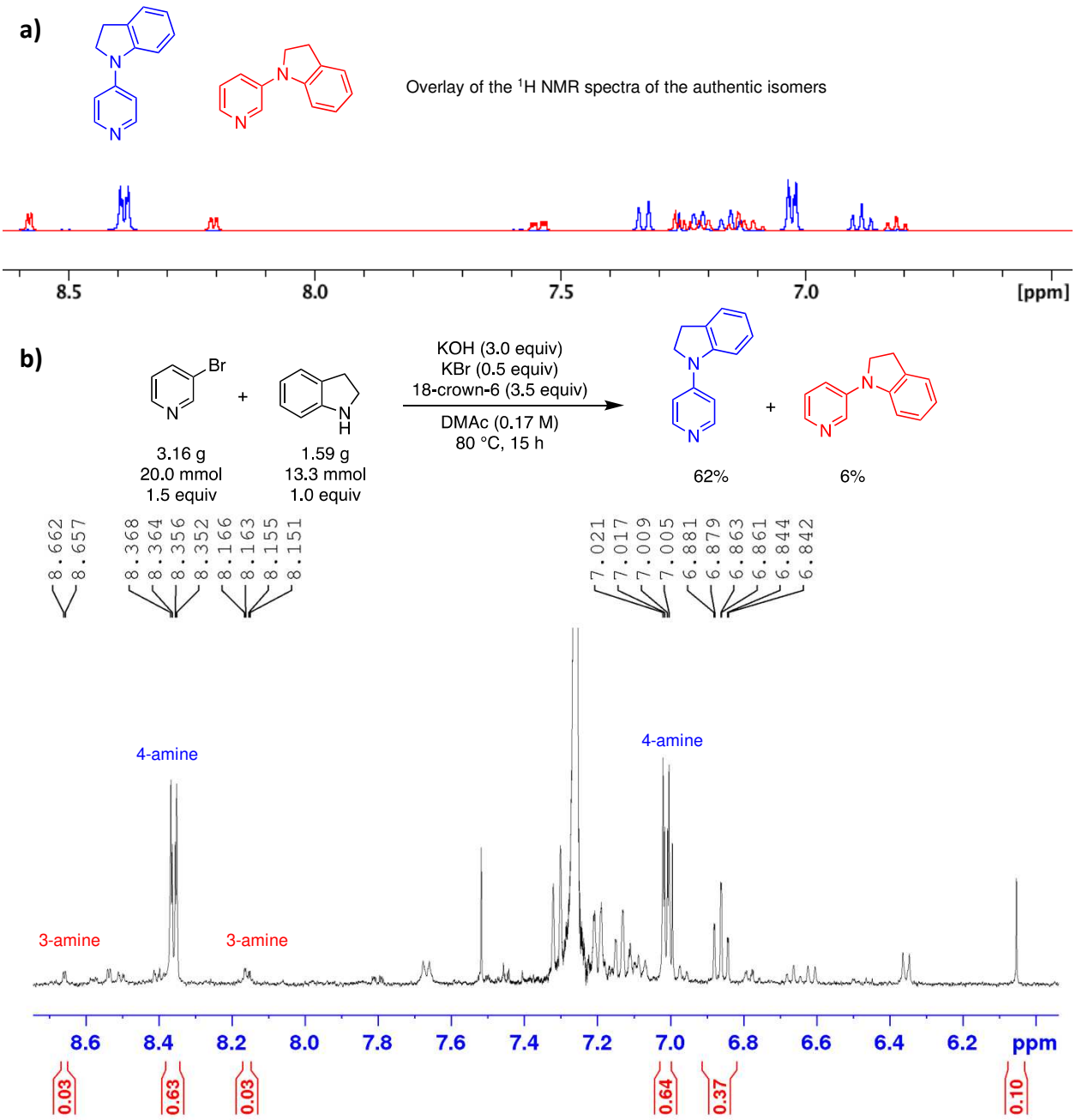

Figure A2–28: **(a)** Overlay of the ^{1}H NMR spectra of authentic 1-(pyridin-4-yl)indoline (blue) and 1-(pyridin-3-yl)indoline (red). **(b)** ^{1}H NMR spectrum of the crude reaction solution. Reaction run according to the procedure described in Section A2.8 on a 13.3 mmol scale; 139.5 mg (0.829 mmol) of TMB was added as internal standard. 62% yield of 1-(pyridin-4-yl)indoline (blue) and 6% yield of 1-(pyridin-3-yl)indoline (>10:1 selectivity).

A2.6 Characterization Data of 4-Substituted Pyridines

4-((2-ethylhexyl)oxy)pyridine (3–11)

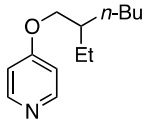

The title product was prepared according to the general procedure using 3-bromopyridine (237.0 mg, 1.5 mmol, 1.5 equiv) and 2-ethyl-1-hexanol (130.2 mg, 1.0 mmol, 1.0 equiv). Silica gel chromatography (50% EtOAc/hexanes) yielded the title compound as a light yellow oil (173.7 mg, 84% yield, >10:1 selectivity). **^{1}H NMR** (400 MHz, $CDCl_3$) δ 8.41 (d, J = 6.2 Hz, 2H), δ 6.80 (d, J = 6.2 Hz, 2H), 3.89 (m, 2H), 1.74 (m, 1H), 1.25-1.55 (m, 8H), 0.89-0.94 (m, 6H). **^{13}C NMR** (101 MHz, $CDCl_3$) δ 165.7, 151.3, 110.7, 70.7, 39.5, 30.8, 29.4, 24.1, 23.3, 14.4, 11.4. **HRMS** (DART) $[M+H]^+$ calcd. for $[C_{13}H_{21}NO]^+$ 208.1696, 208.1754 found. **IR** (neat, cm^{-1}) 2958, 2928, 1590, 1500, 1283, 1210, 1024.

4-((adamantan-1-yl)methoxy)pyridine (3–16)

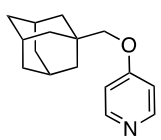

The title product was prepared according to the general procedure using 3-bromopyridine (237.0 mg, 1.5 mmol, 1.5 equiv) and 1-adamantanemethanol (166.3 mg, 1.0 mmol, 1.0 equiv). Silica gel chromatography (40% EtOAc/hexanes) yielded the title compound as an off-white powder (204.3 mg, 84% yield, >10:1 selectivity). **Melting Point**: 75 °C – 77 °C. **^{1}H NMR** (400 MHz, $CDCl_3$) δ 8.39 (m, 2H), 6.79 (m, 2H), 3.53 (s, 2H), 2.02 (m, 3H), 1.64-1.77 (m, 12H). **^{13}C NMR** (101 MHz, $CDCl_3$ δ 165.9, 151.2, 110.7, 78.3, 39.7, 37.4, 34.0, 28.4. **HRMS** (DART) $[M+H]^+$ calcd. for $[C_{16}H_{22}NO]^+$ 244.1696, 244.1754 found. **IR** (neat, cm^{-1}) 2900, 2848, 1590, 1457, 1283, 1212, 1019.

(*S*)-*N*,*N*-dibenzyl-1-phenyl-3-(pyridin-4-yloxy)propan-2-amine (3–17)

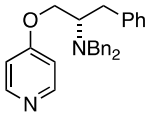

The title product was prepared according to the general procedure using 3-bromopyridine (237.0 mg, 1.5 mmol, 1.5 equiv) and (*S*)-2-(dibenzylamino)-3-phenylpropan-1-ol (331.5 mg, 1.0 mmol, 1.0 equiv). Silica gel chromatography (50% EtOAc/hexanes) yielded the title compound as a viscous yellow oil (346.8 mg, 85% yield, approximately 7:1 selectivity). **^{1}H NMR** (400 MHz, $CDCl_3$) δ 8.36 (m, 2H), 7.17-7.28 (m, 13H), 7.05 (m, 2H), 6.68 (m, 2H), 4.08 (dd, J = 6.3 Hz, 10.0 Hz, 1H), 4.00 (dd, J = 4.4 Hz, 10.0 Hz, 1H), 3.76-3.84 (m, 4H), 3.33 (m, 1H), 3.07 (dd, J = 6.2 Hz, 13.7 Hz, 1H), 2.85 (dd, J = 8.5 Hz, 13.7 Hz, 1H). **^{13}C NMR** (101 MHz, $CDCl_3$) δ 165.1, 151.2, 140.1, 139.7, 129.6, 128.9, 128.8, 128.6, 127.3, 126.6, 110.6, 67.9, 58.5, 54.8, 34.4. **HRMS** (DART) $[M+H]^+$ calcd. for $[C_{28}H_{29}N_2O]^+$ 409.2274, 409.2387 found. **IR** (neat, cm^{-1}) 3026, 2801, 1590, 1494, 1453, 1282, 1026. **Specific Rotation**: $[\alpha]_D^{23}$ = -44.3°.

4-(pent-4-en-1-yloxy)pyridine (3–18)

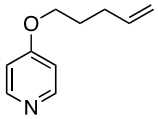

The title product was prepared according to the general procedure using 3-bromopyridine (237.0 mg, 1.5 mmol, 1.5 equiv) and 4-penten-1-ol (86.1 mg, 1.0 mmol, 1.0 equiv). Silica gel chromatography (45% to 50% EtOAc/hexanes) yielded the title compound as a light yellow oil (99.0 mg, 61% yield, >10:1 selectivity). **^{1}H NMR** (400 MHz, $CDCl_3$) δ 8.41 (m, 2H), 6.79 (m, 2H), 5.83 (m, 1H), 5.00-5.08 (m, 2H), 4.01 (t, J = 6.4 Hz, 2H), 2.24 (m, 2H), 1.90 (m, 2H). **^{13}C NMR** (101 MHz, $CDCl_3$) δ 165.3, 151.3, 137.7, 115.9, 110.6, 67.3, 30.2, 28.3. **HRMS** (DART) $[M+H]^+$ calcd. for $[C_{10}H_{14}NO]^+$ 164.1070, 164.1107 found. **IR** (neat, cm^{-1}) 2942, 1591, 1501, 1283, 1210, 1010.

4-(decyloxy)-3-methylpyridine (3–19)

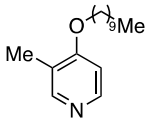

The title product was prepared according to the general procedure using 3-bromo-5-methylpyridine (258.0 mg, 1.5 mmol, 1.5 equiv) and decan-1-ol (158.3 mg, 1.0 mmol, 1.0 equiv). Silica gel chromatography (50% EtOAc/hexanes) yielded the title compound as a light yellow oil (174.6 mg, 70% yield, >10:1 selectivity). **^{1}H NMR** (400 MHz, $CDCl_3$) δ 8.31 (d, J = 5.6 Hz, 1H), 8.24 (s, 1H), 6.70 (d, J = 5.6 Hz, 1H), 4.00 (t, J = 6.5 Hz, 2H), 2.17 (s, 3H), 1.82 (m, 2H), 1.47 (m, 2H), 1.22-1.40 (m, 12H), 0.88 (t, J = 7.0 Hz, 3H). **^{13}C NMR** (101 MHz, $CDCl_3$) δ 163.7, 151.0, 149.4, 122.7, 106.5, 68.2, 32.2, 29.9, 29.9, 29.6, 29.3, 26.3, 23.0, 14.4, 13.4. **HRMS** (DART) $[M+H]^+$ calcd. for $[C_{16}H_{28}NO]^+$ 250.2166, 250.2222 found. **IR** (neat, cm^{-1}) 2923, 2854, 1589, 1501, 1467, 1283, 1186.

4-(isopentyloxy)-2-methylpyridine (3–20)

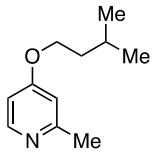

The title product was prepared according to the general procedure using 3-bromo-2-methylpyridine (258.0 mg, 1.5 mmol, 1.5 equiv) and isoamyl alcohol (88.2 mg, 1.0 mmol, 1.0 equiv). Silica gel chromatography (40% EtOAc/hexanes to 50% EtOAc/hexanes) yielded the title compound as a light yellow oil (111.5 mg, 62% yield, >10:1 selectivity). **^{1}H NMR** (400 MHz, $CDCl_3$) δ 8.29 (d, J = 5.8 Hz, 1H), 6.65 (d, J = 2.4 Hz, 1H), 6.62 (dd, J = 2.4 Hz, 5.8 Hz, 1H), 4.01 (t, J = 6.6 Hz, 2H), 2.50 (s, 3H), 1.81 (m, 1H), 1.67 (m, 2H), 0.96 (d, J = 6.6 Hz, 6H). **^{13}C NMR** (101 MHz, $CDCl_3$) δ 165.8, 160.2, 150.5, 109.7, 107.9, 66.5, 37.9, 25.3, 24.9, 22.8. **HRMS** (DART) $[M+H]^+$ calcd. for $[C_{11}H_{18}NO]^+$ 180.1383, 180.1428 found. **IR** (neat, cm^{-1}) 2956, 1595, 1568, 1474, 1284, 1023.

4-(dicyclopropylmethoxy)-2-methylpyridine (3–21)

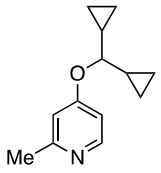

The title product was prepared according to the general procedure using 5-bromo-2-methylpyridine (258.0 mg, 1.5 mmol, 1.5 equiv) and dicyclopropylmethanol (112.2 mg, 1.0 mmol, 1.0 equiv). Silica gel chromatography (50% EtOAc/hexanes) yielded the title compound as a light yellow oil (153.9 mg, 76% yield, >10:1 selectivity). **^{1}H NMR** (400 MHz, $CDCl_3$) δ 8.26 (d, J = 5.8 Hz, 1H), 6.65 (d, J = 2.4 Hz, 1H), 6.60 (dd, J = 2.4 Hz, 5.8 Hz, 1H), 3.66 (t, J = 6.8 Hz, 1H), 2.47 (s, 3H), 1.14 (m, 2H), 0.50-0.58 (m, 4H), 0.32-0.46 (m, 4H). **^{13}C NMR** (101 MHz, $CDCl_3$) δ 165.8, 160.2, 150.5, 111.0, 108.9, 83.5, 24.9, 14.7, 2.8, 2.6. **HRMS** (DART) $[M+H]^+$ calcd. for $[C_{13}H_{18}NO]^+$ 204.1383, 204.1438 found. **IR** (neat, cm^{-1}) 3084, 3008, 1593, 1564, 1281, 1172, 972.

4-(((3a*R*,5*R*,5a*S*,8a*S*,8b*R*)-2,2,7,7-tetramethyltetrahydro-5*H*-bis([1,3]dioxolo)[4,5-*b*:4',5'-*d*]pyran-5-yl)methoxy)pyridine (3–22)

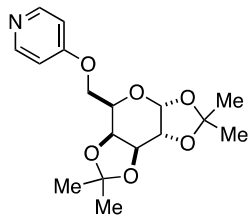

The title product was prepared according to the general procedure on a 0.5 mmol scale using 3-bromopyridine (118.5 mg, 0.75 mmol, 1.5 equiv) and ((3a*R*,5*R*,5a*S*,8a*S*,8b*R*)-2,2,7,7-tetramethyltetrahydro-5*H*-bis([1,3]dioxolo)[4,5-*b*:4',5'-*d*]pyran-5-yl)methanol (130.2 mg, 0.5 mmol, 1.0 equiv). Silica gel chromatography (60% EtOAc/hexanes) yielded the title compound as a white solid (87.5 mg, 52% yield, >10:1 selectivity). **Melting Point**: 111 °C – 114 °C. **^{1}H NMR** (400 MHz, $CDCl_3$) δ 8.43 (d, J = 6.3 Hz, 2H), 6.88 (d, J = 6.3 Hz, 2H), 5.56 (d, J = 5.0 Hz, 1H), 4.66 (dd, J = 2.5 Hz, 8.0 Hz, 1H), 4.33-4.36 (m, 2H), 4.15-4.25 (m, 3H), 1.53 (s, 3H), 1.47 (s, 3H), 1.35 (s, 3H), 1.34 (s, 3H). **^{13}C NMR** (101 MHz, $CDCl_3$) δ 165.4, 150.9, 110.9, 110.0, 109.2, 96.7, 71.2, 71.0, 70.9, 67.1, 66.4, 26.4, 26.3, 25.2, 24.8. **HRMS** (DART) $[M+H]^+$ calcd. for $[C_{17}H_{24}NO_6]^+$

338.1598, 338.1688 found. **IR** (neat, cm^{-1}) 2938, 2905, 1598, 1381, 1283, 1115, 999. **Specific Rotation**: $[\alpha]_D^{23}$ = -52.5°.

(*S*)-4-((1-benzylpyrrolidin-2-yl)methoxy)-2-(cyclopentyloxy)pyridine (3–23)

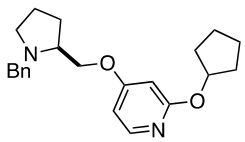

The title product was prepared using a modified procedure. An oven-dried 25 mL round bottom flask was charged with a magnetic stir bar, 3-bromo-2-(cyclopentyloxy)pyridine (90.8 mg, 0.375 mmol, 1.5 equiv), and (*S*)-(1-benzylpyrrolidin-2-yl)methanol (47.8 mg, 0.25 mmol, 1.0 equiv). The flask was then brought into a N_2 filled glovebox and charged with DMAc (1.5 mL, 0.17 M), KBr (14.9 mg, 0.125 mmol, 0.5 equiv), 18-crown-6 (33.0 mg, 0.125 mmol, 0.5 equiv), and P_4-*t*-Bu (407 µl of a 0.8 M solution in hexanes, 0.325 mmol, 1.3 equiv) in that respective order. The flask was then sealed with a Fisherbrand® red septum stopper (Cat. No. FB57875) and the edges of the septum were then sealed with Parafilm®. The flask was then removed from the glovebox, placed into a preheated 40 °C silicon oil bath and stirred for 15 h. The aqueous workup and purification procedures are in accord with the general procedure. Silica gel chromatography (35% EtOAc/hexanes) yielded the title compound as a brown oil (52.4 mg, 60% yield, >10:1 selectivity). **^{1}H NMR** (400 MHz, $CDCl_3$) δ 7.93 (d, J = 5.9 Hz, 1H), 7.28-7.38 (m, 4H), 7.25 (m, 1H), 6.39 (dd, J = 1.8 Hz, 5.9 Hz, 1H), 6.11 (d, J = 1.8 Hz, 1H), 5.35 (m, 1H), 4.08 (m, 1H), 3.93 (m, 1H), 3.83 (m, 1H), 3.54 (m, 1H), 2.92-3.08 (m, 2H), 2.32 (m, 1H), 1.86-2.07 (m, 3H), 1.68-1.85 (m, 7H), 1.56-1.66 (m, 2H). **^{13}C NMR** (101 MHz, $CDCl_3$) δ 167.4, 165.9, 147.9, 129.3, 128.6, 127.4, 106.2, 95.4, 78.2, 71.4, 62.3, 60.0, 54.9, 33.2, 28.9, 24.2, 23.3. **HRMS** (DART) $[M+H]^+$ calcd. for $[C_{22}H_{29}N_2O_2]^+$ 353.2224, 353.2310 found. **IR** (neat, cm^{-1}) 2959, 2871, 1597, 1419, 1165, 1028. **Specific Rotation**: $[\alpha]_D^{23}$ = +9.6°.

2-chloro-10-(3-(4-(2-((2-methylpyridin-4-yl)oxy)ethyl)piperazin-1-yl)propyl)-10*H*-phenothiazine (3–24)

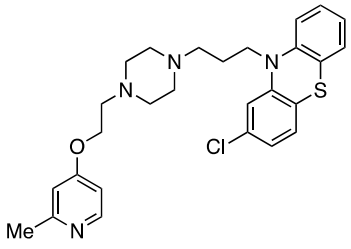

The title product was synthesized according to the general procedure on a 0.5 mmol scale using 5-bromo-2-methylpyridine (129.0 mg, 0.75 mmol, 1.5 equiv) and perphenazine (202.0 mg, 0.50 mmol, 1.0 equiv). The crude organic residue obtained after the aqueous workup was dried *in vacuo* for 24 h. The desired product was purified via chromatography on NEt_3-neutralized silica gel (1% $MeOH/CH_2Cl_2$ to 1.5% $MeOH/CH_2Cl_2$). A small quantity of triethylammonium salt was present in the product after purification. This was removed by diluting the product in EtOAc (50 mL) and washing with H_2O (2 x 50 mL) and with brine (1 x 50 mL). The organic layer was subsequently dried over Na_2SO_4 and concentrated *in vacuo* to afford the purified product as a light yellow oil (130.6 mg, 53% yield, >10:1 selectivity). **^{1}H NMR** (400 MHz, $CDCl_3$) δ 8.29 (d, J = 5.8 Hz, 1H), 7.10-7.16 (m, 2H), 7.01 (d, J = 8.1 Hz, 1H), 6.84-6.94 (m, 4H), 6.66 (d, J = 2.4 Hz, 1H), 6.62 (dd, J = 2.4 Hz, 5.8 Hz, 1H), 4.10 (t, J = 5.8 Hz, 2H), 3.90 (t, J = 6.8 Hz, 2H), 2.79 (t, J = 5.8 Hz, 2H), 2.52-2.67 (m, 4H), 2.37-2.52 (m, 9H), 1.94 (m, 2H). **^{13}C NMR** (101 MHz, $CDCl_3$) δ 165.4, 160.3, 150.6, 146.8, 144.8, 133.5, 128.2, 127.8, 127.7, 125.1,123.8, 123.2, 122.6, 116.2, 116.1, 109.8, 108.0, 66.0, 57.1, 55.8, 53.9, 53.5, 45.6, 24.9, 24.5. **HRMS** (DART) $[M+H]^+$ calcd. for $[C_{27}H_{32}ClN_4OS]^+$ 495.1980, 495.2020 found. **IR** (neat, cm^{-1}) 2939, 2811, 1594, 1566, 1456, 1282, 1039.

4-(4-(1-cyclopropylethoxy)pyridin-2-yl)-*N*,*N*-dimethylaniline (3–25)

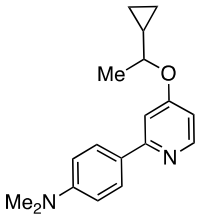

The title product was prepared according to the general procedure on a 0.5 mmol scale using 4-(5-bromopyridin-2-yl)-*N*,*N*-dimethylaniline (207.2 mg, 0.75 mmol, 1.5 equiv) and 1-cyclopropylethanol (43.1 mg, 0.5 mmol, 1.0 equiv). Silica gel chromatography (50% EtOAc/hexanes) yielded the title compound as a light yellow oil (77.0 mg, 55% yield, >10:1 selectivity). **^{1}H NMR** (400 MHz, $CDCl_3$) δ 8.43 (d, J = 5.9 Hz, 1H), 7.89 (d, J = 9.0 Hz, 2H), 7.13 (d, J = 2.4 Hz, 1H), 6.78 (d, J = 9.0 Hz, 2H), 6.64 (dd, J = 2.4 Hz, 5.9 Hz, 1H), 4.03 (m, 1H), 3.02 (s, 6H), 1.42 (d, J = 6.1 Hz, 3H), 1.17 (m, 1H), 0.61 (m, 2H), 0.44 (m, 1H), 0.33 (m, 1H). **^{13}C NMR** (101 MHz, $CDCl_3$) δ 165.4, 159.5, 151.4, 150.7, 128.1, 127.4, 112.5, 108.5, 107.0, 77.8, 40.7, 19.5, 16.9, 3.9, 2.5. **HRMS** (DART) $[M+H]^+$ calcd. for $[C_{18}H_{23}N_2O]^+$ 283.1805, 283.1865 found. **IR** (neat, cm^{-1}) 2976, 1894, 1587, 1526, 1468, 1192, 1064.

4-(((1*R*,2*S*,5*R*)-2-isopropyl-5-methylcyclohexyl)oxy)-2-(*p*-tolyl)pyridine (3–26)

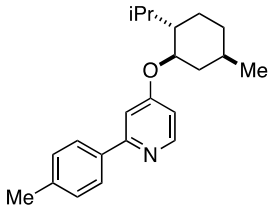

The title product was prepared according to the general procedure on a 0.5 mmol scale using 3-bromo-2-(*p*-tolyl)pyridine (248.1 mg, 0.75 mmol, 1.5 equiv) and (1*R*,2*S*,5*R*)-2-isopropyl-5-methylcyclohexan-1-ol (78.2 mg, 0.5 mmol, 1.0 equiv). Silica gel chromatography (10% EtOAc/hexanes) yielded the title compound as a white solid (124.3 mg, 77% yield, >10:1 selectivity). **Melting Point**: 201 °C – 205 °C **^{1}H NMR** (400 MHz, $CDCl_3$) δ 8.49 (d, J = 5.8 Hz, 1H), 7.86 (d, J = 8.2 Hz, 2H), 7.28 (d, J = 8.2 Hz, 2H), 7.18 (d, J = 3.0 Hz, 1H), 6.75 (dd, J = 3.0 Hz, 5.8 Hz, 1H), 4.21 (td, J = 4.2 Hz, 10.6 Hz, 1H), 2.40 (s, 3H), 2.14 (m, 2H), 1.76 (m, 2H), 1.47-1.60 (m, 2H), 1.03-1.19 (m, 2H), 0.90-1.00 (m, 7H), 0.77 (d, J = 7.0 Hz, 3H). **^{13}C NMR** (101 MHz, $CDCl_3$) δ 165.9, 159.3, 150.7, 139.5, 136.5, 129.8, 127.2,

109.0, 108.3, 77.8, 48.1, 40.2, 34.6, 31.7, 26.5, 24.1, 22.4, 21.6, 21.0, 17.0. **HRMS** (DART) $[M+H]^+$ calcd. for $[C_{22}H_{30}NO]^+$ 324.2322, 323.2371 found. **IR** (neat, cm^{-1}) 2924.45, 2602.04, 1594.40, 1473.69, 1397. 27, 1198.60. **Specific Rotation**: $[\alpha]_D^{23}$ = -2.9°.

4-(((3*S*,4*R*)-4-(4-fluorophenyl)-1-methylpiperidin-3-yl)methoxy)-2-methylpyridine (3–27)

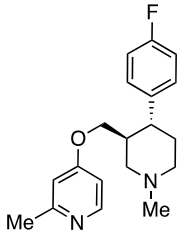

The title product was prepared according to the general procedure using 5-bromo-2-methylpyridine (206.4 mg, 1.2 mmol, 1.2 equiv) and (3*S*, 4*R*)-4-(4-fluorophenyl)-3-hydroxymethyl-1-methylpiperidine (331.5 mg, 1.0 mmol, 1.0 equiv). Chromatography on NEt_3-neutralized silica gel (100% CH_2Cl_2 – 5% MeOH/CH_2Cl_2) yielded the title compound as a light brown oil (172.4 mg, 55% yield, >10:1 selectivity). **^{1}H NMR** (400 MHz, $CDCl_3$) δ 8.22 (d, J = 5.7 Hz, 1H), 7.15 (m, 2H), 6.97 (m, 2H), 6.48 (d, J = 2.2 Hz, 1H), 6.44 (dd, J = 2.2 Hz, 5.7 Hz, 1H), 3.67 (dd, J = 2.9 Hz, 9.7 Hz, 1H), 3.55 (dd, J = 6.7 Hz, 9.7 Hz), 3.21 (m, 1H), 3.03 (m, 1H), 2.27-2.58 (m, 8H), 2.04-2.19 (m, 2H), 1.97 (m, 1H), 1.84 (m, 1H). **^{13}C NMR** (101 MHz, $CDCl_3$) δ 165.4, 163.2, 160.8, 160.3, 150.5, 139.3 (d, J = 3.1 Hz), 129.1 (d, J = 7.8 Hz), 115.9 (d, J = 21.2 Hz), 108.6 (d, J = 173.2 Hz), 68.4, 59.4, 56.3, 46.5, 43.5, 41.9, 34.2, 24.8. **^{19}F NMR** (376 MHz, $CDCl_3$) δ 116.69. **HRMS** (DART) $[M+H]^+$ calcd. for $[C_{19}H_{24}FN_2O]^+$ 315.1867, 315.1946 found. **IR** (neat, cm^{-1}) 2938.27, 2795.74, 1598.89, 1509.84, 1283.33, 1221.45, 1177.06. **Specific Rotation**: $[\alpha]_D^{23}$ = -38.2°.

4-(4-(cyclopropylmethoxy)pyridin-2-yl)morpholine (3–28)

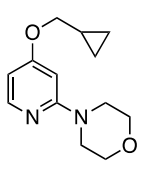

The title product was prepared according to the general procedure using 4-(3-bromopyridin-2-yl)morpholine (291.7 mg, 1.2 mmol, 1.2 equiv) and cyclopropylmethanol (72.1 mg, 1.0 mmol, 1.0 equiv). Silica gel chromatography

(40% EtOAc/hexanes) yielded the title compound as a light yellow oil (122.1 mg, 43% yield, 10:1 selectivity). **^{1}H NMR** (400 MHz, $CDCl_3$) δ 8.03 (d, J = 5.8 Hz, 1H), 6.28 (dd, J = 2.6 Hz, 5.8 Hz, 1H), 6.10 (d, J = 2.6 Hz, 1H), 3.80-3.83 (m, 6H), 3.47 (t, J = 5.0 Hz, 4H), 1.26 (m, 1H), 0.66 (m, 2H), 0.35 (m, 2H). **^{13}C NMR** (101 MHz, $CDCl_3$) δ 167.0, 161.8, 149.3, 102.1, 92.8, 72.7, 67.0, 46.1, 10.3, 3.5. **HRMS** (DART) $[M+H]^+$ calcd. for $[C_{13}H_{19}N_2O_2]^+$ 235.1441, 235.1507 found. **IR** (neat, cm^{-1}) 2963, 2859, 1595, 1553, 1441, 1202, 1118.

***tert*-butyl ((4-(1-cyclopropylethoxy)pyridin-3-yl)methyl)(methyl)carbamate (3–29)**

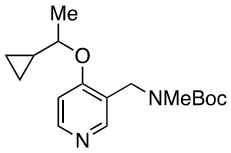

The title product was prepared according to the general procedure using *tert*-butyl ((5-bromopyridin-3-yl)methyl)(methyl)carbamate (343.2 mg, 1.2 mmol, 1.2 equiv) and 1-cyclopropylethanol (86.1 mg, 1.0 mmol, 1.0 equiv). Silica gel chromatography (60% EtOAc/hexanes) yielded the title compound as a light yellow oil (179.0 mg, 61% yield, >10:1 selectivity). **^{1}H NMR** (400 MHz, $CDCl_3$) signal broadening due to mixture of rotamers δ 8.34 (d, J = 5.8 Hz, 1H), 8.29 (br s, 1H), 6.70 (d, J = 5.8 Hz, 1H), 4.41 (m, 2H), 4.01 (m, 1H), 2.75-2.99 (m, 3H), 1.41-153 (m, 9H), 1.38 (m, 3H), 1.13 (m, 1H), 0.65 (m, 2H), 0.37 (m, 1H), 0.29 (m, 1H). **^{13}C NMR** (101 MHz, $CDCl_3$) (mixture of rotamers) δ 162.6, 156.2, 150.9, 150.5, 150.3, 123.1, 122.9, 107.7, 80.2, 78.1, 77.8, 46.0, 45.2, 35.2, 34.7, 28.8, 19.6, 16.9, 3.8, 2.5. **HRMS** (DART) $[M+H]^+$ calcd. for $[C_{17}H_{27}N_2O_3]^+$ 307.2016, 307.2096 found. **IR** (neat, cm^{-1}) 2976, 1688, 1588, 1490, 1390, 1140, 1048.

2-(4-((2-ethylhexyl)oxy)pyridin-2-yl)-1-(pyrrolidin-1-yl)propan-1-one (3–30)

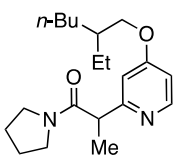

The title product was prepared using a modified procedure. A 4.0 mL oven-dried vial (ThermoFisher, C4015-1) was charged with a magnetic stir bar and 2-(5-

bromopyridin-2-yl)-1-(pyrrolidin-1-yl)propan-1-one (84.6 mg, 0.3 mmol, 1.2 equiv). The vial was then brought into a N_2 filled glovebox and charged with 2-ethyl-1-hexanol (32.6 mg, 0.25 mmol, 1.0 equiv), DMAc (1.5 mL, 0.17 M), KBr (14.9 mg, 0.125 mmol, 0.5 equiv), 18-crown-6 (231.3 mg, 0.875 mmol, 3.5 equiv), and KOH (42.1 mg, 0.75 mmol, 3.0 equiv) in that respective order. The vial was sealed with a PTFE-lined screw cap (ThermoFisher, C4015-1A), removed from the glovebox, and placed into a preheated 80 °C aluminum reaction block. The reaction solution was stirred at 80 °C for 15 h. The solution was then allowed to cool to rt and was quenched with H_2O (ca. 1.0 mL) and diluted with EtOAc (30 mL). The organic layer was washed with H_2O (2 x 30 mL) and brine (1 x 20 mL). The organic layer was then dried over Na_2SO_4 and concentrated *in vacuo*. The crude residue was then loaded onto a preparatory TLC plate and developed with 1% MeOH/CH_2Cl_2 (R_f = 0.7). The band was scrapped off of the plate and the silica was washed with 100 mL 5% MeOH/CH_2Cl_2 to extract the product. The volatiles were removed *in vacuo*. The product remained impure and was therefore loaded onto another preparatory TLC plate neutralized with NEt_3 and developed with 50% EtOAc/hexanes (R_f = 0.4). The band was scrapped off the plate and the silica gel was washed with 100 mL of 5% MeOH/CH_2Cl_2. The volatiles were removed *in vacuo* to yield the title compound as a clear oil (32.0 mg, 44% yield, approximately 9:1 selectivity). **^{1}H NMR** (400 MHz, $CDCl_3$) δ 8.27 (d, J = 5.8 Hz, 1H), 6.89 (d, J = 2.4 Hz, 1H), 6.65 (dd, J = 2.4 Hz, 5.8 Hz, 1H), 3.99 (q, J = 7.0 Hz, 1H), 3.85 (m, 2H), 3.51 (m, 2H), 3.39 (m, 2H), 1.90 (m, 1H), 1.75-1.84 (m, 3H), 1.69 (m, 1H), 1.48 (d, J = 7.0 Hz, 3H), 1.34-1.45 (m, 3H), 1.21-1.34 (m, 5H), 0.81-0.95 (m, 6H). **^{13}C NMR** (101 MHz, $CDCl_3$) δ 171.8, 166.6, 163.4, 150.2, 109.4, 107.7, 70.7, 47.8, 46.9, 46.3, 39.5, 30.7, 29.4, 26.3, 24.6, 24.0, 24.0, 23.3, 18.9, 14.4, 11.4. **HRMS** (DART) $[M+H]^+$ calcd. for $[C_{20}H_{33}N_2O_2]^+$ 333.2537, 333.2604 found. **IR** (neat, cm^{-1}) 2929, 2872, 1640, 2592, 1430, 1301, 1172.

2-(2,6-dimethylphenyl)-6-ethyl-4-(nonyloxy)pyridine (3–31)

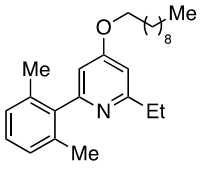

The title product was prepared according to the general procedure inside an N_2 filled glovebox. A 4.0 mL oven-dried vial (ThermoFisher, C4015-1) was charged with a magnetic stir bar and 3-bromo-6-(2,6-dimethylphenyl)-2-ethylpyridine (72.3 mg, 0.25 mmol, 1.0 equiv). The vial was then brought into a N_2 filled glovebox and charged with 1-decanol (39.6 mg, 0.25 mmol, 1.0 equiv), DMAc (1.5 mL, 0.17 M), KBr (14.9 mg, 0.125 mmol, 0.5 equiv), 18-crown-6 (231.3 mg, 0.875 mmol, 3.5 equiv), and KOH (42.1 mg, 0.75 mmol, 3.0 equiv) in that respective order. The vial was sealed with a PTFE-lined screw cap (ThermoFisher, C4015-1A), removed from the glovebox, and placed into a preheated 80 °C aluminum reaction block and stirred for 15 h. The solution was allowed to cool to rt and then loaded directly onto a silica gel column and eluted (1% acetone/hexanes to 2% acetone/hexanes) to yield the purified title compound as a clear oil (51.9 mg, 57% yield, >10:1 selectivity). **^{1}H NMR** (400 MHz, $CDCl_3$) δ 7.16 (m, 1H), 7.08 (m, 2H), 6.66 (d, J = 2.3 Hz, 1H), 6.57 (d, J = 2.3 Hz, 1H), 4.00 (t, J = 6.6 Hz, 2H), 2.81 (q, J = 7.6 Hz, 2H), 2.08 (s, 6H), 1.80 (m, 2H), 1.46 (m, 2H), 1.22-1.38 (m, 13H), 0.89 (m, 3H). **^{13}C NMR** (101 MHz, $CDCl_3$) δ 166.3, 165.4, 161.0, 141.3, 136.1, 127.9, 127.8, 108.0, 106.8, 68.2, 32.2, 32.1, 29.9, 29.7, 29.6, 29.3, 26.3, 23.0, 20.5, 14.8, 14.4. **HRMS** (DART) $[M+H]^+$ calcd. for $[C_{25}H_{38}NO]^+$ 368.2948, 368.2987 found. **IR** (neat, cm^{-1}) 2923, 2854, 1589, 1347, 1172, 1037.

***tert*-butyl 2-(4-((2-ethylhexyl)oxy)pyridin-2-yl)pyrrolidine-1-carboxylate (3–32)**

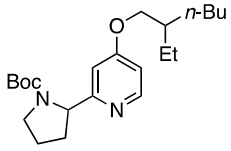

The title product was prepared according to the general procedure using *tert*-butyl 2-(5-bromopyridin-2-yl)pyrrolidine-1-carboxylate (326.1 mg, 1.0 mmol,

1.0 equiv) and 2-ethyl-1-hexanol (130.2 mg, 1.0 mmol, 1.0 equiv). Silica gel chromatography (40% EtOAc/hexanes) yielded the title compound as a clear oil (204.3 mg, 54% yield, >10:1 selectivity). **^{1}H NMR** (400 MHz, $CDCl_3$) Note: broad signals are observed; δ 8.32 (d, J = 5.6 Hz, 1H), 6.58-6.70 (m, 2H), 4.87 (m, 1H), 3.84 (m, 2H), 3.43-3.70 (m, 2H), 2.32 (m, 1H), 2.01 (m, 1H), 1.79-1.93 (m, 2H), 1.70 (m, 1H), 1.35-1.55 (m, 7H), 1.26-1.34 (m, 4H), 1.17-1.26 (m, 6H), 0.85-0.96 (m, 6H). **^{13}C NMR** (101 MHz, CD_3OD) (mixture of rotamers) δ 168.9, 167.3, 166.3, 157.1, 157.0, 151.9, 151.8, 110.7, 108.9, 108.7, 82.0, 81.8, 72.4, 64.8, 64.2, 49.1, 41.3, 36.2, 35.2, 32.4, 31.0, 29.6, 29.3, 25.8, 25.7, 25.5, 25.1, 24.9, 15.3, 12.3. **HRMS** (DART) $[M+H]^+$ calcd. for $[C_{22}H_{37}N_2O_3]^+$ 377.2799, 377.2893 found. **IR** (neat, cm^{-1}) 2960, 2929, 1693, 1594, 1389, 1162, 1114.

4-(1-cyclopropylethoxy)-2-(2-phenyl-1,3-dioxolan-2-yl)pyridine (3–33)

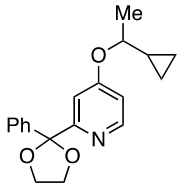

The title product was prepared according to the general procedure using 5-bromo-2-(2-phenyl-1,3-dioxolan-2-yl)pyridine (305.0 mg, 1.0 mmol, 1.0 equiv) and 1-cyclopropylethanol (86.1 mg, 1.0 mmol, 1.0 equiv). Silica gel chromatography (40% EtOAc/hexanes) yielded the title compound as a white solid (181.1 mg, 58% yield, approximately 6:1 selectivity). **Melting Point**: 69 °C – 72 °C. **^{1}H NMR** (400 MHz, $CDCl_3$) δ 8.39 (d, J = 5.7 Hz, 1H), 7.62 (m, 2H), 7.25-7.37 (m, 3H), 7.15 (d, J = 2.5 Hz, 1H), 6.63 (dd, J = 2.5 Hz, 5.7 Hz, 1H), 4.10 (m, 4H), 3.96 (m, 1H), 1.36 (d, J = 6.1 Hz, 3H), 1.12 (m, 1H), 0.58 (m, 2H), 0.39 (m, 1H), 0.30 (m, 1H). **^{13}C NMR** (101 MHz, $CDCl_3$) δ 165.2, 162.3, 151.2, 141.5, 128.4, 128.4, 126.4, 110.2, 108.9, 108.2, 77.8, 65.5, 19.4, 16.8, 3.9, 2.5. **HRMS** (DART) $[M+H]^+$ calcd. for $[C_{19}H_{22}NO_3]^+$ 312.1594, 312.1674 found. **IR** (neat, cm^{-1}) 2973, 2884, 1595, 1561, 1470, 1301, 1072.

***tert*-butyl 2-(4-(5-bromoindolin-1-yl)pyridin-2-yl)pyrrolidine-1-carboxylate (3–39)**

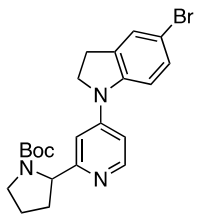

The title product was prepared according to the general procedure using *tert*-butyl 2-(5-bromopyridin-2-yl)pyrrolidine-1-carboxylate (326.1 mg, 1.0 mmol, 1.0 equiv) and 5-bromoindoline (198.1 mg, 1.0 mmol, 1.0 equiv). Silica gel chromatography (40% EtOAc/hexanes – 100% EtOAc) yielded the title compound as a brown oil (220.8 mg, 50% yield, >10:1 selectivity). **^{1}H NMR** (400 MHz, $CDCl_3$) Note: broad signals are observed; δ 8.33 (d, J = 5.6 Hz, 1H), 7.08-7.32 (m, 3H), δ 6.71-7.00 (m, 2H), δ 4.90 (m, 1H), δ 3.88-4.06 (m, 2H), δ 3.44-3.71 (m, 2H), 3.13 (m, 2H), 2.33 (m, 1H), 1.96-2.18 (m, 1H), 1.79-1.95 (m, 2H), 1.47 (s, 4H), 1.24 (s, 5H). **^{13}C NMR** (101 MHz, $CDCl_3$) (mixture of rotamers) δ 164.9, 163.3, 155.0, 154.9, 150.2, 150.0, 144.0, 134.8, 130.2, 130.2, 128.7, 128.6, 113.1, 112.8, 111.9, 111.8, 108.8, 108.6, 106.8, 106.1, 79.6, 63.2, 62.5, 51.5, 47.8, 47.4, 34.4, 33.1, 28.8, 28., 27.9, 24.1, 23.5. **HRMS** (DART) $[M+H]^+$ calcd. for $[C_{22}H_{27}BrN_3O_2]^+$ 444.1281 and , 444.1376 found. **IR** (neat, cm^{-1}) 2973, 2875, 1686, 1584, 1485, 1388, 1158.

2-methyl-1-(2-(2-phenyl-1,3-dioxolan-2-yl)pyridin-4-yl)indoline (3–40)

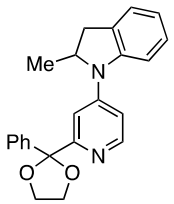

The title product was prepared according to the general procedure using 5-bromo-2-(2-phenyl-1,3-dioxolan-2-yl)pyridine (305.0 mg, 1.0 mmol, 1.0 equiv) and 2-methylindoline (133.1 mg, 1.0 mmol, 1.0 equiv). Silica gel chromatography (40% EtOAc/hexanes – 100% EtOAc) yielded the title compound as a light yellow oil (184.8 mg, 52% yield, >10:1 selectivity). **^{1}H NMR** (400 MHz, $CDCl_3$) δ 8.38 (d, J = 5.8 Hz, 1H), 7.64-7.67 (m, 2H), 7.46 (d, J = 2.4 Hz, 1H), 7.14-7.38 (m, 6H), 6.93 (dd, J = 2.4 Hz, 5.8 Hz, 1H), 6.90 (td, J = 1.0 Hz, 7.4 Hz, 1H), 4.45 (m, 1H), 4.12 (m, 4H), 3.39 (dd, J = 8.8 Hz, 15.3 Hz, 1H), 2.63 (dd, J =

2.6 Hz, 15.3 Hz, 1H), 1.32 (d, J = 6.3 Hz, 3H). **^{13}C NMR** (101 MHz, d_6-DMSO) δ 160.7, 150.0, 148.8, 142.7, 141.6, 131.5, 127.8, 127.7, 127.1, 126.1, 125.9, 121.4, 111.7, 108.9, 108.2, 105.3, 64.8, 58.1, 35.8, 19.4. **HRMS** (DART) $[M+H]^+$ calcd. for $[C_{16}H_{22}NO]^+$ 359.1754, 359.1841 found. **IR** (neat, cm^{-1}) 2969, 2888, 1583, 1485, 1390, 1087, 989.

1-(2-(8-methoxy-1,4-dioxaspiro[4.5]decan-8-yl)pyridin-4-yl)indoline (3–41)

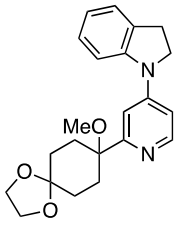

The title product was prepared according to the general procedure using 5-bromo-2-(8-methoxy-1,4-dioxaspiro[4.5]decan-8-yl)pyridine (327.0 mg, 1.0 mmol, 1.0 equiv) and indoline (141.8 mg, 1.2 mmol, 1.2 equiv). Silica gel chromatography (40% EtOAc/hexanes to 60% EtOAc/hexanes) yielded the title compound as a light brown solid (245.5 mg, 67% yield, approximately 9:1 selectivity). **Melting Point**: 113 °C – 115 °C. **^{1}H NMR** (400 MHz, $CDCl_3$) δ 8.38 (d, J = 5.8 Hz, 1H), 7.32 (d, J = 8.0 Hz, 1H), 7.28 (d, J = 2.4 Hz, 1H), 7.21 (m, 1H), 7.15 (m, 1H), 6.94 (dd, J = 5.8 Hz, 2.4 Hz, 1H), 6.87 (m, 1H), 3.94-4.02 (m, 6H), 3.12-3.19 (m, 5H), 2.26 (td, J = 13.5 Hz, 4.3 Hz, 2H), 1.92-2.10 (m, 4H), 1.69 (m, 2H). **^{13}C NMR** (101 MHz, $CDCl_3$) δ 164.9, 150.4, 149.7, 144.9, 132.5, 127.6, 125.7, 121.2, 110.8, 109.2, 108.8, 107.0, 79.1, 64.7, 64.5, 51.4, 50.9, 32.1, 30.8, 28.2. **HRMS** (DART) $[M+H]^+$ calcd. for $[C_{22}H_{27}N_2O_3]^+$ 367.2016, 367.2111 found. **IR** (neat, cm^{-1}) 2945, 2884, 1583, 1487, 1108, 1065, 941.

2-(2-phenyl-1,3-dioxolan-2-yl)pyridin-4(1*H*)-one (3–44)

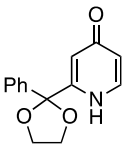

The title product was prepared according to the general procedure inside a N_2 filled glovebox. An oven-dried 4 mL vial (ThermoFisher, C4015-1) was charged with a magnetic stir bar, 5-bromo-2-(2-phenyl-1,3-dioxolan-2-yl)pyridine (76.5 mg, 0.25 mmol, 1.0 equiv), and *N*,*N*-dibenzyl-3-hydroxypropanamide (67.3 mg, 0.25 mmol, 1.0 equiv and

brought into a N_2 filled glovebox. DMAc (1.5 mL, 0.17 M), KBr (14.9 mg, 0.125 mmol, 0.5 equiv), 18-crown-6 (231.3 mg, 0.875 mmol, 3.5 equiv), and KOH (42.1 mg, 0.75 mmol, 3.0 equiv) was then added in successive order. The reaction vial was sealed with a PTFE-lined screw cap (ThermoFisher, C4015-1A), removed from the glovebox and placed into a preheated 80 °C aluminum reaction block. The crude reaction solution was cooled to rt and directly loaded onto a silica gel column that had been neutralized with NEt_3 and eluted on a gradient (1% MeOH/CH_2Cl_2 to 5% MeOH/CH_2Cl_2) to yield the title compound as a light yellow solid (30.1 mg, 0.124 mmol 50% yield, >10:1 selectivity). **Melting Point**: 213 °C – 217 °C. **^{1}H NMR** (400 MHz, CD_3OD) δ 7.75 (d, J = 7.2 Hz, 1H), 7.56 (m, 2H), 7.38-7.45 (m, 3H), 6.54 (d, J = 2.6 Hz, 1H), 6.43 (dd, J = 7.2 Hz, 2.6 Hz, 1H), 4.17 (m, 4H). **^{13}C NMR** (CD_3OD, 101 MHz) δ 182.5, 154.0, 140.6, 140.5, 130.8, 130.1, 127.6, 117.6, 116.0, 108.0, 67.3. **HRMS** (DART) $[M+H]^+$ calcd. for $[C_{14}H_{14}NO_3]^+$ 244.0968, 244.1028 found. **IR** (neat, cm^{-1}) 2894, 1628, 1519, 1215, 1072, 989.

A2.7 Convergence of 3- and 5-Bromopyridine Isomers

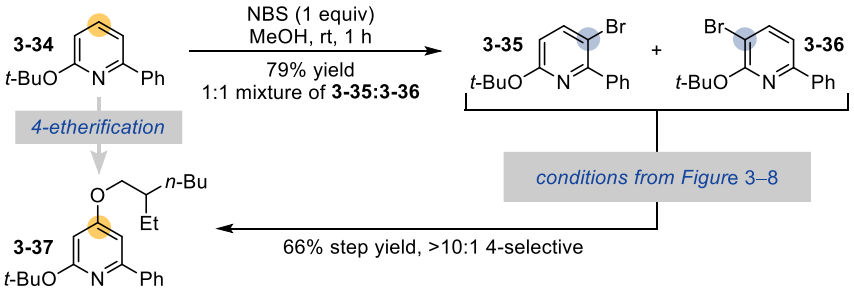

3-bromo-6-(*tert*-butoxy)-2-phenylpyridine (3–35) and 3-bromo-2-(*tert*-butoxy)-6-phenylpyridine (3–36) mixture: Inside a N_2 filled glovebox, an oven-dried 100 mL round bottom flask was charged with 2-(*tert*-butoxy)-6-phenylpyridine (1.32 g, 5.8 mmol, 1.0 equiv) and anhydrous MeOH (20.0 mL, 0.29 M). *N*-Bromosuccinimide (1.03 g, 5.8 mmol, 1.0 equiv) was then added slowly portionwise. The flask was sealed with a red septum (VWR, Cat. No. 89097-

544) and the edges of the septum were sealed with Parafilm®. The flask was removed from the glovebox, put under positive pressure with an N_2 balloon, and stirred at rt for one hour. The reaction solution was then poured into H_2O (70 mL) in a separatory funnel and the product was extracted with EtOAc (3 x 60 mL). The organic layer was dried over Na_2SO_4. The Na_2SO_4 was filtered off and the organic layer was concentrated *in vacuo*. Silica gel chromatography (1% EtOAc/hexanes) yielded the title compounds as a 1.1:1 mixture of isomers (1.39 g, 79% yield). **Melting Point**: 37 °C – 39 °C. **^{1}H NMR** (400 MHz, $CDCl_3$) *mixture of regioisomers δ 7.98 (both isomers) (m, 2H), 7.82 (single isomer) (d, J = 8.0 Hz, 1H), 7.39-7.75 (both isomers) (m, 10H), 7.20 (single isomer) (d, J = 8.0 Hz, 1H), 6.51 (single isomer) (d, J = 8.6 Hz, 1H), 1.71 (s, 9H), 1.59 (s, 9H). **^{13}C NMR** (101 MHz, $CDCl_3$) *mixture of 3- and 5-bromoregioisomers δ 162.5, 159.5, 154.3, 153.5, 143.8, 142.3, 140.1, 138.8, 129.8, 129.3, 129.1, 128.7, 128.0, 126.9, 113.6, 113.6, 109.8, 107.8, 81.6, 80.6, 29.0, 28.9. **HRMS** (DART) $[M+H]^+$ calcd. for $[C_{15}H_{17}BrNO]^+$ 306.0488, 306.0555 found. **IR** (neat, cm^{-1}) 2968, 2360, 1566, 1424, 1322, 1164, 1120.

Note: Provided below are ^{1}H and ^{13}C NMR spectra of the obtained brominated mixture.

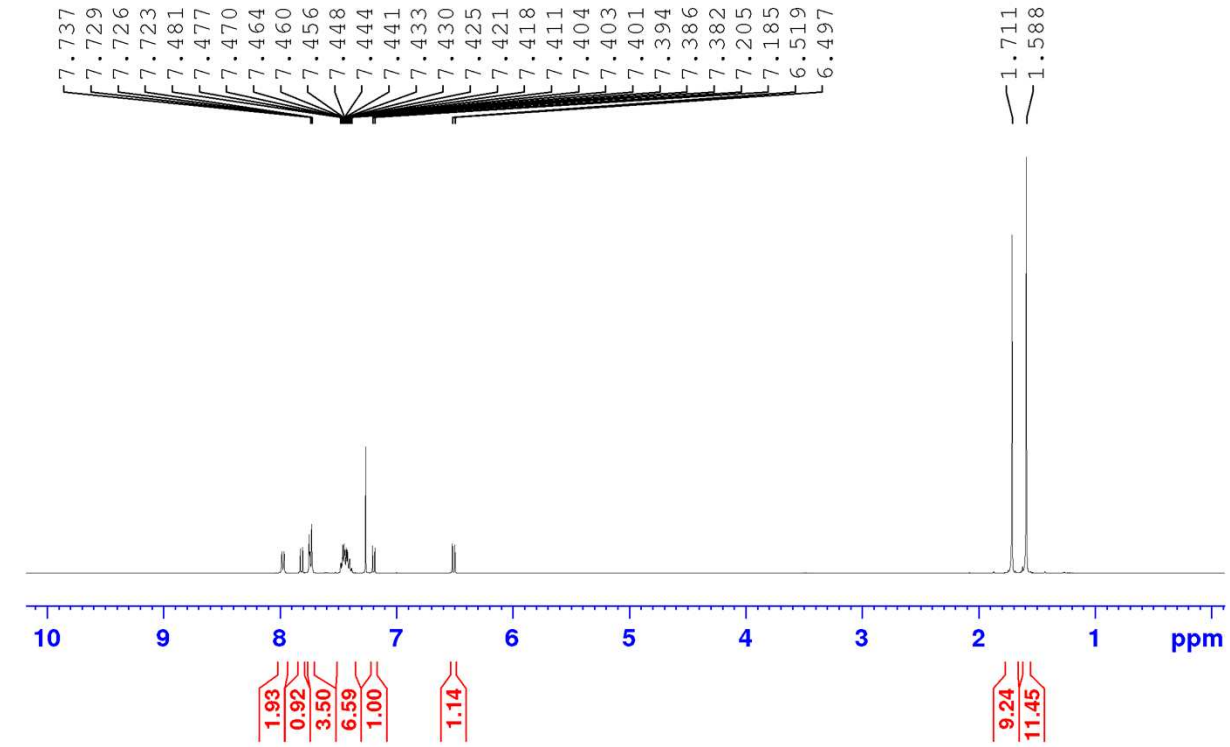

Figure A2–29: ^{1}H NMR spectrum (400 MHz, $CDCl_3$) of the purified 1.1:1 mixture of **3–35** and **3–36**.

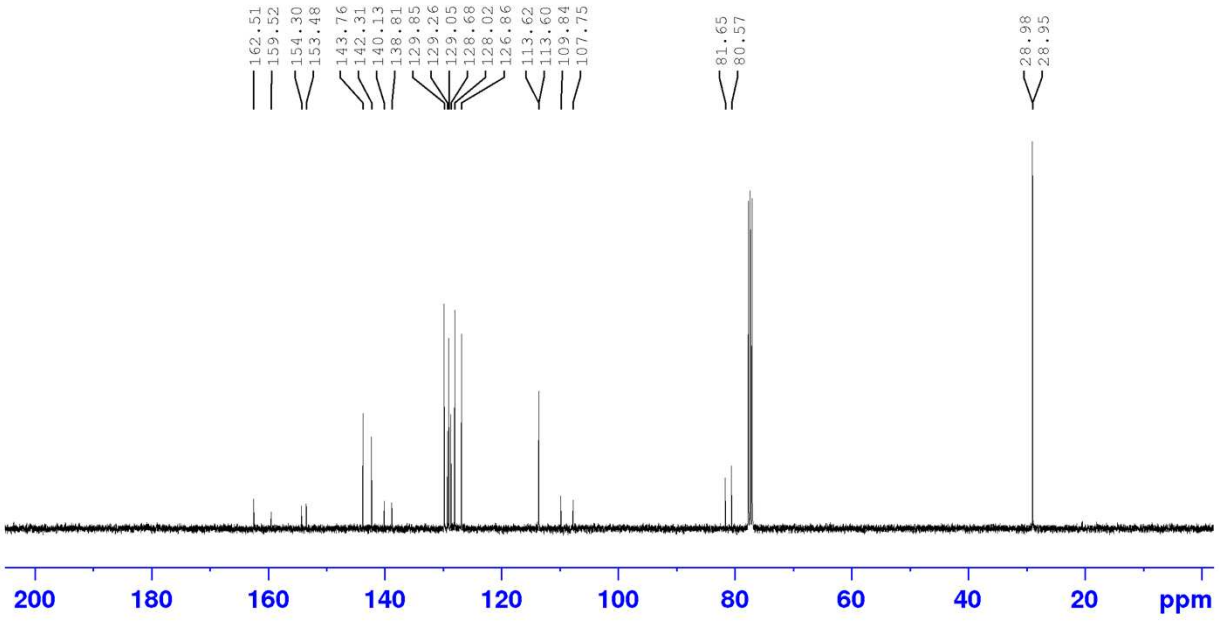

Figure A2–30: ^{13}C NMR spectrum (101 MHz, $CDCl_3$) of the purified 1.1:1 mixture of **3–35** and **3–36**.

2-(*tert*-butoxy)-4-((2-ethylhexyl)oxy)-6-phenylpyridine (3–37)

Procedure: Inside a N_2 filled glovebox, an oven-dried 25 mL round bottom flask was charged with a magnetic stir bar, a 1.1:1 mixture of 3-bromo-2-(*tert*-butoxy)-6-phenylpyridine and 3-bromo-6-(*tert*-butoxy)-2-phenylpyridine (152.5 mg, 0.5 mmol, 1.0 equiv), 2-ethyl-1-hexanol (65.1 mg, 0.5 mmol, 1.0 equiv), DMAc (5.0 mL, 0.10 M), KBr (29.8 mg, 0.25 mmol, 0.5 equiv), 18-crown-6 (594.7 mg, 2.25 mmol, 4.5 equiv), and KOH (98.2 mg, 1.75 mmol, 3.5 equiv) in successive order. The flask was sealed with a Fisherbrand® red septum stopper (Cat. No. FB57875) and the edges of the septum were then sealed with Parafilm®. The flask was then removed from the glovebox, put under positive pressure with N_2 on a Schlenk line, and placed into a preheated 80 °C silicon oil bath. The solution was stirred at 80 °C for 15 h and then allowed to cool to rt. The selectivity was determined according to the general procedure in Section A2.5. The solution was poured into a separatory funnel containing water (50 mL). The product was then extracted with EtOAc (3 x 50 mL). The organic layer was dried over Na_2SO_4. The Na_2SO_4 was then filtered and the solution was concentrated *in vacuo*. Silica gel chromatography (1% EtOAc/hexanes to 2% EtOAc/hexanes) yielded the title compound as a clear oil (117.6 mg, 66% yield, >10:1 selectivity). **^{1}H NMR** (400 MHz, $CDCl_3$) δ 8.00 (m, 2H), 7.45 (m, 2H), 7.38 (m, 1H), 6.92 (d, J = 1.9 Hz, 1H), 6.11 (d, J = 1.9 Hz, 1H), 3.89 (m, 2H), 1.75 (m, 1H), 1.68 (s, 9H), 1.38-1.57 (m, 4H), 1.29-1.37 (m, 4H), 0.88-0.98 (m, 6H). **^{13}C NMR** (101 MHz, $CDCl_3$) δ 168.4, 165.5, 155.3, 139.8, 128.9, 128.8, 127.0, 102.7, 95.4, 79.8, 70.7, 39.5, 30.8, 29.4, 29.2, 24.2, 23.4, 14.4, 11.4. **HRMS** (DART) $[M+H]^+$ calcd. for $[C_{23}H_{34}NO_2]^+$ 356.2584, 356.2668 found. **IR** (neat, cm^{-1}) 2960, 2928, 1596, 1571, 1418, 1151.

A2.8 Preparative scale 4-selective amination of 3-bromopyridine

1-(pyridin-4-yl)indoline (3–38)

Procedure: An oven-dried 250 mL round bottom flask was charged with a magnetic stir bar, 18-crown-6 (12.30 g, 46.6 mmol, 3.5 equiv), KBr (797.4 mg, 6.7 mmol, 0.5 equiv), and KOH (2.24 g, 39.9 mmol, 3.0 equiv). The flask was sealed with a Fisherbrand® red septum stopper (Cat. No. FB57875) and the edges of the septum were then sealed with Parafilm®. The flask was evacuated and backfilled three times with N_2 and then left under positive pressure of N_2 on a Schlenk line. DMAc (68 mL) was then added and the solution was stirred at rt (***Note***: there are some insoluble salts remaining at the bottom of the flask). 3-Bromopyridine (3.16 g, 20.0 mmol, 1.5 equiv) and indoline (1.59 g, 13.3 mmol, 1.0 equiv) were then measured into a 20 mL scintillation vial and constituted in 10 mL of DMAc and sparged with N_2 for 5 min. This solution was then added dropwise via syringe to the 250 mL round bottom flask. The reaction solution was then placed into a preheated 80 °C silicon oil bath and stirred for 15 h. The solution was cooled to rt and 1,3,5-trimethoxybenzene internal standard was added and the 4-selectivity was determined using the general procedure described in Section A2.5. The solution was then poured into a separatory funnel with H_2O (700 mL) and the product was extracted with EtOAc (3 x 250 mL). The organic layers were then pooled and poured back into the separatory funnel and washed with H_2O (1 x 200 mL) and brine (1 x 100 mL). The organic layer was then dried over Na_2SO_4. The Na_2SO_4 was filtered off and the organic layer was concentrated *in vacuo*. Purification by silica gel chromatography (50% EtOAc/hexanes to 100% EtOAc to 5% MeOH/CH_2Cl_2 to 10% MeOH/ CH_2Cl_2) yielded the title compound as a brown solid (1.60 g, 8.2 mmol, 62% yield, >10:1 selectivity). **Melting Point**: 71 °C – 76 °C. **^{1}H NMR** (400 MHz, $CDCl_3$) δ 8.39 (m, 2H), 7.33 (d, J = 8.0 Hz, 1H), 7.22 (dd, J = 0.6 Hz, 7.3 Hz, 1H), 7.15 (m, 1H), 7.03 (m, 2H), 6.89 (td, J = 0.6 Hz, 7.4 Hz, 1H), 4.00 (t, J =

8.4 Hz, 2H), 3.18 (t, J = 8.4 Hz, 2H). **^{13}C NMR** (101 MHz, $CDCl_3$) δ 150.5, 149.8, 144.7, 132.6, 127.5, 125.8, 121.5, 111.0, 110.5, 51.3, 28.2. **HRMS** (DART) $[M+H]^+$ calcd. for $[C_{13}H_{13}N_2]^+$ 197.1073, 197.1083 found. **IR** (neat, cm^{-1}) 3025, 2945, 1581, 1504, 1392, 1222.

A2.9 Preparation of 3- or 5-bromopyridine starting materials

(a) Preparation of simple 3-bromopyridine substrates

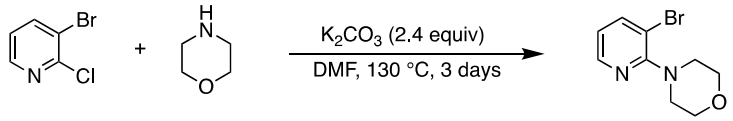

1.0 equiv 2.0 equiv 75% yield

4-(3-bromopyridin-2-yl)morpholine: Title compound was prepared according to a reported procedure.[2] Spectroscopic characterization is consistent with a previous report.[2] **^{1}H NMR** (400 MHz, $CDCl_3$) δ 8.25 (dd, J = 1.6 Hz, 4.7 Hz, 1H), 7.80 (dd, J = 1.6 Hz, 7.7 Hz, 1H), 6.80 (dd, J = 4.7 Hz, 7.7 Hz, 1H), 3.87 (m, 4H), 3.35 (m, 4H).

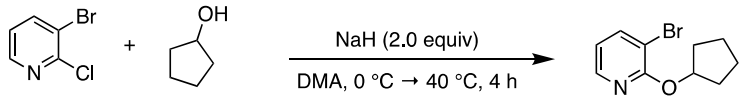

1.0 equiv 1.5 equiv 93% yield

3-bromo-2-(cyclopentyloxy)pyridine: NaH (60% dispersion, 800 mg, 20.0 mmol, 2.0 equiv) was weighed into an oven-dried 100 mL round bottom flask. The flask was sealed with a septum stopper (VWR, Cat. No. 89097-544). The flask was evacuated and backfilled three times with N_2 and then left under positive pressure with a N_2 balloon. The flask was cooled to 0 °C, and then DMAc (20 mL) was added. Cyclopentanol (1.29 g, 15.0 mmol, 1.5 equiv) was then added dropwise to the slurry. The solution was allowed to stir at 0 °C for 10 min, then 3-bromo-2-chloropyridine (1.92g, 10.0 mmol, 1.0 equiv) constituted in DMAc (20 mL) was added dropwise. Upon completion of the addition, the solution was allowed to warm to rt and was then placed into a 40

°C preheated silicon oil bath. The solution was stirred at 40 °C for 4 h. The solution was then allowed to cool to rt and was quenched dropwise with H_2O (ca. 1.0 mL). The mixture was then poured into H_2O (100 mL) in a separatory funnel and the product was extracted with EtOAc (3 x 80 mL). The organic layers were dried over Na_2SO_4. The Na_2SO_4 was filtered off and the organic layer was concentrated *in vacuo*. Purification of the resultant residue by silica gel chromatography (5% EtOAc/hexanes) yielded the title compound as a clear oil (2.23 g, 9.3 mmol, 93% yield). **^{1}H NMR** (400 MHz, $CDCl_3$) δ 8.07 (dd, J = 1.7 Hz, 4.9 Hz, 1H), 7.77 (dd, J = 1.7 Hz, 7.6 Hz, 1H), 6.72 (dd, J = 4.9 Hz, 7.6 Hz, 1H), 5.45 (m, 1H), 1.90-2.04 (m, 2H), 1.77-1.90 (m, 4H), 1.59-1.70 (m, 2H). **^{13}C NMR** (101 MHz, $CDCl_3$) δ 160.1, 145.8, 141.8, 117.5, 108.2, 79.5, 33.1, 24.2. **HRMS** (DART) $[M+H]^+$ calcd. for $[C_{10}H_{13}BrNO]^+$ 242.0175, 242.0194 found. **IR** (neat, cm^{-1}) 2960, 2871, 1580, 1430, 1296, 1025, 971.

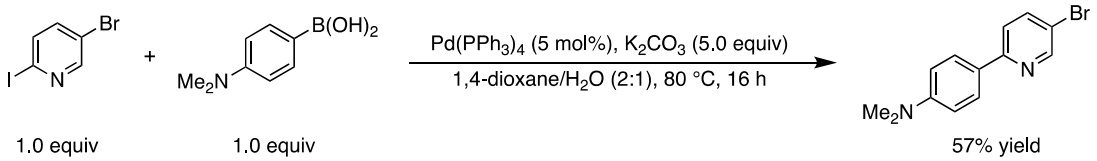

4-(5-bromopyridin-2-yl)-*N*,*N*-dimethylaniline: Inside a N_2 filled glovebox, an oven-dried 100 mL round bottom flask was charged with a magnetic stir bar, 5-bromo-2-iodopyridine (851.7 mg, 3.0 mmol, 1.0 equiv), 4-(*N,N*-dimethylamino)phenylboronic acid (495.0 mg, 3.0 mmol, 1.0 equiv), 1,4-dioxane (13 mL), tetrakis(triphenylphosphine)palladium(0) (173.3 mg, 0.15 mmol, 0.05 equiv), and K_2CO_3 (1.50 g, 15.0 mmol, 5.0 equiv). The flask was sealed with a red septum (VWR, Cat. No. 89097-544) and removed from the glovebox. The system was put under positive pressure with a N_2 balloon, then H_2O (7 mL) was then added via syringe. The flask was then placed into a preheated 80 °C silicon oil bath and stirred for 16 h. The solution was then allowed to cool to rt and was poured into a separatory funnel containing H_2O (70 mL). The product was extracted with

EtOAc (3 x 60 mL). The organic layers were dried over Na_2SO_4. The Na_2SO_4 was filtered out and the organic layer was concentrated *in vacuo*. Silica gel chromatography (3% EtOAc/hexanes to 10% EtOAc/hexanes) yielded the title compound as a light yellow powder (470.6 mg, 1.7 mmol, 57% yield). **Melting Point**: 150 °C – 152 °C. **^{1}H NMR** (400 MHz, $CDCl_3$) δ 8.64 (d, J = 2.4 Hz, 1H), 7.88 (d, J = 9.0 Hz, 2H), 7.76 (dd, J = 2.4 Hz, 8.6 Hz, 1H), 7.53 (d, J = 8.6 Hz, 1H), 6.78 (d, J = 9.0 Hz, 2H), 3.02 (s, 6H). **^{13}C NMR** (101 MHz, $CDCl_3$) δ 156.4, 151.6, 150.6, 139.3, 128.0, 126.2, 120.5, 117.6, 112.5, 40.6. **HRMS** (DART) $[M+H]^+$ calcd. for $[C_{13}H_{14}BrN_2]^+$ 277.0335, 277.0407 found. **IR** (neat, cm^{-1}) 2799, 2360, 2342, 1606, 1454, 1325, 1091.

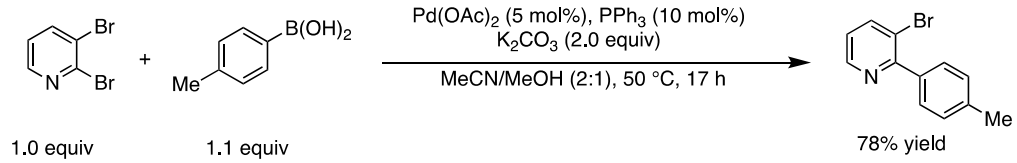

3-bromo-2-(*p*-tolyl)pyridine: Inside a N_2 filled glovebox, an oven-dried 100 mL round bottom flask was charged with a magnetic stir bar, 2,3-dibromopyridine (947.6 mg, 4.0 mmol, 1.0 equiv), *p*-tolylboronic acid (598.2 mg, 4.4 mmol, 1.1 equiv), anhydrous MeCN/MeOH (2:1, 50 mL), palladium(II) acetate (44.9 mg, 0.20 mmol, 0.05 equiv), triphenylphosphine (104.9 mg, 0.4 mmol, 0.1 equiv), and K_2CO_3 (800.9 mg, 8.0 mmol, 2.0 equiv). The flask was sealed with a red septum (VWR, Cat. No. 89097-544) and removed from the glovebox. The system was put under positive pressure with a N_2 balloon and then placed into a preheated 50 °C silicon oil bath and stirred for 17 h. The solution was then allowed to cool to rt and was poured into a separatory funnel containing H_2O (70 mL). The product was extracted with EtOAc (3 x 60 mL). The organic layers were dried over Na_2SO_4. The Na_2SO_4 was filtered out and the organic layer was concentrated *in vacuo*. Silica gel chromatography (8% EtOAc/hexanes) yielded the title compound as a clear oil (774.2 mg, 3.1 mmol, 78% yield). Spectroscopic characterization matches that of reported literature.[3] **^{1}H NMR**

(400 MHz, $CDCl_3$) δ 8.62 (d, J = 4.6 Hz, 1H), 7.98 (d, J = 8.0 Hz, 1H), 7.60 (d, J = 8.0 Hz, 2H), 7.28 (d, J = 8.0 Hz, 2H), 7.13 (dd, J = 4.6 Hz, 8.0 Hz, 1H), 2.43 (s, 3H).

(b) Preparation of 3-bromopyridines where corresponding 4-halopyridine is less available

Note on the commercial availability of 3-bromopyridines vs. 4-halopyridines: For the substrates below, the 3-bromopyridine derivative is more readily available and/or cheaper than a corresponding 4-halogenated derivative. For these substrates, a comparison of the cheapest price for 1 gram of both the 3-bromopyridine and a 4-halopyridine (as reported in the online www.emolecules.com database accessed March 2, 2020) starting material is provided in Figure A2–31 below. The obtained estimated times of delivery are also included. The comparison is meant to provide a general idea of the relative cost and availability of these substrates compared to their 4-halogenated or 4-hydroxylated derivatives.

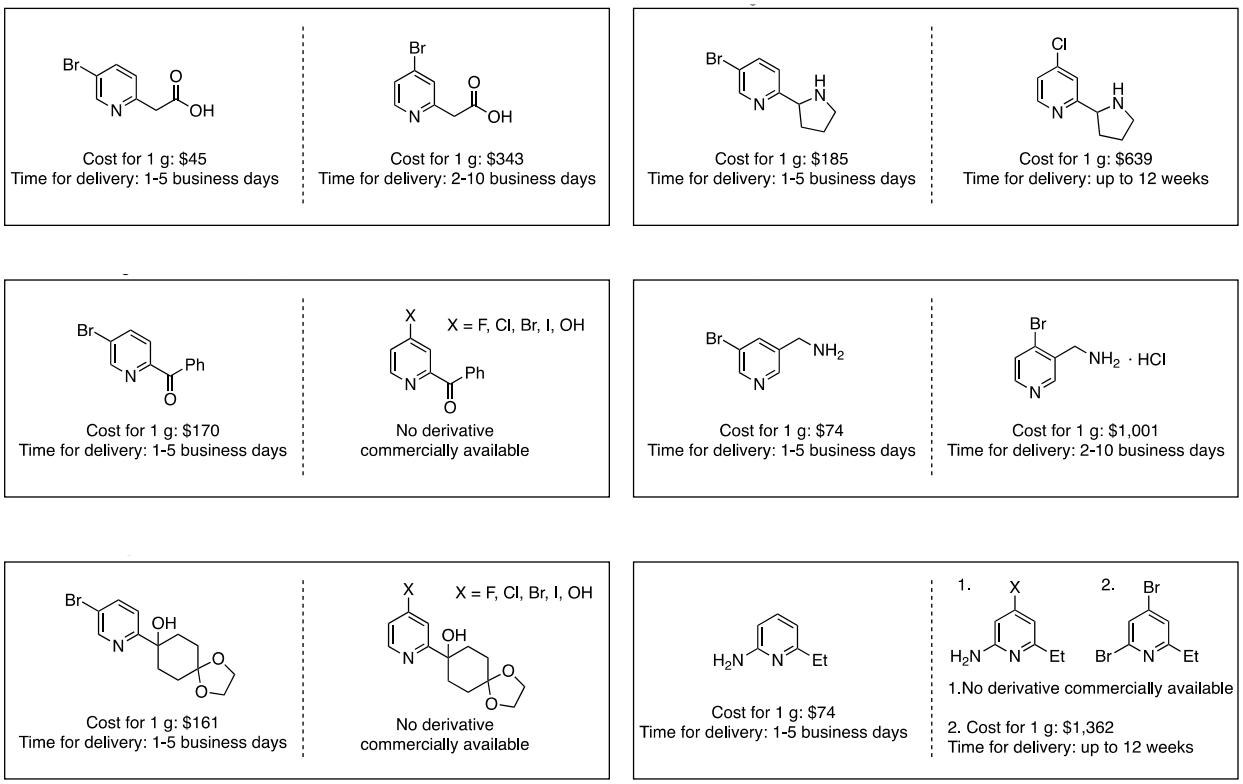

Figure A2–31: Comparison of commercially available 3-bromopyridine starting materials compared to corresponding 4-halogenated or 4-hydroxylated starting materials.

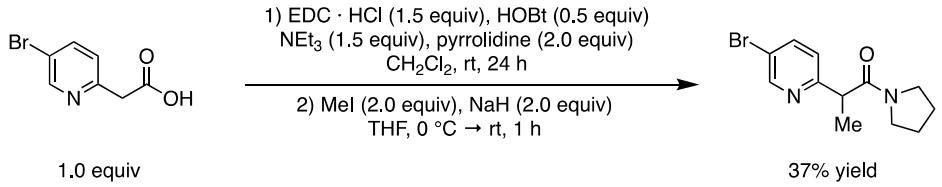

2-(5-bromopyridin-2-yl)-1-(pyrrolidin-1-yl)propan-1-one: A 250 mL round bottom flask was charged with a magnetic stir bar, *N*-(3-dimethylaminopropyl)-*N*'-ethylcarbodiimide hydrochloride (1.34 g, 7.0 mmol, 1.5 equiv), 1-hydroxybenzotriazole hydrate (310.8 mg, 2.3 mmol, 0.5 equiv), anhydrous CH_2Cl_2 (30 mL, 0.16 M), triethylamine (1.0 mL, 7.0 mmol, 1.5 equiv), 2-(5-bromopyridin-2-yl)acetic acid (1.0 g, 4.7 mmol, 1.0 equiv), and pyrrolidine (0.8 mL, 9.3 mmol, 2.0 equiv) in successive order. The solution was stirred at rt for 24 h, and then diluted with CH_2Cl_2 (50 mL). The solution was then washed with saturated aqueous NH_4Cl (1 x 50 mL), H_2O (1 x 50

mL), and brine (1 x 30 mL). The organic layer was dried over Na_2SO_4. The Na_2SO_4 was filtered out and the organic layer was concentrated *in vacuo*. Silica gel chromatography (100% CH_2Cl_2 to 5% MeOH/CH_2Cl_2) yielded 2-(5-bromopyridin-2-yl)-1-(pyrrolidin-1-yl)ethan-1-one as a yellow solid (560.0 mg, 2.1 mmol, 44% yield). **^{1}H NMR** (400 MHz, $CDCl_3$) δ 8.57 (d, J = 2.4 Hz, 1H), 7.76 (dd, J = 2.4 Hz, 8.4 Hz, 1H), 7.31 (d, J = 8.4 Hz, 1H), 3.81 (s, 2H), 3.55 (t, J = 6.7 Hz, 2H), 3.48 (t, J = 6.9 Hz, 2H), 1.95 (m, 2H), 1.86 (m, 2H).

2-(5-bromopyridin-2-yl)-1-(pyrrolidin-1-yl)ethan-1-one (560.0 mg, 2.1 mmol, 1.0 equiv) from the previous step was constituted in 5.0 mL of anhydrous THF in a 25 mL round bottom flask. The solution was cooled to 0 °C and NaH (60% dispersion, 168.0 mg, 4.2 mmol, 2.0 equiv) was added slowly. MeI (260 µl, 4.2 mmol, 2.0 equiv) was then added dropwise. The solution was warmed to rt and stirred for 1 h. The reaction solution was quenched slowly with H_2O (ca. 0.2 mL) until the solution ceased evolving H_2 gas. The solution was then loaded directly onto a silica column and eluted with 2% MeOH/CH_2Cl_2 to yield the title compound as an off-white solid (495.8 mg, 1.76 mmol, 84% yield). **Melting Point**: 62 °C – 64 °C. **^{1}H NMR** (400 MHz, $CDCl_3$) δ 8.55 (m, 1H), 7.77 (dd, J = 2.2 Hz, 8.4 Hz, 1H), 7.34 (d, J = 8.4 Hz, 1H), 4.03 (q, J = 7.0 Hz, 1H), 3.51 (m, 2H), 3.40 (m, 2H), 1.75-1.99 (m, 4H), 1.50 (d, J = 7.0 Hz, 3H). **^{13}C NMR** (101 MHz, $CDCl_3$) δ 171.4, 160.3, 150.2, 139.9, 123.4, 119.3, 47.2, 47.0 (minor rot.), 46.4 (major rot.), 26.4 (minor rot.), 24.6 (major rot.), 18.7. **HRMS** (DART) $[M+H]^+$ calcd. for $[C_{12}H_{16}BrN_2O]^+$ 283.0441, 283.0507 found. **IR** (neat, cm^{-1}) 2966, 2360, 2342, 1637, 1421, 1372, 1008.

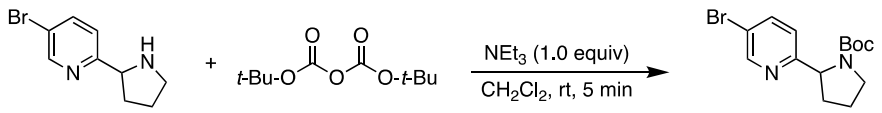

1.0 equiv 2.0 equiv 84% yield

***tert*-butyl 2-(5-bromopyridin-2-yl)pyrrolidine-1-carboxylate** An oven-dried 25 mL round bottom flask was charged with a magnetic stir bar, 5-bromo-2-(pyrrolidin-2-yl)pyridine (500 mg, 2.2 mmol, 1.0 equiv), anhydrous CH_2Cl_2 (4.0 mL), di-*tert*-butyl dicarbonate (960.5 mg, 4.4 mmol, 2.0 equiv), and triethylamine (300 µl, 2.2 mmol, 1.0 equiv) in successive order. The solution was stirred at rt for 5 min and then loaded directly onto silica gel column and eluted (25% EtOAc/hexanes) to afford the title compound as a white solid (603.4 mg, 1.9 mmol, 84% yield). **Melting Point**: 37 °C – 40 °C. **^{1}H NMR** (mixture of rotamers) (400 MHz, $CDCl_3$) δ 8.58 (m, 1H), 7.74 (m, 1H), 7.08 (m, 1H), 4.87 (m, 1H), 3.46-3.68 (m, 2H), 2.34 (m, 1H), 1.81-2.06 (m, 3H), 1.15-1.51 (m, 9H). **^{13}C NMR** (101 MHz, $CDCl_3$) (mixture of rotamers) δ 162.8, 154.7, 150.6, 150.4, 139.3, 139.1, 122.1, 121.5, 118.6, 79.9, 62.6, 62.0, 47.7, 47.4, 34.5, 33.3, 28.8, 28.5, 24.2, 23.5. **HRMS** (DART) $[M+H]^+$ calcd. for $[C_{14}H_{20}BrN_2O_2]^+$ 327.0703, 327.0775 found. **IR** (neat, cm^{-1}) 2974, 2875, 1690, 1463, 1387, 1156, 1113.

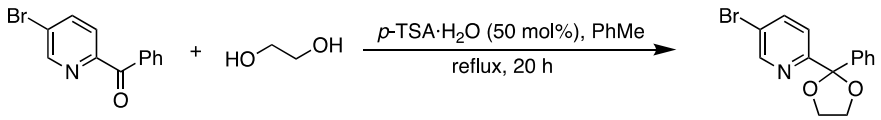

1.0 equiv 30 equiv 68% yield

5-bromo-2-(2-phenyl-1,3-dioxolan-2-yl)pyridine: 5-Bromopyridin-2-yl)(phenyl)methanone (2.13 g, 8.2 mmol, 1.0 equiv) was added to a 100 mL round bottom flask and constituted in anhydrous toluene (25 mL, 0.33 M). *para*-Toluenesulfonic acid monohydrate (779.8 mg, 4.1 mmol, 0.5 equiv) and anhydrous ethylene glycol (14.0 mL, 246 mmol, 30 equiv) were then added. The flask was fitted with a reflux condenser and refluxed for 20 h. The solution was cooled to rt

and then poured into H_2O (80 mL) in a separatory funnel. The product was extracted with EtOAc (3 x 60 mL) and the organic layers were pooled and dried over Na_2SO_4. The Na_2SO_4 was filtered out and the organic layer was concentrated *in vacuo*. Silica gel chromatography yielded the title compound as white crystals (1.69 g, 5.5 mmol, 68% yield). **Melting Point**: 112 °C – 114 °C. **^{1}H NMR** (400 MHz, $CDCl_3$) δ 8.65 (d, J = 2.3 Hz, 1H), 7.80 (dd, J = 2.3 Hz, 8.5 Hz, 1H), 7.55-7.60 (m, 3H), 7.27-7.36 (m, 3H), 4.11 (s, 4H). **^{13}C NMR** (101 MHz, $CDCl_3$) δ 159.3, 150.8, 141.0, 139.5, 128.7, 128.5, 126.3, 122.2, 120.4, 108.7, 65.5. **HRMS** (DART) $[M+H]^+$ calcd. for $[C_{14}H_{13}BrNO_2]^+$ 306.0124, 306.0207 found. **IR** (neat, cm^{-1}) 2993, 2891, 2360, 1571, 1445, 1206, 1091.

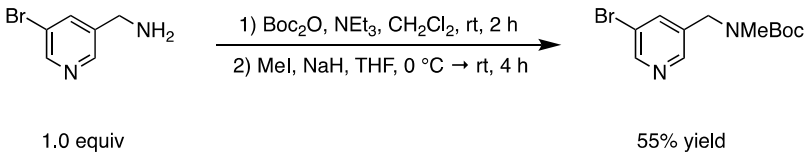

***tert*-butyl ((5-bromopyridin-3-yl)methyl)(methyl)carbamate**: An oven-dried 4 mL vial (ThermoFisher, C4015-1) was charged with a magnetic stir bar, (5-bromopyridin-3-yl)methanamine (187.0 mg, 1.0 mmol, 1.0 equiv), anhydrous CH_2Cl_2 (1.5 mL, 0.67 M), di-*tert*-butyl dicarbonate (261.9 mg, 1.2 mmol, 1.2 equiv), and NEt_3 (210 µl, 1.5 mmol, 1.5 equiv) in successive order. The solution was stirred 2 h at rt. The solution was slowly transferred into H_2O (40 mL) in a separatory funnel and the product was extracted with CH_2Cl_2 (3 x 30 mL). The organic layers were pooled and dried over Na_2SO_4. The Na_2SO_4 was filtered off and the organic layer was concentrated *in vacuo*. Silica gel chromatography (40% EtOAc/hexanes) yielded *tert*-butyl ((5-bromopyridin-3-yl)methyl)carbamate (213.8 mg, 0.75 mmol, 75% yield). **^{1}H NMR** (400 MHz, $CDCl_3$) δ 8.59 (d, J = 2.1 Hz, 1H), 8.46 (m, 1H), 7.79 (m, 1H), 4.92 (s, 1H), 4.32 (s, 2H), 1.47 (s, 9H).

An oven-dried 25 mL round bottom flask was charged with a magnetic stir bar, *tert*-butyl ((5-bromopyridin-3-yl)methyl) (213.8 mg, 0.75 mmol, 1.0 equiv) and anhydrous THF (4.0 mL, 0.19 M). The solution was cooled to 0 °C and then NaH (60% dispersion, 36.0 mg, 0.9 mmol, 1.2 equiv) and iodomethane (51 µl, 0.83 mmol, 1.1 equiv) were added. The reaction solution was warmed to rt and stirred for 4 h. The solution was then slowly quenched with H_2O (ca. 1 mL) and then transferred to a separatory funnel containing H_2O (30 mL). The product was extracted with EtOAc (3 x 30 mL) and the organic layers were pooled and dried over Na_2SO_4. The Na_2SO_4 was filtered out and the organic layer was concentrated *in vacuo*. Silica gel chromatography (30% EtOAc/hexanes) yielded the title compound as an off-white solid (166.2 mg, 0.55 mmol, 77% step yield, 55% overall yield). **Melting Point**: 30 °C – 32 °C. **^{1}H NMR** (400 MHz, $CDCl_3$) δ 8.60 (m 1H), 8.41 (m, 1H), 7.72 (m, 1H), 4.40 (br s, 2H), 2.84 (br s, 3H), 1.47 (br s, 9H). **^{13}C NMR** (101 MHz, $CDCl_3$) 150.2, 147.5, 138.3, 137.9, 135.8, 121.2, 80.7, 50.2, 49.5, 34.6, 28.7. **HRMS** (DART) $[M+H]^+$ calcd. for $[C_{12}H_{18}BrN_2O_2]^+$ 301.0546, 301.0615 found. **IR** (neat, cm^{-1}) 3044, 2972, 1685, 1419, 1387, 1142.

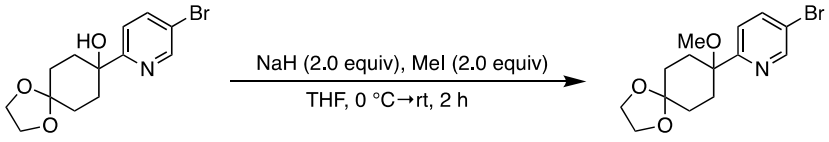

1.0 equiv 92% yield

5-bromo-2-(8-methoxy-1,4-dioxaspiro[4.5]decan-8-yl)pyridine: An oven-dried 50 mL flask was charged with a magnetic stir bar, 8-(5-bromopyridin-2-yl)-1,4-dioxaspiro[4.5]decan-8-ol (2.5 g, 8.0 mmol, 1.0 equiv), and anhydrous THF (16.0 mL, 0.5 M). The solution was cooled to 0 °C and NaH (60% dispersion, 640.0 mg, 16.0 mmol, 2.0 equiv) and iodomethane (1.0 mL, 16.0 mmol, 2.0 equiv) were added slowly. The solution was warmed to rt and stirred for 2 h. The reaction solution was quenched with H_2O (ca. 0.5 mL) and then loaded directly onto a silica gel column

and eluted (30% EtOAc/hexanes) to yield the title compound as a white powder (2.41 g, 7.4 mmol, 92% yield). **Melting Point**: 81 °C – 84 °C. **^{1}H NMR** (400 MHz, $CDCl_3$) δ 8.61 (d, J = 2.4 Hz, 1H), 7.79 (dd, J = 2.4 Hz, 8.6 Hz, 1H), 7.40 (d, J = 8.6 Hz, 1H), 3.97 (m, 4H), 3.07 (s, 3H), 2.18 (m, 2H), 1.92-2.05 (m, 4H), 1.59-1.70 (m, 2H). **^{13}C NMR** (101 MHz, $CDCl_3$) δ 163.0, 150.2, 139.3, 122.3, 119.5, 108.6, 78.8, 64.7, 64.6, 50.9, 32.0, 30.7. **HRMS** (DART) $[M+H]^+$ calcd. for $[C_{14}H_{19}BrNO_3]^+$ 328.0543, 328.0623 found. **IR** (neat, cm^{-1}) 2931, 2869, 1702, 1460, 1360, 1093, 1035.

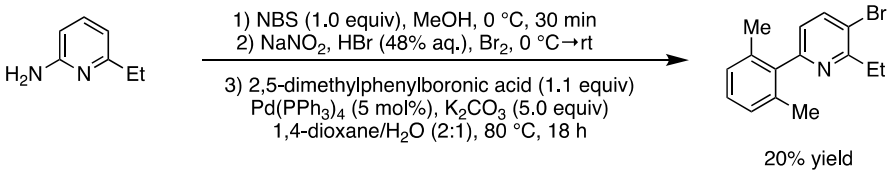

3-bromo-6-(2,6-dimethylphenyl)-2-ethylpyridine: An oven-dried 250 mL round bottom flask was charged with 2-amino-6-ethylpyridine (5.0 g, 41.0 mmol, 1.0 equiv) and anhydrous MeOH (80 mL, 0.51 M). The solution was cooled to 0 °C and *N*-bromosuccinimide (7.3 g, 41.0 mmol, 1.0 equiv) was added portion wise slowly (***Caution****:* addition of *N*-bromosuccinimide is exothermic. Care should be taken to add the reagent very slowly). The solution was stirred at 0 °C for 30 min and was subsequently poured into H_2O (200 mL) in a separatory funnel. The product was extracted with EtOAc (3 x 100 mL). The organic layers were dried over Na_2SO_4. The Na_2SO_4 was filtered off and the organic layer was concentrated *in vacuo*. Purification by silica gel chromatography (20% EtOAc/hexanes to 50% EtOAc/hexanes) yielded 6-amino-3-bromo-2-ethylpyridine as a light orange solid (5.87 g, 29.4 mmol, 70% yield). **^{1}H NMR** (400 MHz, $CDCl_3$) δ 7.48 (d, J = 8.5 Hz, 1H), 6.23 (d, J = 8.5 Hz, 1H), 4.39 (br s, 2H), 2.79 (q, J = 7.6 Hz, 2H), 1.23 (t, J = 7.6 Hz, 3H).

6-amino-3-bromo-2-ethylpyridine (2.83 g, 14.2 mmol, 1.0 equiv) was added to a 50 mL round bottom flask and the flask was cooled to 0 °C; 48% aq. HBr (6.0 mL) was then added slowly and the slurry was stirred for 15 min at 0 °C. Br_2 (2.2 mL, 42.6 mmol, 3.0 equiv) was then added dropwise and the solution was stirred for an additional 15 min at 0 °C. $NaNO_2$ (2.94 g, 42.6 mmol, 3.0 equiv) constituted in H_2O (7.0 mL) was then added dropwise over approximately 10 min (***Caution****:* addition of $NaNO_2$ is highly exothermic and results in the formation of a reactive diazonium salt. A blast shield should be utilized as an additional precaution). The solution was stirred for 1 h at 0 °C and 1 h at rt. The solution was cooled to 0 °C and 4 M NaOH was used to neutralize the reaction. Once the solution was basic, it was transferred to a separatory funnel and the product was extracted with Et_2O (3 x 70 mL). The organic layers were pooled and dried over Na_2SO_4. The Na_2SO_4 was filtered out and the organic layer was concentrated in vacuo. Purification by silica gel chromatography (10% CH_2Cl_2/hexanes to 15% CH_2Cl_2/hexanes) yielded 3,6-dibromo-2-ethylpyridine as a clear oil (1.73 g, 6.6 mmol, 46% yield). **^{1}H NMR** (400 MHz, $CDCl_3$) δ 7.63 (d, J = 8.2 Hz, 1H), 7.18 (d, J = 8.2 Hz, 1H), 2.94 (q, J = 7.5 Hz, 2H), 1.28 (t, J = 7.5 Hz, 3H).

Inside a N_2 filled glovebox, a 50 mL round bottom flask was charged with a magnetic stir bar, 2,6-dimethylphenylboronic acid (627.4 mg, 4.2 mmol, 1.1 equiv), potassium carbonate (1.90 g, 19.0 mmol, 5.0 equiv), palladium tetrakistriphenylphosphine (219.5 mg, 0.19 mmol, 0.05 equiv), 1,4-dioxane (10 mL), and 3,6-dibromo-2-ethylpyridine (1.0 g, 3.8 mmol, 1.0 equiv) in successive order. The flask was removed from the glovebox and put under positive pressure of N_2 on a Schlenk line. H_2O (5.0 mL) was then added via syringe. The solution was then placed into a preheated 80 °C silicon oil bath and stirred for 18 h. The solution was then allowed to cool to rt and poured into H_2O (70 mL) in a separatory funnel. The product was extracted with EtOAc (3 x

70 mL). The organic layers were dried over Na_2SO_4. The Na_2SO_4 was filtered off and the organic layer was concentrated *in vacuo*. Purification by silica gel chromatography (1% CH_2Cl_2/hexanes to 20% CH_2Cl_2/hexanes) yielded the title compound as a clear oil (669.8 mg, 2.3 mmol, 61% yield). **Melting Point**: 43 °C – 44 °C. **^{1}H NMR** (400 MHz, $CDCl_3$) δ 7.86 (d, J = 8.1 Hz, 1H), 7.18 (dd, J = 6.8 Hz, 8.3 Hz, 1H), 7.10 (m, 2H), 6.93 (d, J = 8.1 Hz, 1H), 3.04 (q, J = 7.5 Hz, 2H), 2.06 (s, 6H), 1.30 (t, J = 7.5 Hz, 3H). **^{13}C NMR** (101 MHz, $CDCl_3$) δ 161.9, 158.6, 140.7, 139.9, 136.1, 128.4, 128.0, 123.6, 119.1, 31.4, 20.6, 13.5. **HRMS** (DART) $[M+H]^+$ calcd. for $[C_{15}H_{17}BrN]^+$ 290.0539, 290.0543 found. **IR** (neat, cm^{-1}) 2975, 2172, 1973 1561, 1439, 1044.

A2.10 References

[1] Connon, S. J.; Hegarty, A. F. Substituted 3,4-pyridynes: clean cycloadditions. *J. Chem. Soc., Perkin Trans.* **2000**, *1*, 1245-1249.

[2] Crawford, S. M.; Wheaton, C. A.; Mishra, V.; Stradiotto, M. Probing the effect of donor-fragment substitution in Mor-DalPhos on palladium-catalyzed C-N and C-C cross-coupling reactivity. *Canadian Journal of Chemistry* **2018**, *96*, 578-586.

[3] Fan, J.; Zhang, W.; Gao, W.; Wang, T.; Duan, W.-L.; Liang, Y.; Zhang, Z. Syntheses of Benzofuranoquinolines and Analogues via Photoinduced Acceptorless Dehydrogenative Annulation of *o*-Phenylfuranylpyridines. *Org. Lett.* **2019**, *21*, 9183-9187.

A2.11 Copies of NMR Spectra

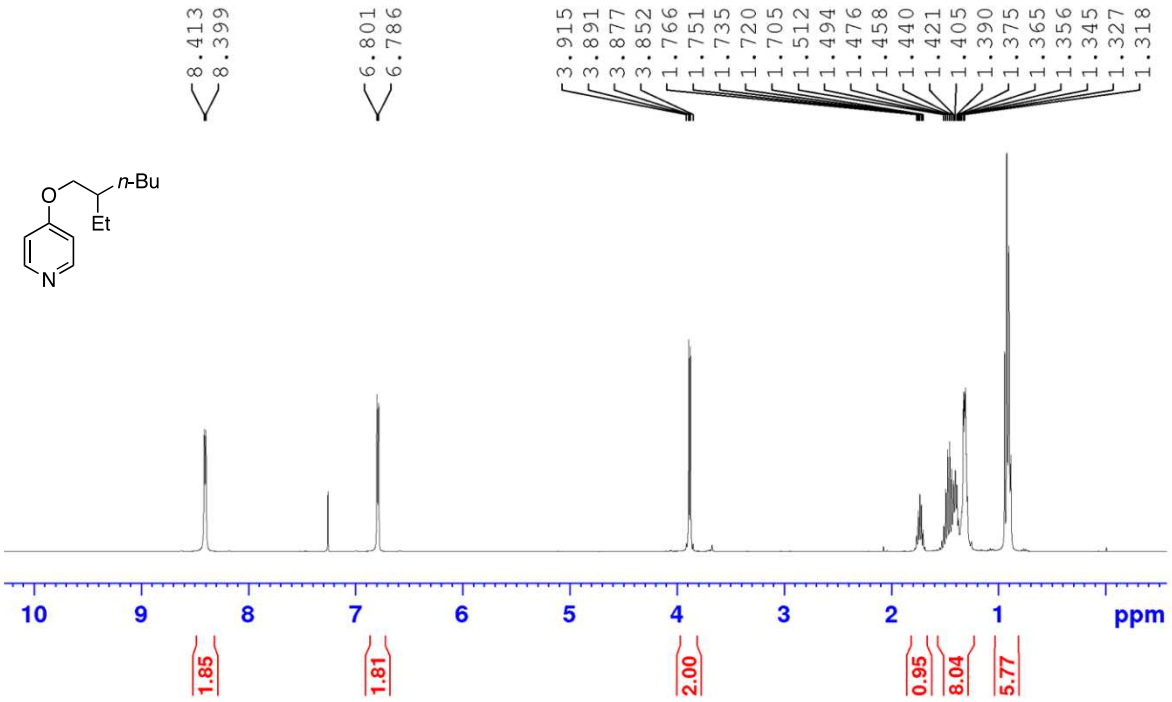

^{1}H NMR spectrum ($CDCl_3$, 400 MHz)

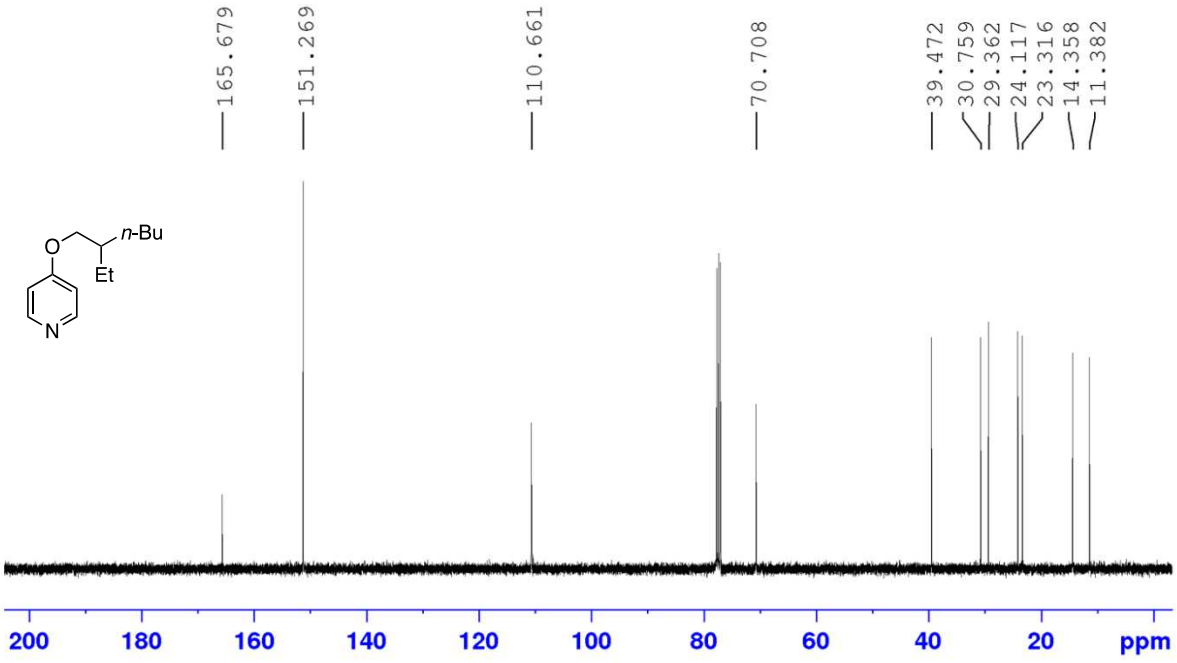

^{13}C NMR spectrum ($CDCl_3$, 101 MHz)

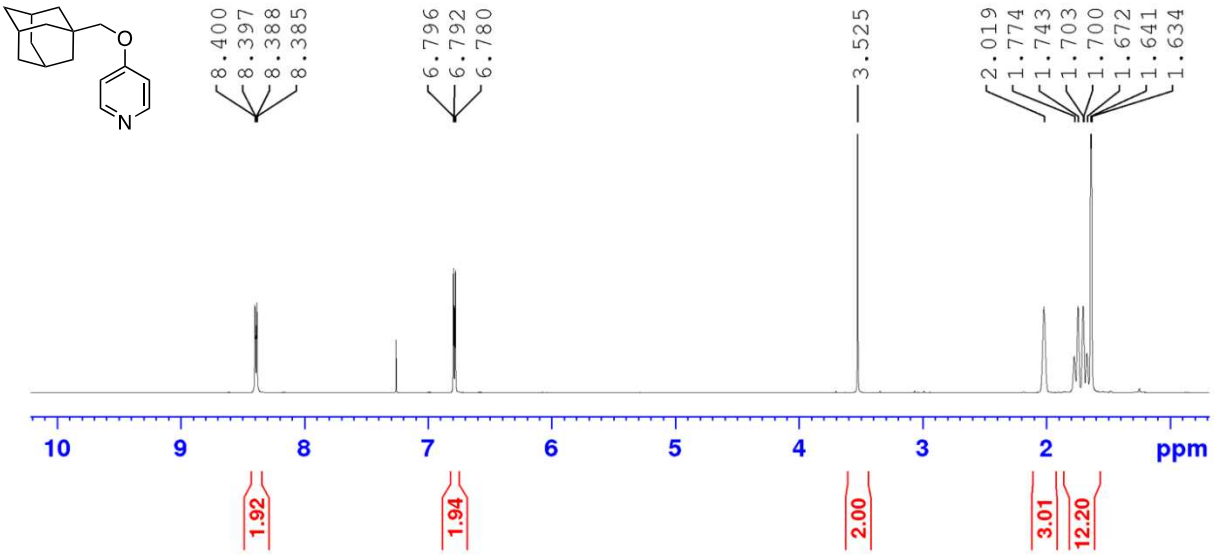

^{1}H NMR spectrum ($CDCl_3$, 400 MHz)

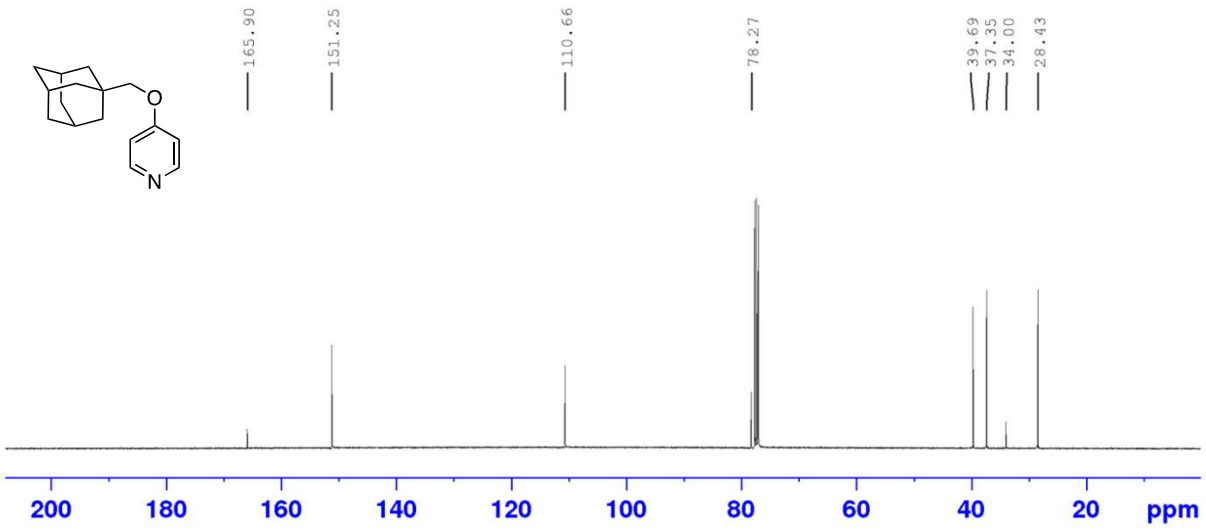

^{13}C NMR spectrum ($CDCl_3$, 101 MHz)

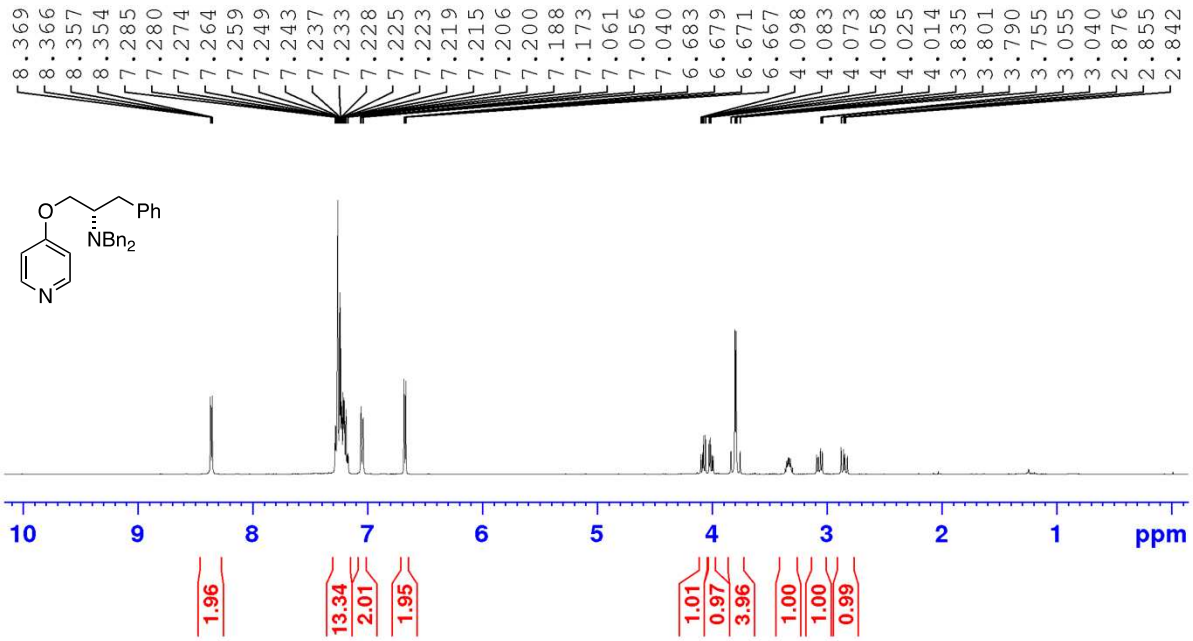

^{1}H NMR spectrum ($CDCl_3$, 400 MHz)

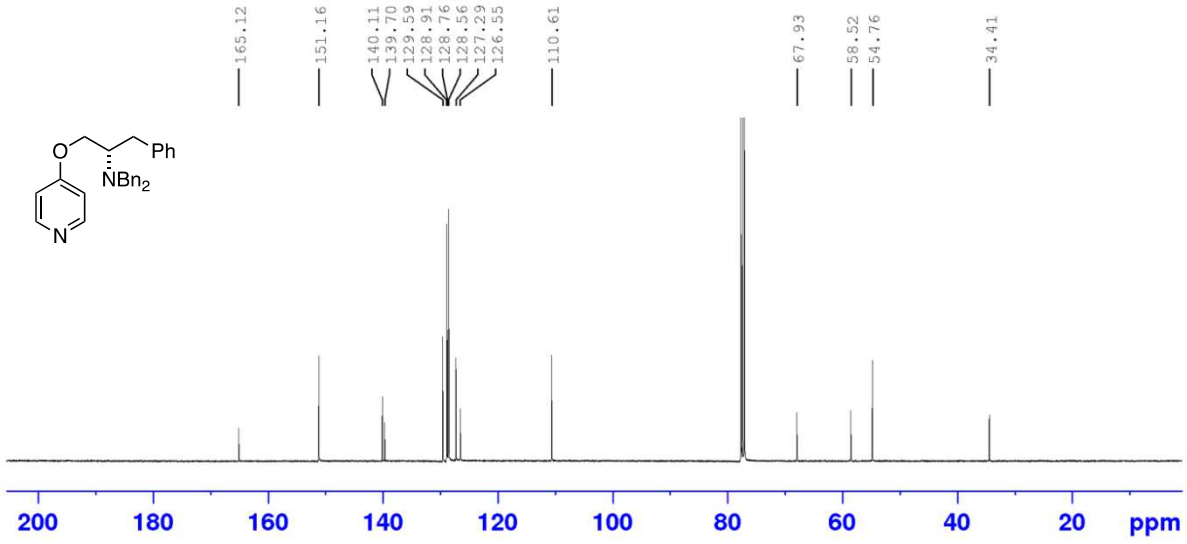

^{13}C NMR spectrum ($CDCl_3$, 101 MHz)

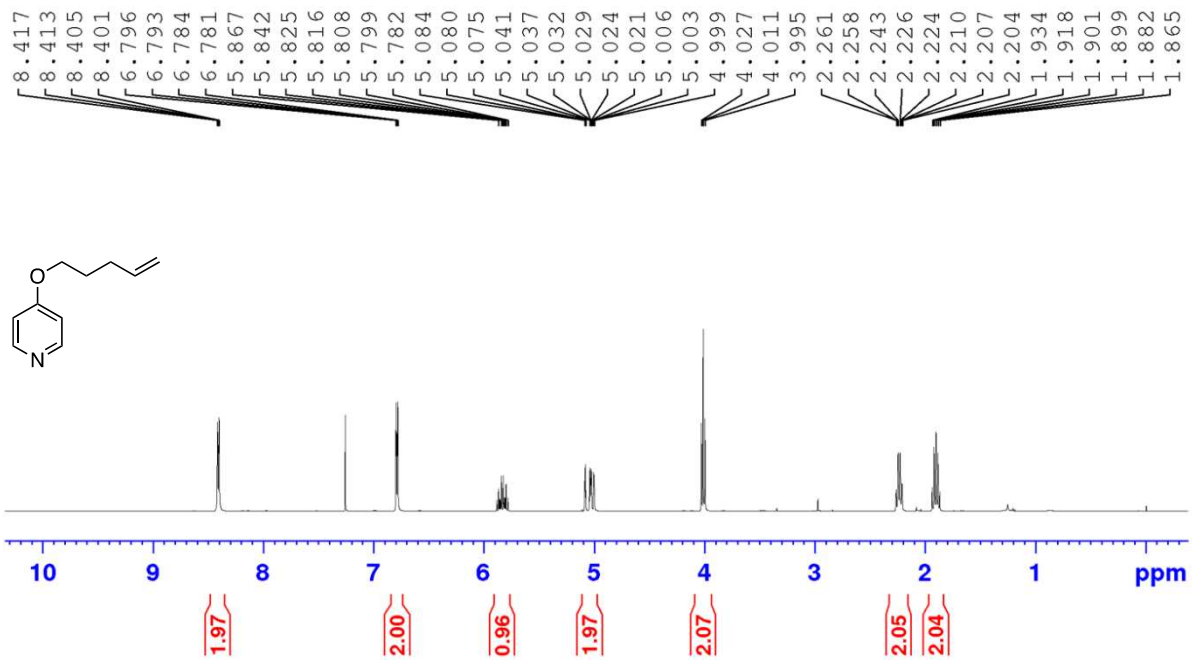

^{1}H NMR spectrum ($CDCl_3$, 400 MHz)

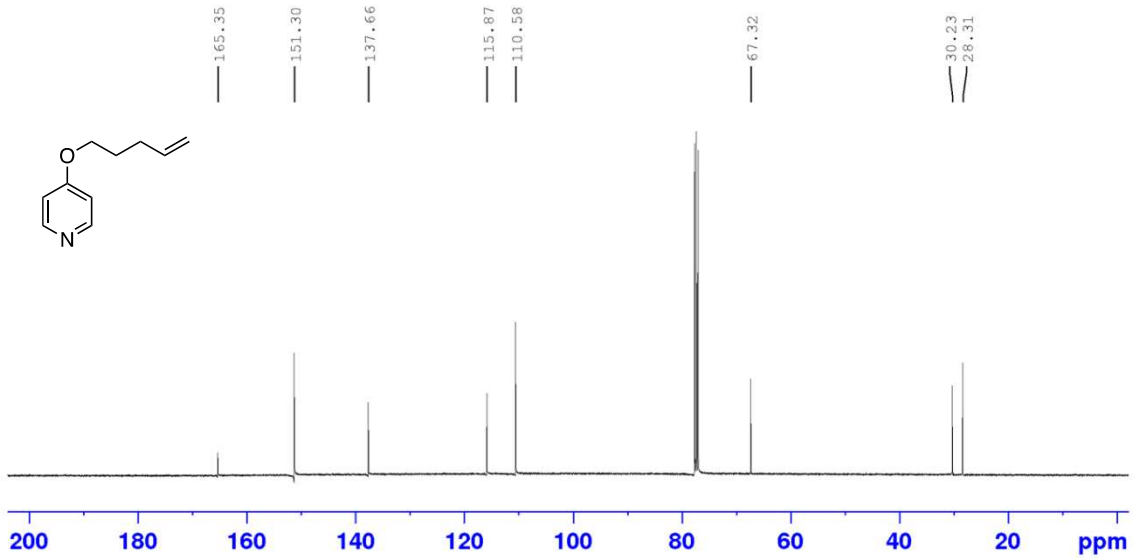

^{13}C NMR spectrum ($CDCl_3$, 101 MHz)

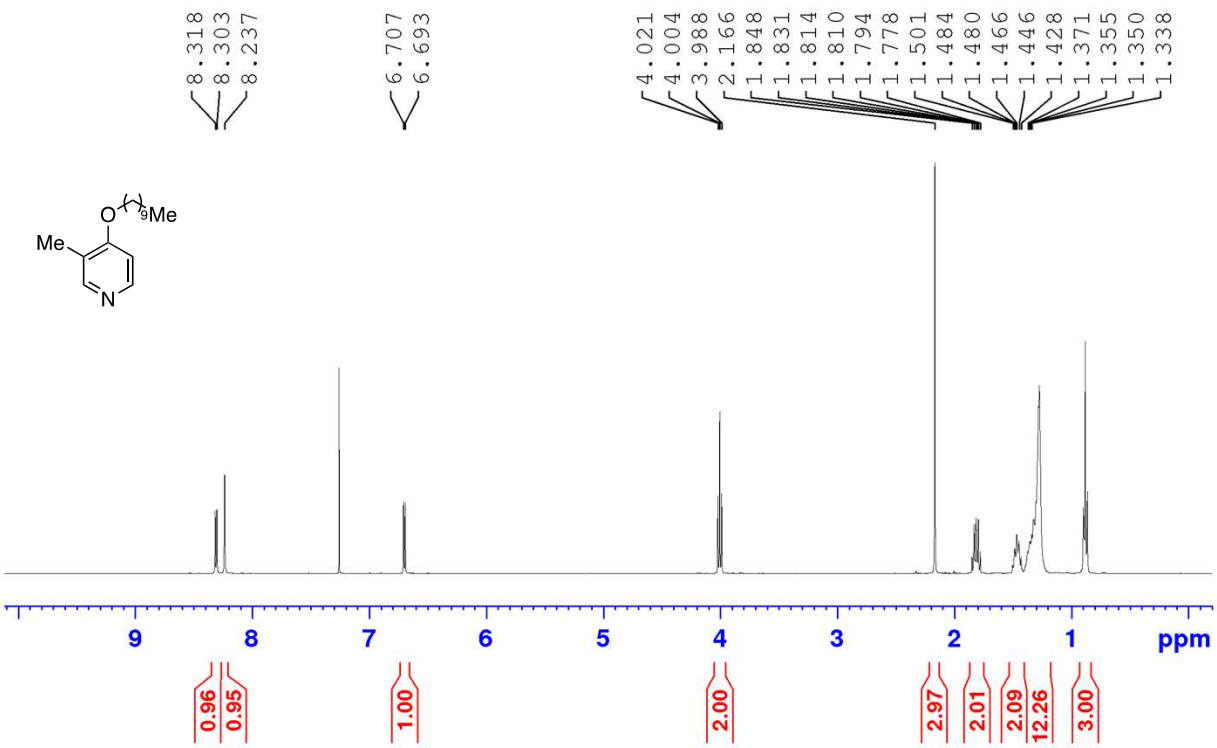

^{1}H NMR spectrum ($CDCl_3$, 400 MHz)

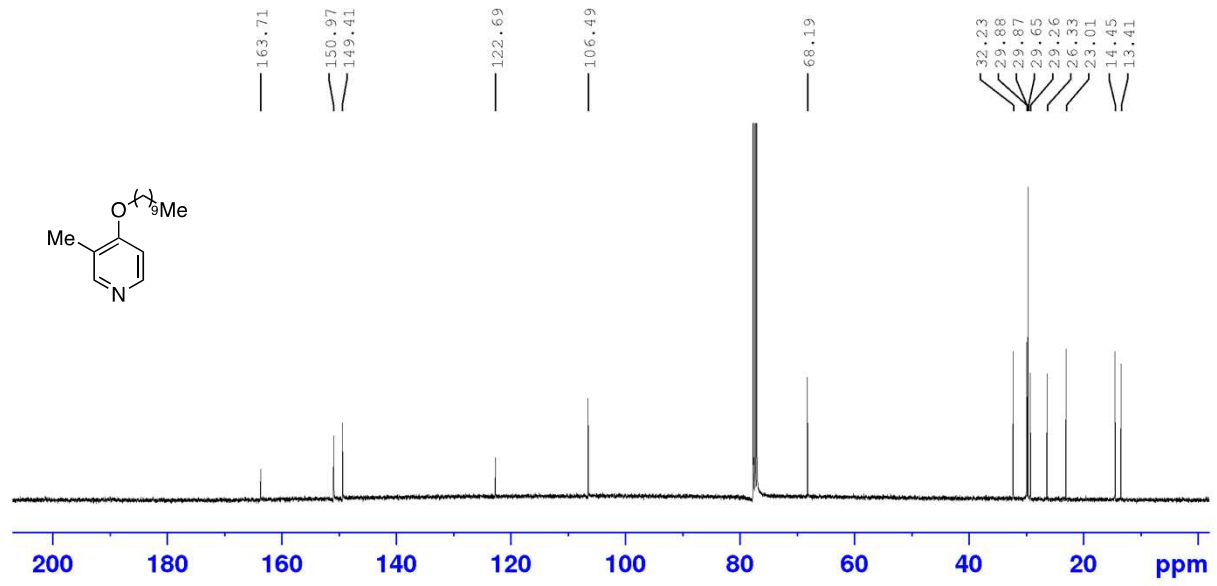

^{13}C NMR spectrum ($CDCl_3$, 101 MHz)

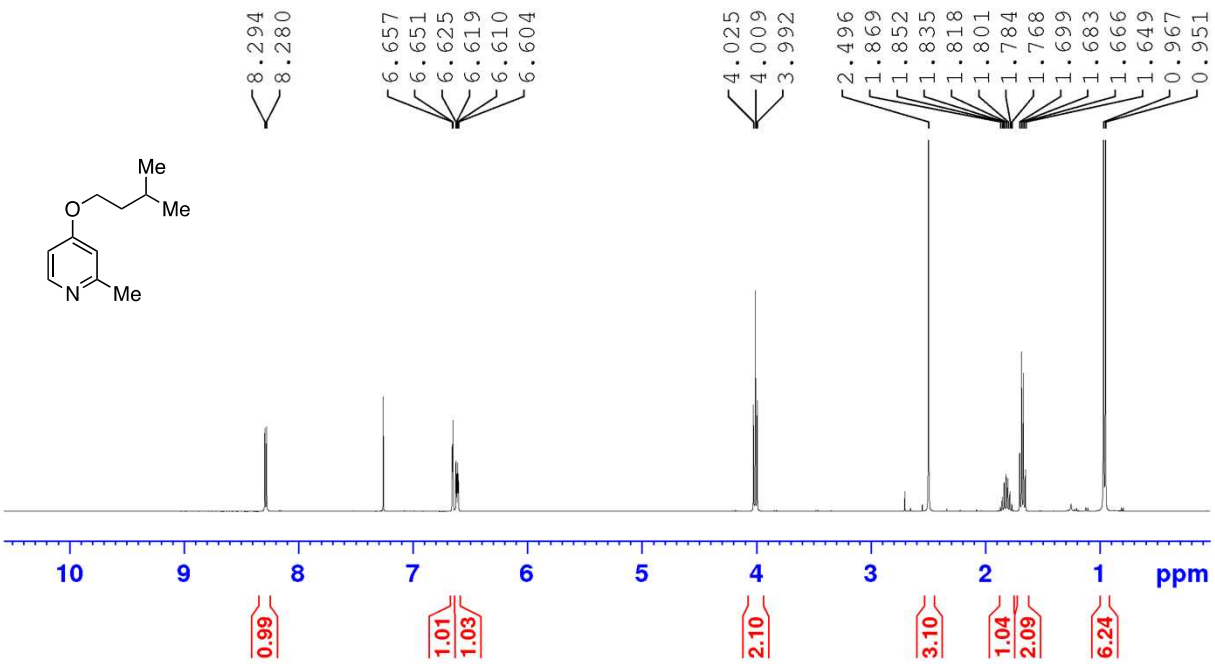

^{1}H NMR spectrum ($CDCl_3$, 400 MHz)

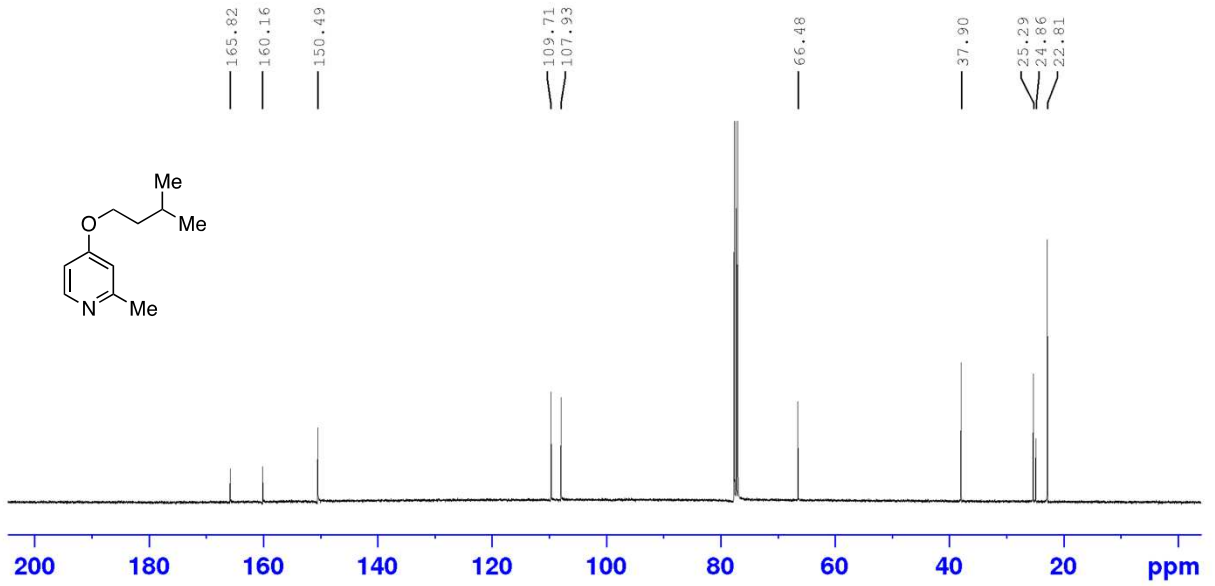

^{13}C NMR spectrum ($CDCl_3$, 101 MHz)

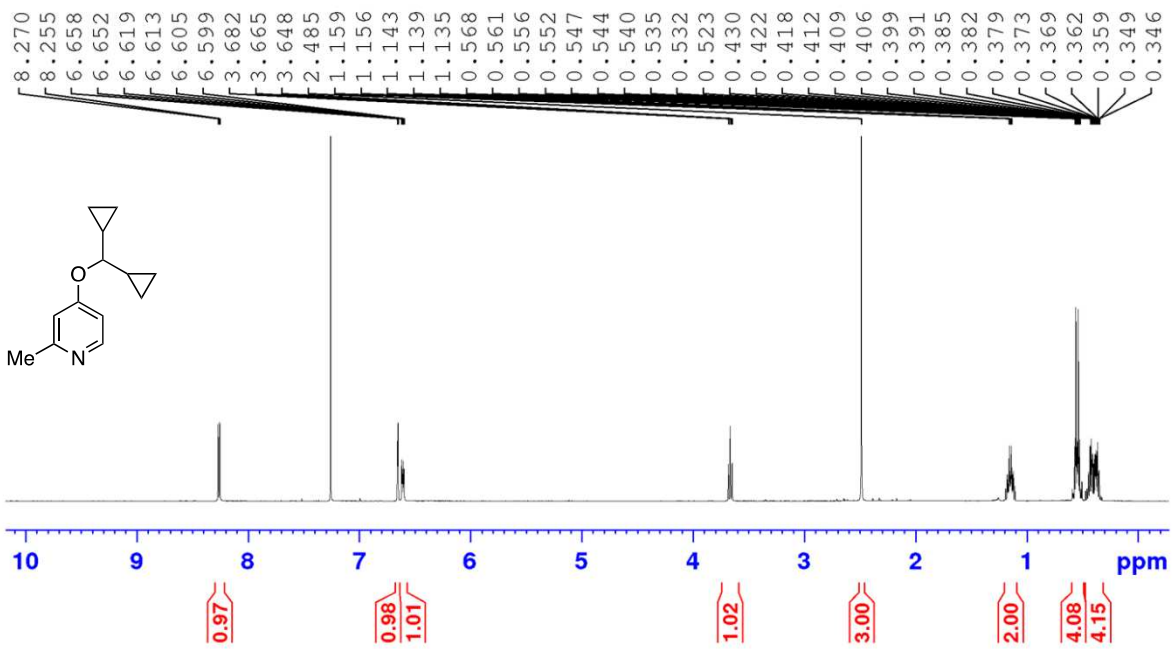

^{1}H NMR spectrum ($CDCl_3$, 400 MHz)

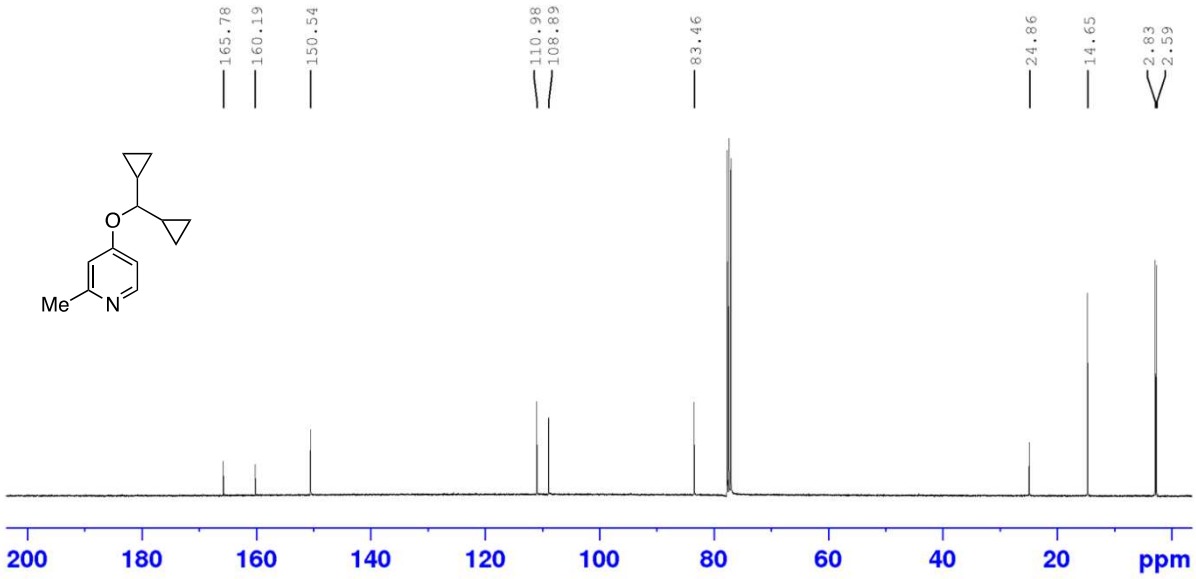

^{13}C NMR spectrum ($CDCl_3$, 101 MHz)

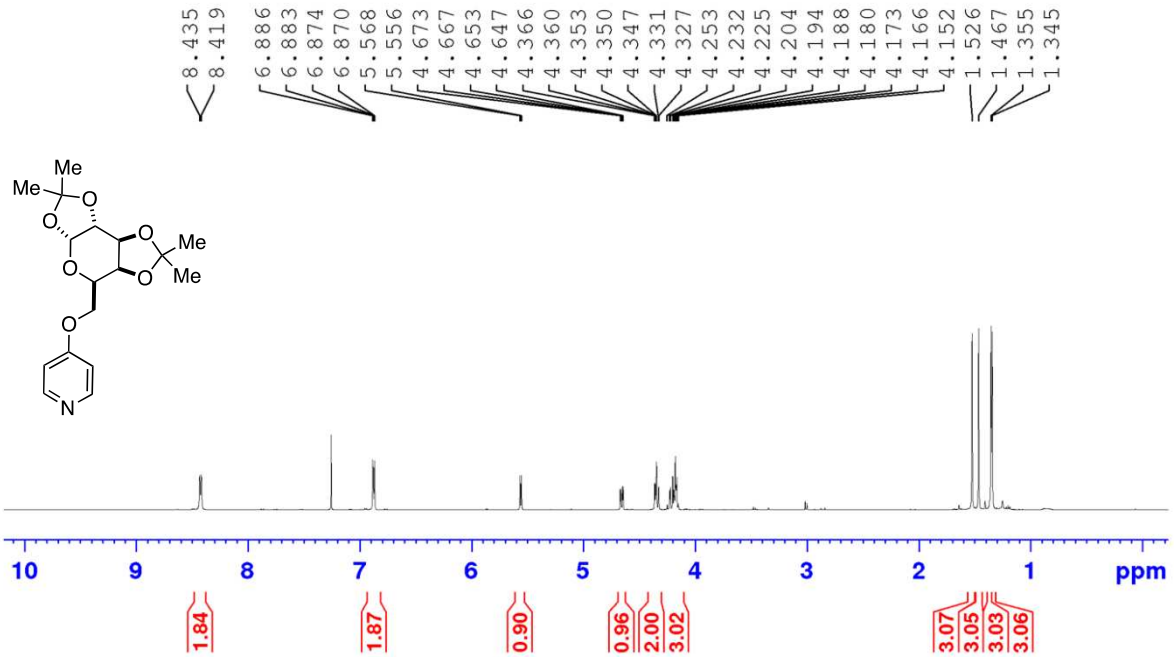

^{1}H NMR spectrum ($CDCl_3$, 400 MHz)

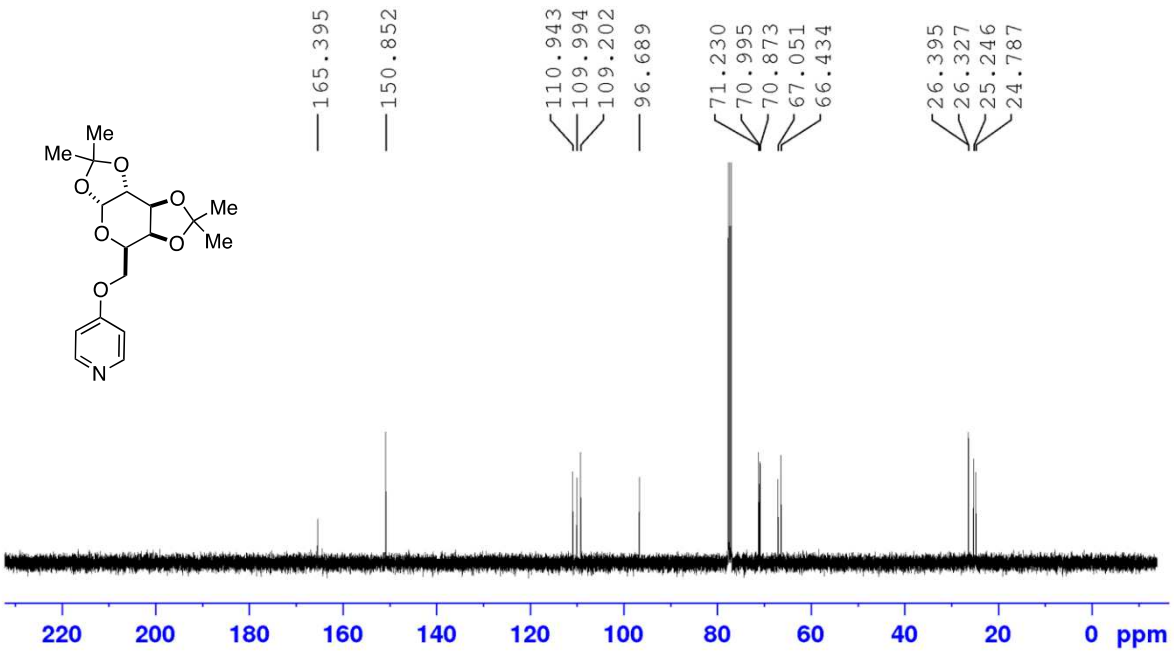

^{13}C NMR spectrum ($CDCl_3$, 101 MHz)

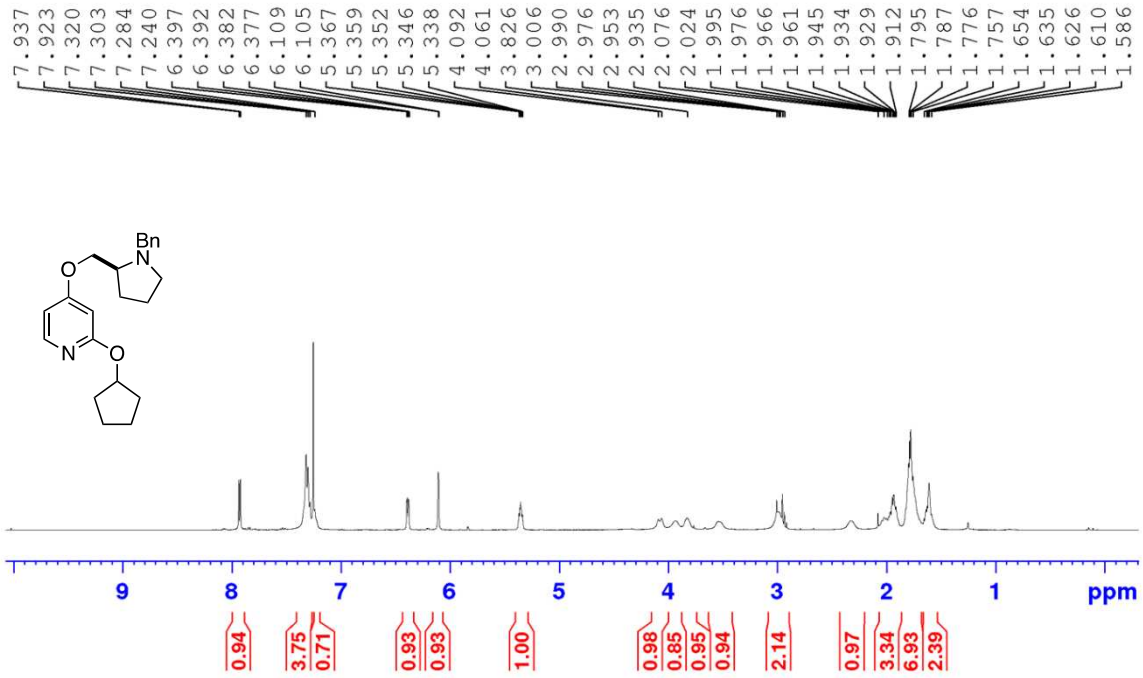

^{1}H NMR spectrum ($CDCl_3$, 400 MHz)

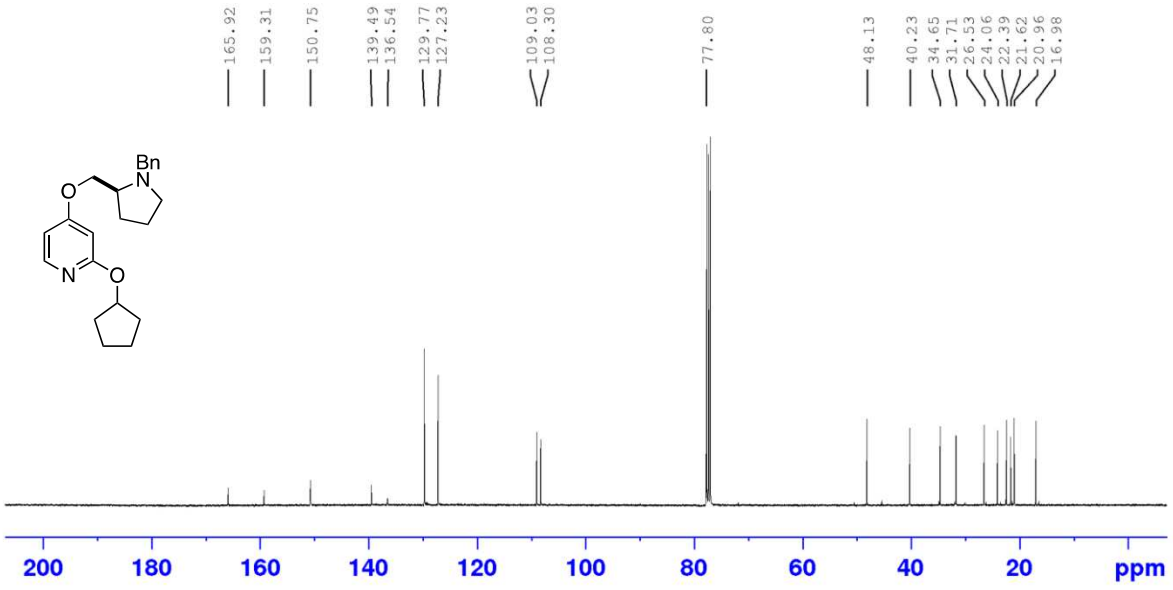

^{13}C NMR spectrum ($CDCl_3$, 101 MHz)

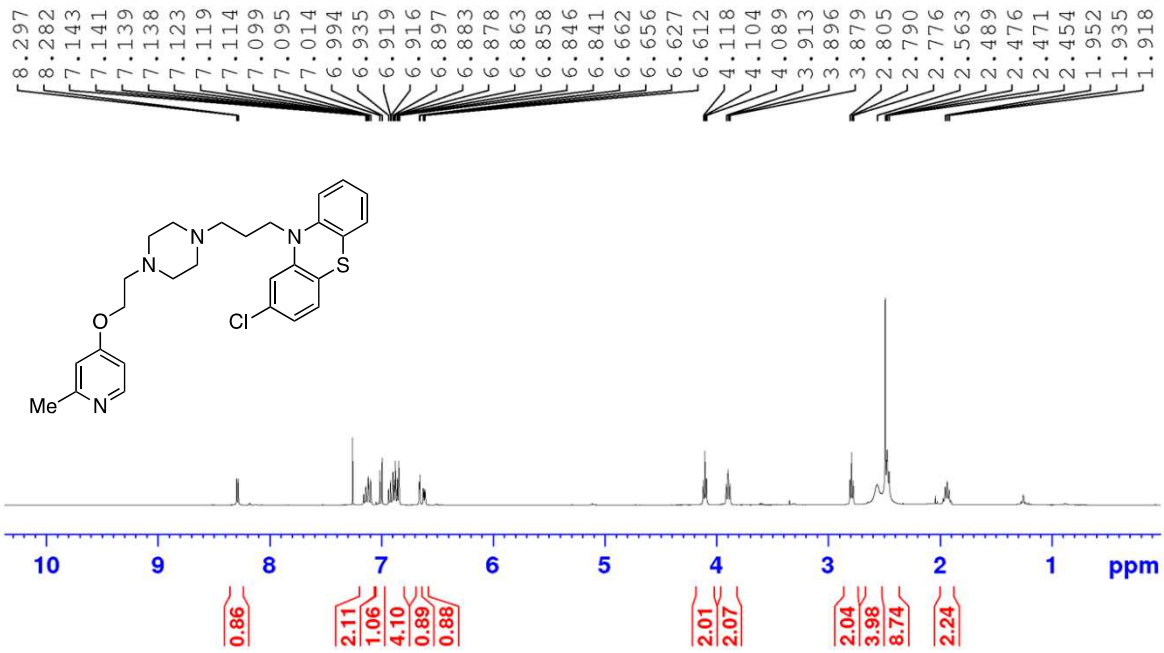

^{1}H NMR spectrum ($CDCl_3$, 400 MHz)

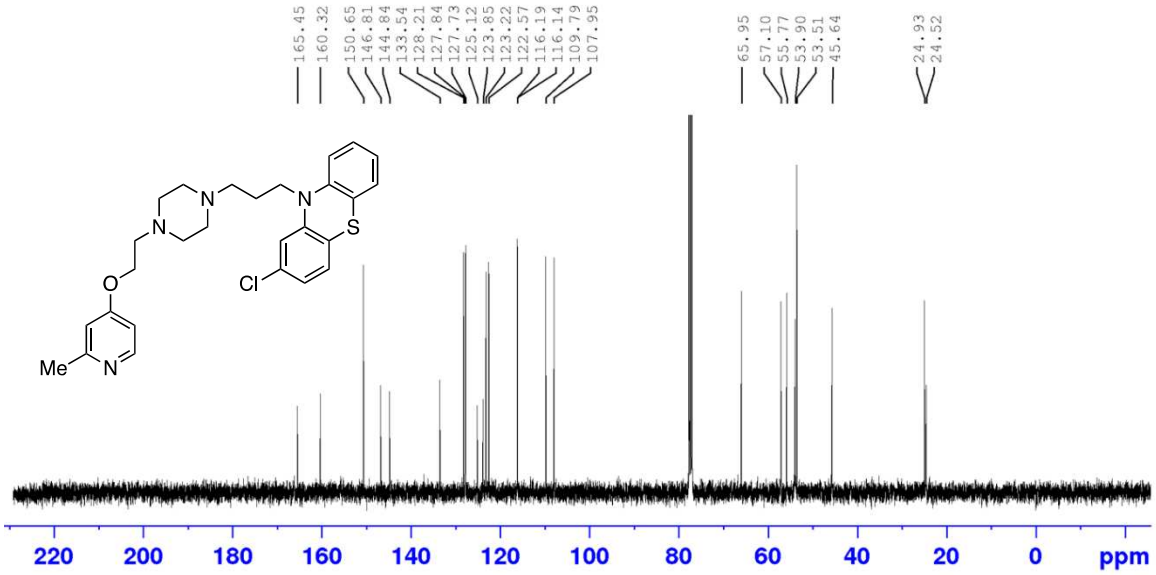

^{13}C NMR spectrum ($CDCl_3$, 101 MHz)

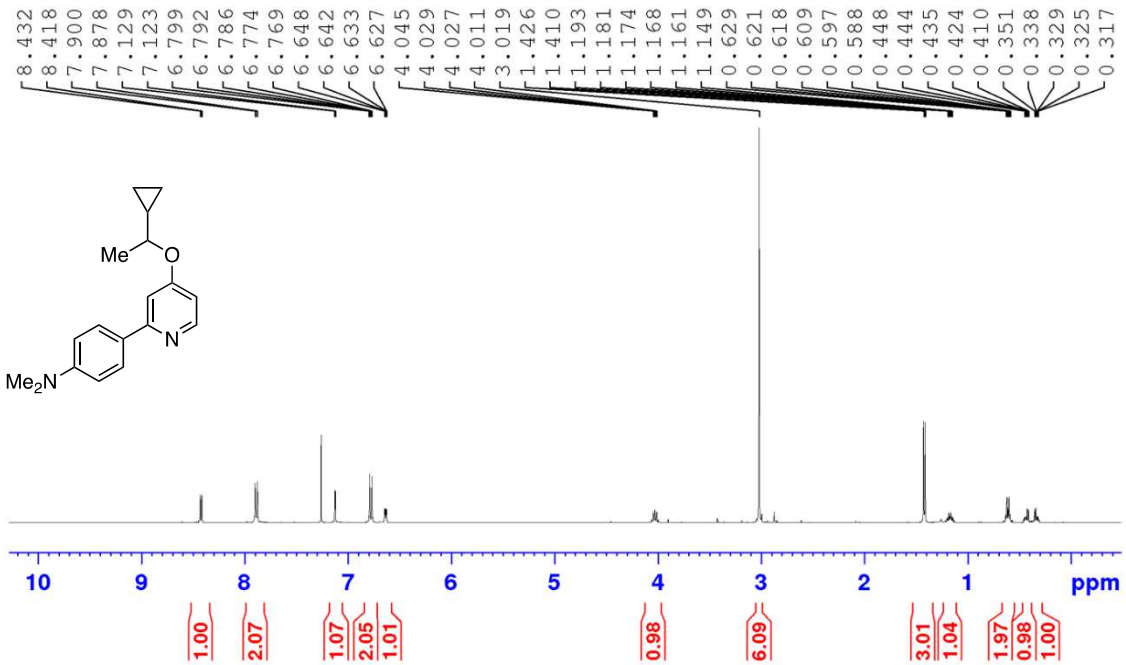

^{1}H NMR spectrum (400 MHz, $CDCl_3$)

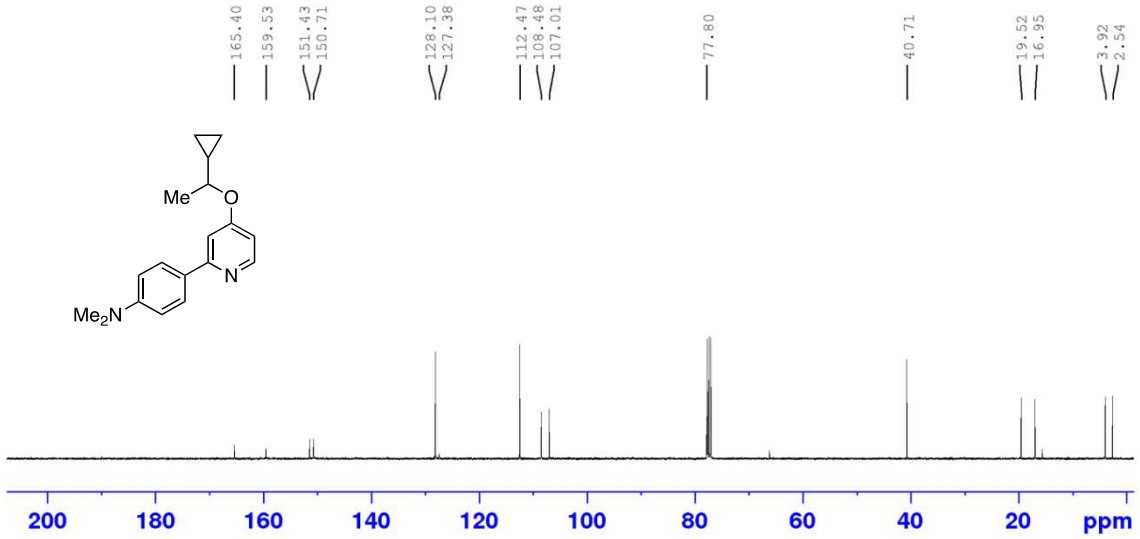

^{13}C NMR spectrum (101 MHz, $CDCl_3$)

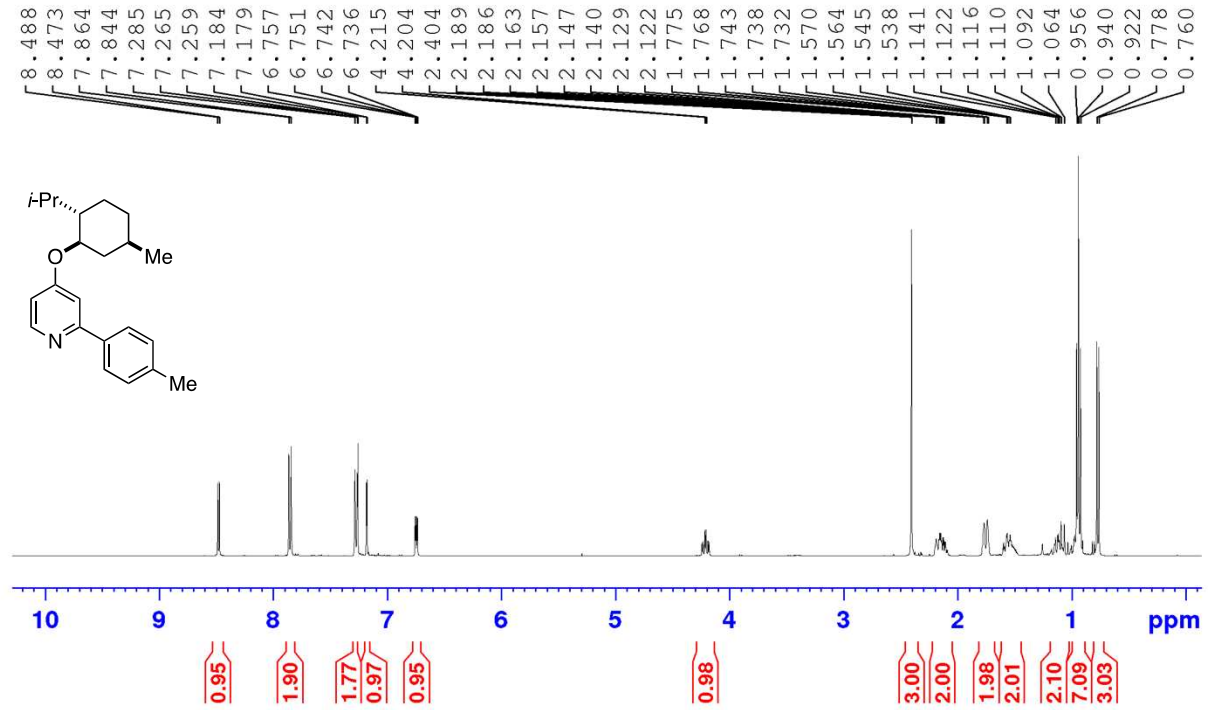

^{1}H NMR spectrum ($CDCl_3$, 400 MHz)

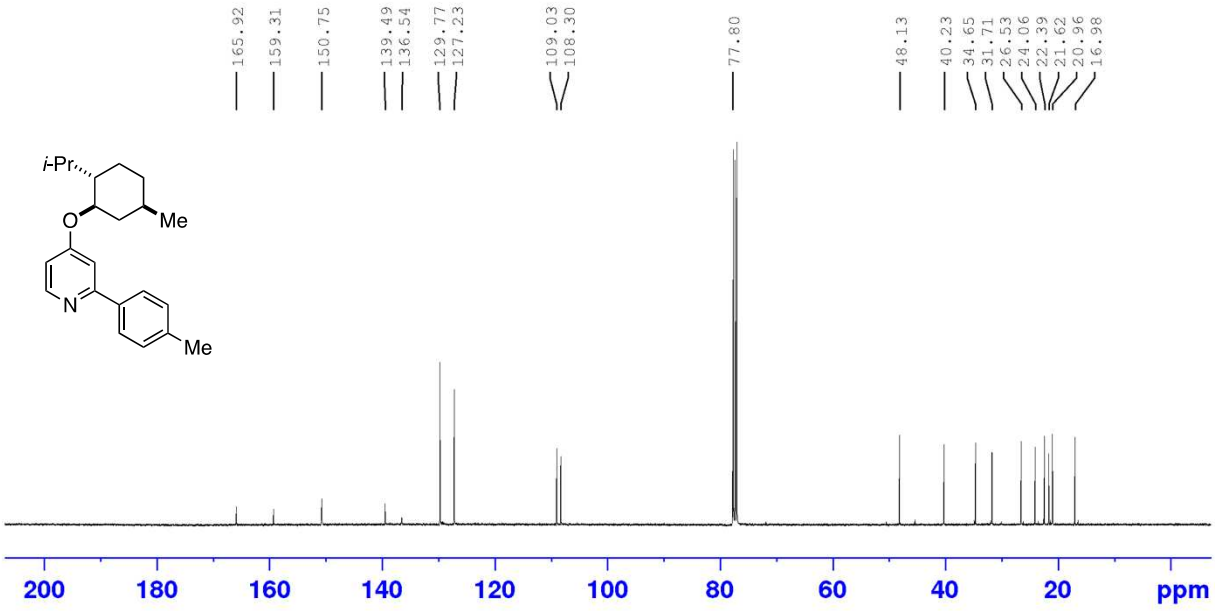

^{13}C NMR spectrum (101 MHz, $CDCl_3$)

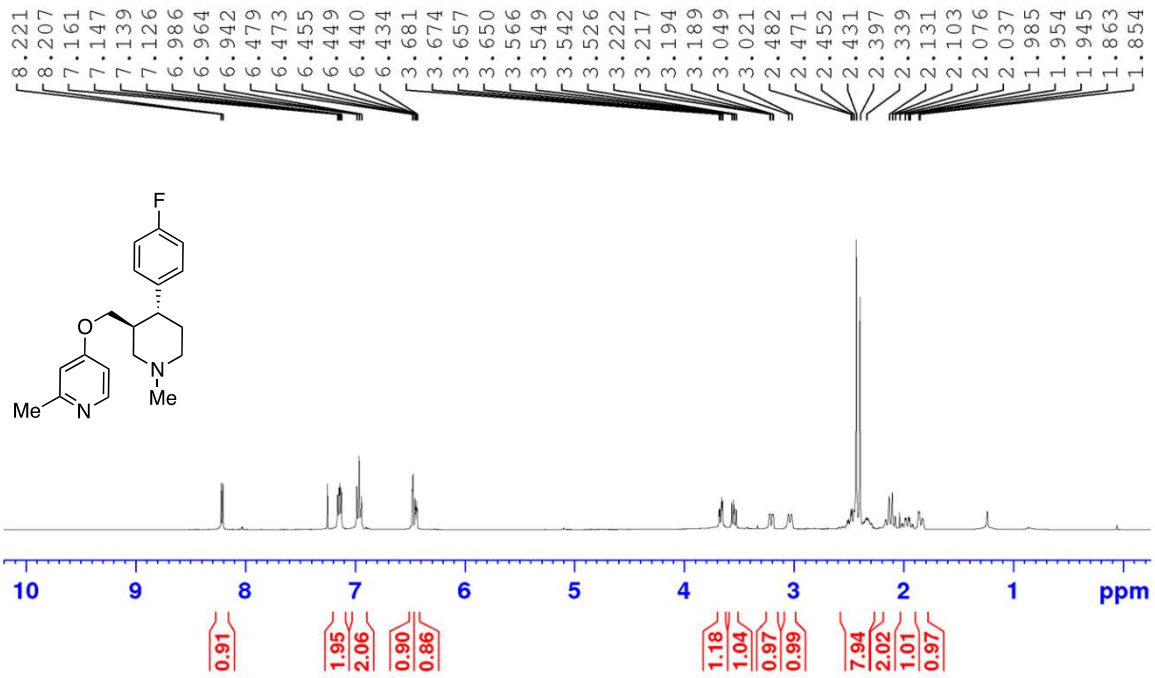

^{1}H NMR spectrum ($CDCl_3$, 400 MHz)

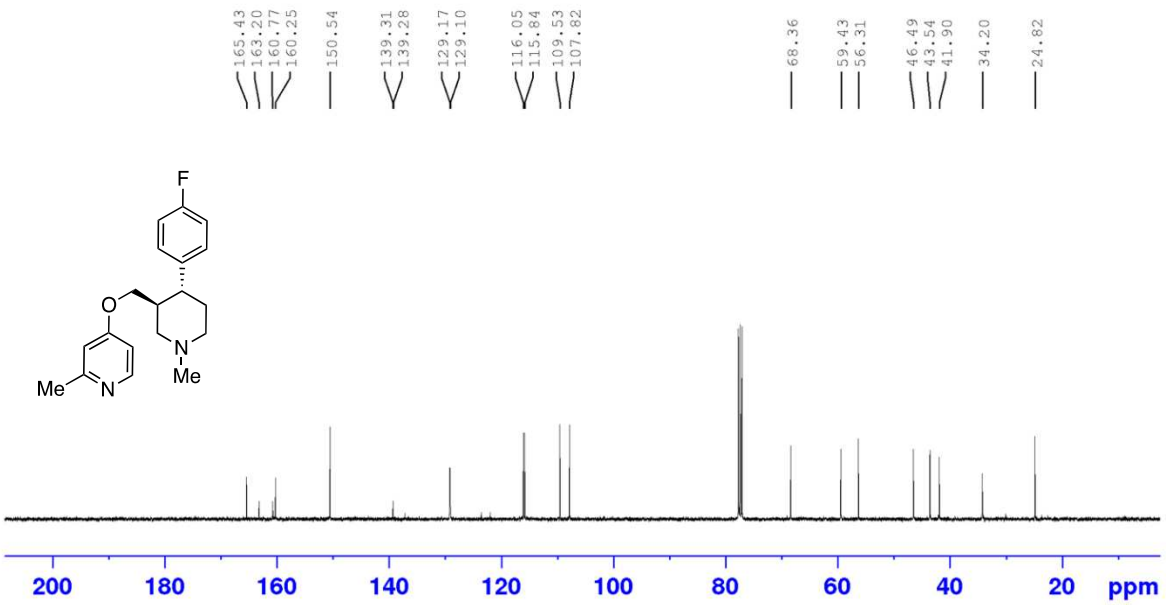

^{13}C NMR spectrum ($CDCl_3$, 101 MHz)

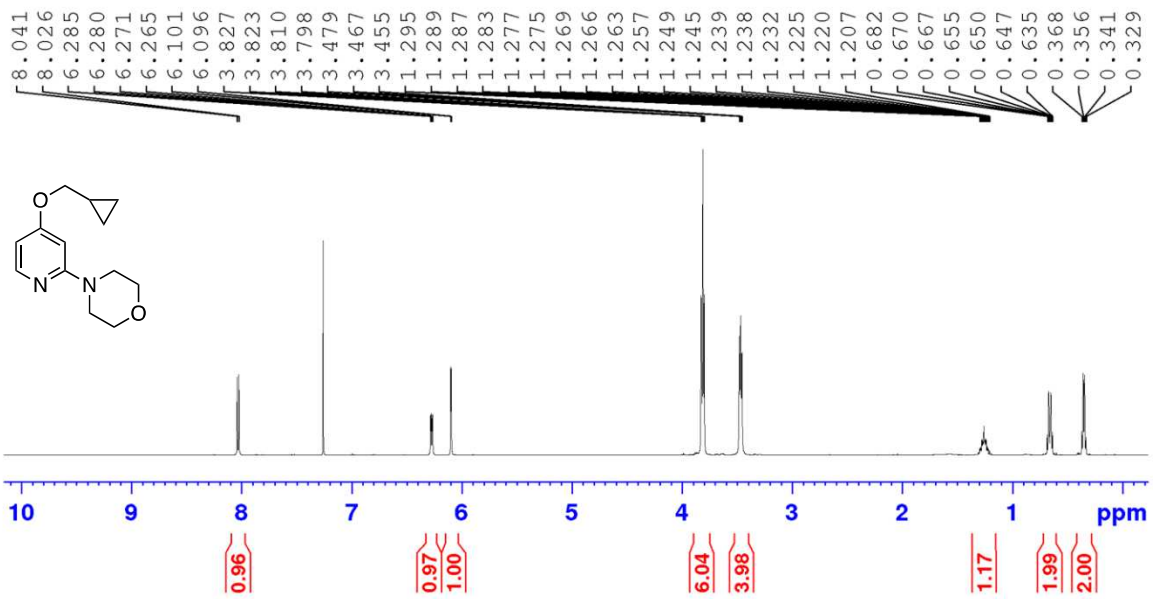

^{1}H NMR spectrum ($CDCl_3$, 400 MHz)

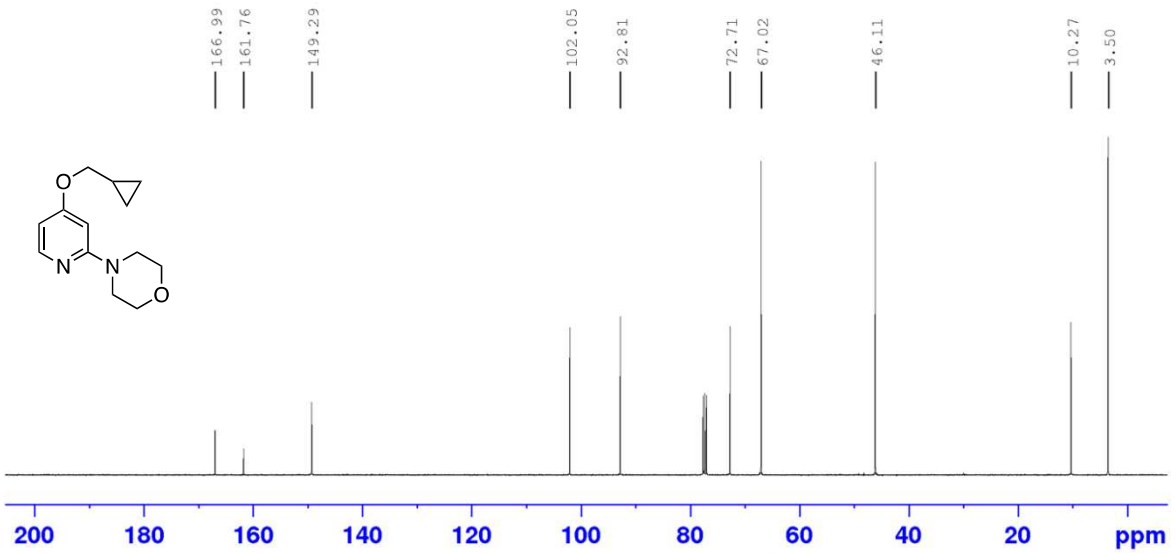

^{13}C NMR spectrum ($CDCl_3$, 101 MHz)

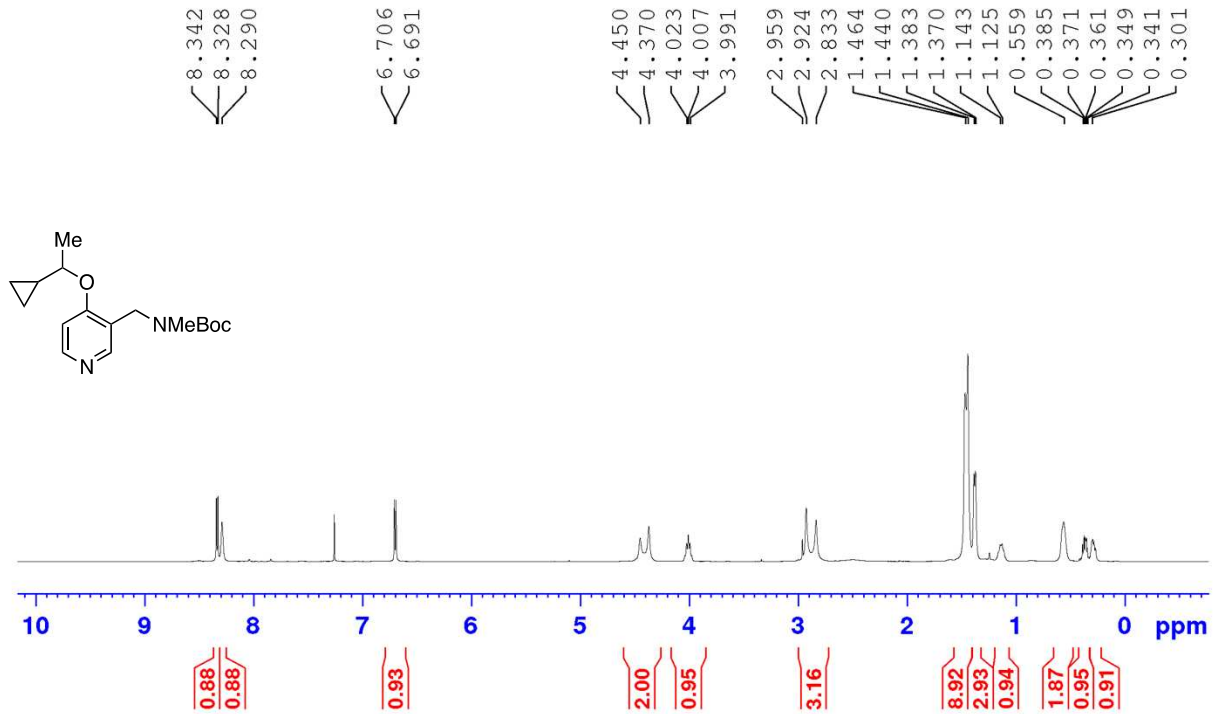

^{1}H NMR spectrum ($CDCl_3$, 400 MHz)

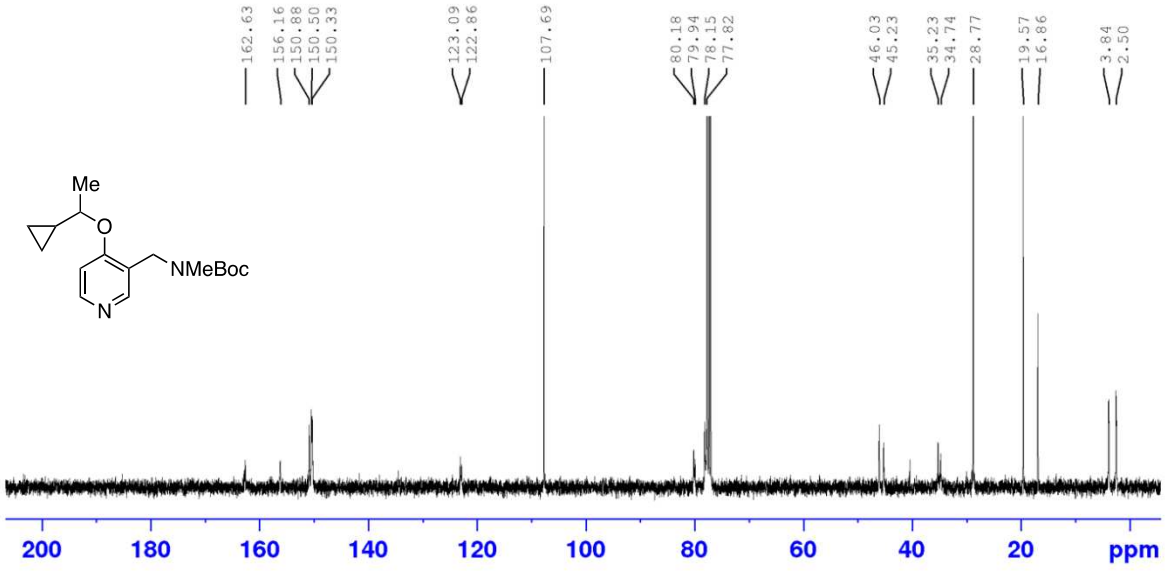

^{13}C NMR spectrum ($CDCl_3$, 101 MHz)

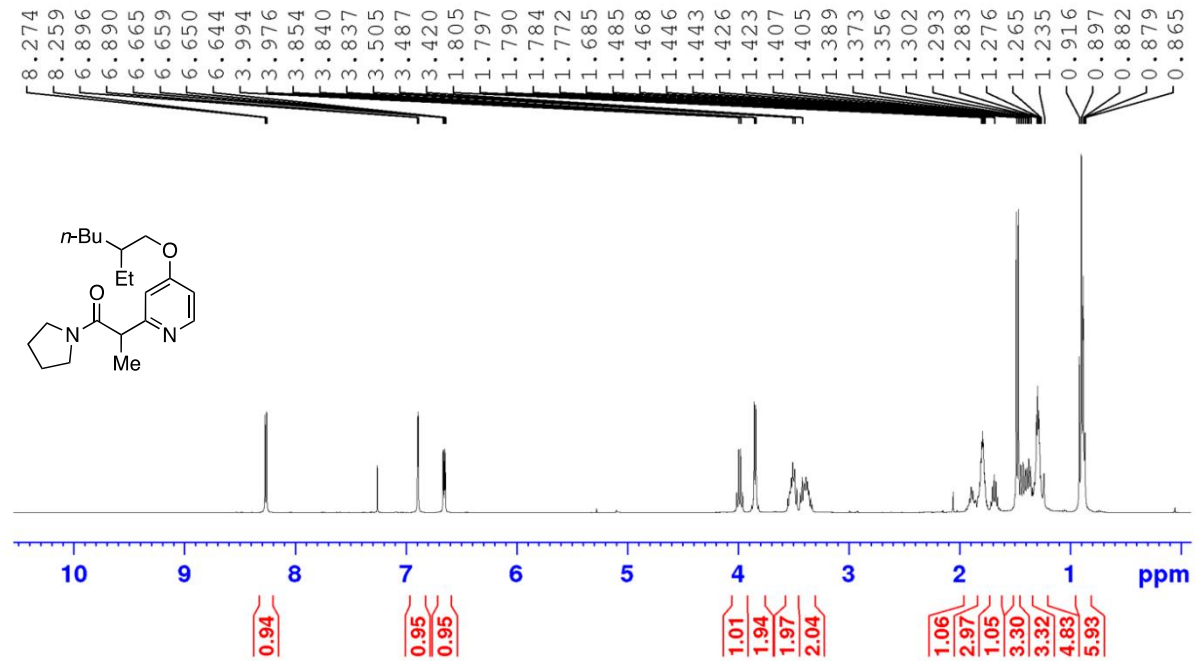

^{1}H NMR spectrum ($CDCl_3$, 400 MHz)

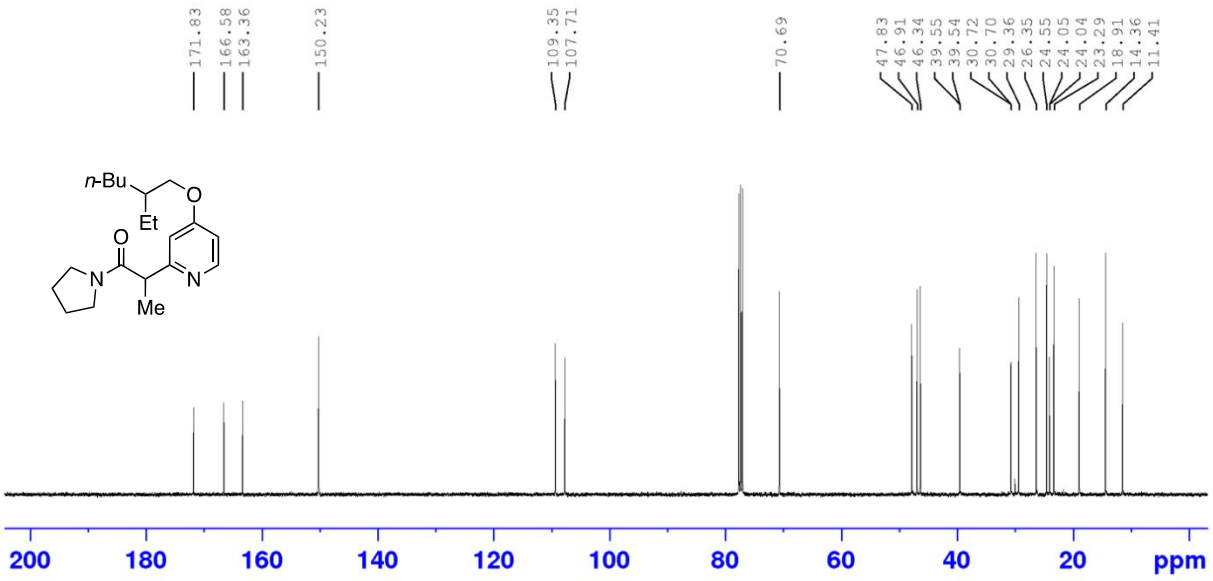

^{13}C NMR spectrum ($CDCl_3$, 101 MHz)

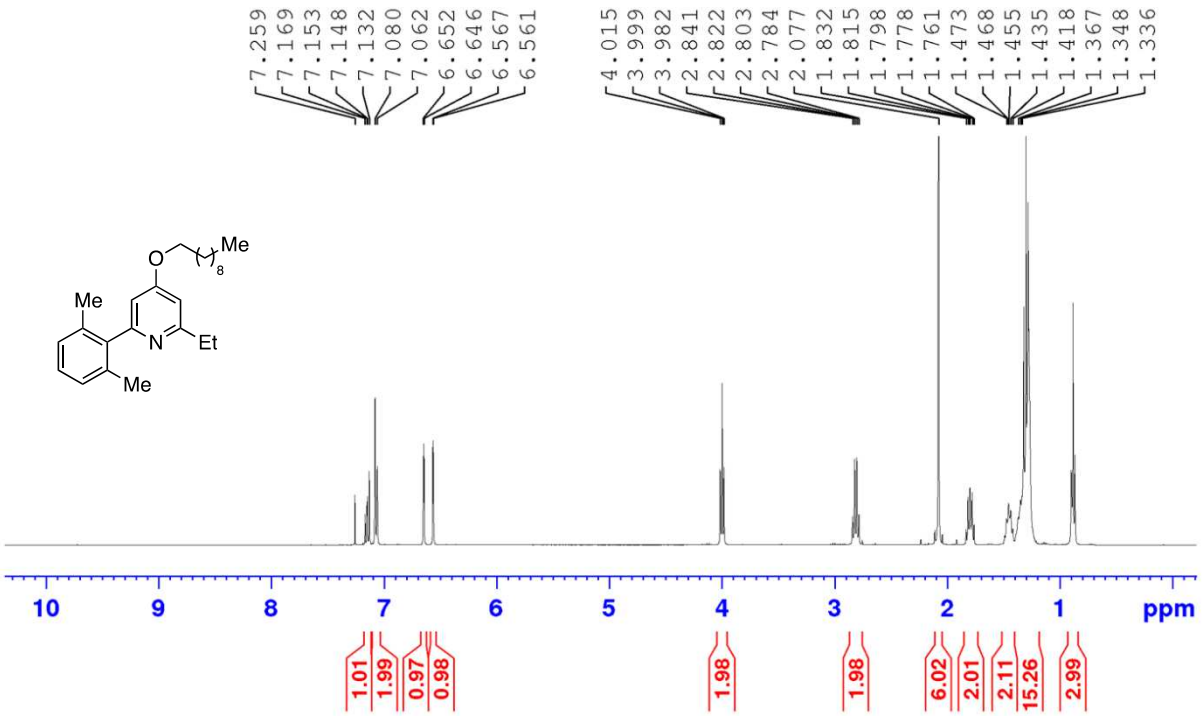

^{1}H NMR spectrum (400 MHz, $CDCl_3$)

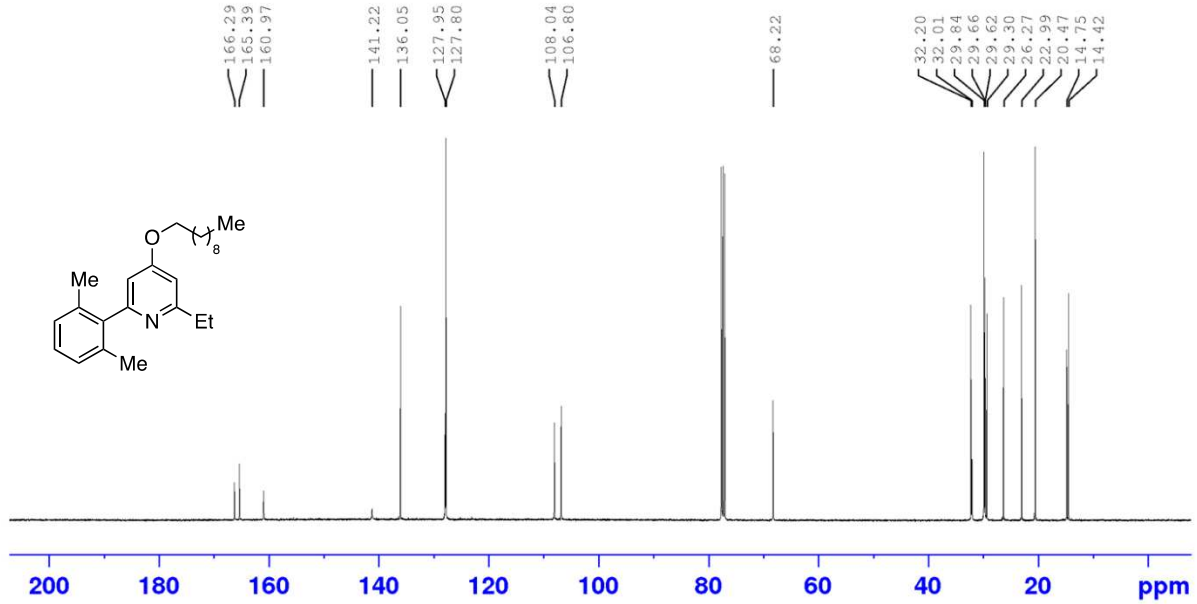

^{13}C NMR spectrum (101 MHz, $CDCl_3$)

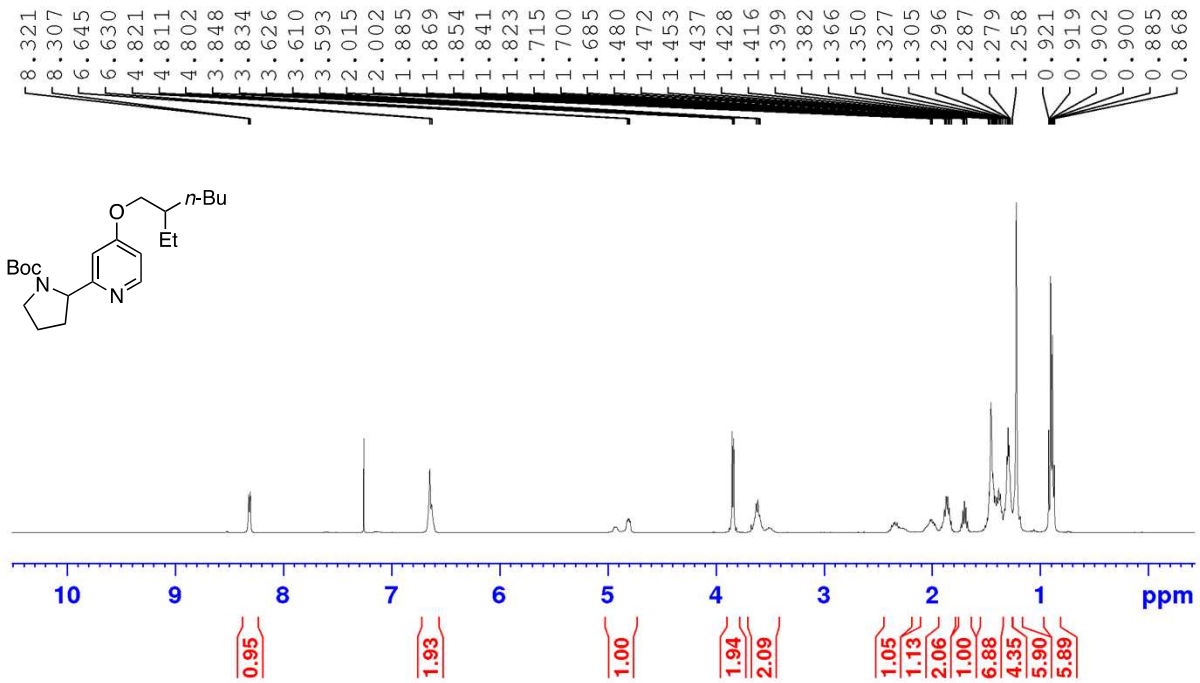

^{1}H NMR spectrum ($CDCl_3$, 400 MHz)

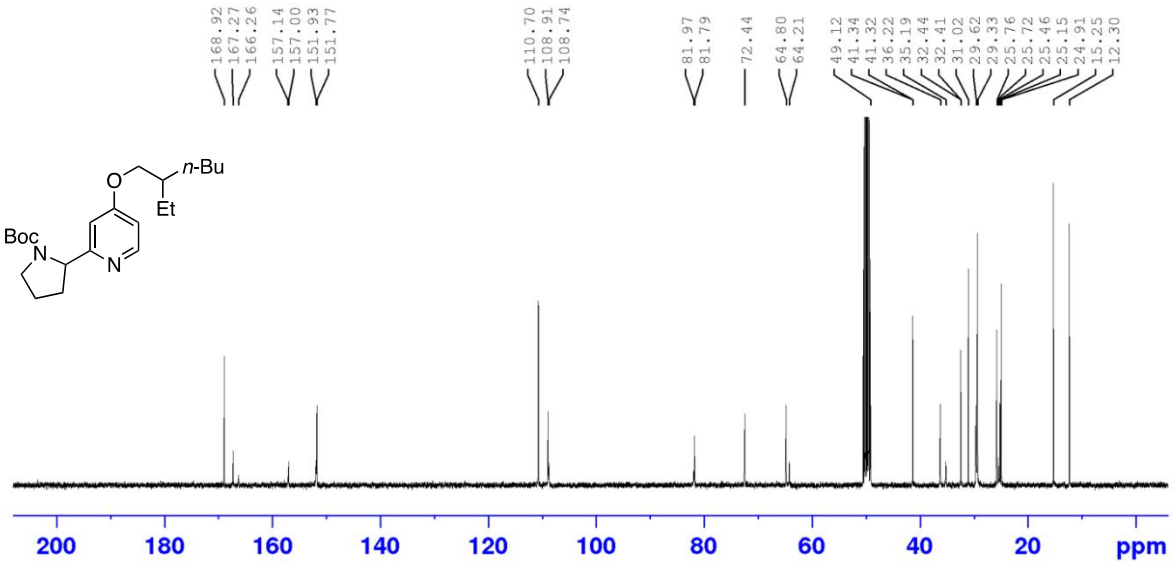

^{13}C NMR spectrum (CD_3OD, 101 MHz)

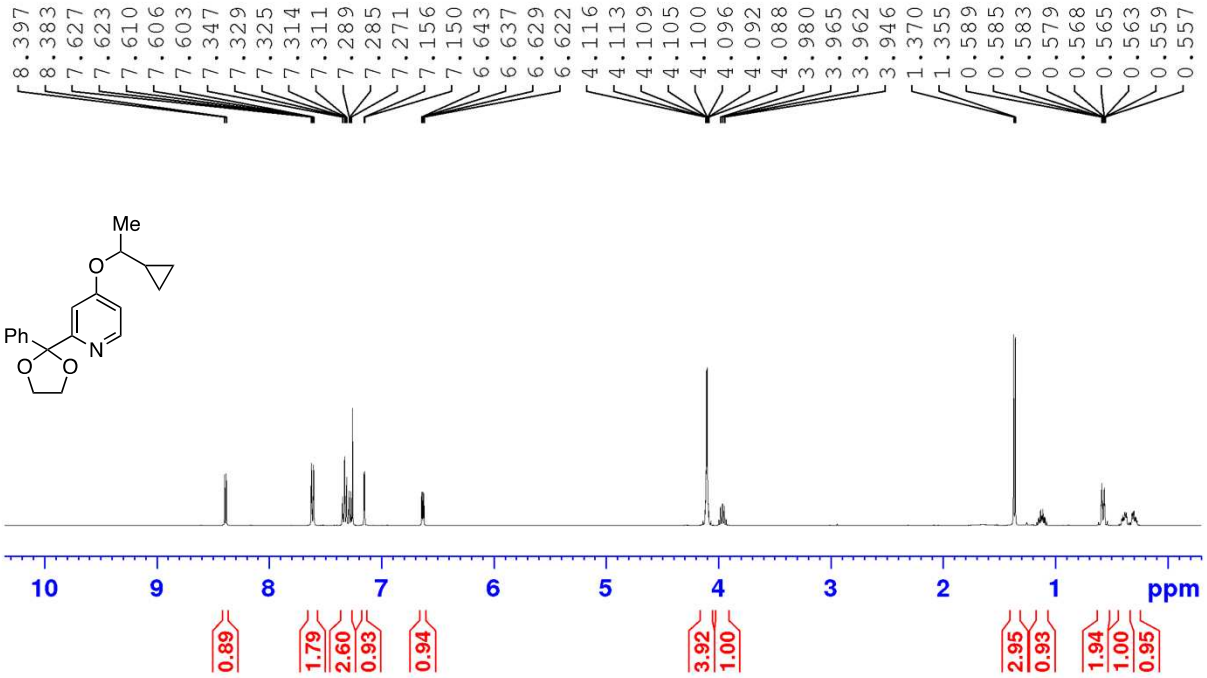

^{1}H NMR spectrum ($CDCl_3$, 400 MHz)

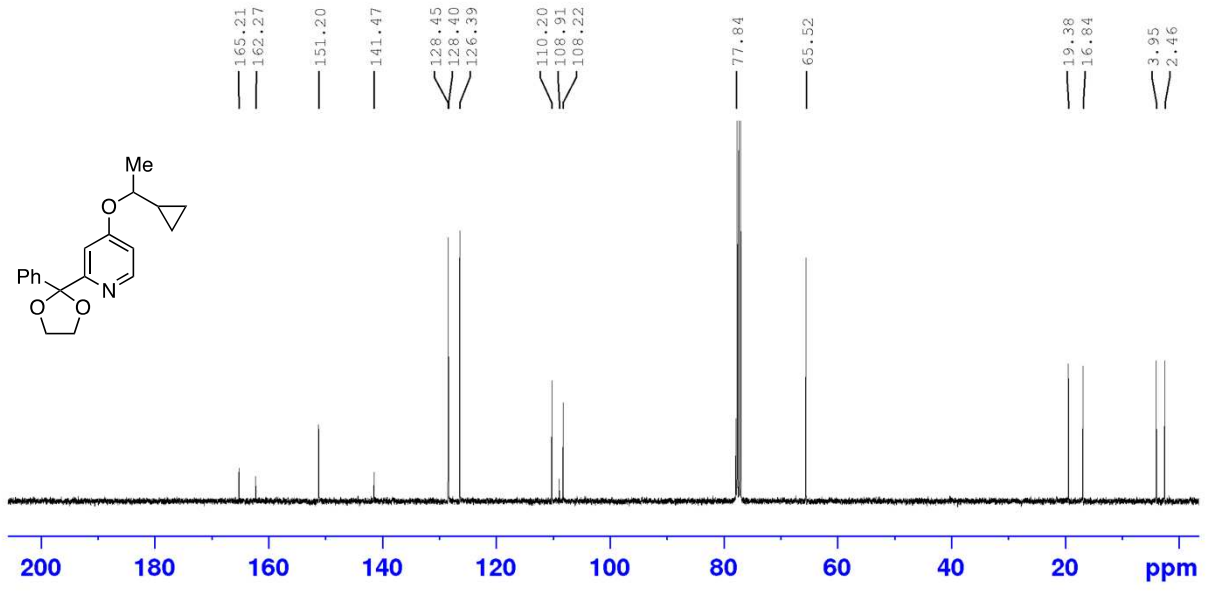

^{13}C NMR spectrum ($CDCl_3$, 101 MHz)

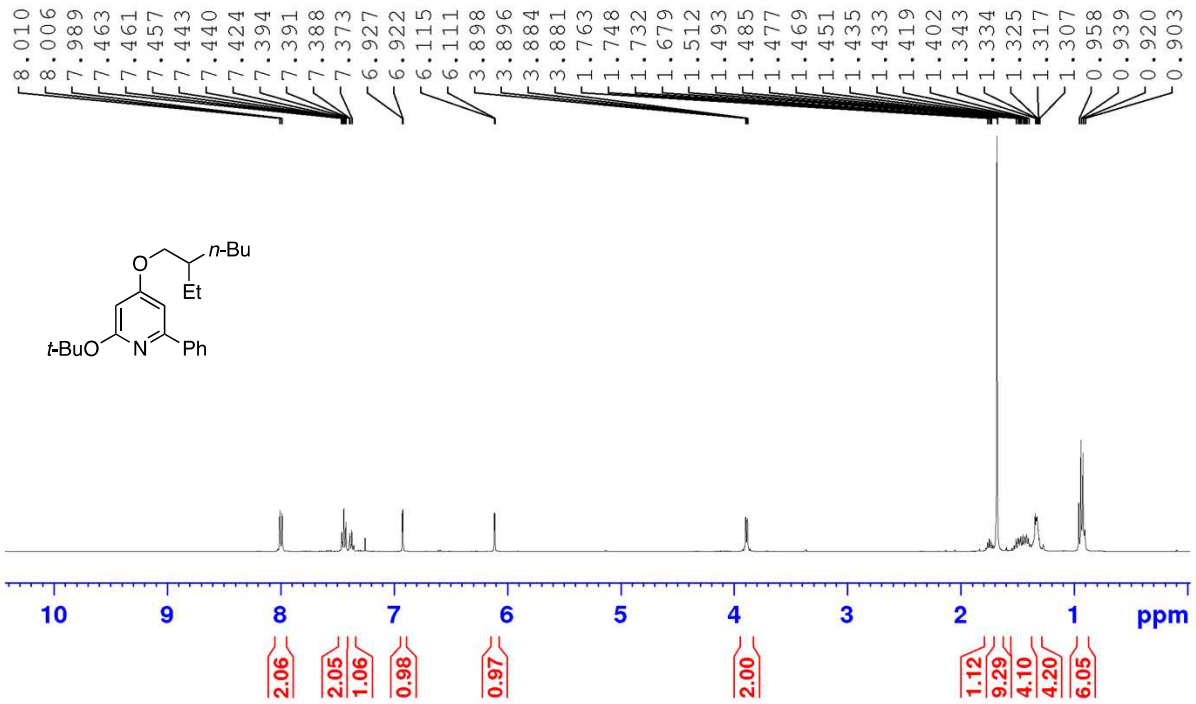

^{1}H NMR spectrum ($CDCl_3$, 400 MHz)

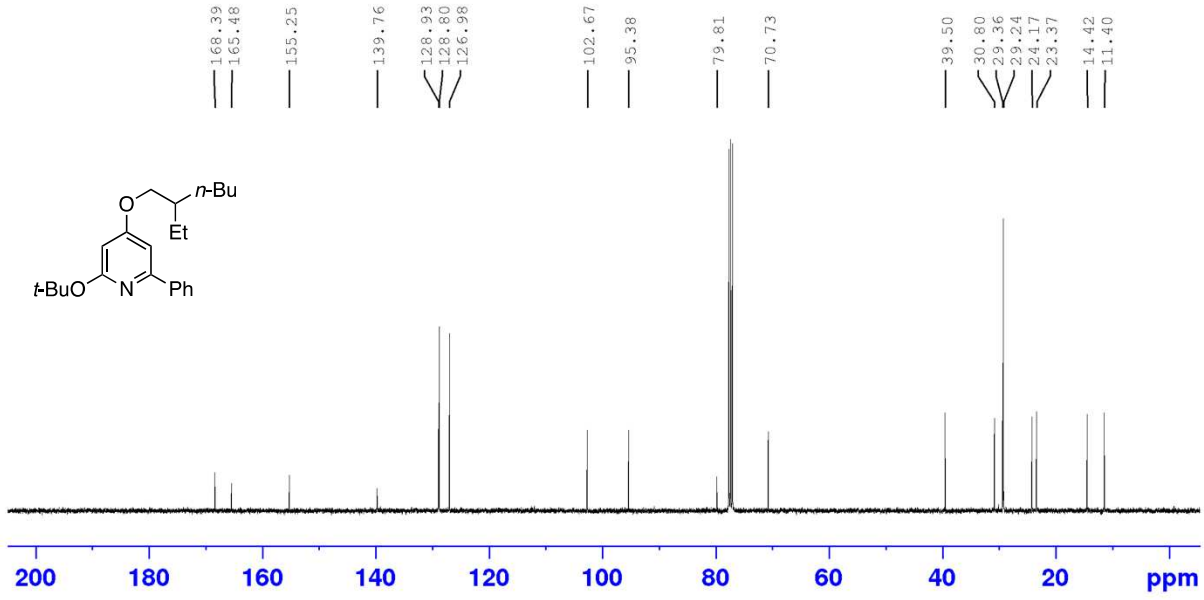

^{13}C NMR spectrum ($CDCl_3$, 101 MHz)

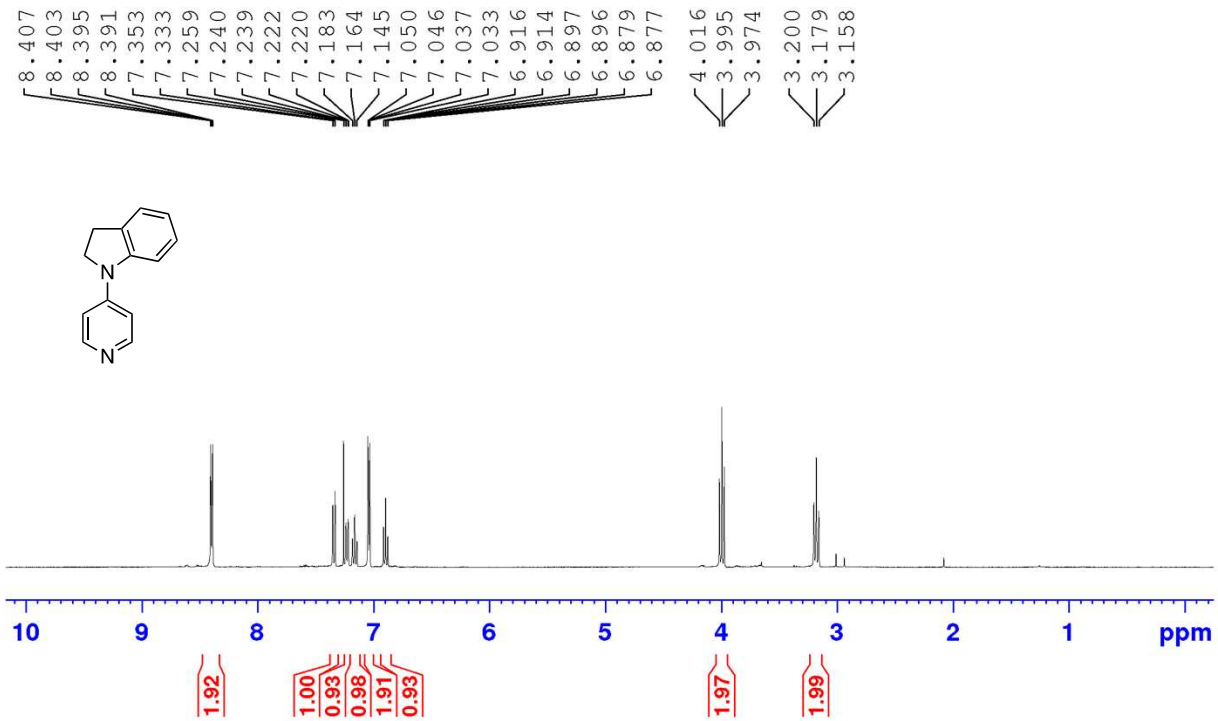

^{1}H NMR spectrum (400 MHz, $CDCl_3$)

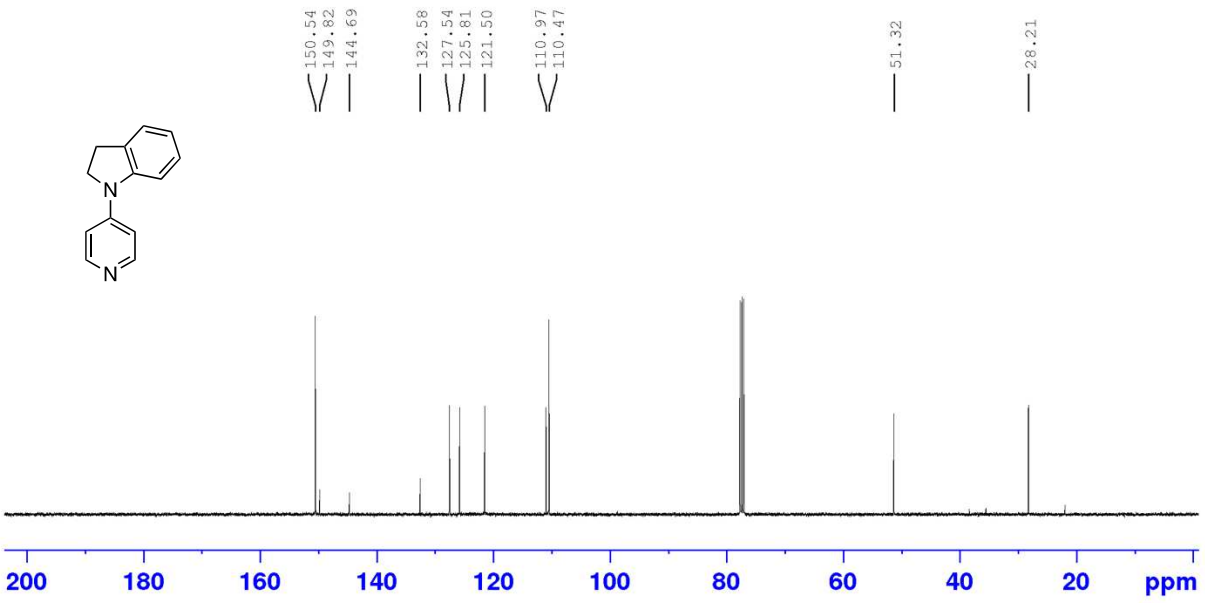

^{13}C NMR spectrum (101 MHz, $CDCl_3$)

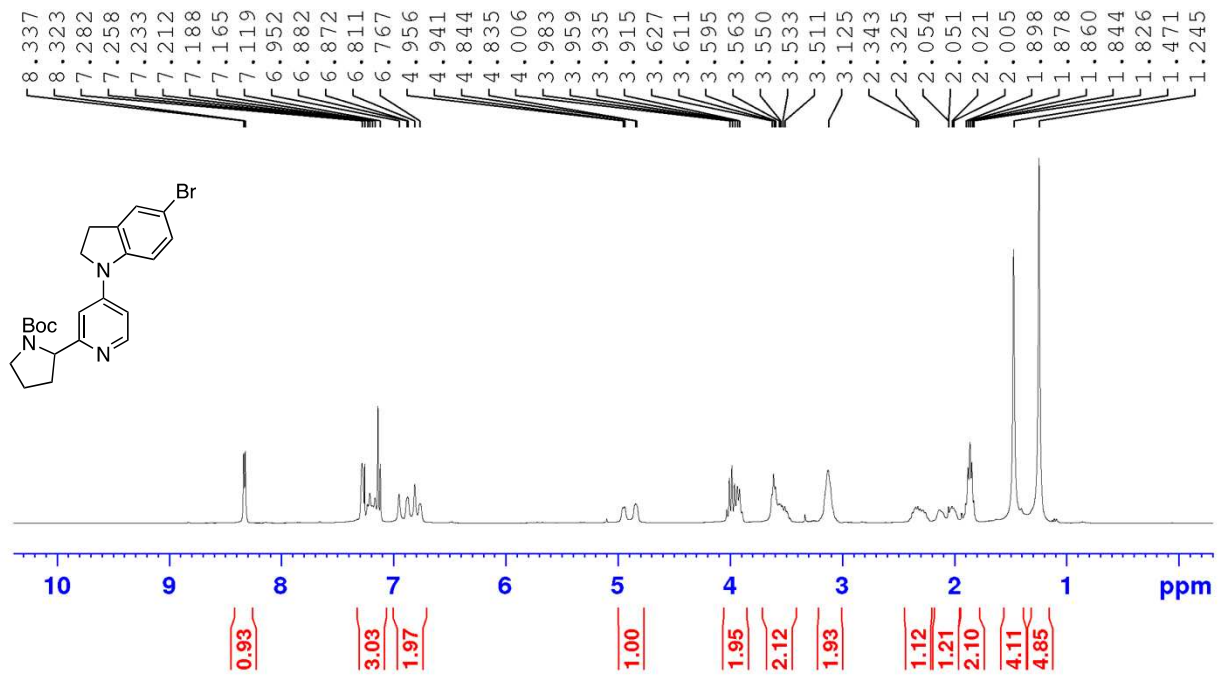

^{1}H NMR spectrum ($CDCl_3$, 400 MHz)

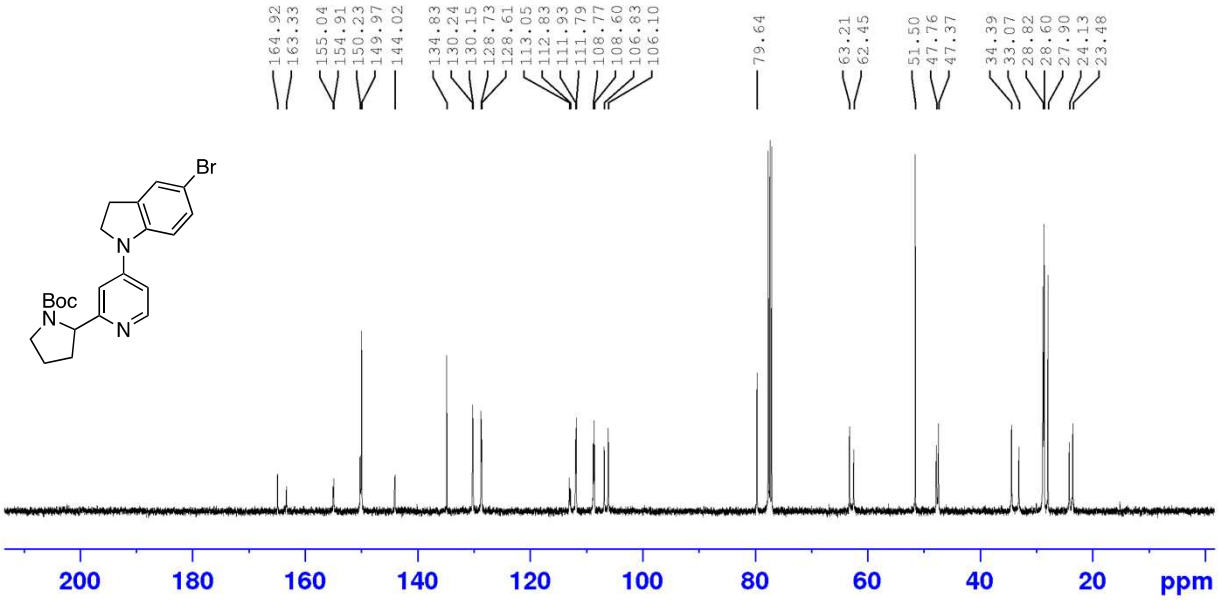

^{13}C NMR spectrum ($CDCl_3$, 101 MHz)

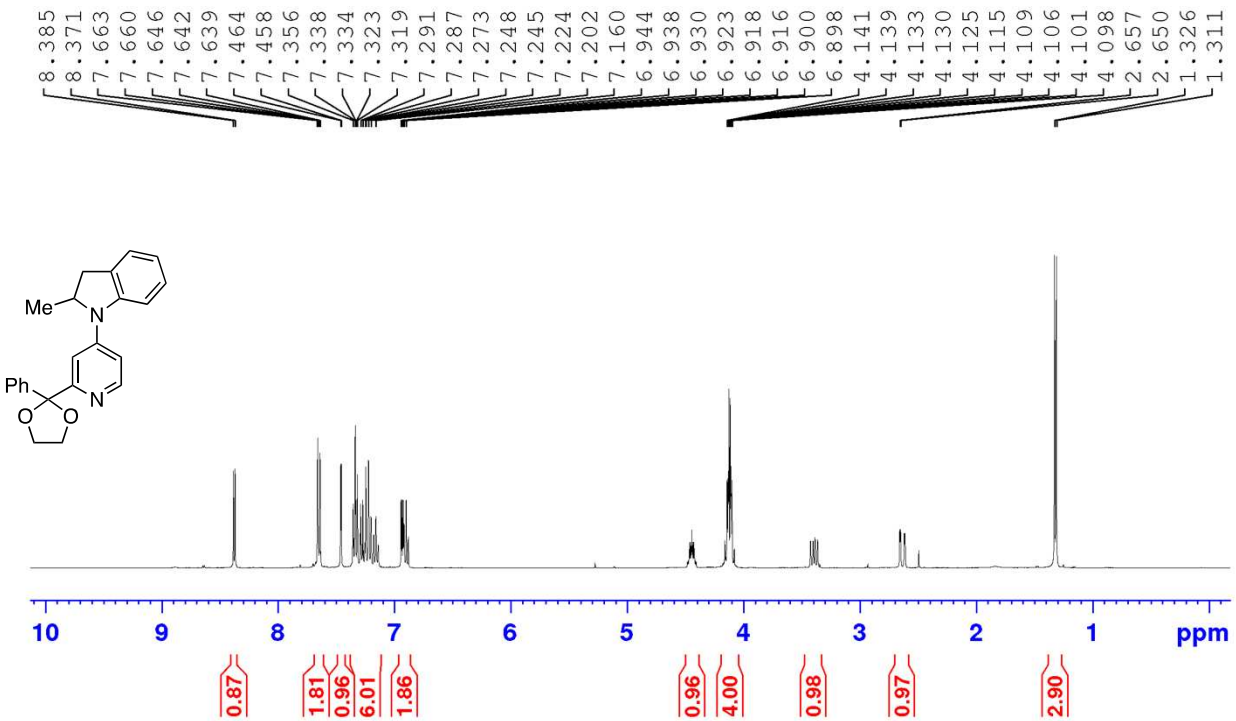

^{1}H NMR spectrum ($CDCl_3$, 400 MHz)

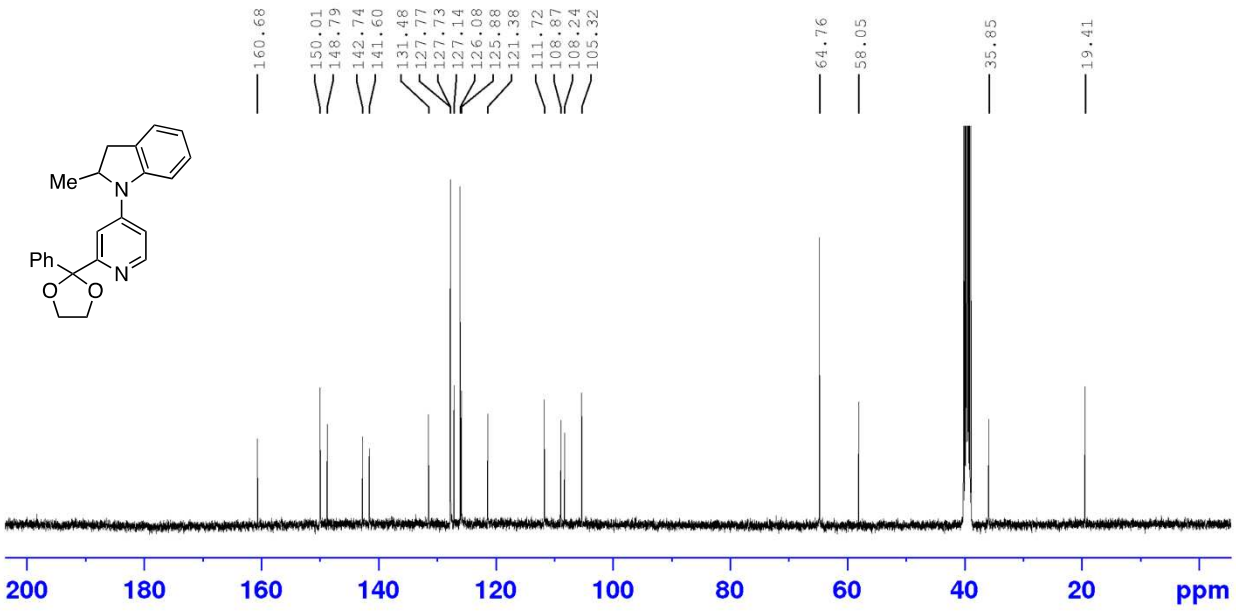

^{13}C NMR spectrum (d_6-DMSO, 101 MHz)

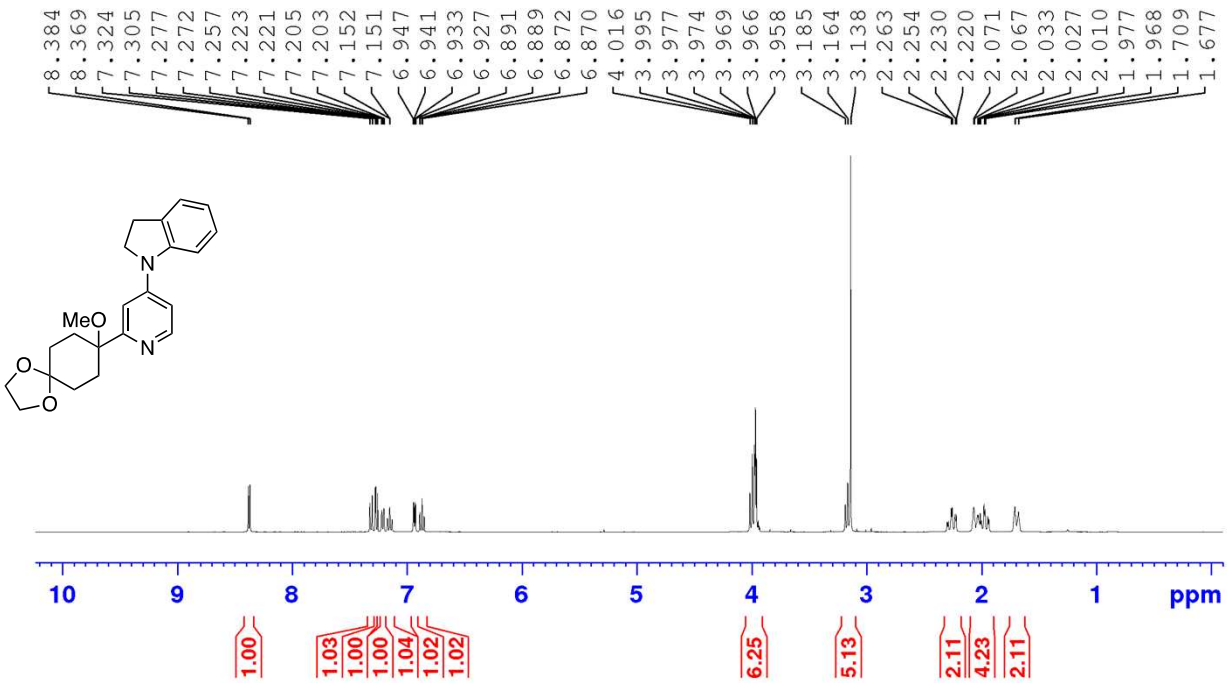

^{1}H NMR spectrum ($CDCl_3$, 400 MHz)

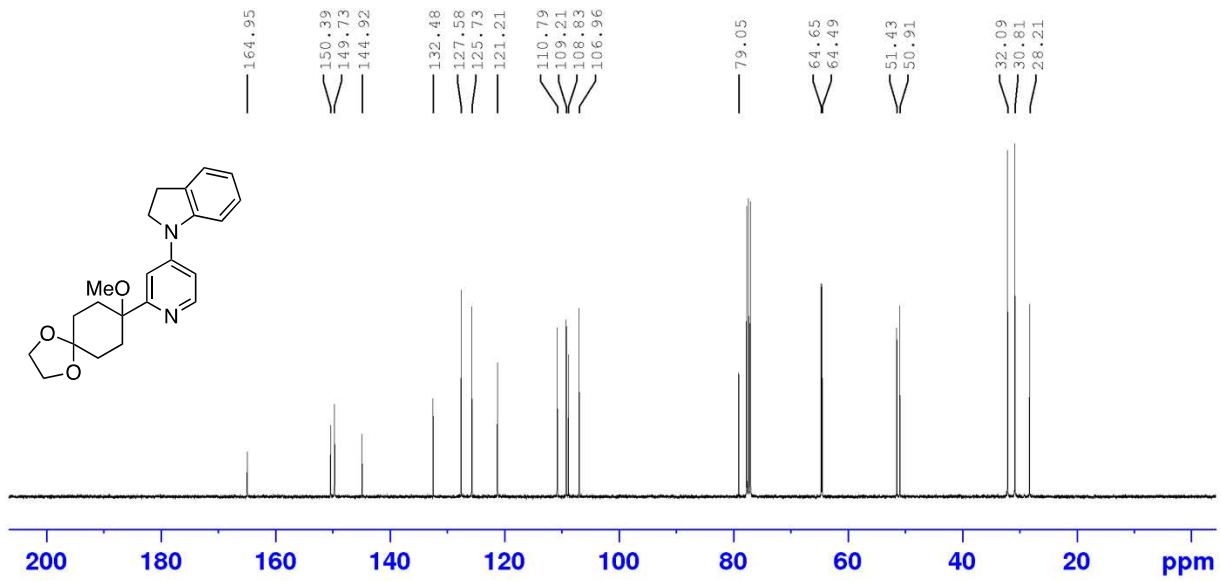

^{13}C NMR spectrum ($CDCl_3$, 101 MHz)

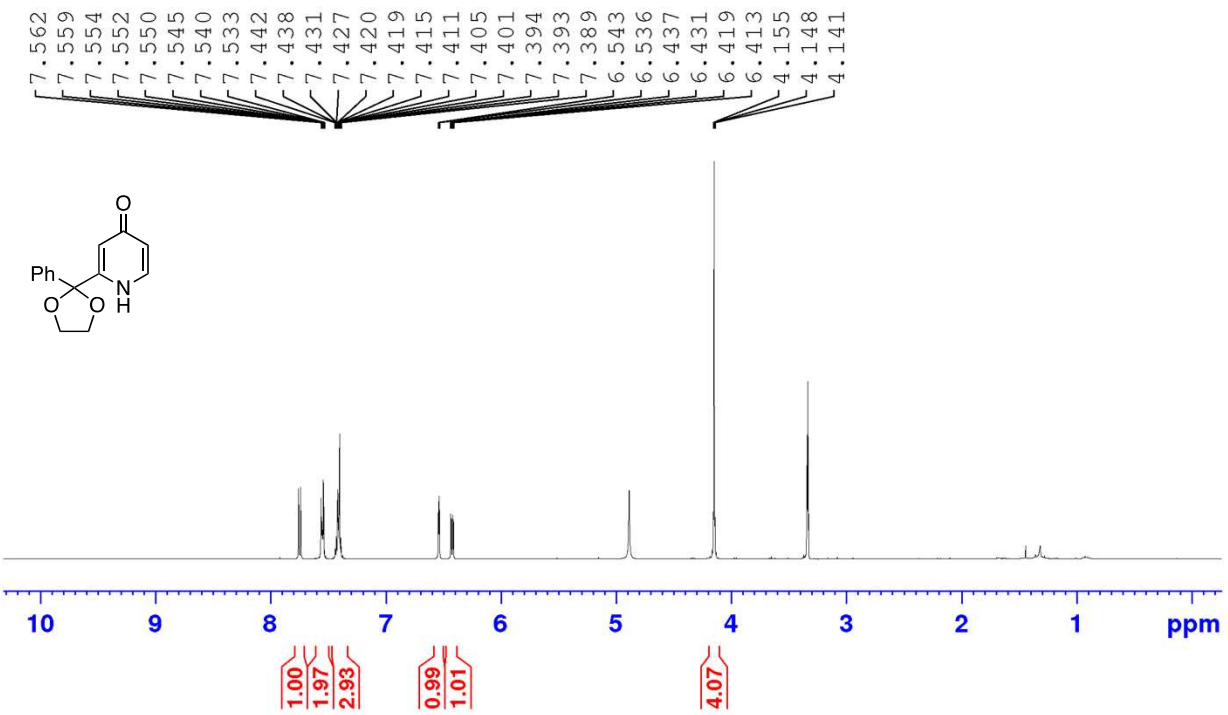

^{1}H NMR spectrum (CD_3OD, 400 MHz)

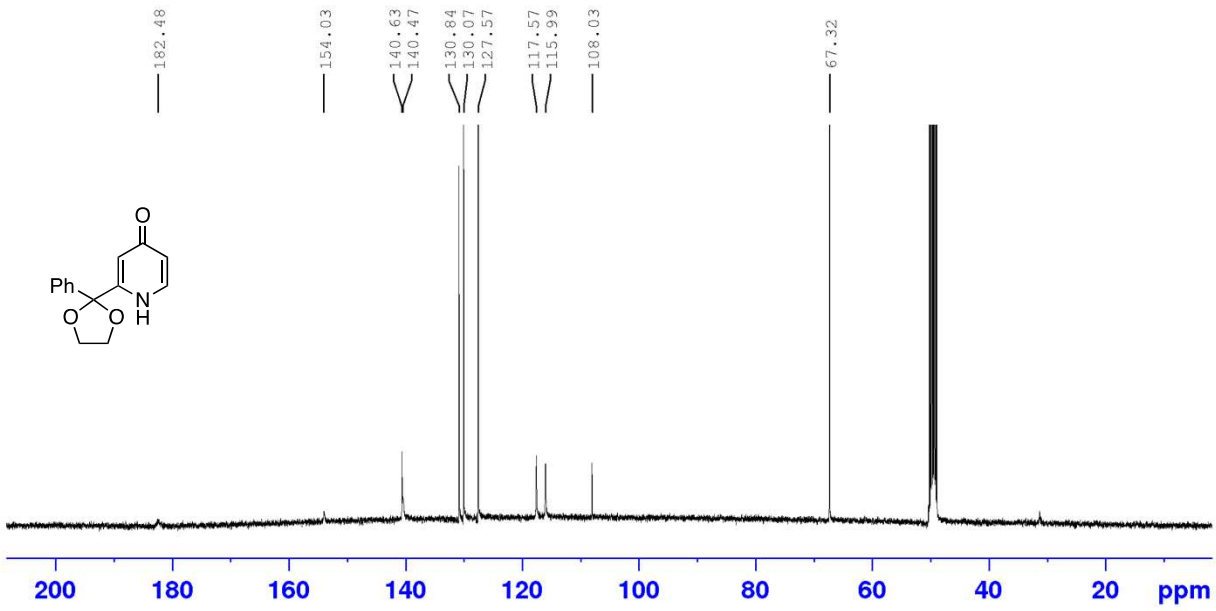

^{13}C NMR spectrum (CD_3OD, 101 MHz)

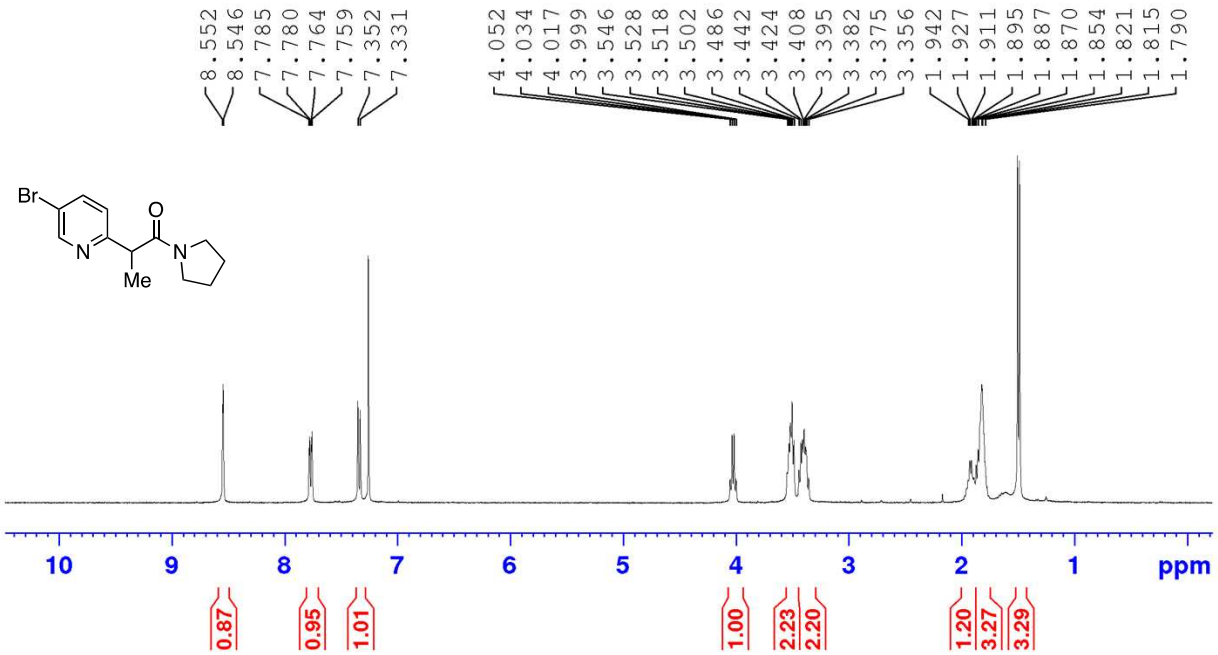

^{1}H NMR spectrum of 2-(5-bromopyridin-2-yl)-1-(pyrrolidin-1-yl)propan-1-one ($CDCl_3$, 400 MHz)

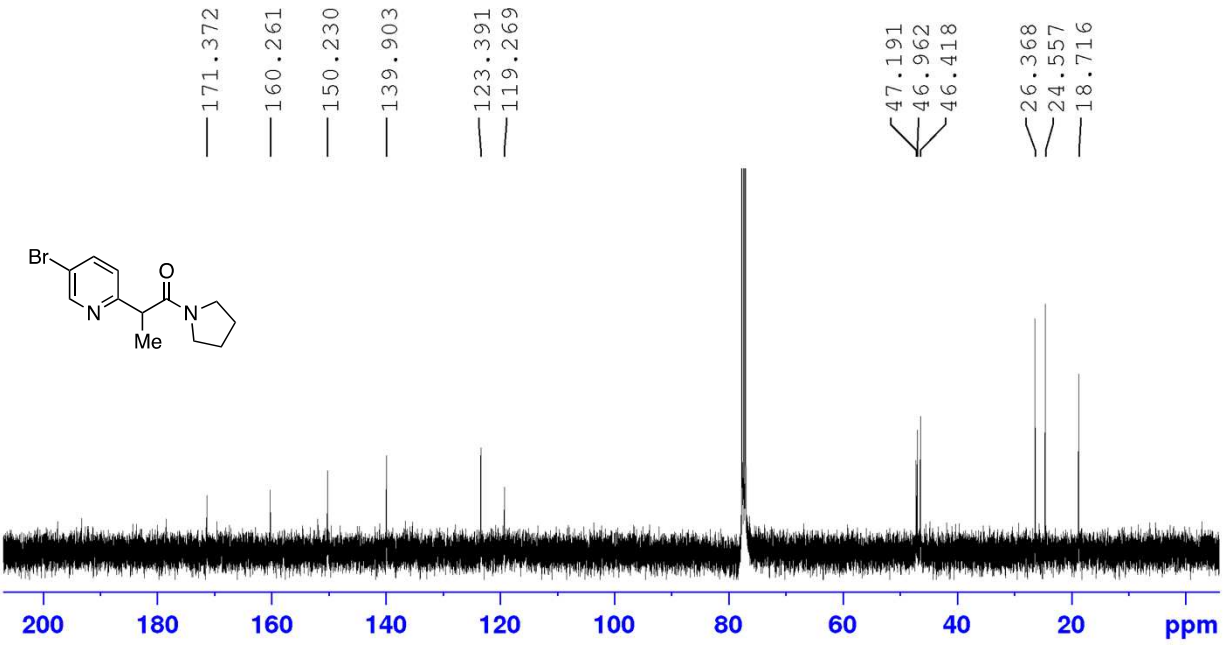

^{13}C NMR spectrum of 2-(5-bromopyridin-2-yl)-1-(pyrrolidin-1-yl)propan-1-one ($CDCl_3$, 101 MHz)

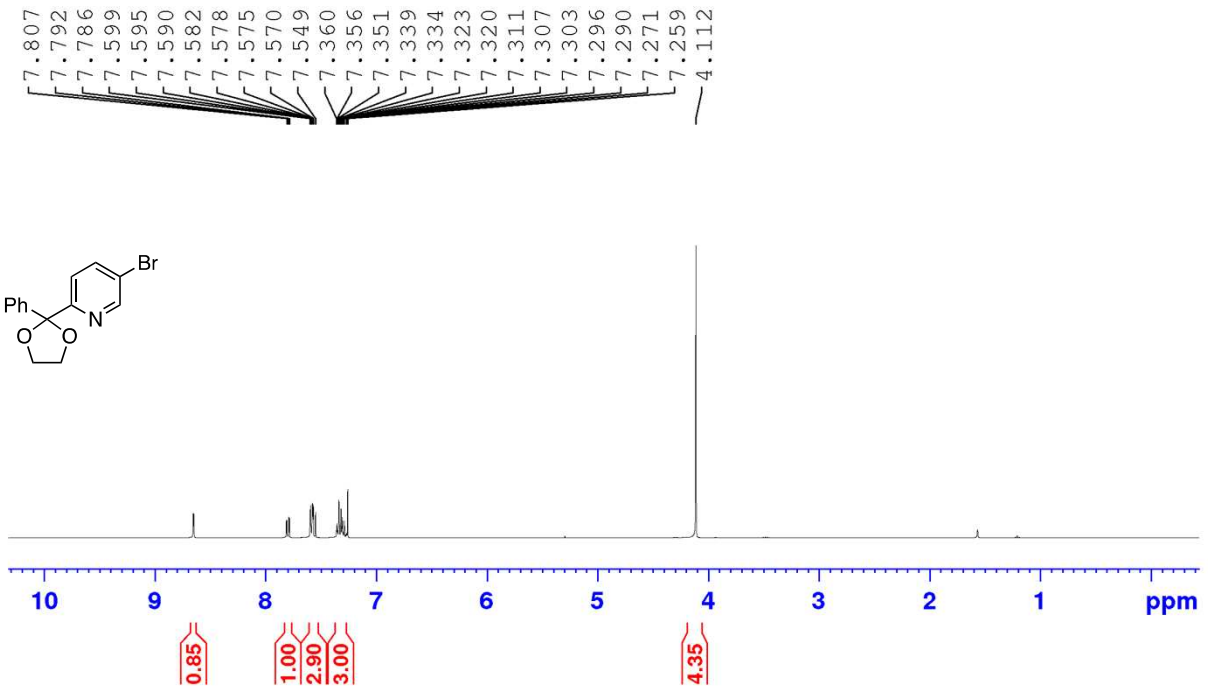

^{1}H NMR spectrum of 5-bromo-2-(2-phenyl-1,3-dioxolan-2-yl)pyridine ($CDCl_3$, 400 MHz)

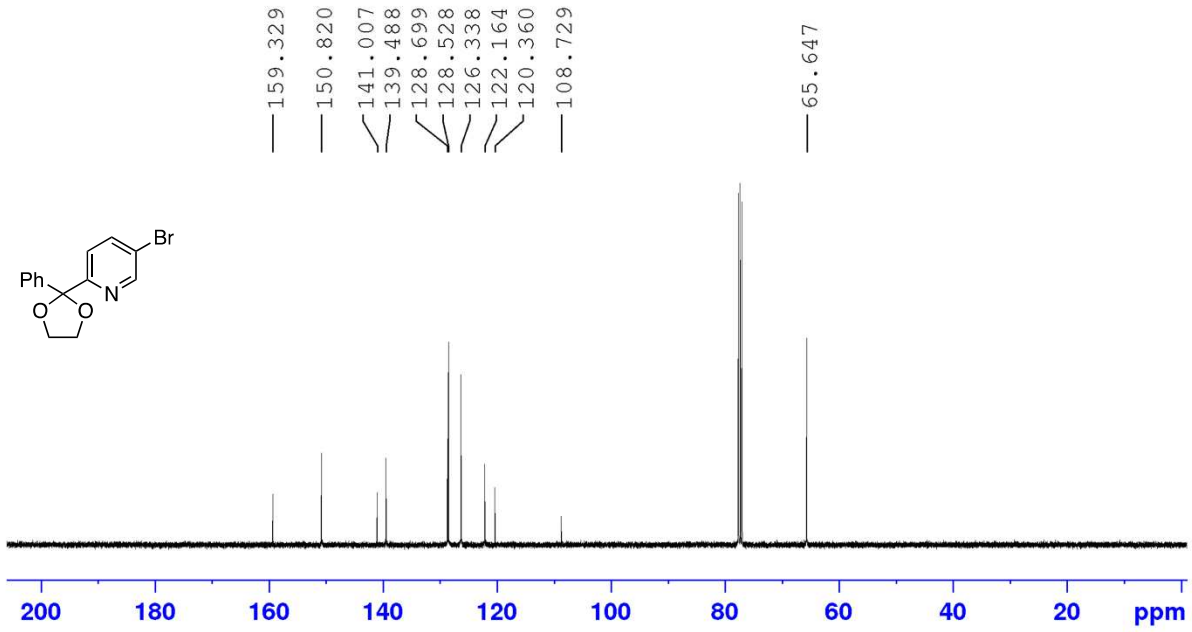

^{13}C NMR spectrum of 5-bromo-2-(2-phenyl-1,3-dioxolan-2-yl)pyridine ($CDCl_3$, 101 MHz)

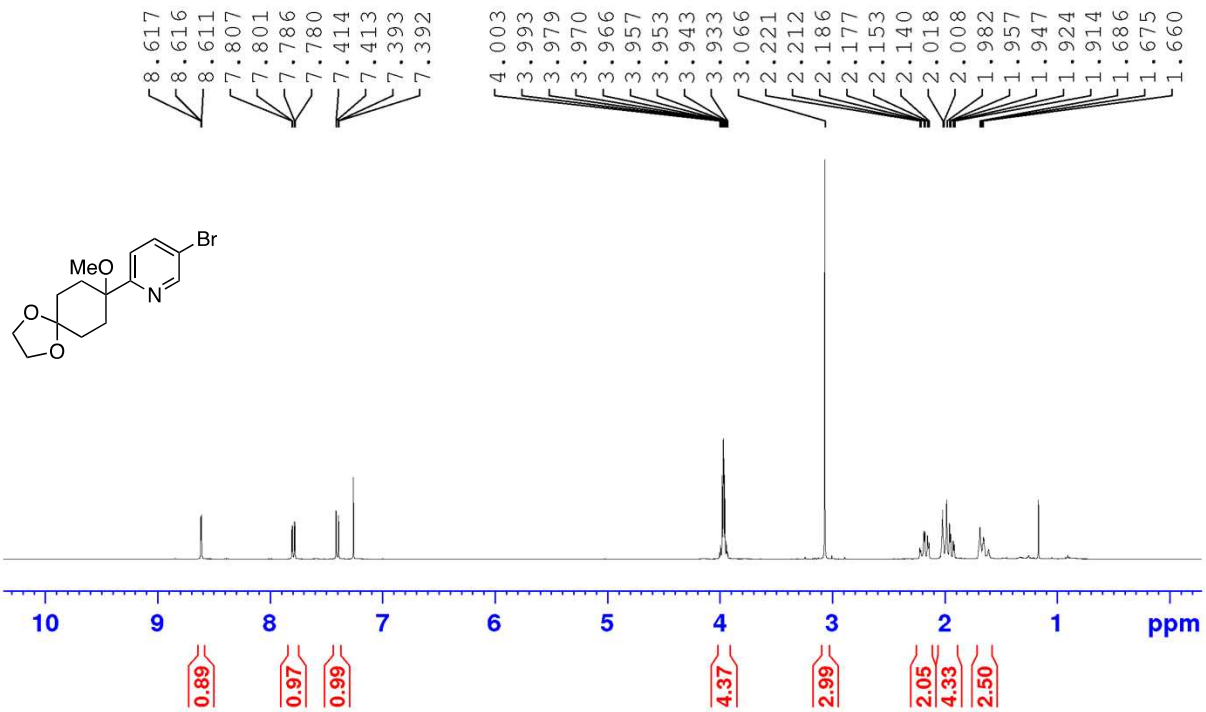

^{1}H NMR spectrum of 5-bromo-2-(8-methoxy-1,4-dioxaspiro[4.5]decan-8-yl)pyridine ($CDCl_3$, 400 MHz)

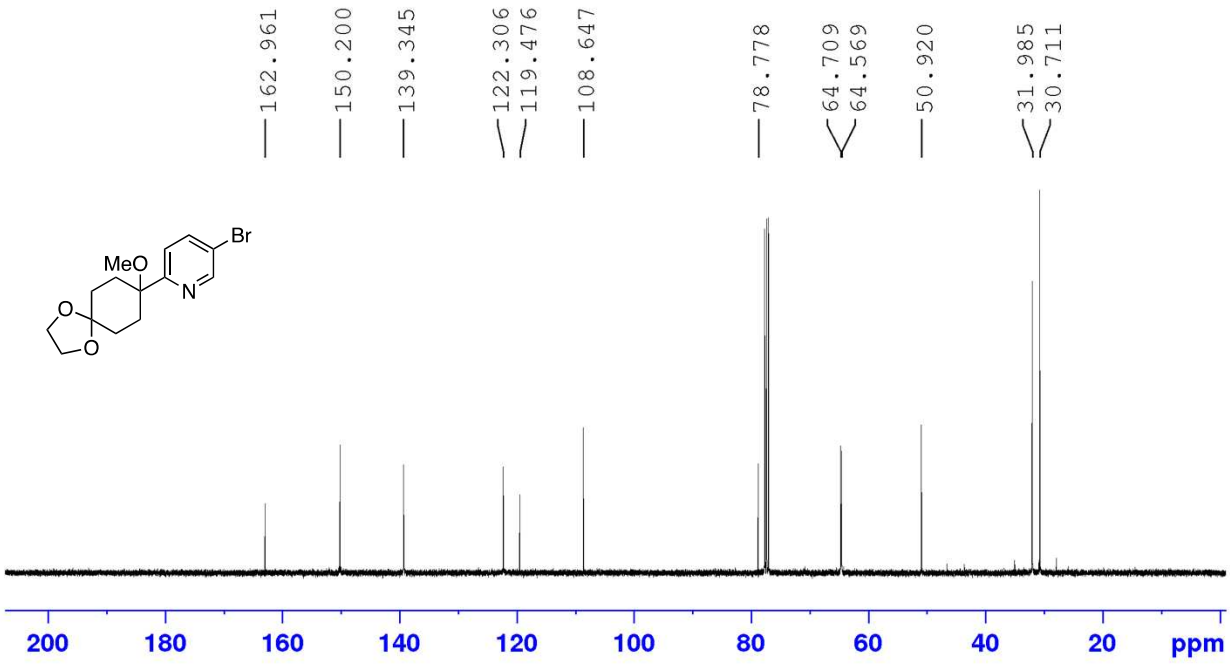

^{13}C NMR spectrum of 5-bromo-2-(8-methoxy-1,4-dioxaspiro[4.5]decan-8-yl)pyridine ($CDCl_3$, 101 MHz)

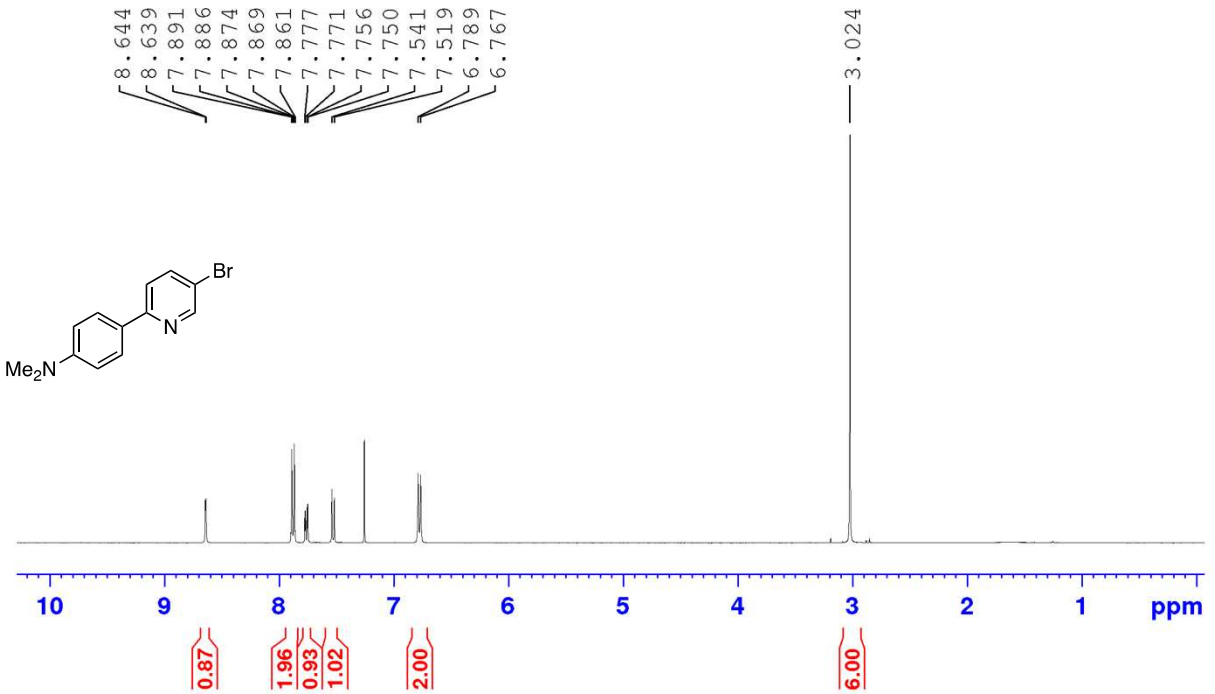

^{1}H NMR spectrum of 4-(5-bromopyridin-2-yl)-*N*,*N*-dimethylaniline ($CDCl_3$, 400 MHz)

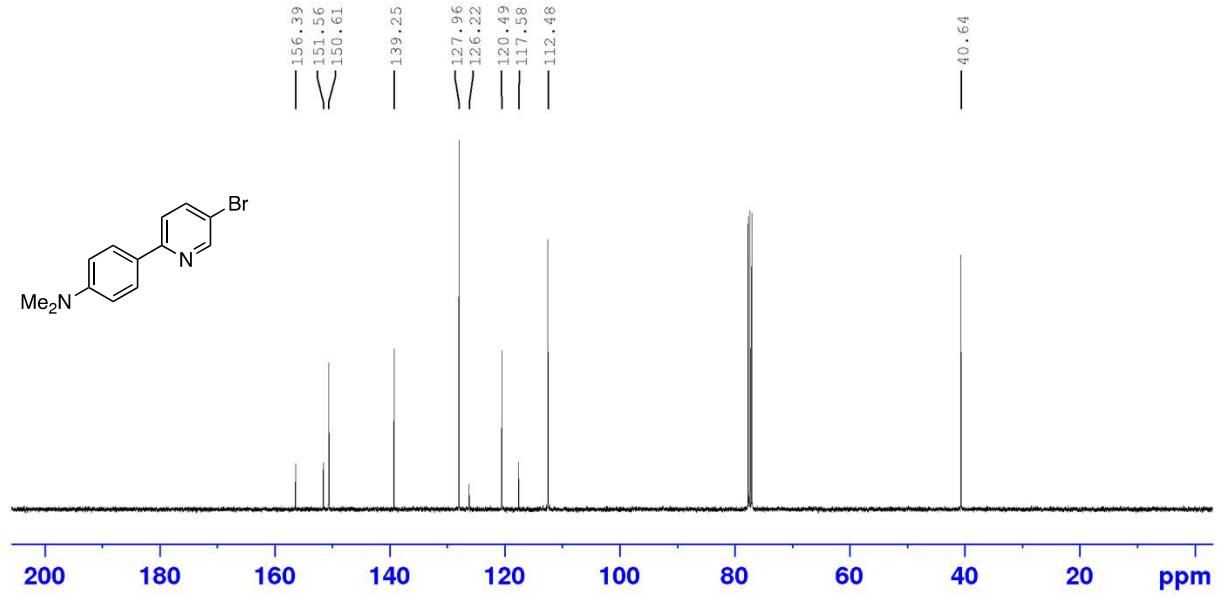

^{13}C NMR spectrum of 4-(5-bromopyridin-2-yl)-*N*,*N*-dimethylaniline ($CDCl_3$, 101 MHz)

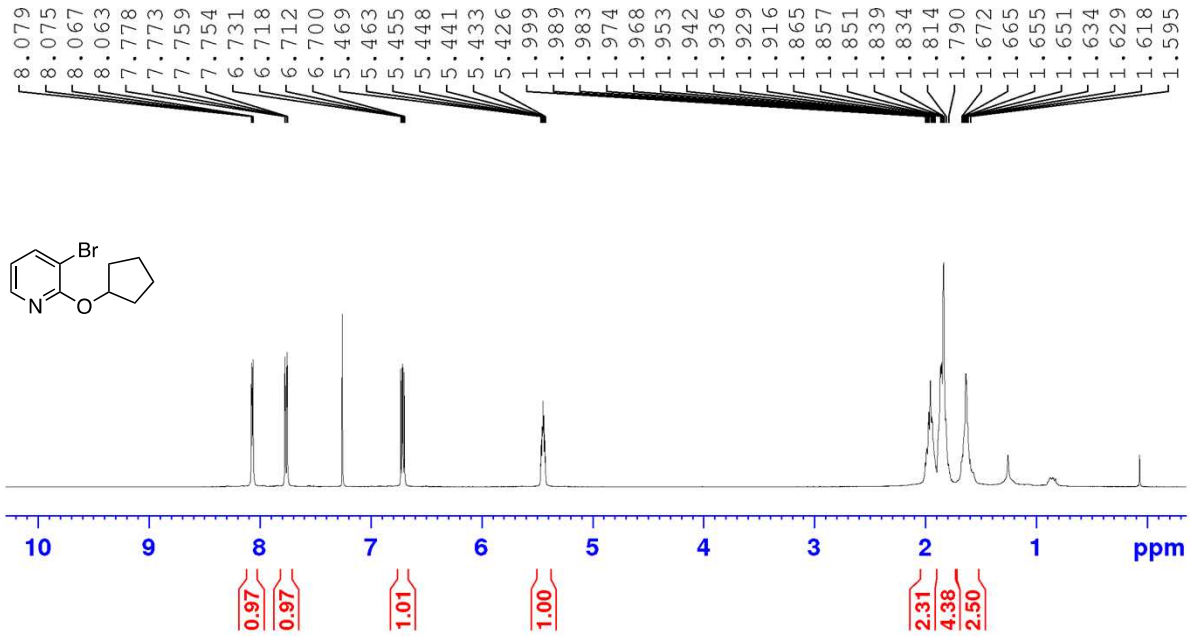

^{1}H NMR spectrum of 3-bromo-2-(cyclopentyloxy)pyridine ($CDCl_3$, 400 MHz)

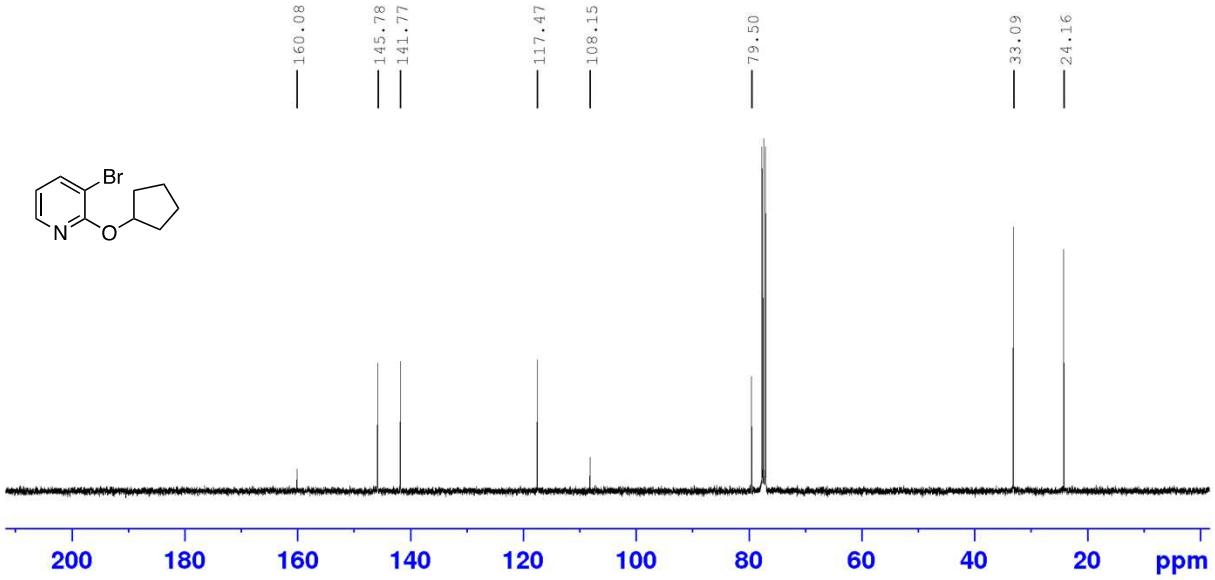

^{13}C NMR spectrum of 3-bromo-2-(cyclopentyloxy)pyridine ($CDCl_3$, 101 MHz)

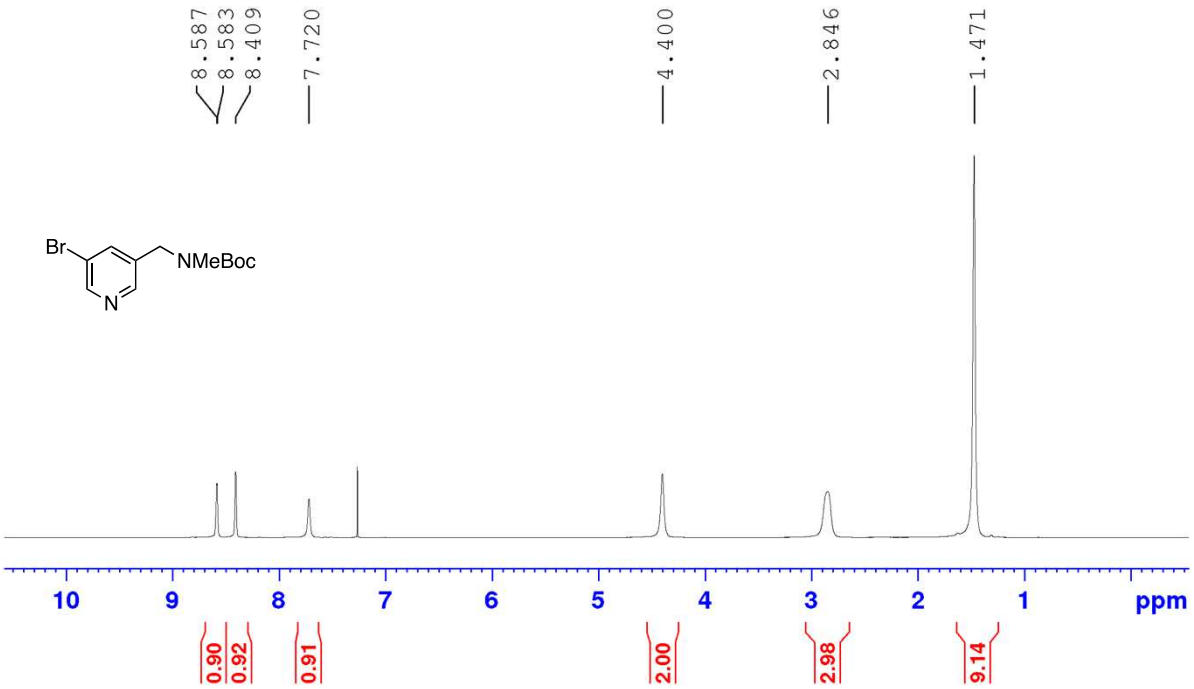

^{1}H NMR spectrum of *tert*-butyl ((5-bromopyridin-3-yl)methyl)(methyl)carbamate ($CDCl_3$, 400 MHz)

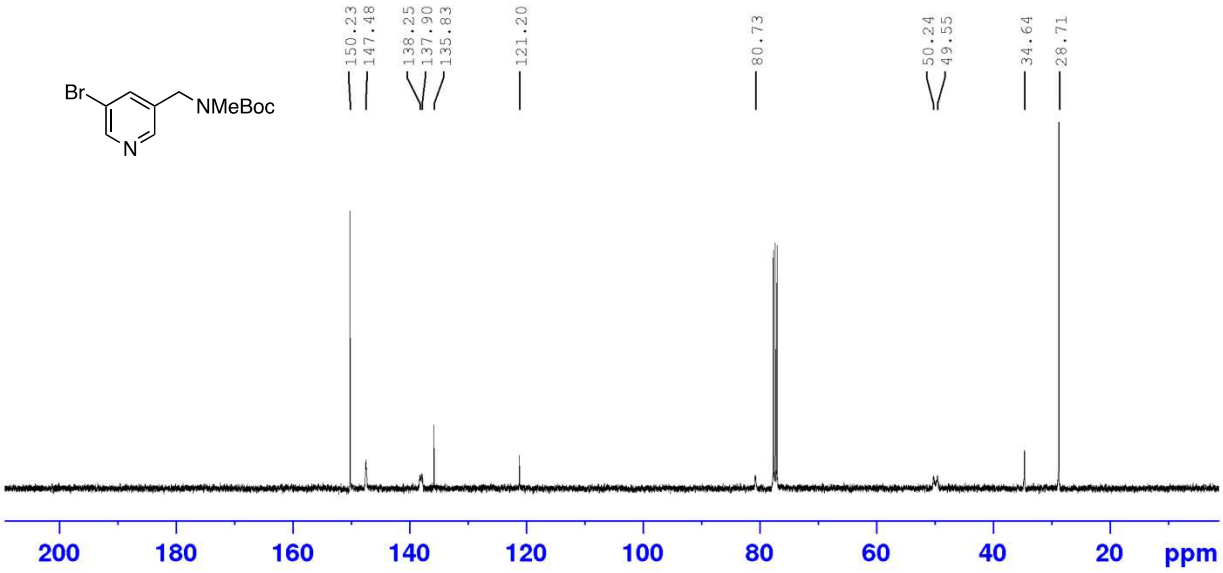

^{13}C NMR spectrum of *tert*-butyl ((5-bromopyridin-3-yl)methyl)(methyl)carbamate ($CDCl_3$, 101 MHz)

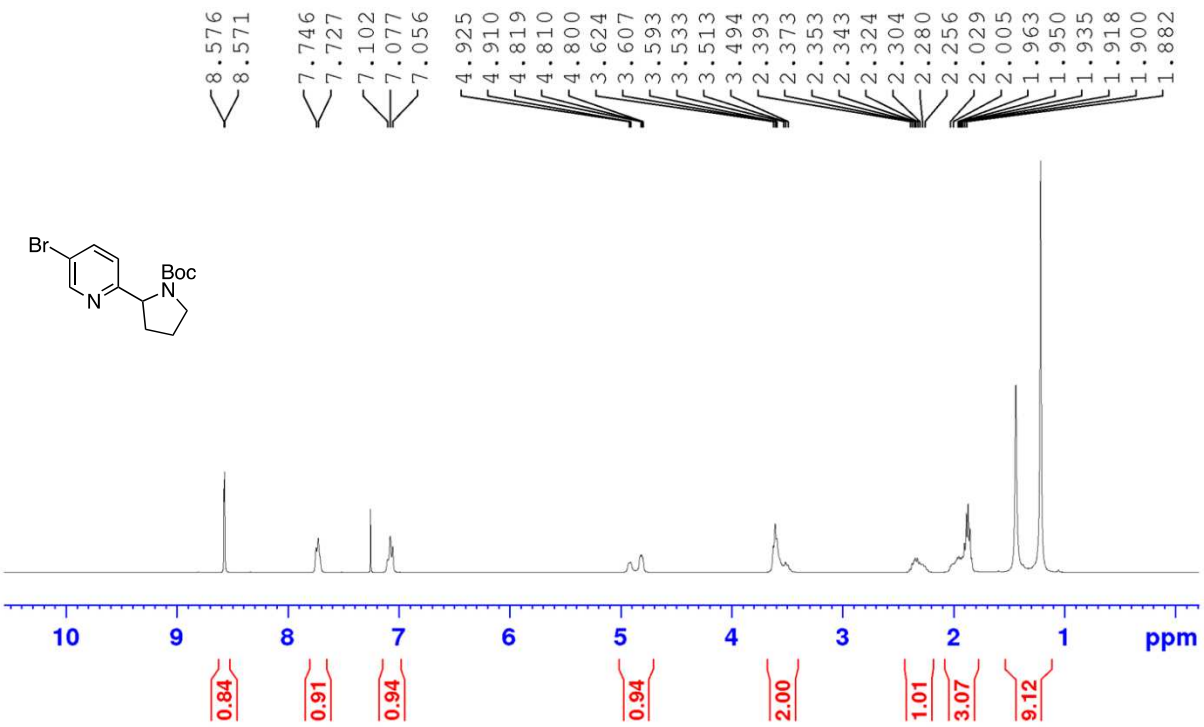

^{1}H NMR spectrum of *tert*-butyl 2-(5-bromopyridin-2-yl)pyrrolidine-1-carboxylate ($CDCl_3$, 400 MHz)

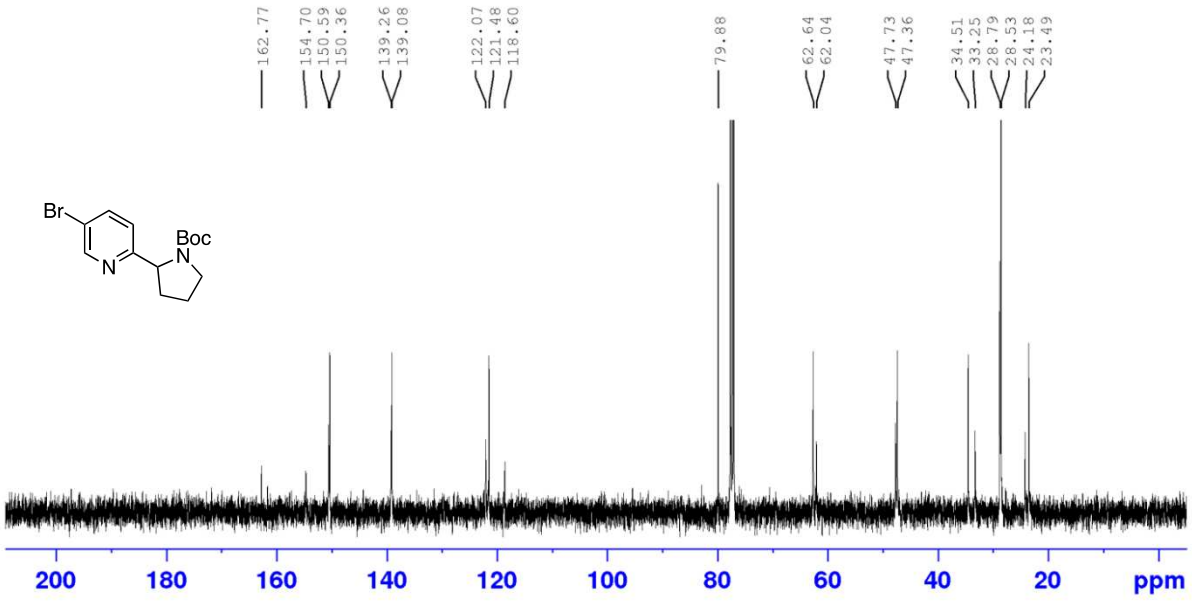

^{13}C NMR spectrum of *tert*-butyl 2-(5-bromopyridin-2-yl)pyrrolidine-1-carboxylate ($CDCl_3$, 101 MHz)

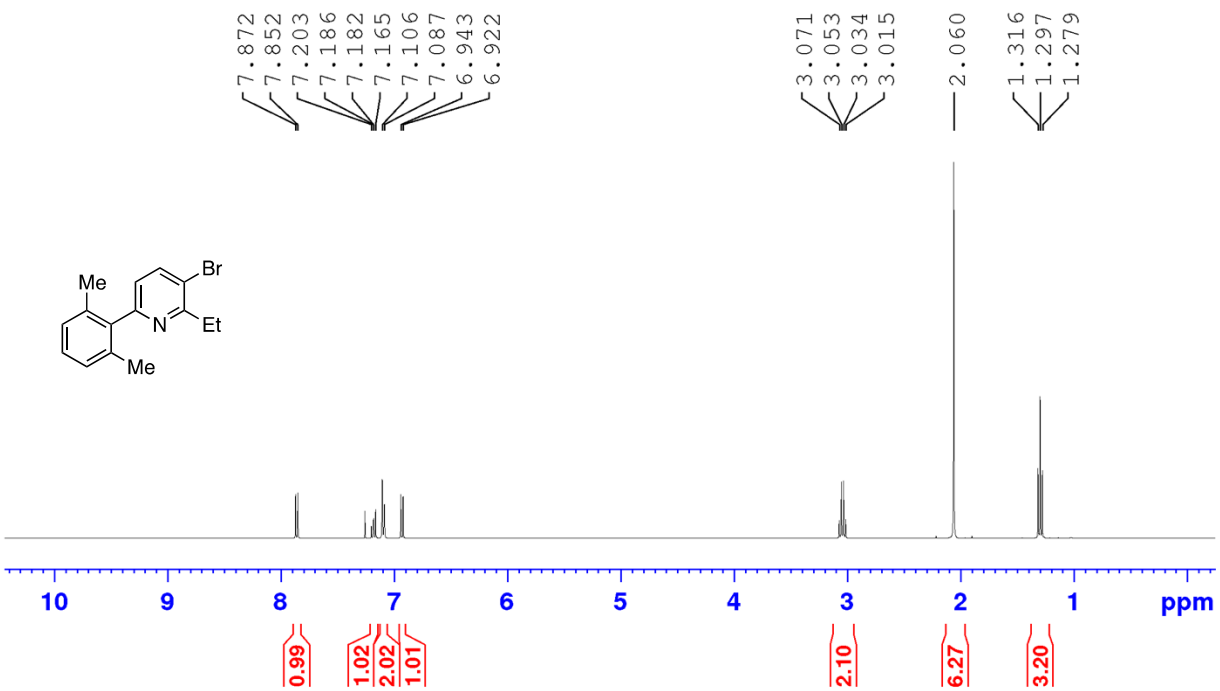

^{1}H NMR spectrum of 3-bromo-6-(2,6-dimethylphenyl)-2-ethylpyridine ($CDCl_3$, 400 MHz)

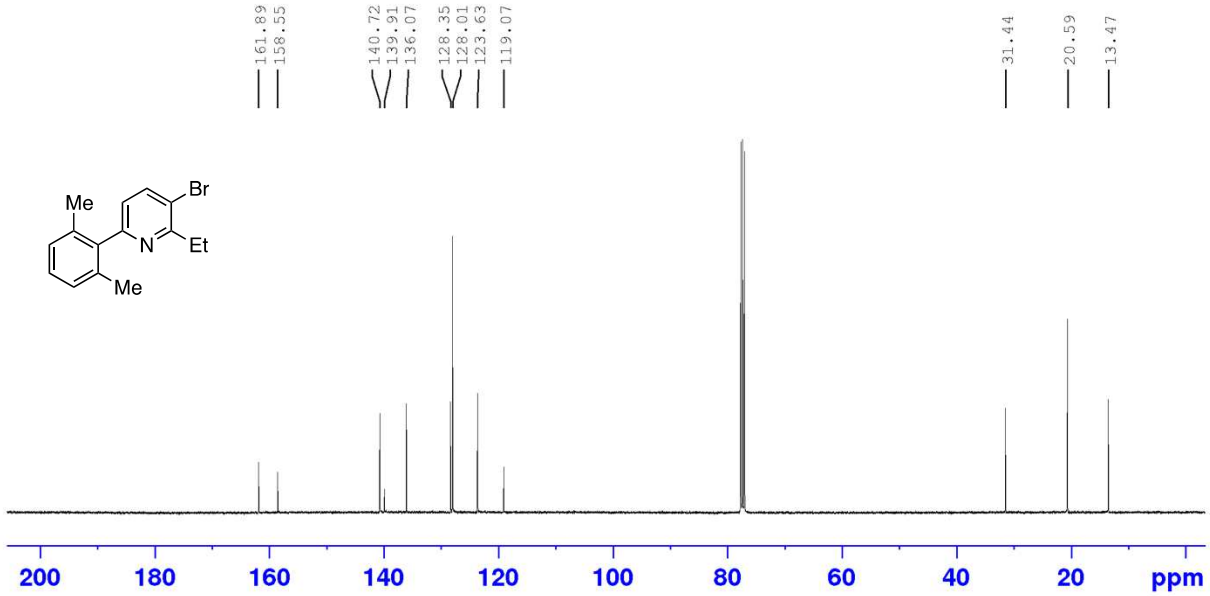

^{13}C NMR spectrum of 3-bromo-6-(2,6-dimethylphenyl)-2-ethylpyridine ($CDCl_3$, 101 MHz)

APPENDIX THREE

NUCLEOPHILIC C–H ETHERIFICATION OF *N*-HETEROARENES ENABLED BY BASE-CATALYZED HALOGEN TRANSFER: EXPERIMENTAL

A3.1 General Information

General Reagent Information: All reactions were performed under a nitrogen (N_2) atmosphere unless otherwise noted. Thiazole (Catalog #ST-5418) was purchased from Combi-Blocks and used as received. Potassium *tert*-butoxide (KO-*t*-Bu) was purchased from Chem-Impex (Catalog #27317) as a 99.8% pure powder and used as received. 1,4,7,10,13,16-Hexaoxacyclooctadecane (18-crown-6) was purchased from Chem-Impex (Catalog #03901) and used as received. Anhydrous 2-ethyl-1-hexanol was purchased from Sigma-Aldrich (Catalog #538051) and stored over oven-dried 4 Å molecular sieves. 3-Bromopyridine was purchased from Chem-Impex (Catalog #27044) and used as received. 2,5-Dibromothiophene was purchased from Matrix Scientific (Catalog #004596) and used as received. 2-Iodothiophene was purchased from Combi-Blocks (Catalog #OR-1024) and used as received. KO-*t*-Bu and 18-crown-6 were stored at room temperature (rt) inside a N_2 filled glovebox and used immediately if brought outside the glovebox. Tetrahydrofuran (THF) was deoxygenated and dried by passage over packed columns of neutral alumina and copper (II) oxide under positive pressure of N_2. All other solvents and reagents were purchased from Millipore Sigma, Combi-Blocks, TCI, Acros Organics, Matrix Scientific, Alfa-Aesar, or Synthonix and used as received unless otherwise noted. Flash chromatography was performed on 40-63 μm silica gel (SiliaFlash® F60 from Silicycle). Preparative thin-layer chromatography (PTLC) was performed on silica gel 60 Å F_{254} plates (20 x 20 cm, 1000 μm, SiliaPlate from Silicycle, #TLG-R10011B-341) and visualized with UV light (254 nm). Celite® 545 (Product # CX0574-3) was purchased from Millipore Sigma.

General Analytical Information: All reported compounds were characterized by ^{1}H, ^{13}C, and ^{19}F (if applicable) NMR spectroscopy, FTIR spectroscopy and mass spectrometry. Melting point analysis was conducted if the compound was solid. ^{1}H NMR, ^{13}C NMR, and ^{19}F NMR spectra were obtained on a Bruker NEO400, Bruker US400, Bruker Ascend 400, or Varian Inova 400 spectrometer. ^{1}H NMR data is reported as follows: chemical shift (δ ppm), multiplicity (s = singlet, br s = broad singlet, d = doublet, t = triplet, q = quartet, dd = doublet of doublets, td = triplet of doublets, m = multiplet), coupling constant (Hz), and integration. ^{13}C NMR data is reported as follows: chemical shift (δ ppm), multiplicity (if applicable, d = doublet, t = triplet, q = quartet), and coupling constant (Hz). All ^{1}H NMR signals are reported as chemical shifts (δ ppm) relative to residual $CHCl_3$ at 7.26 ppm.[1] ^{13}C NMR signals are reported as chemical shifts (δ ppm) relative to $CDCl_3$ at 77.16 ppm.[1] ^{19}F NMR signals are reported as chemical shifts relative to added α,α,α-trifluorotoluene internal standard calibrated to -63.72 ppm. High resolution mass spectra (HRMS) were recorded on an Agilent 6210 TOF interfaced to a DART 100 source or an Agilent 6230 LC-MS B-TOF equipped with a dual ESI source provided by Colorado State University Materials and Molecular Analysis Center. IR spectra were recorded using a Thermo Scientific Nicolet iS-50 FTIR Spectrometer and reported as frequency of absorption (cm^{-1}). Samples were sent to Atlantic Microlab in Norcross, GA for combustion elemental analysis and analyzed for carbon, hydrogen, and nitrogen composition. Melting point analyses were conducted using a Mel-Temp capillary melting point apparatus. The specific rotation of chiral molecules was measured using a Rudolph Research Analytical Autopol III polarimeter. Thin-layer chromatography analysis was performed on silica gel 60 Å F_{254} plates (250 μm, SiliaPlate from Silicycle, #TLG-R10014B-323) and interpreted using UV light (254 nm). Preparatory thin-layer chromatography purification was

performed on silica gel 60 Å (1000 µm, Silicycle, #TLG-R10011B-341) and interpreted using UV light (254 nm).

Note on nomenclature: The names provided for the structures below were obtained from ChemDraw Professional 16.0.

A3.2 Optimization of C-H Etherification of 1,3-Azoles and (Di)Azines

a. Evaluation of optimal base, solvent, temperature, concentration, reaction time, and 2-bromothiophene structure for 2-selective thiazole C-H etherification

General procedure for condition variation: Inside an N_2 filled glovebox, an oven-dried 8 mL vial (Thermo Fisher Scientific, Product #033405P) was charged with a magnetic stir bar, thiazole (21.3 mg, 0.25 mmol, 1.0 equiv), 2-ethyl-1-hexanol (48.8 mg, 0.375 mmol, 1.5 equiv), 2-brominated thiophene (0.5 mmol, 2.0 equiv), anhydrous solvent (1.0 mL, 0.25 M), and base (0.375 mmol, 1.5 equiv) in that order. The vial was sealed with a screw cap (Thermo Fisher Scientific, Product #03392A) lined with a PTFE septum (Thermo Fisher Scientific, Product #B7995-15), removed from the glovebox, and placed into a preheated silicon oil bath at the indicated temperature and the reaction mixture was stirred for 3 h. The reaction solution was cooled to rt, then 1,3,5-trimethoxybenzene internal standard was weighed into the vial. For each experiment, the mass of 1,3,5-trimethoxybenzene weighed into the vial was recorded separately. ^{1}H NMR spectroscopy (400 MHz, $CDCl_3$) of the crude reaction solution was used to determine the yield of 2-((2-ethylhexyl)oxy)thiazole (**4**–**3**). The aromatic C-H signal of 1,3,5-trimethoxybenzene at 6.08 ppm was integrated against the aromatic C-H signal of **3** at 6.62 ppm to determine the yield. Each spectrum was calibrated to residual $CHCl_3$ at 7.26 ppm. The results are summarized in Figure A3–1 below. **Note:** for the optimized procedure (entry 1), no *tert*-butyl aryl ether (2-(*tert*-

butoxy)thiazole) was observed by ^{1}H NMR spectroscopy and MS analysis of the crude reaction mixture.

Standard Conditions

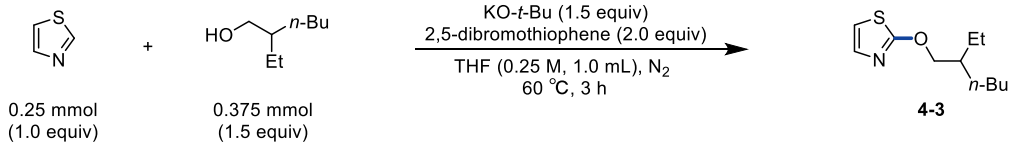

Entry	Change from the "standard conditions"	Yield
1	none	74%
2	rt for 12 h instead of 60 °C for 3 h	57%
3	NaO-*t*-Bu used instead of KO-*t*-Bu	8%
4	1.0 equiv of KO-*t*-Bu used instead of 1.5 equiv	64%
5	KO-*t*-Bu received from TCI used instead of KO-*t*-Bu from Chem-Impex	74%
6	KO-*t*-Bu received from Millipore Sigma used instead of KO-*t*-Bu from Chem-Impex	74%
7	cyclohexane used as solvent instead of THF	25%
8	PhMe used as solvent instead of THF	23%
9	DMSO used as solvent instead of THF	0%
10	1,4-dioxane used as solvent instead of THF	73%
11	0.5 M in THF instead of 0.25 M	70%
12	1.0 M in THF instead of 0.25 M	58%
13	no 2,5-dibromothiophene	0%
14	2,5-dibromothiophene received from Millipore Sigma used instead of 2,5-dibromothiophene from Matrix Scientific	75%
15	2-bromothiophene used instead of 2,5-dibromothiophene	16%
16	2,3,5-tribromothiophene used instead of 2,5-dibromothiophene	6%
17	2,3-dibromothiophene used instead of 2,5-dibromothiophene	29%
18	tetrabromothiophene used instead of 2,5-dibromothiophene	0%
19	2-iodothiophene used instead of 2,5-dibromothiophene[a]	0%
20	Reaction run open to air instead of under N_2	51%

Figure A3–1: Condition variation of base, solvent, temperature, concentration, reaction time, and 2-brominated thiophene for 2-selective thiazole C-H etherification. [a] Reaction of 2-iodothiazole with KO-*t*-Bu (1.5 equiv) and 2-ethylhexan-1-ol (1.5 equiv) in THF at 60 °C for 20 h produced no **4–3** and mostly protodeiodonated product was observed.

2-((2-ethylhexyl)oxy)thiazole (4–3)

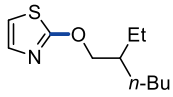

^{1}H NMR (400 MHz, $CDCl_3$) δ 7.12 (d, *J* = 3.8 Hz, 1H), 6.65 (d, *J* = 3.8 Hz, 1H), 4.29 (m, 2H), 1.75 (m, 1H), 1.36-1.53 (m, 4H), 1.25-1.35 (m, 4H), 0.88-0.95 (m, 6H). **^{13}C NMR** (101 MHz, $CDCl_3$) δ 175.7, 136.9, 110.8, 74.6, 39.3, 30.4, 29.1, 23.8, 23.1, 14.2,

11.1. **IR** (neat, cm^{-1}) 2958, 2929, 1521, 1460, 1308, 1233, 1164. **HRMS** (DART) $[M+H]^+$ calcd. for $[C_{11}H_{20}NOS]^+$ = 214.1260, 214.1268 found.

b. Evaluation of optimal base, solvent, temperature, concentration, reaction time, and 2-halothiophene structure for 4-selective 3-bromopyridine C-H etherification

General procedure for condition variation: Inside an N_2 filled glovebox, an oven-dried 4 mL vial (KIMBLE®, Product #60910-1) was charged with a magnetic stir bar, 3-bromopyridine (39.5 mg, 0.25 mmol, 1.0 equiv), 2-ethyl-1-hexanol (48.8 mg, 0.375 mmol, 1.5 equiv), 18-crown-6 (99.1 mg, 0.375 mmol, 1.5 equiv), the appropriate 2-halogenated thiophene (0.5 mmol, 2.0 equiv), anhydrous THF (1.0 mL, 0.25 M), and KO-*t*-Bu (42.1 mg, 0.375 mmol, 1.5 equiv) in that order. The vial was sealed with a screw cap (Thermo Fisher Scientific, Product #C4015-1A) lined with a PTFE septum (Thermo Fisher Scientific, Product #B7995-13), removed from the glovebox, and placed into a preheated 25 °C aluminum reaction block and the reaction mixture was stirred for 20 h. 1,3,5-Trimethoxybenzene internal standard was then weighed into the vial. For each experiment, the mass of 1,3,5-trimethoxybenzene weighed into the vial was recorded separately. ^{1}H NMR spectroscopy (400 MHz, $CDCl_3$) of the crude reaction solution was used to determine the yield of 3-bromo-4-((2-ethylhexyl)oxy)pyridine (**4–9**). The aromatic C-H signal of 1,3,5-trimethoxybenzene at 6.08 ppm was integrated against the aromatic C-H signal of **4–9** at 8.35 ppm to determine the yield. The chemical shift of each spectrum was calibrated to residual $CHCl_3$ at 7.26 ppm. The results are summarized in A3–2 below. **Note:** for the optimized procedure (entry 1), no *tert*-butyl aryl ether (3-bromo-4-(*tert*-butoxy)pyridine) was observed by ^{1}H NMR spectroscopy and MS analysis of the crude reaction mixture.

Standard Conditions

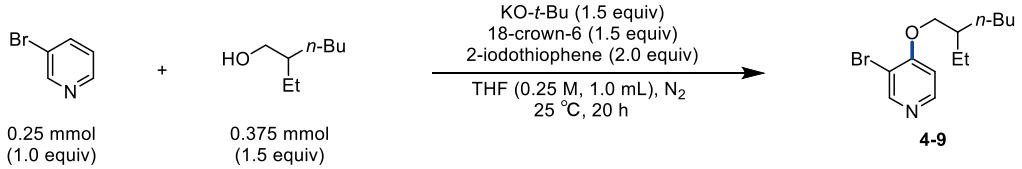

Entry	Change from the "standard conditions"	Yield
1	none	84%
2	no 18-crown-6	65%
3	0.2 equiv 18-crown-6 used instead of 1.5 equiv	71%
4	0.5 equiv 18-crown-6 used instead of 1.5 equiv	74%
5	1.0 equiv 18-crown-6 used instead of 1.5 equiv	71%
6	NaO-*t*-Bu used instead of KO-*t*-Bu	56%
7	1.0 equiv of KO-*t*-Bu and 18-crown-6 used instead of 1.5 equiv	73%
8	KO-*t*-Bu received from TCI used instead of KO-*t*-Bu from Chem-Impex	81%
9	KO-*t*-Bu received from Millipore Sigma used instead of KO-*t*-Bu from Chem-Impex	81%
10	3 h instead of 20 h	60%
11	PhMe used as solvent instead of THF	43%
12	DMSO used as solvent instead of THF	0%
13	1,4-dioxane used as solvent instead of THF	70%
14	0.5 M in THF instead of 0.25 M	73%
15	no 2-iodothiophene	0%
16	2-iodothiophene received from Matrix Scientific used instead of 2-iodothiophene from Combi-Blocks	81%
17	2,5-dibromothiophene used instead of 2-iodothiophene	8%
18	2,5-diiodothiophene used instead of 2-iodothiophene	82%
19	2,3-diiodobenzothiophene used instead of 2-iodothiophene	86%
20	Reaction run open to air instead of under N_2	64%

Figure A3–2: Condition variation of base, solvent, temperature, concentration, reaction time, and 2-halogenated thiophene for 4-selective 3-bromopyridine C-H etherification.

c. Observed 2,5-dibromothiophene byproducts in thiazole C-H etherification

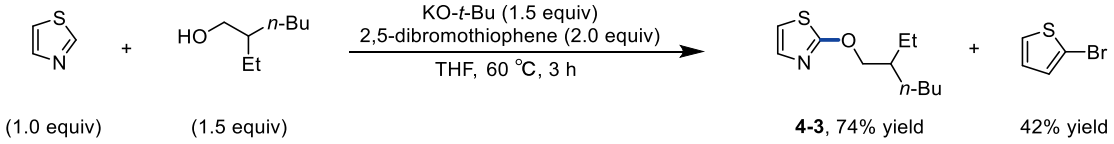

Procedure: The reaction was set up according to the general procedure described in Section A3.2a on a 0.25 mmol scale using thiazole (21.3 mg, 0.25 mmol, 1.0 equiv), 2-ethyl-1-hexanol (48.8 mg, 0.375 mmol, 1.5 equiv), 2,5-dibromothiophene (121.0 mg, 0.5 mmol, 2.0 equiv), KO-*t*-Bu (42.1 mg, 0.375 mmol, 1.5 equiv), and anhydrous THF (1.0 mL). 1,3,5-Trimethoxybenzene (42.0 mg,

0.25 mmo1) internal standard was weighed into the vial at the end of the reaction time and ^{1}H NMR spectroscopy (400 MHz, $CDCl_3$) was used to determine the yield of all products; 74% yield of **4–3**, 42% yield of 2-bromothiophene. The ^{1}H NMR spectrum of the crude reaction solution is shown below.

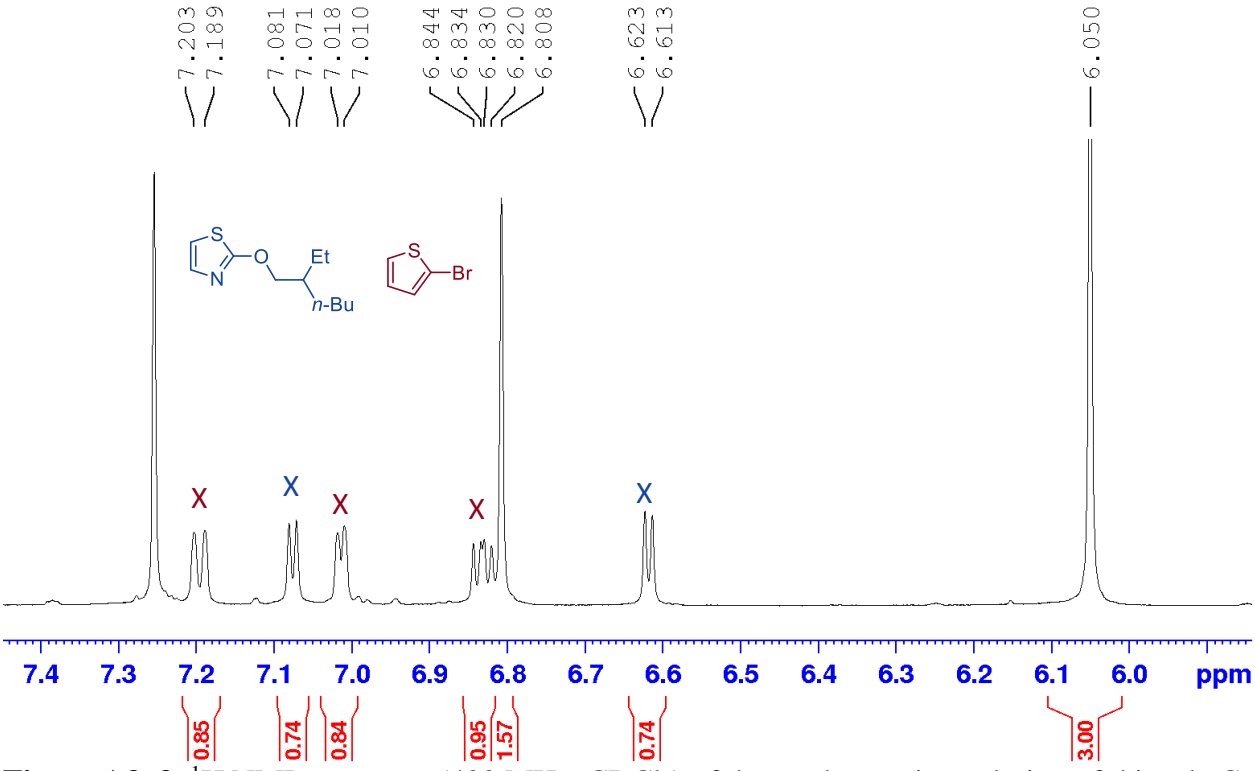

Figure A3–3: ^{1}H NMR spectrum (400 MHz, $CDCl_3$) of the crude reaction solution of thiazole C-H etherification using 2,5-dibromothiophene as the halogen transfer reagent. 1,3,5-Trimethoxybenzene (42.0 mg, 0.25 mmol, signal at 6.05 ppm integrated to 3.0 for 0.25 mmol scale reaction) added as internal standard. The ^{1}H NMR signal at 6.62 ppm was used to determine the yield of **3**; 74% yield of **3** (marked with X). The ^{1}H NMR signal at 7.20 ppm was used to determine the yield of 2-bromothiophene; 42% yield of 2-bromothiophene (marked with X). The ^{1}H NMR signal at 6.81 ppm is 2,5-dibromothiophene; 79% yield of 2,5-dibromothiophene.

d. Observed 2-iodothiophene byproducts in 3-bromopyridine C-H etherification

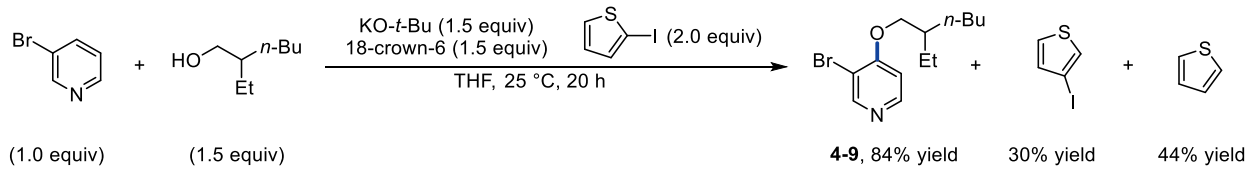

Procedure: The reaction was set up according to the general procedure described in Section A3.2b on a 0.1 mmol scale using 3-bromopyridine (15.8 mg, 0.1 mmol, 1.0 equiv), 2-ethyl-1-hexanol (19.5 mg, 0.15 mmol, 1.5 equiv), 2-iodothiophene (42.0 mg, 0.2 mmol, 2.0 equiv), 18-crown-6 (39.6 mg, 0.15 mmol, 1.5 equiv), KO-*t*-Bu (16.8 mg, 0.15 mmol, 1.5 equiv), and anhydrous THF (0.4 mL). 1,3,5-Trimethoxybenzene (16.6 mg, 0.099 mmo1) internal standard was weighed into the vial at the end of the reaction and ^{1}H NMR spectroscopy (400 MHz, $CDCl_3$) was used to determine the yield of all products; 84% yield of **4–9**, 30% yield of 3-iodothiophene, 44% yield of thiophene. The ^{1}H NMR spectrum of the crude reaction solution is shown below.

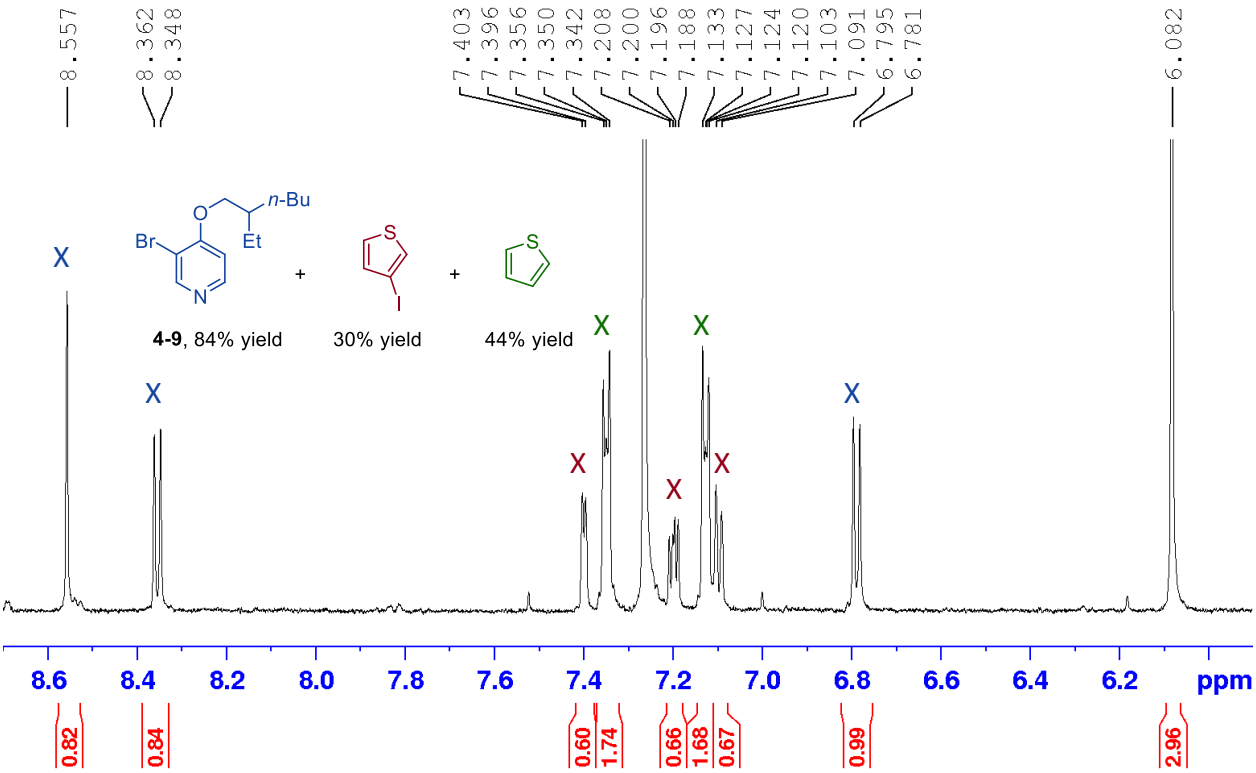

Figure A3–4: ^{1}H NMR spectrum (400 MHz, $CDCl_3$) of the crude reaction solution of 3-bromopyridine C-H etherification using 2-iodothiophene as the halogen transfer reagent. 1,3,5-Trimethoxybenzene (16.6 mg, 0.099 mmol, signal at 6.08 ppm integrated to 2.96 for 0.1 mmol scale reaction) added as internal standard. The ^{1}H NMR signal at 8.35 ppm was used to determine the yield of **4–9**; 84% yield of **4–9** (marked with X). The ^{1}H NMR signal at 7.40 ppm was used to determine the yield of 3-iodothiophene; 30% yield of 3-iodothiophene (marked with X). The ^{1}H

NMR signal at 7.13 ppm was used to determine the yield of thiophene; 44% yield of thiophene (marked with X).

e. Relative stability of 2,3-diiodobenzothiophene under basic conditions

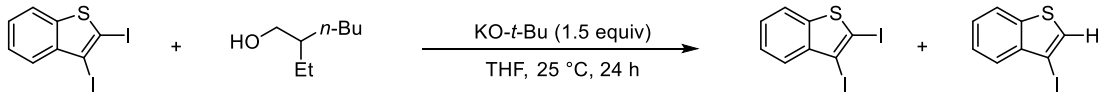

3-12, (1.0 equiv) (1.5 equiv) **3-12**, 92% 8%

Procedure: Inside an N_2 filled glovebox, an oven-dried 4 mL vial (KIMBLE®, Product #60910-1) was charged with a magnetic stir bar, 2,3-diiodobenzothiophene (38.6 mmol, 0.1 mmol, 1.0 equiv), anhydrous THF (0.4 mL, 0.25 M), 2-ethyl-1-hexanol (19.5 mg, 0.15 mmol, 1.5 equiv), and KO-*t*-Bu (16.8 mg, 0.15 mmol, 1.5 equiv) in successive order. The vial was sealed with a screw cap (Thermo Fisher Scientific, Product #C4015-1A) lined with a PTFE septum (Thermo Fisher Scientific, Product #B7995-13), removed from the glovebox, and placed into a preheated 25 °C aluminum reaction block and the reaction mixture was stirred for 24 h. 1,3,5-Trimethoxybenzene (21.4 mg, 0.13 mmol) was measured into the reaction solution. ^{1}H NMR spectroscopy (400 MHz, $CDCl_3$) of the crude reaction solution was used to determine the yield of remaining 2,3-diiodobenzothiophene (92% yield) and 3-iodobenzothiophene (8% yield).

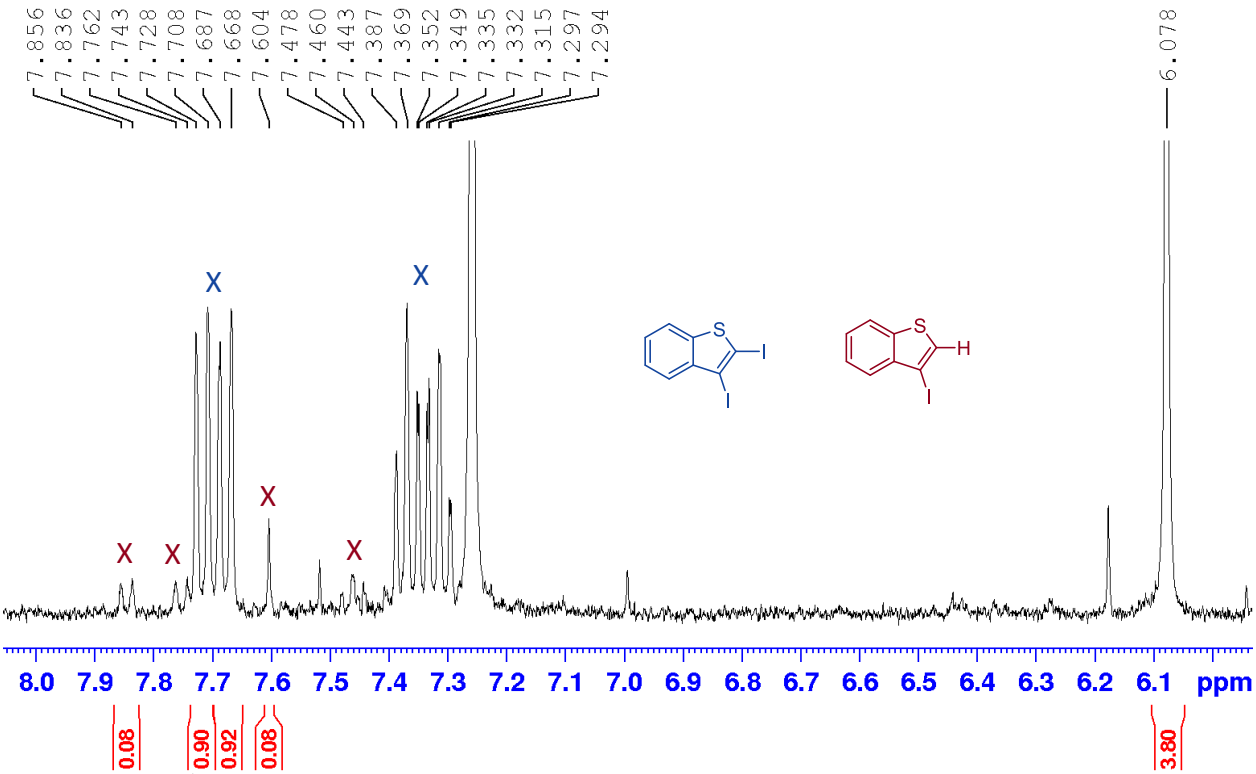

Figure A3–5: ^{1}H NMR spectrum of the crude reaction solution of 2,3-diiodobenzothiophene under basic conditions. 1,3,5-Trimethoxybenzene internal standard (21.4 mg, 0.13 mmol, signal at 6.08 ppm calibrated to 3.80 for 0.1 mmol scale reaction) was used to determine the yield of remaining 2,3-diiodobenzothiophene (signal at 7.68 ppm used to determine yield, 92% yield) and 3-iodobenzothiophene (signal at 7.60 ppm used to determine yield, 8% yield).

f. Examination of other common halogenating reagents in place of 2-halothiophenes

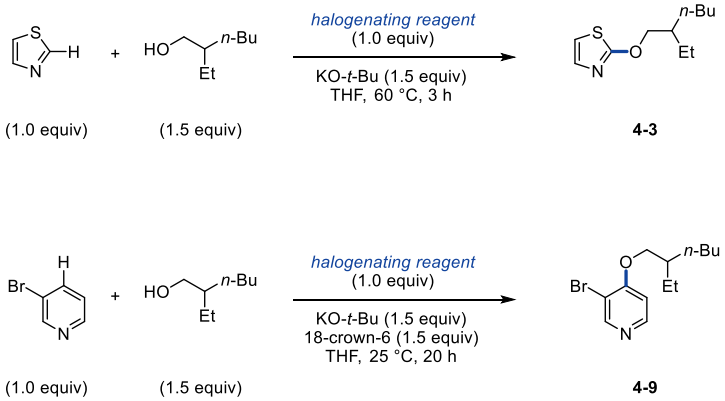

halogenating reagent	%yield **4-3**	% yield **4-9**
N-bromosuccinimide	0	0
N-iodosuccinimide	0	0
Br_2/I_2	0	0
Cl_3CN	0	0
CCl_4/CBr_4	0	0
$(BrCF_2)_2$	0	0
C_6F_5I/C_6F_5Br	0	0
C_4F_9I	0	2

Procedure: Inside an N_2 filled glovebox, an oven-dried 4 mL vial (KIMBLE®, Product #60910-1) was charged with a magnetic stir bar, the appropriate halogenating regent (0.1 mmol, 1.0 equiv), anhydrous THF (0.4 mL, 0.25 M), 2-ethyl-1-hexanol (19.5 mg, 0.15 mmol, 1.5 equiv), 3-

bromopyridine (15.8 mg, 0.1 mmol, 1.0 equiv) or thiazole (8.5 mg, 0.1 mmol, 1.0 equiv), 18-crown-6 (only for 3-bromopyridine, 39.6 mg, 0.15 mmol, 1.5 equiv), and KO-*t*-Bu (16.8 mg, 0.15 mmol, 1.5 equiv) in successive order. The vial was sealed with a screw cap (Thermo Fisher Scientific, Product #C4015-1A) lined with a PTFE septum (Thermo Fisher Scientific, Product #B7995-13), removed from the glovebox, and placed into a preheated 25 °C (for 3-bromopyridine) or 60 °C (for thiazole) aluminum reaction block and the reaction mixture was stirred for 20 h (for 3-bromopyridine) or 3 h (for thiazole). ^{1}H NMR spectroscopy (400 MHz, $CDCl_3$) of the crude reaction solution was used to determine the yield of 3-bromo-4-((2-ethylhexyl)oxy)pyridine (**4–9**) or 2-((2-ethylhexyl)oxy)thiazole (**3–3**). Most halogenating reagents resulted in no yield of **4–9** or **4–3** with only C_4F_9I producing a 2% yield of **4–9**.

A3.3 Synthesis of 2,3-Diiodobenzo[*b*]thiophene

Step 1: Trimethyl((2-(methylthio)phenyl)ethynyl)silane

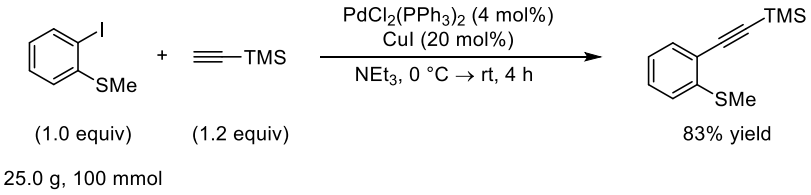

Procedure: This procedure was adapted from a previous literature report.[2] An oven-dried 1 L round bottom flask was charged with a magnetic stir bar, $PdCl_2(PPh_3)_2$ (2.81 g, 4.0 mmol, 0.04 equiv), and CuI (3.81 g, 20 mmol, 0.2 equiv). The flask was sealed with a red septum stopper (Chemglass, Product #CG-3022-08), evacuated and backfilled with N_2 three times, then left under positive pressure of N_2 on a manifold Schlenk line. The flask was inserted into a 0 °C ice-bath and triethylamine (400 mL) was added *via* syringe. Trimethylsilylacetylene (16.6 mL, 120 mmol, 1.2 equiv) followed by 2-iodothioanisole (25.0 g, 100 mmol, 1.0 equiv) were then sequentially added dropwise *via* syringe. The flask was allowed to warm to rt and the solution was stirred for 4 h. The

reaction solution was filtered through a pad of Celite® and transferred to a separatory funnel. The solution was diluted with EtOAc (300 mL) and then washed with H_2O (2 x 200 mL) and brine (1 x 200 mL). The organic layer was dried over Na_2SO_4, filtered, and then concentrated *in vacuo*. Silica gel chromatography (hexanes to 2% EtOAc/hexanes) yielded the title compound as a light-yellow oil (18.2 g, 82.7 mmol, 83% yield). **^{1}H NMR** (400 MHz, $CDCl_3$) δ 7.42 (dd, *J* = 1.4 Hz, 7.6 Hz, 1H), 7.28 (m, 1H), 7.13 (m, 1H), 7.06 (td, *J* = 1.1 Hz, 7.5 Hz, 1H), 2.48 (s, 3H), 0.28 (s, 9H).

Step 2: (3-iodobenzo[*b*]thiophen-2-yl)trimethylsilane

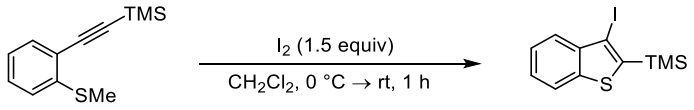

(1.0 equiv) 92% yield

Procedure: This procedure was adapted from a previous literature report.[2] An oven-dried 500 mL round bottom flask was charged with a magnetic stir bar, trimethyl((2-(methylthio)phenyl)ethynyl)silane (18.2 g, 82.7 mmol, 1.0 equiv), and anhydrous CH_2Cl_2 (300 mL) open to air. The solution was cooled to 0 °C in an ice-bath and iodine (31.5 g, 124 mmol, 1.5 equiv) was added slowly over approximately 15 min. No significant exotherm was observed. The solution was allowed to warm to rt and stirred for 1 h. The solution was transferred to a separatory funnel containing H_2O (300 mL). Na_2SO_3 (ca. 11 g) was added to the separatory funnel and the solution was agitated until it became light-yellow in color. The aqueous layer was extracted with CH_2Cl_2 (3 x 200 mL). The organic layer was dried over Na_2SO_4, filtered, and then concentrated *in vacuo*. Silica gel chromatography (hexanes) yielded the title compound as a clear oil (25.1 g, 75.6 mmol, 92% yield). **^{1}H NMR** (400 MHz, $CDCl_3$) δ 7.79-7.84 (m, 2H), 7.44 (m, 1H), 7.37 (m, 1H), 0.51 (s, 9H).

Step 3: 2,3-diiodobenzo[*b*]thiophene (4–12)

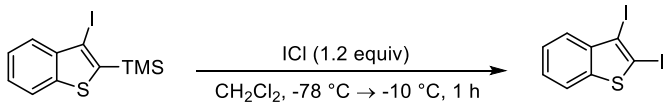

Procedure: An oven-dried 500 mL round bottom flask was charged with a magnetic stir bar and (3-iodobenzo[*b*]thiophen-2-yl)trimethylsilane (25.1 g, 75.6 mmol, 1.0 equiv). The flask was sealed with a red septum stopper (Chemglass, Product #CG-3022-08), evacuated and backfilled three times with N_2, then left under positive pressure of N_2 on a manifold Schlenk line. Anhydrous CH_2Cl_2 (150 mL) was then added *via* syringe. The solution was cooled to -78 °C with a dry ice/acetone bath, then ICl (14.7 g, 90.7 mmol, 1.2 equiv) constituted in anhydrous CH_2Cl_2 (50 mL) was added dropwise *via* syringe. After approximately half of the ICl solution was added, large quantities of solid precipitated that inhibited stirring. At this point, the solution was warmed to -10 °C in an ice water/salt bath to allow for adequate stirring. The remainder of the ICl solution was added dropwise at -10 °C. The solution was stirred for an additional 1 h at -10 °C and then transferred to a separatory funnel containing H_2O (300 mL). Na_2SO_3 (ca. 10 g) was added to the separatory funnel and the solution was agitated until it turned a light-yellow color. The aqueous layer was extracted with CH_2Cl_2 (3 x 200 mL). The organic layer was dried over Na_2SO_4, filtered, and concentrated *in vacuo*. Silica gel chromatography (hexanes) yielded the title compound as a fluffy white solid (22.8 g, 60 mmol, 78% step yield, 60% overall yield). Spectroscopic characterization is consistent with a previous report.[2] **^{1}H NMR** (400 MHz, $CDCl_3$) δ 7.70 (m, 2H), 7.35 (m, 2H). **^{13}C NMR** (101 MHz, $CDCl_3$) δ 144.1, 141.8, 127.0, 126.1, 125.8, 121.8, 95.4, 89.5. **EA**: Anal. Calcd. for $C_8H_4I_2S$: C, 24.89; H, 1.04; Found: C, 24.90; H, 0.94. **Note on Storage**: We found 2,3-diiodothiophene was most effectively stored at room temperature in a dark environment. Upon extended exposure to light (ca. 2 weeks) in a desiccator the solid progressively

turns a light pink color, although no detectable decomposition can be observed by ^{1}H NMR spectroscopy. If desired, the compound can be recrystallized using 3% CH_2Cl_2/hexanes solvent.

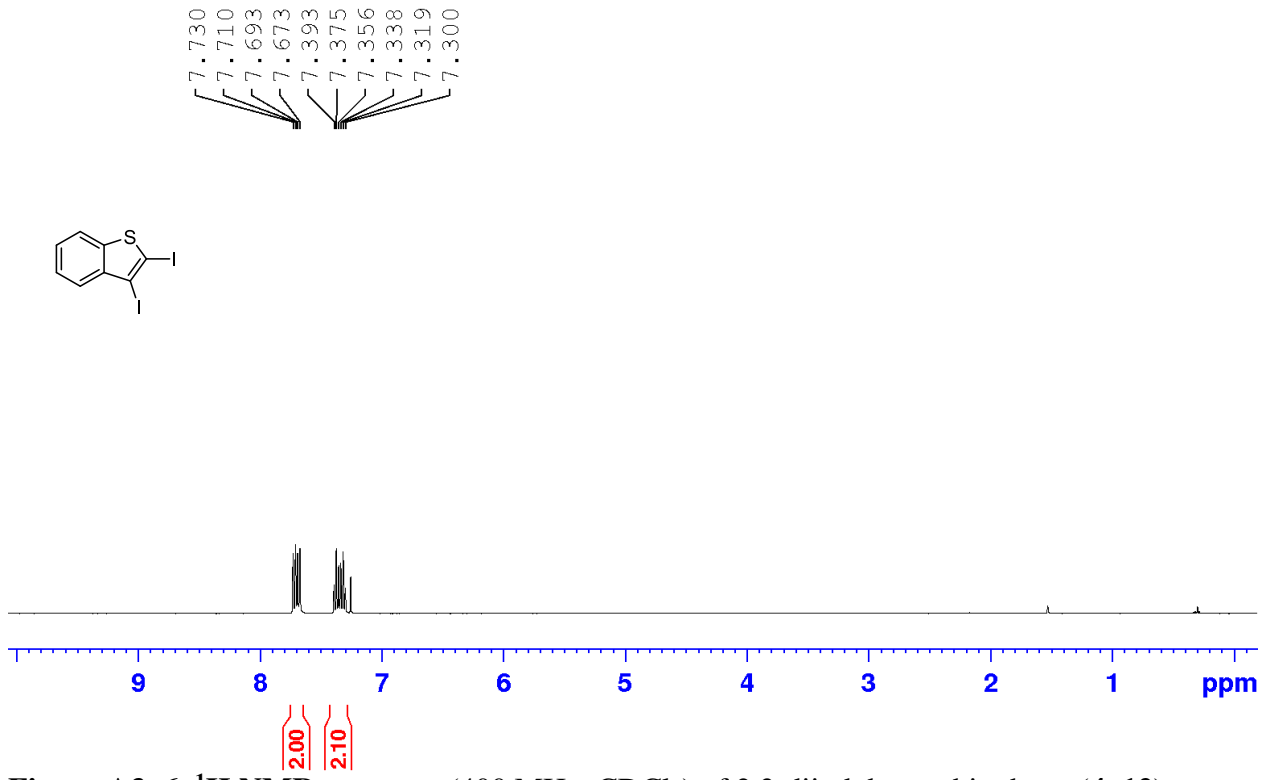

Figure A3–6: **^{1}H NMR** spectrum (400 MHz, $CDCl_3$) of 2,3-diiodobenzothiophene (**4–12**).

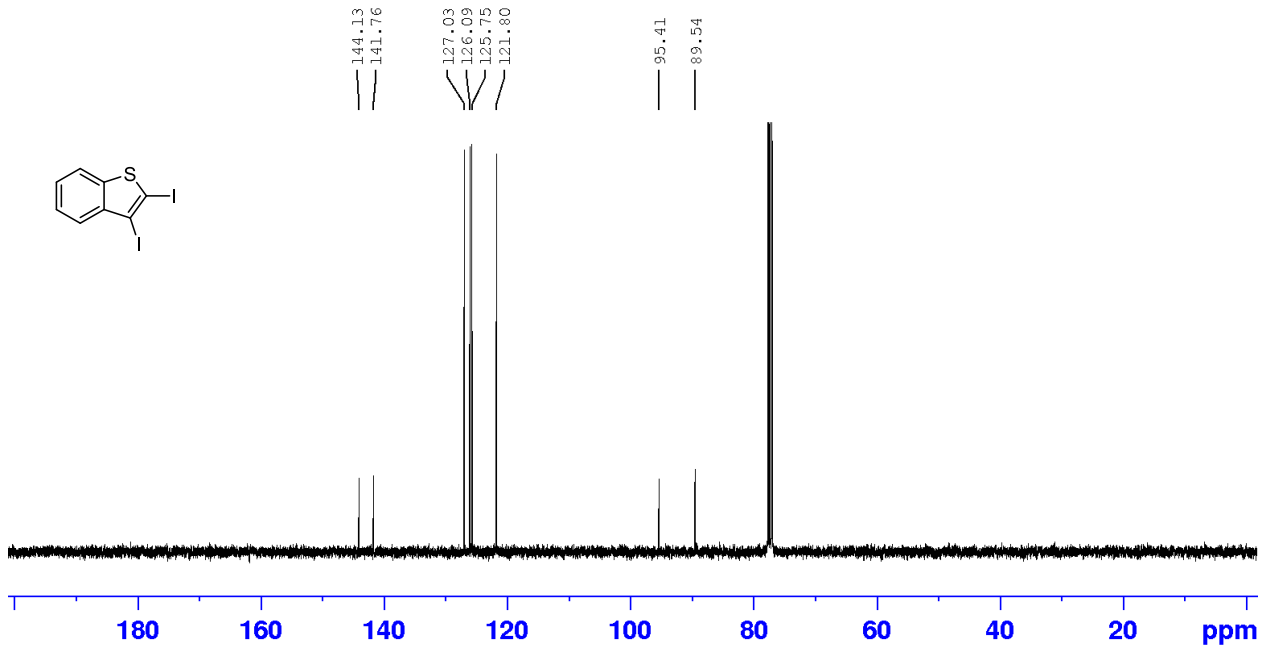

Figure A3–7: **^{13}C NMR** spectrum of 2,3-diiodobenzothiophene (**4–12**).

A3.4 General Procedures for 1,3-Azole and (Di)Azine C-H Etherification

General Procedure for 1,3-Azole C-H Etherification: Open to air, an 8 mL oven-dried vial (Thermo Fisher Scientific, Product #033405P) was charged with a magnetic stir bar along with the appropriate 1,3-azole (1.0 mmol, 1.0 equiv), alcohol (1.5 mmol, 1.5 equiv), and 2,5-dibromothiophene (483.8 mg, 2.0 mmol, 2.0 equiv). The vial was sealed with a screw cap (Thermo Fisher Scientific, Product #03392A) lined with a PTFE septum (Thermo Fisher Scientific, Product #B7995-15), evacuated and backfilled three times with N_2, and left under positive pressure of N_2 on a manifold Schlenk line. Anhydrous THF (2.0 mL) was then added to the vial *via* syringe. A 0.75 M solution of KO-*t*-Bu in anhydrous THF (2.0 mL, 1.5 mmol, 1.5 equiv, see procedure below for preparation) was then added to the reaction vial *via* syringe. The reaction vial was placed into a preheated 60 °C silicon oil bath with stirring for 3 h. The reaction solution was allowed to cool to rt and subsequently transferred into separatory funnel containing H_2O (40 mL). The aqueous mixture was extracted with EtOAc (3 x 40 mL). The organic layer was dried over Na_2SO_4. The Na_2SO_4 was removed by filtration and the organic layer was concentrated under reduced pressure. The resulting crude material was purified using flash silica gel chromatography using the conditions given below.

General Procedure for (Di)azine C-H Etherification: Open to air, an 8 mL oven-dried vial (Thermo Fisher Scientific, Product #033405P) was charged with a magnetic stir bar along with the appropriate (di)azine (1.0 mmol, 1.0 equiv), alcohol (1.5 mmol, 1.5 equiv), and either 2-iodothiophene (420.1 mg, 2.0 mmol, 2.0 equiv) or 2,3-diiodobenzothiophene (577.7 mg, 1.5 mmol, 1.5 equiv). 18-crown-6 (396.5 mg, 1.5 mmol, 1.5 equiv) was added for certain substrates as indicated below. The vial was sealed with a screw cap (Thermo Fisher Scientific, Product

#03392A) lined with a PTFE septum (Thermo Fisher Scientific, Product #B7995-15), evacuated and backfilled three times with N_2, and left under positive pressure of N_2 on a manifold Schlenk line. Anhydrous THF 2.0 mL was then added *via* syringe. A 0.75 M solution of KO-*t*-Bu in anhydrous THF (2.0 mL, 1.5 mmol, 1.5 equiv, see procedure for preparation below) was then added to the reaction vial *via* syringe. The reaction vial was placed into a 25 °C silicon oil bath with stirring for 20 h. The reaction mixture was then transferred into a separatory funnel containing H_2O (40 mL). The aqueous mixture was extracted with EtOAc (3 x 40 mL). The organic layer was dried over Na_2SO_4. The Na_2SO_4 was removed by filtration and the organic layer was concentrated under reduced pressure. The resulting crude material was purified using flash silica gel chromatography using the conditions given below. **Note**: For the preparation of compounds that utilize 2,3-diiodobenzothiophene, we found 1.5 equiv of the reagent rather 2.0 equiv was generally sufficient. This is ideal because independent preparation of this reagent is necessary. For the substrates where 2,3-diiodbenzothiophene was employed, a 20% to 60% yield increase was observed relative to use of 2-iodothiophene (2 equiv) as the halogen transfer reagent. For example, when 2-iodothiophene was used in place of 2,3-diiodobenzothiophene for **4–12**, only a 2% yield of **4–40** was obtained (68% yield with 2,3-diiodobenzothiophene).

Preparation of 0.75 M Solution of KO-*t*-Bu in THF: Open to air, an 8 mL oven-dried vial (Thermo Fisher Scientific, Product #033405P) was charged with a magnetic stir bar and KO-*t*-Bu (420.7 mg, 3.75 mmol). The vial was sealed with a screw cap (Thermo Fisher Scientific, Product #03392A) lined with a PTFE septum (Thermo Fisher Scientific, Product #B7995-15), evacuated and backfilled three times with N_2, and left under positive pressure of N_2 on a manifold Schlenk line. Anhydrous THF (5.0 mL) was added *via* syringe and the solution was stirred for

approximately 1 min until homogenous. This solution was used immediately upon preparation and not stored for extended use in the above procedures. The scale of this preparation can be adjusted as necessary for the use of this solution for multiple reactions or larger scale reactions.

Verification and of Product Regioselectivity: The regioselectivity of the C-H etherification reaction could usually be determined through analysis of the ^{1}H NMR spectrum of each compound. The ^{1}H NMR spectrum of the crude reaction mixture for each compound was analyzed to determine if the major product was formed in high selectivity. In cases where other *N*-heteroaryl ethers or *N*-heteroaryl halides are observed we include a note below the characterization data with more details. For compounds where the regioselectivity of the major product is more ambiguous, experimental verification of the product structure is provided below the characterization data.

A3.5 Characterization Data of Heteroaryl Ether Products

a) Characterization data for 1,3-Azole Substrates in Figure 4–15

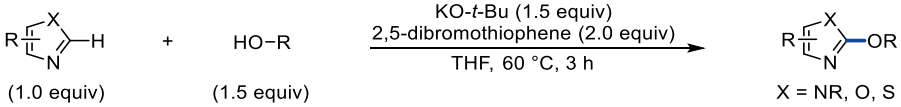

4,5-dimethyl-2-((*cis*-3-methylcyclohexyl)oxy)thiazole (4–13)

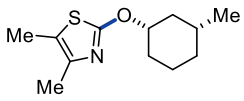

The title product was prepared according to the general procedure for 1,3-azole C-H etherification using 4,5-dimethylthiazole (113.0 mg, 1.0 mmol, 1.0 equiv), *cis*-3-methylcyclohexan-1-ol (171.1 mg, 1.5 mmol, 1.5 equiv), 2,5-dibromothiophene (483.8 mg, 2.0 mmol, 2.0 equiv), KO-*t*-Bu (0.75 M solution in THF, 2.0 mL, 1.5 mmol, 1.5 equiv), and anhydrous THF (2.0 mL). Silica gel chromatography (1% EtOAc/hexanes) afforded the title compound as a light-yellow oil (160.0 mg, 0.71 mmol, 71% yield). **^{1}H NMR** (400 MHz, $CDCl_3$)

δ 4.72 (m, 1H), 2.13-2.20 (m, 8H), 1.78 (m, 1H), 1.63 (m, 1H), 1.53 (m, 1H), 1.23-1.42 (m, 2H), 1.06 (m, 1H), 0.93 (d, J = 6.6 Hz, 3H), 0.84 (m, 1H). **^{13}C NMR** (101 MHz, $CDCl_3$) δ 170.1, 141.2, 116.8, 80.3, 40.6, 34.2, 31.7, 31.4, 24.0, 22.4, 14.8, 11.4. **IR** (neat, cm^{-1}) 2923, 2860, 1515, 1260 1224, 968. **HRMS** (ESI) $[M+H]^+$ calcd. for $[C_{12}H_{20}NOS]^+$ = 226.1260, 226.1246 found.

2-(benzo[*d*][1,3]dioxol-5-ylmethoxy)thiazole (4–14)

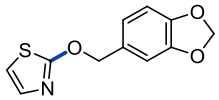

The title product was prepared according to the general procedure for 1,3-azole C-H etherification using thiazole (85.1 mg, 1.0 mmol, 1.0 equiv), benzo[*d*][1,3]dioxol-5-ylmethanol (228.0 mg, 1.5 mmol, 1.5 equiv), 2,5-dibromothiophene (483.8 mg, 2.0 mmol, 2.0 equiv), KO-*t*-Bu (0.75 M solution in THF, 2.0 mL, 1.5 mmol, 1.5 equiv), and anhydrous THF (2.0 mL). Silica gel chromatography (5% EtOAc/hexanes) afforded the title compound as a light-yellow oil (138.0 mg, 0.59 mmol, 59% yield). **^{1}H NMR** (400 MHz, $CDCl_3$) δ 7.14 (d, J = 3.8 Hz, 1H), 6.91-6.96 (m, 2H), 6.81 (d, J = 7.9 Hz, 1H), 6.68 (d, J = 3.8 Hz, 1H), 5.97 (s, 2H), 5.34 (s, 2H). **^{13}C NMR** (101 MHz, $CDCl_3$) δ 174.9, 148.0, 148.0, 136.9, 129.4, 122.6, 111.4, 109.3, 108.4, 101.3, 73.2. **IR** (neat, cm^{-1}) 3115, 2892, 1647, 1487, 1243, 1034, 924. **EA**: Anal. Calcd. for $C_{11}H_9NO_3S$: C, 56.16; H, 3.86; N, 5.95. Found: C, 56.02; H, 3.99; N, 5.79.

5-(2-bromophenyl)-2-((2-ethylhexyl)oxy)oxazole (4–15)

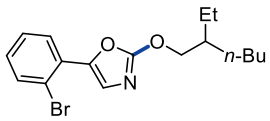

The title product was prepared according to the general procedure for 1,3-azole C-H etherification using 5-(2-bromophenyl)oxazole (223.0 mg, 1.0 mmol, 1.0 equiv), 2-ethylhexan-1-ol (195.3 mg, 1.5 mmol, 1.5 equiv), 2,5-dibromothiophene (483.8 mg, 2.0 mmol, 2.0 equiv), KO-*t*-Bu (0.75 M solution in THF, 2.0 mL, 1.5 mmol, 1.5 equiv), and anhydrous THF (2.0 mL). Silica gel chromatography (5% EtOAc/hexanes) afforded the title compound as a light-yellow oil (175.0 mg, 0.50 mmol, 50% yield). **^{1}H NMR** (400 MHz, $CDCl_3$) δ 7.65 (m, 2H), 7.60 (s, 1H), 7.35 (m, 1H), 7.11 (m, 1H), 4.36 (m, 2H), 1.78 (m, 1H), 1.38-1.56

(m, 4H), 1.26-1.38 (m, 4H), 0.89-0.97 (m, 6H). **^{13}C NMR** (101 MHz, $CDCl_3$) δ 162.0, 143.8, 134.2, 128.8, 128.5, 127.7, 127.6, 126.3, 119.1, 74.4, 39.2, 30.2, 29.0, 23.6, 23.1, 14.2, 11.1. **IR** (neat, cm^{-1}) 2958, 2929, 2872, 1584, 1469, 1343, 1015. **EA**: Anal. Calcd. for $C_{17}H_{22}BrNO_2$: C, 57.96; H, 6.30; N, 3.98. Found: C, 58.23; H, 6.36; N, 4.09.

1,3,7-trimethyl-8-(3-(piperidin-1-yl)propoxy)-3,7-dihydro-1*H*-purine-2,6-dione (4–16)

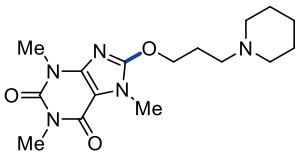

The title product was prepared according to the general procedure for 1,3-azole C-H etherification using 1,3,7-trimethyl-3,7-dihydro-1*H*-purine-2,6-dione (194.0 mg, 1.0 mmol, 1.0 equiv), 3-(piperidin-1-yl)propan-1-ol (215.0 mg, 1.5 mmol, 1.5 equiv), 2,5-dibromothiophene (483.8 mg, 2.0 mmol, 2.0 equiv), KO-*t*-Bu (0.75 M solution in THF, 2.0 mL, 1.5 mmol, 1.5 equiv), and anhydrous THF (2.0 mL). Silica gel chromatography (5% MeOH/CH_2Cl_2) afforded the title compound as an off-white solid (278.0 mg, 0.83 mmol, 83% yield). **Mp**: 156 ºC – 164 ºC, solid turned dark red prior to melting. **^{1}H NMR** (400 MHz, $CDCl_3$) δ 4.53 (t, *J* = 6.3 Hz, 2H), 3.69 (s, 3H), 3.50 (s, 3H), 3.38 (s, 3H), 2.32-3.07 (m, 6H), 2.10-2.32 (m, 2H), 1.62-1.86 (m, 4H), 1.38-1.61 (m, 2H). **^{13}C NMR** (101 MHz, $CDCl_3$) δ 155.6, 154.9, 151.8, 146.3, 103.5, 69.4, 55.3, 54.4, 29.9, 29.8, 27.8, 25.8, 25.1, 23.8. **IR** (neat, cm^{-1}) 2933, 2772, 1697, 1668, 1538, 1458, 1027. **HRMS** (ESI) $[M+H]^+$ calcd. for $[C_{16}H_{26}N_5O_3]^+$ = 336.2030, 336.2030 found.

2-((4-methoxybenzyl)oxy)-4-(pyridin-3-yl)thiazole (4–17)

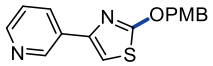

The title product was prepared according to the general procedure for 1,3-azole C-H etherification on a 0.5 mmol scale using 4-(pyridin-3-yl)thiazole (81.0 mg, 0.5 mmol, 1.0 equiv), (4-methoxyphenyl)methanol (103.7 mg, 0.75 mmol, 1.5 equiv), 2,5-dibromothiophene (241.9 mg, 1.0 equiv, 2.0 equiv), KO-*t*-Bu (0.75 M solution, 1.0 mL, 0.75 mmol, 1.5 equiv), and anhydrous THF (1.0 mL). Silica gel chromatography (50% EtOAc/hexanes) yielded the title

compound as a white solid (75.8 mg, 0.25 mmol, 51% yield). **Mp**: 72 °C – 73 °C. **^{1}H NMR** (400 MHz, $CDCl_3$) δ 9.08 (s, 1H), 8.54 (m, 1H), 8.10 (m, 1H), 7.44 (d, *J* = 8.6 Hz, 2H), 7.32 (dd, *J* = 4.8 Hz, 7.9 Hz, 1H), 6.95 (s, 1H), 6.92 (d, *J* = 8.6 Hz, 2H), 5.46 (s, 2H), 3.81 (s, 3H). **^{13}C NMR** (101 MHz, $CDCl_3$) δ 174.4, 160.1, 148.9, 147.6, 146.1, 133.2, 130.7, 130.5, 127.6, 123.6, 114.1, 106.3, 73.5, 55.4. **IR** (neat, cm^{-1}) 2959, 2931, 1611, 1513, 1229, 1033, 818. **HRMS** (ESI) $[M+H]^+$ calcd. for $[C_{24}H_{23}N_2OS]^+$ = 299.0849, 299.0847 found.

5-chloro-1-methyl-2-(pentyloxy)-1*H*-imidazole (4–18)

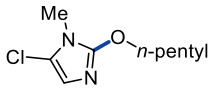

The title product was prepared using a modified procedure. Inside an N_2 filled glovebox, an 8 mL oven-dried vial (Thermo Fisher Scientific, Product #033405P) was charged with a magnetic stir bar along with 5-chloro-1-methyl-1*H*-imidazole (116.0 mg, 1.0 mmol, 1.0 equiv), pentan-1-ol (132.3 mg, 1.5 mmol, 1.5 equiv), 2,5-dibromothiophene (483.8 mg, 2.0 mmol, 2.0 equiv), anhydrous THF (4.0 mL), and KO-*t*-Bu (168.3 mg, 1.5 mmol, 1.5 equiv) in successive order. The vial was sealed a screw cap (Thermo Fisher Scientific, Product #03392A) lined with a PTFE septum (Thermo Fisher Scientific, Product #B7995-15), removed from the glovebox, put under positive pressure of N_2 on a manifold Schlenk line, placed into a preheated 60 °C silicon oil bath with stirring for 3 h. The title product was purified according to the general procedure. Silica gel chromatography (5% to 10% EtOAc/hexanes) afforded the title compound as a light-yellow oil (102.2 mg, 0.51 mmol, 51% yield). **^{1}H NMR** (400 MHz, $CDCl_3$) δ 6.50 (s, 1H), 4.30 (t, *J* = 6.7 Hz, 2H), 3.32 (s, 3H), 1.77 (m, 2H), 1.33-1.44 (m, 4H), 0.92 (t, *J* = 7.0 Hz, 3H). **^{13}C NMR** (101 MHz, $CDCl_3$) δ 151.7, 119.1, 112.4, 69.5, 28.8, 28.3, 28.1, 22.5, 14.1. **IR** (neat, cm^{-1}) 2956, 2872, 1545, 1491, 1257, 1095, 707. **HRMS** (ESI) $[M+H]^+$ calcd. for $[C_9H_{16}ClN_2O]^+$ = 203.0946, 203.0946 found. **Note on observed side product**: The title product represents the only heteroaryl ether observed in the ^{1}H NMR

spectrum of the crude reaction solution although a brominated imidazole ($C_4H_4ClBrN_2$) was also observed in approximately 19% yield. Isolation and subjection of this material to the standard reaction conditions (in the absence of 2,5-dibromothiophene) produces **4–18** in 70% yield, indicating it is an intermediate en route to **4–18**.

1-methyl-2-(pent-4-en-1-yloxy)-1*H*-benzo[*d*]imidazole (4–19)

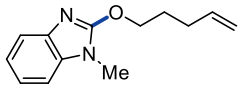

The title product was prepared according to the general procedure for 1,3-azole C-H etherification using *N*-methylbenzimidazole (132.1 mg, 1.0 mmol, 1.0 equiv), pent-4-en-1-ol (129.2 mg, 1.5 mmol, 1.5 equiv), 2,5-dibromothiophene (483.8 mg, 2.0 mmol, 2.0 equiv), KO-*t*-Bu (0.75 M solution in THF, 2.0 mL, 1.5 mmol, 1.5 equiv), and anhydrous THF (2.0 mL). Silica gel chromatography (10% to 20% EtOAc/hexanes) afforded the title compound as a light-yellow oil (147.0 mg, 0.68 mmol, 68% yield). **^{1}H NMR** (400 MHz, $CDCl_3$) δ 7.54 (m, 1H), 7.13-7.19 (m, 3H), 5.87 (m, 1H), 5.00-5.11 (m, 2H), 4.56 (t, J = 6.6 Hz, 2H), 3.56 (s, 3H), 2.26 (m, 2H), 1.97 (m, 2H). **^{13}C NMR** (101 MHz, $CDCl_3$) δ 157.7, 140.2, 137.6, 134.4, 121.6, 120.9, 117.7, 115.6, 108.0, 69.7, 30.1, 28.4, 28.1. **IR** (neat, cm^{-1}) 3063, 2939, 1623, 1534, 1453, 1375, 1284, 737. **HRMS** (ESI) $[M+H]^+$ calcd. for $[C_{13}H_{17}N_2O]^+$ = 217.1335, 217.1333 found.

2-((1-benzhydrylazetidin-3-yl)methoxy)benzo[*d*]thiazole (4–20)

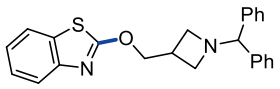

The title product was prepared according to the general procedure for 1,3-azole C-H etherification using benzothiazole (135.2 mg, 1.0 mmol, 1.0 equiv), (1-benzhydrylazetidin-3-yl)methanol (379.7 mg, 1.5 mmol, 1.5 equiv), 2,5-dibromothiophene (483.8 mg, 2.0 mmol, 2.0 equiv), KO-*t*-Bu (0.75 M solution in THF, 2.0 mL, 1.5 mmol, 1.5 equiv), and anhydrous THF (2.0 mL). Silica gel chromatography (5% to 20% EtOAc/hexanes) afforded the title compound as a clear oil (289.6 mg, 0.75 mmol, 75% yield). **^{1}H**

NMR (400 MHz, $CDCl_3$) δ 7.67 (d, *J* = 8.0 Hz, 1H), 7.62 (d, *J* = 7.9 Hz, 1H), 7.34-7.41 (m, 5H), 7.21-7.27 (m, 5H), 7.15-7.19 (m, 2H), 4.73 (d, *J* = 6.9 Hz, 2H), 4.36 (s, 1H), 3.31 (t, *J* = 7.5 Hz, 2H), 3.02 (m, 2H), 2.94 (m, 1H). **^{13}C NMR** (101 MHz, $CDCl_3$) δ 173.0, 149.4, 142.2, 132.0, 128.6, 127.6, 127.2, 126.2, 123.7, 121.4, 120.9, 78.0, 74.0, 56.1, 29.2. **IR** (neat, cm^{-1}) 3060, 3025, 2949, 2830, 1532, 1442, 1248, 1213. **HRMS** (ESI) $[M+H]^+$ calcd. for $[C_{24}H_{23}N_2OS]^+$ = 387.1526, 387.1526 found.

(*S*)-*N*,*N*-dibenzyl-1-((4-(1-methyl-1*H*-benzo[*d*]imidazol-2-yl)thiazol-2-yl)oxy)-3-phenylpropan-2-amine (4–21)

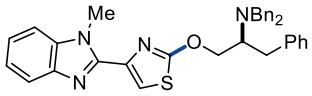

The title product was prepared according to the general procedure for 1,3-azole C-H etherification using 4-(1-methyl-1*H*-benzo[*d*]imidazol-2-yl)thiazole (215.0 mg, 1.0 mmol, 1.0 equiv), (*S*)-2-(dibenzylamino)-3-phenylpropan-1-ol (497.0 mg, 1.5 mmol, 1.5 equiv), 2,5-dibromothiophene (483.8 mg, 2.0 mmol, 2.0 equiv), KO-*t*-Bu (0.75 M solution in THF, 2.0 mL, 1.5 mmol, 1.5 equiv), and anhydrous THF (2.0 mL). Silica gel chromatography (25% EtOAc/hexanes) afforded the title compound as a light-yellow oil (323.0 mg, 0.59 mmol, 59% yield). **^{1}H NMR** (400 MHz, $CDCl_3$) δ 7.82 (br s, 1H), 7.31-7.38 (m, 3H), 7.17-7.30 (m, 12H), 7.08-7.14 (m, 4H), 4.58 (d, *J* = 6.1 Hz, 2H), 3.88 (d, *J* = 9.8 Hz, 2H), 3.73-3.78 (m, 5H), 3.52 (m, 1H), 3.14 (dd, *J* = 13.5, 5.5 Hz, 1H), 2.74 (dd, *J* = 13.6, 8.9 Hz, 1H). **^{13}C NMR** (101 MHz, $CDCl_3$) δ 174.0, 139.7, 139.3, 136.2, 129.3, 128.7, 128.6, 128.3, 127.0, 126.4, 123.0, 122.9, 119.4, 109.7, 71.3, 58.0, 54.2, 33.8, 31.9. **IR** (neat, cm^{-1}) 3024, 2933, 2800, 1735, 1522, 1230, 738. **HRMS** (ESI) $[M+H]^+$ calcd. for $[C_{34}H_{33}N_4OS]^+$ = 545.2370, 545.2354 found. **Specific Rotation**: $[\alpha]_D^{23}$ = -19.9°

b) Characterization data for (di)azine Substrates in Figure 4–15

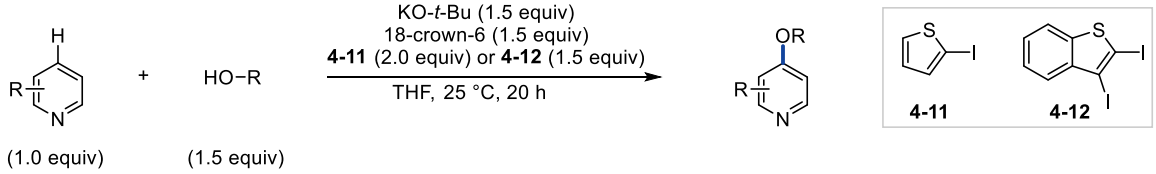

3-bromo-4-((2-ethylhexyl)oxy)pyridine (4–9)

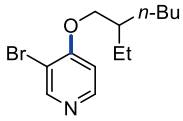

The title product was prepared according to the general procedure for (di)azine C-H etherification using 3-bromopyridine (158.0 mg, 1.0 mmol, 1.0 equiv), 2-ethylhexan-1-ol (195.3 mg, 1.5 mmol, 1.5 equiv), 2-iodothiophene (420.1 mg, 2.0 mmol, 2.0 equiv), 18-crown-6 (396.5 mg, 1.5 mmol, 1.5 equiv), KO-*t*-Bu (0.75 M solution in THF, 2.0 mL, 1.5 mmol, 1.5 equiv), and anhydrous THF (2.0 mL). Silica gel chromatography (10% to 20% EtOAc/hexanes) afforded the title compound as an amber oil (246.4 mg, 0.85 mmol, 85% yield). **^{1}H NMR** (400 MHz, $CDCl_3$) δ 8.56 (s, 1H), 8.36 (d, *J* = 5.6 Hz, 1H), 6.79 (d, *J* = 5.6 Hz, 1H), 3.97 (d, *J* = 5.6 Hz, 2H), 1.81 (m, 1H), 1.41-1.58 (m, 4H), 1.31-1.36 (m, 4H), 0.89-0.97 (m, 6H). **^{13}C NMR** (101 MHz, $CDCl_3$) δ 161.7, 152.4, 150.0, 110.7, 108.3, 71.5, 39.2, 30.5, 29.1, 24.0, 23.1, 14.2, 11.3. **IR** (neat, cm^{-1}) 2958, 2928, 1575, 1460, 1296, 1014, 812. **HRMS** (DART) $[M+H]^+$ calcd. for $[C_{13}H_{21}BrNO]^+$ = 286.0801, 286.0853 found.

4-((1-benzylpiperidin-4-yl)oxy)-3,5-dichloropyridine (4–22)

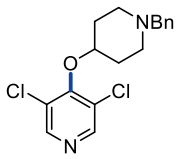

The title product was prepared according to the general procedure for (di)azine C-H etherification using 3,5-dichloropyridine (147.0 mg, 1.0 mmol, 1.0 equiv), 1-benzylpiperidin-4-ol (286.7 mg, 1.5 mmol, 1.5 equiv), 2-iodothiophene (420.1 mg, 2.0 mmol, 2.0 equiv), 18-crown-6 (396.5 mg, 1.5 mmol, 1.5 equiv), KO-*t*-Bu (0.75 M solution in THF, 2.0 mL, 1.5 mmol, 1.5 equiv), and anhydrous THF (2.0 mL). Silica gel chromatography (20% EtOAc/hexanes to 60% EtOAc/hexanes) afforded the title compound as an amber oil (266.2 mg, 0.79 mmol, 79% yield). **^{1}H NMR** (400 MHz, $CDCl_3$) δ 8.42 (s, 2H), 7.24-7.33 (m, 5H), 4.55

(m, 1H), 3.54 (s, 2H), 2.84 (m, 2H), 2.24 (m, 2H), 1.99 (m, 4H) **^{13}C NMR** (101 MHz, $CDCl_3$) δ 157.2, 149.3, 129.2, 128.4, 127.3, 126.8, 81.0, 62.9, 50.7, 31.8. **IR** (neat, cm^{-1}) 3027, 2949, 2801, 1551, 1453, 1270, 1004. **HRMS** (DART) $[M+H]^+$ calcd. for $[C_{17}H_{19}Cl_2N_2O]^+$ = 337.0869, 337.0871 found.

5-bromo-2-iodo-4-propoxypyridine (4–23)

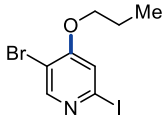

Due to the volatility of propan-1-ol, the title product was prepared using a modified procedure. An 8 mL oven-dried vial was charged with a magnetic stir bar, KO-*t*-Bu (168.3 mg, 1.5 mmol, 1.5 equiv), and 18-crown-6 (396.4 mg, 1.5 mmol, 1.5 equiv). The vial was evacuated and backfilled three times with N_2 and left under positive pressure with an N_2 balloon. A separate 8 mL vial was charged with 5-bromo-2-iodopyridine (282.8 mg, 1.0 mmol, 1.0 equiv), propan-1-ol (90.2 mg, 1.5 mmol, 1.5 equiv), 2-iodothiophene (420.1 mg, 2.0 mmol, 2.0 equiv), and anhydrous THF (4.0 mL). The solution was sparged with N_2 for 3 min then added to the vial containing KO-*t*-Bu *via* syringe. The vial was placed into a preheated 25 °C silicon oil bath and stirred for 20 h. The purification protocols were carried out in accordance with the general procedure for (di)azine C-H etherification. Silica gel chromatography (2% EtOAc/hexanes) afforded the title compound as a white solid (203.8 mg, 0.60 mmol, 60% yield). **Mp**: 48 °C – 50 °C. **^{1}H NMR** (400 MHz, $CDCl_3$) δ 8.28 (s, 1H), 7.15 (s, 1H), 4.02 (t, *J* = 6.4 Hz, 2H), 1.87 (m, 2H), 1.07 (t, *J* = 7.4 Hz, 3H). **^{13}C NMR** (101 MHz, $CDCl_3$) δ 161.6, 152.3, 119.1, 116.5, 111.7, 71.1, 22.2, 10.5. **IR** (neat, cm^{-1}) 2964, 2924, 1557, 1525, 1447, 1336, 1264, 1091. **HRMS** $[M+H]^+$ calcd. for $[C_8H_{10}BrINO]^+$ = 341.8985, 341.8989 found. **Note on reaction selectivity**: Two other heteroaryl ether side products were observed in this reaction and identified as 5-bromo-2,4-dipropoxypyridine (formed in 5% yield) and 5-bromo-2-propoxypyridine (formed in 15% yield). No heteroaryl ether regioisomers that could arise from C-H etherification were observed.

Verification of regioselectivity: To verify that 4-substitution of iodine occurred over 2-substitution, we subjected the isolated material to the protodeiodination conditions below. Formation of one of two possible products, 3-bromo-4-propoxypyridine or 5-bromo-2-propoxypyridine, was used to determine the regioselectivity of the etherification reaction.

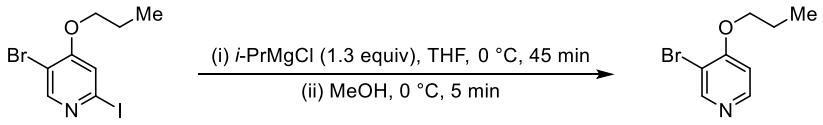

Procedure: An oven-dried 4 mL vial (KIMBLE®, Product #60910-1) was charged with a magnetic stir bar and 5-bromo-2-iodo-4-propoxypyridine (50.0 mg, 0.12 mmol, 1.0 equiv). The vial was sealed with a screw cap (Thermo Fisher Scientific, Product #C4015-1A) lined with a PTFE septum (Thermo Fisher Scientific, Product #B7995-13), evacuated and backfilled three times with N_2, and left under positive pressure of N_2 on a manifold Schlenk line. Anhydrous THF (0.4 mL) was then added via syringe and the solution was cooled to 0 °C in an ice bath. *i*-PrMgCl (2.0 M in THF, 0.08 mL, 0.16 mmol, 1.3 equiv) was then added *via* syringe and the solution was stirred for 45 min at 0 °C. MeOH (0.5 mL) was then added *via* syringe and the solution was stirred for 5 min at 0 °C. The crude reaction solution was loaded directly onto a preparatory thin layer chromatography plate and developed with 50% EtOAc/hexanes. The isolated product is 3-bromo-4-propoxypyridine (see ^{1}H NMR spectrum below), confirming 4-substitution of iodine occurred over 2-substitution of iodine. Additionally, ^{1}H NMR spectroscopy of the crude reaction solution revealed complete conversion to 3-bromo-4-propoxypyridine. Furthermore, 3-bromo-4-propoxypyridine was synthesized separately from 3-bromo-4-iodopyridine and that spectrum is

also shown below. **^{1}H NMR** (400 MHz, $CDCl_3$) δ 8.57 (s, 1H), 8.37 (d, *J* = 5.6 Hz, 1H), 6.80 (d, *J* = 5.6 Hz, 1H), 4.06 (t, *J* = 6.4 Hz, 2H), 1.89 (m, 2H), 1.08 (t, *J* = 7.4 Hz, 3H).

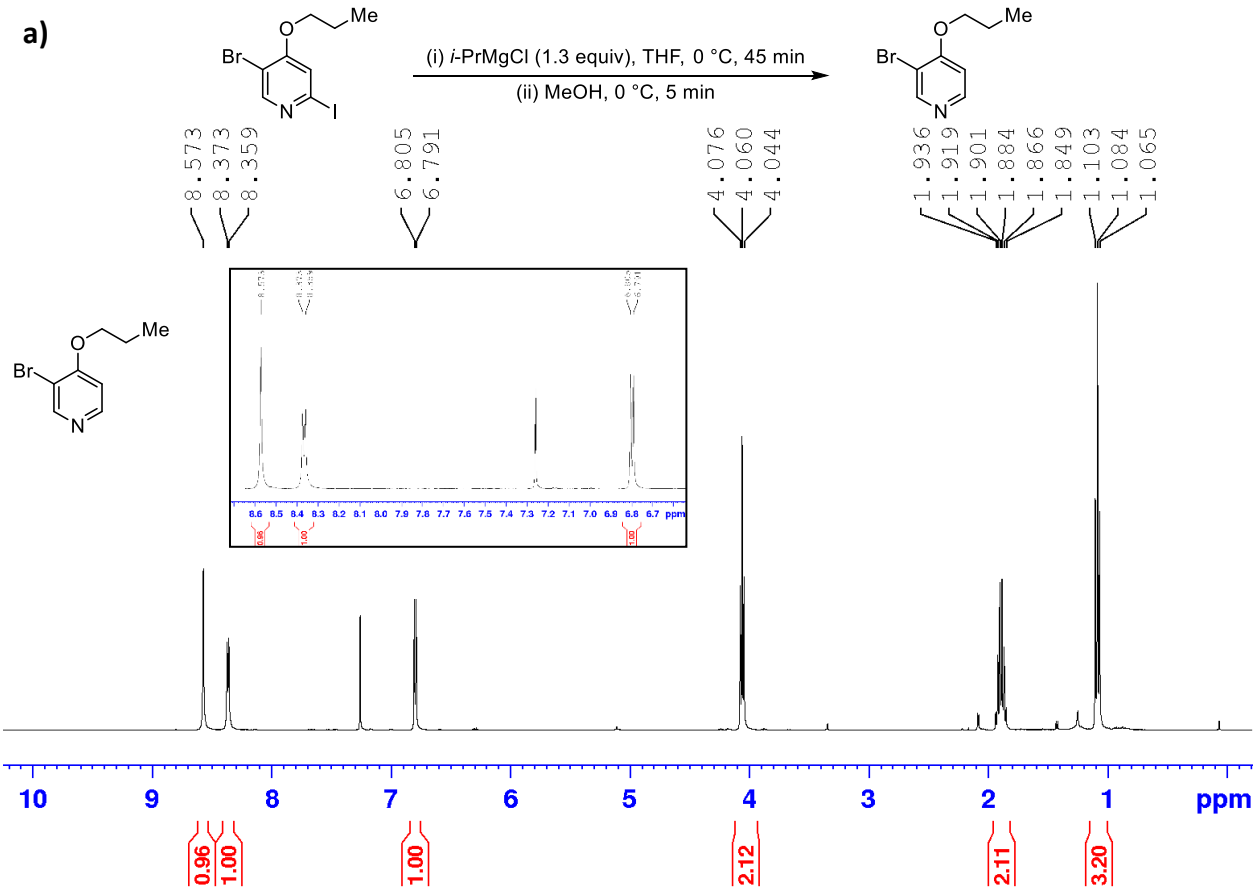

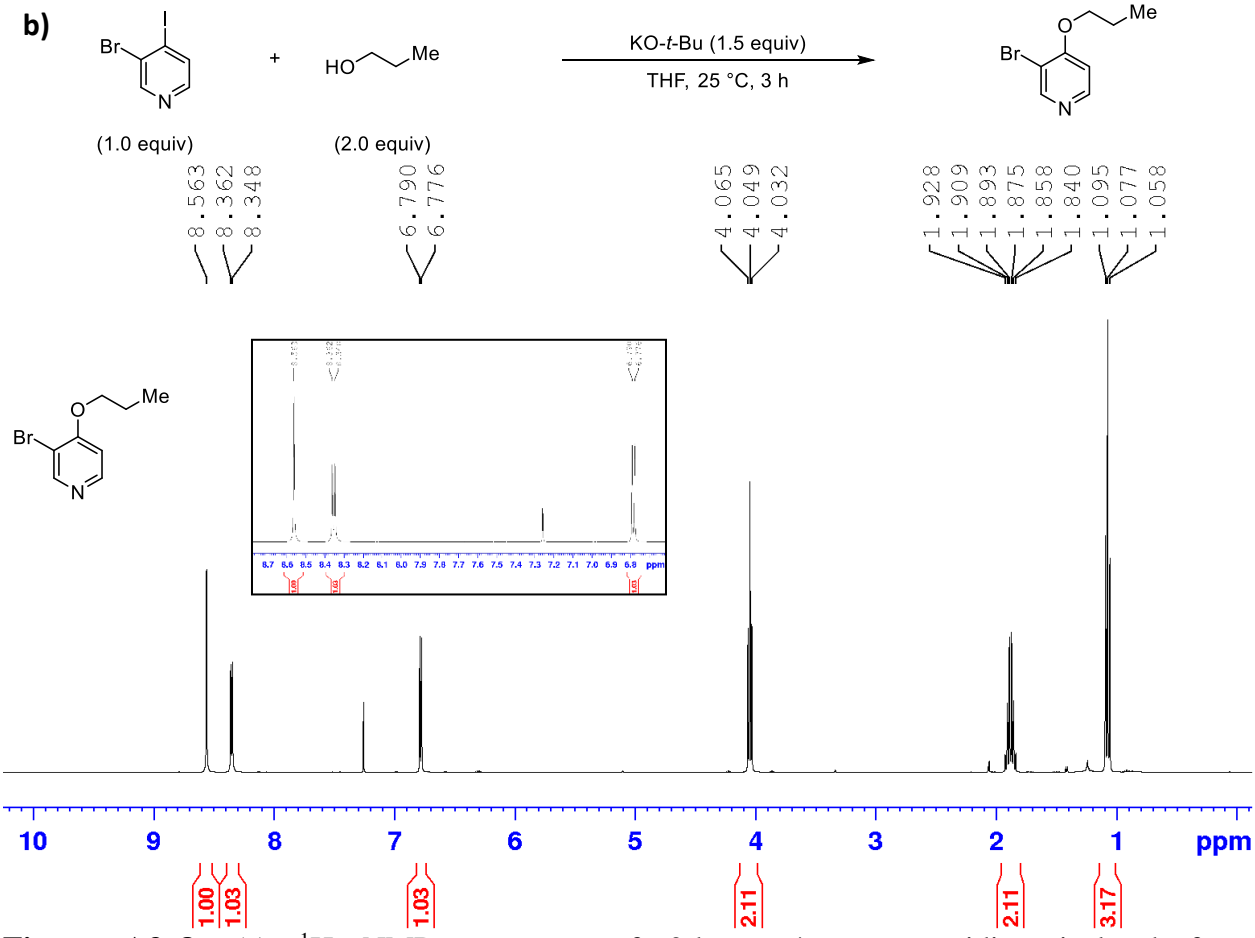

Figure A3–8: (a) ^{1}H NMR spectrum of 3-bromo-4-propoxypyridine isolated from protodeiodination of 5-bromo-2-iodo-4-propoxypyridine (**4–23**). (b) ^{1}H NMR spectrum of 3-bromo-4-propoxypyridine isolated from substitution of 3-bromo-4-iodopyridine with propan-1-ol.

5-fluoro-2-methoxy-4-(3-methoxy-3-methylbutoxy)pyridine (4–24)

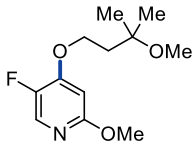

The title product was prepared according to the general procedure for (di)azine C-H etherification using 5-fluoro-2-methoxypyridine (127.0 mg, 1.0 mmol, 1.0 equiv), 3-methoxy-3-methylbutan-1-ol (177.2 mg, 1.5 mmol, 1.5 equiv), 2-iodothiophene (420.1 mg, 2.0 mmol, 2.0 equiv), 18-crown-6 (396.5 mg, 1.5 mmol, 1.5 equiv), KO-*t*-Bu (0.75 M solution in THF, 2.0 mL, 1.5 mmol, 1.5 equiv), and anhydrous THF (2.0 mL). Silica gel chromatography (5% EtOAc/hexanes to 10% EtOAc/hexanes) afforded the title compound as a white solid (157.0 mg, 0.65 mmol, 65% yield). **Mp**: 47 ºC - 50 ºC. **^{1}H NMR** (400 MHz, $CDCl_3$)

δ 7.84 (d, *J* = 3.0 Hz, 1H), 6.28 (d, *J* = 5.8 Hz, 1H), 4.13 (t, *J* = 7.0 Hz, 2H), 3.87 (s, 3H), 3.21 (s, 3H), 2.04 (t, *J* = 7.0 Hz, 2H), 1.23 (s, 6H). **^{13}C NMR** (101 MHz, $CDCl_3$) δ 161.5 (d, *J* = 1.6 Hz), 155.6 (d, *J* = 11.3 Hz), 147.0 (d, *J* = 245.9 Hz), 132.5 (d, *J* = 23.1 Hz), 95.0, 73.6, 65.5, 53.8, 49.5, 38.7, 25.4. **^{19}F NMR** (376 MHz, $CDCl_3$) δ -161.7. **IR** (neat, cm^{-1}) 2973, 2941, 2826, 1616, 1505, 1381, 1212, 1014. **HRMS** (DART) $[M+H]^+$ calcd. for $[C_{12}H_{19}FNO_3]^+$ = 244.1343, 244.1345 found.

2-chloro-4-((2-ethylhexyl)oxy)-5-methoxypyridine (4–25)

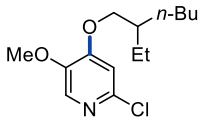

The title product was prepared according to the general procedure for (di)azine C-H etherification using 2-chloro-5-methoxypyridine (143.1 mg, 1.0 mmol, 1.0 equiv), 2-ethylhexan-1-ol (195.3 mg, 1.5 mmol, 1.5 equiv), 2-iodothiophene (420.1 mg, 2.0 mmol, 2.0 equiv), KO-*t*-Bu (0.75 M solution in THF, 2.3 mL, 2.0 mmol, 2.0 equiv), and anhydrous THF (1.7 mL). Silica gel chromatography (4% EtOAc/hexanes) afforded the title compound as a light-yellow oil (88.1 mg, 0.32 mmol, 32% yield). **^{1}H NMR** (400 MHz, $CDCl_3$) δ 7.84 (s, 1H), 6.78 (s, 1H), 3.89-3.92 (m, 5H), 1.83 (m, 1H), 1.39-1.57 (m, 4H), 1.25-1.37 (m, 4H), 0.89-0.95 (m, 6H). **^{13}C NMR** (101 MHz, $CDCl_3$) δ 157.1, 145.8, 144.4, 129.9, 107.7, 72.0, 57.2, 39.0, 30.4, 29.1, 23.8, 23.1, 14.2, 11.1. **IR** (neat, cm^{-1}) 2958, 2929, 2872, 1580, 1501, 1461, 1245, 1013. **HRMS** (DART) $[M+H]^+$ calcd. for $[C_{14}H_{23}ClNO_2]^+$ = 272.1412, 272.1413 found.

4-(isopentyloxy)-3-(phenylthio)pyridine (4–26)

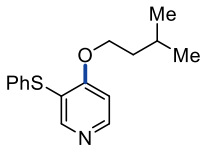

The title product was prepared according to the general procedure for (di)azine C-H etherification using 3-(phenylthio)pyridine (187.0 mg, 1.0 mmol, 1.0 equiv), 3-methylbutan-1-ol (176.2 mg, 2.0 mmol, 2.0 equiv), KO-*t*-Bu (0.75 M in THF, 4.0 mL, 3.0 mmol, 3.0 equiv), 2-iodothiophene (630.1 mg, 3.0 mmol, 3.0 equiv), and 18-crown-6 (793.0 mg, 3.0 mmol, 3.0 equiv). Prior to addition of the KO-*t*-Bu solution, the reagents

were constituted in 0.5 mL of THF instead of 2.0 mL of THF. Silica gel chromatography (25% EtOAc/hexanes to 50% EtOAc/hexanes) afforded the title compound as a brown oil (134.8 mg, 0.49 mmol, 49% yield). **^{1}H NMR** (400 MHz, $CDCl_3$) δ 8.39 (d, *J* = 5.6 Hz, 1H), 8.31 (s, 1H), 7.21-7.32 (m, 5H), 6.78 (d, *J* = 5.6 Hz, 1H), 4.04 (t, *J* = 6.2 Hz, 2H), 1.56-1.66 (m, 3H), 0.86 (d, *J* = 6.0 Hz, 6H). **^{13}C NMR** (101 MHz, $CDCl_3$) δ 163.5, 152.8, 150.6, 134.1, 130.9, 129.3, 127.2, 121.1, 107.1, 67.1, 37.4, 24.8, 22.5. **IR** (neat, cm^{-1}) 2962, 2877, 1546, 1436, 1394, 1054, 998, 960. **HRMS** (ESI) $[M+H]^+$ calcd. for $[C_{16}H_{20}NOS]^+$ = 274.1260, 274.1249 found.

***N*,*N*-dimethyl-2-((2-phenyl-6-(trifluoromethyl)pyridin-4-yl)oxy)ethan-1-amine (4–27)**

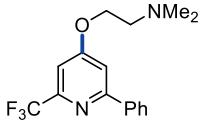

The title product was prepared according to the general procedure for (di)azine C-H etherification using 2-phenyl-6-(trifluoromethyl)pyridine (223.1 mg, 1.0 mmol, 1.0 equiv), 2-(dimethylamino)ethan-1-ol (133.7 mg, 1.5 mmol, 1.5 equiv), 2-iodothiophene (420.1 mg, 2.0 mmol, 2.0 equiv), 18-crown-6 (396.5 mg, 1.5 mmol, 1.5 equiv), KO-*t*-Bu (0.75 M solution in THF, 2.0 mL, 1.5 mmol, 1.5 equiv), and anhydrous THF (2.0 mL). Silica gel chromatography (7% MeOH/CH_2Cl_2) afforded the title compound as a brown oil (177.4 mg, 0.57 mmol, 57% yield). **^{1}H NMR** (400 MHz, $CDCl_3$) δ 8.01 (m, 2H), 7.41-7.50 (m, 3H), 7.40 (m, 1H), 7.15 (d, *J* = 2.1 Hz, 1H), 4.24 (m, 2H), 2.81 (m, 2H), 2.38 (br s, 6H). **^{13}C NMR** (101 MHz, $CDCl_3$) δ 166.7, 159.8, 149.8 (q, *J* = 34.6 Hz), 138.2, 129.9, 129.0, 127.3, 121.6 (q, *J* = 275.5 Hz), 109.1, 105.9 (q, *J* = 2.9 Hz), 66.6, 57.9, 45.9. **^{19}F NMR** (376 MHz, $CDCl_3$) δ -69.2. **IR** (neat, cm^{-1}) 2947, 2824, 2773, 1605, 1445, 1130, 775. **HRMS** (DART) $[M+H]^+$ calcd. for $[C_{16}H_{18}F_3N_2O]^+$ = 311.1366, 311.1395 found.

4-(cyclopropylmethoxy)-2,6-bis(trifluoromethyl)pyridine (4–28)

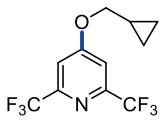

The title product was prepared according to the general procedure for (di)azine C-H etherification using 2,6-bis(trifluoromethyl)pyridine (215.0 mg, 1.0 mmol, 1.0

equiv), cyclopropylmethanol (108.2 mg, 1.5 mmol, 1.5 equiv), 2-iodothiophene (420.1 mg, 2.0 mmol, 2.0 equiv), 18-crown-6 (396.5 mg, 1.5 mmol, 1.5 equiv), KO-*t*-Bu (0.75 M solution in THF, 2.0 mL, 1.5 mmol, 1.5 equiv), and anhydrous THF (2.0 mL). Silica gel chromatography (1% EtOAc/hexanes to 2% EtOAc/hexanes) afforded the title compound as a clear oil (205.4 mg, 0.72 mmol, 72% yield). **^{1}H NMR** (400 MHz, $CDCl_3$) δ 7.31 (s, 2H), 3.98 (d, *J* = 7.1 Hz, 2H), 1.31 (m, 1H), 0.73 (m, 2H), 0.41 (m, 2H). **^{13}C NMR** (101 MHz, $CDCl_3$) δ 167.4, 150.4 (q, *J* = 35.7 Hz), 120.9 (q, *J* = 275.8 Hz), 109.9 (q, *J* = 2.3 Hz), 74.3, 9.7, 3.6. **^{19}F NMR** (376 MHz, $CDCl_3$) δ -69.3. **IR** (neat, cm^{-1}) 3094, 3015, 2891, 1612, 1390, 1271, 1135, 1005. **EA**: Anal. Calcd. for $C_{11}H_9F_6NO$: C, 46.33; H, 3.18; N, 4.91. Found: C, 46.57; H, 3.05; N, 5.01.

2,6-bis(difluoromethyl)-4-(pentyloxy)pyridine (4–29)

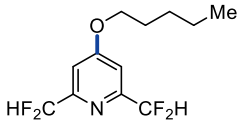

The title product was prepared according to the general procedure for (di)azine C-H etherification on a 0.25 mmol scale using 2,6-bis(difluoromethyl)pyridine (31.7 mg, 0.25 mmol, 1.0 equiv), pentan-1-ol (33.0 mg, 0.375 mmol, 1.5 equiv), 2-iodothiophene (105.0 mg, 0.5 mmol, 2.0 equiv), 18-crown-6 (132.2 mg, 0.5 mmol, 2.0 equiv), KO-*t*-Bu (0.75 M solution in THF, 0.67 mL, 2.0 mmol, 2.0 equiv), and anhydrous THF (0.3 mL). Preparatory thin layer chromatography (4% EtOAc/hexanes) afforded the title compound as a clear oil (31.7 mg, 0.12 mmol, 48% yield). **^{1}H NMR** (400 MHz, $CDCl_3$) δ 7.21 (s, 2H), 6.59 (t, *J* = 55.3 Hz, 2H), 4.10 (t, *J* = 6.5 Hz, 2H), 1.84 (m, 2H), 1.35-1.50 (m, 4H), 0.95 (t, *J* = 6.8 Hz, 3H). **^{13}C NMR** (101 MHz, $CDCl_3$) δ 167.5, 154.6 (t, *J* = 25.8 Hz), 113.5 (t, *J* = 242.1 Hz), 108.4, 69.1, 28.5, 28.1, 22.5, 14.1. **^{19}F NMR** (376 MHz, $CDCl_3$) δ -117.1 (d, *J* = 55.3 Hz). **IR** (neat, cm^{-1}) 3051, 2921, 1637, 1573, 1461, 1433, 1097. **HRMS** (DART) $[M+H]^+$ calcd. for $[C_{12}H_{16}F_4NO]^+$ = 266.1163, 266.1157 found. **Note on reaction selectivity**: The title product represents the major product formed in the reaction. Another unidentified ether side product can

be observed in the ^{1}H NMR spectrum (see below) of the crude reaction solution as the signal at 4.10 ppm is not a clean triplet. No aromatic signals corresponding to this signal were identified suggesting this compound is not a separate aryl ether regioisomer.

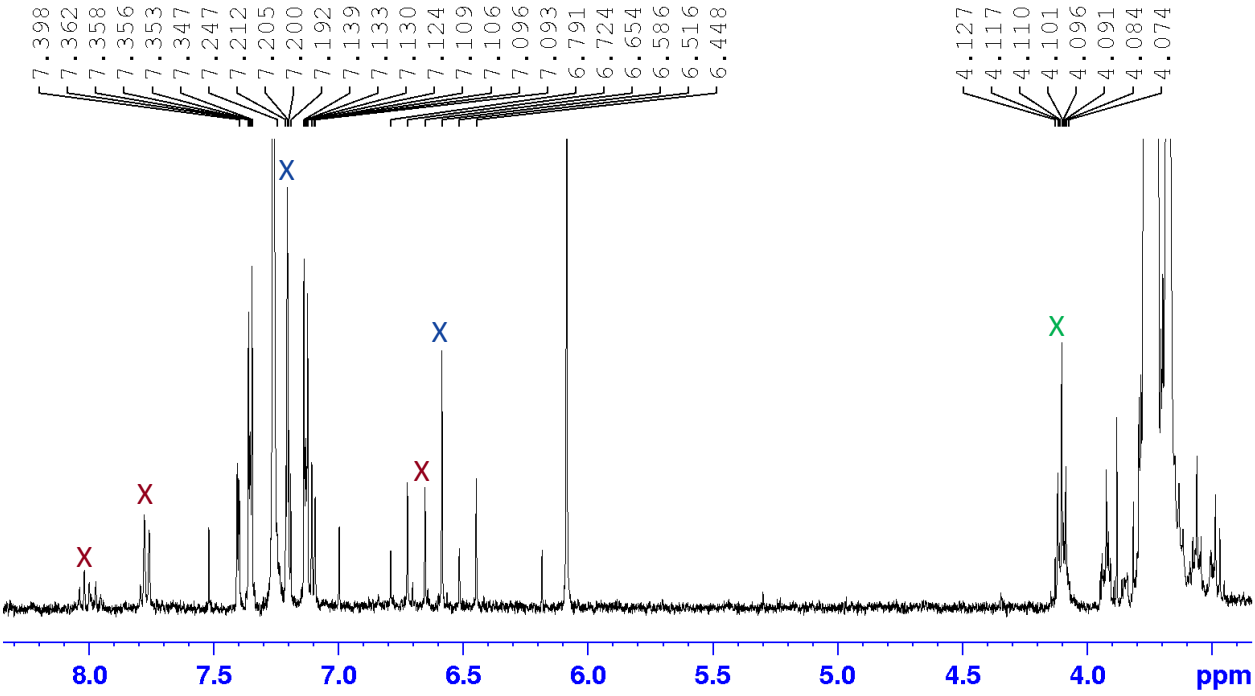

Figure A3–9: ^{1}H NMR spectrum of the crude reaction solution of C-H etherification of **4–29**. Signals corresponding to **4–29**are marked with X. Signals corresponding to the starting material are marked with X. The signal corresponding to the methylene next to the heteroaryl ether oxygen (4.10 ppm) is marked with X.

2-phenyl-7-((tetrahydro-2*H*-pyran-4-yl)methoxy)furo[3,2-*b*]pyridine (4–30)

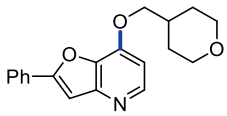

The title product was prepared according to the general procedure for (di)azine C-H etherification using 2-phenylfuro[3,2-*b*]pyridine (194.1 mg, 1.0 mmol, 1.0 equiv), (tetrahydro-2*H*-pyran-4-yl)methanol (174.2 mg, 1.5 mmol, 1.5 equiv), 2-iodothiophene (420.1 mg, 2.0 mmol, 2.0 equiv), 18-crown-6 (396.5 mg, 1.5 mmol, 1.5 equiv), KO-*t*-Bu (0.75 M solution in THF, 2.0 mL, 1.5 mmol, 1.5 equiv), and anhydrous THF (2.0 mL). Silica gel chromatography (25% EtOAc/hexanes to EtOAc) afforded the title compound as a light-yellow

solid (174.2 mg, 0.57 mmol, 57% yield). **Mp**: 142 ºC – 144 ºC; **^{1}H NMR** (400 MHz, $CDCl_3$) δ 8.35 (d, *J* = 5.4 Hz, 1H), 7.89 (m, 2H), 7.47 (m, 2H), 7.40 (m, 1H), 7.17 (s, 1H), 6.71 (d, *J* = 5.5 Hz, 1H), 4.16 (d, *J* = 6.5 Hz, 2H), 4.06 (dd, *J* = 3.3 Hz, 10.9 Hz, 2H), 3.48 (td, *J* = 2.0 Hz, 11.9 Hz, 2H), 2.22 (m, 1H), 1.84 (m, 2H), 1.54 (m, 2H). **^{13}C NMR** (101 MHz, $CDCl_3$) δ 158.9, 150.8, 150.1, 147.8, 137.9, 129.9, 129.5, 129.0, 125.4, 104.2, 102.8, 73.8, 67.7, 35.2, 29.7. **IR** (neat, cm^{-1}) 3101, 2921, 2844, 1627, 1301, 1114, 992. **HRMS** (DART) $[M+H]^+$ calcd. for $[C_{19}H_{20}NO_3]^+$ = 310.1438, 310.1454 found.

3-bromo-4-((3-methyloxetan-3-yl)methoxy)quinoline (4–31)

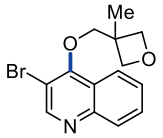

The title product was prepared according to the general procedure for (di)azine C-H etherification using 3-bromoquinoline (207.0 mg, 1.0 mmol, 1.0 equiv), (3-methyloxetan-3-yl)methanol (153.2 mg, 1.5 mmol, 1.5 equiv), 2-iodothiophene (420.1 mg, 2.0 mmol, 2.0 equiv), 18-crown-6 (396.5 mg, 1.5 mmol, 1.5 equiv), KO-*t*-Bu (0.75 M solution in THF, 2.0 mL, 1.5 mmol, 1.5 equiv), and anhydrous THF (2.0 mL). Silica gel chromatography (15% EtOAc/hexanes to 30% EtOAc/hexanes) afforded the title compound as a light-yellow powder (185.0 mg, 0.60 mmol, 60% yield). **Mp**: 105 ºC – 107 ºC; **^{1}H NMR** (400 MHz, $CDCl_3$) δ 8.92 (s, 1H), 8.11 (m, 2H), 7.75 (m, 1H), 7.60 (m, 1H), 4.81 (d, *J* = 6.1 Hz, 2H), 4.57 (d, *J* = 6.1 Hz, 2H), 4.36 (s, 2H), 1.63 (s, 3H). **^{13}C NMR** (101 MHz, $CDCl_3$) δ 159.1, 153.5, 149.0, 130.2, 129.8, 127.5, 125.1, 121.6, 109.1, 79.8, 78.8, 40.7, 21.4. **IR** (neat, cm^{-1}) 2959, 2869, 1574, 1359, 1075, 981, 767. **HRMS** (DART) $[M+H]^+$ calcd. for $[C_{14}H_{15}BrNO_2]^+$ = 308.0281, 308.0291 found.

(*S*)-4-((1-benzylpyrrolidin-2-yl)methoxy)pyridazine (4–32)

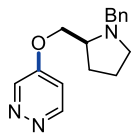

The title product was prepared according to the procedure described for **4–34** using pyridazine (160.2 mg, 2.0 mmol, 2.0 equiv), (*S*)-(1-benzylpyrrolidin-2-yl)methanol (191.1 mg, 1.0 mmol, 1.0 equiv), 2-iodothiophene (420.1 mg, 2.0 mmol, 2.0 equiv), KO-*t*-Bu

(168.3 mg, 1.5 mmol, 1.5 equiv), and DMF (4.0 mL). The reaction solution was stirred in a 60 °C silicon oil bath for 20 h. Silica gel chromatography (2% MeOH/CH_2Cl_2 to 3% MeOH/CH_2Cl_2) afforded the title compound as an amber oil (102.6 mg, 0.38 mmol, 38% yield). **^{1}H NMR** (400 MHz, $CDCl_3$) δ 8.89 (m, 1H), 8.85 (m, 1H), 7.28-7.40 (m, 4H), 7.22-7.26 (m, 1H), 6.70 (dd, *J* = 3.1 Hz, 6.1 Hz. 1H), 3.96 (d, *J* = 13.1 Hz, 1H), 3.91 (dd, *J* = 5 Hz, 9.4 Hz, 1H), 3.82 (dd, *J* = 6.6 Hz, 9.4 Hz, 1H), 3.65 (d, *J* = 13.0 Hz, 1H), 3.04 (m, 2H), 2.39 (m, 1H), 2.05 (m, 1H), 1.71-1.84 (m, 3H). **^{13}C NMR** (101 MHz, $CDCl_3$) δ 157.2, 151.6, 144.2, 139.5, 129.0, 128.5, 127.3, 108.8, 71.5, 61.9, 60.2, 55.2, 28.8, 23.4. **IR** (neat, cm^{-1}) 2945, 2874, 2793, 1574, 1304, 1266, 1016, 740. **HRMS** (ESI) $[M+H]^+$ calcd. for $[C_{16}H_{20}N_3O]^+$ = 270.1601, 270.1599 found. $[\alpha]_D^{23}$ = -50.5°. **Note on reaction selectivity**: Heteroaryl ether minor side products are observed in the ^{1}H NMR spectrum of the crude reaction solution. These products were identified as the 3-ether of pyridazine (5% yield) and the 4,5-diether of pyridazine (8% yield).

3,6-diisopropoxy-4-(2-(piperidin-1-yl)ethoxy)pyridazine (4–33)

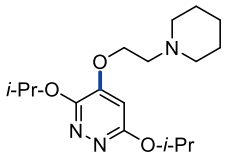

The title product was prepared according to the procedure described for **4–34** using 3,6-diisopropoxypyridazine (196.1 mg, 1.0 mmol, 1.0 equiv), 2-(piperidin-1-yl)ethan-1-ol (193.7 mg, 1.5 mmol, 1.5 equiv), 2-iodothiophene (420.1 mg, 2.0 mmol, 2.0 equiv), KO-*t*-Bu (168.3 mg, 1.5 mmol, 1.5 equiv), and anhydrous DMF (4.0 mL). The reaction solution was stirred in a 25 °C silicon oil bath for 20 h. Silica gel chromatography (1% MeOH/CH_2Cl_2 to 4% MeOH/CH_2Cl_2) afforded the title compound as an amber oil (156.3 mg, 0.48 mmol, 48% yield). **^{1}H NMR** (400 MHz, $CDCl_3$) δ 6.20 (s, 1H), 5.40 (m, 2H), 4.12 (t, *J* = 6.1 Hz, 2H), 2.82 (t, *J* = 6.0 Hz, 2H), 2.52 (m, 4H), 1.56-1.62 (m, 4H), 1.41-1.48 (m, 2H), 1.39 (d, *J* = 6.2 Hz, 6H), 1.36 (d, *J* = 6.2 Hz, 6H). **^{13}C NMR** (101 MHz, $CDCl_3$) δ 162.0, 154.1, 150.5, 99.5, 69.9, 69.3, 67.2, 56.9, 55.2, 26.1, 24.2, 22.2, 22.1. **IR** (neat, cm^{-1}) 2977,

2934, 1606, 1444, 1420, 1254, 1186, 1105. **HRMS** (ESI) $[M+H]^+$ calcd. for $[C_{17}H_{30}N_3O_3]^+$ = 324.2282, 324.2292 found. **Note on reaction regioselectivity**: Another unidentified ether side product is observed in the ^1H NMR spectrum of the crude reaction mixture in 8% yield. We speculate that this product may arise from substitution of the product with another equivalent of 2-(piperidin-1-yl)ethan-1-ol or from C-H etherification of **4–33**.

5-(decyloxy)-*N*,*N*-diethylpyridazine-4-carboxamide (4–34)

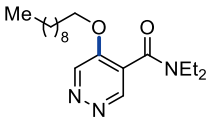

The title product was prepared using a slightly modified procedure on a 0.5 mmol scale. Open to air, an 8 mL oven-dried vial (Thermo Fisher Scientific, Product #033405P) was charged with a magnetic stir bar along with KO-*t*-Bu (84.2 mg, 0.75 mmol, 1.5 equiv). The vial was sealed a screw cap (Thermo Fisher Scientific, Product #03392A) lined with a PTFE septum (Thermo Fisher Scientific, Product #B7995-15), evacuated and backfilled three times with N_2, and left under positive pressure of N_2 on a manifold Schlenk line. A separate vial was charged with *N*,*N*-diethylpyridazine-4-carboxamide (89.6 mg, 0.5 mmol, 1.0 equiv), decan-1-ol (118.7 mg, 0.75 mmol, 1.5 equiv), 2-iodothiophene (420.1 mg, 2.0 mmol, 2.0 equiv), and anhydrous DMF (4.0 mL). This solution was sparged with N_2 for 3 minutes and then added to the vial containing KO-*t*-Bu *via* syringe. The reaction vial was placed into a preheated 25 °C silicon oil bath with stirring for 20 h. The title compound was purified according to the general procedure for (di)azine C-H etherification. Silica gel chromatography (70% EtOAc/hexanes to EtOAc) afforded the title compound as an amber oil (88.8 mg, 0.26 mmol, 53% yield). **^{1}H NMR** (400 MHz, $CDCl_3$) δ 9.07 (br s, 1H), 8.92 (br s, 1H), 4.21 (t, *J* = 6.4 Hz, 2H), 3.30 - 3.82 (m, 2H), 3.12 (q, *J* = 7.1 Hz, 2H), 1.81 (m, 2H), 1.42 (m, 2H), 1.22-1.36 (m, 15H), 1.07 (t, *J* = 7.1 Hz, 3H), 0.87 (t, *J* = 7.0 Hz, 3H). **^{13}C NMR** (101 MHz, $CDCl_3$) Note: aromatic signals depressed in spectrum; δ 163.6, 69.4, 50.4, 42.9, 39.3, 31.8, 29.5, 29.3, 29.2, 28.8, 25.6, 22.6, 14.2, 14.1, 12.7. **IR** (neat, cm^-

[1]) 2926, 2855, 2240, 1633, 1549, 1329, 728. **HRMS** (DART) $[M+H]^+$ calcd. for $[C_{19}H_{34}N_3O_2]^+$ = 336.2646, 336.2677 found.

Verification of Regioselectivity: The ^{1}H NMR spectrum of the isolated product makes it difficult to identify the regioisomer formed due to significant aromatic signal broadening. This broadening was not observed in the ^{1}H NMR spectrum of the crude reaction solution. The ^{1}H NMR spectrum of the crude solution is consistent with the proposed structure for the title product and is provided below along with the ^{1}H NMR spectrum of the isolated product.

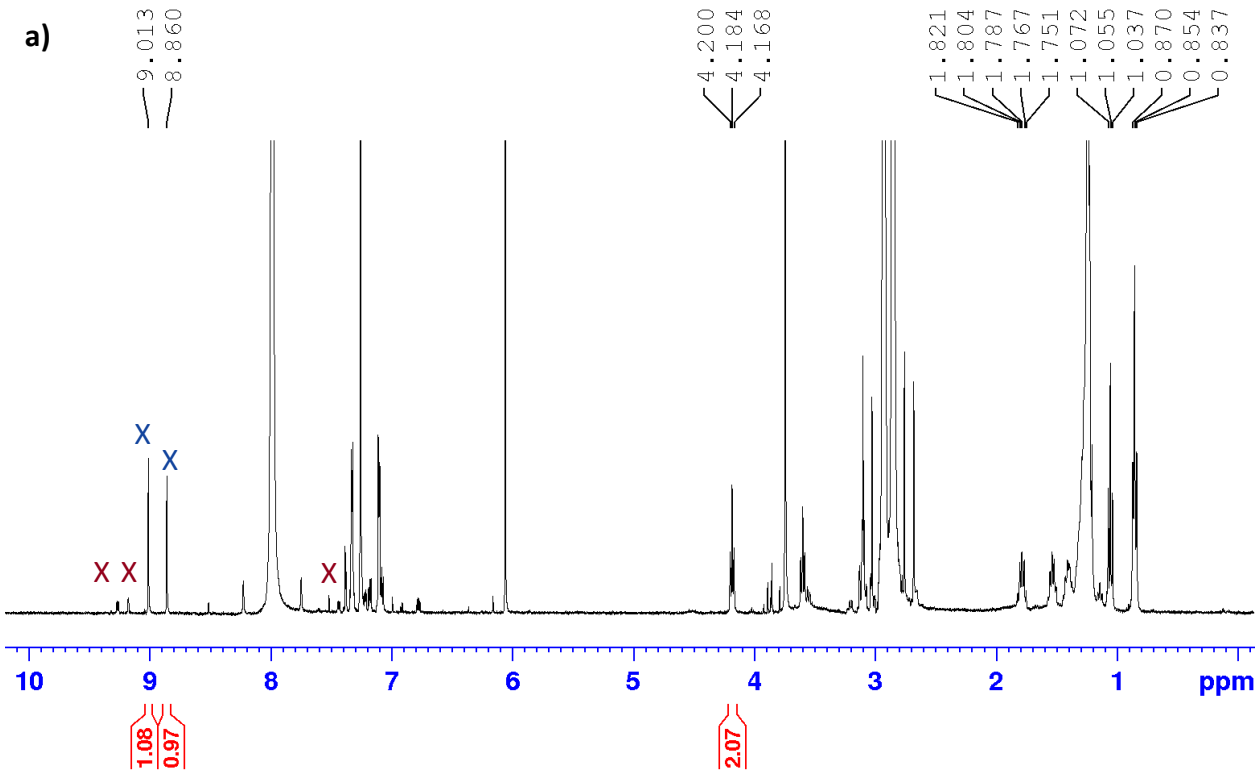

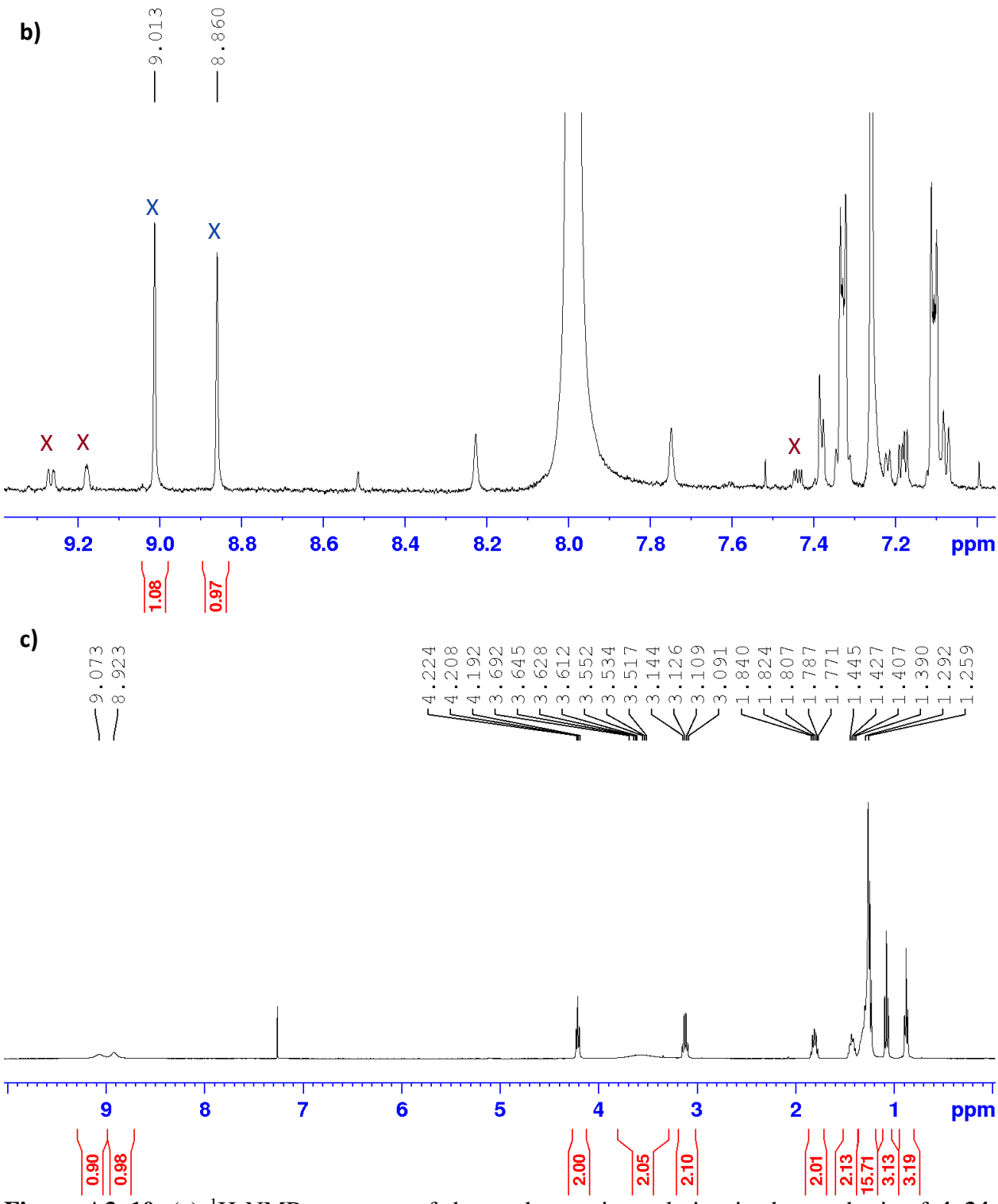

Figure A3–10: (a) ^{1}H NMR spectrum of the crude reaction solution in the synthesis of **4–34**. Aromatic signals corresponding to the product are labelled with X. Aromatic signals corresponding to the starting material are labelled with X (b) Zoomed in ^{1}H NMR spectrum of the crude reaction solution in the synthesis of **4–34**. Aromatic signals corresponding to the product are labelled with X. (c) ^{1}H NMR spectrum of purified **4–34**.

7-butoxypyrazolo[1,5-*a*]pyrimidine (4–35)

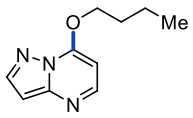

The title product was prepared according to the general procedure for (di)azine C-H etherification using pyrazolo[1,5-*a*]pyrimidine (119.1 mg, 1.0 mmol, 1.0 equiv), butan-1-ol (111.2 mg, 1.5 mmol, 1.5 equiv), 2-iodothiophene (420.1 mg, 2.0 mmol, 2.0 equiv), KO-*t*-Bu (0.75 M solution in THF, 2.0 mL, 1.5 mmol, 1.5 equiv), and anhydrous THF (2.0 mL). Silica gel chromatography (50% EtOAc/hexanes to 70% EtOAc/hexanes) afforded the title compound as an orange semi-solid (71.1 mg, 0.37 mmol, 37% yield). **^{1}H NMR** (400 MHz, $CDCl_3$) δ 8.30 (d, *J* = 5.0 Hz, 1H), 8.07 (d, *J* = 2.2 Hz, 1H), 6.58 (d, *J* = 2.3 Hz, 1H), 6.11 (d, *J* = 5.0 Hz, 1H), 4.32 (t, *J* = 6.6 Hz, 2H), 1.90-1.97 (m, 2H), 1.53 (m, 2H), 0.95 (t, *J* = 7.4 Hz, 3H). **^{13}C NMR** (101 MHz, $CDCl_3$) δ 155.5, 150.9, 150.5, 145.0, 96.5, 86.8, 70.4, 30.4, 19.0, 13.7. **IR** (neat, cm^{-1}) 3060, 2957, 2872, 1610, 1538, 1461, 1323, 1119. **HRMS** (ESI) $[M+H]^+$ calcd. for $[C_{10}H_{14}N_3O]^+$ = 192.1131, 192.1129 found.

Verification of Regioselectivity: To determine the regioselectivity of the etherification reaction, an authentic sample of **4–35** was prepared *via* substitution of 7-chloropyrazolo[1,5-*a*]pyrimidine with butan-1-ol.

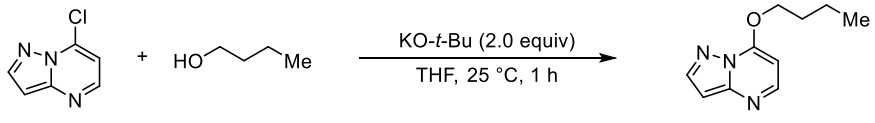

Procedure: Open to air, an oven-dried 4 mL vial (KIMBLE®, Product #60910-1) was charged with a magnetic stir bar, 7-chloropyrazolo[1,5-*a*]pyrimidine (38.3 mg, 0.25 mmol, 1.0 equiv), butan-1-ol (37.1 mg, 0.5 mmol, 2.0 equiv), anhydrous THF (1.0 mL), and KO-*t*-Bu (56.1 mg, 0.5 mmol, 2.0 equiv) in successive order. The vial was sealed with a screw cap (Thermo Fisher Scientific, Product #C4015-1A) lined with a PTFE septum (Thermo Fisher Scientific, Product

#B7995-13) and the solution was stirred for 1 h at 25 °C. The crude solution was loaded directly onto a preparatory thin layer chromatography plate and developed with 80% EtOAc/hexanes. Comparison of the ^{1}H NMR spectrum of the isolated product is consistent with the proposed title product structure. **^{1}H NMR** (400 MHz, $CDCl_3$) δ 8.36 (d, *J* = 5.0 Hz, 1H), 8.11 (d, *J* = 2.2 Hz, 1H), 6.63 (d, *J* = 2.2 Hz, 1H), 6.16 (d, *J* = 5.0 Hz, 1H), 4.38 (t, *J* = 6.6 Hz, 2H), 1.99 (m, 2H), 1.57 (m, 2H), 1.00 (t, *J* = 7.4 Hz, 3H).

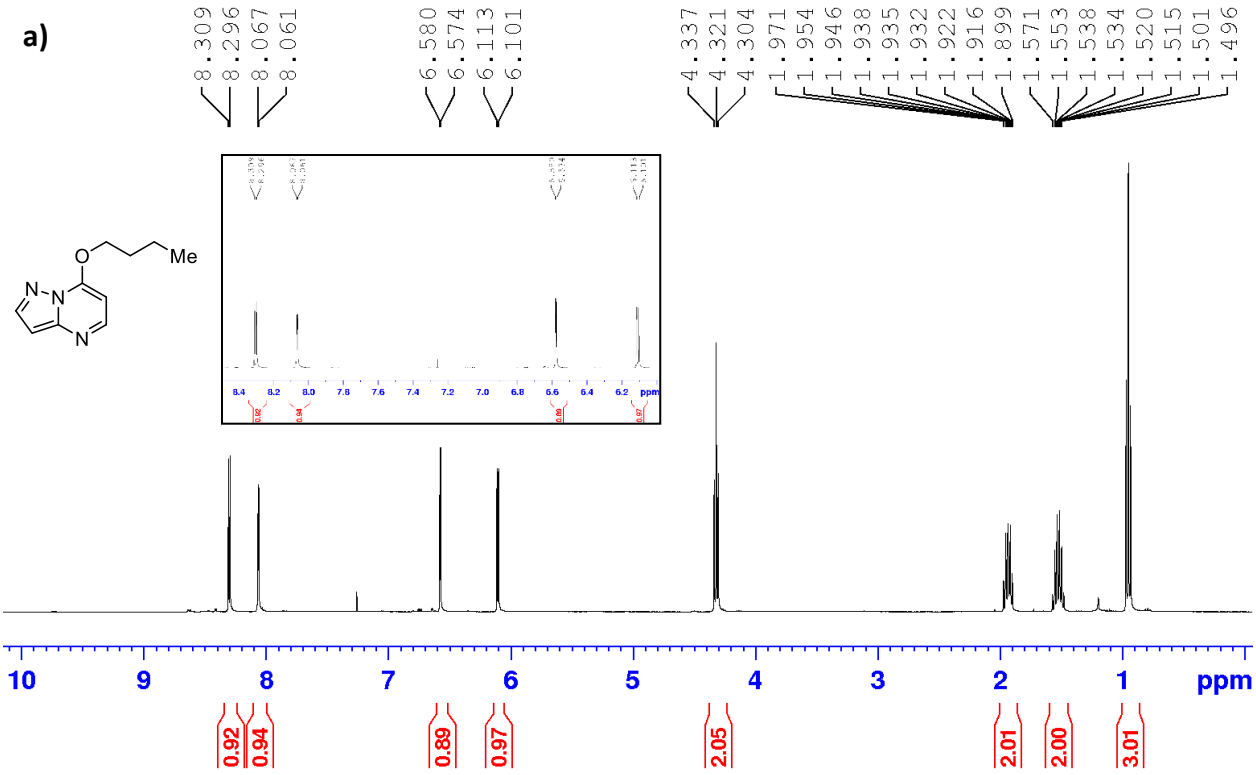

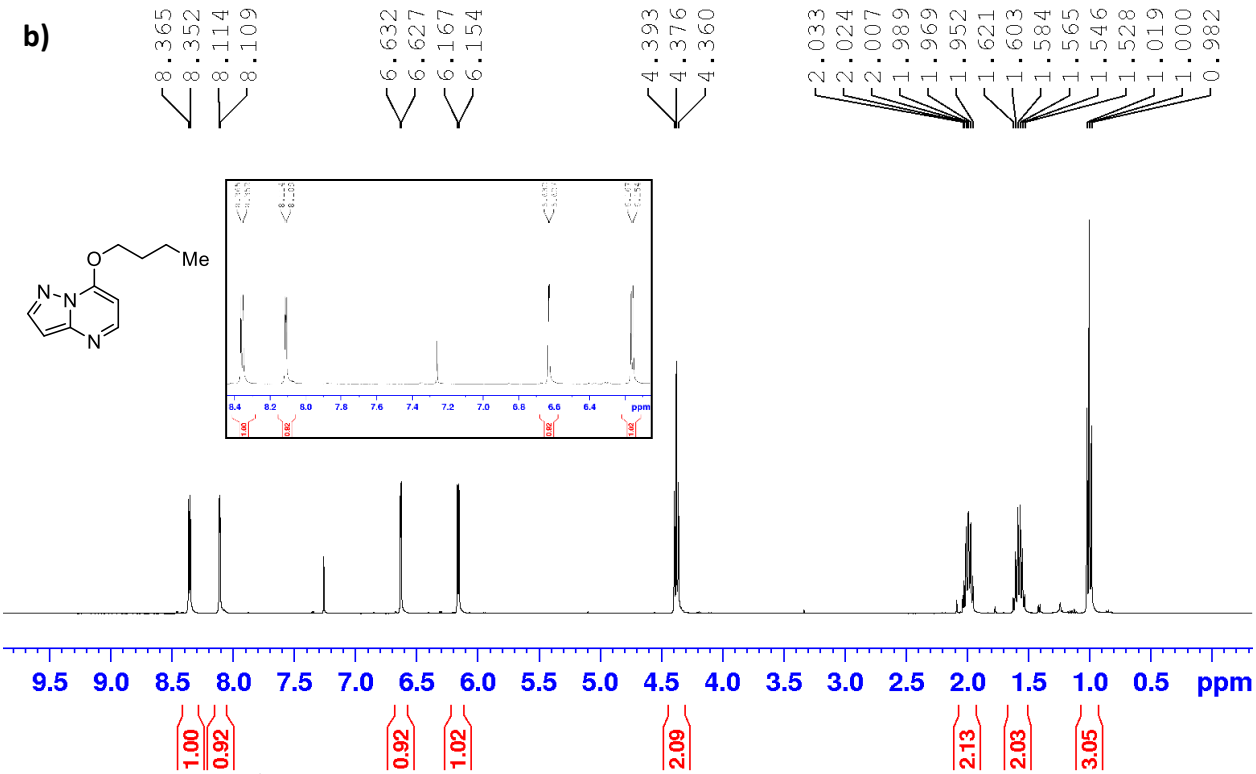

Figure A3–11: (a) ^{1}H NMR spectrum of **4–35** isolated from C-H etherification of pyrazolo[1,5-*a*]pyrimidine with butan-1-ol. (b) ^{1}H NMR spectrum of **4–35** isolated from substitution of 7-chloropyrazolo[1,5-*a*]pyrimidine with 1-butanol.

2-chloro-10-(3-(4-(2-((3-iodopyridin-4-yl)oxy)ethyl)piperazin-1-yl)propyl)-10*H*-phenothiazine (4–36)

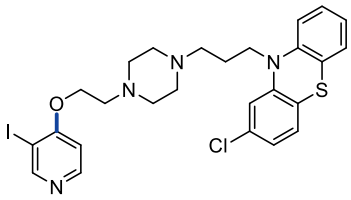

The title product was prepared according to the general procedure for (di)azine C-H etherification on 0.4 mmol scale using 3-iodopyridine (102.5 mg, 0.5 mmol, 1.25 equiv), perphenazine (161.6 mg, 0.4 mmol, 1.0 equiv), 2-iodothiophene (168.0 mg, 0.8 mmol, 2.0 equiv), 18-crown-6 (158.6 mg, 0.6 mmol, 1.5 equiv), anhydrous THF (1.2 mL), and KO-*t*-Bu (0.75 M solution in THF, 0.8 mL, 0.6 mmol, 1.5 equiv), and anhydrous THF (1.2 mL). Silica gel chromatography (15% acetone/hexanes to acetone on silica gel neutralized with NEt_3) afforded the title compound as a light-brown oil (196.0 mg, 0.32 mmol, 80% yield). **^{1}H NMR** (400 MHz, $CDCl_3$) δ 8.74 (s, 1H), 8.35 (d, *J* = 5.6 Hz, 1H), 7.10-7.16 (m, 2H), 7.00 (d, *J* = 8.1 Hz, 1H), 6.84-6.94 (m, 4H), 6.71 (d,

J = 5.6, 1H), 4.20 (t, *J* = 5.6 Hz, 2H), 3.90 (t, *J* = 6.7 Hz, 2H), 2.90 (t, *J* = 5.5 Hz, 2H), 2.67 (m, 4H), 2.50 (m, 6H), 1.96 (m, 2H). **^{13}C NMR** (101 MHz, $CDCl_3$) δ 163.4, 157.9, 150.8, 146.6, 144.5, 133.3, 128.0, 127.6, 127.5, 124.9, 123.7, 123.0, 122.4, 116.0, 116.0, 107.8, 85.4, 67.8, 56.4, 55.5, 53.7, 53.2, 45.3, 24.1. **IR** (neat, cm^{-1}) 2938, 2810, 1568, 1456, 1295, 1014. **HRMS** (DART) $[M+H]^+$ calcd. for $[C_{26}H_{29}ClN_4OS]^+$ = 607.0790, 607.0788 found.

3-(phenylsulfonyl)-4-propoxypyridine (4–40)

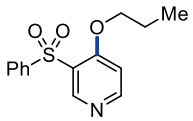

Due to the volatility of 1-propanol, the title product was prepared using a modified procedure. An 8 mL oven-dried vial was charged with a magnetic stir bar and KO-*t*-Bu (168.3 mg, 1.5 mmol, 1.5 equiv). The vial was evacuated and backfilled three times with N_2 and left under positive pressure with an N_2 balloon. A separate 8 mL vial was charged with 3-(phenylsulfonyl)pyridine (219.0 mg, 1.0 mmol, 1.0 equiv), propan-1-ol (90.2 mg, 1.5 mmol, 1.5 equiv), 2,3-diiodobenzothiophene (962.8 mg, 2.5 mmol, 2.5 equiv), and anhydrous THF (4.0 mL). The solution was sparged with N_2 for 3 min then added to vial containing KO-*t*-Bu *via* syringe. The vial was placed into a preheated 25 °C silicon oil bath with stirring for 20 h. The purification protocols were carried out in accordance with the general procedure for (di)azine C-H etherification. Silica gel chromatography (50% EtOAc/hexanes to 80% EtOAc/hexanes) afforded the title compound as a light-yellow solid (189.0 mg, 0.68 mmol, 68% yield). **Mp**: 148 °C – 150 °C. **^{1}H NMR** (400 MHz, $CDCl_3$) δ 9.18 (s, 1H), 8.60 (d, *J* = 5.9 Hz, 1H), 7.96 (m, 2H), 7.59 (m, 1H), 7.49 (m, 2H), 6.80 (d, *J* = 5.9 Hz, 1H), 3.96 (t, *J* = 6.5 Hz, 2H), 1.74 (m, 2H), 0.96 (t, *J* = 7.4 Hz, 3H). **^{13}C NMR** (101 MHz, $CDCl_3$) δ 162.7, 156.2, 150.8, 140.9, 133.5, 128.8, 128.6, 125.7, 108.2, 71.1, 22.0, 10.4. **IR** (neat, cm^{-1}) 2977, 2934, 1607, 1447, 1420, 1255, 1188. **HRMS** (ESI) $[M+H]^+$ calcd. for $[C_{14}H_{16}NO_3S]^+$ = 278.0845, 278.0846 found.

4-(cyclopentyloxy)-*N*,*N*-diethylpyridine-3-sulfonamide (4–41)

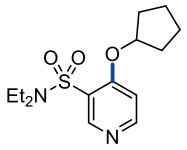

The title product was prepared according to the general procedure for (di)azine C-H etherification on a 0.5 mmol scale using *N*,*N*-diethylpyridine-3-sulfonamide (106.6 mg, 0.5 mmol, 1.0 equiv), cyclopentanol (64.6 mg, 0.75 mmol, 1.5 equiv), 2,3-diiodobenzothiophene (288.8 mg, 0.75 mmol, 1.5 equiv), anhydrous THF (1.0 mL), and KO-*t*-Bu (0.75 M solution in THF, 1.0 mL, 0.75 mmol, 1.5 equiv). Silica gel chromatography (50% EtOAc/hexanes to 80% EtOAc/hexanes) afforded the title compound as a light-brown solid (92.6 mg, 0.31 mmol, 62% yield). **Mp**: 47 ºC – 50 ºC. **^{1}H NMR** (400 MHz, $CDCl_3$) δ 8.95 (s, 1H), 8.55 (d, *J* = 5.8 Hz, 1H), 6.88 (d, *J* = 5.8 Hz, 1H), 4.96 (m, 1H), 3.35 (q, *J* = 7.1 Hz, 4H), 1.80-2.05 (m, 6H), 1.70 (m, 2H), 1.12 (t, *J* = 7.1 Hz, 6H). **^{13}C NMR** (101 MHz, $CDCl_3$) δ 161.7, 154.6, 152.1, 126.4, 109.3, 81.8, 41.8, 32.9, 24.1, 14.5. **IR** (neat, cm^{-1}) 2971, 2874, 1575, 1477, 1326, 1149, 1015, 937. **EA**: Anal. Calcd. for $C_{14}H_{22}N_2O_3S$: C, 56.35; H, 7.43; N, 9.39. Found: C, 56.61; H, 7.51; N, 9.25.

5-chloro-4-(2-ethylbutoxy)-2-phenylpyrimidine (4–42)

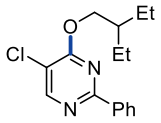

The title product was prepared according to the general procedure for (di)azine C-H etherification on a 0.5 mmol scale using 5-chloro-2-phenylpyrimidine (94.5 mg, 0.5 mmol, 1.0 equiv), 2-ethylbutan-1-ol (76.6 mg, 0.75 mmol, 1.5 equiv), 2,3-diiodobenzothiophene (288.8 mg, 0.75 mmol, 1.5 equiv), KO-*t*-Bu (0.75 M solution in THF, 1.0 mL, 0.75 mmol, 1.5 equiv), and anhydrous THF (1.0 mL). The reaction solution was stirred in a 60 °C silicon oil bath for 20 h. Silica gel chromatography (2% EtOAc/hexanes) afforded the title compound as a light-yellow solid (64.6 mg, 0.22 mmol, 45% yield). **Mp**: 39 ºC – 41 ºC; **^{1}H NMR** (400 MHz, $CDCl_3$) δ 8.49 (s, 1H), 8.38-8.40 (m, 2H), 7.46-7.49 (m, 3H), 4.50 (d, *J* = 5.8 Hz, 2H),

1.79 (m, 1H), 1.52 (m, 4H), 0.99 (t, J = 7.5 Hz, 6H). **^{13}C NMR** (101 MHz, $CDCl_3$) δ 164.6, 162.2, 155.8, 136.9, 130.9, 128.6, 128.3, 115.8, 69.6, 40.6, 23.6, 11.3. **IR** (neat, cm^{-1}) 2962, 2877, 1546, 1436, 1394, 1054, 998, 960. **HRMS** (ESI) $[M+H]^+$ calcd. for $[C_{16}H_{20}ClN_2O]^+$ = 291.1259, 291.1262 found. **Note on reaction selectivity**: 5-chloro-4,6-bis(2-ethylbutoxy)-2-phenylpyrimidine (a product arising from C-H etherification of **4–42**) was observed in the crude reaction mixture in 3% yield as determined by ^{1}H NMR spectroscopy.

8-((1-benzhydrylazetidin-3-yl)methoxy)imidazo[1,2-*b*]pyridazine (4–43)

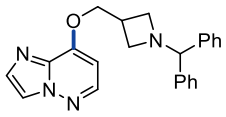

The title product was prepared according to the general procedure for (di)azine C-H etherification using imidazo[1,2-*b*]pyridazine (119.0 mg, 1.0 mmol, 1.0 equiv), (1-benzhydrylazetidin-3-yl)methanol (379.8 mg, 1.5 mmol, 1.5 equiv), 2,3-diiodobenzothiophene (577.7 mg, 1.5 mmol, 1.5 equiv), KO-*t*-Bu (0.75 M solution in THF, 2.0 mL, 1.5 mmol, 1.5 equiv), and anhydrous THF (2.0 mL). Silica gel chromatography (2% MeOH/CH_2Cl_2 to 3% MeOH/CH_2Cl_2) afforded the title compound as a light-brown solid (265.4 mg, 0.72 mmol, 72% yield). **Mp**: 145 ºC – 147 ºC; **^{1}H NMR** (400 MHz, $CDCl_3$) δ 8.15 (d, J = 5.4 Hz, 1H), 7.91 (d, J = 1.1 Hz, 1H), 7.65 (m, 1H), 7.42 (m, 4H), 7.28 (m, 4H), 7.19 (m, 2H), 6.36 (d, J = 5.5 Hz, 1H), 4.50 (d, J = 7.1 Hz, 2H), 4.42 (br s, 1H), 3.36 (m, 2H), 3.12 (m, 2H), 3.05 (m, 1H). **^{13}C NMR** (101 MHz, $CDCl_3$) δ 154.8, 144.2, 142.1, 134.7, 132.3, 128.5, 127.6, 127.2, 117.4, 95.6, 77.8, 72.1, 56.1, 29.0. **IR** (neat, cm^{-1}) 2901, 2824, 1550, 1305, 1121, 1082, 813. **HRMS** (DART) $[M+H]^+$ calcd. for $[C_{23}H_{23}N_4O]^+$ = 371.1866, 371.1898 found.

1-(3-phenylpropoxy)phthalazine (4–44)

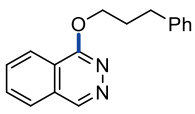

The title product was prepared according to the general procedure for (di)azine C-H etherification using phthalazine (130.1 mg, 1.0 mmol, 1.0 equiv), 3-phenylpropan-1-ol (204.2 mg, 1.5 mmol, 1.5 equiv), 2,3-diiodobenzothiophene (577.7 mg, 1.5

mmol, 1.5 equiv), KO-*t*-Bu (0.75 M solution in THF, 2.0 mL, 1.5 mmol, 1.5 equiv), and anhydrous THF (2.0 mL). Silica gel chromatography (30% EtOAc/hexanes to 50% EtOAc/hexanes) afforded the title compound as a brown oil (84.2 mg, 0.32 mmol, 32% yield). **^{1}H NMR** (400 MHz, $CDCl_3$) δ 9.16 (s, 1H), 8.19 (m, 1H), 7.84-7.88 (m, 3H), 7.17-7.31 (m, 5H), 4.71 (t, *J* = 6.4 Hz, 2H), 2.89 (m, 2H), 2.28 (m, 2H). **^{13}C NMR** (101 MHz, $CDCl_3$) δ 160.6, 148.0, 141.6, 132.3, 132.1, 128.9, 128.6, 128.6, 126.1, 125.9, 123.1, 120.1, 67.0, 32.6, 30.7. **IR** (neat, cm^{-1}) 3060, 3025, 2950, 1553, 1407, 1337, 1111. **HRMS** (ESI) $[M+H]^+$ calcd. for $[C_{17}H_{17}N_2O]^+$ = 265.1335, 265.1325 found.

c) Characterization data of polyazine substrates from Scheme 2

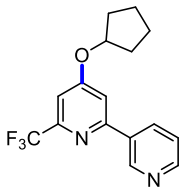

4-(cyclopentyloxy)-6-(trifluoromethyl)-2,3'-bipyridine (4–47)

The title product was prepared according to a modified procedure. Inside an N_2 filled glovebox, an oven-dried 4 mL vial was charged with a magnetic stir bar, 6-(trifluoromethyl)-2,3'-bipyridine (112.0 mg, 0.5 mmol, 1.0 equiv), cyclopentanol (64.6 mg, 0.75 mmol, 1.5 equiv), 2,3-diiodobenzothiophene (385.1 mg, 1.0 mmol, 2.0 equiv), 18-crown-6 (264.3mg, 1.0 mmol, 2.0 equiv), anhydrous THF (2.0 mL), and KO-*t*-Bu (112.2 mg, 1.0 mmol, 2.0 equiv) in successive order. The vial was sealed with screw cap (Thermo Fisher Scientific, Product #C4015-1A) lined with PTFE septum (Thermo Fisher Scientific, Product #B7995-13), removed from the glovebox, and placed into a 25 °C aluminum reaction block. The reaction solution was stirred for 3 h. The crude reaction mixture was then loaded directly onto a silica gel column and eluted using a 20% EtOAc/hexanes to 40% EtOAc/hexanes solvent gradient to afford the title compound as a brown solid (94.8 mg, 0.31 mmol, 62% yield). **Mp**: 44 °C – 47 °C. **IR** (neat, cm^{-1}) 2964, 1603, 1387, 1184, 1139, 996, 852. **^{1}H NMR** (400 MHz, $CDCl_3$) δ 9.16 (d, *J* = 1.9 Hz, 1H), 8.66 (dd, *J* = 4.8 Hz, 1.4 Hz, 1H), 8.35 (m, 1H), 7.40 (dd, *J* = 4.8 Hz, 7.9 Hz, 1H), 7.33 (d, *J* = 2.0 Hz, 1H), 7.13 (d, *J* = 2.0 Hz, 1H), 4.96 (m, 1H), 1.98 – 2.07 (m, 2H), 1.80 – 1.95

(m, 4H), 1.65 – 1.77 (m, 2H). **^{13}C NMR** (101 MHz, $CDCl_3$) δ 166.3, 156.9, 150.7, 150.0 (q, *J* = 34.5 Hz), 148.3, 134.9, 133.9, 123.8, 121.5 (q, *J* = 275.6 Hz), 110.0, 107.3 (q, *J* = 2.9 Hz), 80.9, 32.8, 24.1. **^{19}F NMR** (376 MHz, $CDCl_3$) δ -69.3. **HRMS** (ESI) $[M+H]^+$ calcd. for $[C_{16}H_{16}F_3N_2O]^+$ = 309.1209, 309.1206 found. **Note on reaction selectivity**: Other unidentified side products were observed in the ^{19}F NMR spectrum of the crude reaction solution. The title product was formed in approximately 7:1 selectivity. We speculate the observed side products could arise from C-H etherification adjacent to the trifluoromethyl functional group or C-H etherification of the other pyridine ring. The ^{1}H NMR signals at 7.33 (d, *J* = 2.0 Hz, 1H) and 7.13 (d, *J* = 2.0 Hz, 1H) ppm are consistent with the 2,4,6-trisubstituted pattern of the title product.

5-chloro-4-(3-(pyridin-3-yl)propoxy)-2,3'-bipyridine (4–50)

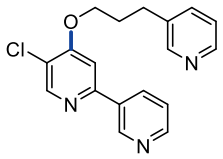

The title product was prepared according to the general procedure using 5-chloro-2,3'-bipyridine (190.0 mg, 1.0 mmol, 1.0 equiv), 3-(pyridin-3-yl)propan-1-ol (206.2 mg, 1.5 mmol, 1.5 equiv), 2,3-diiodobenzothiophene (577.7 mg, 1.5 mmol, 1.5 equiv), and 18-crown-6 (396.5 mg, 1.5 mmol, 1.5 equiv). Silica gel chromatography (2% MeOH/CH_2Cl_2 to 4% MeOH/CH_2Cl_2) afforded the title compound as a white solid (226.0 mg, 0.70 mmol, 70% yield). **Mp**: 93 ºC - 95 ºC; **IR** (neat, cm^{-1}) 3024, 2921, 1586, 1415, 1364, 1024, 704. **^{1}H NMR** (400 MHz, $CDCl_3$) δ 9.09 (s, 1H), 8.65 (d, *J* = 4.7 Hz, 1H), 8.55 (s, 1H), 8.51 (s, 1H), 8.47 (d, *J* = 4.7 Hz, 1H), 8.24 (m, 1H), 7.56 (m, 1H), 7.39 (dd, *J* = 4.8 Hz, 8.0 Hz, 1H), 7.24 (dd, *J* = 4.9 Hz, 7.7 Hz, 1H), 7.17 (s, 1H), 4.18 (t, *J* = 6.0 Hz, 2H), 2.91 (t, *J* = 7.4 Hz, 2H), 2.24 (m, 2H). **^{13}C NMR** (101 MHz, $CDCl_3$) δ 160.9, 155.2, 150.4, 150.1, 150.0, 148.2, 147.9, 136.2, 136.2, 134.6, 134.4, 123.7, 123.6, 120.4, 104.9, 67.5, 30.1, 29.1. **HRMS** (ESI) $[M+H]^+$ calcd. for $[C_{18}H_{16}ClN_3O]^+$ = 326.1055, 326.1053 found. **Note on Regioselectivity**: The title product represents the only regioisomer observed in the ^{1}H NMR spectrum of the crude

reaction solution. The ^{1}H NMR signals at 8.55 (s, 1H) and 7.17 (s, 1H) ppm are consistent with the trisubstituted pyridine structure of the title product. Additionally, the splitting pattern and number of the other ^{1}H NMR signals are consistent with the monosubstituted pyridine structures of the title product.

8-(8-(hex-5-en-1-yloxy)imidazo[1,2-*b*]pyridazin-6-yl)quinoline (4–51)

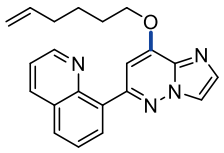

The title product was prepared according to the general procedure on a 0.5 mmol scale with a modified purification procedure using 8-(imidazo[1,2-*b*]pyridazin-6-yl)quinoline (123.1 mg, 0.5 mmol, 1.0 equiv), hex-5-en-1-ol (75.1 mg, 0.75 mmol, 1.5 equiv), KO-*t*-Bu (0.75 M in THF, 2.0 mL, 1.5 mmol, 1.5 equiv), and 2,3-diiodobenzothiophene (288.8 mg, 0.75 mmol, 1.5 equiv). After silica gel chromatography (30% EtOAc/hexanes to 80% EtOAc/hexanes), the isolated material was transferred into a separatory funnel containing 1M $HCl_{(aq)}$ (40 mL) and agitated to ensure efficient mixing. The aqueous mixture was washed with CH_2Cl_2 (3 x 40 mL) then made basic by adding solid portions of Na_2CO_3 slowly. The aqueous mixture was then washed with CH_2Cl_2 (3 x 40 mL) and the organic layers were combined and dried over Na_2SO_4. The Na_2SO_4 was removed by filtration and the organic layer was concentrated *in vacuo* to afford the title compound as a light-yellow solid (80.6 mg, 0.23 mmol, 47% yield). **Mp**: decomposition to a brown sludge occurred before melting point could be observed. **IR** (neat, cm^{-1}) 3052, 2923, 1574, 1461, 1434, 1117, 743. **^{1}H NMR** (400 MHz, $CDCl_3$) δ 8.96 (m, 1H), 8.26 (m, 1H), 8.04 (m, 1H), 7.96-7.98 (m, 2H), 7.65-7.69 (m, 2H), 7.48 (dd, *J* = 4.2 Hz, 8.3 Hz, 1H), 7.08-7.11 (m, 1H), 5.80 (m, 1H), 4.97 (m, 2H), 4.29 (t, *J* = 6.5 Hz, 2H), 2.13 (m, 2H), 1.98 (m, 2H), 1.65 (m, 2H). **^{13}C NMR** (101 MHz, $CDCl_3$) δ 154.3, 153.2, 150.8, 146.1, 138.4, 136.7, 135.9, 134.3, 132.1, 131.1, 130.0, 128.8, 126.5, 121.6, 117.5, 115.1, 100.6, 69.4, 33.5, 28.3, 25.3. **HRMS** (ESI) $[M+H]^+$ calcd. for $[C_{21}H_{21}N_4O]^+$ = 345.1710, 345.1710 found.

Note on reaction selectivity: The title product represents the major product observed in the ^{1}H NMR spectrum of the crude reaction solution. A side product, identified as an iodinated derivative ($C_{21}H_{19}IN_4O$) of the title product, is observed in the ^{1}H NMR spectrum of the crude reaction solution in 11% yield.

Verification of Regioselectivity: To verify the substitution selectivity, an authentic sample of **4–51** was synthesized from 8-bromo-6-chloroimidazo[1,2-*b*]pyridazine.

Step 1: 6-chloro-8-(hex-5-en-1-yloxy)imidazo[1,2-*b*]pyridazine

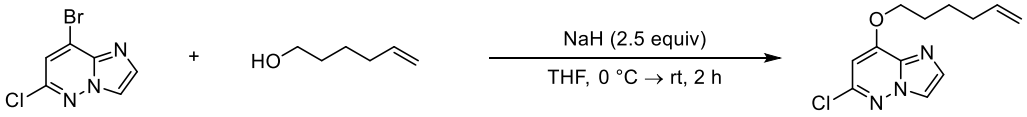

(1.0 equiv) (1.0 equiv) 86% yield

Procedure: Open to air, an oven-dried 8 mL vial (KIMBLE®, Product #60910-1) was charged with a magnetic stir bar, NaH (60% dispersion in mineral oil, 100.0 mg, 2.5 mmol, 2.5 equiv), and anhydrous THF (4.0 mL) in successive order. The solution was placed into a 0 °C ice water bath then 5-hexen-1-ol (100.1 mg, 1.0 mmol, 1.0 equiv) and 8-bromo-6-chloroimidazo[1,2-*b*]pyridazine (232.5 mg, 1.0 mmol, 1.0 equiv) were added in successive order. The vial was sealed with a screw cap (Thermo Fisher Scientific, Product #C4015-1A) lined with a PTFE septum (Thermo Fisher Scientific, Product #B7995-13), warmed to rt, and stirred for 2 h. The reaction mixture was then transferred into a separatory funnel containing H_2O (40 mL). The aqueous mixture was extracted with EtOAc (3 x 40 mL). The organic layer was dried over Na_2SO_4. The Na_2SO_4 was filtered off and the organic layer was concentrated. Silica gel chromatography (35% EtOAc/hexanes) yielded the title product as a clear oil (217.2 mg, 0.86 mmol, 86% yield). **^{1}H NMR** (400 MHz, $CDCl_3$) δ 7.83 (m, 1H), 7.64 (m, 1H), 6.38 (s, 1H), 5.81 (m, 1H), 4.97-5.06 (m, 2H), 4.27 (t, J = 6.5 Hz, 2H), 2.15 (m, 2H), 1.98 (m, 2H), 1.64 (m, 2H). **HRMS** $[M+H]^+$ calcd. for

$[C_{12}H_{15}ClN_3O]^+$ = 252.0898, 252.0908 found. **Note**: HRMS confirms regioselectivity of alcohol substitution of bromine over chlorine.

Step 2: 8-(8-(hex-5-en-1-yloxy)imidazo[1,2-*b*]pyridazin-6-yl)quinoline (4–51)

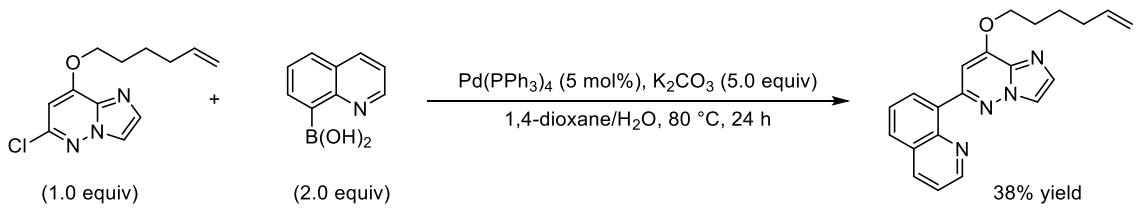

(1.0 equiv) (2.0 equiv) 38% yield

Procedure: Inside an N_2 filled glovebox, an oven-dried 4 mL vial (KIMBLE®, Product #60910-1) was charged with a magnetic stir bar, 6-chloro-8-(hex-5-en-1-yloxy)imidazo[1,2-*b*]pyridazine (62,8 mg, 0.25 mmol, 1.0 equiv), 1,4-dioxane (0.7 mL), quinolin-8-ylboronic acid (86.6 mg, 0.50 mmol, 2.0 equiv), $Pd(PPh_3)_4$ (14.4 mg, 0.013 mmol, 0.05 equiv), and K_2CO_3 (125.2 mg, 1.25 mmol, 5.0 equiv) in successive order. The vial was sealed with a screw cap (Thermo Fisher Scientific, Product #C4015-1A) lined with a PTFE septum (Thermo Fisher Scientific, Product #B7995-13), removed from the glovebox, and placed into a preheated 80 °C aluminum reaction block and the reaction mixture was stirred for 24 h. The reaction solution was cooled to rt. The crude solution was loaded directly onto preparatory thin layer chromatography (plate developed with 5% MeOH/CH_2Cl_2 solvent) for isolation (32.6 mg, 0.095 mmol, 38% yield). ^{1}H NMR of the isolated compound is consistent with the ^{1}H NMR of **4–51** (see figure below for comparison of the ^{1}H NMR spectra). **^{1}H NMR** (400 MHz, $CDCl_3$) δ 8.96 (m, 1H), 8.26 (m, 1H), 8.04 (dd, *J* = 1.4 Hz, 7.1 Hz, 1H), 7.96-7.98 (m, 2H), 7.66-7.70 (m, 2H), 7.49 (dd, *J* = 4.2 Hz, 8.3 Hz, 1H), 7.00 Hz (s, 1H), 5.81 (m, 1H), 4.93-5.04 (m, 2H), 4.29 (t, *J* = 6.5 Hz, 2H), 2.14 (m, 2H), 1.99 (m, 2H), 1.65 (m, 2H).

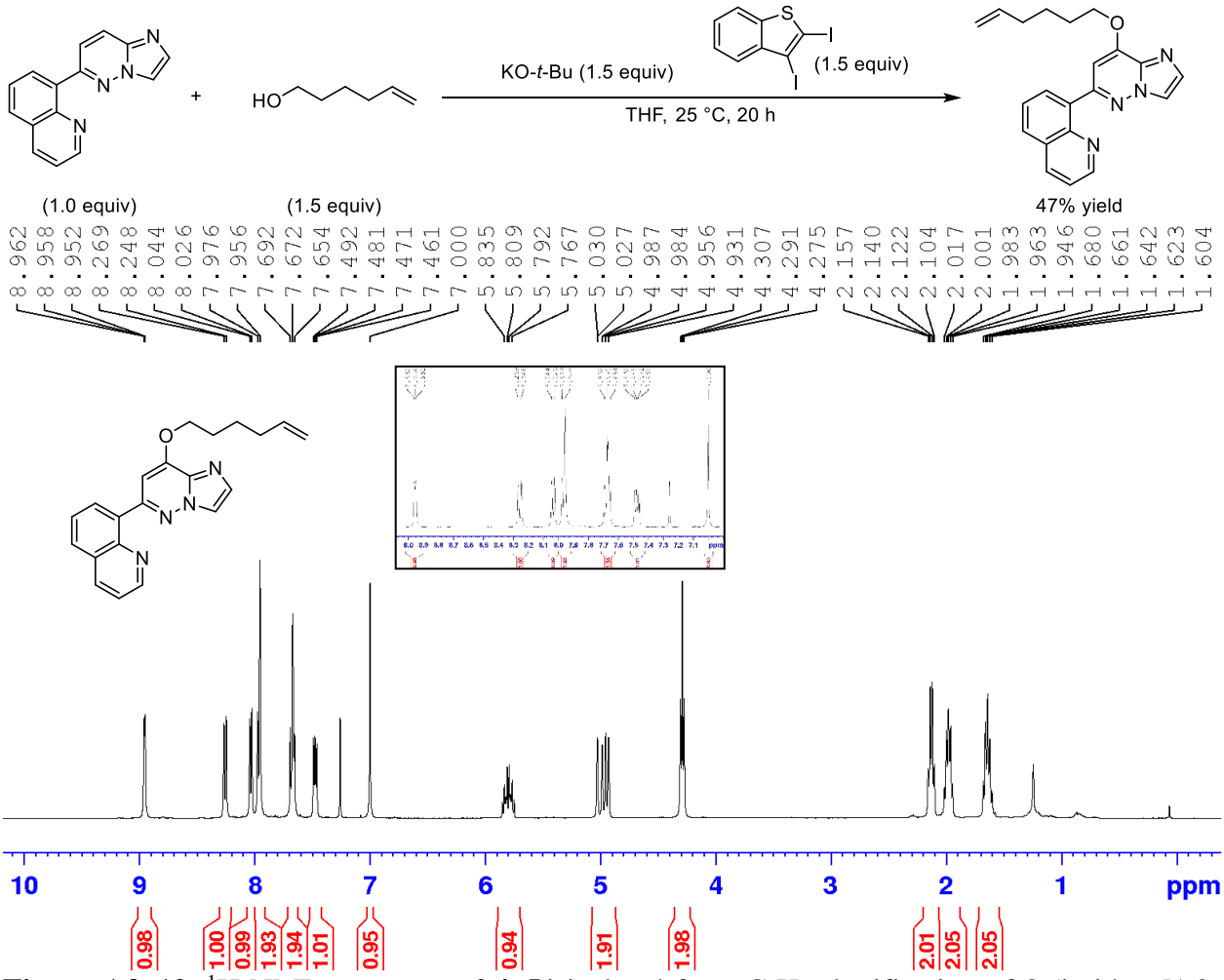

Figure A3–12: ^{1}H NMR spectrum of **4–51** isolated from C-H etherification of 8-(imidazo[1,2-*b*]pyridazin-6-yl)quinoline.

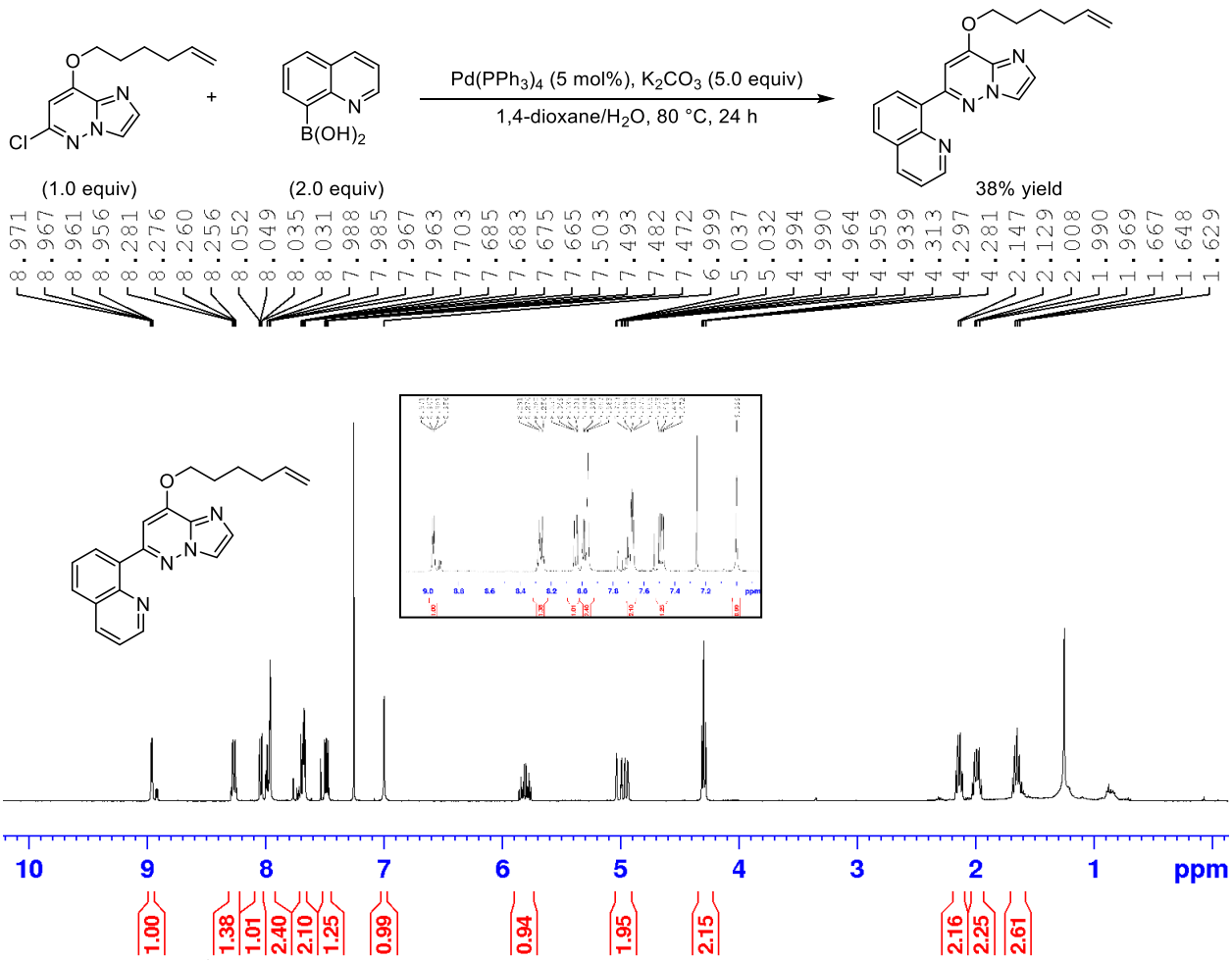

Figure A3–13: ^{1}H NMR spectrum of **4–51** isolated from coupling quinolin-8-ylboronic acid with 6-chloro-8-(hex-5-en-1-yloxy)imidazo[1,2-*b*]pyridazine.

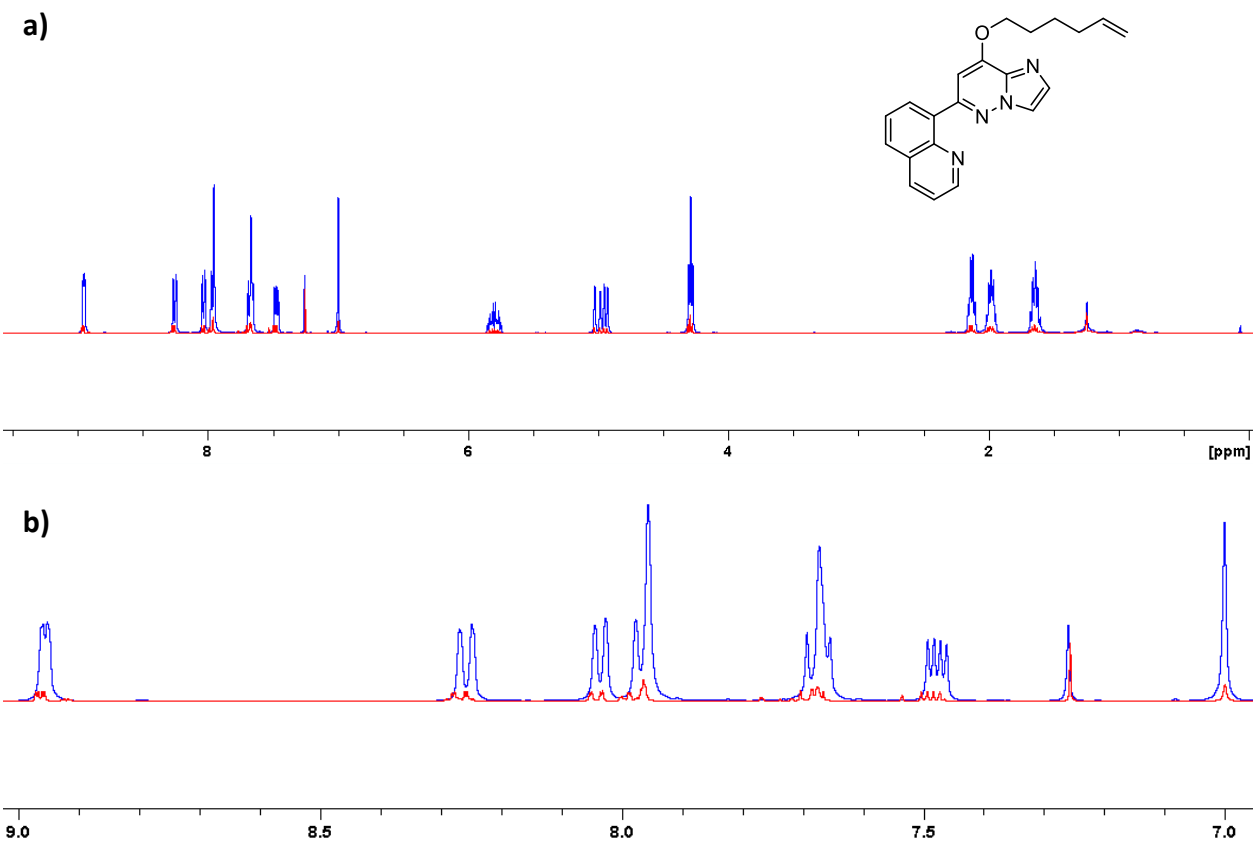

Figure A3–14: (a) Overlay of ^{1}H NMR spectra of **4–51** isolated from the (di)azine C-H etherification protocol (blue spectrum) and from the nucleophilic aromatic substitution and Suzuki cross-coupling protocol (red spectrum) described above. (b) Zoomed in ^{1}H NMR spectrum from (a).

***N*,*N*'-(((4-(2-(dimethylamino)ethoxy)pyridazine-3,6-diyl)bis(oxy))bis(ethane-2,1-diyl))bis(*N*-methylpyridin-2-amine) (4–52)**

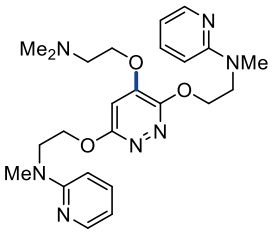

The title product was prepared according to the procedure described for **4–34** using *N*,*N*'-((pyridazine-3,6-diylbis(oxy))bis(ethane-2,1-diyl))bis(*N*-methylpyridin-2-amine) (380.2 mg, 1.0 mmol, 1.0 equiv), 2-(dimethylamino)ethan-1-ol (133.5 mg, 1.5 mmol, 1.5 equiv), 2-iodothiophene (420.1 mg, 2.0 mmol, 2.0 equiv), KO-*t*-Bu (224.4 mg, 2.0 mmol, 2.0 equiv), and anhydrous DMF (4.0 mL). The reaction solution was stirred in a 25 °C silicon oil bath for 20 h. Silica gel chromatography (5% MeOH/CH_2Cl_2 to 10% MeOH/CH_2Cl_2) afforded the title

compound as an amber oil (405.6 mg, 0.87 mmol, 87% yield). **IR** (neat, cm^{-1}) 2941, 2821, 2770, 1594, 1496, 1421, 1182, 767. **^{1}H NMR** (400 MHz, $CDCl_3$) δ 8.11 (m, 2H), 7.42 (m, 2H), 6.52 (m, 4H), 6.18 (s, 1H), 4.61 (m, 4H), 4.00 (m, 6H), 3.13 (s, 3H), 3.10 (s, 3H), 2.74 (t, *J* = 5.8 Hz, 2H), 2.31 (s, 6H). **^{13}C NMR** (101 MHz, $CDCl_3$) δ 162.8, 158.6, 158.6, 154.7, 150.3, 148.0, 148.0, 137.3, 137.2, 111.8, 111.7, 105.9, 98.9, 67.4, 65.4, 65.0, 57.5, 49.1, 49.0, 46.2, 37.5, 37.4. **HRMS** (ESI) $[M+H]^+$ calcd. for $[C_{24}H_{34}N_7O_3]^+$ = 468.2718, 468.2712 found. **Note on reaction selectivity**: The title product represents the only regioisomer observed in the ^{1}H NMR spectrum of the crude reaction solution. The signal at 6.18 (s, 1H) ppm is consistent with the trisubstituted pyridazine structure of the title product.

d) Characterization data of 4–39 from Figure 4–16

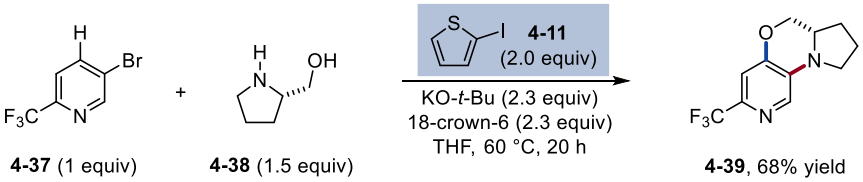

4-37 (1 equiv) **4-38** (1.5 equiv) **4-39**, 68% yield

(*S*)-3-(trifluoromethyl)-6a,7,8,9-tetrahydro-6*H*-pyrido[4,3-*b*]pyrrolo[1,2-*d*][1,4]oxazine (4–39)

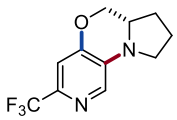

The title product was prepared according to the general procedure for (di)azine C-H etherification using 5-bromo-2-(trifluoromethyl)pyridine (224.9 mg, 1.0 mmol, 1.0 equiv), (*S*)-pyrrolidin-2-ylmethanol (151.8 mg, 1.5 mmol, 1.5 equiv), 2-iodothiophene (420.1 mg, 2.0 mmol, 2.0 equiv), KO-*t*-Bu (0.75 M in THF, 3.1 mL, 2.3 mmol, 2.3 equiv), 18-crown-6 (607.9 mg, 2.3 mmol, 2.3 equiv), and anhydrous THF (0.9 mL). Silica gel chromatography (15% EtOAc/hexanes) afforded the title compound as a white solid (166.8 mg, 0.68 mmol, 68% yield). **Mp**: 64 ºC – 67 ºC; **^{1}H NMR** (400 MHz, $CDCl_3$) δ 8.03 (s, 1H), 6.73 (s, 1H), 4.57 (dd, *J* = 3.6 Hz, 10.4 Hz, 1H), 3.64 (m, 1H), 3.56 (m, 1H), 3.39 (m, 1H), 3.30 (m, 1H), 2.16-2.23 (m, 2H), 2.00-

2.13 (m, 1H), 1.46 (m, 1H). **^{13}C NMR** (101 MHz, $CDCl_3$) δ 142.0 (q, *J* = 34.4 Hz), 140.9, 140.7, 135.5, 121.9 (q, *J* = 274.8 Hz), 103.0 (q, *J* = 2.8 Hz), 68.2, 55.6, 46.8, 28.6, 23.8. **^{19}F NMR** (376 MHz, $CDCl_3$) δ -68.2. **IR** (neat, cm^{-1}) 2955, 2880, 1608, 1526, 1457, 1306, 1116. **HRMS** (DART) $[M+H]^+$ calcd. for $[C_{11}H_{12}F_3N_2O]^+$ = 245.0896, 245.0940 found. **Specific Rotation**: $[\alpha]_D^{23}$ = 32.6°

Verification of Regioselectivity: To verify that etherification (as opposed to amination) occurs at the 4-position, we devised a multi-step pathway to synthesize an authentic sample of **4–39**.

Step 1: 5-bromo-4-iodo-2-(trifluoromethyl)pyridine

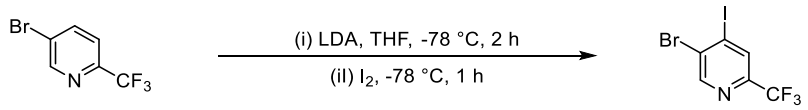

(1.0 equiv) 40% yield

Procedure: An oven-dried 100 mL round bottom flask was charged with a magnetic stir bar, sealed with a red septum stopper (Chemglass, Product #CG-3022-08). The flask was evacuated and backfilled three times with N_2, and left under positive pressure of N_2 on a manifold Schlenk line then diisopropylamine (620 µl, 4.4 mmol, 1.0 equiv, freshly distilled over NaH) and anhydrous THF (5.0 mL) were added *via* syringe. The solution was cooled to -78 °C using a dry ice/acetone bath, then *n*-BuLi (1.6 M in hexanes, 2.8 mL, 4.4 mmol, 1.0 equiv) was added *via* syringe and the solution was stirred for 20 min. 5-Bromo-2-(trifluoromethyl)pyridine (1.0 g, 4.4 mmol, 1.0 equiv) constituted in 2.0 mL of anhydrous THF was then added dropwise *via* syringe. The solution was stirred for 15 min at -78 °C and then iodine (1.24 g, 4.9 mmol, 1.0 equiv) constituted in 3.0 mL of anhydrous THF was added dropwise *via* syringe. The reaction solution was stirred for 1 h at -78 °C and then warmed to rt before being transferred to a separatory funnel containing H_2O (40 mL). Na_2SO_3 was added in portions (ca. 500 mg per portion) with agitation until no discernable color change was observed. The aqueous layer was extracted with EtOAc (3 x 40 mL) and the organic

layers were combined and dried over Na_2SO_4. The Na_2SO_4 was removed by filtration and the organic layer was concentrated *in vacuo*. Silica gel chromatography yielded the title product as a white solid (622.0 mg, 1.8 mmol, 40% yield). **^{1}H NMR** (400 MHz, $CDCl_3$) δ 8.76 (s, 1H), 8.13 (s, 1H).

Step 2: *tert*-butyl (*S*)-2-(((5-bromo-2-(trifluoromethyl)pyridin-4-yl)oxy)methyl)pyrrolidine-1-carboxylate

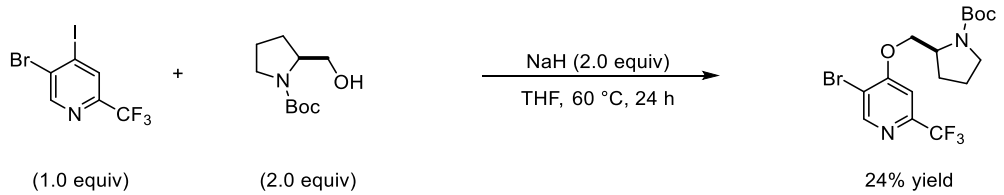

(1.0 equiv) (2.0 equiv) 24% yield

Procedure: Inside an N_2 filled glovebox, an oven-dried 8 mL vial (Thermo Fisher Scientific, Product #033405P) was charged with a magnetic stir bar, 5-bromo-4-iodo-2-(trifluoromethyl)pyridine (500.0 mg, 1.4 mmol, 1.0 equiv), *tert*-butyl (*S*)-2-(hydroxymethyl)pyrrolidine-1-carboxylate (563.1 mg, 2.8 mmol, 2.0 equiv), anhydrous THF (5.0 mL), and NaH (60% dispersion in mineral oil, 112.0 mg, 2.8 mmol, 2.0 equiv) in that order. The vial was sealed with a screw cap (Thermo Fisher Scientific, Product #03392A) lined with a PTFE septum (Thermo Fisher Scientific, Product #B7995-15), removed from the glovebox and placed into a preheated 60 °C silicon oil bath with stirring for 24 h at 60 °C. The solution was allowed to cool to rt and transferred to a separatory funnel containing H_2O (40 mL). The aqueous layer was extracted with EtOAc (3 x 40 mL) and the organic layers were combined and dried over Na_2SO_4. The Na_2SO_4 was removed by filtration and the organic layer was concentrated *in vacuo*. Silica gel chromatography (50% EtOAc/hexanes) yielded the title compound as a light-yellow oil (145.6 mg, 0.34 mmol, 24% yield. **^{1}H NMR** (400 MHz, $CDCl_3$) δ 8.66 (s, 1H), 7.31 (s, 1H), 4.21-4.33 (m, 3H), 3.36-3.50 (m, 2H), 2.05-2.15 (m, 3H), 1.90 (m, 1H), 1.46 (s, 9H). **MS** $[M+H]^+$ calcd. for $[C_{16}H_{21}BrF_3N_2O_3]^+$ = 425.1, 425.1 found. **Note**: bromine isotope pattern observed in MS analysis.

Mass and isotope pattern confirms the regioselectivity of this step (alkoxide substitution of iodine in the 4-position occurs over substitution of bromine in the 3-position).

Step 3: (*S*)-5-bromo-4-(pyrrolidin-2-ylmethoxy)-2-(trifluoromethyl)pyridine

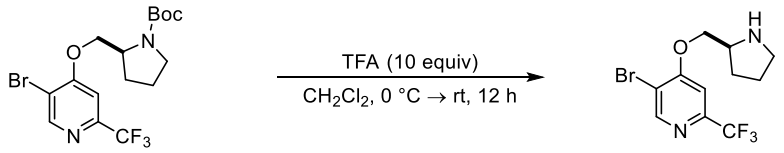

(1.0 equiv) 76% yield

Procedure: Open to air, an oven-dried 4 mL vial (KIMBLE®, Product #60910-1) was charged with *tert*-butyl (*S*)-2-(((5-bromo-2-(trifluoromethyl)pyridin-4-yl)oxy)methyl)pyrrolidine-1-carboxylate (145.6 mg, 0.34 mmol, 1.0 equiv) and anhydrous CH_2Cl_2 (2.0 mL) and cooled to 0 °C using an ice water bath. Trifluoroacetic acid (0.25 mL, 3.4 mmol, 10.0 equiv) was then added slowly to the solution and the vial was sealed with a screw cap (Thermo Fisher Scientific, Product #C4015-1A) lined with a PTFE septum (Thermo Fisher Scientific, Product #B7995-13). The solution was warmed to rt and stirred for 12 h. The reaction solution was then made basic by addition of triethylamine (ca. 0.5 mL), loaded directly onto a silica gel column, and then eluted with a 2% MeOH/CH_2Cl_2 to 6% MeOH/CH_2Cl_2 solvent gradient to yield the title compound as an amber oil (83.4 mg, 0.26 mmol, 76% yield). **^{1}H NMR** (400 MHz, $CDCl_3$) δ 8.67 (s, 1H), 7.17 (s, 1H), 4.23 (m, 1H), 4.12 (m, 1H), 3.75 (m, 1H), 3.12 (m, 2H), 2.06 (m, 1H), 1.97 (m, 1H), 1.88 (m, 1H), 1.73 (m, 1H). **HRMS** $[M+H]^+$ calcd. for $[C_{11}H_{13}BrF_3N_2O]^+$ = 325.0158, 325.0177 found.

Step 4: (*S*)-3-(trifluoromethyl)-6a,7,8,9-tetrahydro-6*H*-pyrido[4,3-*b*]pyrrolo[1,2-*d*][1,4]oxazine (4–39)

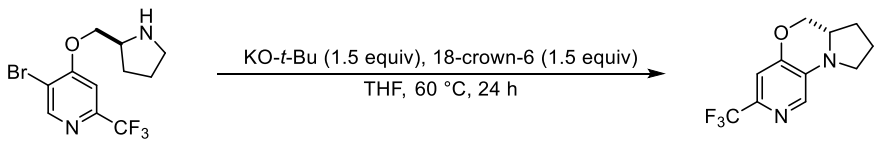

(1.0 equiv) 40% yield

Procedure: Inside a N_2 filled glovebox, and oven-dried 4 mL (KIMBLE®, Product #60910-1) vial was charged with a magnetic stir bar, (*S*)-5-bromo-4-(pyrrolidin-2-ylmethoxy)-2-(trifluoromethyl)pyridine (83.4 mg, 0.26 mmol, 1.0 equiv), 18-crown-6 (105.7 mg, 0.4 mmol, 1.5 equiv), anhydrous THF (1.0 mL), and KO-*t*-Bu (43.8 mg, 0.4 mmol, 1.5 equiv) in successive order. The vial was sealed with a screw cap (Thermo Fisher Scientific, Product #C4015-1A) lined with a PTFE septum (Thermo Fisher Scientific, Product #B7995-13), removed from the glovebox, placed into an aluminum reaction block preheated to 60 °C with stirring for 24 h. The reaction solution was allowed to cool to rt and then transferred to separatory funnel containing H_2O (30 mL). The aqueous layer was extracted with EtOAc (3 x 30 mL) and the organic layers were combined and dried over Na_2SO_4. The Na_2SO_4 was removed by filtration and the organic layers were concentrated *in vacuo*. Preparatory thin layer chromatography (15% EtOAc/hexanes) yielded the title compound as a white solid (25.2 mg, 0.10 mmol, 40% yield). The ^{1}H NMR spectrum of the isolated product is consistent with **4–39** isolated from C-H etherification of 5-bromo-2-(trifluoromethyl)pyridine with L-prolinol. **^{1}H NMR** (400 MHz, $CDCl_3$) δ 8.03 (s, 1H), 6.73 (s, 1H), 4.56 (dd, *J* = 10.9 Hz, 3.5 Hz, 1H), 3.63 (m, 1H), 3.54 (m, 1H), 3.38 (m, 1H), 3.28 (m, 1H), 2.14-2.23 (m, 2H), 2.07 (m, 1H), 1.46 (m, 1H).

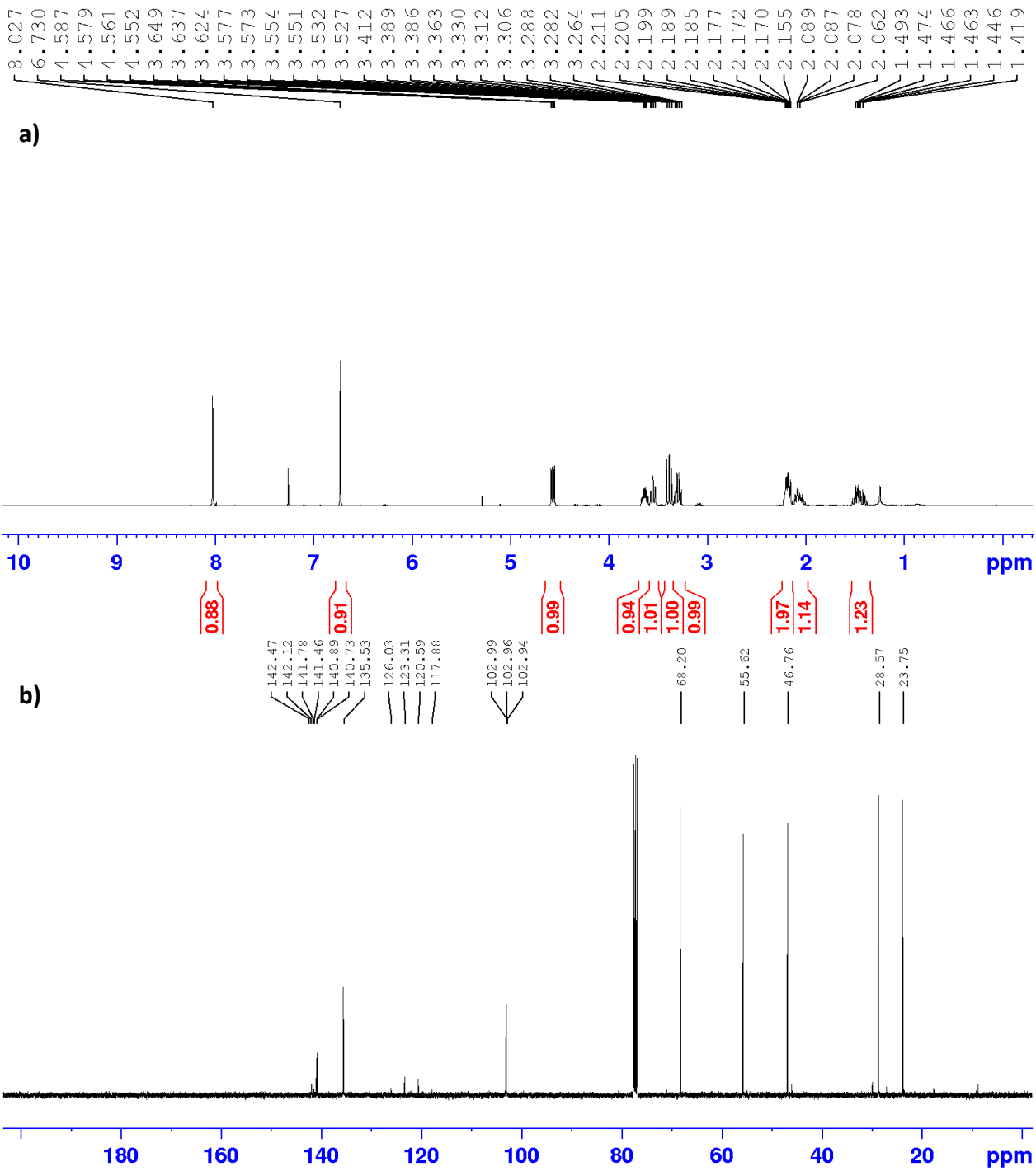
8.027
6.730
4.587
4.579
4.561
4.552
3.649
3.637
3.624
3.577
3.573
3.554
3.551
3.532
3.527
3.412
3.389
3.386
3.363
3.330
3.312
3.306
3.288
3.282
3.264
2.211
2.205
2.199
2.189
2.185
2.177
2.172
2.170
2.155
2.089
2.087
2.078
2.062
1.493
1.474
1.466
1.463
1.446
1.419
a)
10
9
8
7
6
5
4
3
2
1
ppm
0.88
0.91
0.99
0.94
1.01
1.00
0.99
1.97
1.14
1.23
b)
142.47
142.12
141.78
141.46
140.89
140.73
135.53
126.03
123.31
120.59
117.88
102.99
102.96
102.94
68.20
55.62
46.76
28.57
23.75
180
160
140
120
100
80
60
40
20
ppm

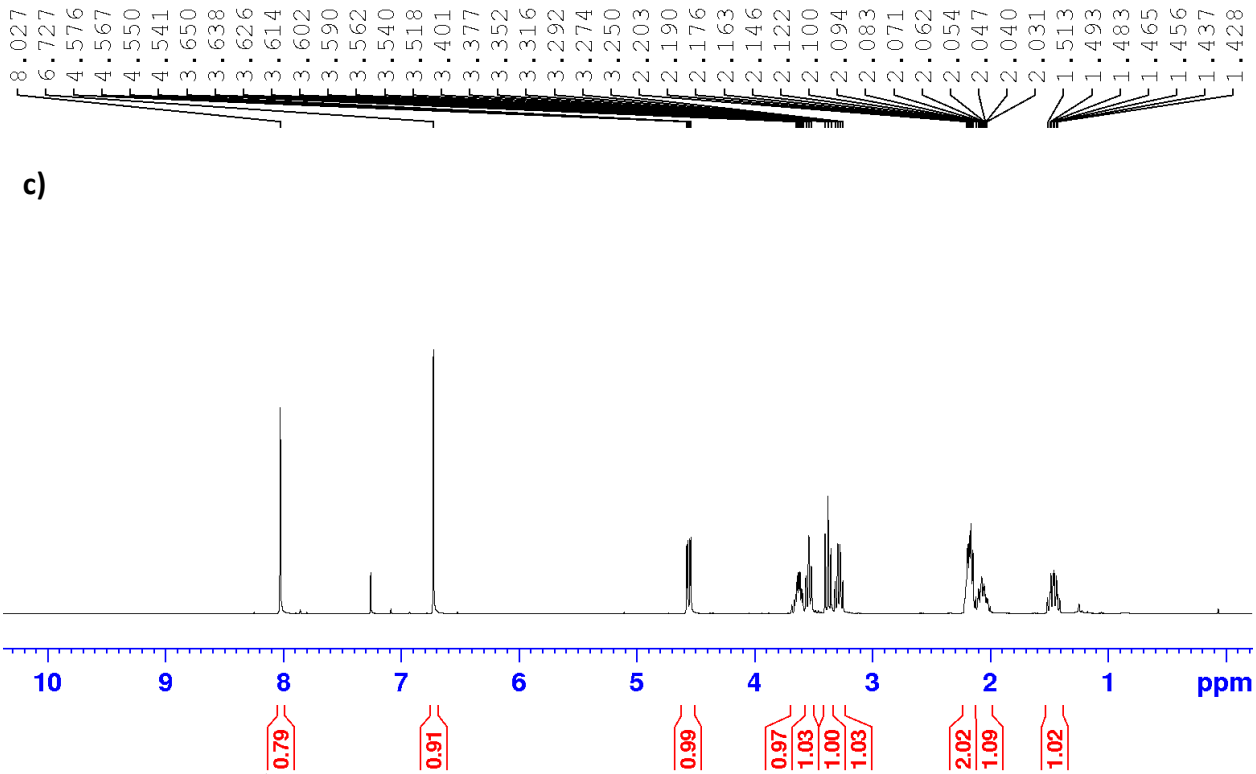

Figure A3–15: (a) ^{1}H NMR spectrum of purified **4–39** from 5-bromo-2-(trifluoromethyl) C-H etherification and C–Br amination with L-prolinol. (b) ^{13}C NMr spectrum of purified **4–39** from 5-bromo-2-(trifluoromethyl) C-H etherification and C–Br amination with L-prolinol. (c) ^{1}H NMR spectrum of purified **4–39** from amination of (*S*)-5-bromo-4-(pyrrolidin-2-ylmethoxy)-2-(trifluoromethyl)pyridine.

VI. Lithiation/Halogenation of Bipyridine Substrate 4–46

(a) Unselective metalation/halogenation of 4–46 with LiTMP and Iodine

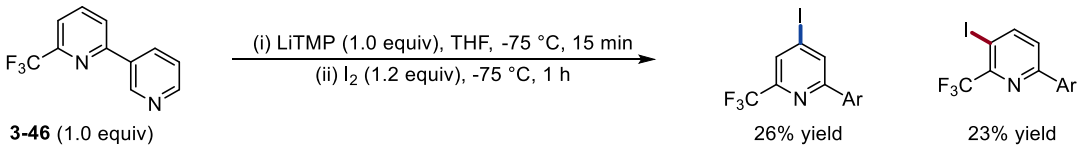

3-46 (1.0 equiv) — 26% yield — 23% yield

Procedure for the metalation/halogenation of 4–46: This procedure was adapted from a reported procedure for 2-trifluoromethylpyridine metalation/carboxylation.[3] An 8 mL oven-dried vial (Thermo Fisher Scientific, Product #033405P) was charged with a magnetic stir bar and sealed with a screw cap (Thermo Fisher Scientific, Product #03392A) lined with a PTFE septum (Thermo Fisher Scientific, Product #B7995-15), evacuated and backfilled three times with N_2, and left under

positive pressure of N_2 on a manifold Schlenk line. 1,1,2,2-Tetramethylpiperidine (freshly distilled over NaH) was added to the vial *via* syringe (0.17 mL, 1.0 mmol, 1.0 equiv) followed by 0.5 mL of anhydrous THF. The solution was cooled to -75 °C using a dry ice in MeOH bath and *n*-BuLi (1.6 M in hexanes, 0.63 mL, 1.0 mmol, 1.0 equiv) was added dropwise *via* syringe. The solution was stirred for 15 min. 6-(Trifluoromethyl)-2,3'-bipyridine (223.1 mg, 1.0 mmol, 1.0 equiv) constituted in anhydrous THF (0.5 mL) was then added dropwise *via* syringe. The solution was stirred 15 min at -75 °C before iodine (304.6 mg, 1.2 mmol, 1.2 equiv) constituted in anhydrous THF (1.0 mL) was added dropwise *via* syringe. The solution was stirred 1 h at -75 °C and then quenched with H_2O (ca. 1.0 mL). The solution was allowed to warm to rt and transferred into a separatory funnel containing H_2O (40 mL), and then Na_2SO_3 was added in portions (ca. 500 mg per portion) with agitation until addition of more Na_2SO_3 resulted in no discernable color change. The aqueous layer was extracted with EtOAc (3 x 40 mL). The organic layers were combined and dried over Na_2SO_4. The Na_2SO_4 was removed by filtration and the organic layer was concentrated under reduced pressure. The crude residue was transferred from the flask to a 20 mL scintillation vial using Et_2O and concentrated under reduced pressure. 1,3,5-Trimethoxybenzene (33.6 mg, 0.20 mmol) was added as a ^1H NMR internal standard to the residue and the residue was homogenized with $CDCl_3$. ^1H NMR (400 MHz, $CDCl_3$) spectroscopy of the homogenized crude residue was used to determine the yield of 5-iodo-6-(trifluoromethyl)-2,3'-bipyridine and 4-iodo-6-(trifluoromethyl)-2,3'-bipyridine. Pure samples of 5-iodo-6-(trifluoromethyl)-2,3'-bipyridine and 4-iodo-6-(trifluoromethyl)-2,3'-bipyridine were isolated using preparatory thin layer chromatography developed with 60% EtOAc/hexanes solvent.

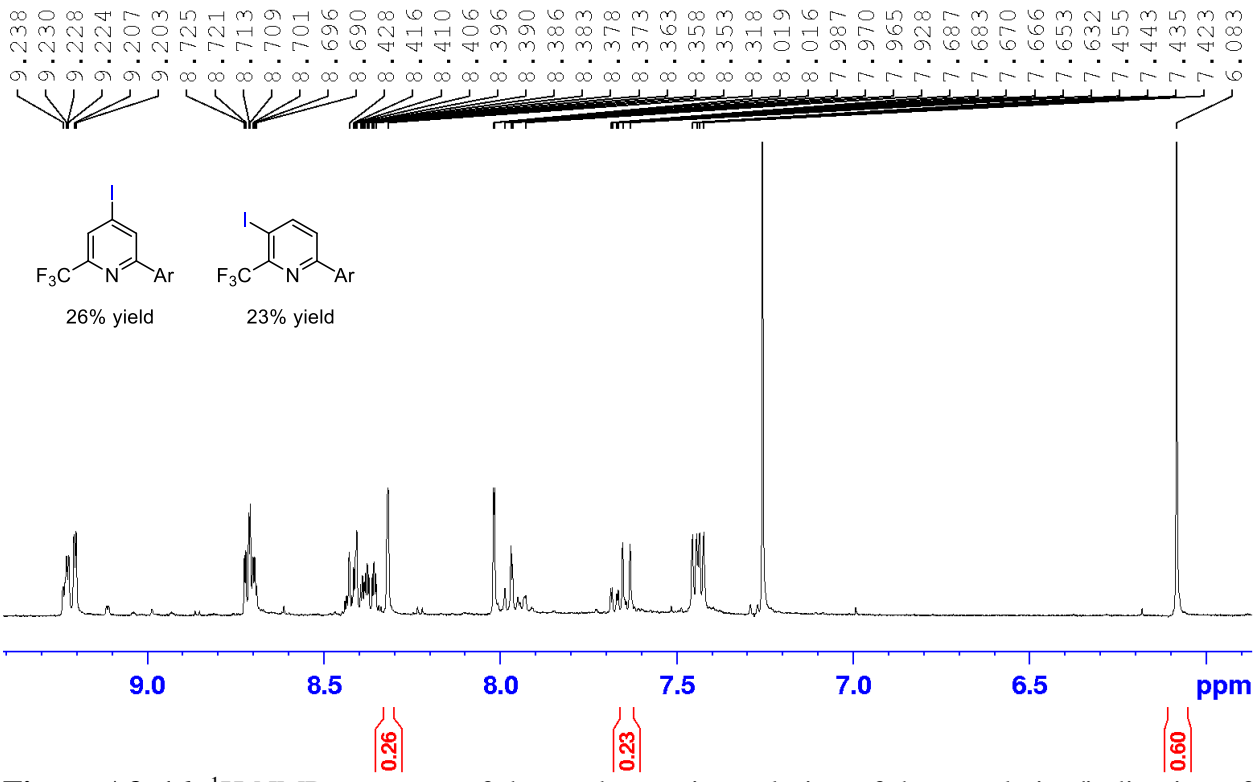

Figure A3–16: ^{1}H NMR spectrum of the crude reaction solution of the metalation/iodination of **4–46**. 1,3,5-Trimethoxybenzene (33.6 mg, 0.20 mmol) used as internal standard (chemical shift at 6.08 ppm). Yields determined by ^{1}H NMR: 26% yield of 4-iodo-6-(trifluoromethyl)-2,3'-bipyridine and 23% yield of 5-iodo-6-(trifluoromethyl)-2,3'-bipyridine.

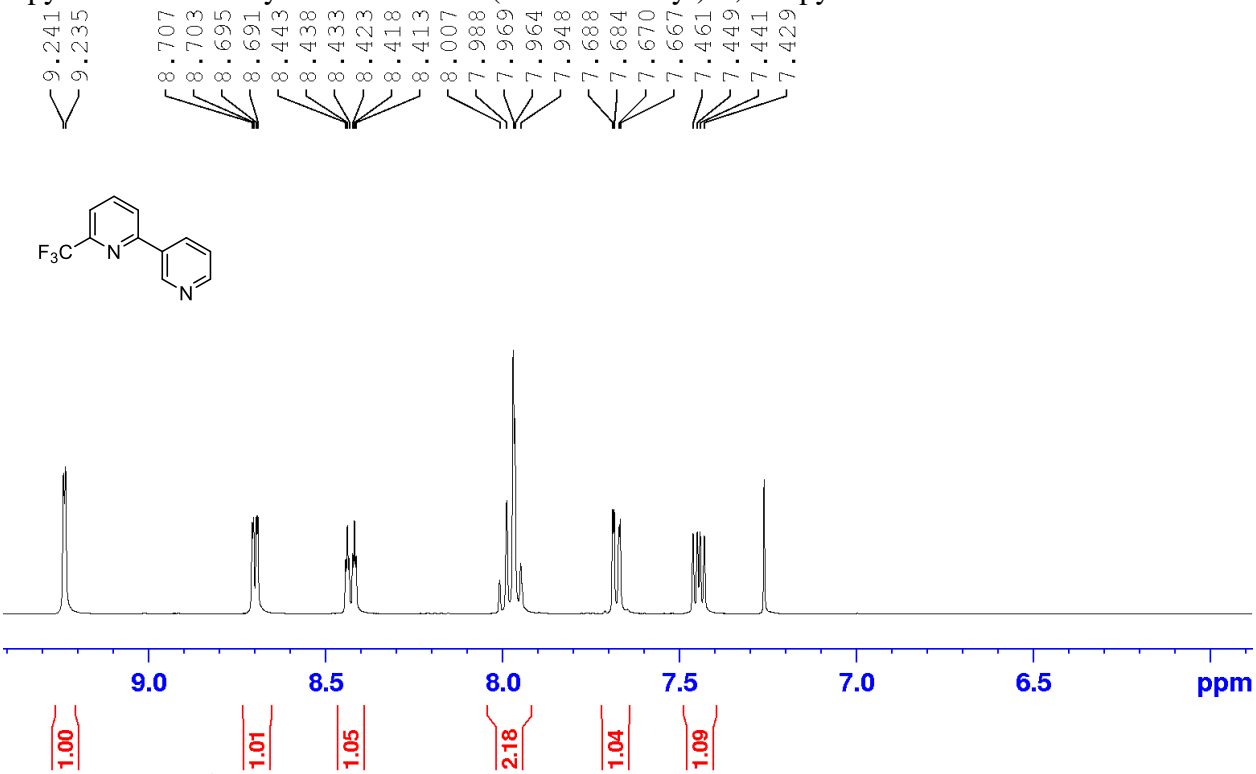

Figure A3–17: ^{1}H NMR spectrum of pure 6-(trifluoromethyl)-2,3'-bipyridine.

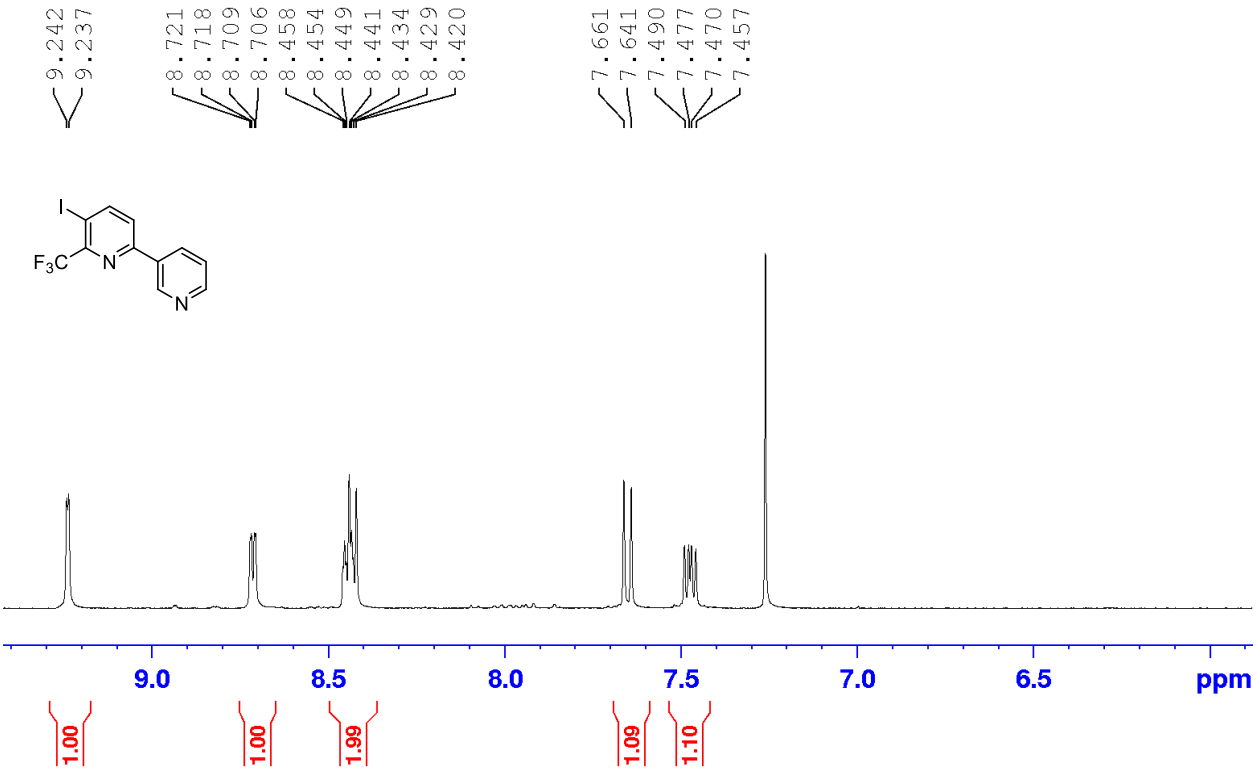

Figure A3–18: ^{1}H NMR spectrum of isolated 5-iodo-6-(trifluoromethyl)-2,3'-bipyridine.

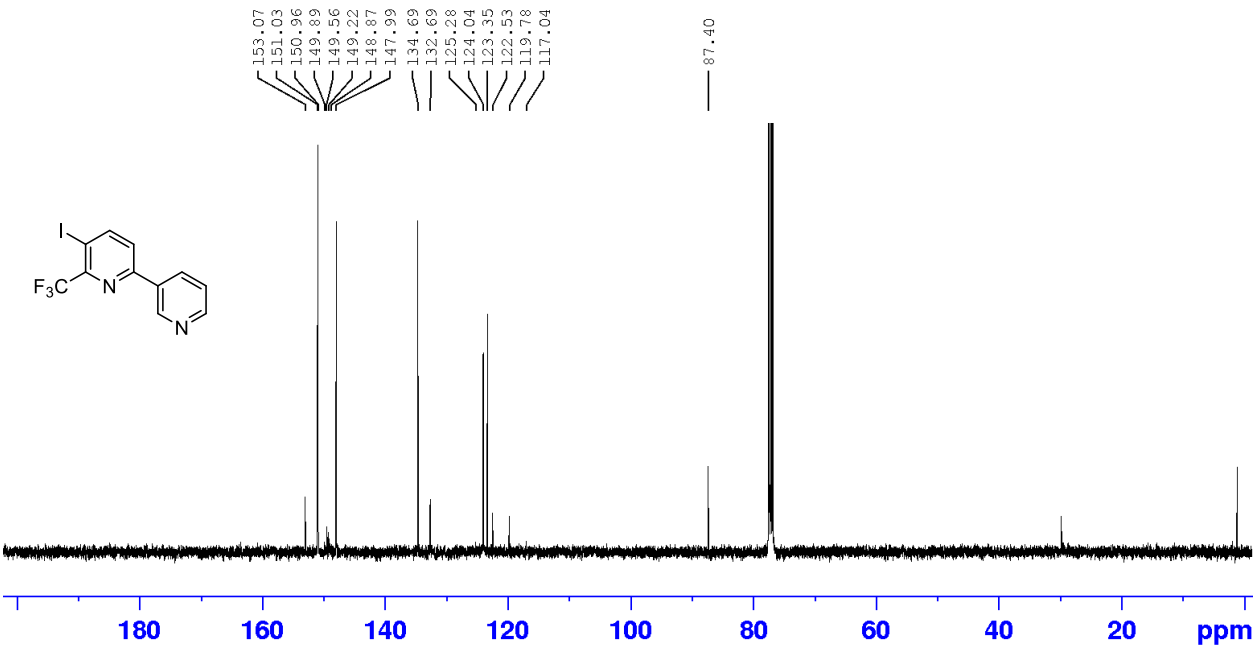

Figure A3–19: ^{13}C NMR of isolated 5-iodo-6-(trifluoromethyl)-2,3'-bipyridine.

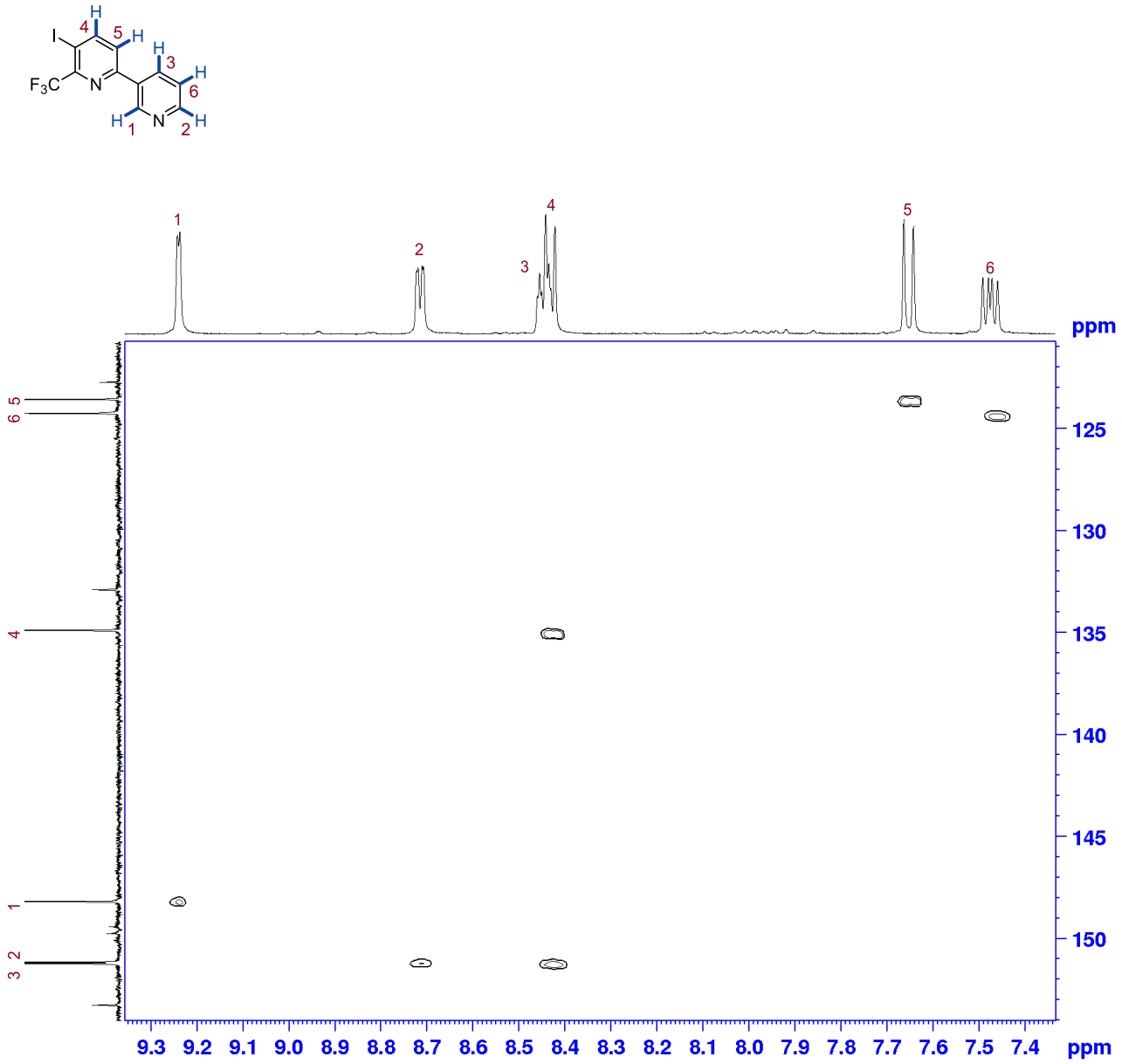

Figure A3–20: HSQC spectrum of 5-iodo-6-(trifluoromethyl)-2,3'-bipyridine.

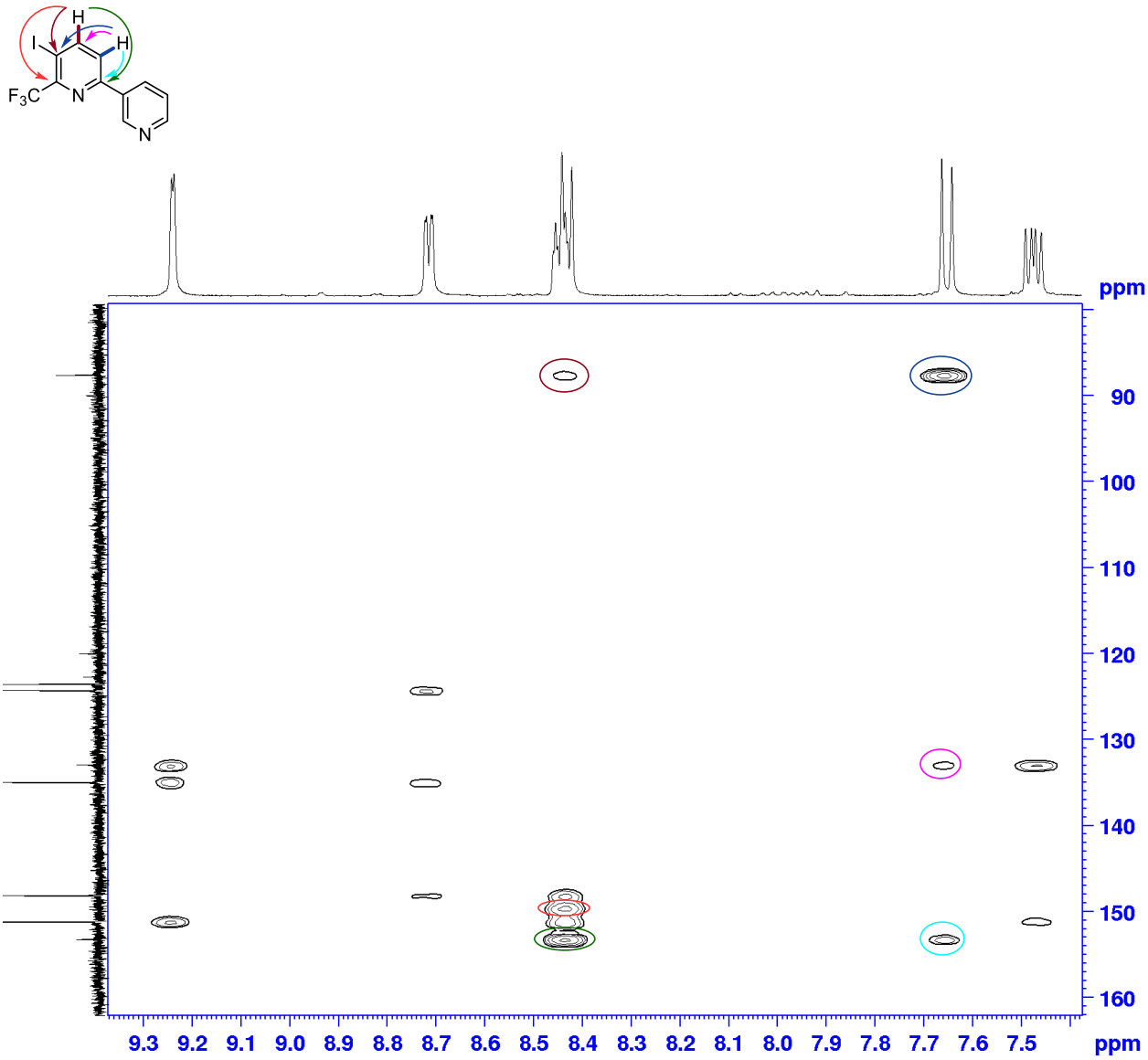

Figure A3–21: HMBC spectrum of 5-iodo-6-(trifluoromethyl)-2,3'-bipyridine.

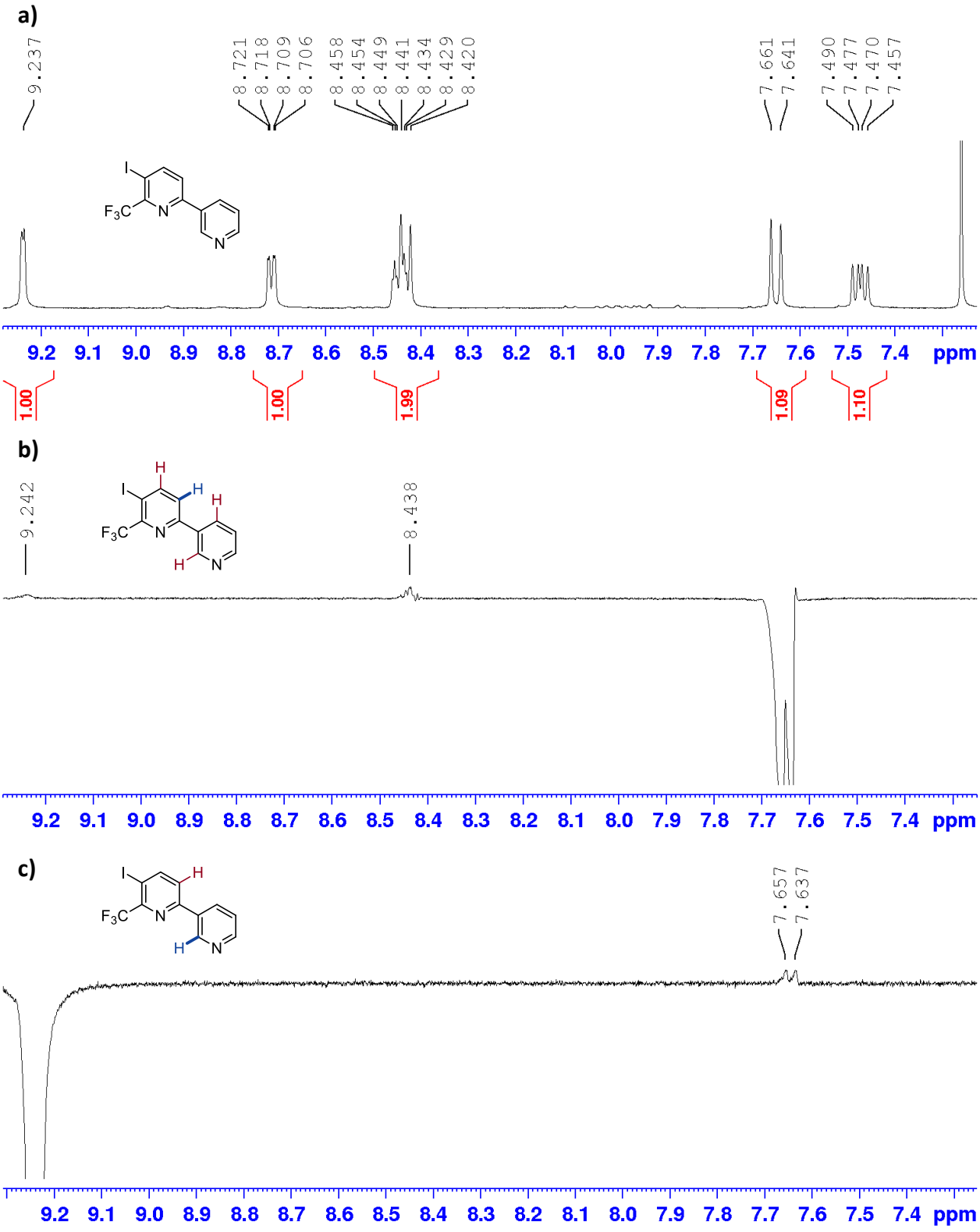

Figure A3–22: 1D NOESY NMR spectra of 5-iodo-6-(trifluoromethyl)-2,3'-bipyridine. Proton highlighted in blue (H) was irradiated and protons highlighted in red (H) correlate to the irradiated proton. (a) ^{1}H NMR spectrum of 5-iodo-6-(trifluoromethyl)-2,3'-bipyridine. (b/c) 1D NOESY NMR spectra of 5-iodo-6-(trifluoromethyl)-2,3'-bipyridine**.**

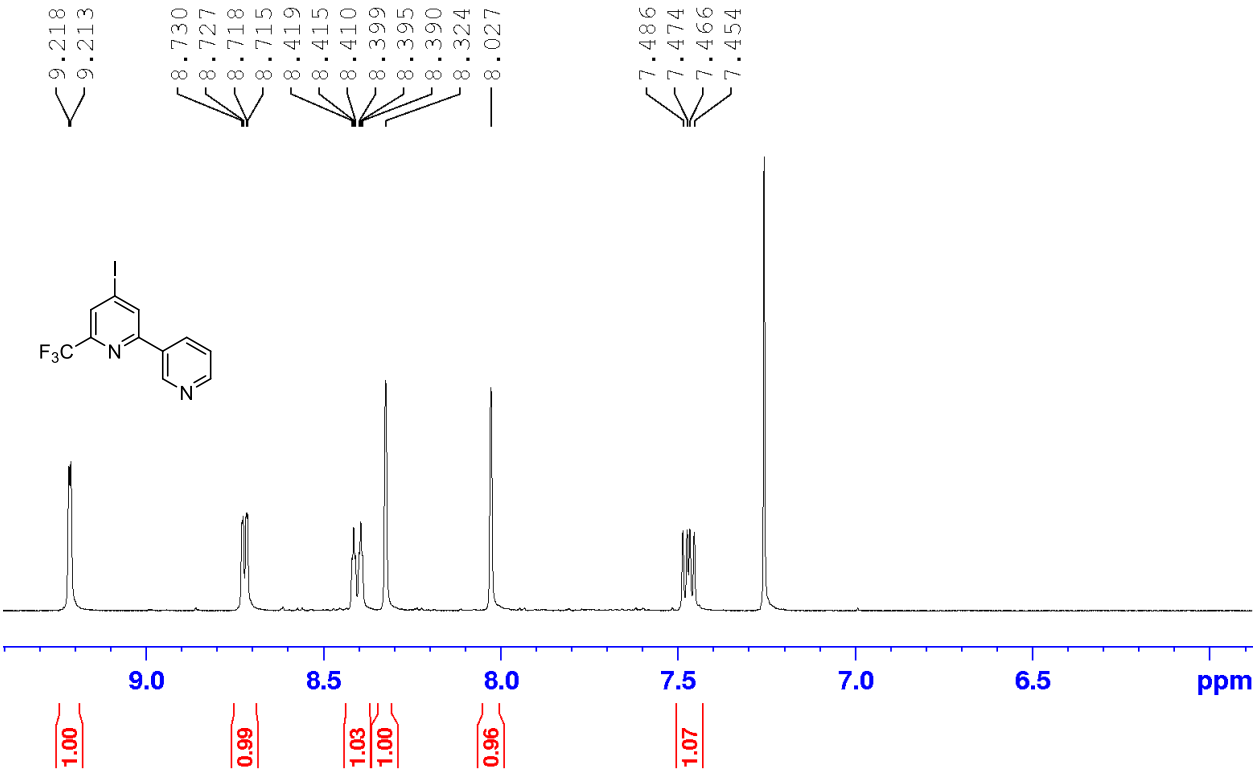

Figure A3–23: ^{1}H NMR spectrum of isolated 4-iodo-6-(trifluoromethyl)-2,3'-bipyridine.

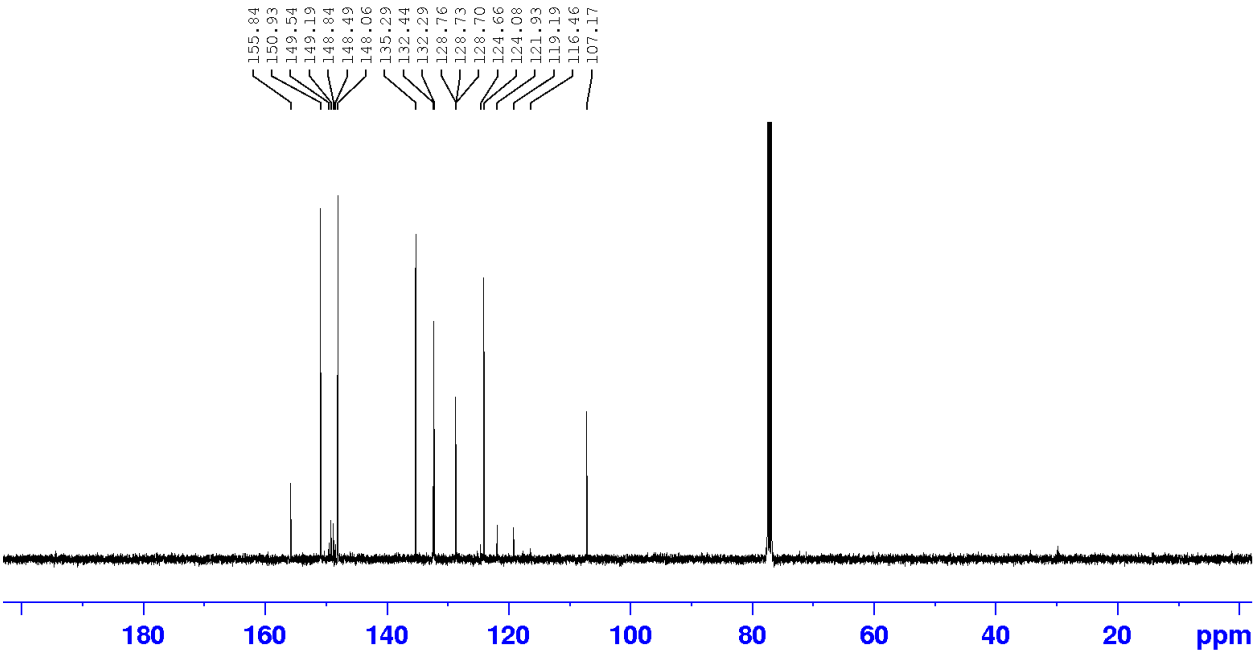

Figure A3–24: ^{13}C NMR spectrum of isolated 4-iodo-6-(trifluoromethyl)-2,3'-bipyridine.

(b) Characterization data of 5-iodo-6-(trifluoromethyl)-2,3'-bipyridine and 4-iodo-6-(trifluoromethyl)-2,3'-bipyridine

5-iodo-6-(trifluoromethyl)-2,3'-bipyridine

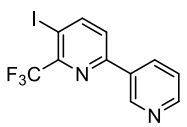

^{1}H NMR (400 MHz, $CDCl_3$) δ 9.24 (d, *J* = 2.0 Hz, 1H), 8.72 (m, 1H), 8.42-8.46 (m, 2H), 7.65 (d, *J* = 8.3 Hz, 1H), 7.47 (dd, *J* = 4.9 Hz, 8.0 Hz, 1H). **^{13}C NMR** (101 MHz, $CDCl_3$) δ 153.1, 151.0, 150.9, 149.4 (q, *J* = 34.2 Hz), 148.0, 134.7, 132.7, 124.0, 123.3, 121.1 (q, *J* = 277.1 Hz), 87.4. Light yellow solid, **Mp**: 99 ºC – 104 °C. **IR** (neat, cm^{-1}) 2962, 2360, 1423, 1261, 1136, 1012, 810. **HRMS** (ESI) $[M+H]^+$ calcd. for $[C_{11}H_7F_3IN_2]^+$ = 350.9601, 350.9604 found

4-iodo-6-(trifluoromethyl)-2,3'-bipyridine

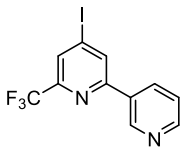

^{1}H NMR (400 MHz, $CDCl_3$) δ 9.22 (d, *J* = 2.0 Hz, 1H), 8.72 (m, 1H), 8.41 (m, 1H), 8.32 (m, 1H), 8.02 (m, 1H), 7.47 (dd, *J* = 4.9 Hz, 8.0 Hz, 1H). **^{13}C NMR** (101 MHz, $CDCl_3$) δ 155.8, 150.9, 149.0 (q, *J* = 35.4 Hz), 148.1, 135.3, 132.4, 132.3, 128.7 (q, *J* = 2.8 Hz), 124.1, 120.6 (q, *J* = 276.2 Hz), 107.2. Light yellow solid, **Mp**: 127 ºC – 129 ºC. **IR** (neat, cm^{-1}) 2948, 1701, 1662, 1564, 1333, 1177, 1133. **HRMS** (ESI) $[M+H]^+$ calcd. for $[C_{11}H_7F_3IN_2]^+$ = 350.9601, 350.9601 found

VII. Mechanistic Studies on *N*-Heteroarene C-H Etherification Reactions

a) Observation of halogen transfer to thiazole from 2,5-dibromothiophene

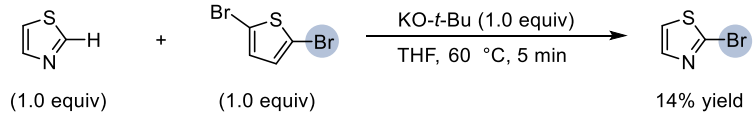

Procedure: Inside an N_2 filled glovebox, an oven-dried 4 mL vial (KIMBLE®, Product #60910-1) was charged with a magnetic stir bar, thiazole (21.3 mg, 0.25 mmol, 1.0 equiv), 2,5-

dibromothiophene (60.5 mg, 0.25 mmol, 1.0 equiv), 1,3,5-trimethoxybenzene (42.0 mg, 0.25 mmol, 1.0 equiv), anhydrous THF (1.0 mL), and KO-*t*-Bu (28.1 mg, 0.25 mmol, 1.0 equiv) in successive order. The vial was sealed with a screw cap (Thermo Fisher Scientific, Product #C4015-1A) lined with a PTFE septum (Thermo Fisher Scientific, Product #B7995-13), removed from the glovebox, put under positive pressure of N_2 on a manifold Schlenk line, and placed into an aluminum reaction block preheated to 60 °C with stirring for 5 min. An aliquot of the reaction mixture was removed *via* syringe, plunged into separate vial, and constituted in $CDCl_3$. ^1H NMR spectroscopy (400 MHz, $CDCl_3$) of the aliquot constituted in $CDCl_3$ was employed to determine the yield of 2-bromothiazole using 1,3,5-trimethoxybenzene as an internal standard (14% yield). We note that longer reaction times do not result in a higher yield of 2-bromothiazole.

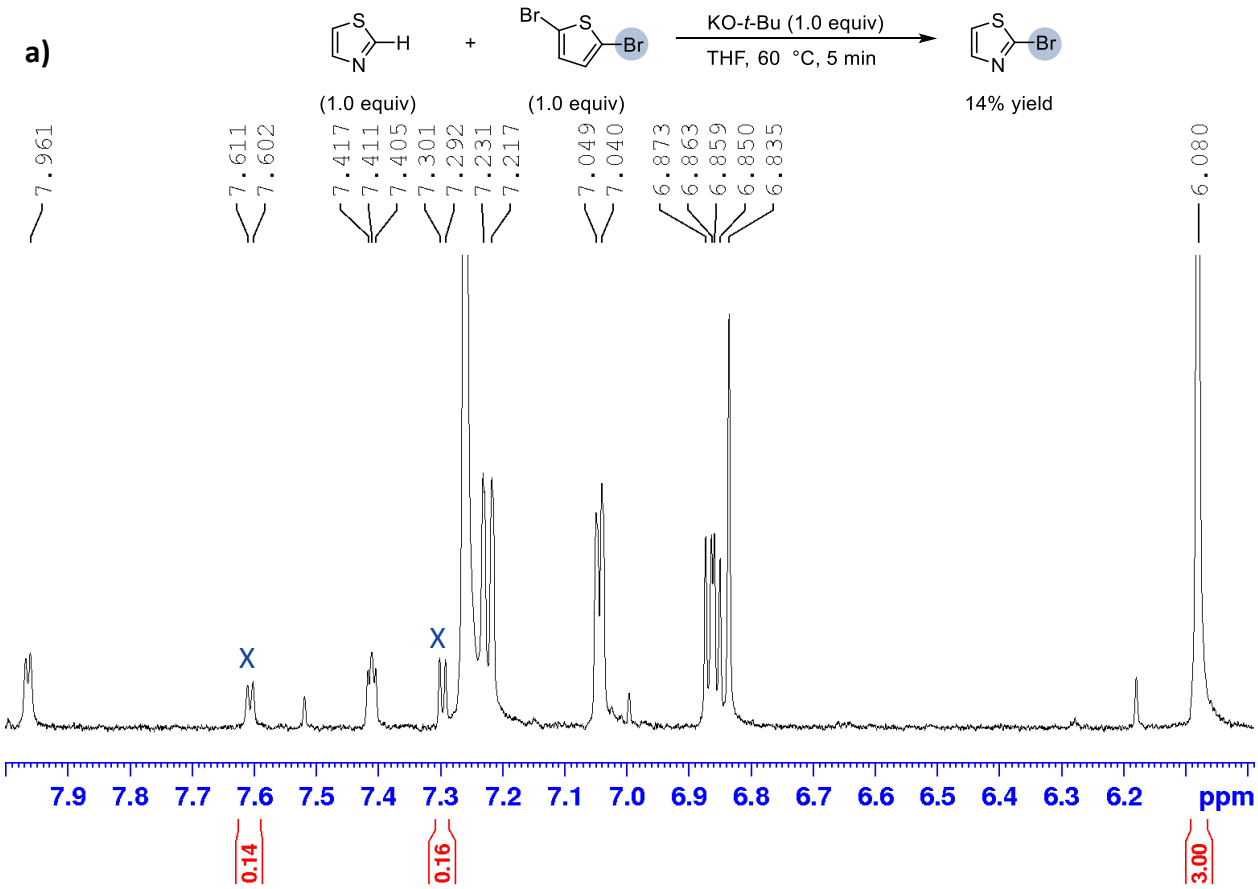

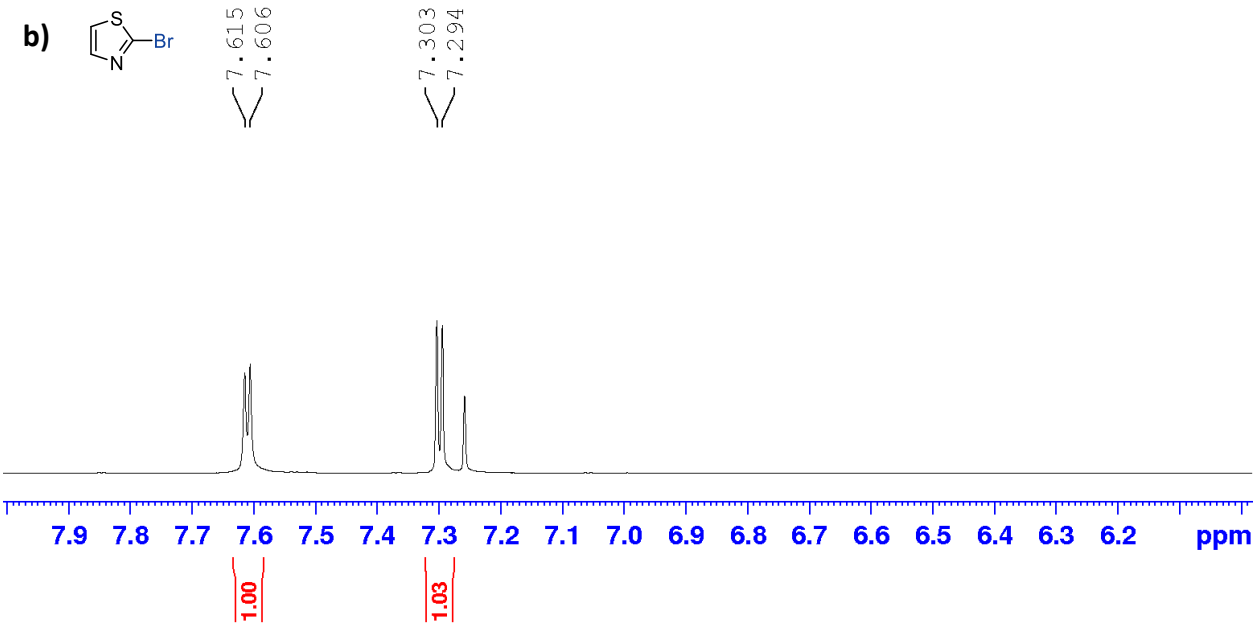

Figure A3–25: (a) ^{1}H NMR spectrum (400 MHz, $CDCl_3$) of the crude reaction solution of halogen transfer from 2,5-dibromothiophene to thiazole. 1,3,5-Trimethoxybenzene (42.0 mg, 0.25 mmol, signal at 6.08 ppm) internal standard was used to determine the yield of 2-bromothiazole (signal at 7.60 used to determine yield, 14% yield, marked with X in the spectrum). (b) ^{1}H NMR spectrum (400 MHz, $CDCl_3$) of authentic 2-bromothiazole.

b) Observation of Halogen Transfer to 3-Bromopyridine from 2-iodothiophene

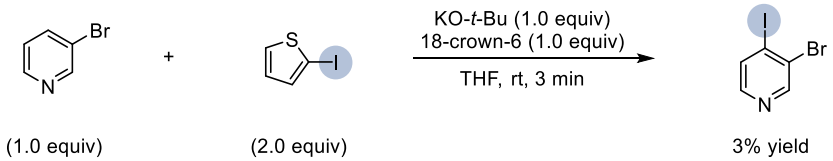

Procedure: Inside a N_2 filled glovebox, an oven-dried 4 mL vial (KIMBLE®, Product #60910-1) was charged with a magnetic stir bar, 3-bromopyridine (15.8 mg, 0.1 mmol, 1.0 equiv), 2-iodothiophene (42.0 mg, 0.2 mmol, 2.0 equiv), anhydrous THF (0.4 mL), 18-crown-6 (26.4 mg, 0.1 mmol, 1.0 equiv), 1,3,5-trimethoxybenzene internal standard (16.8 mg, 0.1 mmol), and KO-*t*-Bu (11.2 mg, 0.1 mmol, 1.0 equiv) in successive order. The vial was sealed with a screw cap (Thermo Fisher Scientific, Product #C4015-1A) lined with a PTFE septum (Thermo Fisher Scientific, Product #B7995-13) and the solution was stirred inside the glovebox for 3 min. ^{1}H NMR analysis (400 MHz, $CDCl_3$) of the crude reaction solution was used to determine the yield

of 3-bromo-4-iodopyridine (3% yield). It was confirmed 3-bromo-4-iodopyridine was produced in the reaction by spiking a small quantity of an authentic 3-bromo-4-iodopyiridine sample into a ^{1}H NMR sample of the crude reaction solution (*vide infra)*. Additionally, we observed the mass of 3-bromo-4-iodopyridine ($[M+H]^+$ calcd. for $[C_5H_3BrIN]^+$ = 283.9, 283.9 found) by mass spectrometry analysis of the crude reaction mixture. We note that longer reaction times do not result in a higher yield of 3-bromo-4-iodopyridine.

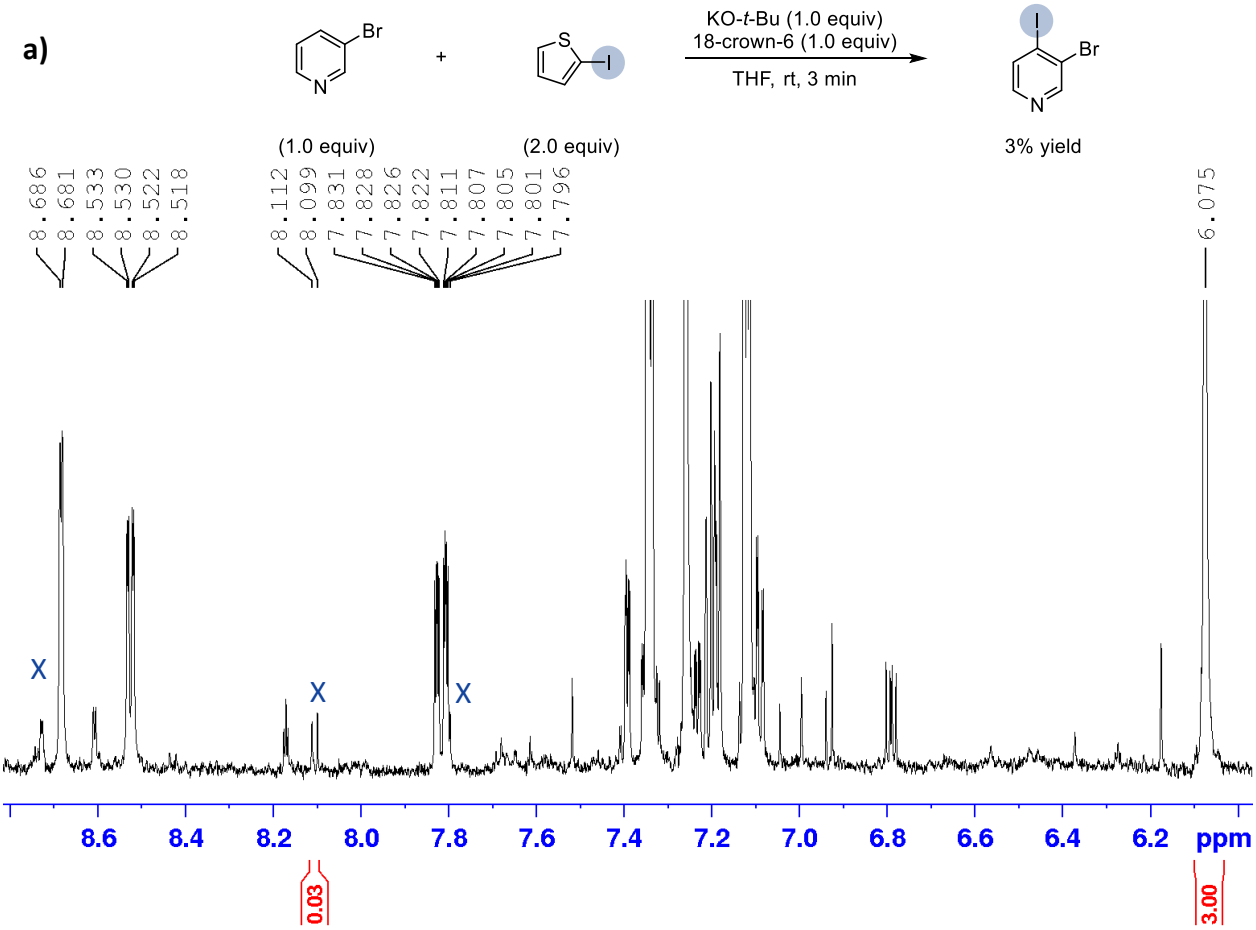

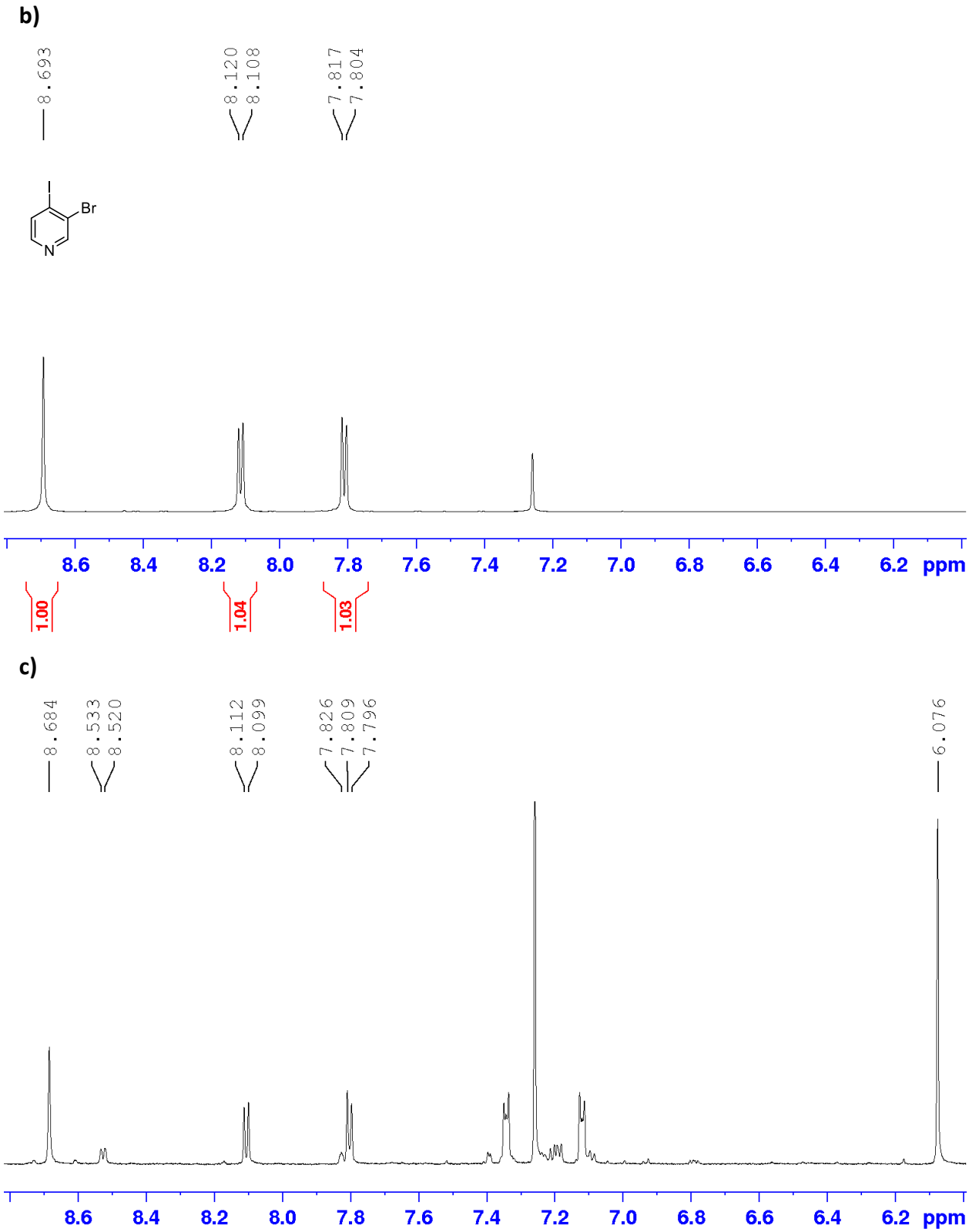

Figure A3–26: (a) ^{1}H NMR spectrum (400 MHz, $CDCl_3$) of the crude reaction solution of 3-bromopyridine 4-selective iodination with 2-iodothiophene. 1,3,5-Trimethoxybenzene used as internal standard (16.8 mg, 0.1 mmol). 3% Yield of 3-bromo-4-iodopyridine (marked with X). (b)

^{1}H NMR spectrum (400 MHz, $CDCl_3$) of authentic 3-bromo-4-iodopyridine. (c) ^{1}H NMR spectrum (400 MHz, $CDCl_3$) of the crude reaction solution from Figure S23a spiked with authentic 3-bromo-4-iodopyridine.

c) 4-Iodination and 3-Selective Substitution of 3-Fluoropyridine under the Standard Reaction Conditions

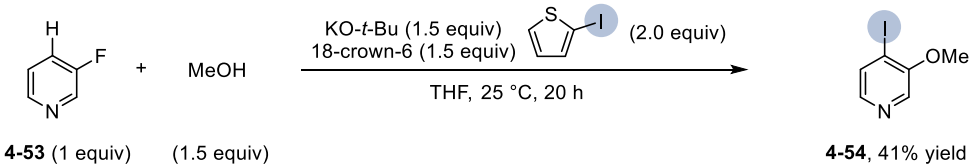

4-53 (1 equiv) (1.5 equiv) **4-54**, 41% yield

Procedure: Inside a N_2 filled glovebox, an oven-dried 4 mL vial (KIMBLE®, Product #60910-1) was charged with a magnetic stir bar, 3-fluoropyridine (48.5 mg, 0.5 mmol, 1.0 equiv), methanol (24.0 mg, 0.75 mmol, 1.5 equiv), 2-iodothiophene (210.0 mg, 1.0 mmol, 2.0 equiv), anhydrous THF (2.0 mL), 18-crown-6 (198.2 mg, 0.75 mmol, 1.5 equiv), and KO-*t*-Bu (84.2 mg, 0.75 mmol, 1.5 equiv) in successive order. The vial was sealed with a screw cap (Thermo Fisher Scientific, Product #C4015-1A) lined with a PTFE septum (Thermo Fisher Scientific, Product #B7995-13), removed from the glovebox, and placed into an aluminum reaction block preheated to 25 °C with stirring for 20 h. 1,3,5-Trimethoxybenzene (21.2 mg, 0.126 mmol) internal standard was then added to the solution. ^{1}H NMR spectroscopy (400 MHz, $CDCl_3$) of the crude reaction solution was utilized to determine the yield of 4-iodo-3-methoxypyridine (**4–54**, 41% yield). A pure sample of 4-iodo-3-methoxypyridine was obtained by loading a portion of the crude reaction solution (ca. 1.0 mL) onto a preparatory thin layer chromatography plate that was developed using 5% EtOAc/hexanes solvent.

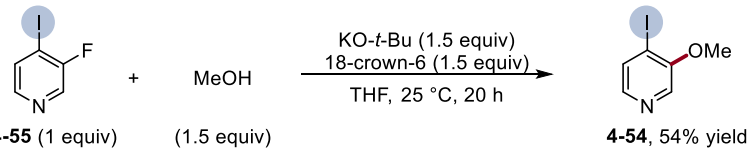

4-55 (1 equiv) (1.5 equiv) **4-54**, 54% yield

Procedure: 3-Selective fluorine substitution of 3-fluoro-4-iodopyridine (**4–55**) was carried out in accordance with the above procedure using 3-fluoro-4-iodopyridine (111.5 mg, 0.5 mmol, 1.0

equiv) instead of 3-fluoropyridine and no 2-iodothiophene was included in the reaction. 1,3,5-Trimethoxybenzene (31.0 mg, 0.184 mmol) internal standard was added to the solution. ^{1}H NMR spectroscopy (400 MHz, $CDCl_3$) of the crude reaction solution was used to determine the yield of 4-iodo-3-methoxypyridine (**4–54**, 54% yield).

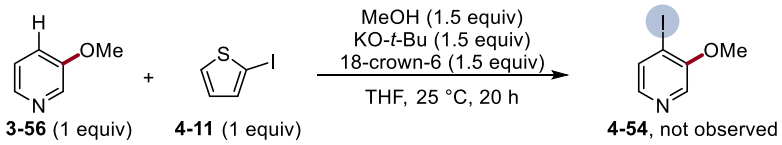

Procedure: Attempted 4-iodination of 3-methoxypyridine (**4–56**) was carried out in accordance with the above procedure on a 0.1 mmol scale using 3-methoxypyridine (10.9 mg, 0.1 mmol, 1.0 equiv), methanol (6.4 mg, 0.15 mmol, 1.5 equiv), 2-iodothiophene (42.0 mg, 0.2 mmol, 2.0 equiv), 18-crown-6 (39.6 mg, 0.15 mmol, 1.5 equiv) KO-*t*-Bu (16.8 mg, 0.15 mmol, 1.5 equiv), and anhydrous THF (0.4 mL). Trimethoxybenzene (15.8 mg, 0.094 mmol) internal standard was added to the solution. ^{1}H NMR spectroscopy (400 MHz, $CDCl_3$) of the crude reaction solution showed no 4-iodo-3-methoxypyridine (**4–54**).

4-iodo-3-methoxypyridine (4–54)

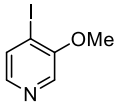

^{1}H NMR (400 MHz, $CDCl_3$) δ 8.11 (s, 1H), 7.88 (d, *J* = 4.9 Hz, 1H), 7.72 (d, *J* = 4.9 Hz, 1H), 3.99 (s, 3H). **^{13}C NMR** (101 MHz, $CDCl_3$) δ 155.2, 143.3, 134.4, 133.2, 97.2, 57.2. Orange solid. **HRMS** (ESI) $[M+H]^+$ calcd. for $[C_6H_6INO]^+$ = 235.9567, 235.9567 found. This mass is consistent with fluorine substitution over iodine substation. Spectroscopic characterization is consistent with a previous report.[4] **Note**: No signal is observed in ^{19}F NMR spectrum of this isolated material.

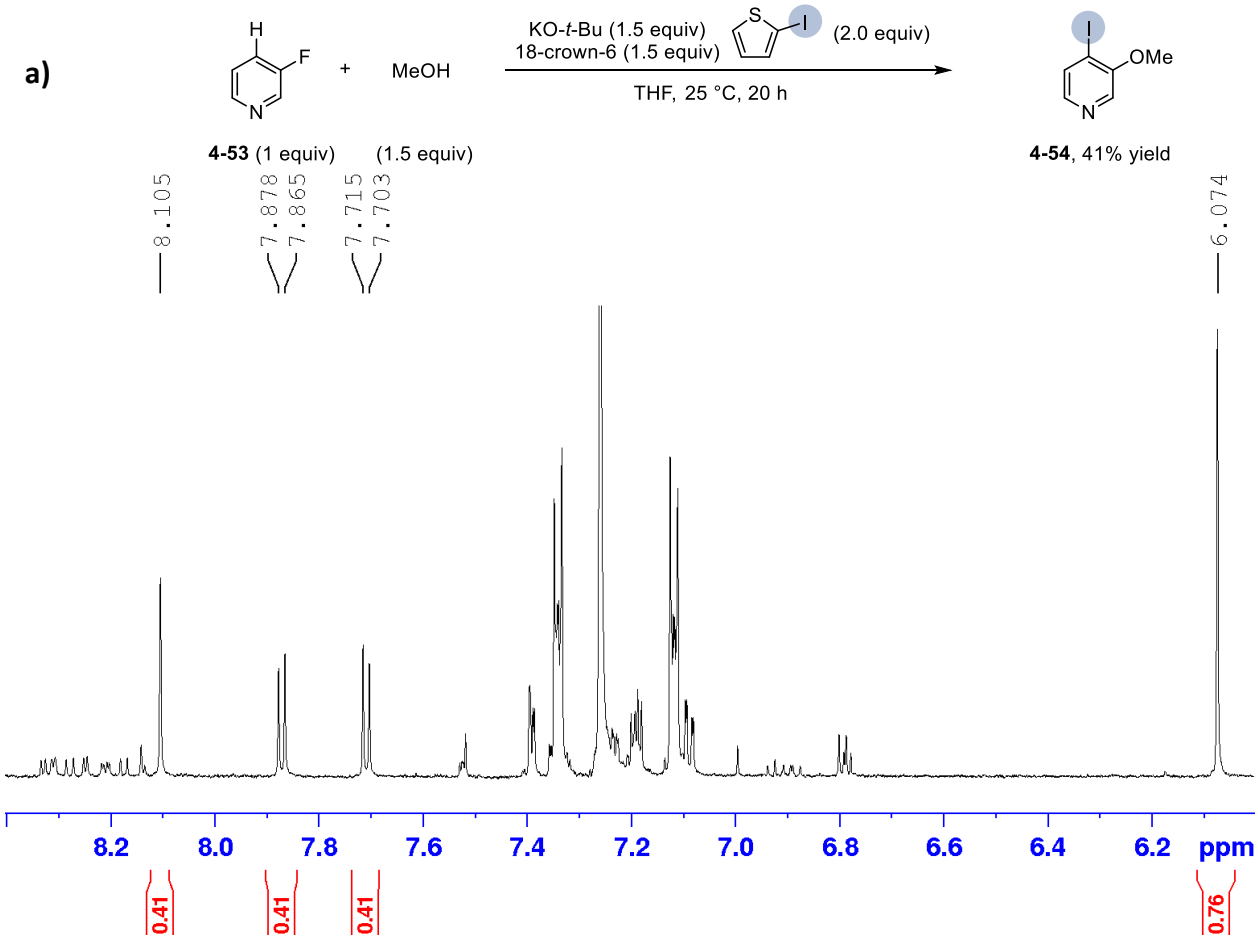
a)
H
F
N
+
MeOH
KO-t-Bu (1.5 equiv)
18-crown-6 (1.5 equiv)
S
I
(2.0 equiv)
THF, 25 °C, 20 h
OMe
N
4-53 (1 equiv)
(1.5 equiv)
4-54, 41% yield
8.105
7.878
7.865
7.715
7.703
6.074
8.2
8.0
7.8
7.6
7.4
7.2
7.0
6.8
6.6
6.4
6.2
ppm
0.41
0.41
0.41
0.76

b)

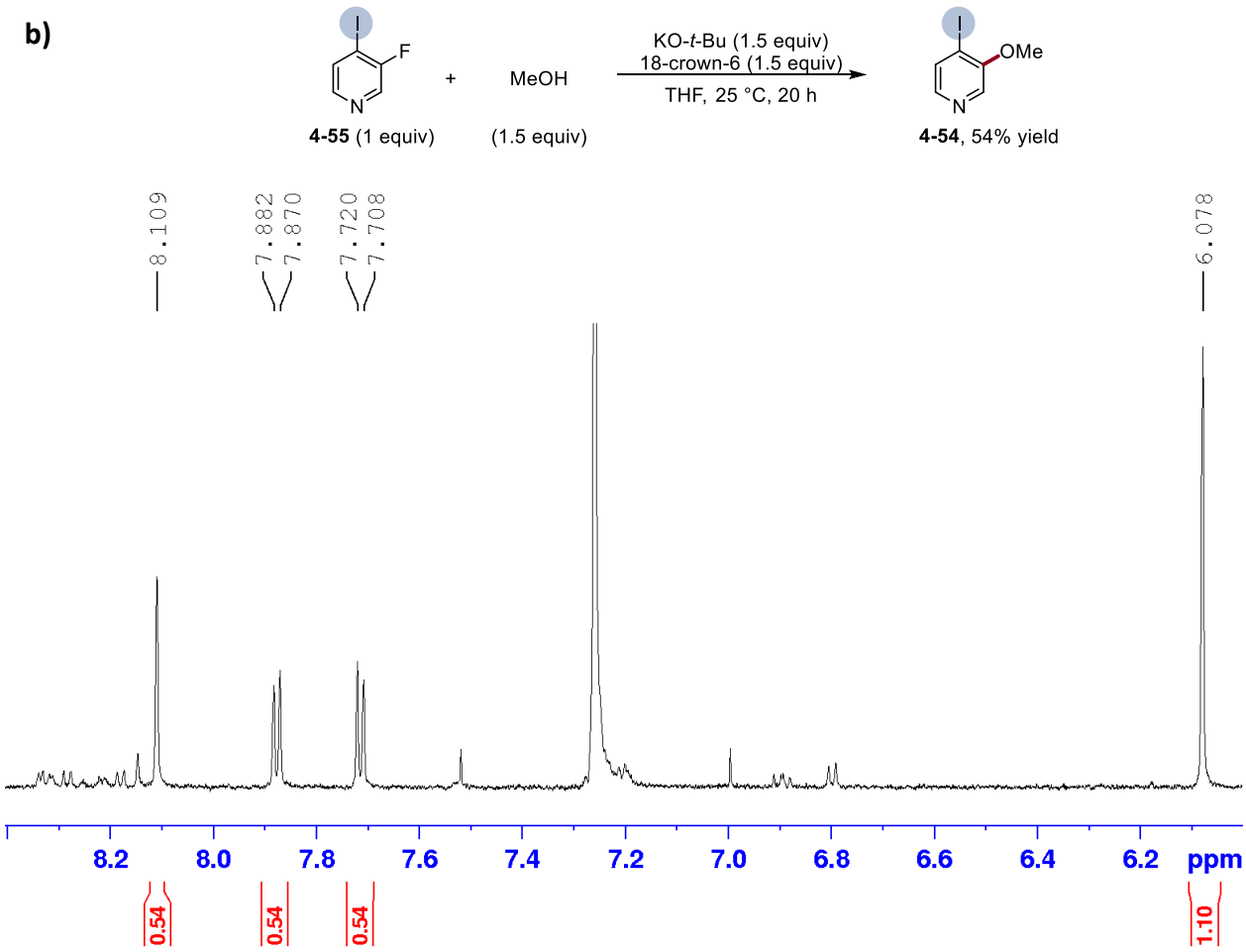
F
N
+
MeOH
KO-t-Bu (1.5 equiv)
18-crown-6 (1.5 equiv)
THF, 25 °C, 20 h
OMe
N
4-55 (1 equiv)
(1.5 equiv)
4-54, 54% yield
8.109
7.882
7.870
7.720
7.708
6.078
8.2
8.0
7.8
7.6
7.4
7.2
7.0
6.8
6.6
6.4
6.2
ppm
0.54
0.54
0.54
1.10

c)

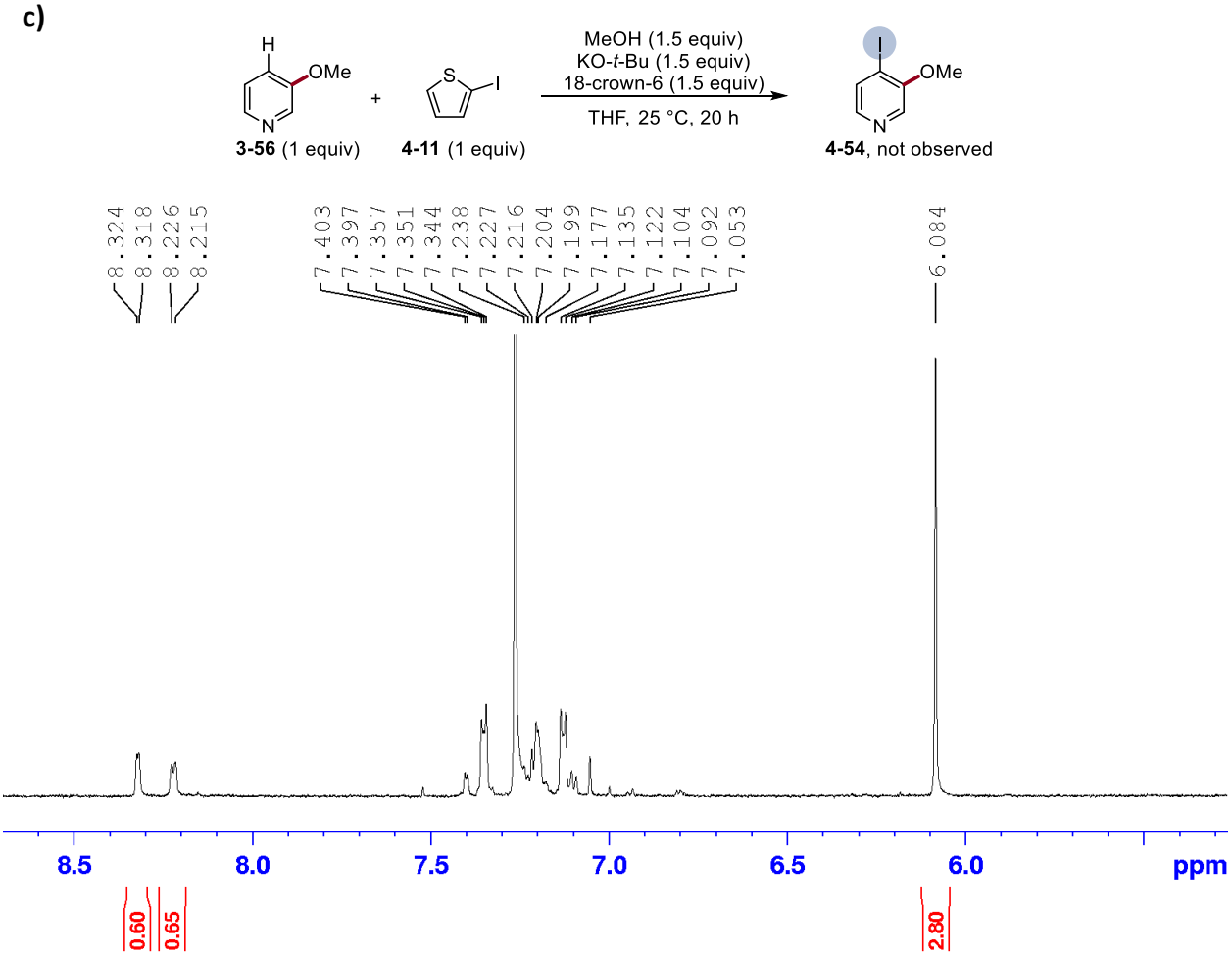
MeOH (1.5 equiv)
KO-t-Bu (1.5 equiv)
18-crown-6 (1.5 equiv)
THF, 25 °C, 20 h
OMe
3-56 (1 equiv)
4-11 (1 equiv)
4-54, not observed
8.324
8.318
8.226
8.215
7.403
7.397
7.357
7.351
7.344
7.238
7.227
7.216
7.204
7.199
7.177
7.135
7.122
7.104
7.092
7.053
6.084
8.5
8.0
7.5
7.0
6.5
6.0
ppm
0.60
0.65
2.80

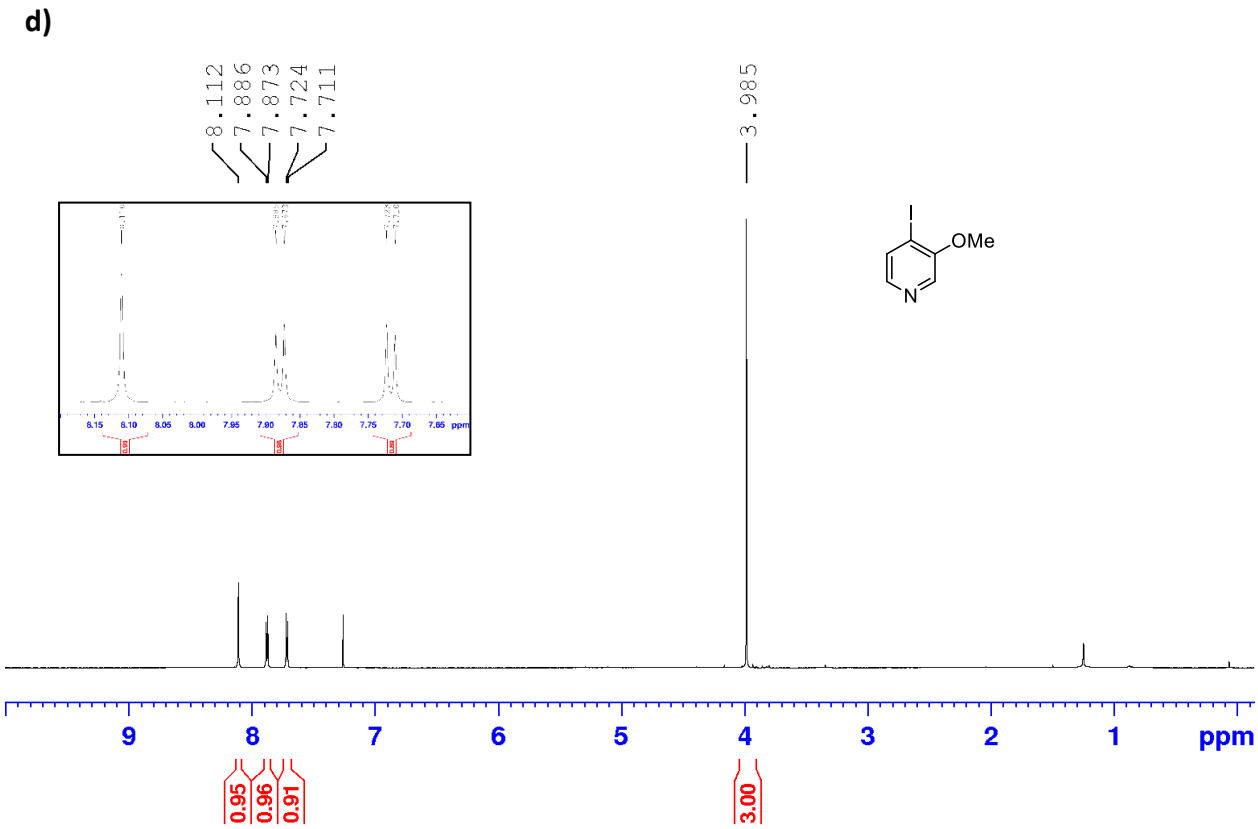

Figure A3–27: (a) ^{1}H NMR spectrum (400 MHz, $CDCl_3$) of the crude reaction solution for 4-selective iodination and 3-selective substitution of 3-fluoropyridine with methanol. 1,3,5-Trimethoxybenzene (21.2 mg, 0.126 mmol, signal at 6.07 ppm calibrated to 0.76 for a 0.5 mmol scale reaction) internal standard was used to determine the yield of 4-iodo-3-methoxypyridine (41% yield). (b) ^{1}H NMR spectrum (400 MHz, $CDCl_3$) of the crude reaction solution for 3-selective substitution of 3-fluoro-4-iodopyridine with methanol. 1,3,5-Trimethoxybenzene (31.0 mg, 0.184 mmol, signal at 6.08 ppm calibrated to 1.10 for a 0.5 mmol scale reaction) internal standard was used to determine the yield of 4-iodo-3-methoxypyridine (54% yield). (c) ^{1}H NMR spectrum (400 MHz, $CDCl_3$) of the crude reaction solution for attempted 4-selective iodination of 3-methoxypyridine. 1,3,5-Trimethoxybenzene (15.8 mg, 0.184 mmol, signal at 6.08 ppm calibrated to 2.80 for a 0.1 mmol scale reaction) was added as an internal standard (0% yield of 4-iodo-3-methoxypyridine). (d) ^{1}H NMR spectrum (400 MHz, $CDCl_3$) of isolated 4-iodo-3-methoxypyridine (**4–54**).

A3.8 Preparation of 1,3-Azole and (Di)azine Starting Materials

N,*N*-diethylpyridazine-4-carboxamide

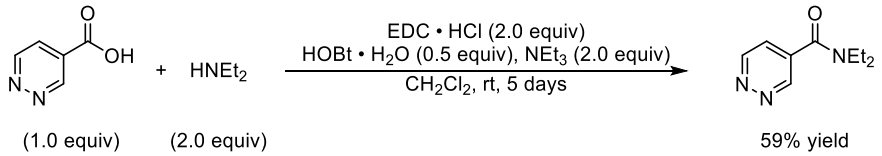

Procedure: Open to air, a 100 mL round bottom flask was charged with a magnetic stir bar, *N*-(3-dimethylaminopropyl)-*N*′-ethylcarbodiimide hydrochloride (3.11 g, 16.2 mmol, 2.0 equiv), 1-hydroxybenzotriazole hydrate (540.5 mg, 4.0 mmol, 0.5 equiv), pyridazine-4-carboxylic acid (1.0 g, 8.1 mmol, 1.0 equiv), diethylamine (1.7 mL, 16.2 mmol, 2.0 equiv), and triethylamine (2.3 mL, 16.2 mmol, 2.0 equiv) in successive order. The solution was stirred 24 h at rt. The solution was then transferred to separatory funnel containing H_2O (50 mL). The organic layer was washed with H_2O (2 x 50 mL) and brine (1 x 30 mL) and then dried over Na_2SO_4. The Na_2SO_4 was removed by filtration and the organic layer was concentrated *in vacuo*. Silica gel chromatography (1% MeOH/CH_2Cl_2 to 5% MeOH/CH_2Cl_2) yielded the title compound as an amber oil. **^{1}H NMR** (400 MHz, $CDCl_3$) δ 9.29 (m, 1H), 9.20 (m, 1H), 7.47 (dd, *J* = 2.2 Hz, 5.2 Hz, 1H), 3.57 (q, *J* = 7.1 Hz, 2H), 3.22 (q, *J* = 7.1 Hz, 2H), 1.28 (t, *J* = 7.1 Hz, 3H), 1.16 (t, *J* = 7.1 Hz, 3H). **^{13}C NMR** (101 MHz, $CDCl_3$) δ 166.0, 151.6, 148.5, 135.2, 123.4, 43.4, 39.9, 14.5, 12.9. **IR** (neat, cm^{-1}) 3050, 2921, 1637, 1573, 1433, 822, 694. **HRMS** (DART) $[M+H]^+$ calcd. for $[C_9H_{14}N_3O]^+$ = 180.1311, 180.1310 found.

3-(phenylthio)pyridine

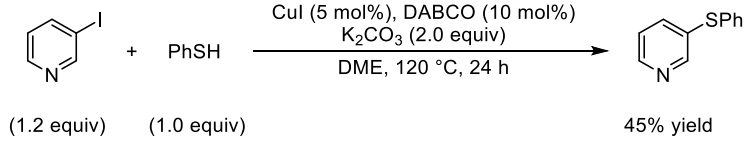

Procedure: The title compound was prepared according to a modified literature procedure.[5] An oven-dried 100 mL round bottom flask was charged with a magnetic stir bar, CuI (76.2 mg, 0.4 mmol, 0.05 equiv), DABCO (89.1 mg, 0.81 mmol, 0.1 equiv), K_2CO_3 (1.96 g, 19.6 mmol, 2.0 equiv), and 3-iodopyridine (2.0 g, 9.8 mmol, 1.2 equiv). The flask was fitted with a reflux condenser and sealed with a red septum stopper (Chemglass, Product #CG-3022-08), evacuated and backfilled three times with N_2, and left under positive pressure of N_2 on a manifold Schlenk line. Anhydrous 1,2-dimethoxyethane (20 mL) followed by thiophenol (0.85 mL, 8.1 mmol, 1.0 equiv) were then added *via* syringe. The flask was placed into a silicon oil bath preheated to 120 °C and the reaction solution was refluxed for 24 h. The solution was allowed to cool to rt, then transferred to a separatory funnel containing H_2O (50 mL). The aqueous layer was extracted with EtOAc (3 x 40 mL) and the organic layers were combined and dried over Na_2SO_4. The Na_2SO_4 was removed by filtration and the organic layer was concentrated *in vacuo*. Silica gel chromatography (10% EtOAc/hexanes to 20% EtOAc/hexanes) yielded the title compound as a clear oil. Spectroscopic characterization of this compound is consistent with a previous literature report.[5] **^{1}H NMR** (400 MHz, $CDCl_3$) δ 8.55 (m, 1H), 8.46 (dd, *J* = 1.5 Hz, 4.8 Hz, 1H), 7.60 (m, 1H), 7.28-7.39 (m, 5H), 7.21 (m, 1H).

3-(phenylsulfonyl)pyridine

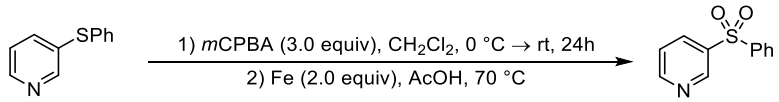

(1.0 equiv) 41% yield

Step 1: 3-(phenylsulfonyl)pyridine 1-oxide

Procedure: A 100 mL round bottom flask was charged with a magnetic stir bar, 3-(phenylthio)pyridine (2.21 g, 11.3 mmol, 1.0 equiv) and CH_2Cl_2 (30 mL). The solution was cooled to 0 °C in an ice-bath, then *m*CPBA (70%-75% balance with water, 8.39 g, 34.0 mmol, 3.0 equiv)

was added slowly in solid portions. The reaction solution was warmed to rt, stirred for 24 h, then poured into a separatory funnel containing H_2O (100 mL). The aqueous layer was extracted with CH_2Cl_2 (3 x 50 mL) and the organic layers were combined and dried over Na_2SO_4. The Na_2SO_4 was removed by filtration and the organic layer was concentrated *in vacuo*. Silica gel chromatography (3% MeOH/CH_2Cl_2) yielded the title compound as a white powder (1.95 g, 8.3 mmol, 73% yield). **^{1}H NMR** (400 MHz, $CDCl_3$) δ 8.65 (m, 1H), 8.26 (m, 1H), 7.96 (m, 2H), 7.66-7.72 (m, 2H), 7.57-7.60 (m, 2H), 7.39 (dd, *J* = 6.6 Hz, 7.8 Hz, 1H).

Step 2: 3-(phenylsulfonyl)pyridine

Procedure: A 100 mL round bottom flask was charged with a magnetic stir bar, 3-(phenylsulfonyl)pyridine 1-oxide (1.95 g, 8.3 mmol, 1.0 equiv), glacial acetic acid (20.0 mL), and Fe powder (923.0 mg, 16.4 mmol, 2.0 equiv) in successive order. The flask was placed into a silicon oil bath preheated to 70 °C with stirring for 24 h. The reaction solution was allowed to cool to rt and then poured into a separatory funnel containing H_2O (50 mL). EtOAc (100 mL) was added to the separatory funnel and the organic layer was washed with H_2O (2 x 50 mL) and brine (1 x 40 mL). The organic layer was dried over Na_2SO_4. The Na_2SO_4 was removed by filtration and the organic layer was concentrated *in vacuo*. Silica gel chromatography (50% EtOAc/hexanes) yielded the title compound as a white powder (1.02 g, 4.7 mmol, 56% yield). Spectroscopic characterization of this compound is consistent with a previous literature report.[6] **^{1}H NMR** (400 MHz, $CDCl_3$) δ 9.15 (m, 1H), 8.79 (dd, *J* = 1.6 Hz, 4.8 Hz, 1H), 8.22 (m, 1H), 7.98 (m, 2H), 7.62 (m, 1H), 7.55 (m, 2H), 7.45 (m, 1H).

***N,N*-diethylpyridine-3-sulfonamide**

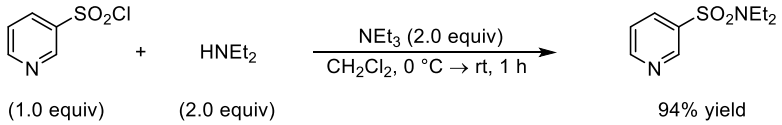

Procedure: An oven-dried 50 mL round bottom flask was charged with a magnetic stir bar, pyridine-3-sulfonyl chloride (1.5 g, 8.5 mmol, 1.0 equiv), and anhydrous CH_2Cl_2 (15.0 mL). The solution was cooled to 0 °C in an ice-bath then triethylamine (2.4 mL, 17.0 mmol, 2.0 equiv) and diethylamine (1.8 mL, 17.0 mmol, 2.0 equiv) were added dropwise *via* syringe. The reaction solution was warmed to rt and stirred for 1 h. The solution was then poured into a separatory funnel containing H_2O (50 mL). The aqueous layer was extracted with EtOAc (3 x 50 mL) and the organic layers were pooled and dried over Na_2SO_4. The Na_2SO_4 was removed by filtration and the organic layer was concentrated *in vacuo*. Silica gel chromatography (80% EtOAc/hexanes) yielded the title compound as a white solid (1.73 g, 8.0 mmol, 94% yield). Spectroscopic characterization of this compound is consistent with a previous literature report.[7] **^{1}H NMR** (400 MHz, $CDCl_3$) δ 9.03 (m, 1H), 8.78 (dd, *J* = 1.6 Hz, 4.8 Hz, 1H), 8.10 (m, 1H), 7.44 (m, 1H), 3.28 (q, *J* = 7.1 Hz, 4H), 1.16 (t, *J* = 7.1 Hz, 6H).

2-phenyl-6-(trifluoromethyl)pyridine

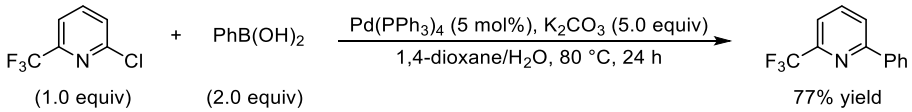

Procedure: Inside an N_2 filled glovebox, a 100 mL round bottom flask was charged with K_2CO_3 (4.50 g, 45.0 mmol, 5.0 equiv), phenylboronic acid (2.19 g, 18.0 mmol, 2.0 equiv), $Pd(PPh_3)_4$ (519.8 mg, 0.45 mmol, 0.05 equiv), 2-chloro-6-(trifluoromethyl)pyridine (1.63 g, 9.0 mmol, 1.0 equiv), and 1,4-dioxane (20 mL). The flask was sealed with a red septum stopper (Chemglass,

Product #CG-3022-08), removed from the glovebox, and put under positive pressure of N_2 on a manifold Schlenk line. H_2O (10 mL) was then added *via* syringe and the flask was placed into a silicon oil bath preheated to 80 °C. The reaction solution was stirred 24 h and then cooled to rt. The resulting solution was then poured into a separatory funnel containing H_2O (50 mL) and the aqueous layer was extracted with EtOAc (3 x 40 mL). The organic layers were combined and dried over Na_2SO_4. The Na_2SO_4 was removed by filtration and the organic layer was concentrated *in vacuo*. Silica gel chromatography yielded the title compound as a white solid (1.53 g, 6.9 mmol, 77% yield). Spectroscopic characterization of this compound is consistent with a previous literature report.[8] **^{1}H NMR** (400 MHz, $CDCl_3$) δ 8.07 (m, 2H), 7.92 (m, 2H), 7.61 (m, 1H), 7.44-7.52 (m, 3H).

3,6-diisopropoxypyridazine

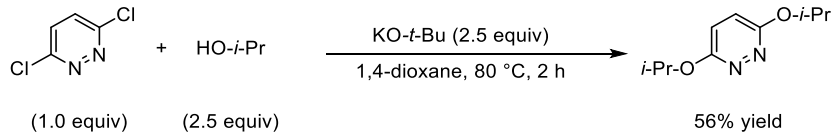

(1.0 equiv) (2.5 equiv) 56% yield

Procedure: Inside an N_2 filled glovebox, an oven-dried 100 mL round bottom flask was charged with 3,6-dichloropyridazine (1.5 g, 10.3 mmol, 1.0 equiv), anhydrous 1,4-dioxane (40 mL), isopropanol (1.55 g, 25.9 mmol, 2.5 equiv), and KO-*t*-Bu (3.17 g, 25.9 mmol, 2.5 equiv) in successive order. The flask was sealed with a red septum stopper (Chemglass, Product #CG-3022-08), removed from the glovebox, put under positive pressure of N_2 on a manifold Schlenk line, and placed into a silicon oil bath preheated to 80 °C. The reaction solution was stirred for 2 h then cooled to rt and transferred to a separatory funnel containing H_2O (50 mL). The aqueous layer was extracted with EtOAc (3 x 40 mL), and the organic layers were combined and dried over Na_2SO_4. The Na_2SO_4 was removed by filtration and the organic layer was concentrated *in vacuo*. Silica gel chromatography (10% EtOAc/hexanes) yielded the title compound as a clear oil (1.13 g, 5.7 mmol,

56% yield). **^{1}H NMR** (400 MHz, $CDCl_3$) δ 6.83 (s, 2H), 5.42 (m, 2H), 1.38 (d, *J* = 6.2 Hz, 12H). **^{13}C NMR** (101 MHz, $CDCl_3$) δ 161.1, 122.1, 69.6, 22.1. **IR** (neat, cm^{-1}) 2977, 2938, 1437, 1263, 1106, 942, 837. **HRMS** (ESI) $[M+H]^+$ calcd. for $[C_{10}H_{17}N_2O_2]^+$ = 197.1285, 197.1282 found.

5-chloro-2-phenylpyrimidine

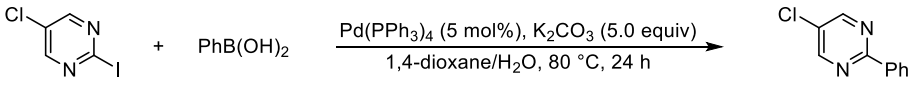

(1.0 equiv) (1.2 equiv) 27% yield

Procedure: The title compound was prepared according to the procedure used for 2-phenyl-6-(trifluoromethyl)pyridine (see above) using 5-chloro-2-iodopyrimidine (2.0 g, 8.3 mmol, 1.0 equiv), phenylboronic acid (1.21 g, 10.0 mmol, 1.2 equiv), $Pd(PPh_3)_4$ (479.4 mg, 0.42 mmol, 0.05 equiv), K_2CO_3 (4.15 g, 41.5 mmol, 5.0 equiv), 1,4-dioxane (35 mL), and H_2O (15 mL). Silica gel chromatography (2% EtOAc/hexanes to 5% EtOAc/hexanes) yielded the title compound as a white solid (421.3 mg, 2.2 mmol, 27% yield). Spectroscopic characterization of this compound is consistent with a previous literature report.[9] **^{1}H NMR** (400 MHz, $CDCl_3$) δ 8.75 (s, 2H), 8.41 (m, 2H), 7.50 (m, 3H).

6-(trifluoromethyl)-2,3'-bipyridine (42)

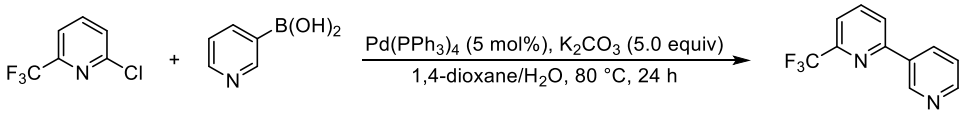

(1.0 equiv) (2.0 equiv) **42**, 91% yield

Procedure: The title compound was prepared according to the procedure used for 2-phenyl-6-(trifluoromethyl)pyridine (see above) using 2-chloro-6-(trifluoromethyl)pyridine (1.5 g, 8.3 mmol, 1.0 equiv), pyridine-3-boronic acid (2.04 g, 16.6 mmol, 2.0 equiv), K_2CO_3 (4.15 g, 41.5 mmol, 5.0 equiv), $Pd(PPh_3)_4$ (479.4 mg, 0.42 mmol, 0.05 equiv), 1,4-dioxane (20 mL), and H_2O (10 mL).

Silica gel chromatography (50% EtOAc/hexanes to EtOAc) yielded the title compound as a white solid (1.69 g, 7.5 mmol, 91% yield). **Mp**: 51 °C – 53 °C. **^{1}H NMR** (400 MHz, $CDCl_3$) δ 9.24 (d, *J* = 2.2 Hz, 1H), 8.70 (dd, *J* = 1.5 Hz, 4.8 Hz, 1H), 8.43 (m, 1H), 7.95-8.01 (m, 2H), 7.68 (m, 1H), 7.45 (dd, *J* = 4.8 Hz, 8.0 Hz, 1H). **^{13}C NMR** (101 MHz, $CDCl_3$) δ 155.4, 150.8, 148.7 (q, *J* = 35.0 Hz), 148.4, 138.6, 134.8, 133.5, 123.9, 122.9, 121.5 (q, *J* = 275.4 Hz), 119.4 (q, *J* = 2.8 Hz). **^{19}F NMR** (376 MHz, $CDCl_3$) δ -69.2. **IR** (neat, cm^{-1}) 3046, 2158, 1594, 1436, 1343, 1115, 792. **HRMS** $[M+H]^+$ calcd. for $[C_{11}H_8F_3N_2]^+$ = 225.0634, 225.0636 found.

5-chloro-2,3'-bipyridine

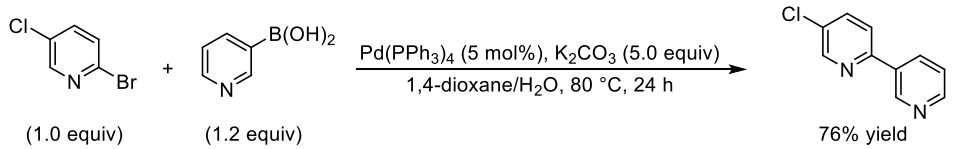

Procedure: The title compound was prepared according to the procedure used for 2-phenyl-6-(trifluoromethyl)pyridine (see above) using 2-bromo-5-chloropyridine (2.0 g, 10.5 mmol, 1.0 equiv), pyridine-3-boronic acid (1.55 g, 12.6 mmol, 1.2 equiv), K_2CO_3 (5.26 g, 52.5 mmol, 5.0 equiv), $Pd(PPh_3)_4$ (612.2 mg, 0.53 mmol, 0.05 equiv), 1,4-dioxane (20 mL), and H_2O (10 mL). Silica gel chromatography (30% EtOAc/hexanes to 60% EtOAc/hexanes) yielded the title compound as a light yellow solid (1.52 g, 8.0 mmol, 76% yield). Spectroscopic characterization of this compound is consistent with a previous literature report.[10] **^{1}H NMR** (400 MHz, $CDCl_3$) δ 9.17 (m, 1H), 8.66 (m, 2H), 8.30 (m, 1H), 7.78 (m, 1H), 7.71 (m, 1H), 7.41 (m, 1H).

8-(imidazo[1,2-*b*]pyridazin-6-yl)quinoline

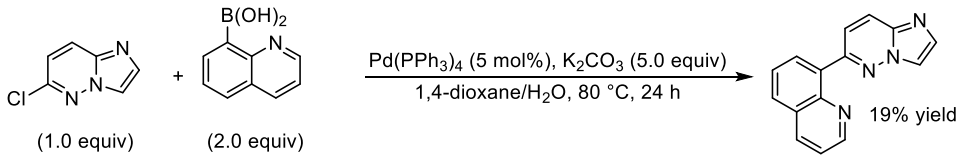

Procedure: The title compound was prepared according to the procedure used for 2-phenyl-6-(trifluoromethyl)pyridine (see above) using 6-chloroimidazo[1,2-*b*]pyridazine (1.0 g, 6.5 mmol, 1.0 equiv), quinolin-8-ylboronic acid (2.25 g, 13.0 mmol, 2.0 equiv), K_2CO_3 (3.27 g, 32.6 mmol, 5.0 equiv), $Pd(PPh_3)_4$ (375.4 mg, 0.325 mmol, 0.05 equiv), 1,4-dioxane (13 mL), and H_2O (7 mL). Silica gel chromatography (3% MeOH/CH_2Cl_2) yielded the title compound as a yellow solid (303.0 mg, 1.23 mmol, 19% yield). **Mp**: 198 ºC – 200 ºC. **^{1}H NMR** (400 MHz, $CDCl_3$) δ 8.96 (dd, *J* = 1.8 Hz, 4.2 Hz, 1H), 8.27 (dd, *J* = 1.8 Hz, 8.3 Hz, 1H), 7.99-8.09 (m, 4H), 7.68-7.80 (m, 3H), 7.49 (dd, *J* = 4.2 Hz, 8.3 Hz, 1H). **^{13}C NMR** (101 MHz, $CDCl_3$) δ 153.1, 150.8, 146.1, 138.6, 136.7, 135.3, 133.8, 131.2, 130.2, 128.8, 126.6, 123.9, 122.1, 121.7, 116.9. **IR** (neat, cm^{-1}) 3106, 2885, 1654, 1502, 1291, 1131, 811. **HRMS** (DART) $[M+H]^+$ calcd. for $[C_{15}H_{11}N_4]^+$ = 247.0978, 247.0983 found.

4-(pyridin-3-yl)thiazole

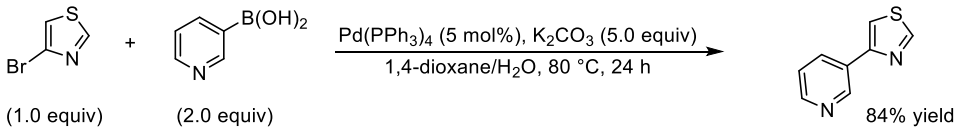

Procedure: The title compound was prepared according to the procedure used for 2-phenyl-6-(trifluoromethyl)pyridine (see above) using 4-bromothiazole (1.0 g, 6.1 mmol, 1.0 equiv), pyridine-3-boronic acid (1.51 g, 12.2 mmol, 2.0 equiv), K_2CO_3 (3.05 g, 30.5 mmol, 5.0 equiv), $Pd(PPh_3)_4$ (352.3 mg, 0.31 mmol, 0.05 equiv), 1,4-dioxane (17 mL), and H_2O (8 mL). Silica gel chromatography (50% EtOAc/hexanes to EtOAc) yielded the title compound as an orange oil (833.4 mg, 5.1 mmol, 84% yield). **^{1}H NMR** δ 9.14 (s, 1H), 8.90 (s, 1H), 8.57 (d, *J* = 4.6 Hz, 1H), 8.23 (m, 1H), 7.63 (m, 1H), 7.37 (dd, *J* = 4.8 Hz, 7.9 Hz, 1H). **^{13}C NMR** (101 MHz, $CDCl_3$) δ 153.6, 153.3, 149.0, 147.6, 134.1, 130.3, 123.9, 114.1. **IR** (neat, cm^{-1}) 3106, 2885, 1654, 1502, 1291, 1131, 811. **HRMS** (ESI) $[M+H]^+$ calcd. for $[C_8H_7N_2S]^+$ = 163.0324, 163.0322 found.

***N*,*N*'-((pyridazine-3,6-diylbis(oxy))bis(ethane-2,1-diyl))bis(*N*-methylpyridin-2-amine)**

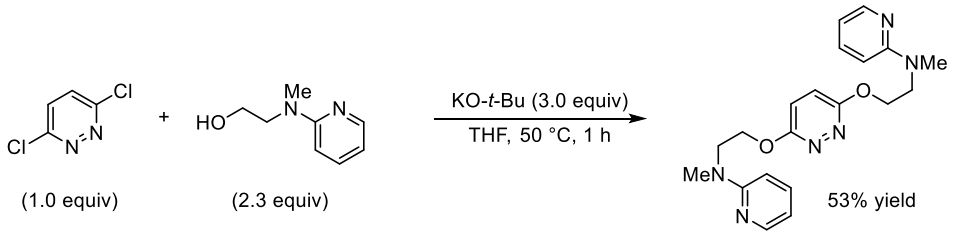

Procedure: An oven-dried 100 mL round bottom flask was charged with a magnetic stir bar and KO-*t*-Bu (4.51 g, 40.2 mmol, 3.0 equiv). The flask was sealed with a red septum stopper (Chemglass, Product #CG-3022-08), evacuated and backfilled three times with N_2, and left under positive pressure of N_2 on a manifold Schlenk line. Anhydrous THF (10 mL) was then added to flask. 2,6-Dichloropyridazine (2.0 g, 13.4 mmol, 1.0 equiv) and 2-(methyl(pyridin-2-yl)amino)ethan-1-ol (4.68 g, 30.8 mmol, 2.3 equiv) were then measured into a 20 mL scintillation vial, constituted in anhydrous THF (15 mL), and then added to the KO-*t*-Bu solution dropwise *via* syringe. The resulting solution was then placed into a silicon oil bath preheated to 50 °C and stirred for 1 h. The solution was allowed to cool to rt and then poured into a separatory funnel containing H_2O (50 mL). The aqueous layer was extracted with EtOAc (3 x 40 mL) and the organic layers were pooled and dried over Na_2SO_4. The Na_2SO_4 was removed by filtration and the organic layer was concentrated *in vacuo*. Silica gel chromatography (50% EtOAc/hexanes) yielded the title compound as a white powder (2.69 g, 7.1 mmol, 53% yield). **Mp**: 106 °C – 108 °C. **^{1}H NMR** (400 MHz, $CDCl_3$) δ 8.13 (m, 2H), 7.43 (m, 2H), 6.85 (s, 2H), 6.52-6.55 (m, 4H), 4.63 (t, *J* = 5.8 Hz, 4H), 3.99 (t, *J* = 5.8 Hz, 4H), 3.11 (s, 6H). **^{13}C NMR** (101 MHz, $CDCl_3$) δ 161.8, 158.6, 148.0, 137.3, 121.7, 111.9, 105.9, 65.2, 49.0, 37.4. **IR** (neat, cm^{-1}) 2942, 1594, 1504, 1424, 1326, 1264, 1155, 998. **HRMS** (DART) $[M+H]^+$ calcd. for $[C_{20}H_{25}N_6O_2]^+$ = 381.2034, 381.2031 found.

4-(1-methyl-1H-benzo[*d*]imidazol-2-yl)thiazole

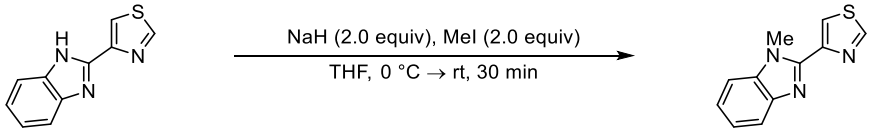

Procedure: An oven-dried 100 mL round-bottom flask was charged with a magnetic stir bar, 4-(1H-benzo[*d*]imidazol-2-yl)thiazole (1.0 g, 5.0 mmol, 1.0 equiv), and anhydrous THF (20 mL). The solution was cooled to 0 °C using an ice water bath, then NaH (60% dispersion in mineral oil, 400.0 mg, 10 mmol, 2.0 equiv) was added slowly in small portions. The solution was warmed to rt and stirred for 30 min. The reaction solution was quenched slowly with H_2O and poured into a separatory funnel containing H_2O (40 mL). The aqueous mixture was extracted with CH_2Cl_2 (3 x 40 mL). The organic layers were pooled and dried over Na_2SO_4. The Na_2SO_4 was filtered off and the organic layer was concentrated *in vacuo*. Silica gel chromatography (10% EtOAc/hexanes) yielded the title compound as a light-yellow powder (741.6 mg, 3.4 mmol, 69% yield). Spectroscopic characterization is consistent with a previous report.[11] **^{1}H NMR** (400 MHz, $CDCl_3$) δ 8.95 (d, *J* = 2.1 Hz, 1H), 8.41 (m, 1H), 7.82 (m, 1H), 7.44 (m, 1H), 7.31-7.38 (m, 2H), 4.25 (s, 3H).

2,6-bis(difluoromethyl)pyridine

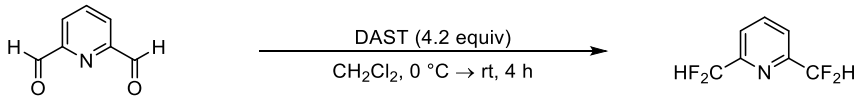

Procedure: An oven-dried 100 mL round bottom flask was charged with a magnetic stir bar, pyridine-2,6-dicarbaldehyde (500.0 mg, 3.7 mmol, 1.0 equiv), and anhydrous CH_2Cl_2 (15.0 mL). The solution was cooled to 0 °C using an ice water bath, then diethylaminosulfur trifluoride (2.1 mL, 15.5 mmol, 4.2 equiv) was added dropwise. The solution was warmed to rt and stirred for 4 h. The reaction solution was cooled back to 0 °C and then quenched slowly with H_2O. The solution

was poured into a separatory funnel containing H_2O. The aqueous mixture was extracted with CH_2Cl_2 (3 x 30 mL). The organic layers were pooled and dried over Na_2SO_4. The Na_2SO_4 was filtered off and the organic layer was concentrated *in vacuo*. Silica gel chromatography (55% CH_2Cl_2/hexanes) yielded the title compound as a clear oil (281.8 mg, 1.57 mmol, 43% yield). **^{1}H NMR** (400 MHz, $CDCl_3$) δ 8.02 (t, *J* = 7.8 Hz, 1H), 7.77 (d, *J* = 7.8 Hz, 2H), 6.66 (t, *J* = 55.2 Hz, 2H). **^{13}C NMR** (101 MHz, $CDCl_3$) δ 152.9 (t, *J* = 26.6 Hz), 139.0, 122.0, 113.6 (t, *J* = 241.7 Hz). **^{19}F NMR** (376 MHz, $CDCl_3$) δ -116.8 (d, *J* = 55.2 Hz). **IR** (neat, cm^{-1}) 3053, 2923, 1574, 1360, 1114, 1042, 823. **EA**: Anal. Calcd. for $C_7H_5F_4N$: C, 46.94; H, 2.81; N, 7.82. Found: C, 46.66; H, 2.82; N, 7.82.

A3.9 References

[1] Fulmer, G. R.; Miller, A. J. M.; Sherden, N. H.; Gottlieb, H. E.; Nudelman, A.; Stoltz, B. M.; Bercaw, J. E.; Goldberg, K. I. *Organometallics* **2010**, *29*, 2176-2179.

[2] Mehta, S.; Larock, R. C. *J. Org. Chem.* **2010**, *75*, 1652-1658.

[3] Schlosser, M.; Marull, M. *Eur. J. Org. Chem.* **2003**, 1569-1575.

[4] Blair, V. L.; Blakemore, D. C.; Hay, D.; Hevia, E.; Pryde, D. C. *Tetrahedron Lett.* **2011**, *52*, 4590-4594.

[5] Thomas, A. M.; Asha, S.; Sindhu, K. S.; Anilkumar, G. *Tetrahedron Lett.* **2015**, *56*, 6560-6564.

[6] Liu, N.-W.; Hofman, K.; Herbert, A.; Manolikakes, G. *Org. Lett.* **2018***, 20*, 760-763.

[7] Pandya, R.; Murashima, T.; Tedeschi, L.; Barrett, A. G. M. *J. Org. Chem.* **2003**, *68*, 8274-8276.

[8] Zinser, C. M.; Warren, K. G.; Meadows, R. E.; Nahra, F.; Al-Majid, A. M.; Barakat, A.; Islam, M. S.; Nolan, S. P.; Cazin, C. S. J. *Green Chem.* **2018**, *20*, 3246-3252.

[9] Yuan, H.; Chen, P.-W.; Li, M.-Y.; Zhang, Y.; Peng, Z.-W.; Liu, W.; Paton, R. S.; Cao, C. *Journal of Molecular Structure* **2020**, *1204*, 127489.

[10] Simkovsky, N. M.; Ermann, M.; Roberts, S. M.; Parry, D. M.; Baxter, A. D. *J. Chem. Soc. Perkin Trans. 1* **2002**, 1847-1849.

[11] Zhang, C.; Zhong, B.; Yang, S.; Pan, L.; Yu, S.; Li, Z.; Li, S.; Su, B.; Meng, X. *Bioorg. Med. Chem.* **2015**, *23*, 3774-3780.

A3.10 Copies of NMR Spectra

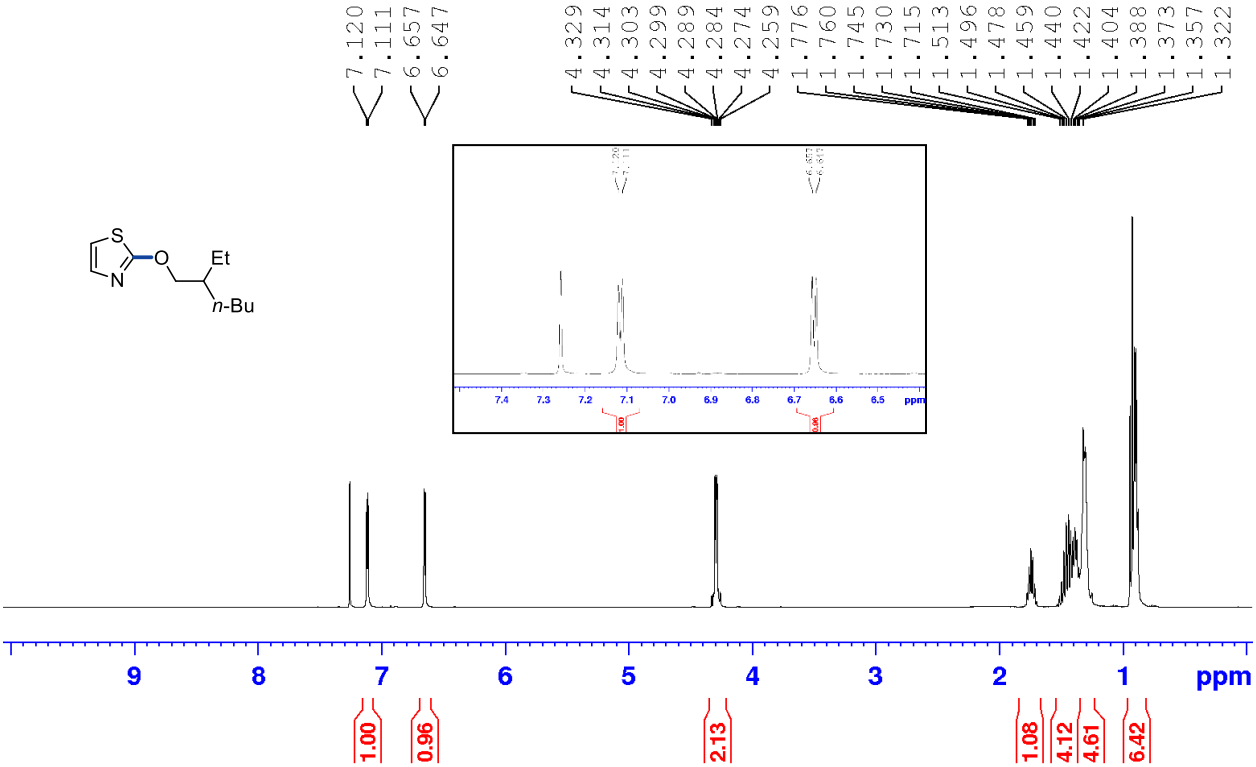

^{1}H NMR spectrum (400 MHz, $CDCl_3$)

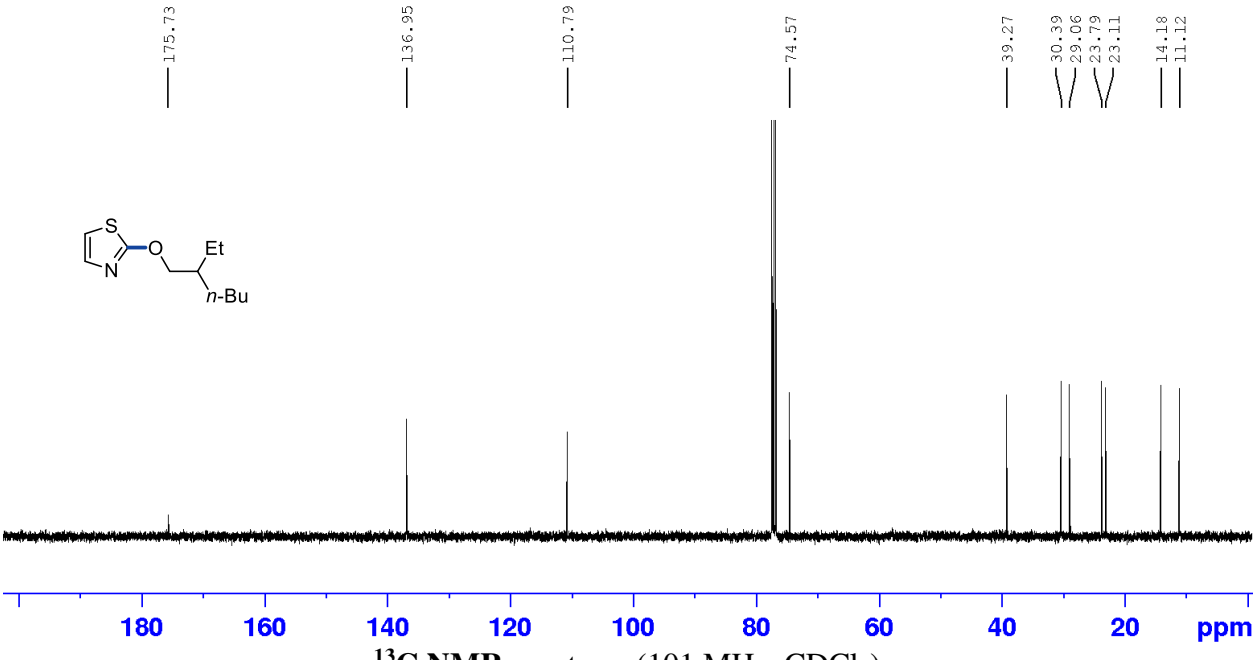

^{13}C NMR spectrum (101 MHz, $CDCl_3$)

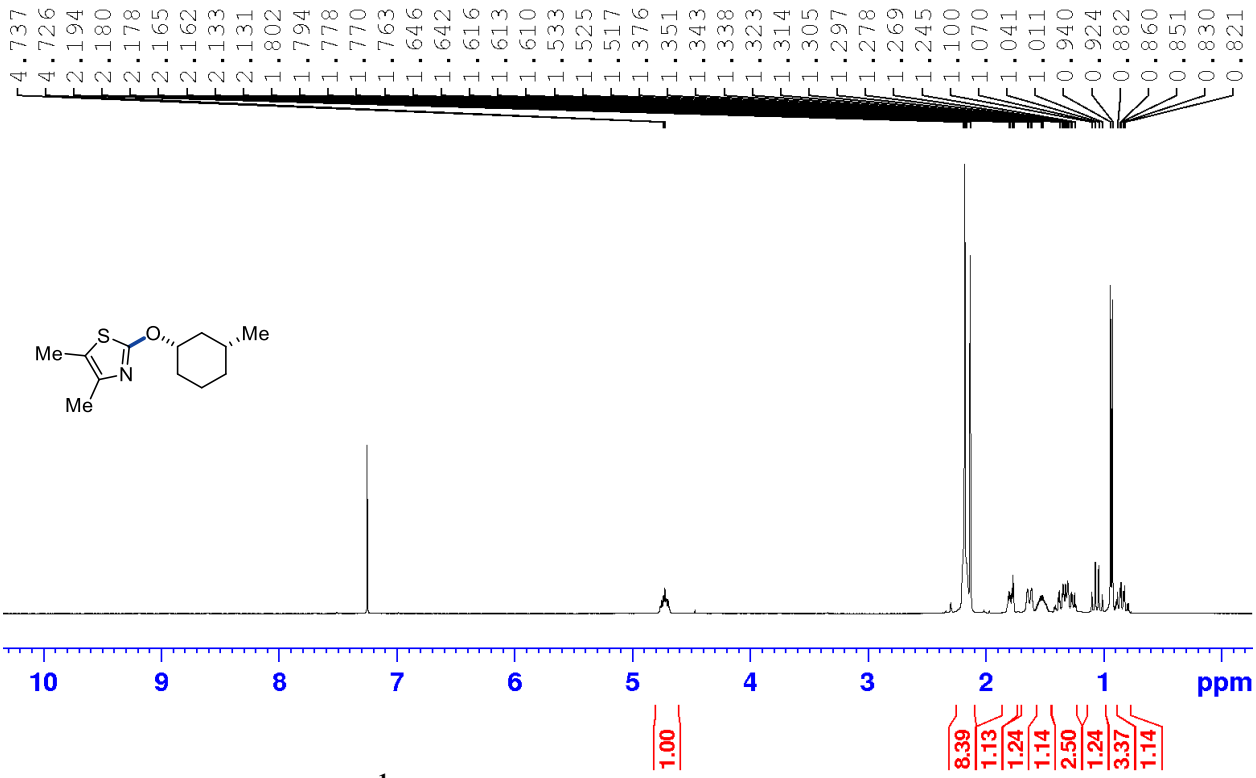

^{1}H NMR spectrum (400 MHz, $CDCl_3$)

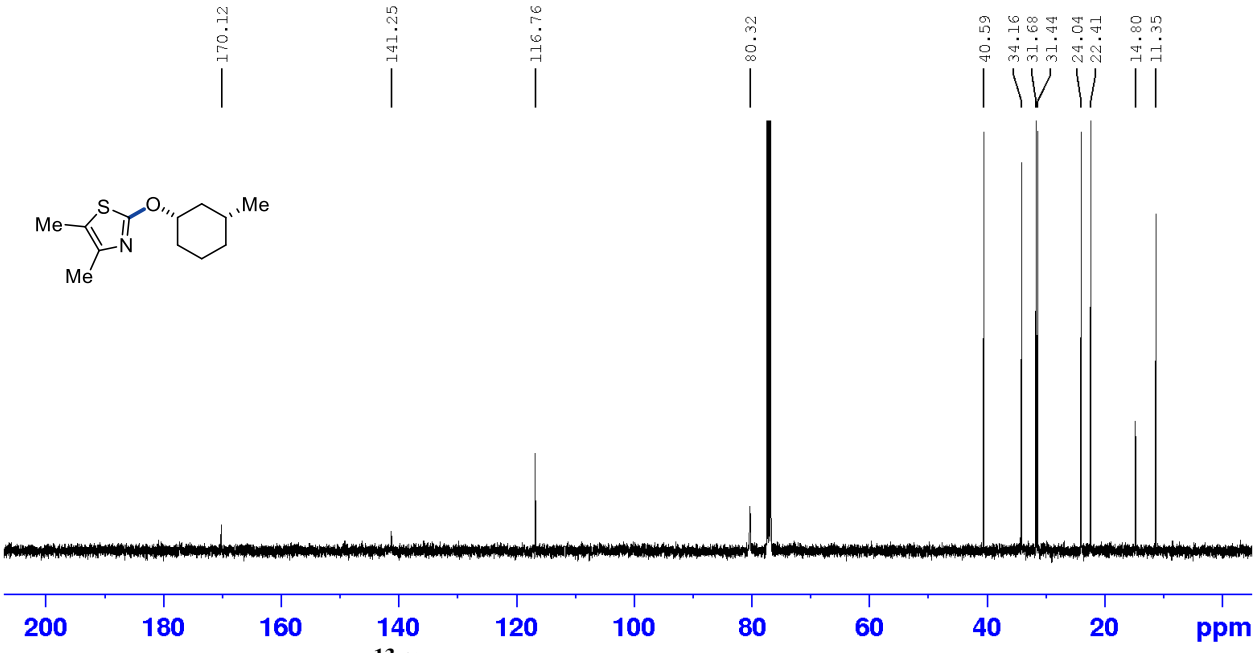

^{13}C NMR spectrum (101 MHz, $CDCl_3$)

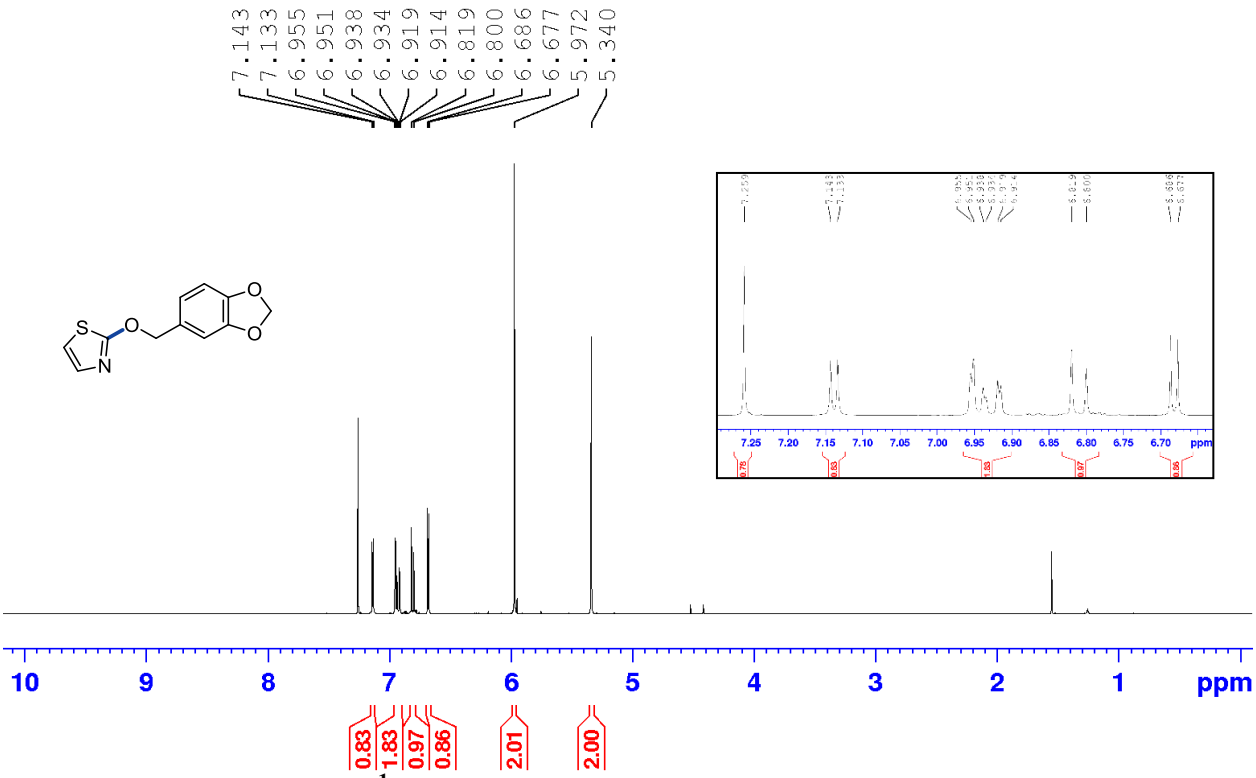

^{1}H NMR spectrum (400 MHz, $CDCl_3$)

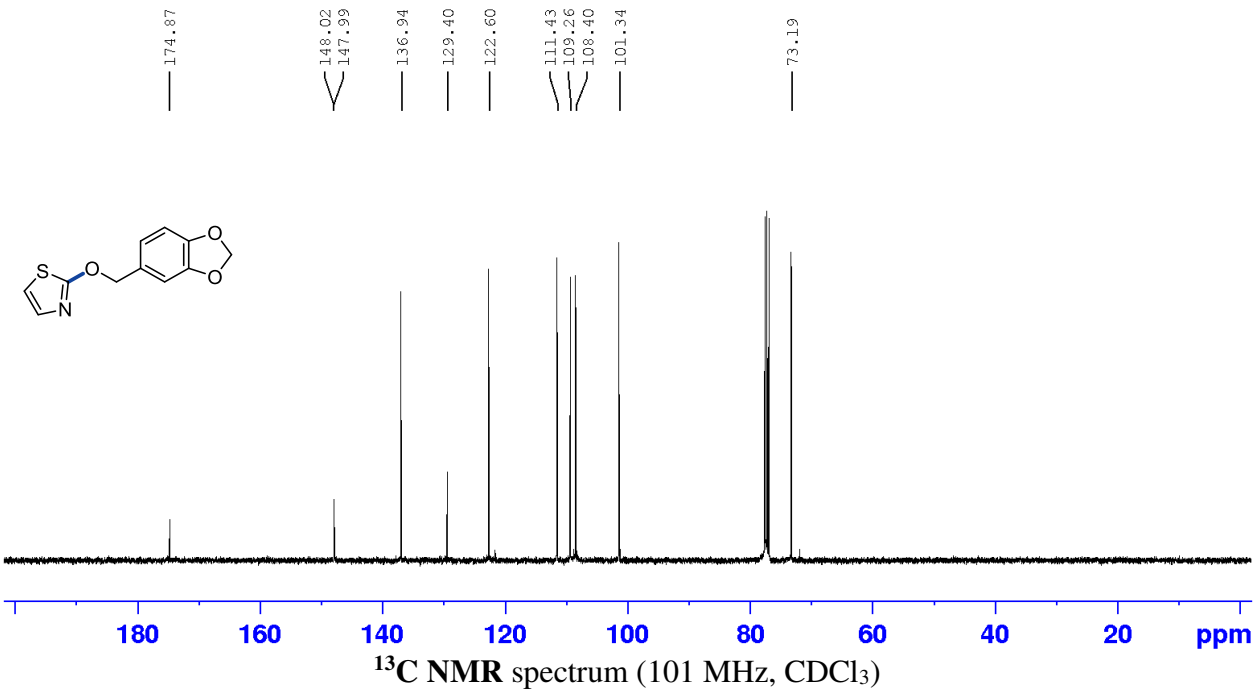

^{13}C NMR spectrum (101 MHz, $CDCl_3$)

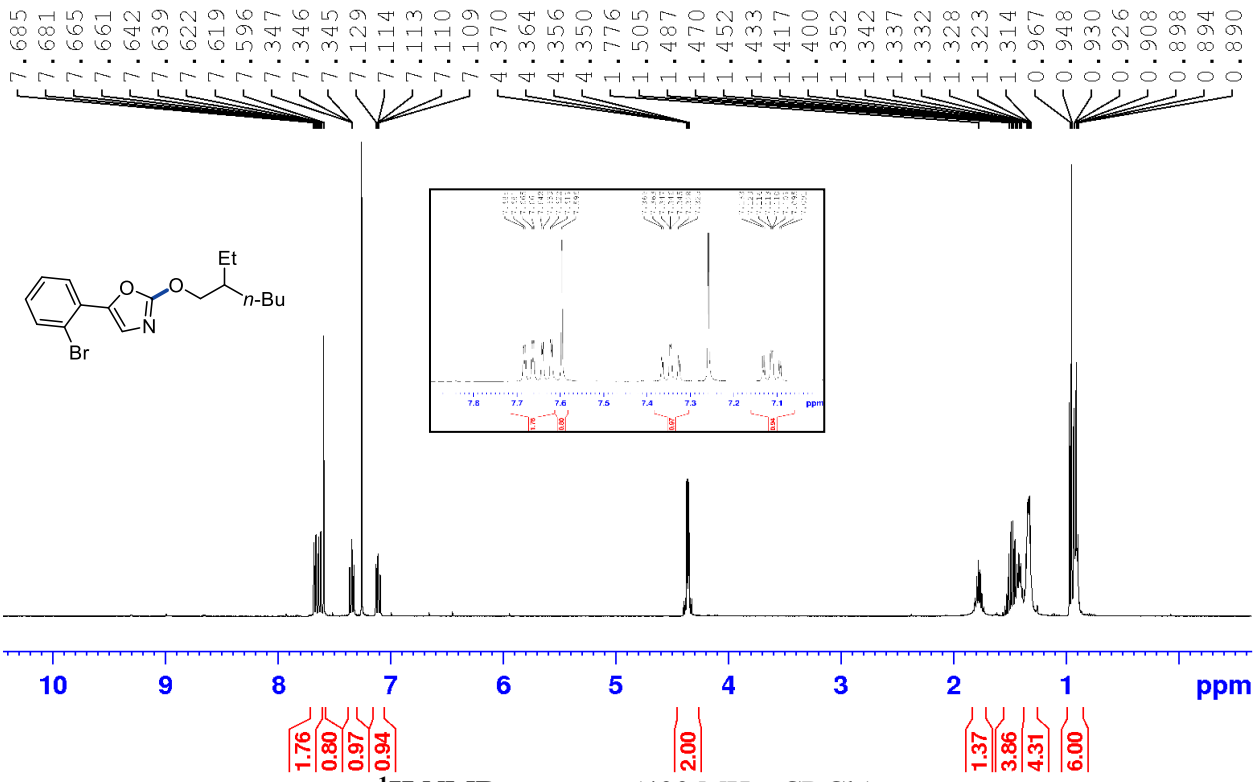

^{1}H NMR spectrum (400 MHz, $CDCl_3$)

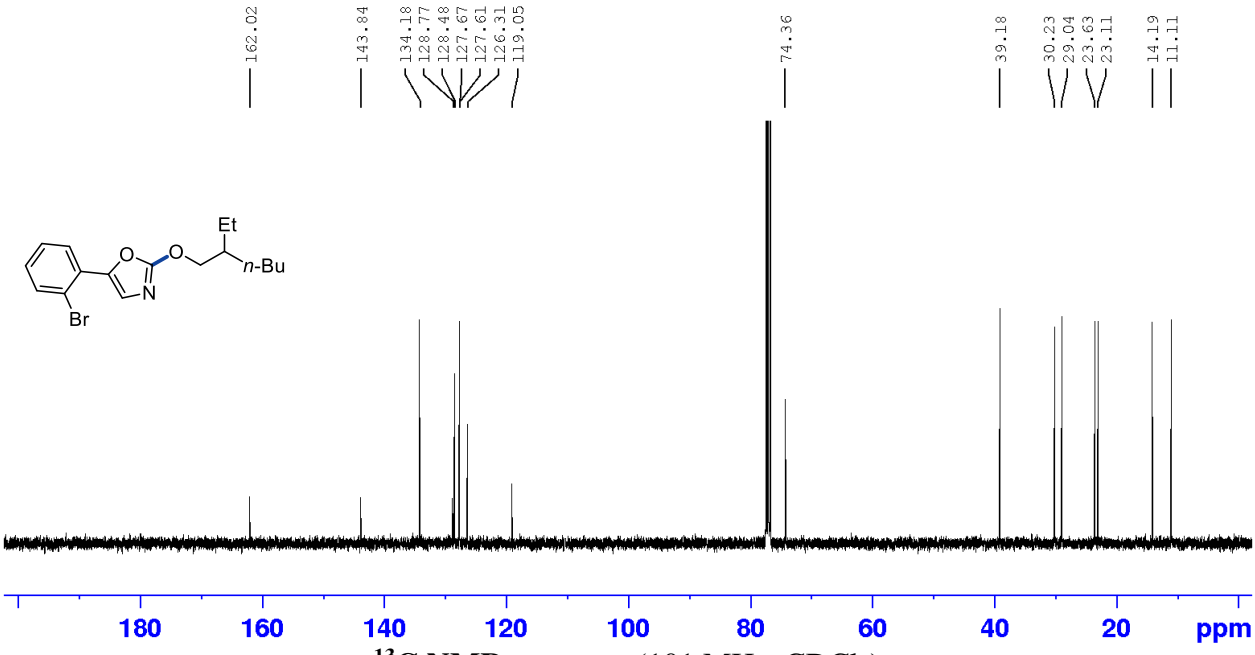

^{13}C NMR spectrum (101 MHz, $CDCl_3$)

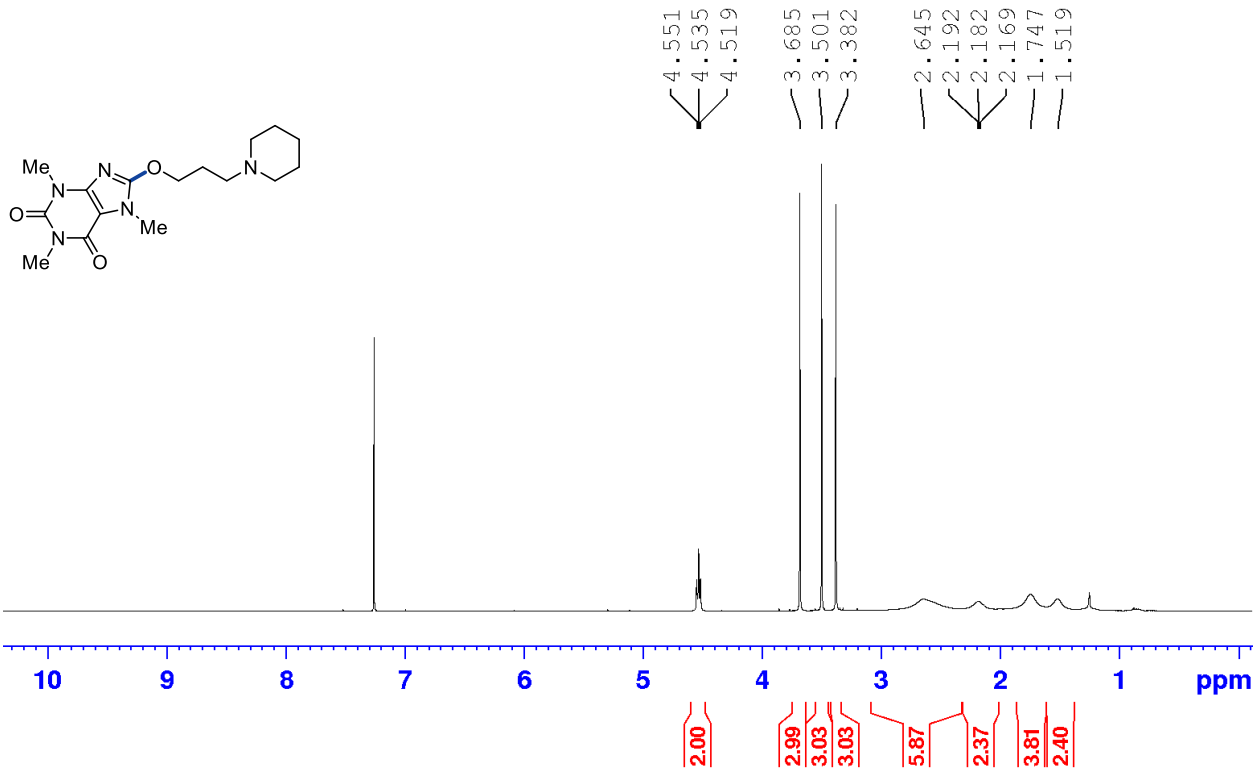

^{1}H NMR spectrum (400 MHz, $CDCl_3$)

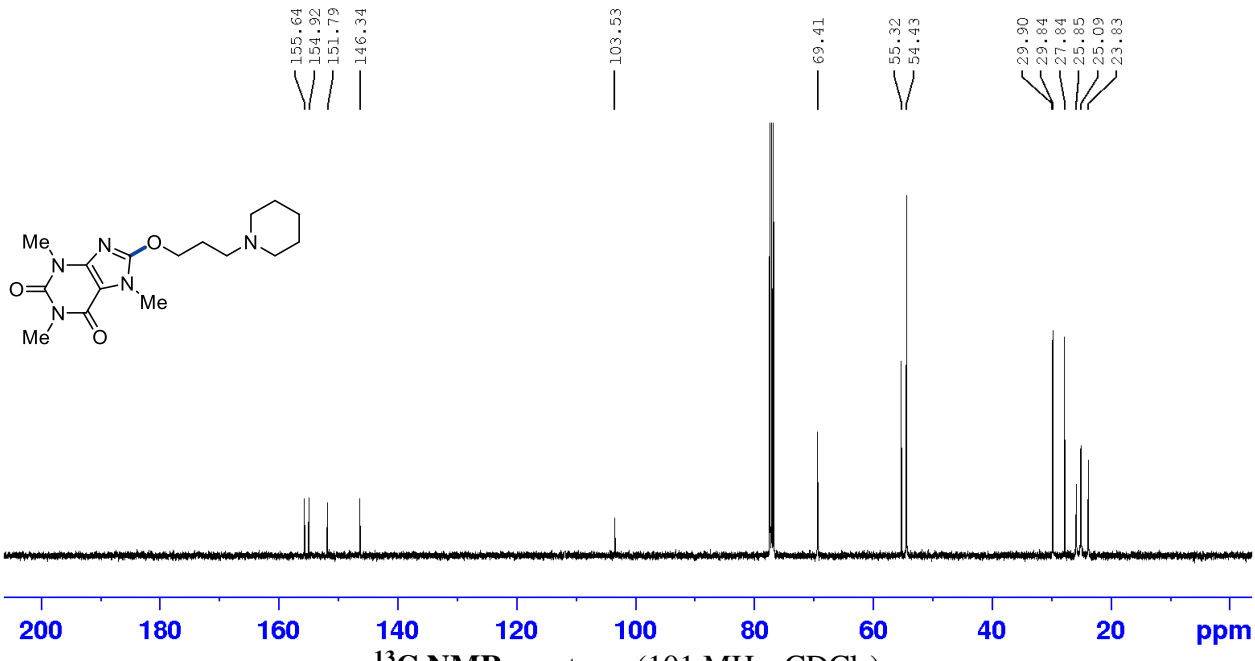

^{13}C NMR spectrum (101 MHz, $CDCl_3$)

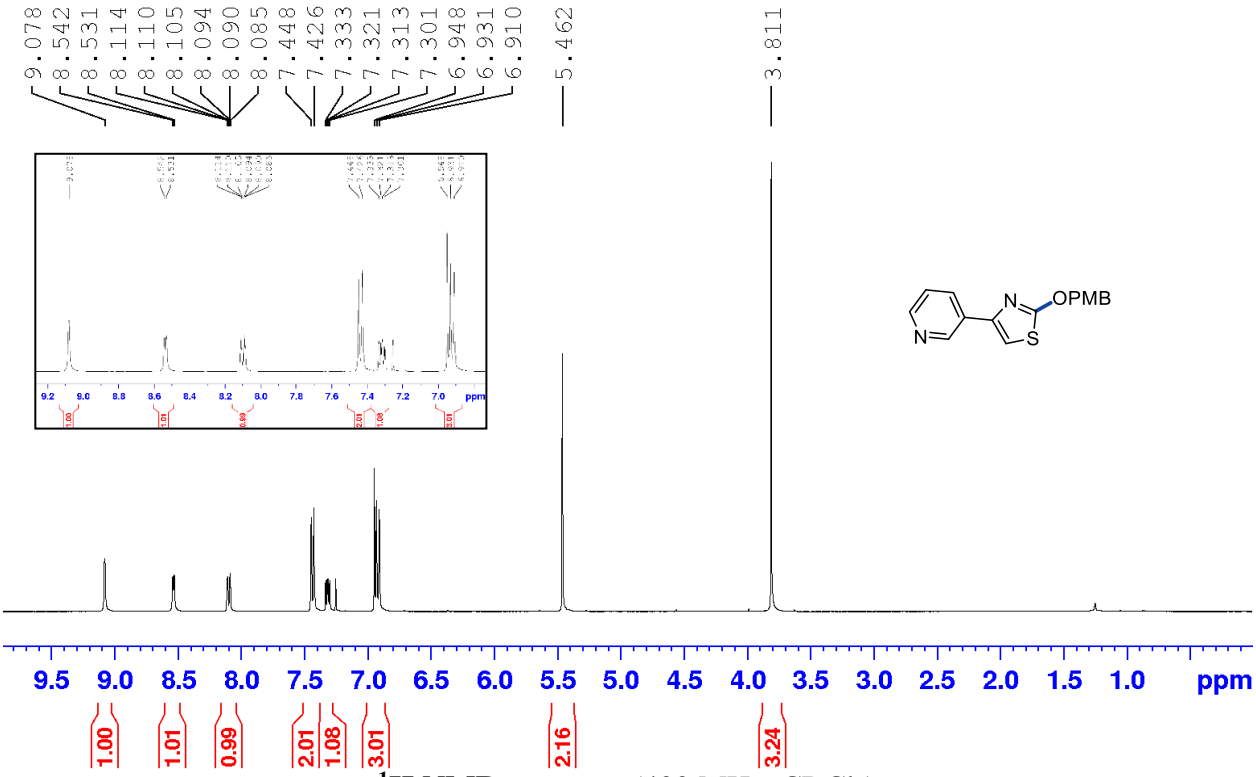

^{1}H NMR spectrum (400 MHz, $CDCl_3$)

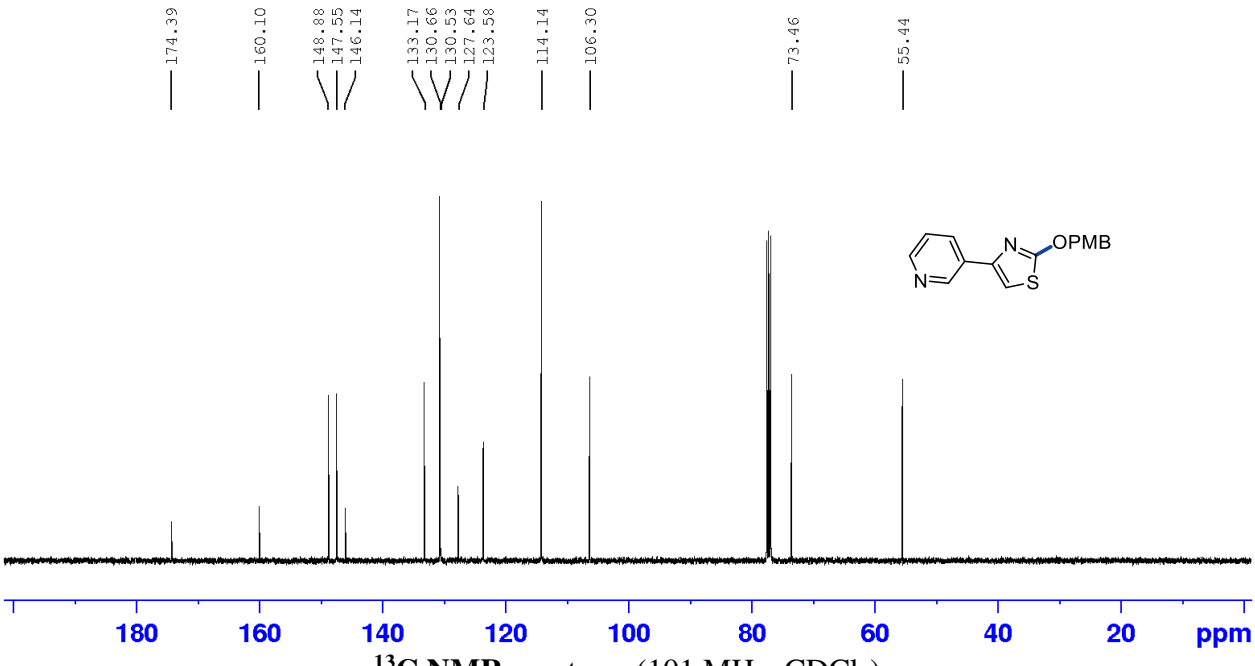

^{13}C NMR spectrum (101 MHz, $CDCl_3$)

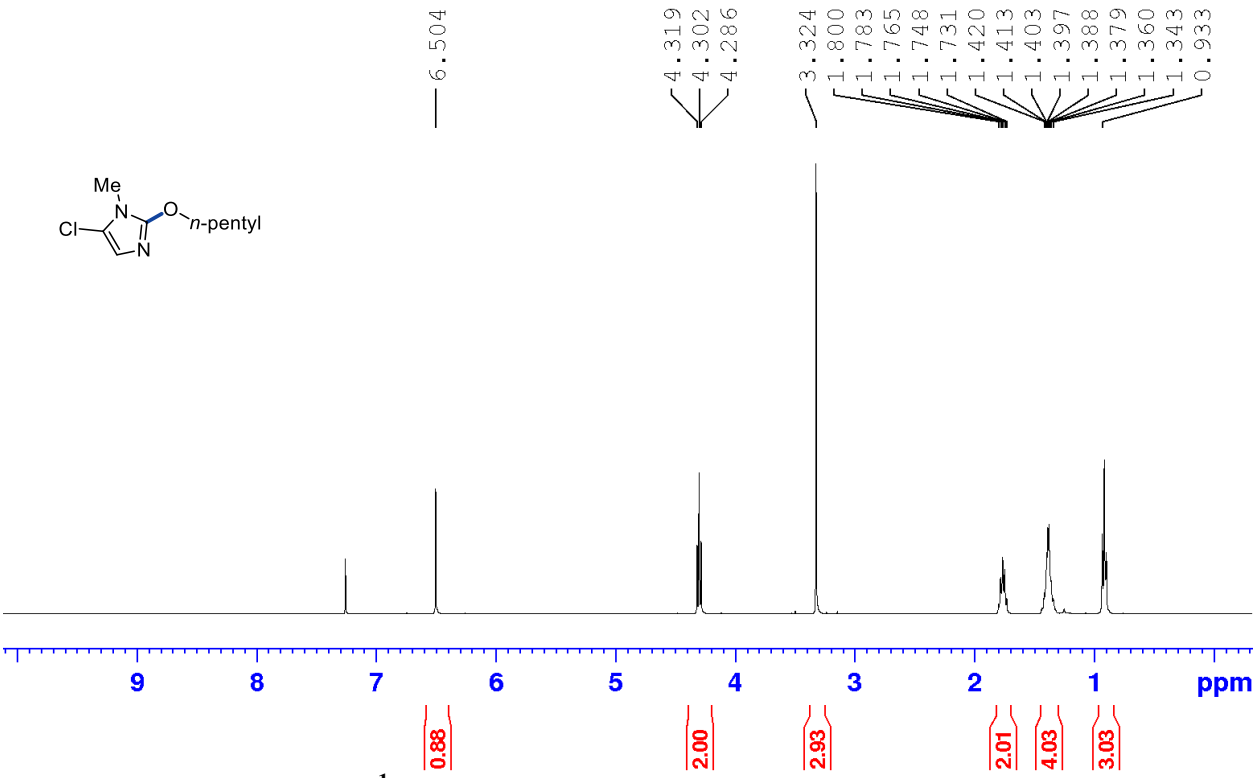

^{1}H NMR spectrum (400 MHz, $CDCl_3$)

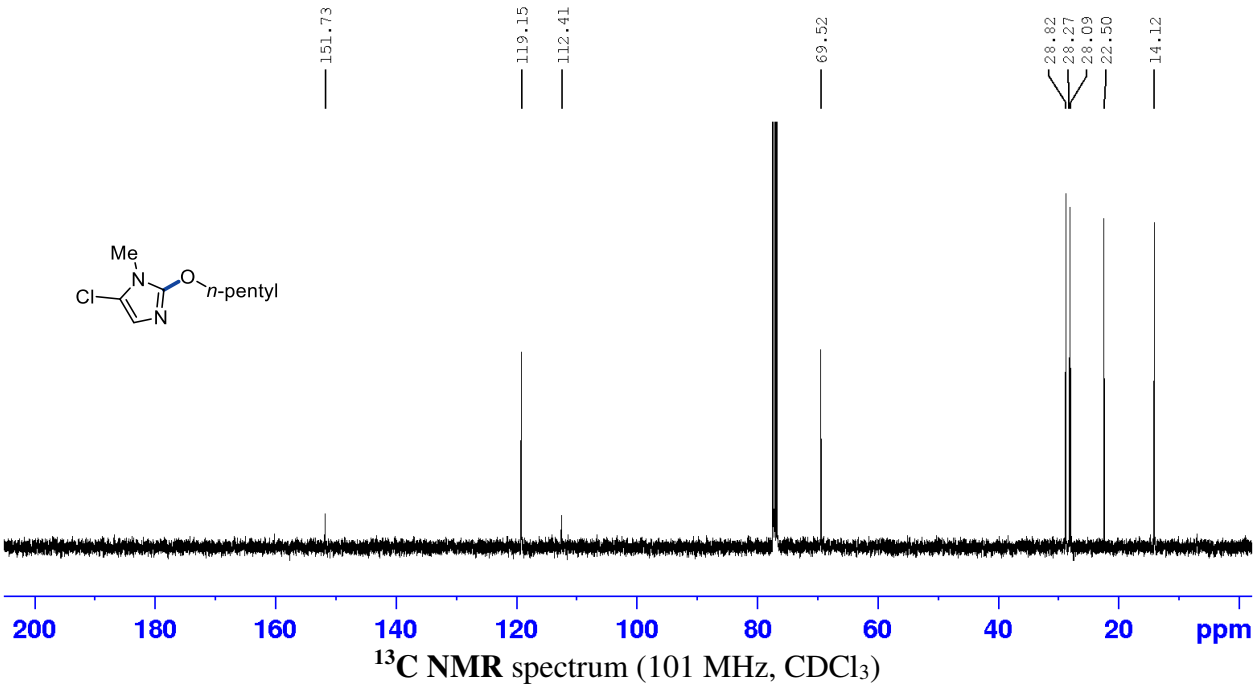

^{13}C NMR spectrum (101 MHz, $CDCl_3$)

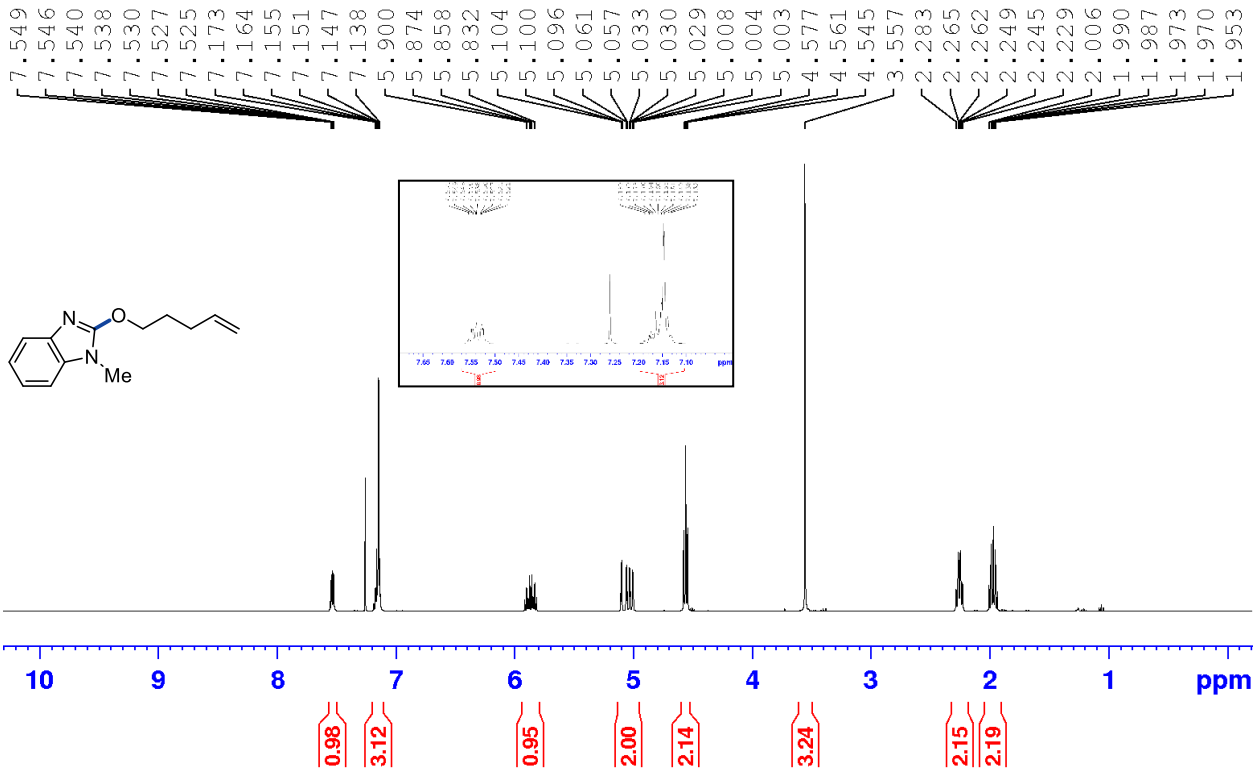

^{1}H NMR spectrum (400 MHz, $CDCl_3$)

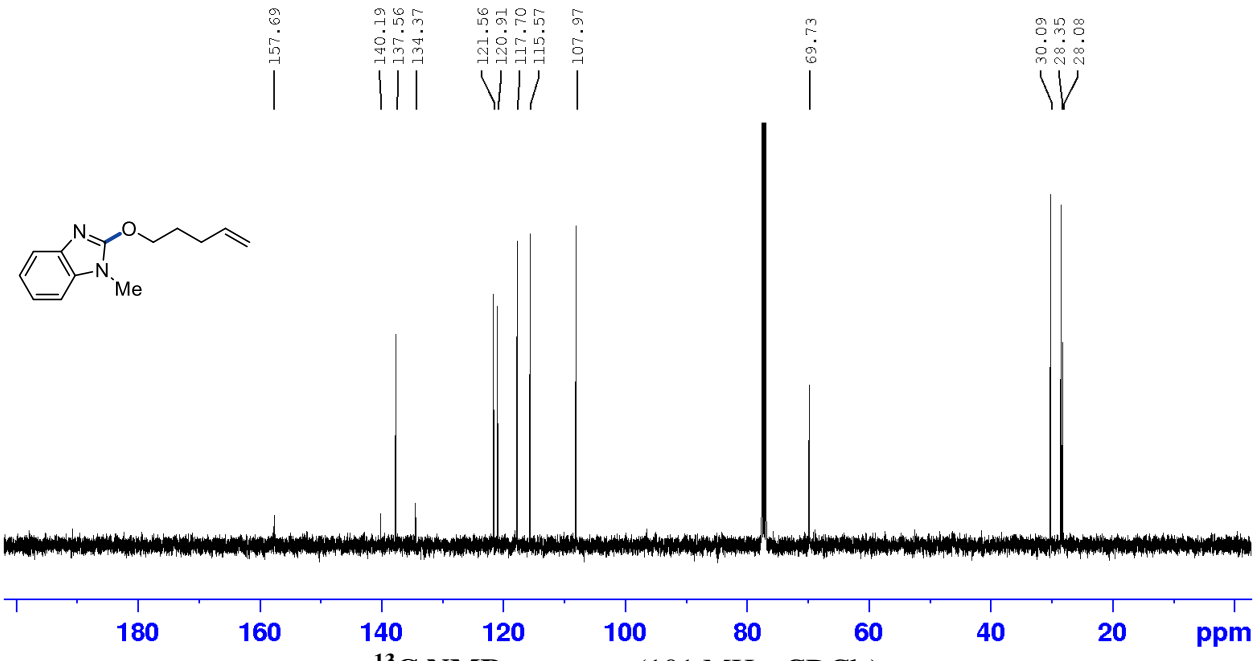

^{13}C NMR spectrum (101 MHz, $CDCl_3$)

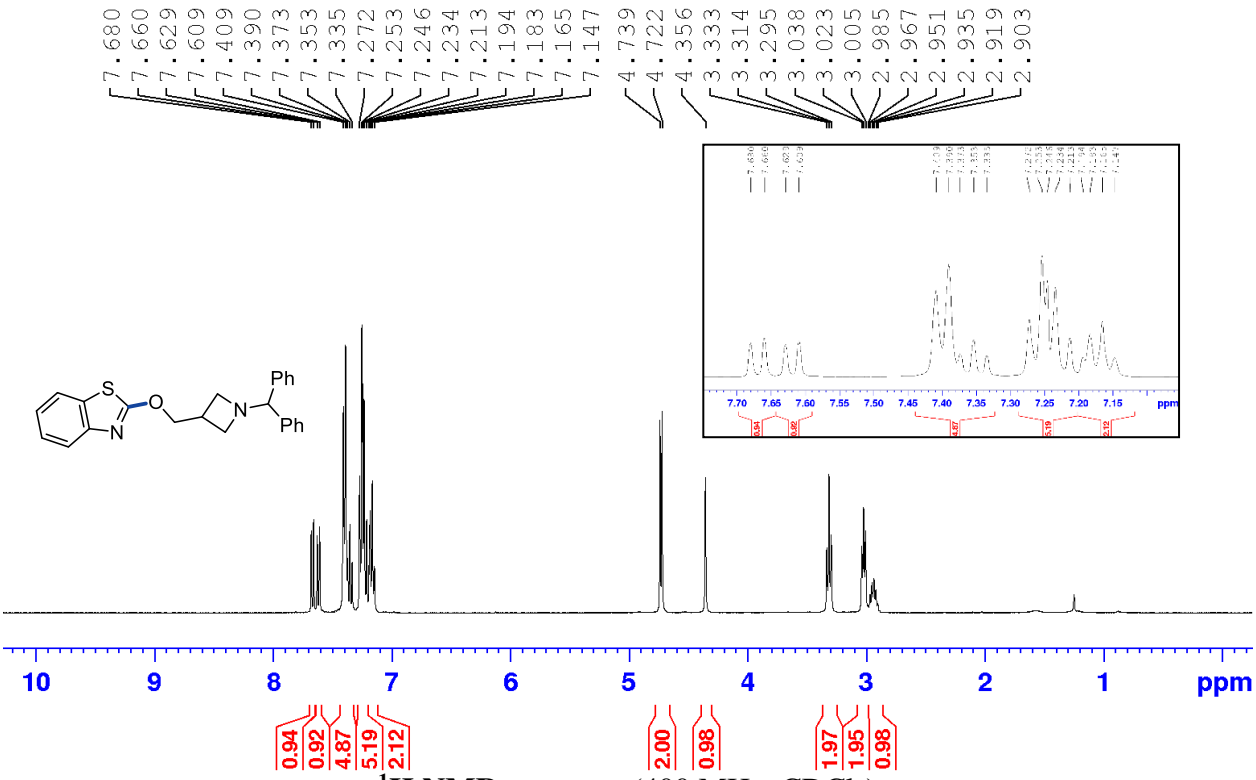

^{1}H NMR spectrum (400 MHz, $CDCl_3$)

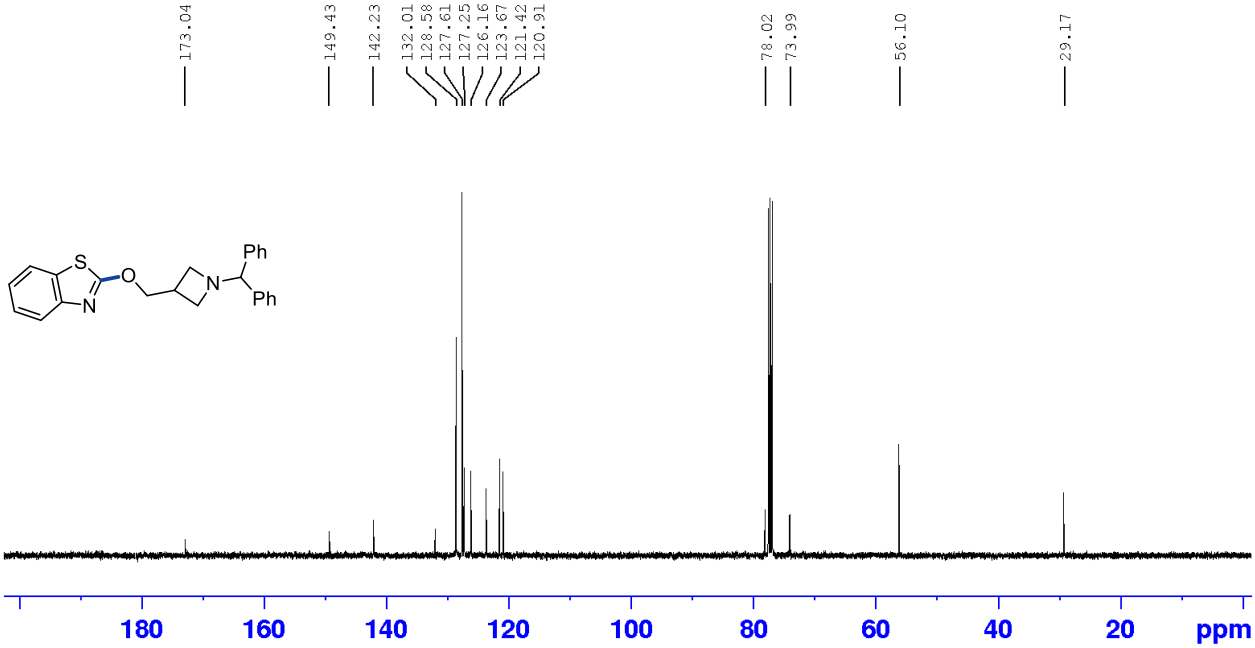

^{13}C NMR spectrum (101 MHz, $CDCl_3$)

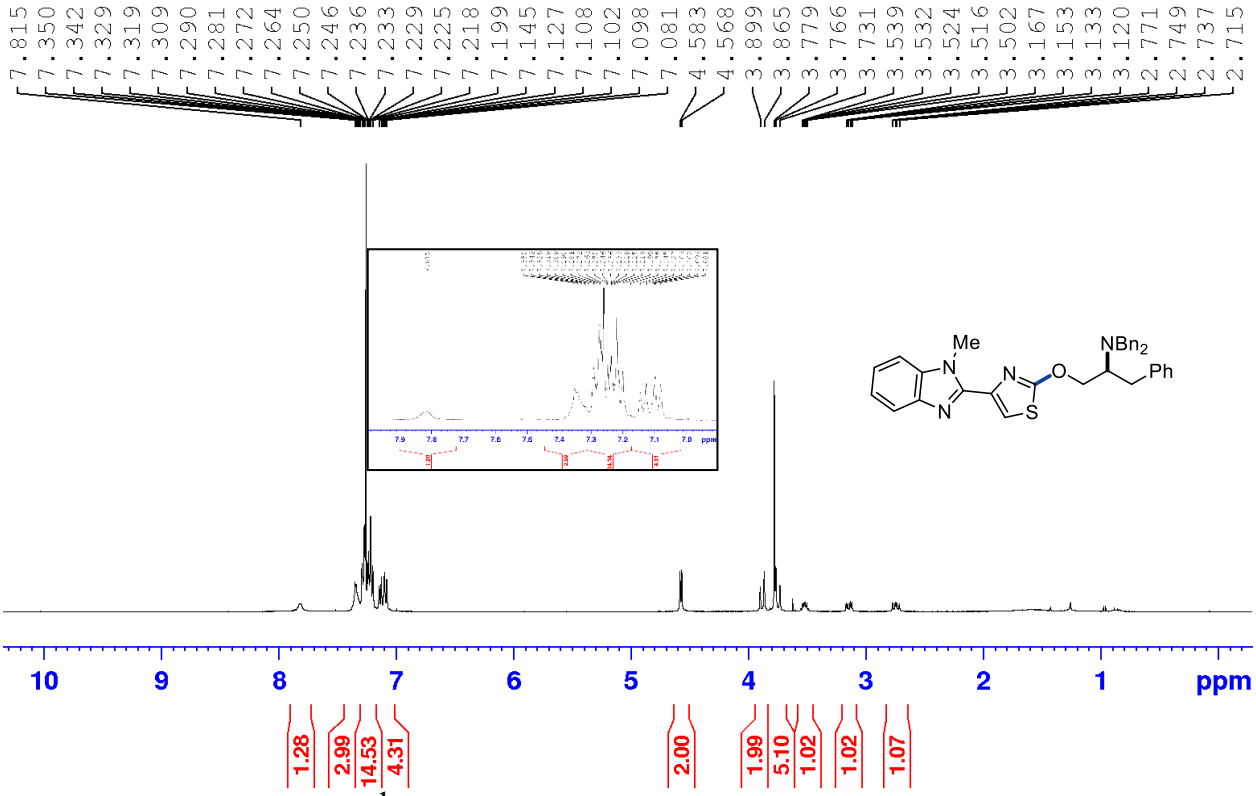

^{1}H NMR spectrum (400 MHz, $CDCl_3$)

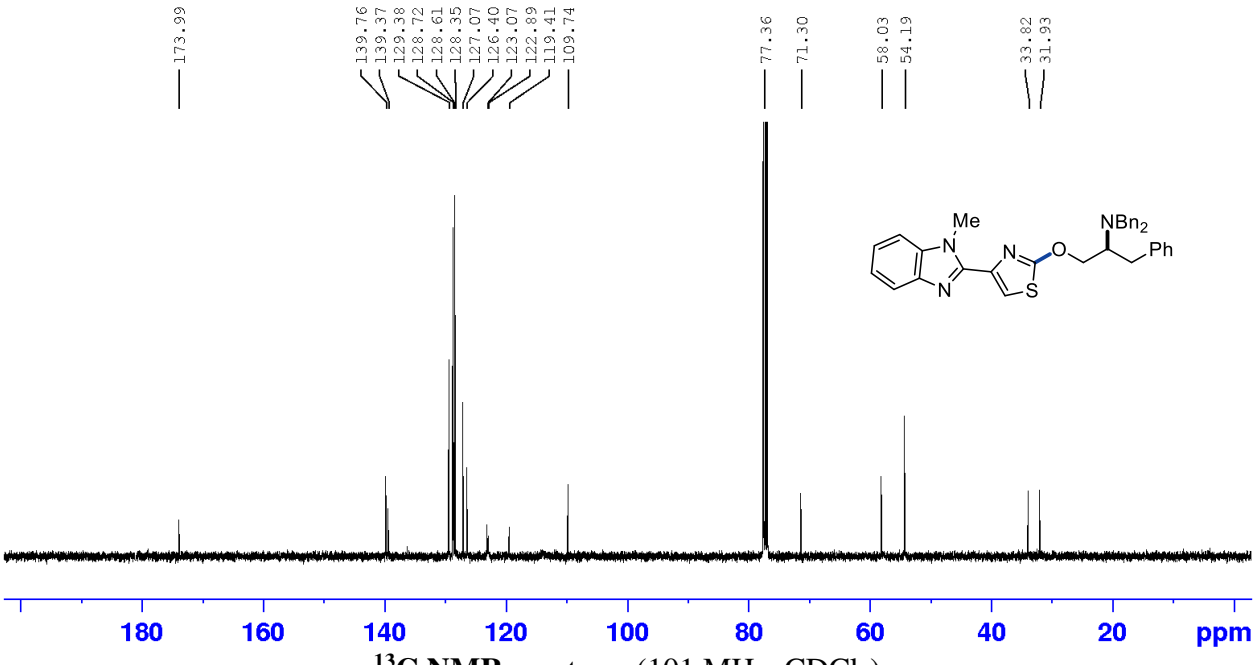

^{13}C NMR spectrum (101 MHz, $CDCl_3$)

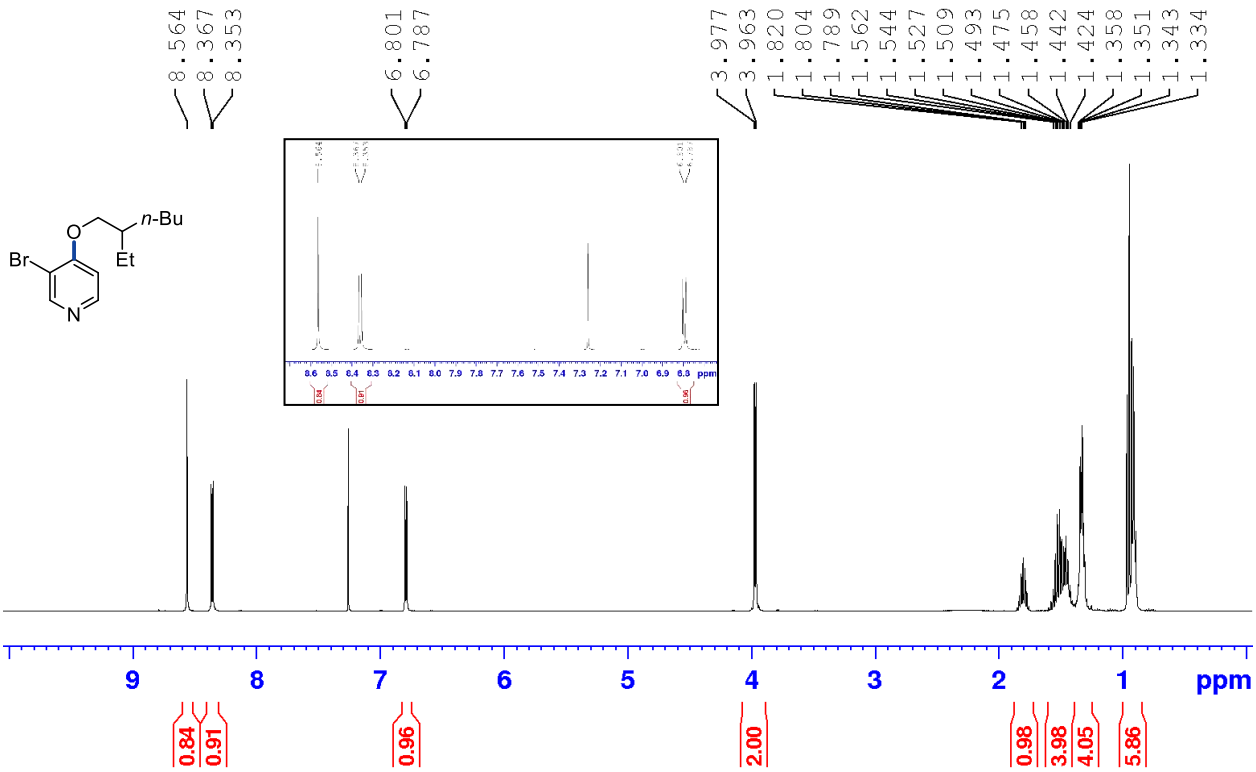

^{1}H NMR spectrum (400 MHz, $CDCl_3$)

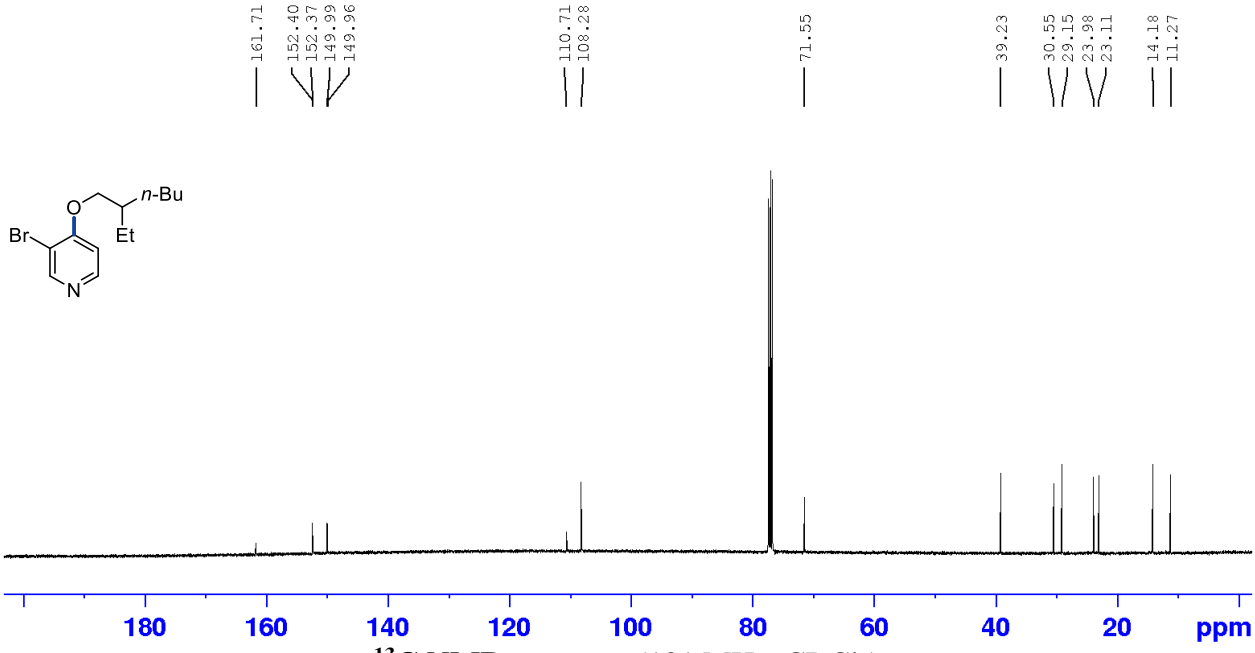

^{13}C NMR spectrum (101 MHz, $CDCl_3$)

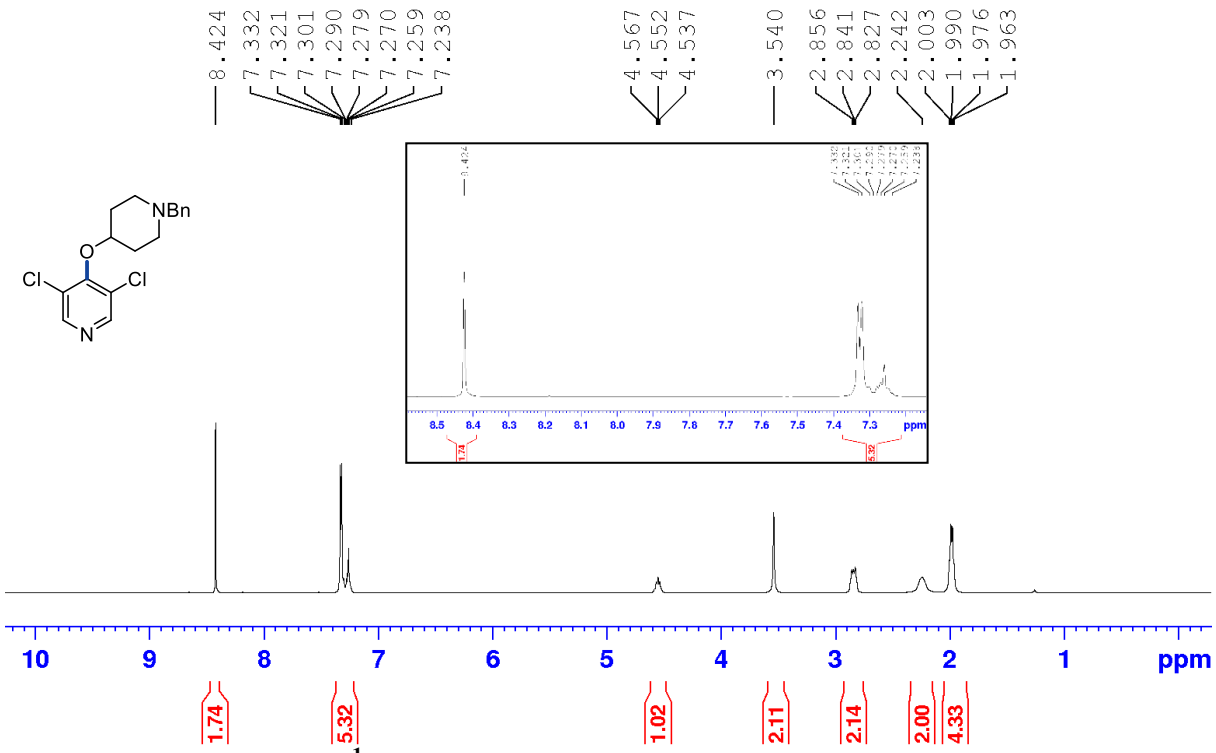

^{1}H NMR spectrum (400 MHz, $CDCl_3$)

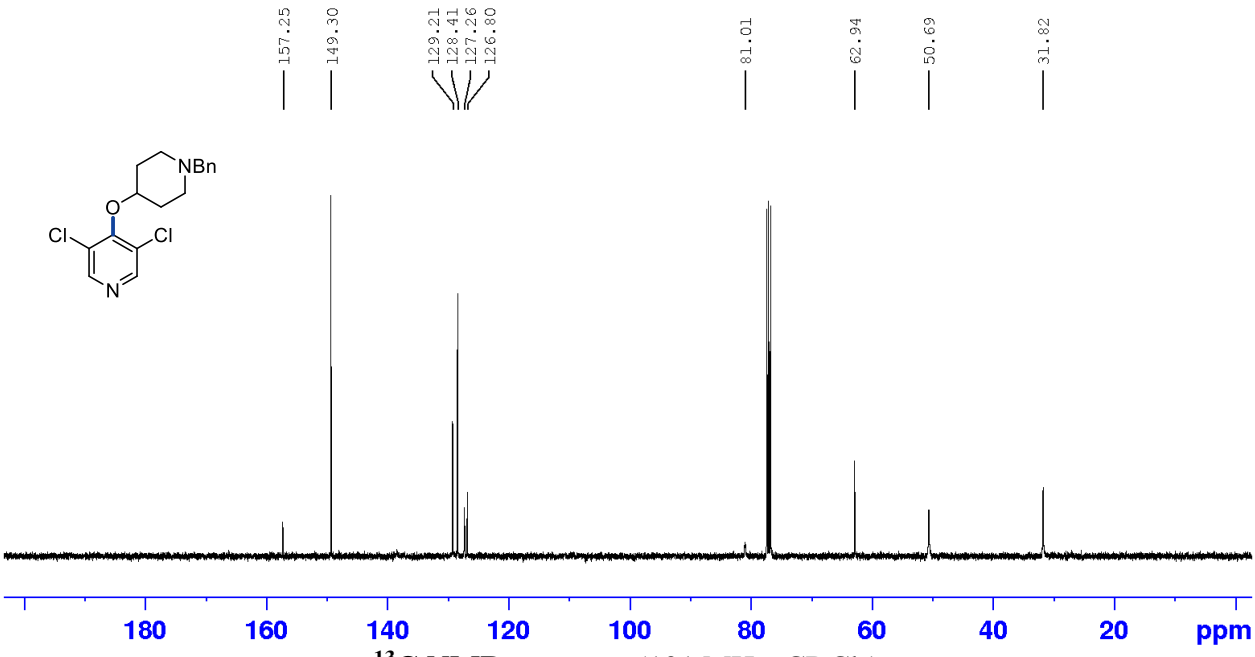

^{13}C NMR spectrum (101 MHz, $CDCl_3$)

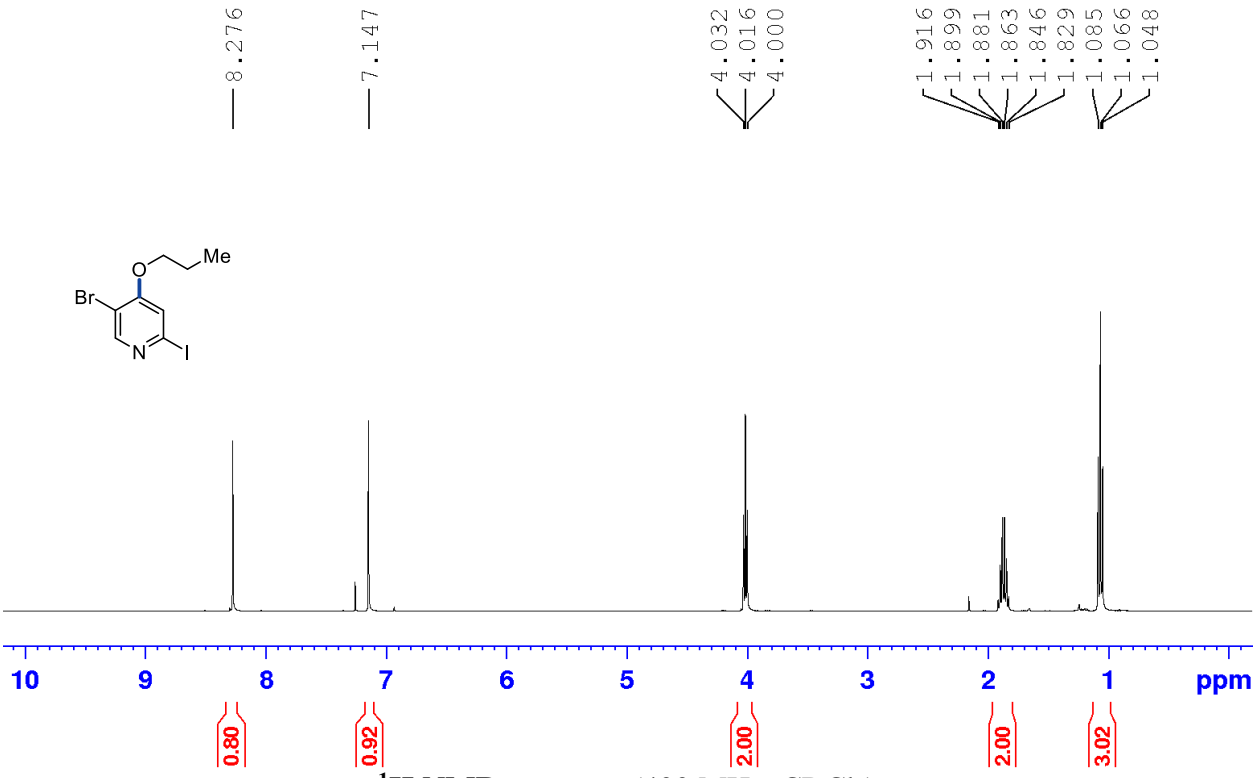

^{1}H NMR spectrum (400 MHz, $CDCl_3$)

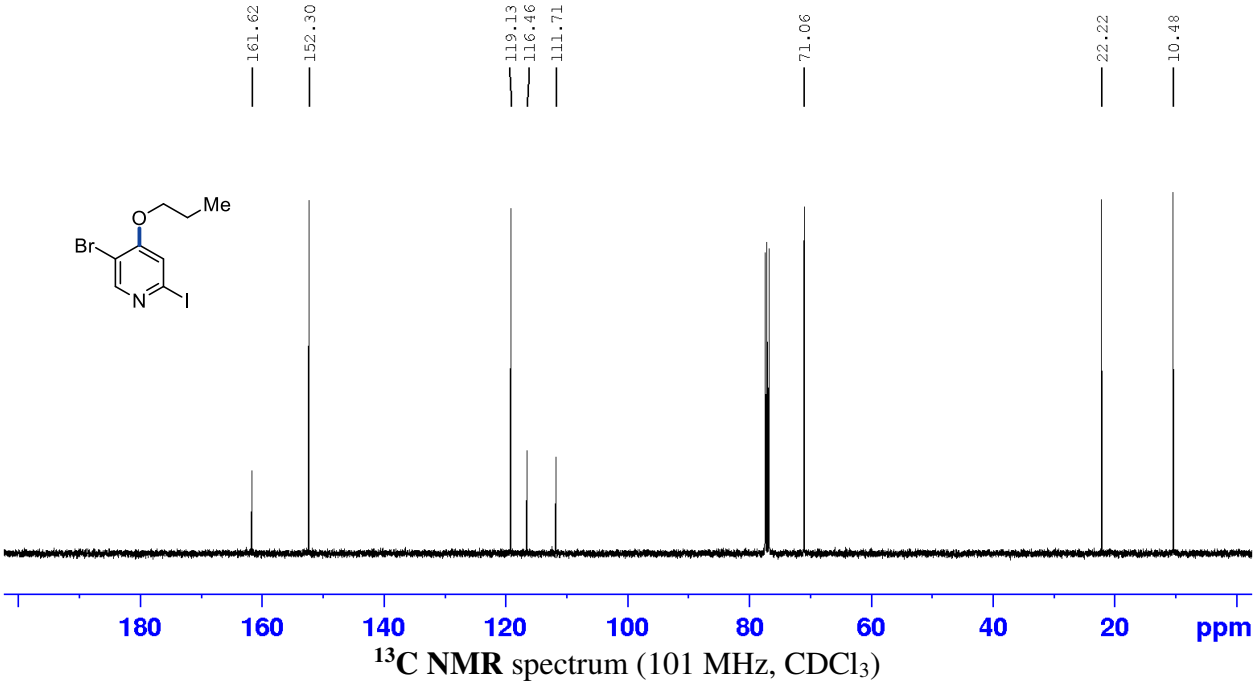

^{13}C NMR spectrum (101 MHz, $CDCl_3$)

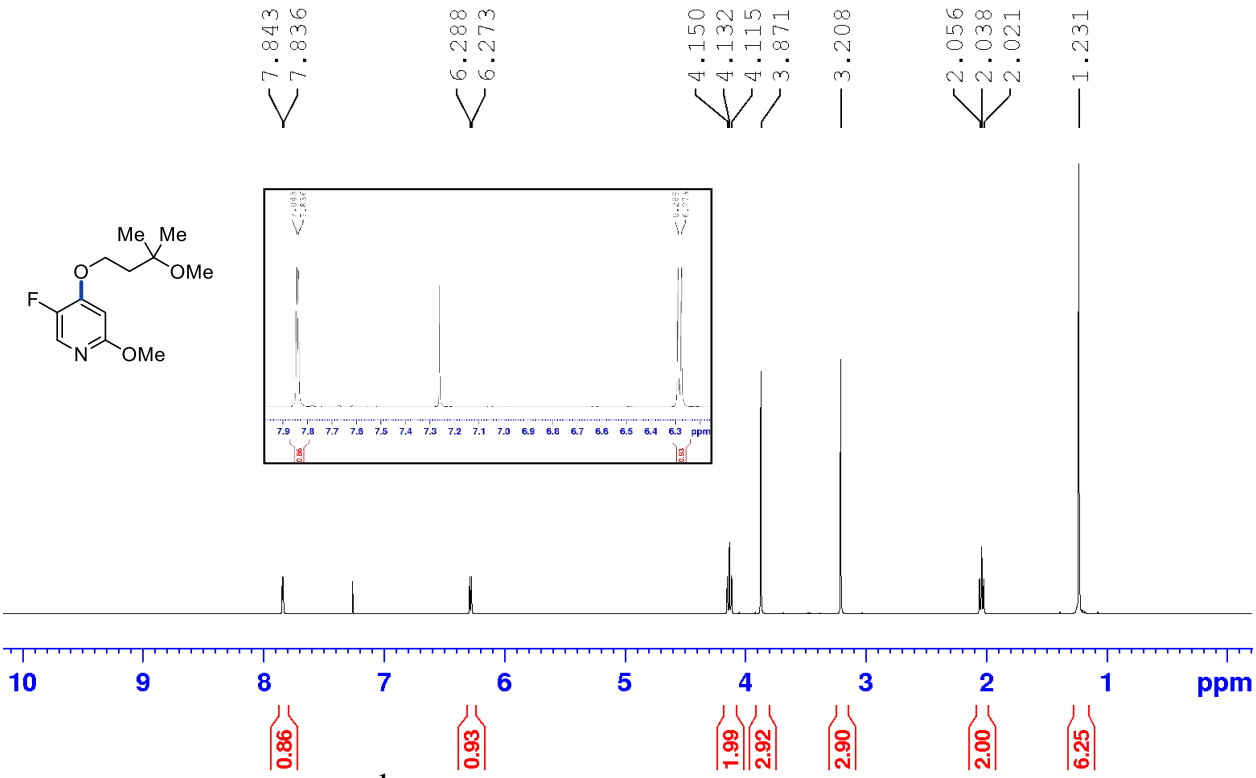

^{1}H NMR spectrum (400 MHz, $CDCl_3$)

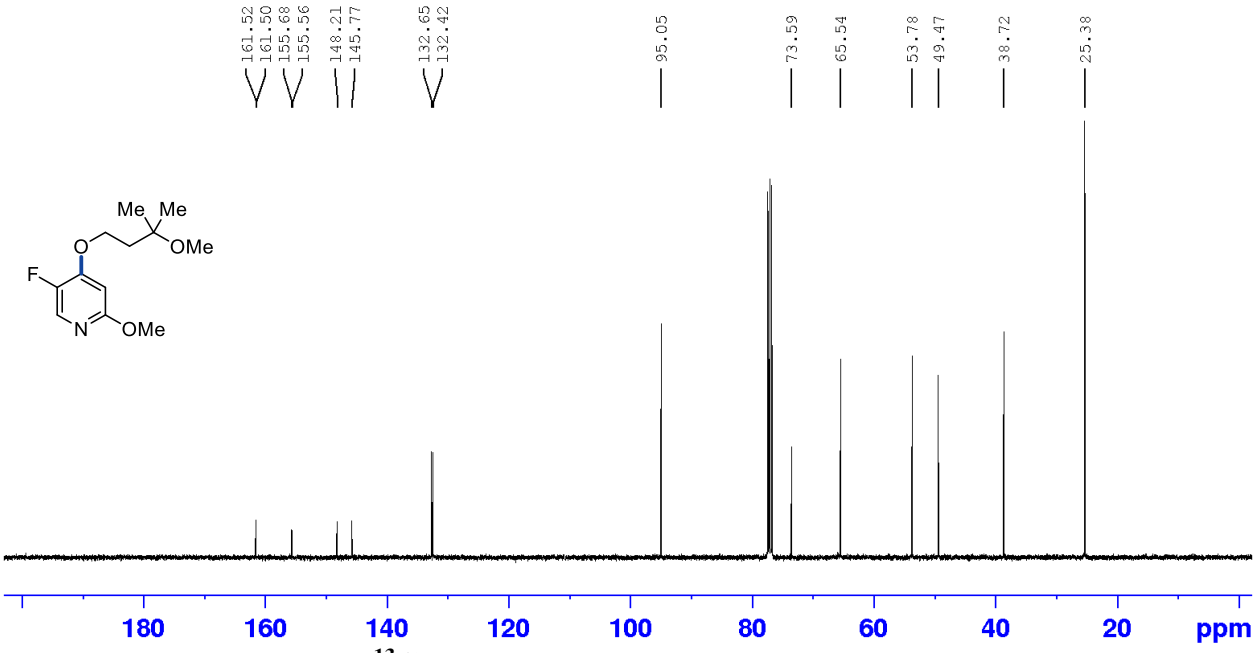

^{13}C NMR spectrum (101 MHz, $CDCl_3$)

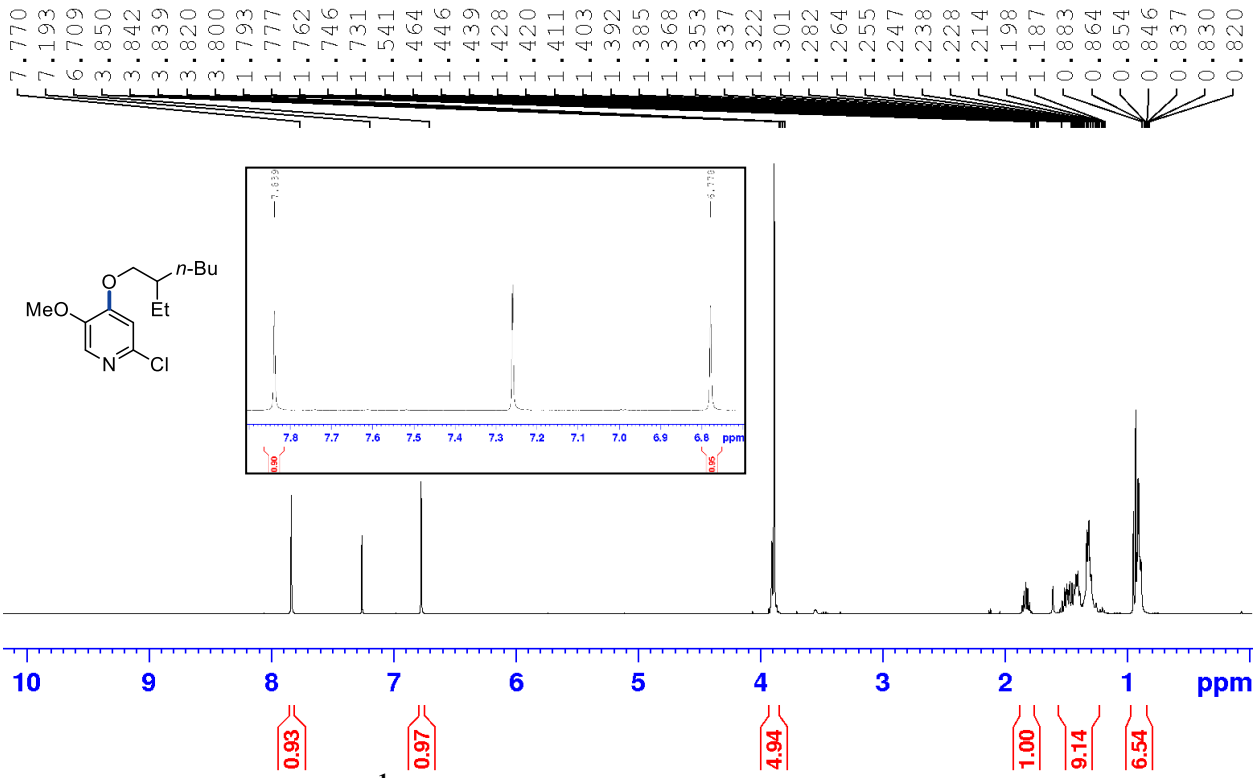

^{1}H NMR spectrum (400 MHz, $CDCl_3$)

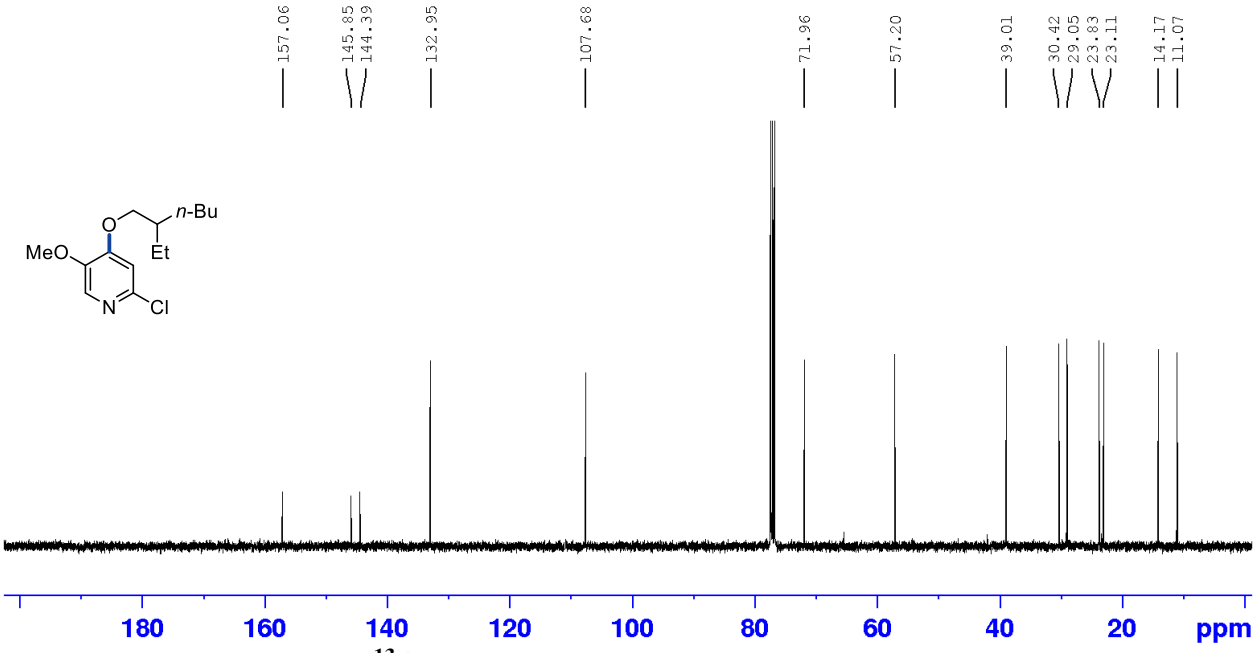

^{13}C NMR spectrum (101 MHz, $CDCl_3$)

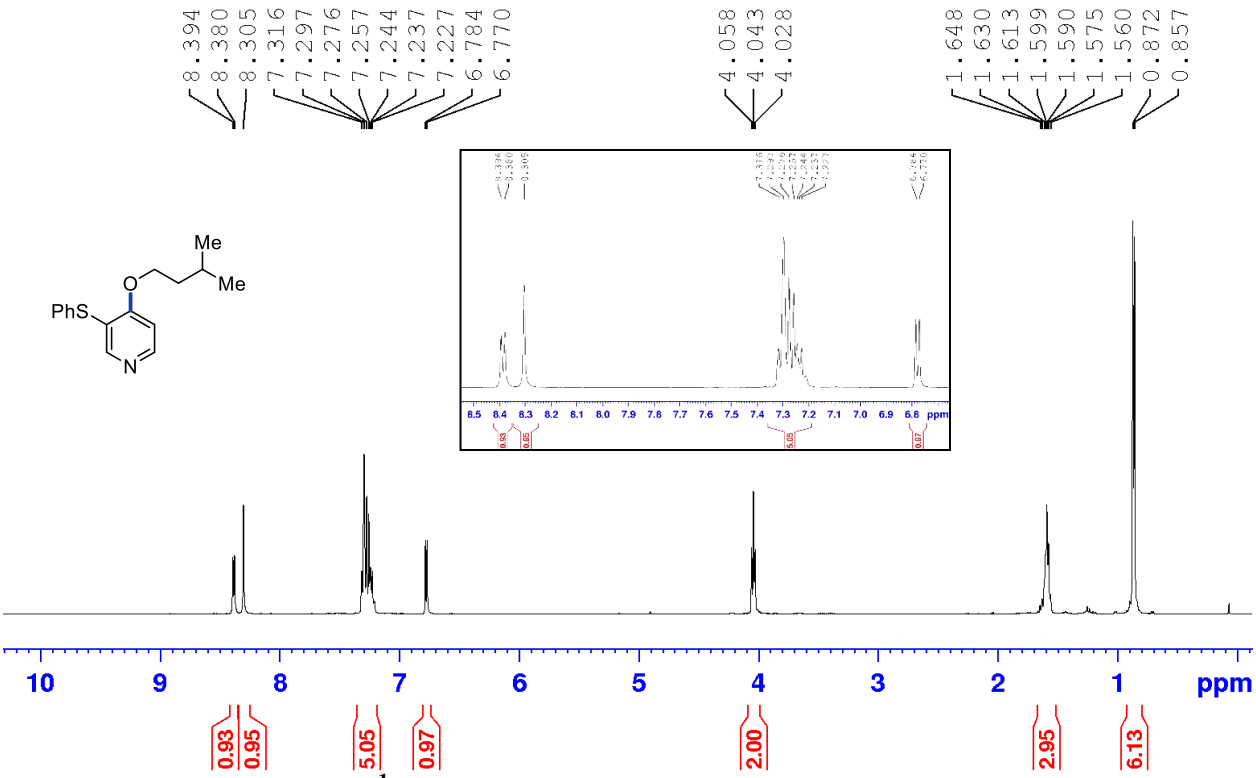

^{1}H NMR spectrum (400 MHz, $CDCl_3$)

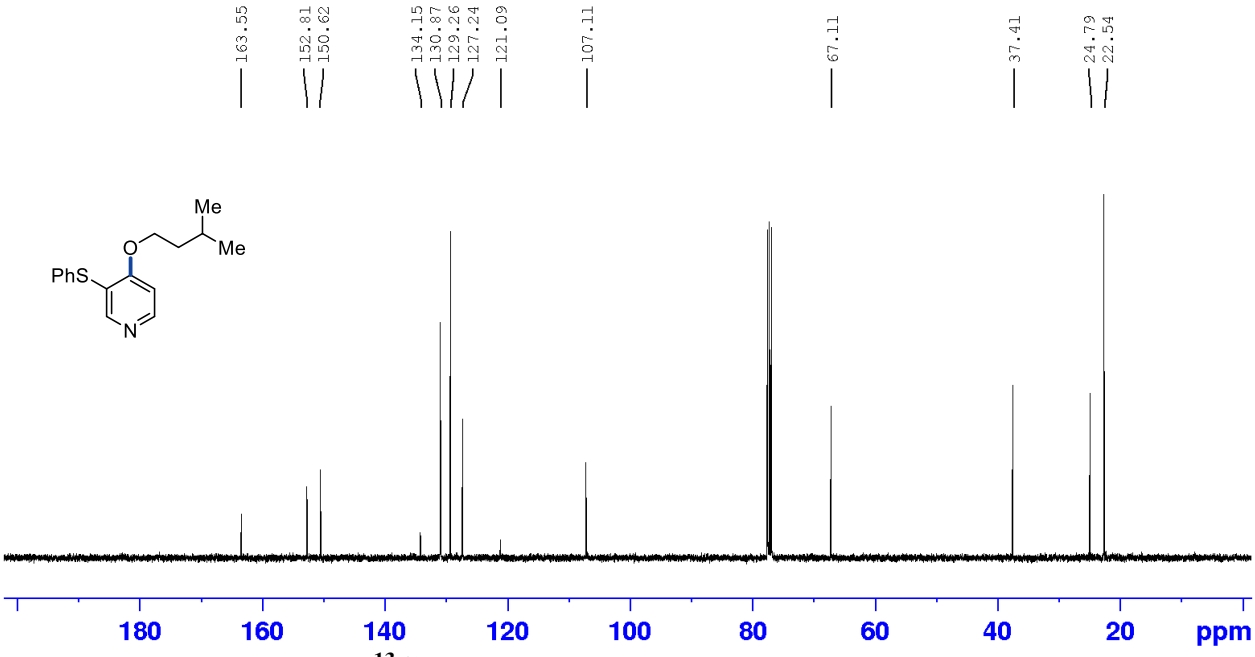

^{13}C NMR spectrum (101 MHz, $CDCl_3$)

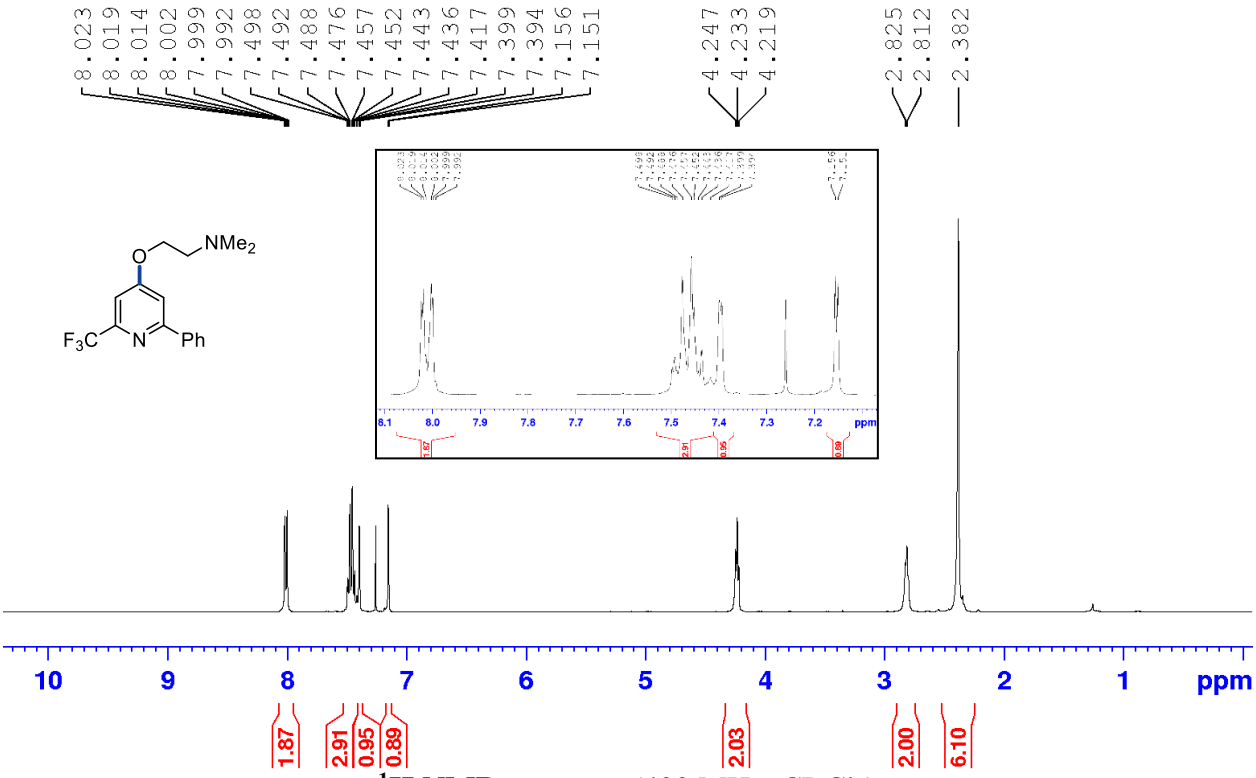

^{1}H NMR spectrum (400 MHz, $CDCl_3$)

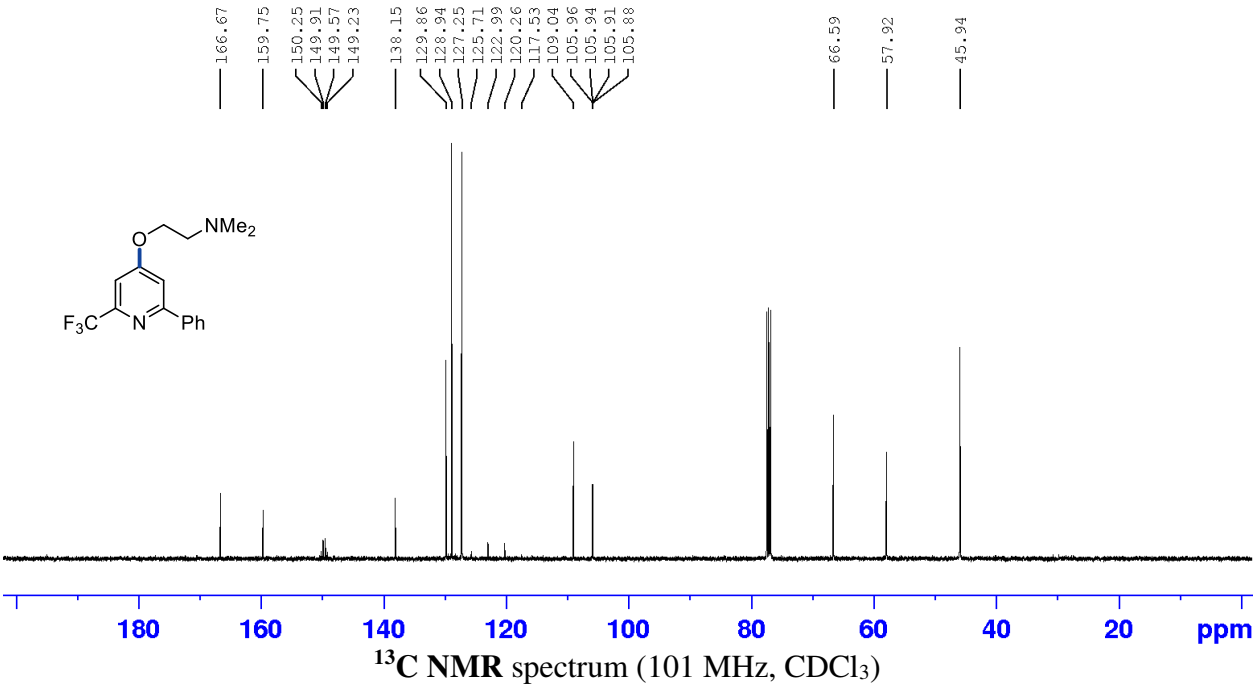

^{13}C NMR spectrum (101 MHz, $CDCl_3$)

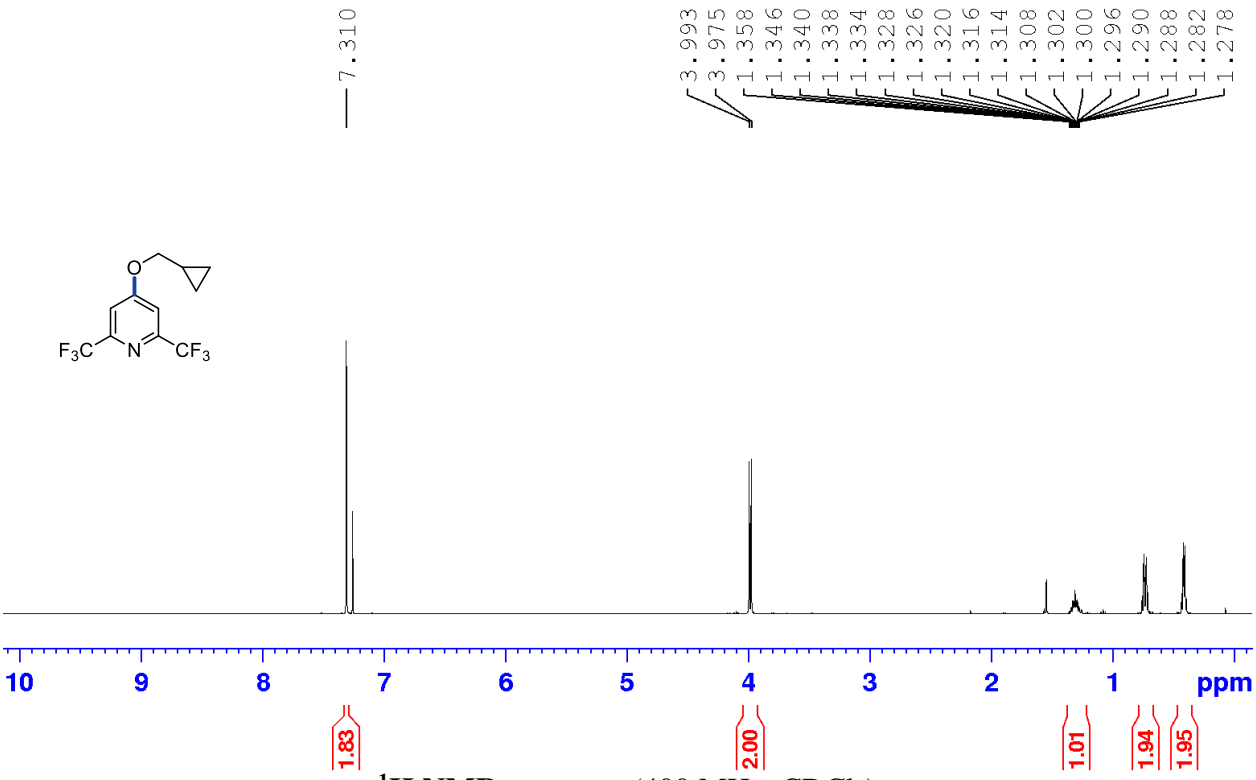

^{1}H NMR spectrum (400 MHz, $CDCl_3$)

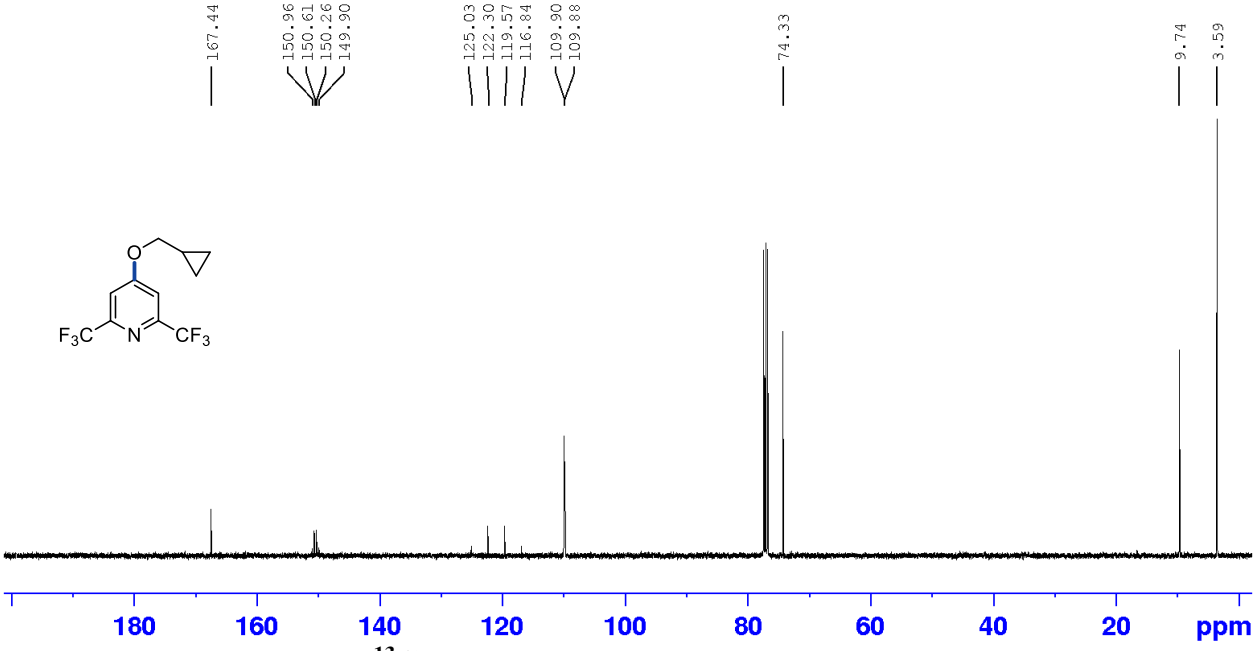

^{13}C NMR spectrum (101 MHz, $CDCl_3$)

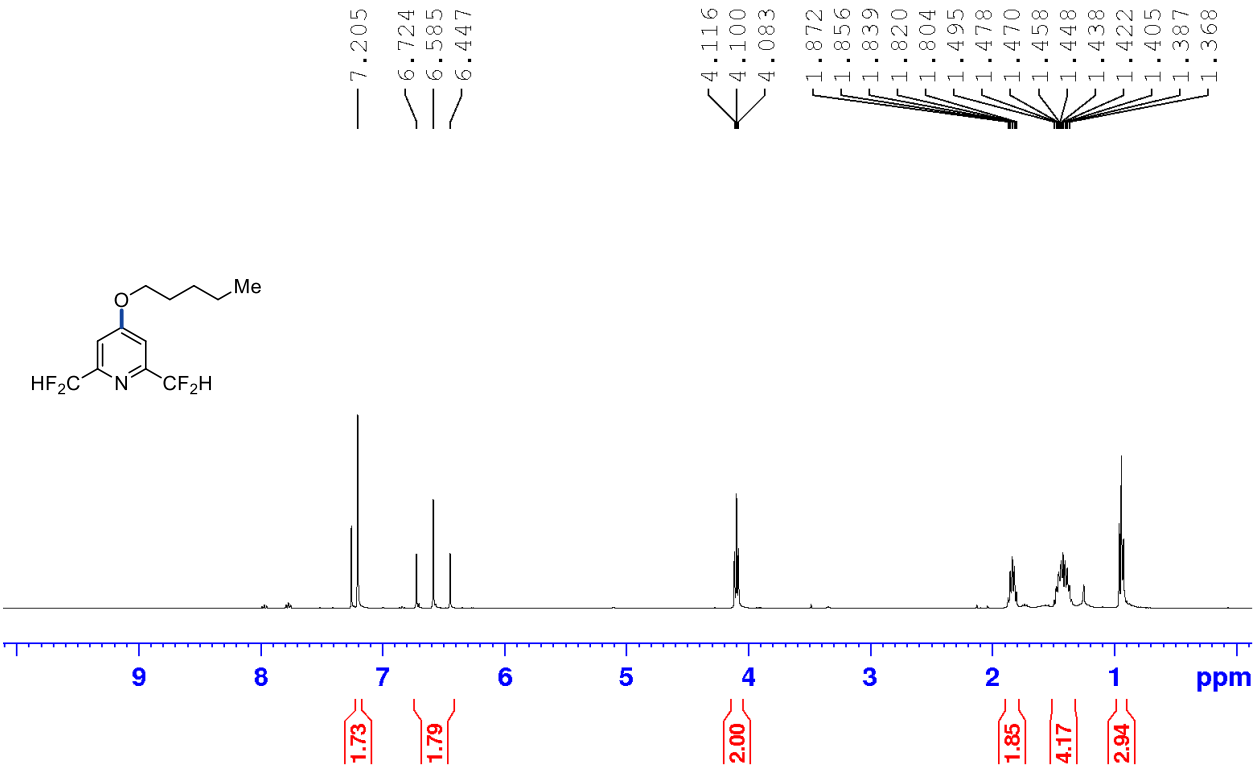

^{1}H NMR spectrum (400 MHz, $CDCl_3$)

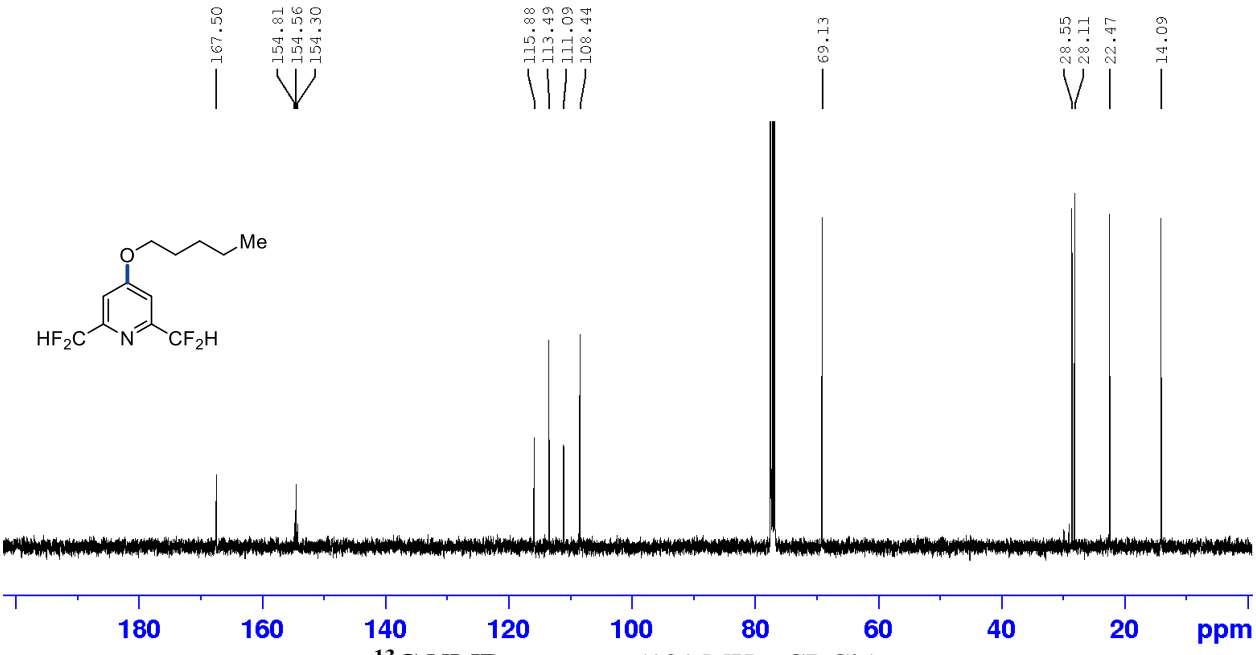

^{13}C NMR spectrum (101 MHz, $CDCl_3$)

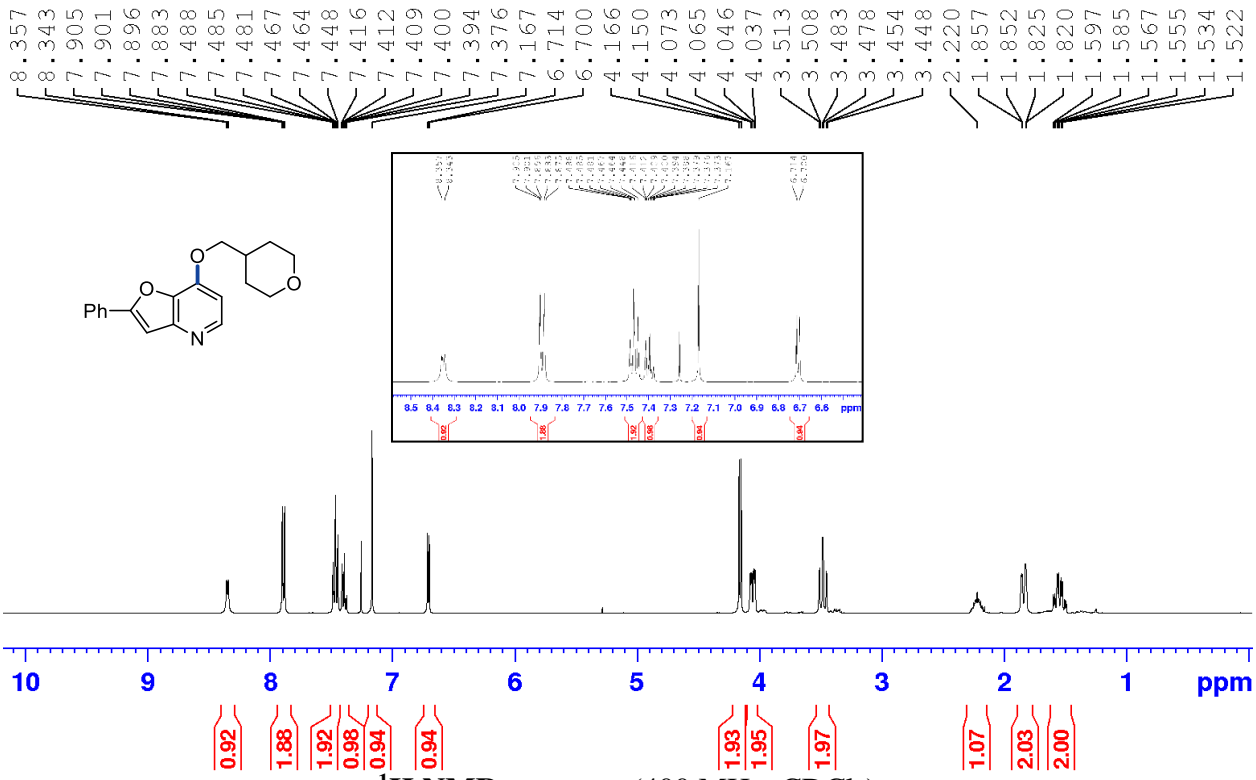

^{1}H NMR spectrum (400 MHz, $CDCl_3$)

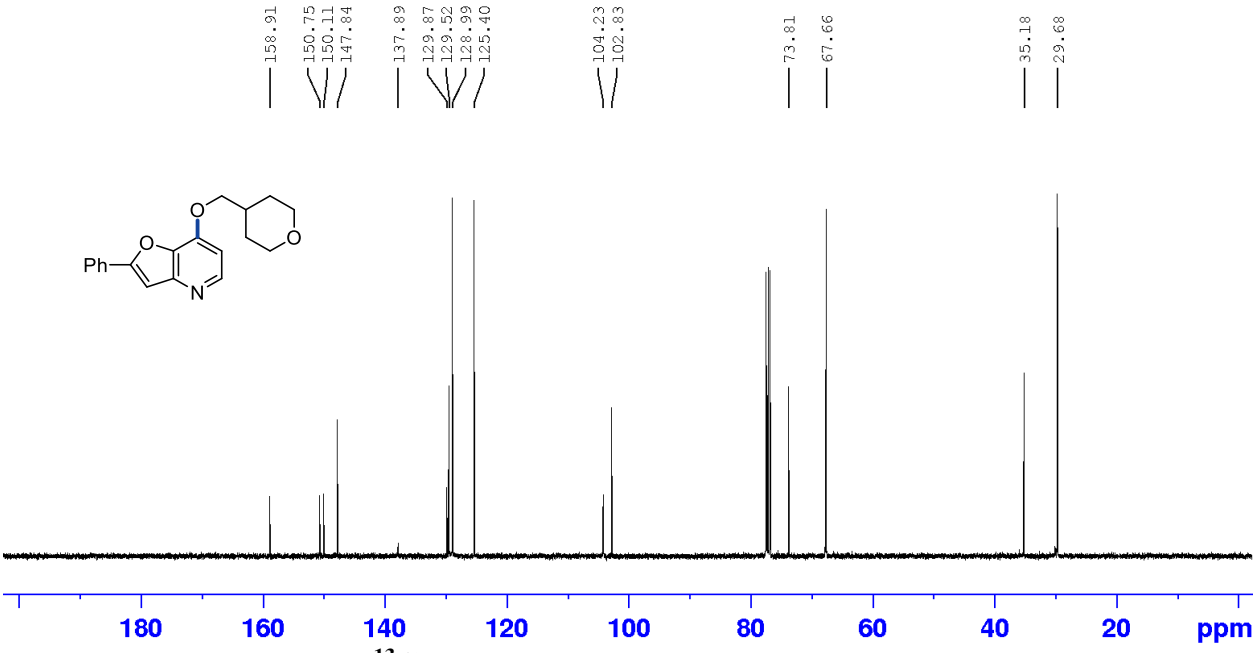

^{13}C NMR spectrum (101 MHz, $CDCl_3$)

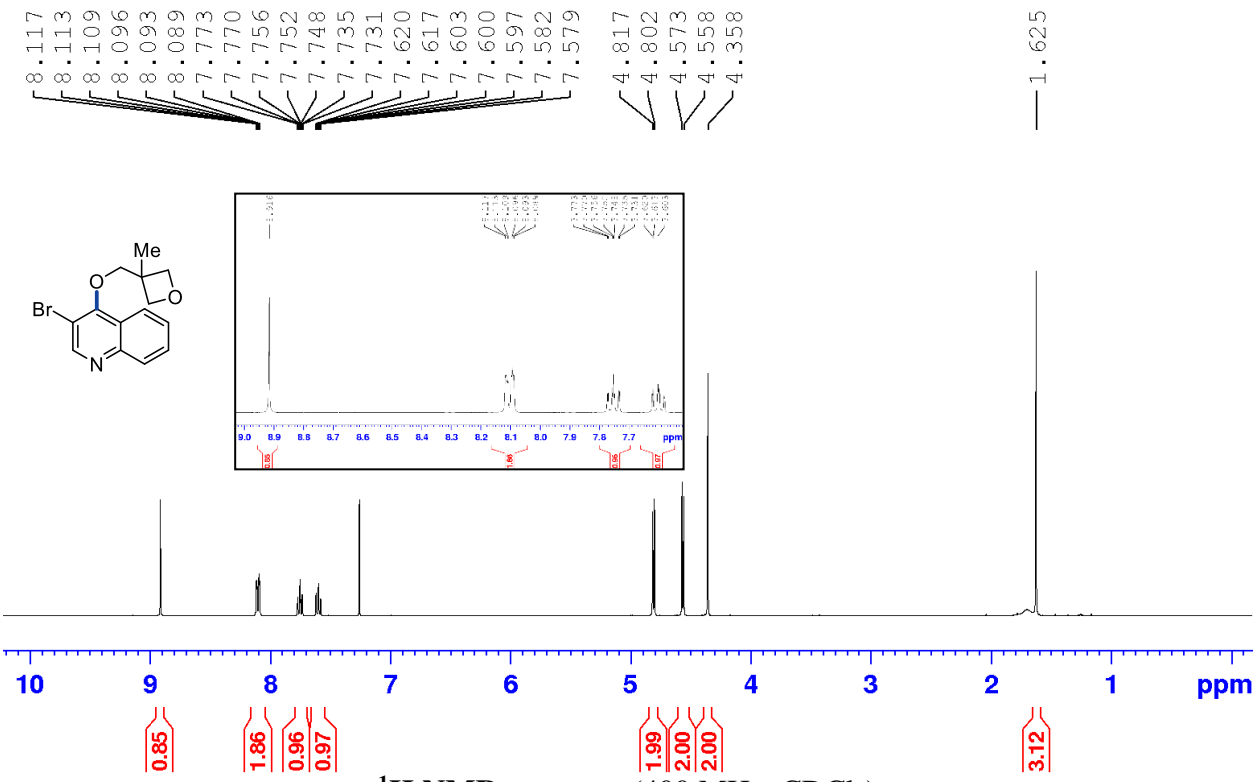

^{1}H NMR spectrum (400 MHz, $CDCl_3$)

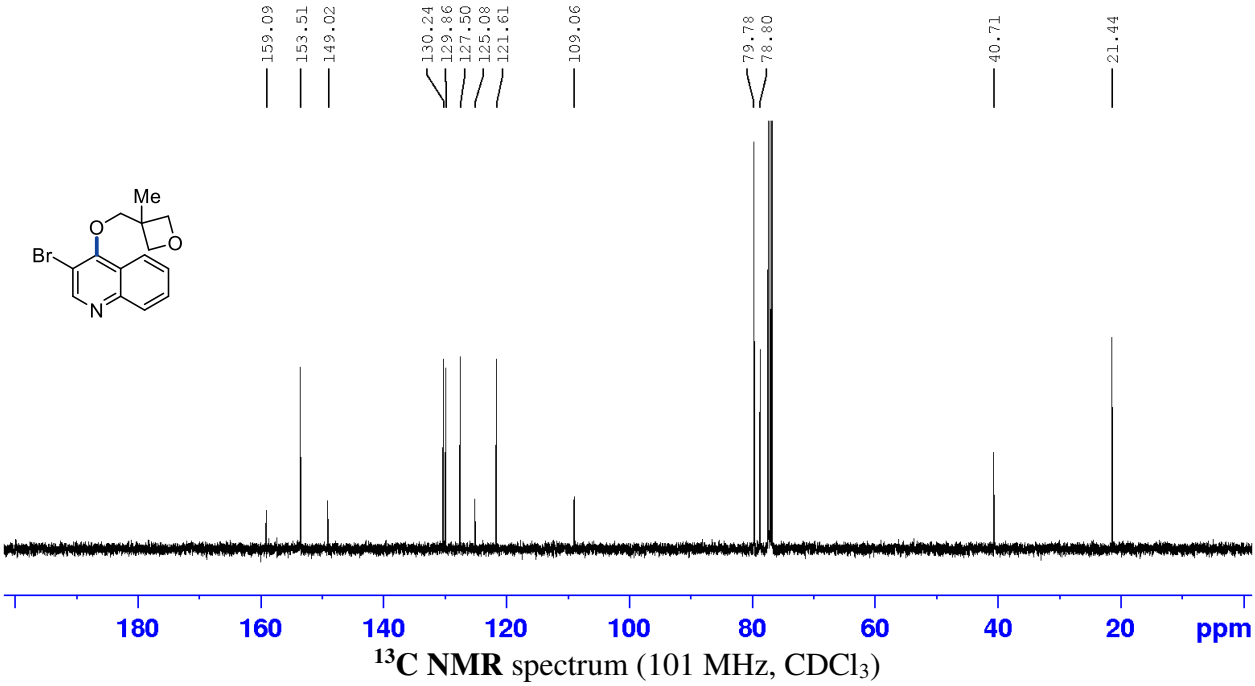

^{13}C NMR spectrum (101 MHz, $CDCl_3$)

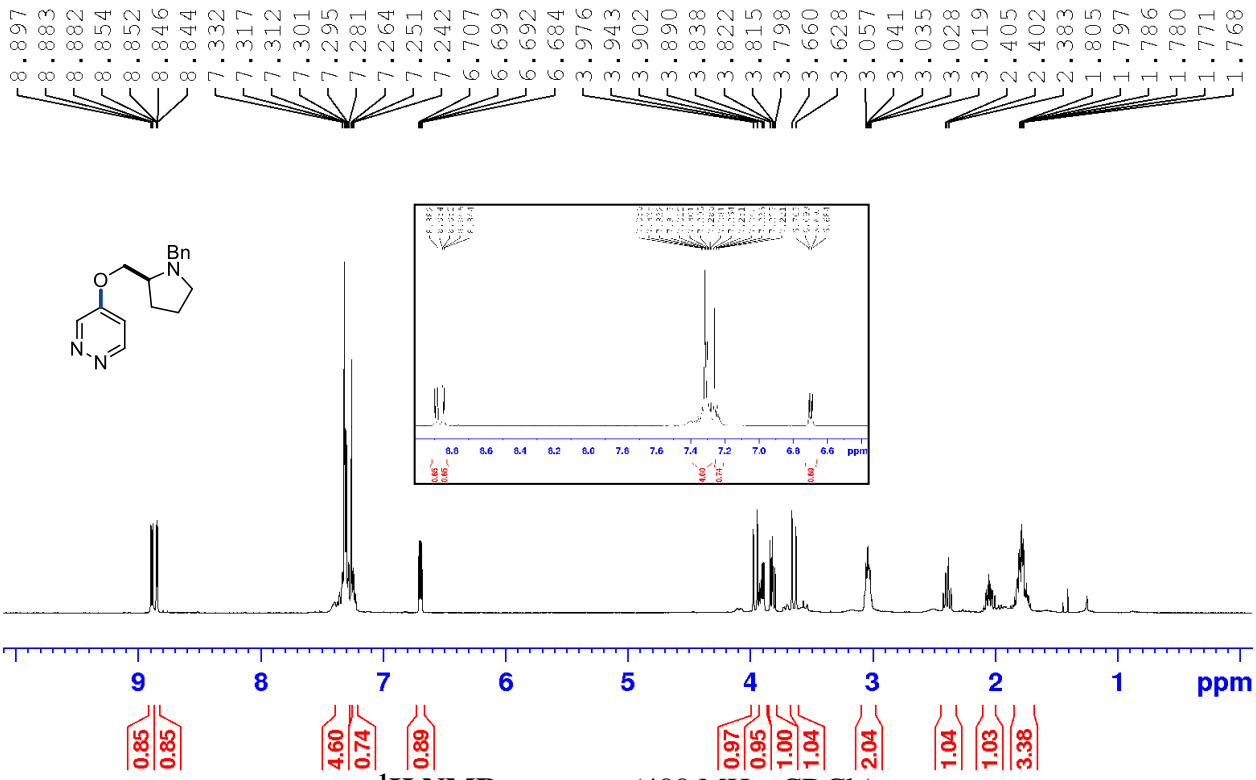

^{1}H NMR spectrum (400 MHz, $CDCl_3$)

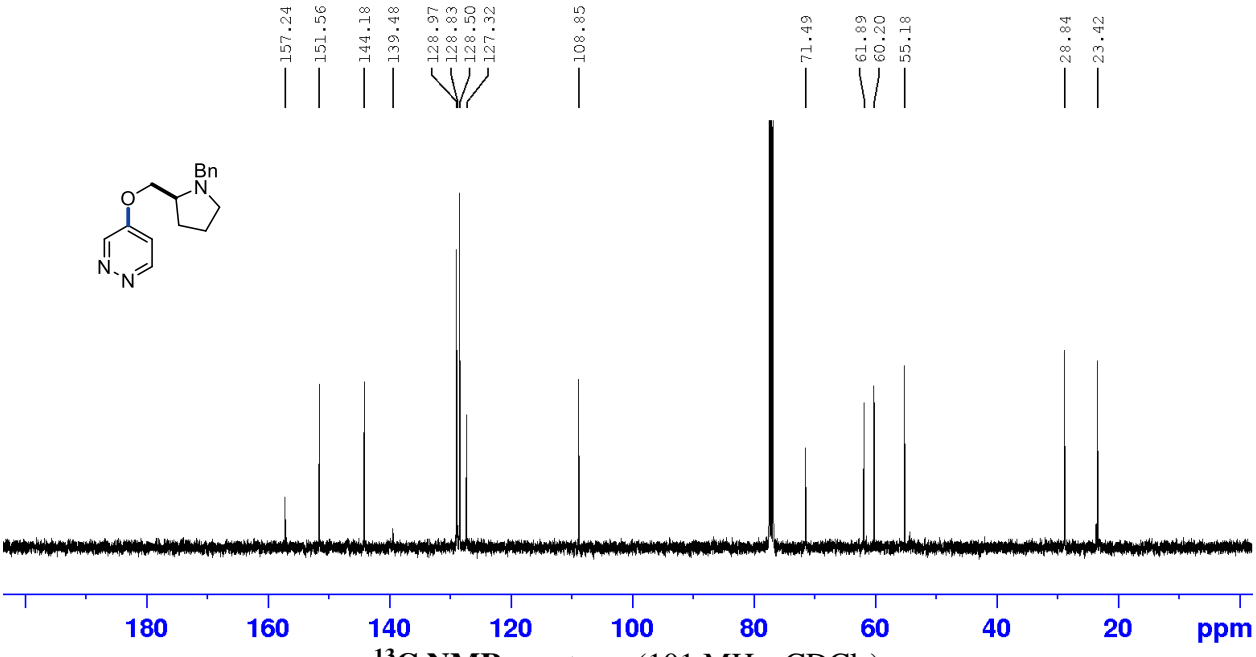

^{13}C NMR spectrum (101 MHz, $CDCl_3$)

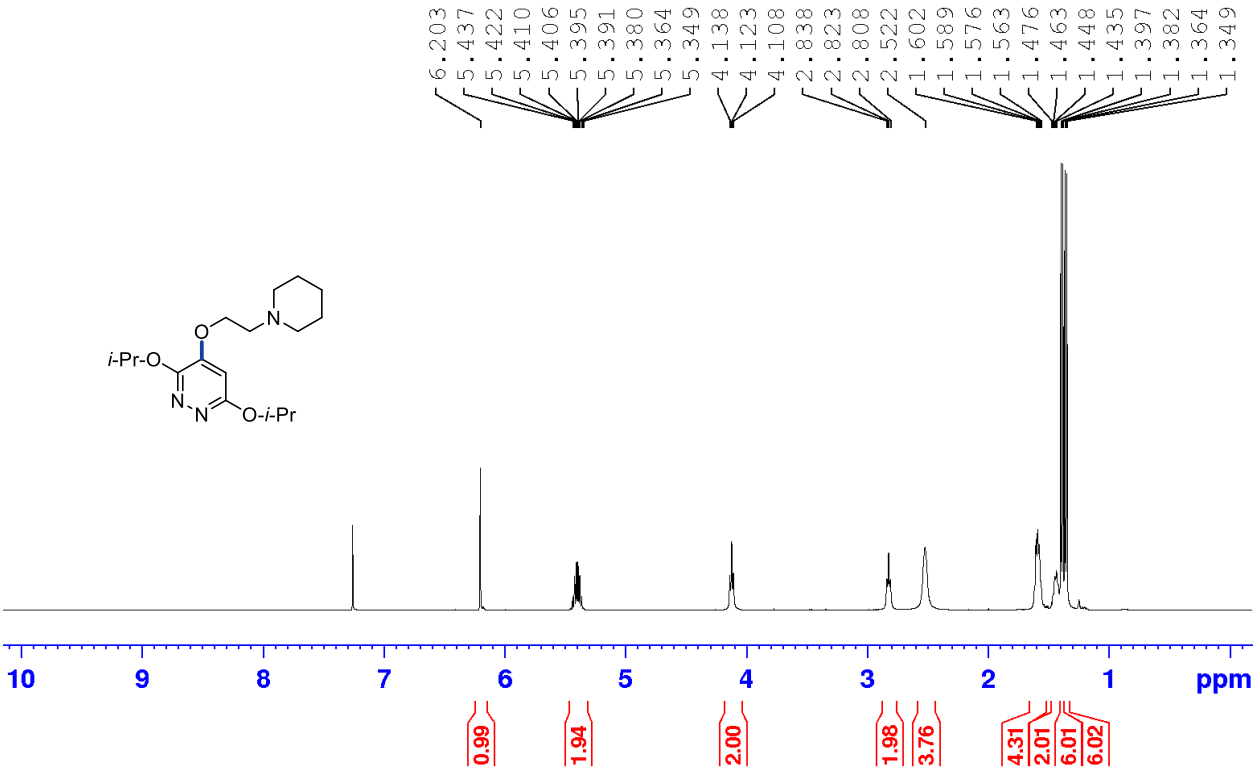

^{1}H NMR spectrum (400 MHz, $CDCl_3$)

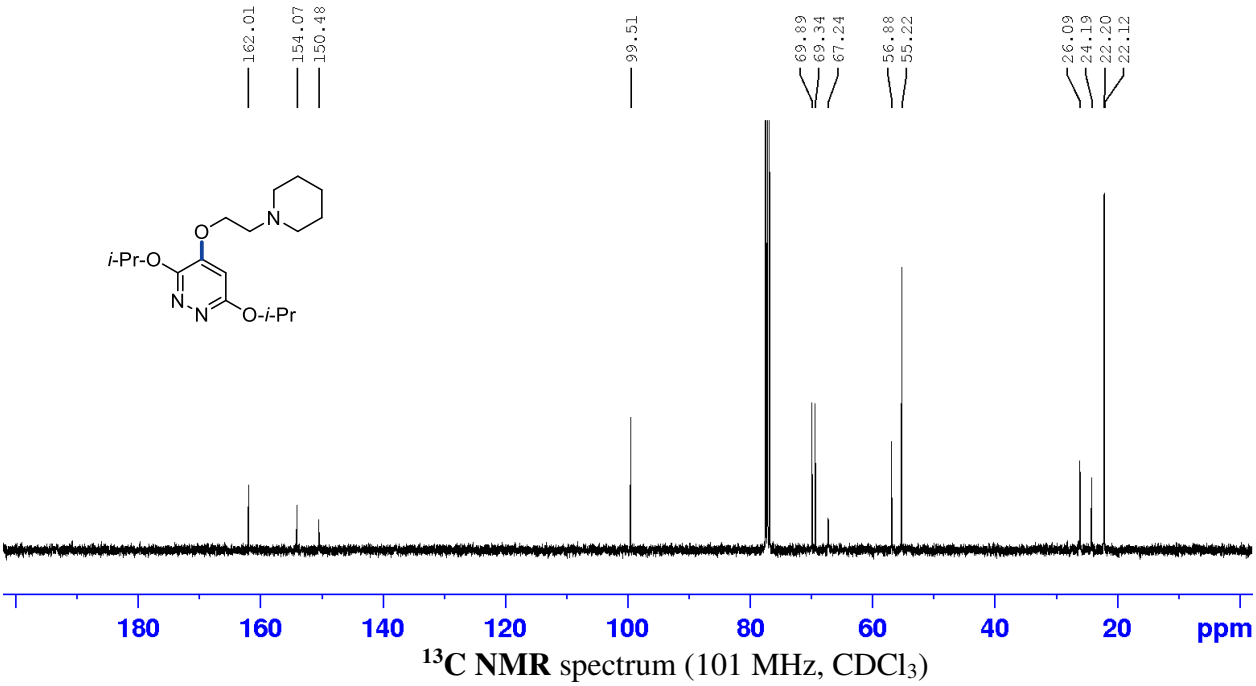

^{13}C NMR spectrum (101 MHz, $CDCl_3$)

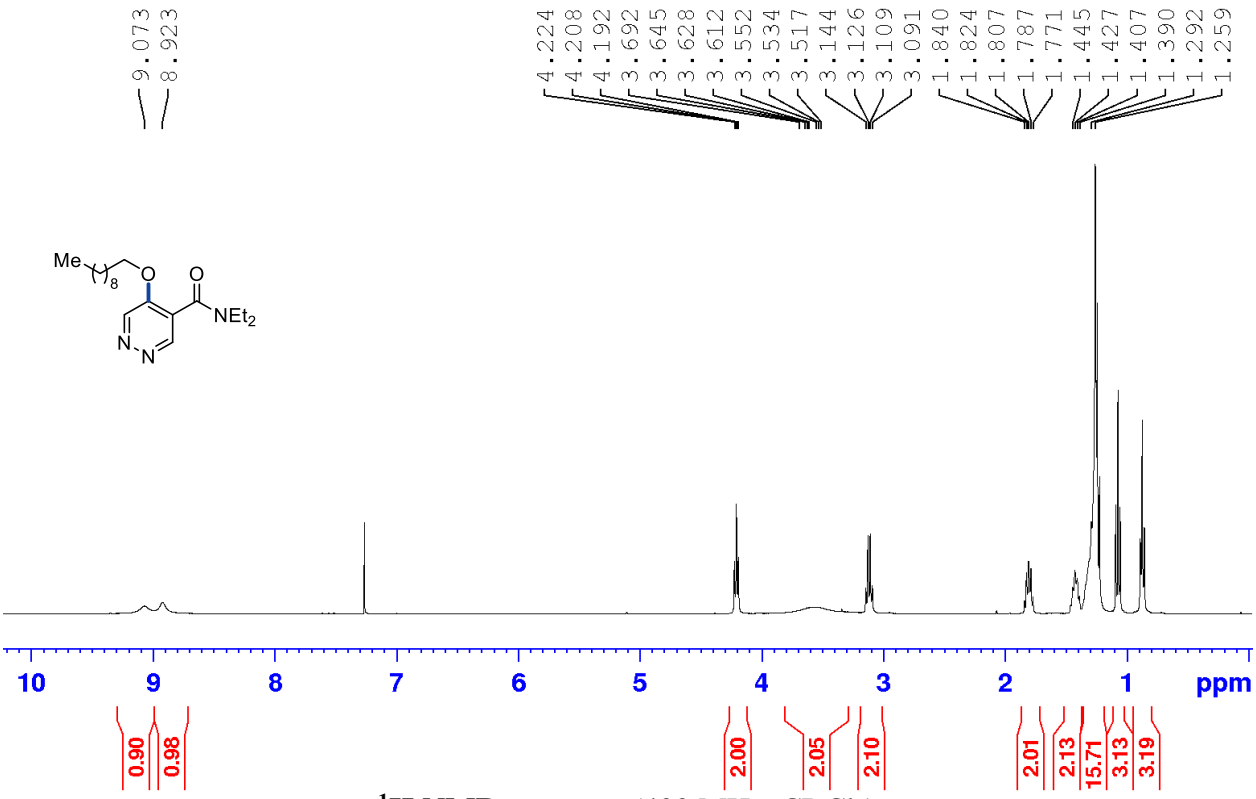

^{1}H NMR spectrum (400 MHz, $CDCl_3$)

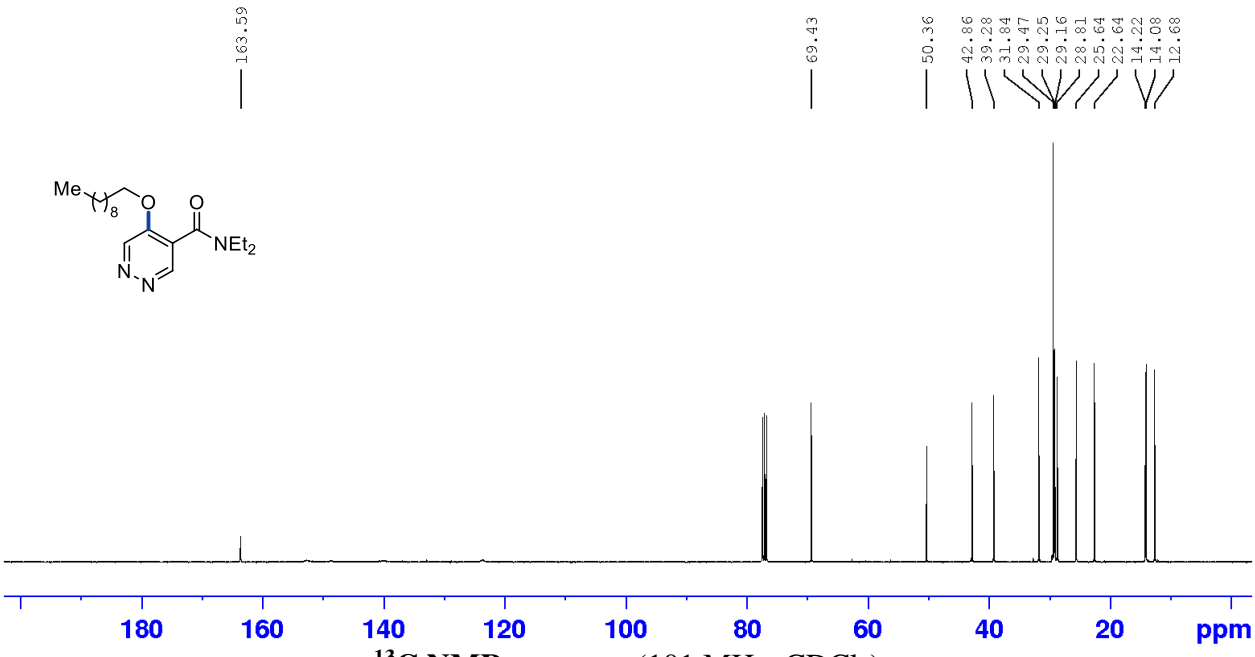

^{13}C NMR spectrum (101 MHz, $CDCl_3$)

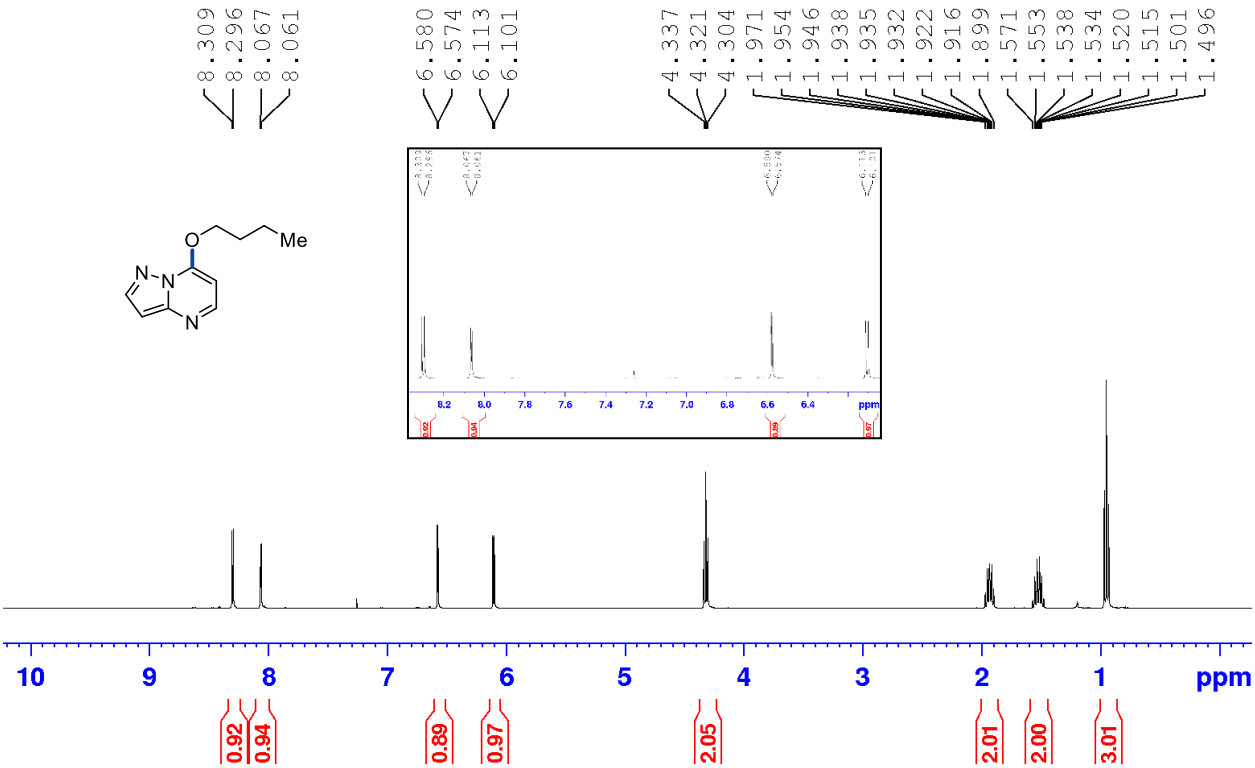

^{1}H NMR spectrum (400 MHz, $CDCl_3$)

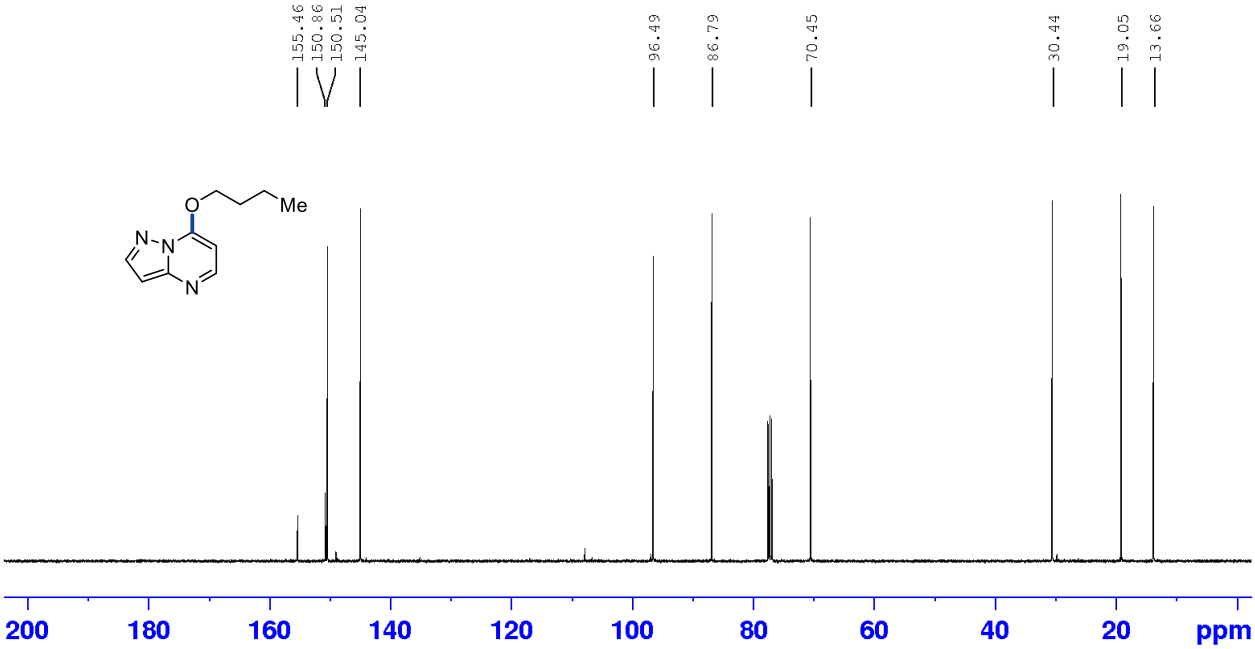

^{13}C NMR spectrum (101 MHz, $CDCl_3$)

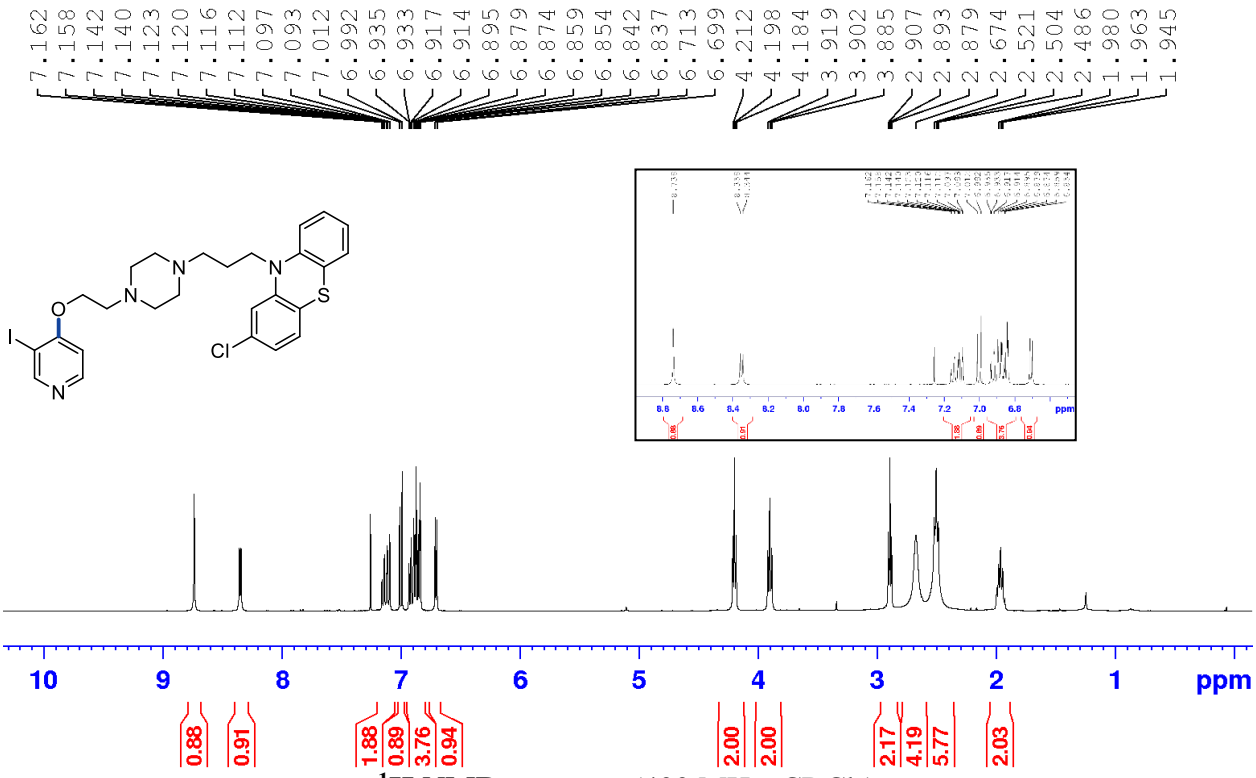

^{1}H NMR spectrum (400 MHz, $CDCl_3$)

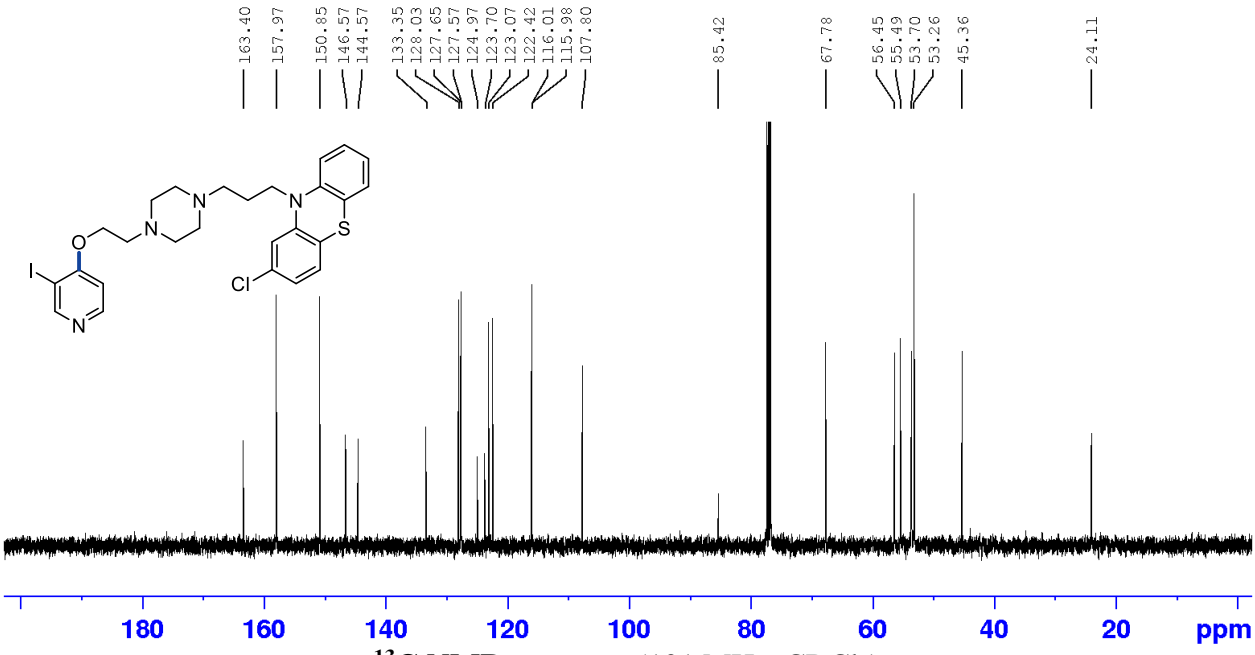

^{13}C NMR spectrum (101 MHz, $CDCl_3$)

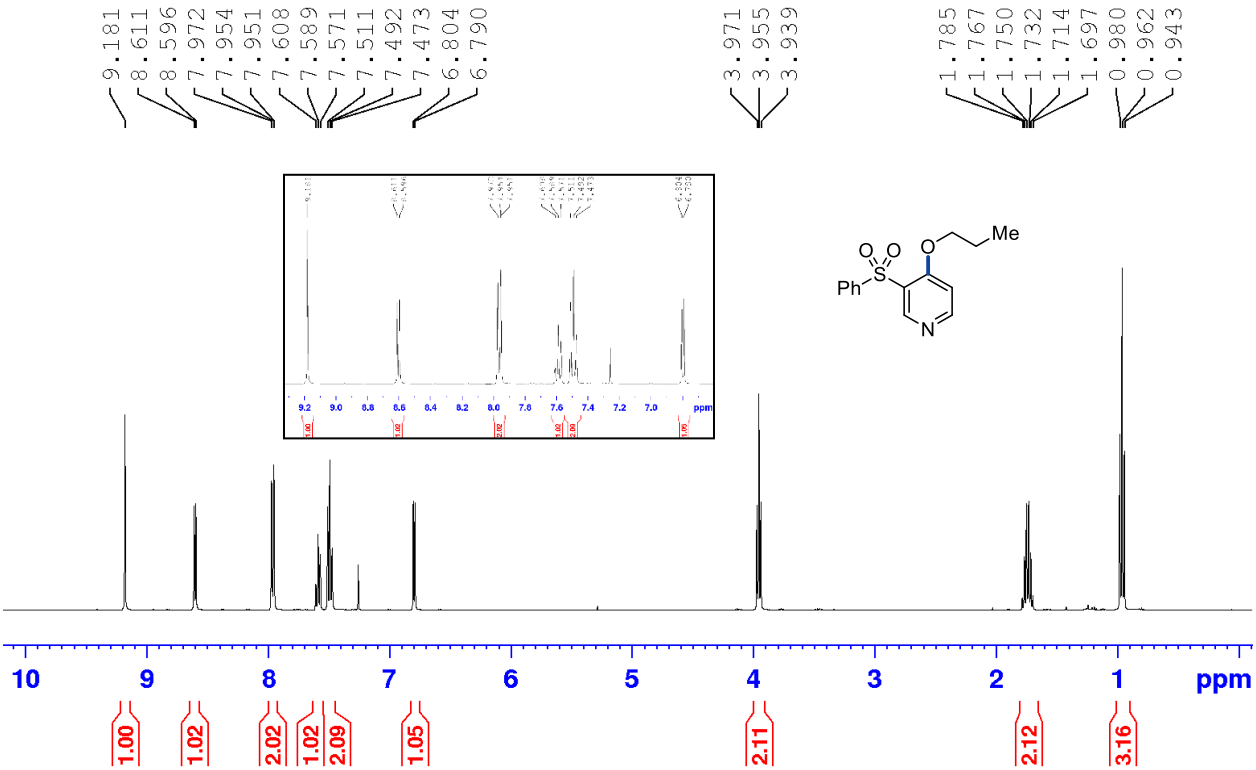

^{1}H NMR spectrum (400 MHz, $CDCl_3$)

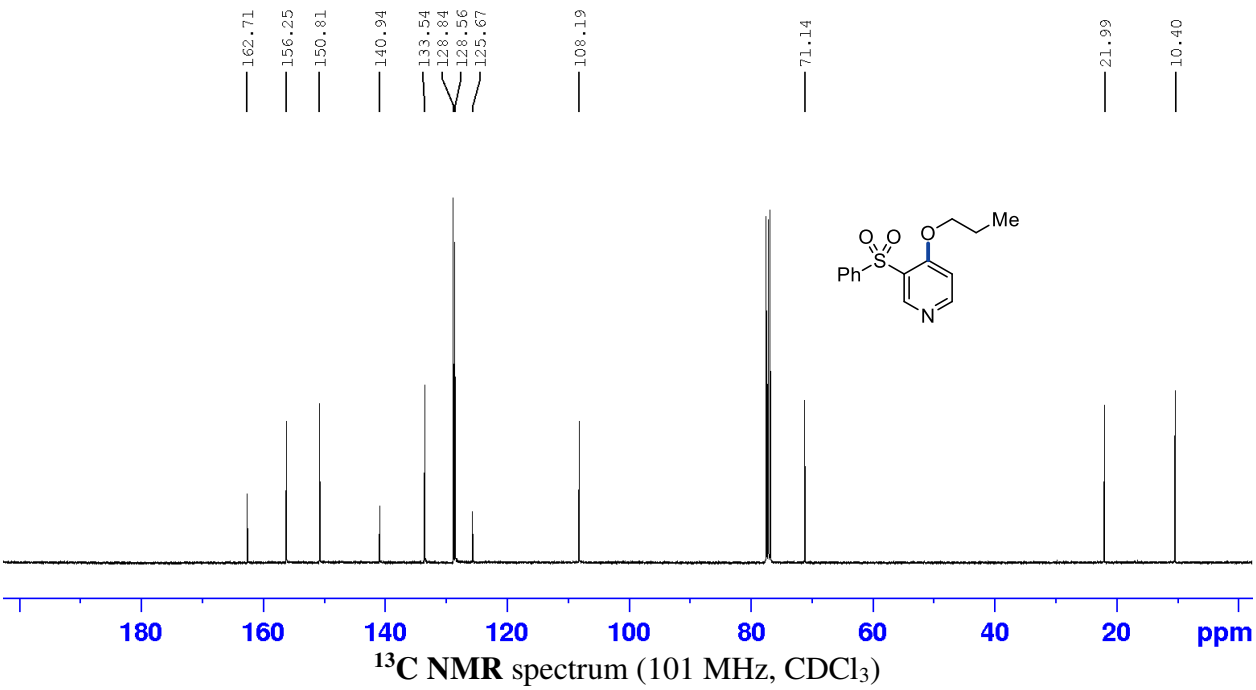

^{13}C NMR spectrum (101 MHz, $CDCl_3$)

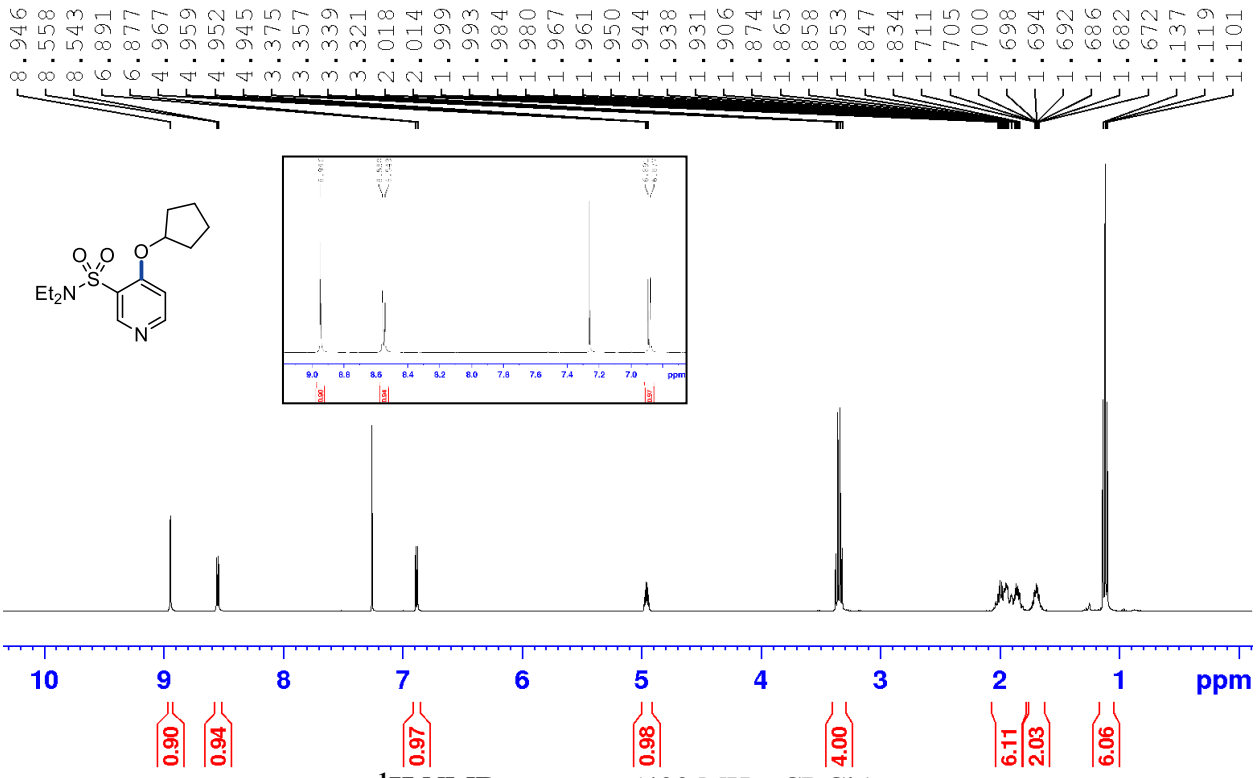

^{1}H NMR spectrum (400 MHz, $CDCl_3$)

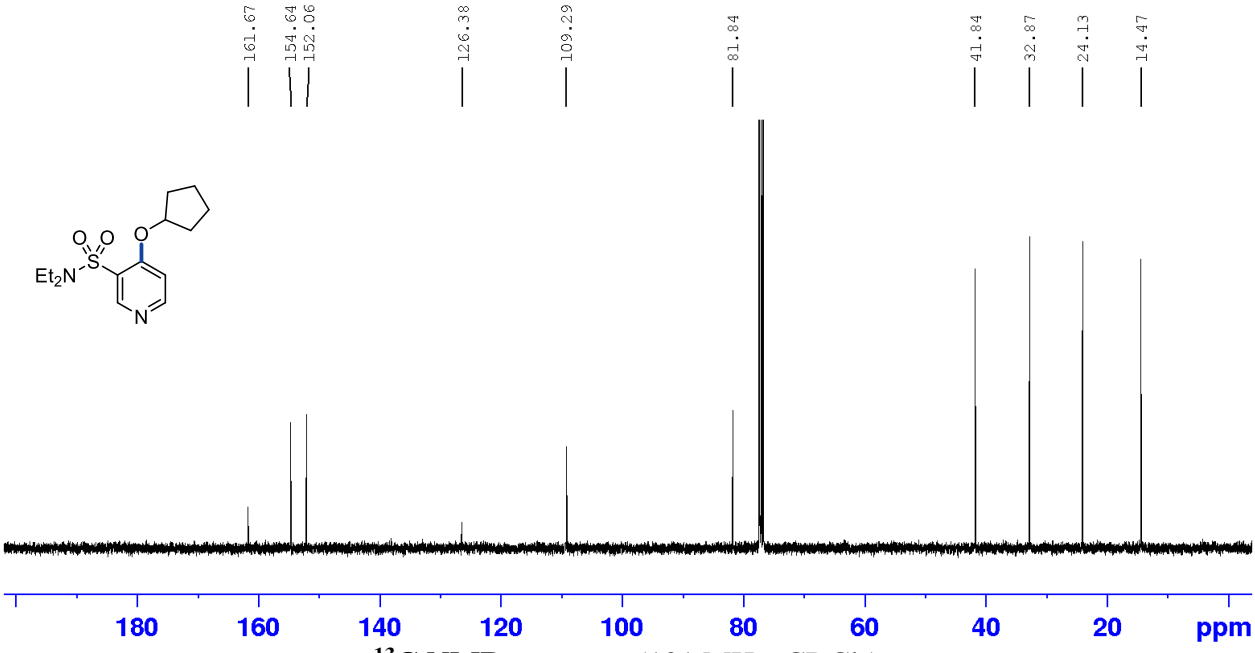

^{13}C NMR spectrum (101 MHz, $CDCl_3$)

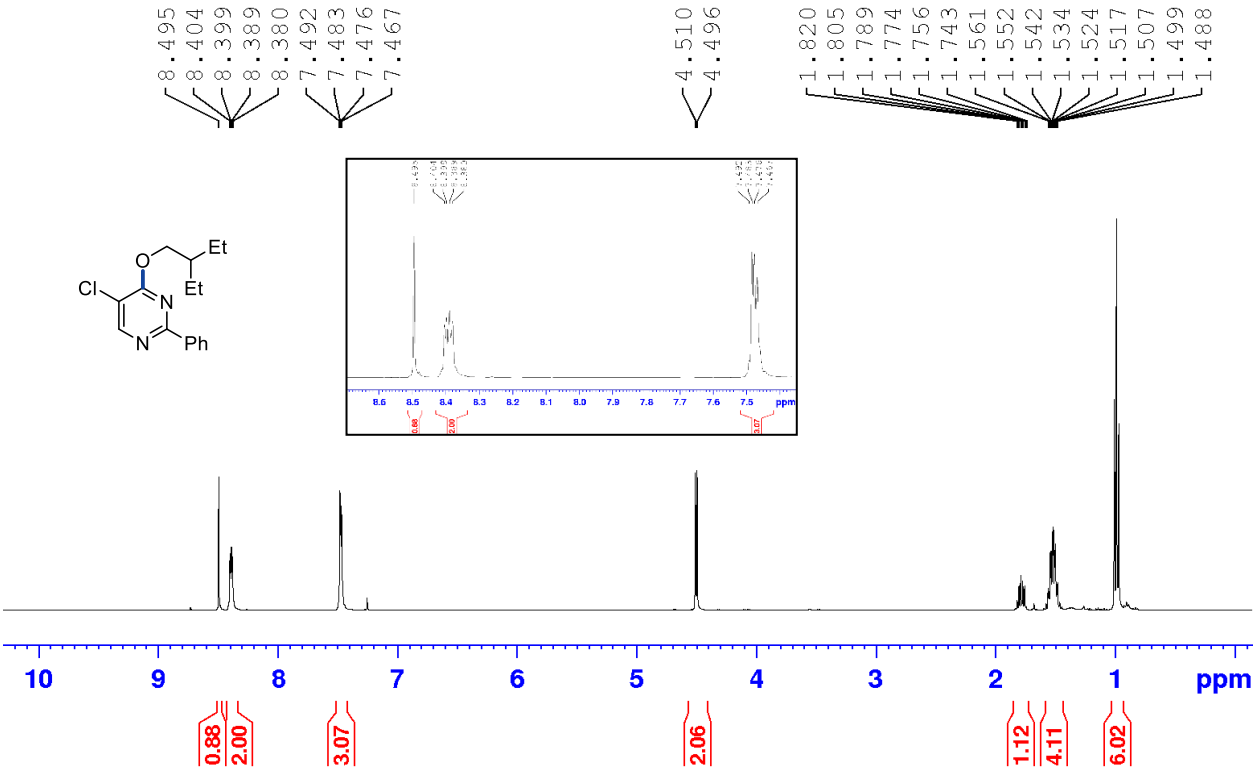

^{1}H NMR spectrum (400 MHz, $CDCl_3$)

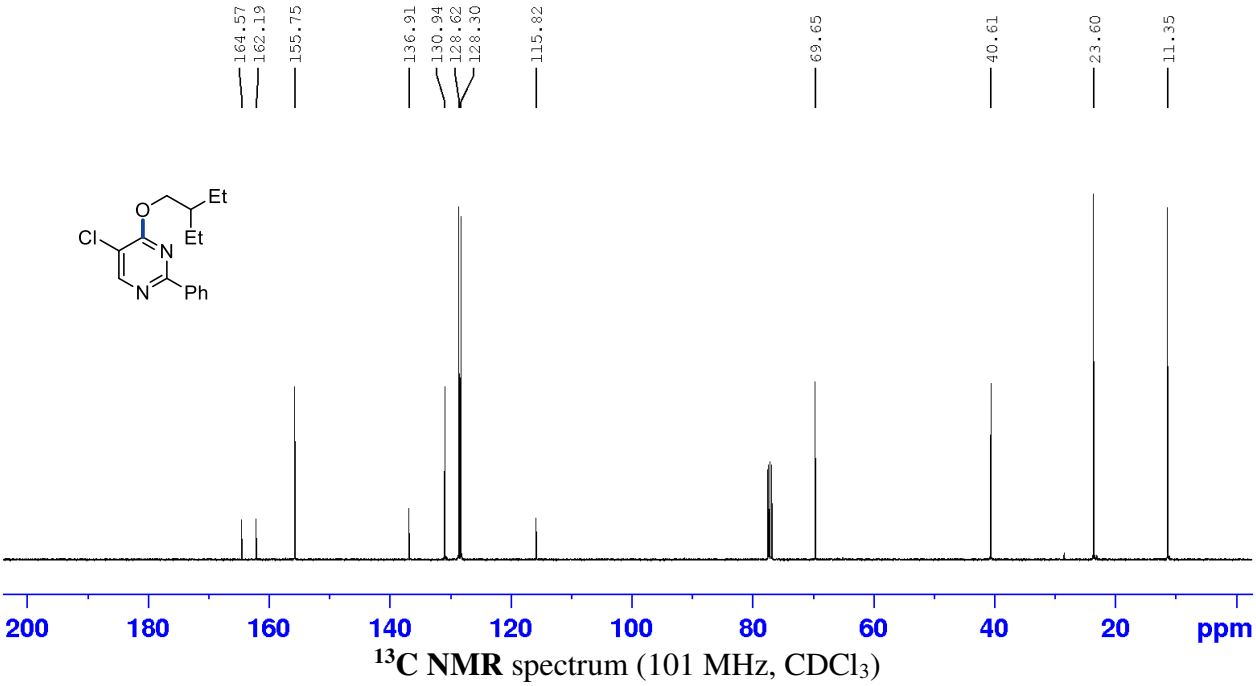

^{13}C NMR spectrum (101 MHz, $CDCl_3$)

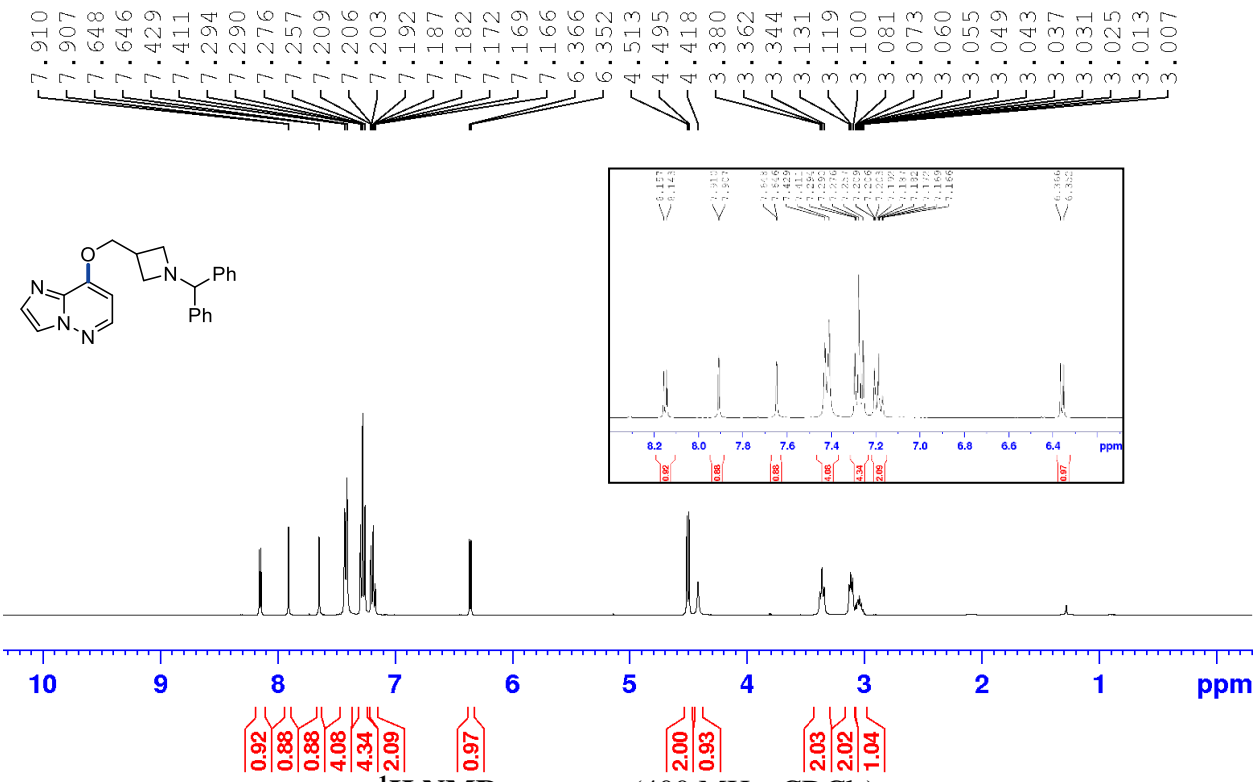

^{1}H NMR spectrum (400 MHz, $CDCl_3$)

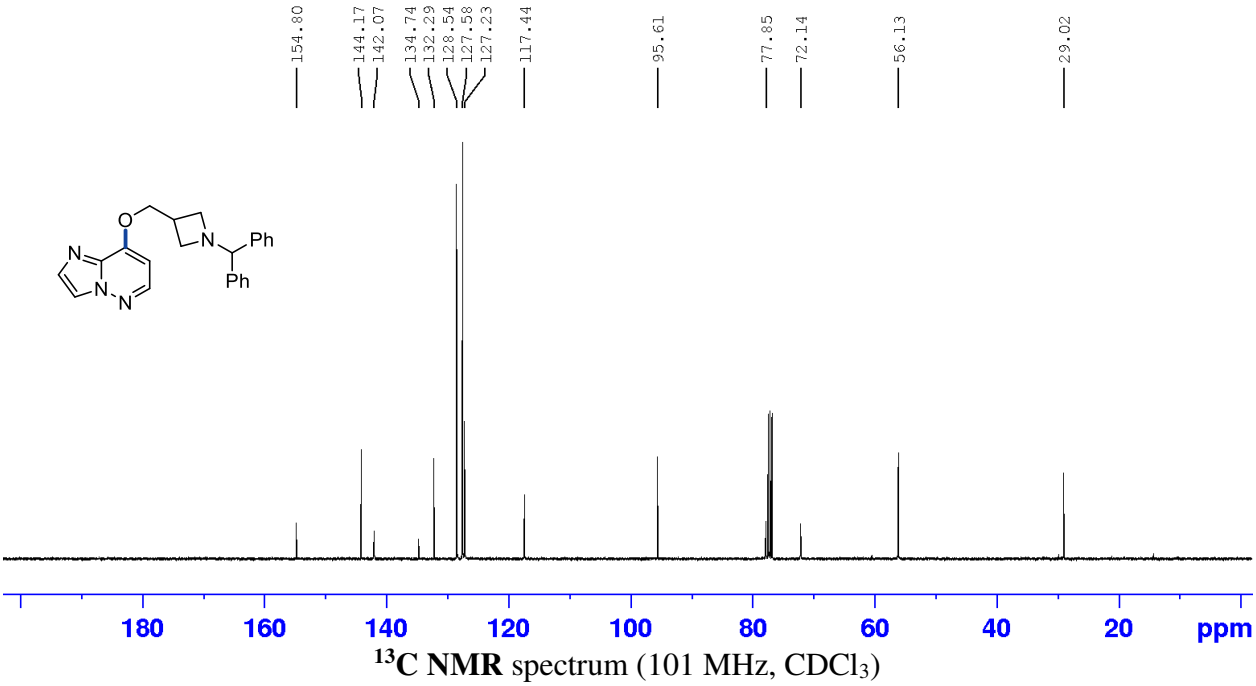

^{13}C NMR spectrum (101 MHz, $CDCl_3$)

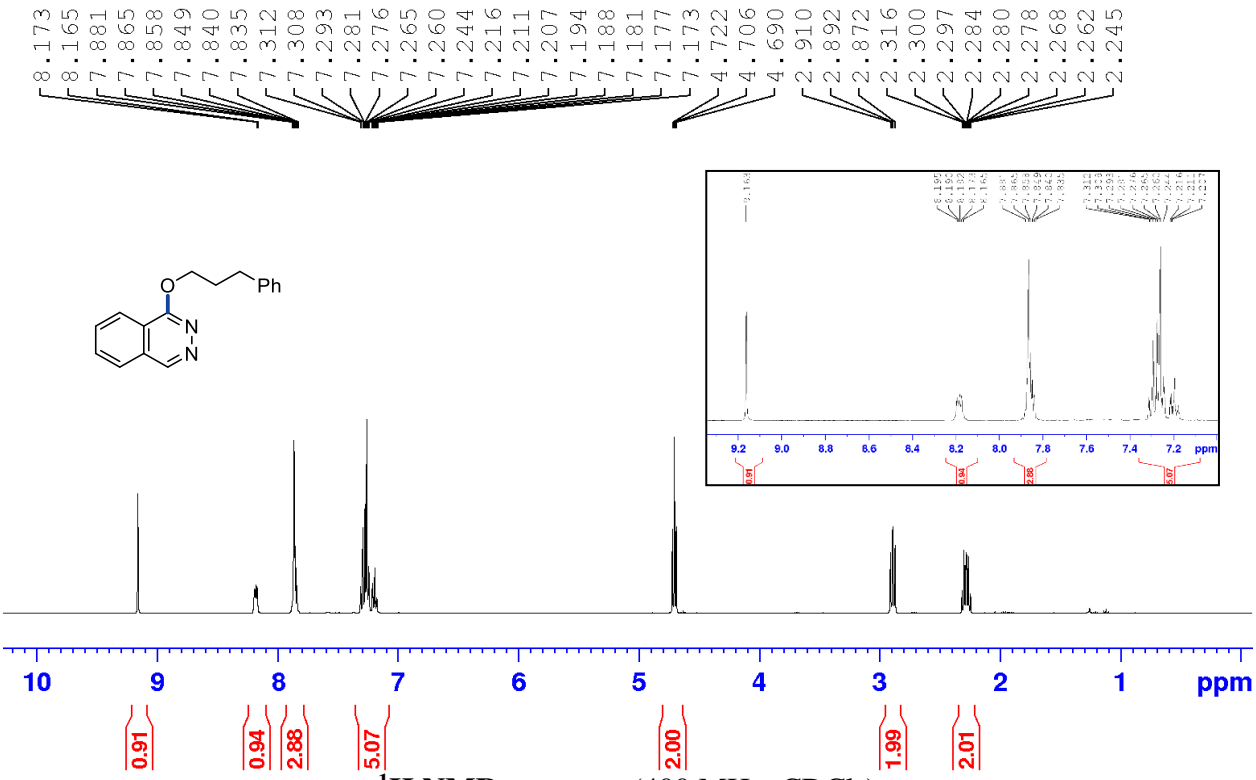

^{1}H NMR spectrum (400 MHz, $CDCl_3$)

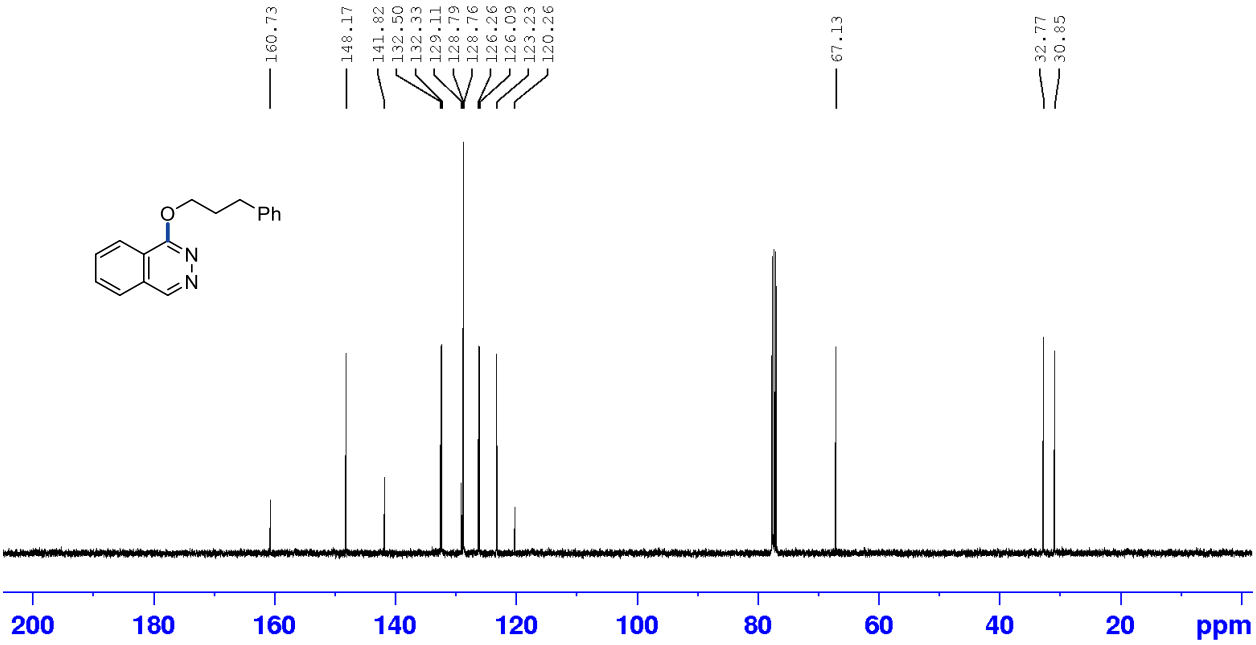

^{13}C NMR spectrum (101 MHz, $CDCl_3$)

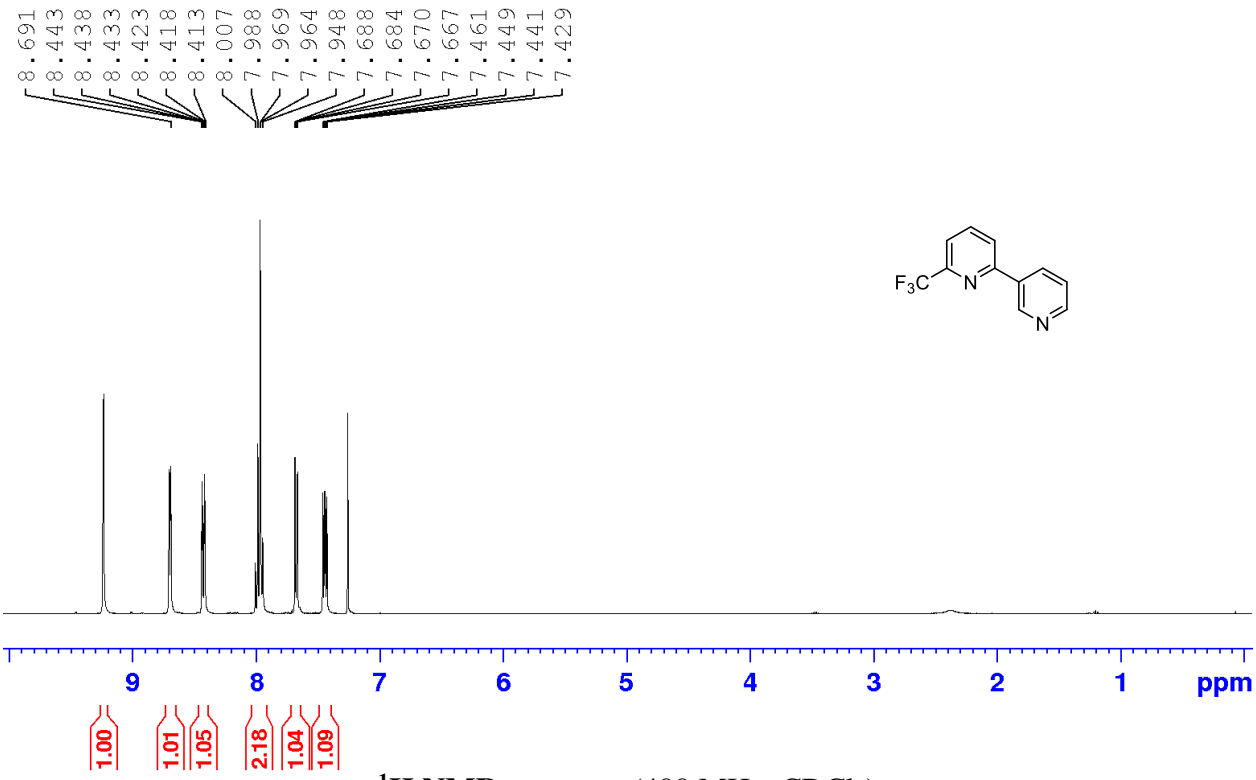

^{1}H NMR spectrum (400 MHz, $CDCl_3$)

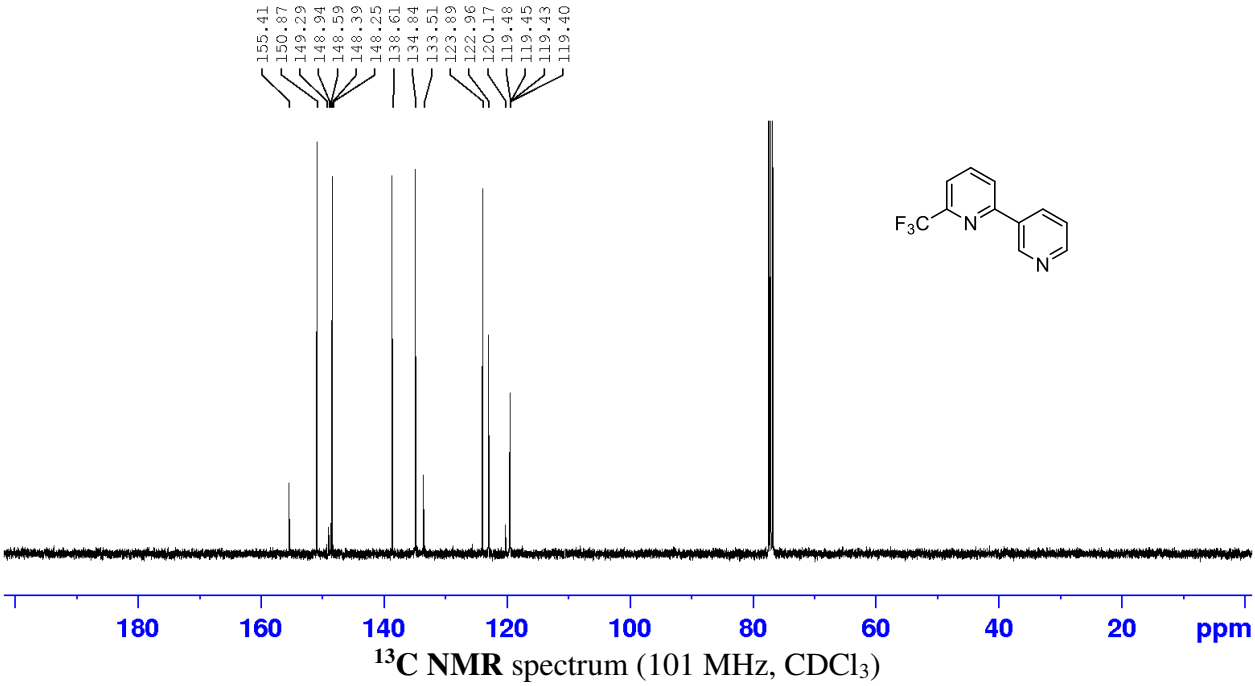

^{13}C NMR spectrum (101 MHz, $CDCl_3$)

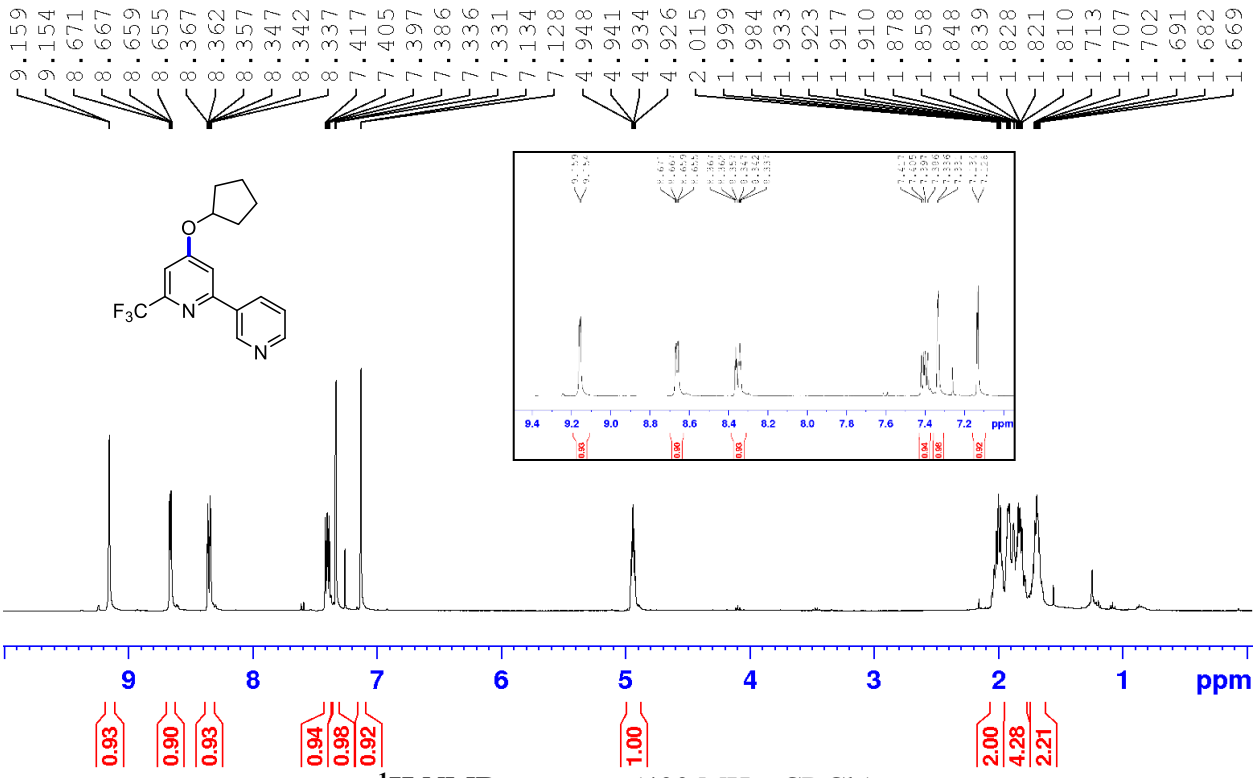

^{1}H NMR spectrum (400 MHz, $CDCl_3$)

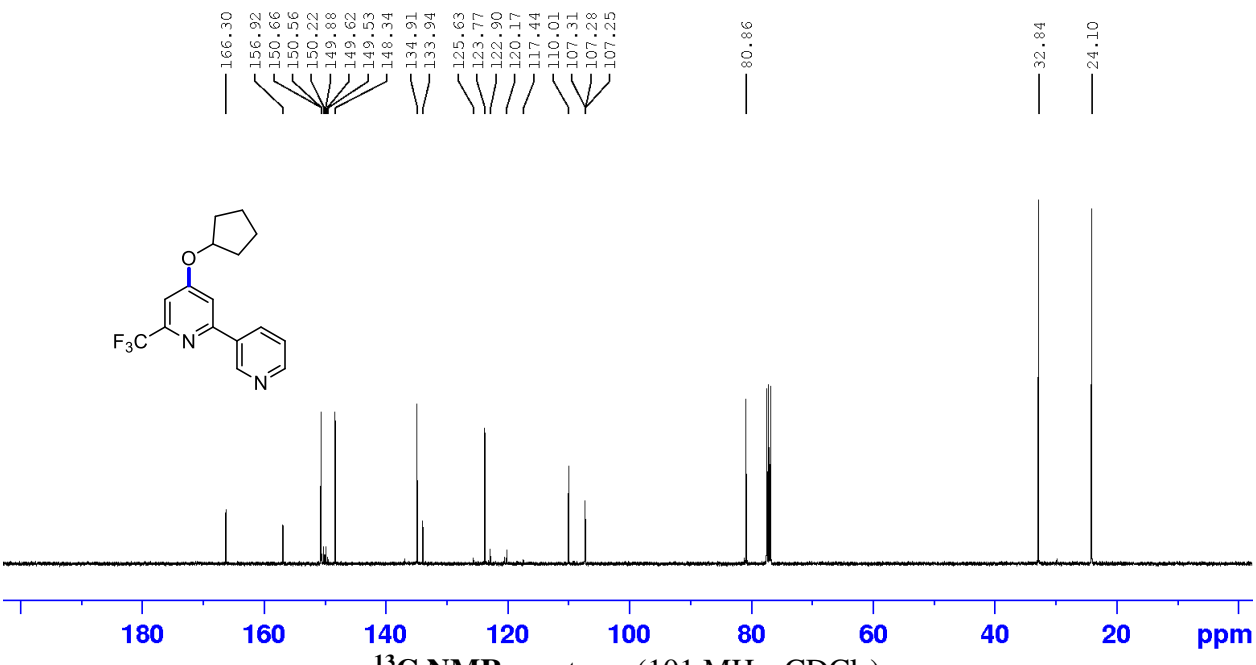

^{13}C NMR spectrum (101 MHz, $CDCl_3$)

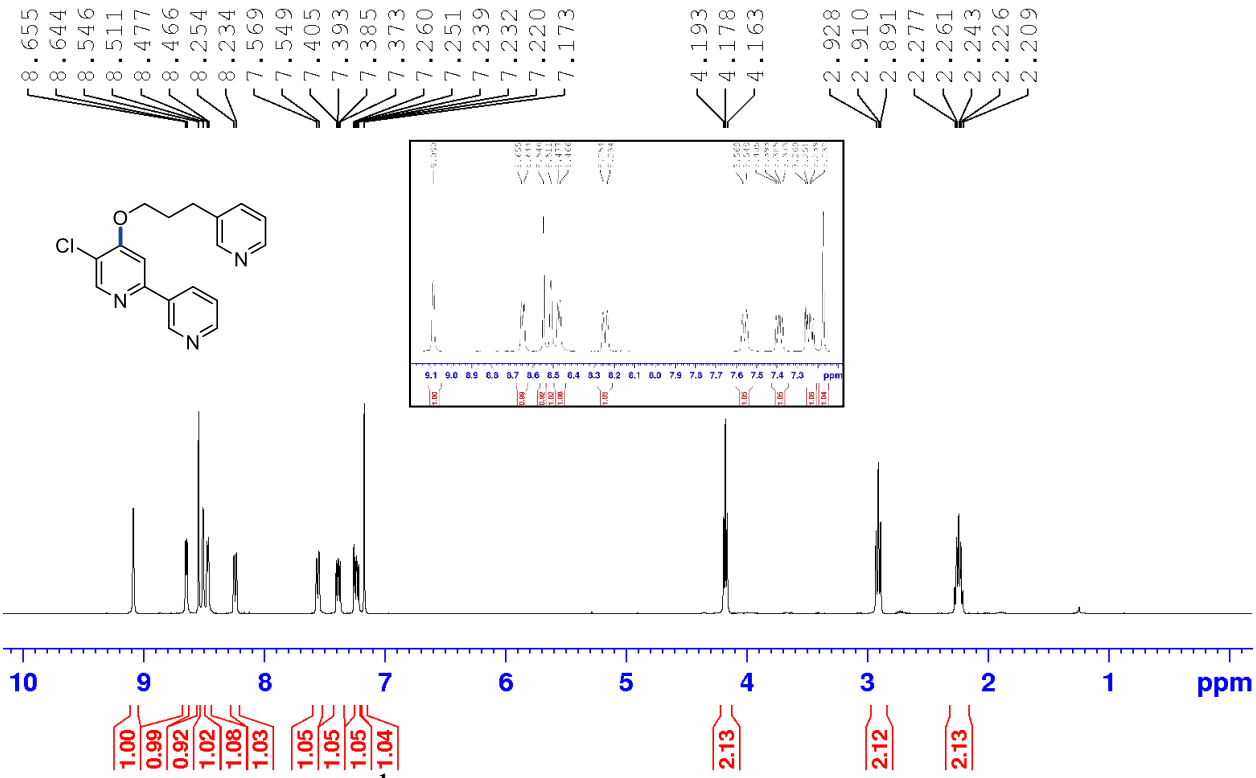

^{1}H NMR spectrum (400 MHz, $CDCl_3$)

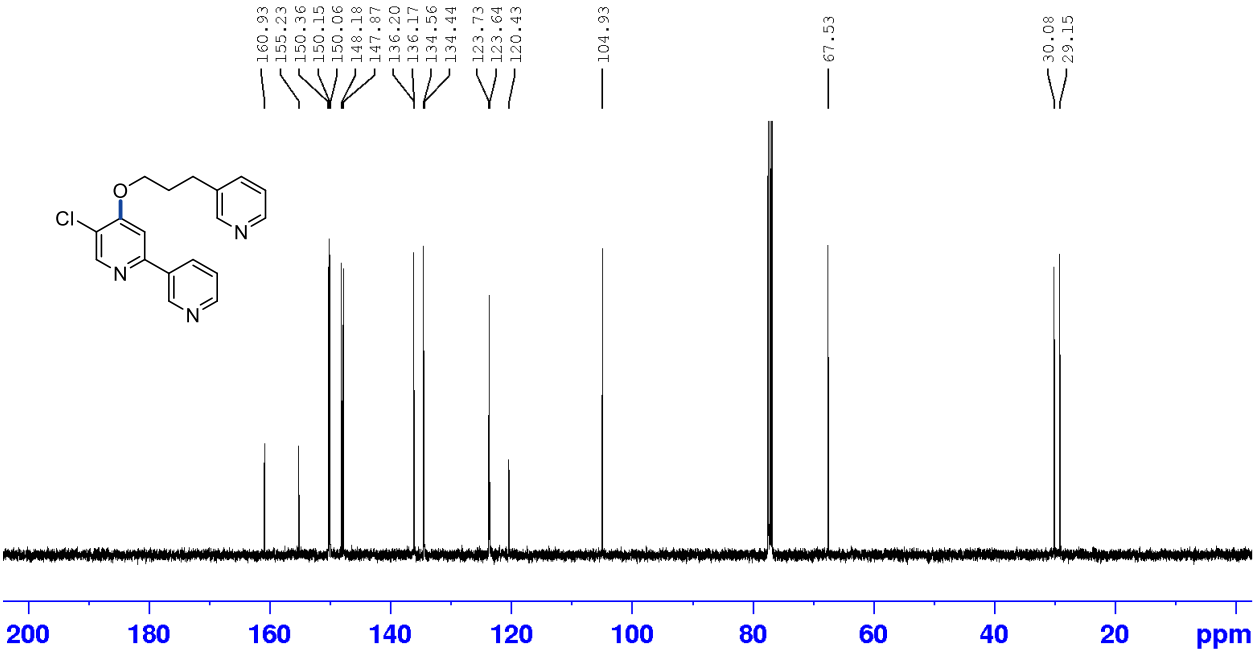

^{13}C NMR spectrum (101 MHz, $CDCl_3$)

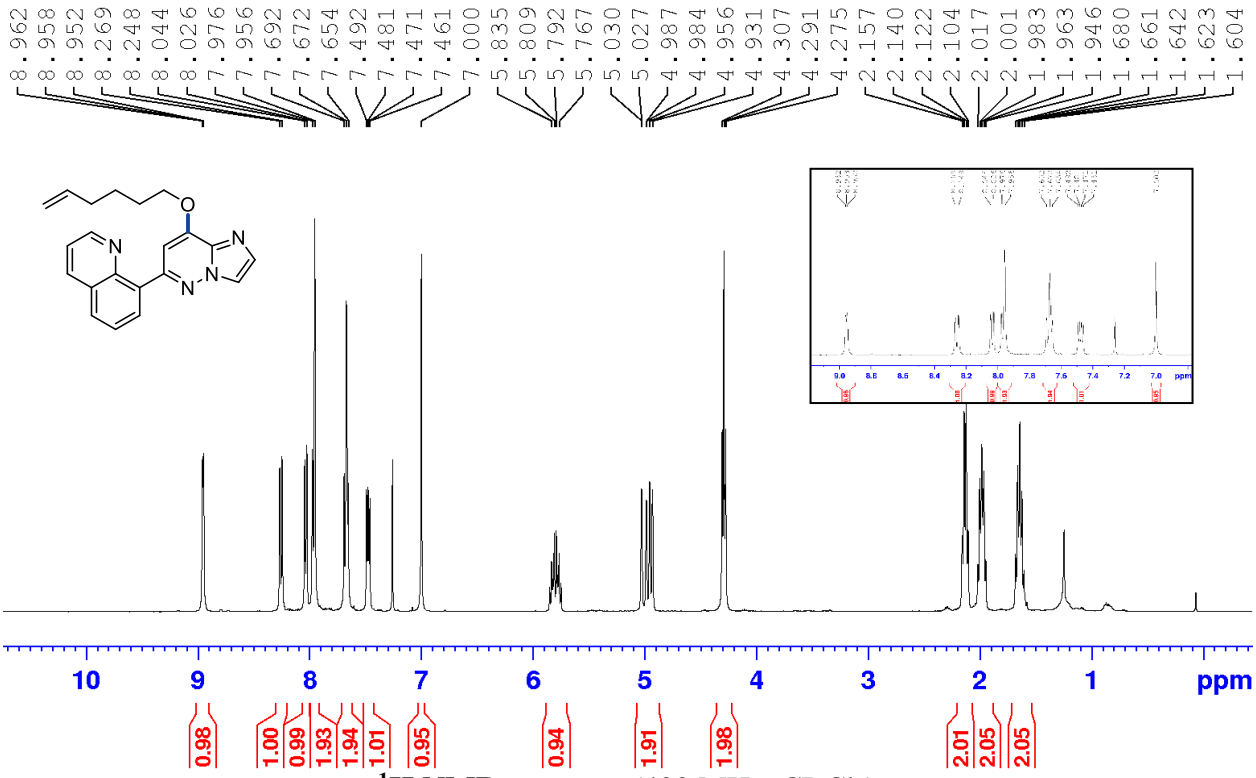

^{1}H NMR spectrum (400 MHz, $CDCl_3$)

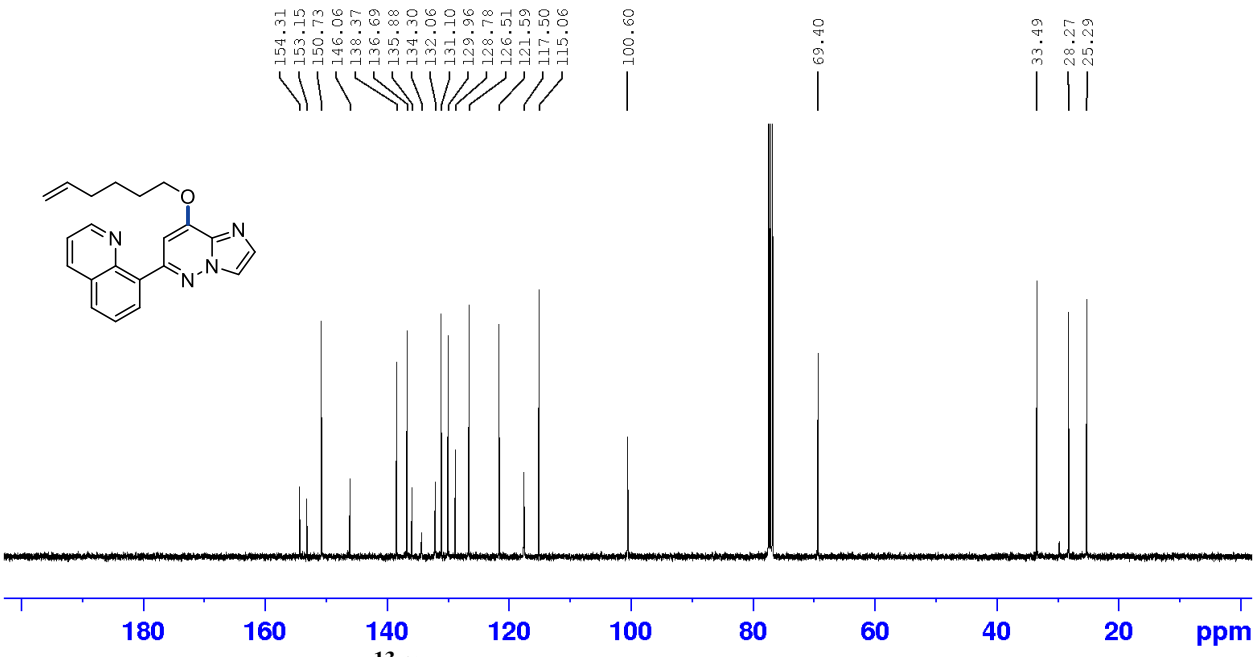

^{13}C NMR spectrum (101 MHz, $CDCl_3$)

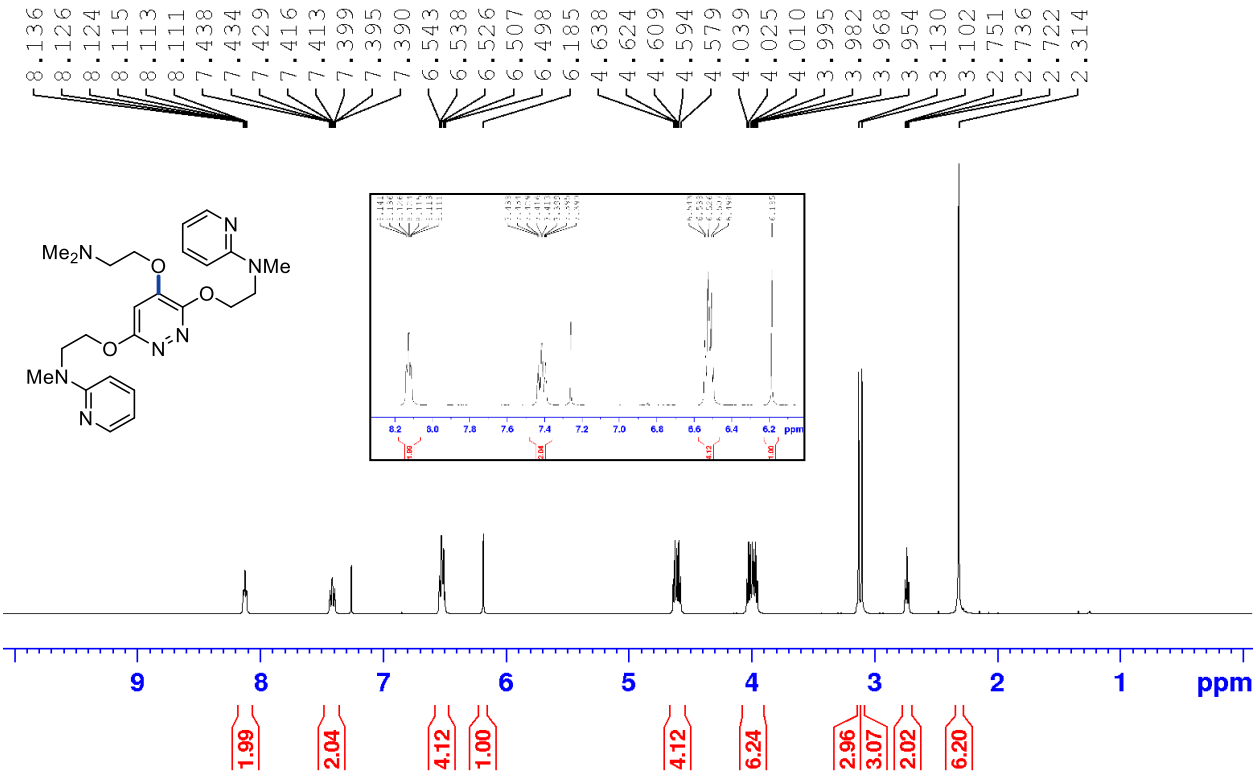

^{1}H NMR spectrum (400 MHz, $CDCl_3$)

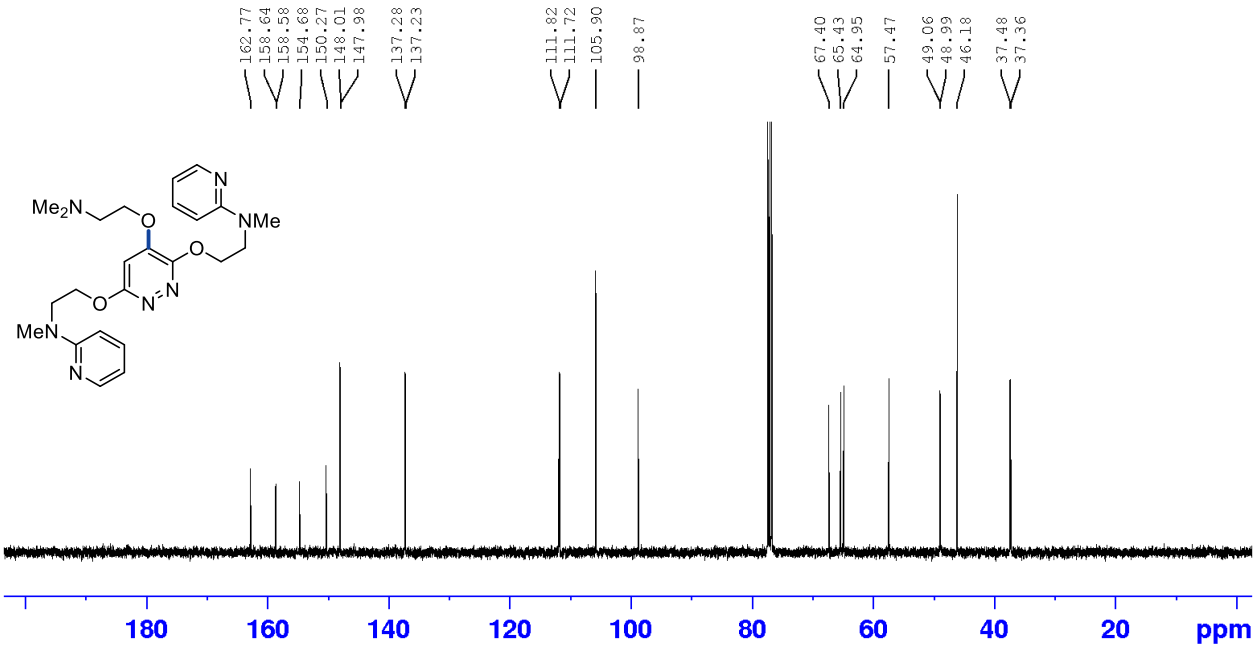

^{13}C NMR spectrum (101 MHz, $CDCl_3$)

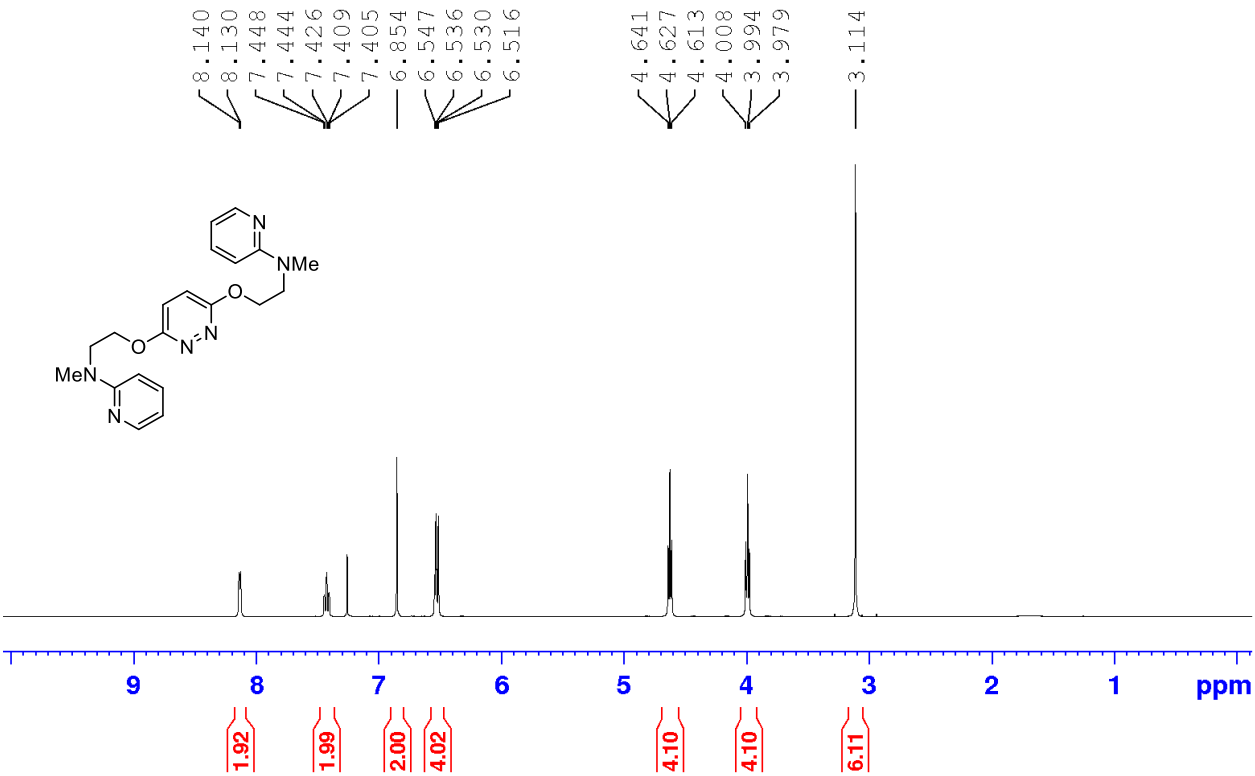

^{1}H NMR spectrum of *N*,*N*'-((pyridazine-3,6-diylbis(oxy))bis(ethane-2,1-diyl))bis(N-methylpyridin-2-amine) (400 MHz, $CDCl_3$)

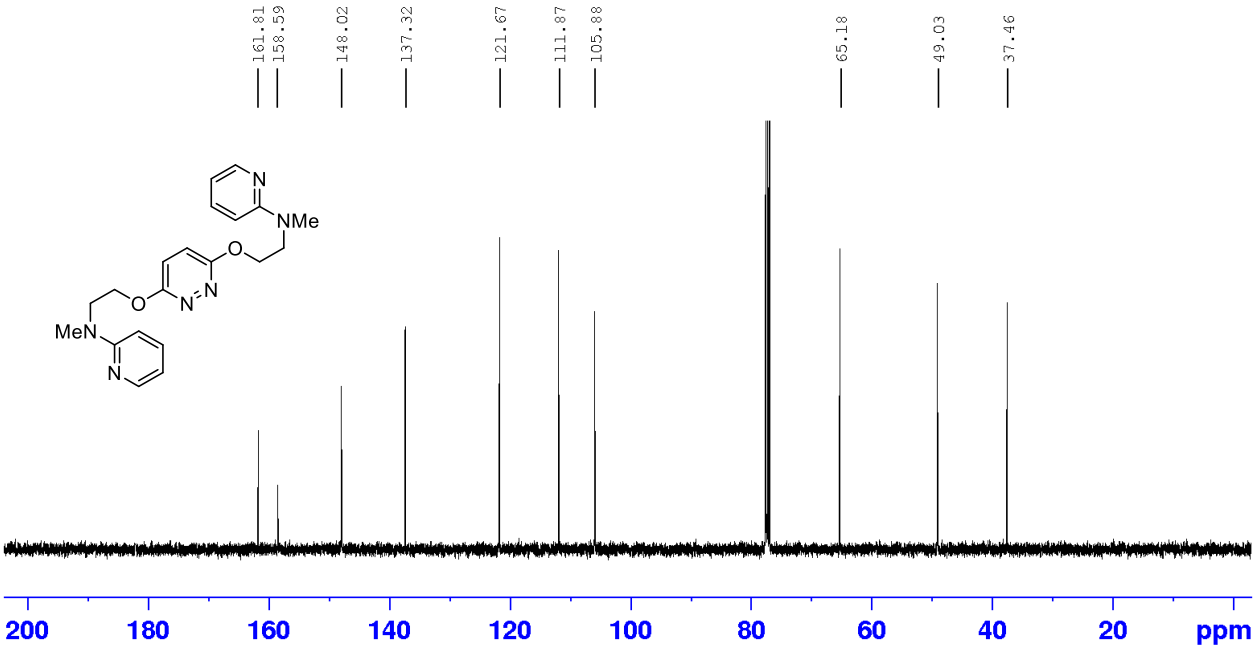

^{13}C NMR spectrum of *N*,*N*'-((pyridazine-3,6-diylbis(oxy))bis(ethane-2,1-diyl))bis(N-methylpyridin-2-amine) (101 MHz, $CDCl_3$)

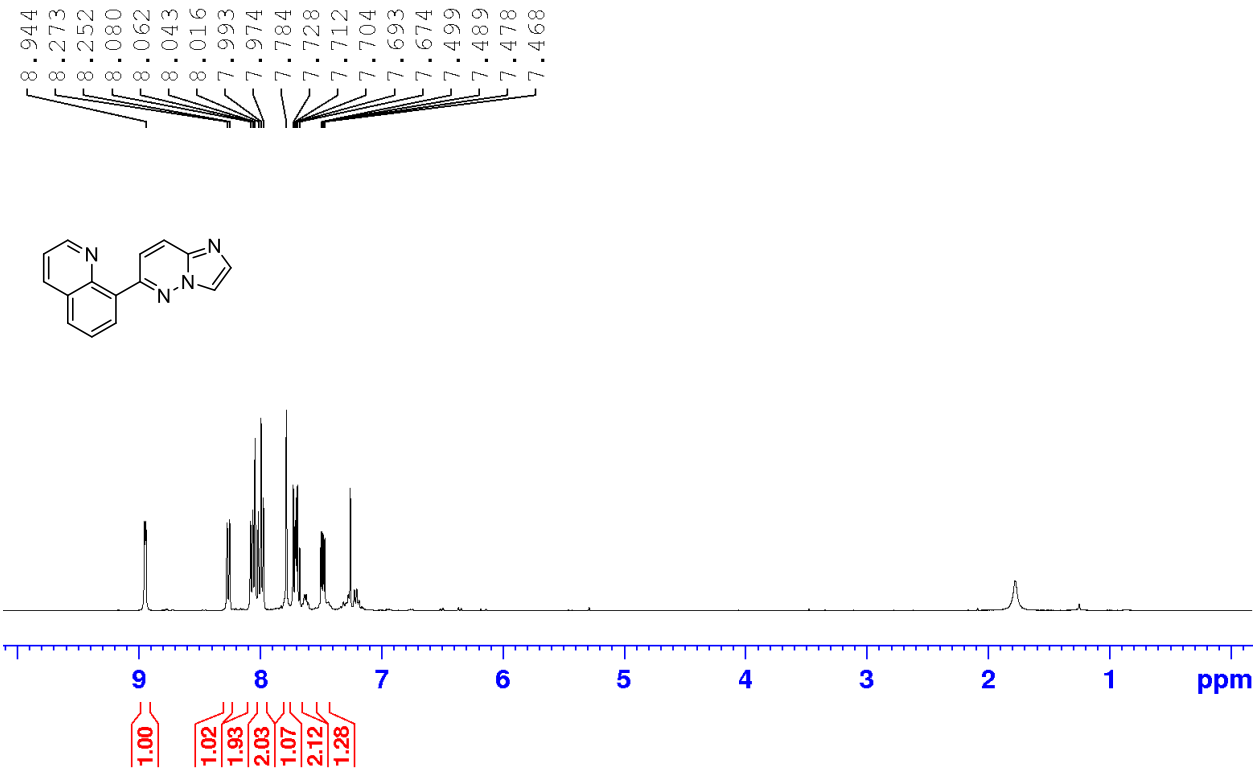

^{1}H NMR spectrum of 8-(imidazo[1,2-*b*]pyridazin-6-yl)quinoline (400 MHz, $CDCl_3$)

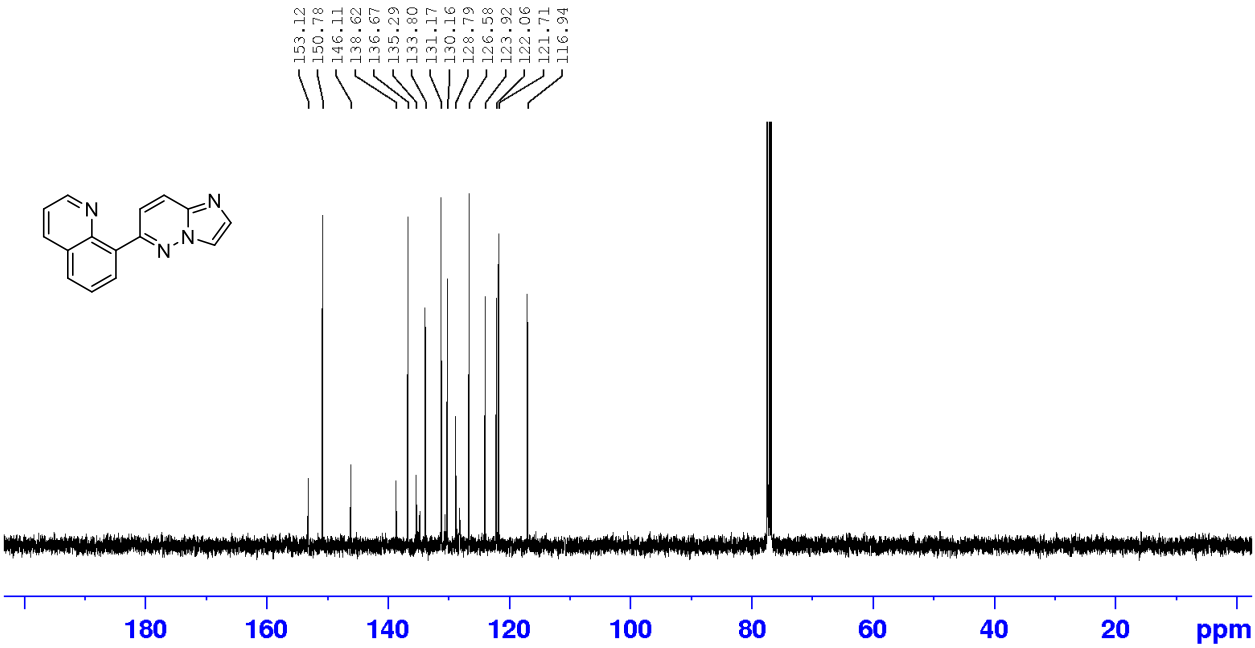

^{13}C NMR spectrum of 8-(imidazo[1,2-*b*]pyridazin-6-yl)quinoline (101 MHz, $CDCl_3$)

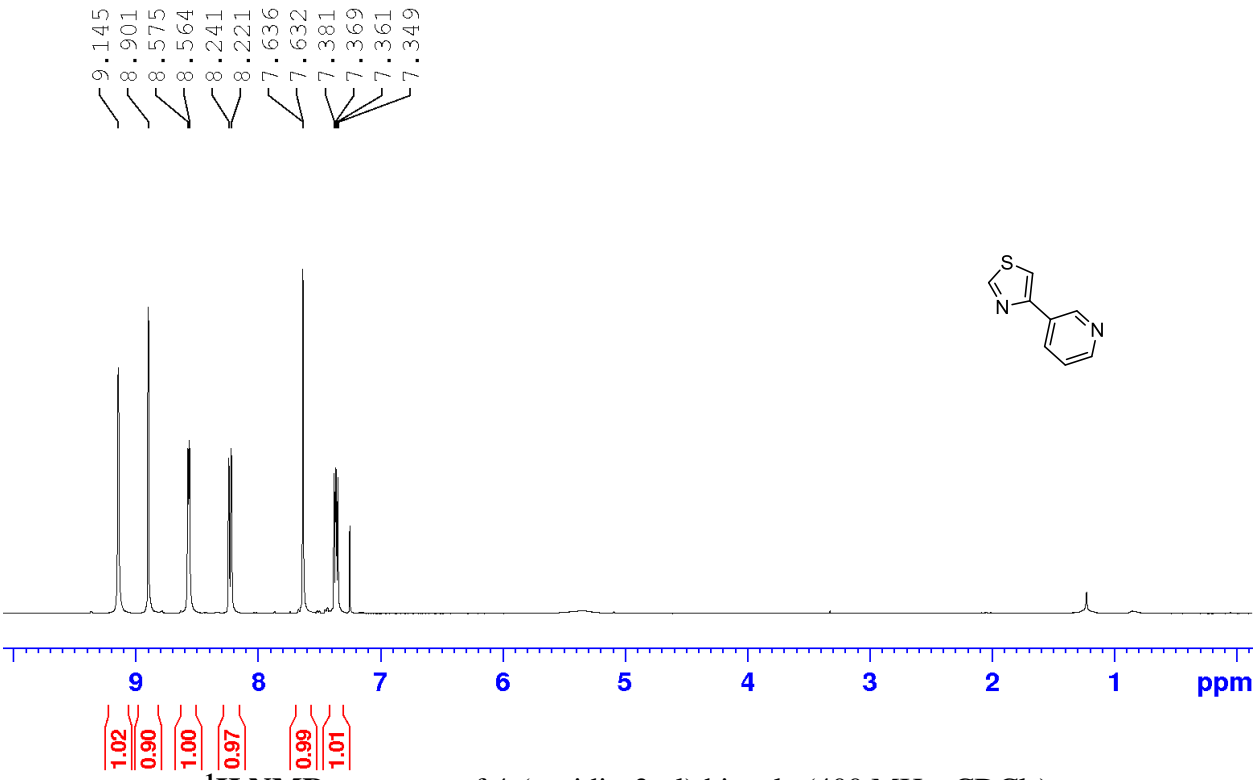

^{1}H NMR spectrum of 4-(pyridin-3-yl)thiazole (400 MHz, $CDCl_3$)

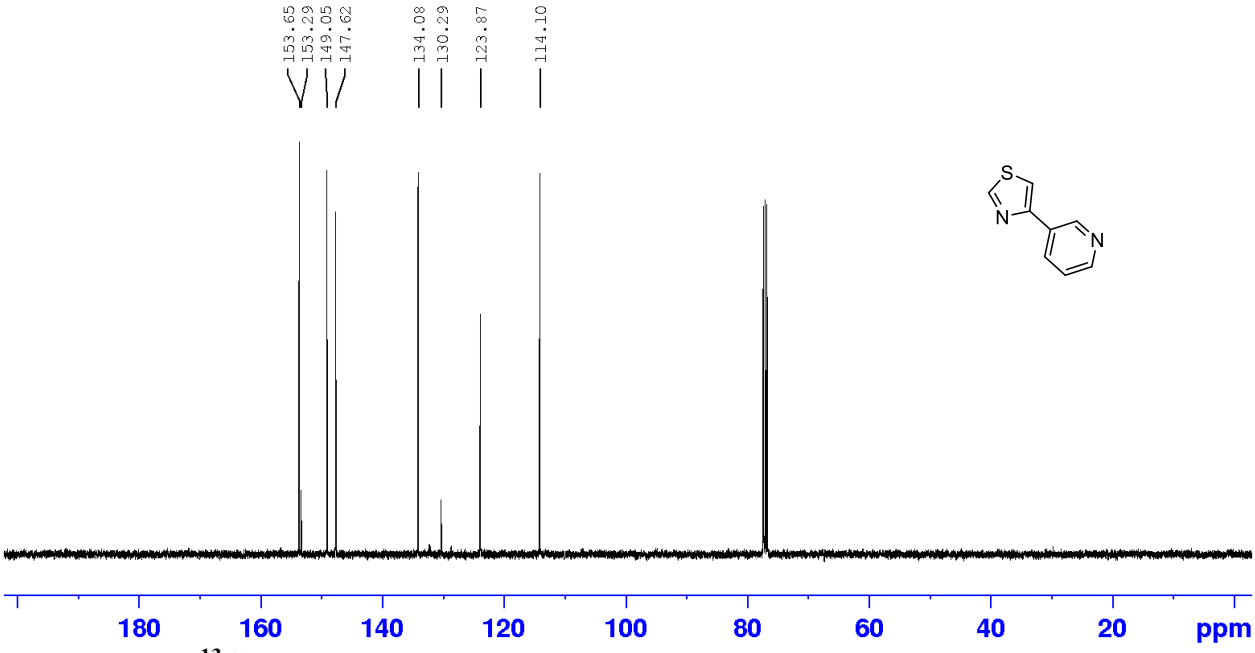

^{13}C NMR spectrum of 4-(pyridin-3-yl)thiazole (101 MHz, $CDCl_3$)

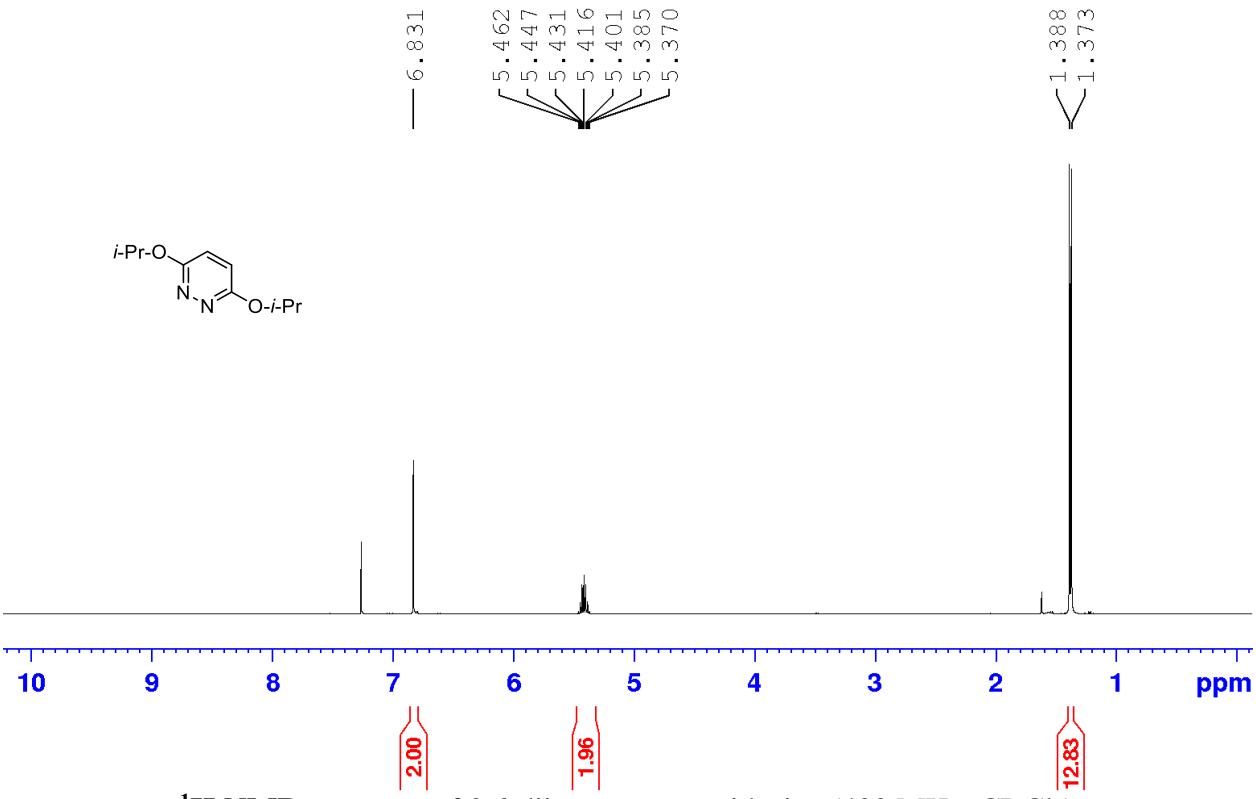

^{1}H NMR spectrum of 3,6-diisopropoxypyridazine (400 MHz, $CDCl_3$)

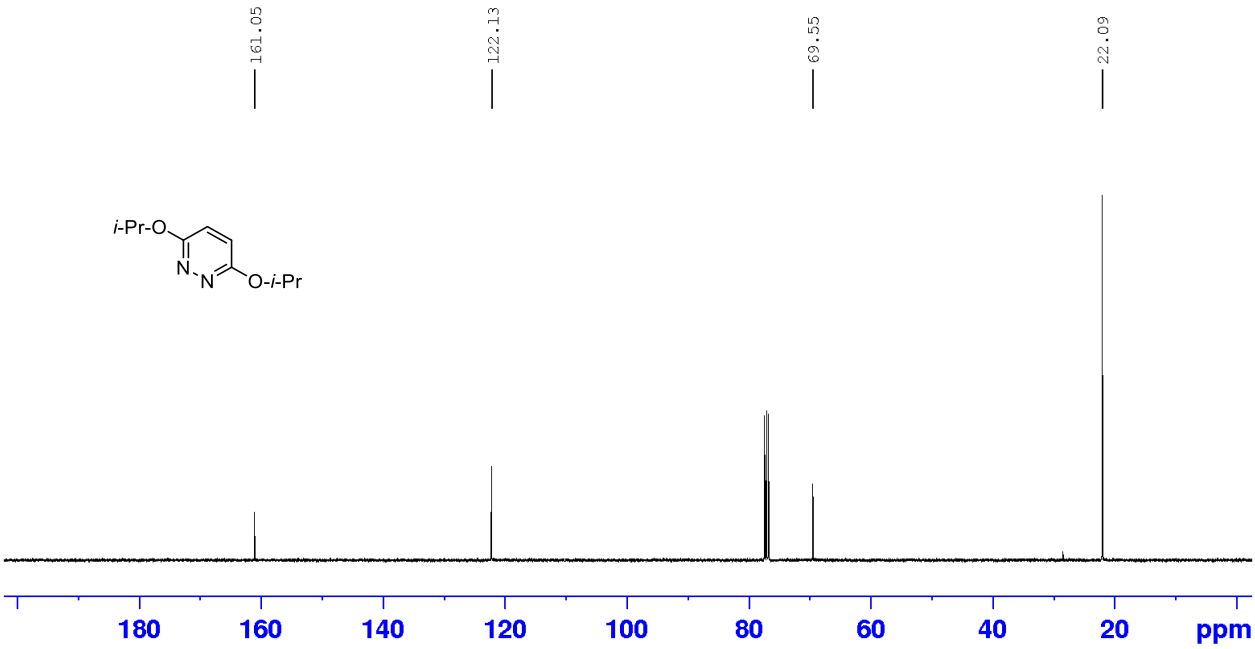

^{13}C NMR spectrum of 3,6-diisopropoxypyridazine (101 MHz, $CDCl_3$)

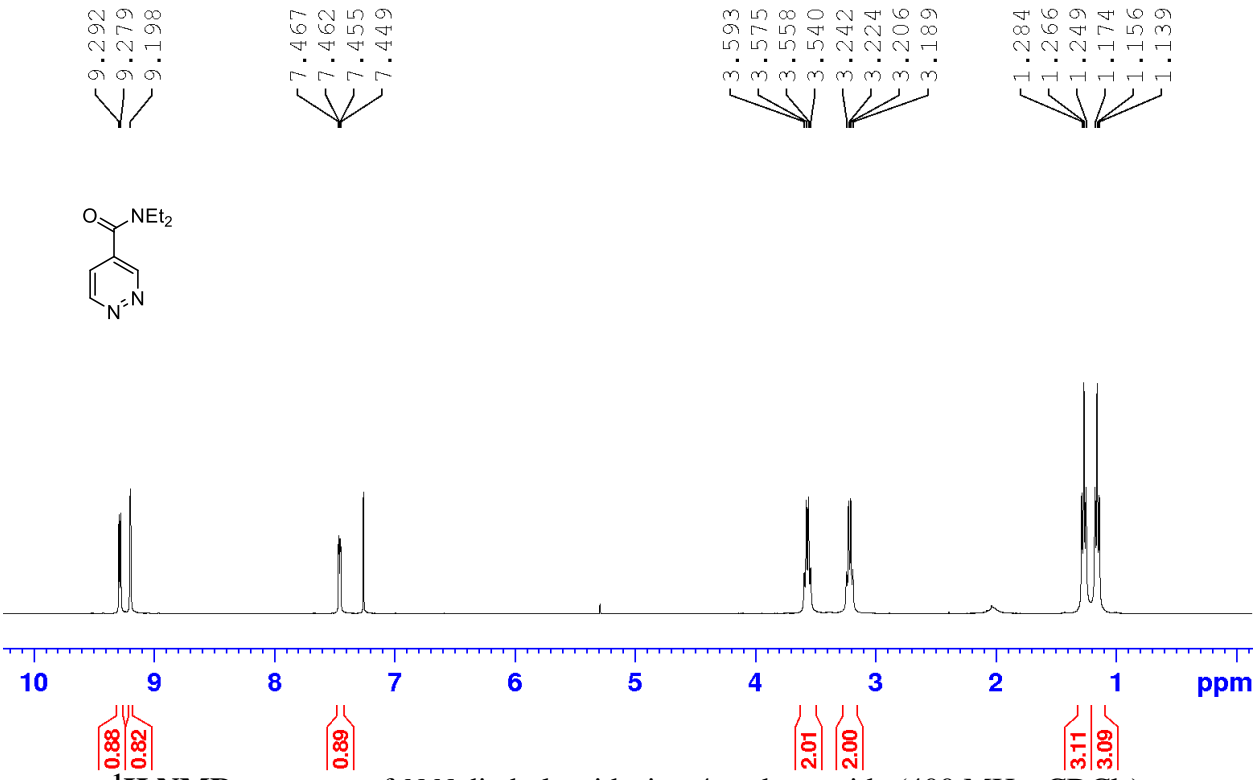

^{1}H NMR spectrum of *N*,*N*-diethylpyridazine-4-carboxamide (400 MHz, $CDCl_3$)

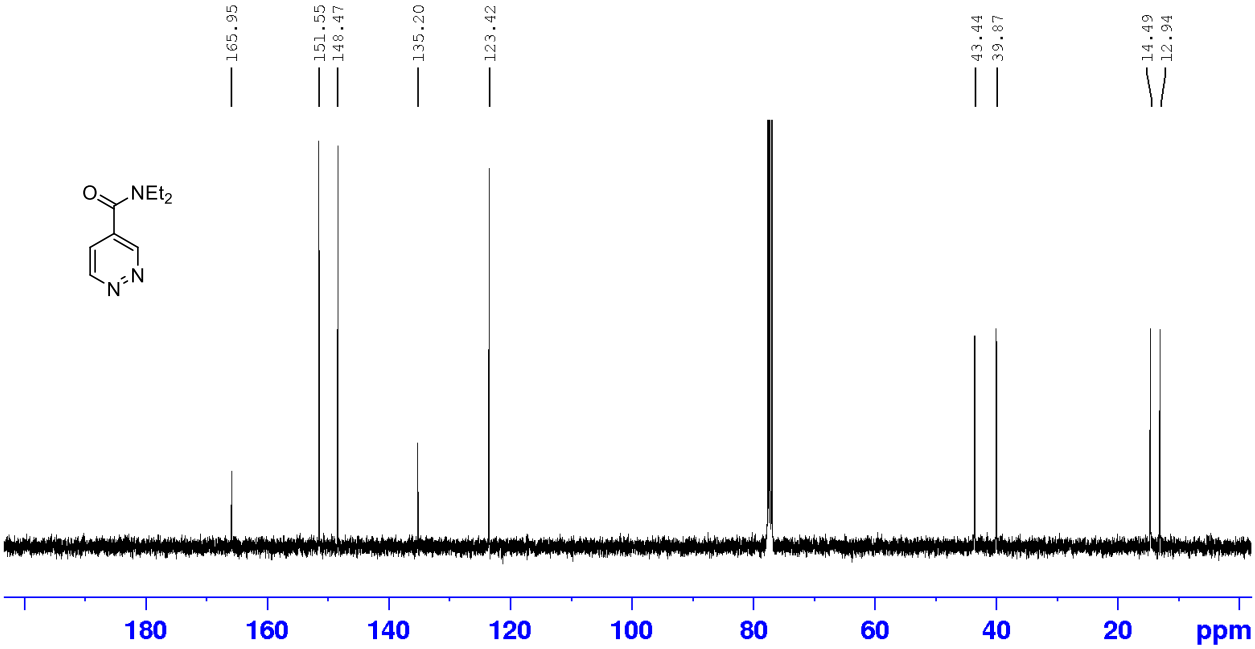

^{13}C NMR spectrum of *N*,*N*-diethylpyridazine-4-carboxamide (101 MHz, $CDCl_3$)

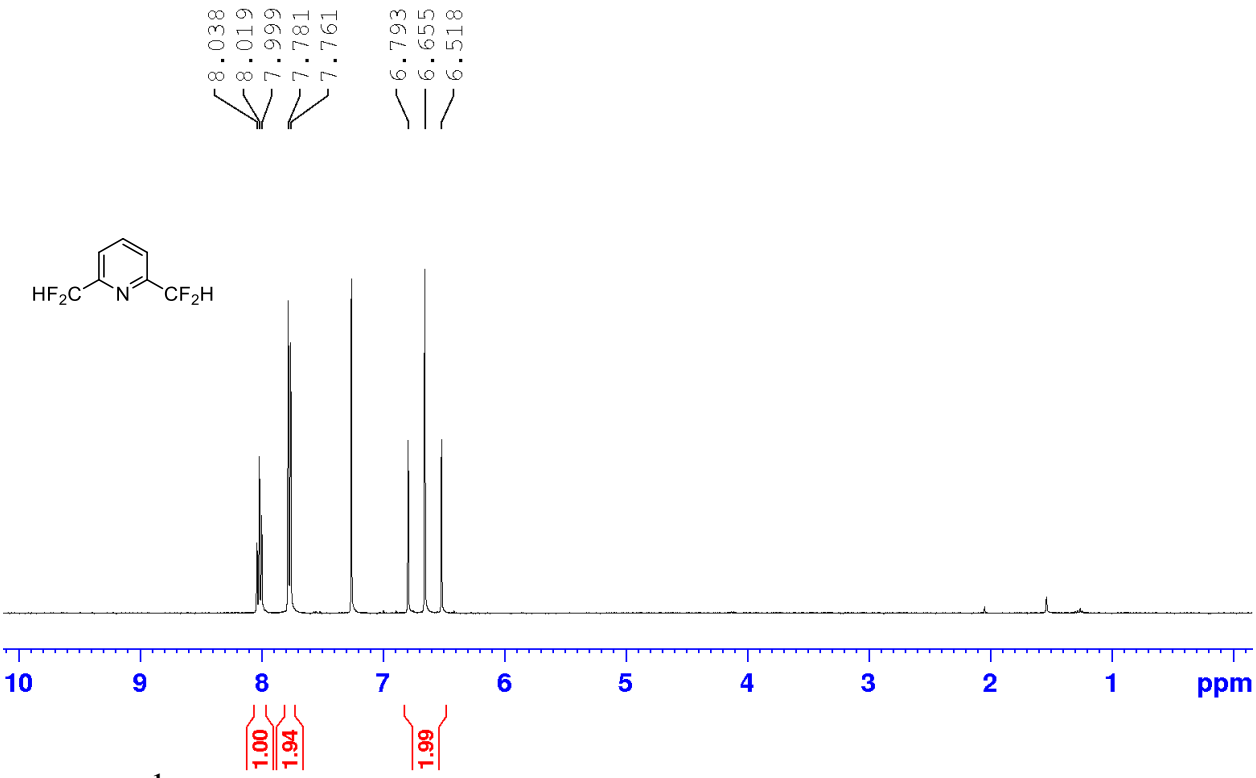

^{1}H NMR spectrum of 2,6-bis(difluoromethyl)pyridine (400 MHz, $CDCl_3$)

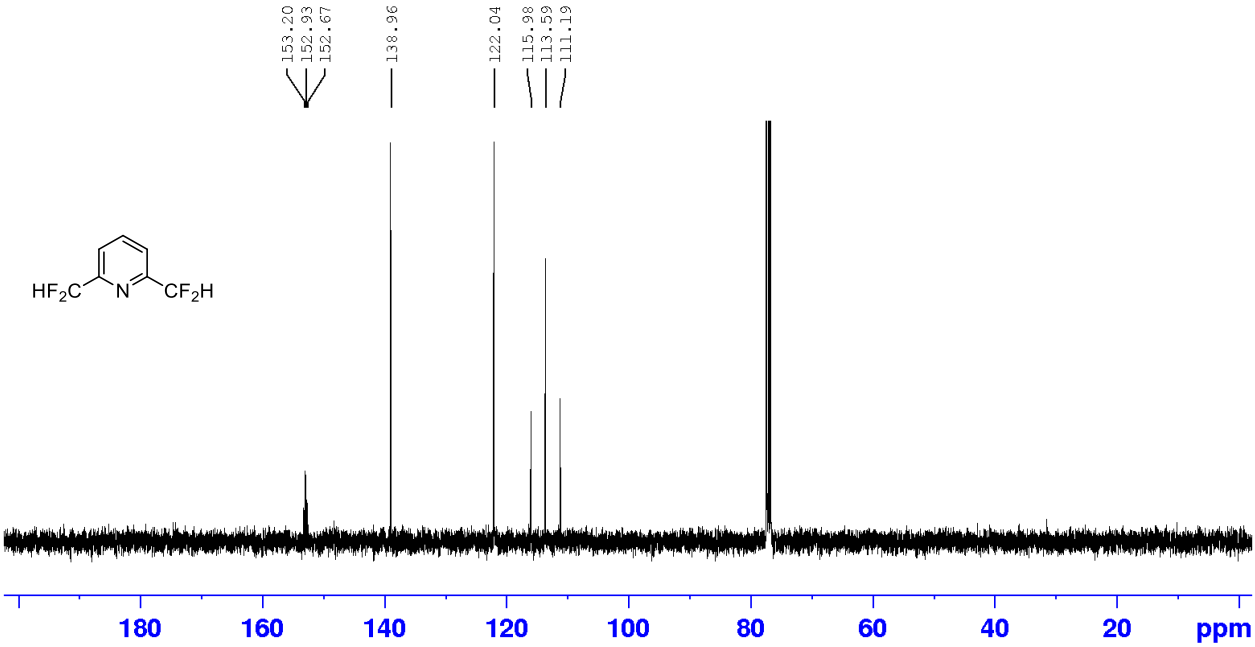

^{13}C NMR spectrum of 2,6-bis(difluoromethyl)pyridine (101 MHz, $CDCl_3$)

LIST OF ABBREVIATIONS

ADME	absorption, distribution, metabolism, and excretion
AIBN	azobisisobutyronitrile
API	active pharmaceutical ingredient
amu	atomic mass unit
CYP-450	cytochrome P450
DBU	1,8-diazabicyclo[5.4.0]undec-7-ene
DG	directing group
DMAc	*N*,*N*-dimethylacetamide
DMF	*N*,*N*-dimethylformamide
DMPU	*N*,*N*′-dimethylpropyleneurea
DMSO	dimethyl sulfoxide
dppp	1,3-bis(diphenylphosphino)propane
ee	enantiomeric excess
EWG	electron-withdrawing group
g	gram
h	hour
HFIP	hexafluoroisopropanol
HIE	hydrogen isotope exchange
HX	hydrogen halide
K_{eq}	equilibrium constant
KIE	kinetic isotope effect
LIDA	lithium diisopropylamide
LiTMP	lithium 2,2,6,6-tetramethylpiperidine
MeOH	methanol
min	minute
MsCl	methanesulfonyl chloride
NBS	*N*-bromosuccinimide
NFSI	*N*-fluorobenzenesulfonimide
NMR	nuclear magnetic resonance

Nu-H	nucleophile
p-TSA	*para*-toluene sulfonic acid
S_NAr	nucleophilic aromatic substitution
Tf_2O	triflic anhydride
TFA	trifluoroacetic acid
THF	tetrahydrofuran
TMPH	2,2,6,6-tetramethylpiperidine
X-Transfer	halogen transfer